"A COMPARATIVE STUDY OF THE PARAGENESIS GEOCHEMISTRY AND FLUID INCLUSIONS OF SELECTED PRIMARY TIN DEPOSITS OF WEST MALAYSIA".

by

BAN NYEN FOO,
B.A.(Mod.)(Trin.Coll., Dublin University);
M.Sc., (Oxon).

Thesis submitted for the degree of
Doctor of Philosophy in the
University of London.

March 1979.

Mining Geology Section,
Imperial College of
Science and Technology,
London S. W. 7.

This thesis and the work it

relates to

is dedicated to

my wife

SHAO SHAN

and my son

POR LIN

with grateful thanks for all

their patience

and understanding.

****

ABSTRACT.

A description is given of the paragenetic sequence of mineralisation in relationship to the host rocks and structures at two of the principal hypogene tin deposits within the Eastern Belt of the S.E. Asian Tin Province in its extension in the Peninsula of Western Malaysia. The specific mines on which this paragenetic, geochemical and thermometric study has been based are the Hantu and Gakak Mines at Sungei Lembing, (State of Pahang), and the Waterfall Mine at Pelapah Kanan, (State of Johore). Additional mineralogical, petrochemical and thermal data have been obtained from selected mineralised localities in the Western and Eastern Belts and comparisons are presented.

Special emphasis is placed upon the determination and interpretation of homogenisation temperatures, salinity and phase chemistry of fluid inclusions in hydrothermal minerals notably cassiterite, quartz, fluorite and topaz and conclusions are drawn regarding the nature of the hydrothermal systems. The compositional and mineralogical results obtained by the use of Scanning Electron Microscopy on opened fluid inclusions are also discussed.

The major, minor and trace element chemistries of cassiterites from the quartz-chlorite, and quartz-feldspar-fluorite veins respectively at the Hantu and Gakak Mines of Sg. Lembing, and the Waterfall Mine are compared with those of the cassiterites from greisenised granite and alluvial and primary deposits from other areas. Regional and local differences in the contents of certain elements in the cassiterites are presented and are interpreted in terms of gross differences in the chemistries of the tin-rich mineralising fluids.

The green ferroan chlorites are the principal gangue mineral of the tin lodes in the Sg. Lembing Area. They have been chemically analysed in order to assess their role as a fluorine species. Their combined chemical and XRD data showed them to be a ferroan daphnite.

A comparative survey of published data on the contents of incompatible and compatible trace elements between the "tin-granites" and the granitoids which have no known associated tin mineralisation is made and the role of various chemical and mineral discriminants in defining "tin-granites" is discussed.

LIST OF FIGURES

LIST OF FIGURES Page

LIST OF FIGURES Page

Cont:-

LIST OF FIGURES

LIST OF FIGURES

Cont:-

LIST OF TABLES

List of Tables

ACKNOWLEDGEMENTS.

I am most grateful for the financial and moral support given to me by my family and also to Professor G. R. Davis and Dr. C. Halls of the Mining Geology Division at Imperial College who have given me this opportunity to carry out this research project. I thank Dr. C. Halls, my research supervisor, who has given much attention and time to my research, and also Dr. A. Rankin for discussion on some aspects of fluid inclusion study and Mr. R. Aldous for giving me his time to help me with the S.E.M. work. Appreciations are also extended to the technical staff of the Mining Geology Department; the Petrology and Mineralogy Sections and Geochemistry Section. I thank Mrs. Ela Ng for supervision and help given to my figure drafting and to Miss J. Crawley for typing this thesis.

Ban Nyen Foo.

25th March, 1979.

Contents

Contents Page

Contents Page

Cont:-

Contents

Contents Page

Contents Page

Contents Page

Contents Page

Contents Page

Contents Page

Contents Page

CHAPTER 1.

Introduction to the Geology of the West Malaysian Tin Province.

1.1. The Granitoids.

The tin-bearing belt of West Malaysia is the southward extension from the Burma-Thai tin belt which together with the tin-bearing Indonesian islands of Bangka and Billiton constitute the important S.E. Asian Tin Province (Fig. 1). The main axis of the West Malaysian Tin Province is constituted by three almost north-south trending parallel belts of acid intrusives known as the Western Belt (the Main Range and West Coast granites), the Central Belt and the Eastern Belt, (Fig. 2).

The typically equigranular granites (C. K. Burton, personal communication in Hutchison,1973b, pg. 222) of the Eastern Belt have been dated to give Rb/Sr ages which vary from 280 to 300 m.y. (Upper Carboniferous age) (Snelling et. al., 1968) which is compatible with their emplacement into Upper Palaeozoic metasediments. Limestones form only an insignificant part of the Upper Palaeozoic country rocks in the Eastern Belt. Hutchison (1973a) has argued that most of these granites were epizonally emplaced within 5 km. of the surface. The evidence for this is given by (a) their emplacement in Lower Carboniferous (Visean) sediments in places (Hutchison and Snelling, 1971) and (b) the presence of well developed contact thermal aureoles in the Gambang (Lim, 1971) and Sg.Lembing areas (Yeap, 1966). Hutchison's (1973a) third argument relating

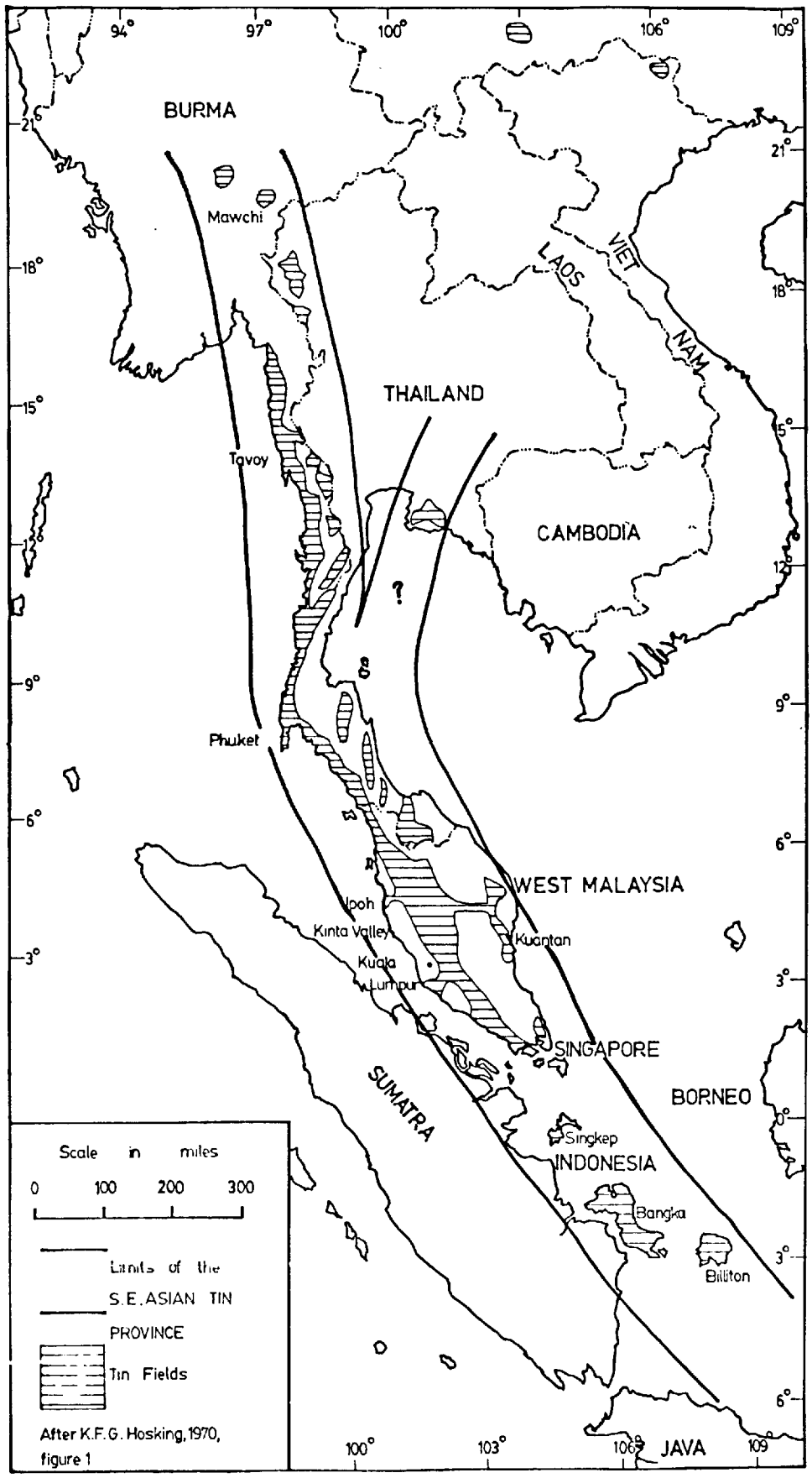

FIGURE 1 The Tin Province Of South-East Asia.

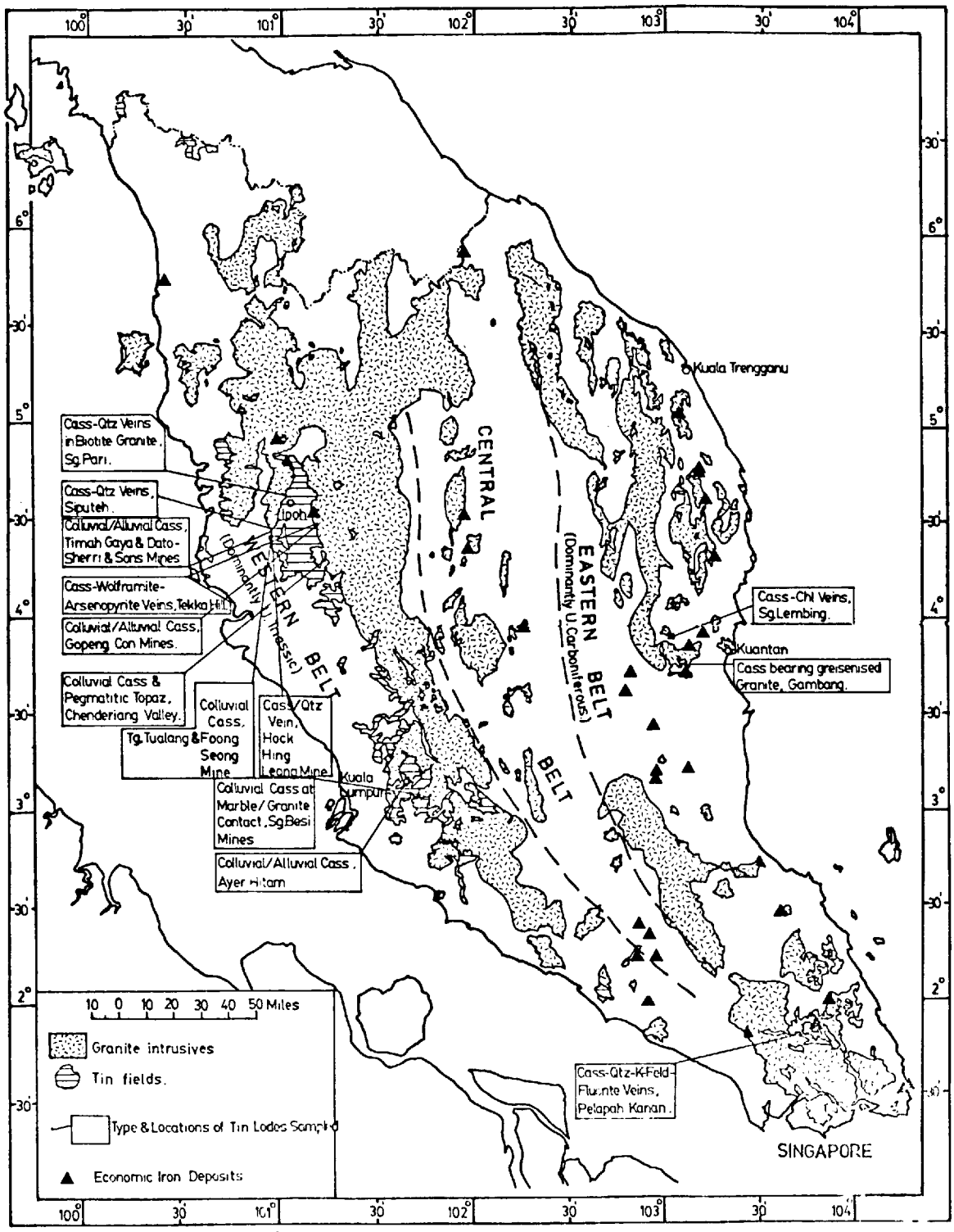

(Map from Hosking, 1973 b)

Figure 2. The distribution of the acid intrusives and the economic iron deposits and the localities and types of the tin deposits studied in Western Malaysia.

the frequency of occurrence of primary euhedral amphibole in granitic rocks to the relatively "dry" (presumably undersaturated) condition of the melt is incorrect. The presence of amphibole implies only that H_2O was present as a component of the system and by itself cannot be used as a criterion of relative "dryness" or saturation. In all probability it is likely that the water content of the original melt was of the order of 1 - 5% H_2O (Harris, Kennedy and Scarfe, 1970; Carmichael, Turner and Verhoogen, 1974). Such melts H_2O undersaturated at their source could be expected to rise to higher levels in the crust than H_2O saturated melts (Harris, Kennedy and Scarfe, 1970; Cann, 1970; Fyfe, Price and Thomson, 1978).

The average Sn contents of some granites with which tin deposits are associated is 7.5 p.p.m. (2 samples) with a range from 5 - 10 p.p.m. (Hosking, 1973b, pg. 343); those without such association have a lower average of 4.2 p.p.m. (44 samples) with a range from 2.5 - 7.5 p.p.m.

The intrusives of the Central Belt consist of several elongate bodies of equigranular microgranite and 'quartz porphyry' as at Raub and Lanchang. These were emplaced in Permo-Triassic volcanics and sandstones, however, their ages are presently not known. This belt is characterised by gold mineralisation and also by the general absence of tin mineralisation. At present this

belt is being investigated for possible lead-zinc mineralisation, (Personal communication, Jaafar, 1976).

The typically grey porphyritic biotite granites with large phenocrysts of microcline and plagioclase, (Scrivenor, 1931) from the Main Range batholith and the west coast form the intrusives of the Western Belt which is the largest of the three granitic belts. The intrusives were dated using the rubidium-strontium method and gave dominantly Upper Triassic ages although some gave Upper Carboniferous ages and others gave Upper Cretaceous ages, (Snelling et. al., 1968). Hutchison (1973b) concluded that the Main Range batholith was emplaced at a mesozonal level within 5 - 11 km from the surface. The points in favour of this conclusion are (a) that the host rocks within which the intrusives were emplaced are isoclinally folded metasediments of Upper Palaeozoic age which lie within the greenschist facies. Such greenschists, if of continental tectonic origin, would probably have formed in the depth range 8 - 15 km (Fyfe, Price and Thompson, 1978). (b) there is an apparent lack of non-developed contact thermal metamorphic aureoles suggesting that the gramites were close to thermal equilibrium with the host rocks. The greenschist grade of the country rocks supports this view, however, the abundance of calcareous rocks and allochemical alteration (tourmalinisation, fluoritisation,

greisenization and possibly hypogene kaolinisation) which is typical of the Western Belt could obscure the development of classical hornfelsed aureoles. The absence of primary amphibole from the granites of the Western Belt is used by Hutchison (1973a) as a third point in favour of the 'wet' condition of the granitic rocks. This is not valid evidence, although if all the general geological features under points (a) and (b) are considered it seems possible that the granite melts of the Western Belt were to some degree higher in water content than those of the Eastern Belt.

Marmorised limestones of various ages (Carboniferous and Permian) are common in the Kinta and Kuala Lumpur Valleys. The average Sn content of "fresh" vein free granites with which tin deposits are associated is 6.5 p.p.m. (average of 25 samples) with a range from 2.5 to 12.5 p.p.m. In contrast, a lower average Sn content of 5.1 p.p.m. (average of 109 samples) with a range from 2.5 to 12.5 p.p.m. was recorded for granites without associated tin deposits (Hosking, 1973b), p.343)

The genesis of these granitic belts has been interpreted in terms of plate tectonic mechanisms by Hutchison (1973 and 1973b). He proposed that the Upper Carboniferous granites from the Eastern Belt and the Western Belt were generated at a westward dipping Benioff Zone which

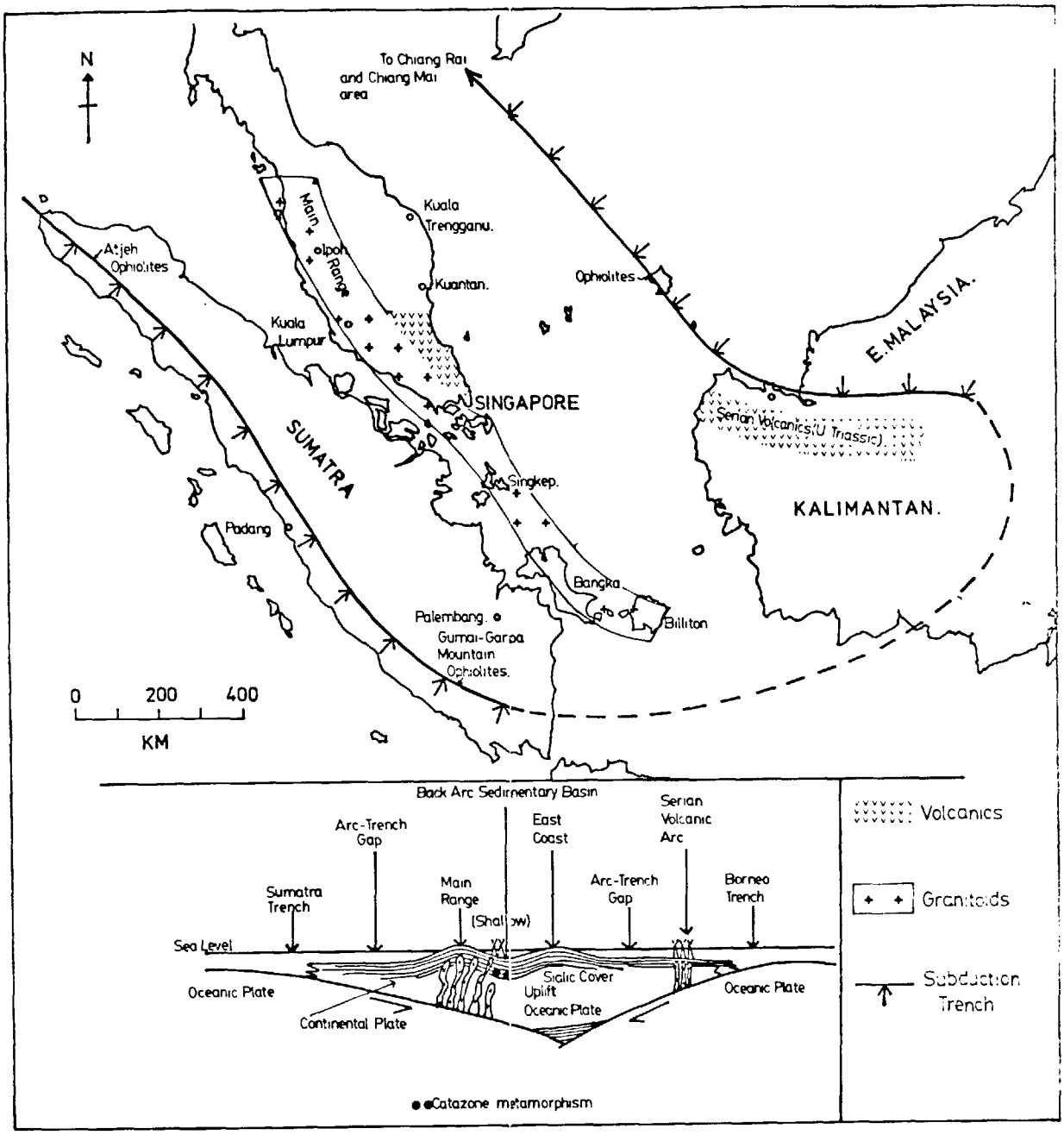

After Hutchison, 1973.

Figure 3 Palaeo-tectonic scheme for Late Triassic to Early Jurassic for the Sundaland region, The diagrammatic cross section shows the two igneous arcs in relation to the opposite-facing subduction pattern.

trended roughly parallel to the long axis of the West Malaysian Peninsula, (Fig.3). This proposal is in agreement with the suggestion of Hutchison and Jeacocke (1971) that a dioritic magma was the parent of these differentiated Upper Carboniferous granites. A significant body of petrochemical data revealed in a later part of this thesis shows that the majority of the granitic rocks of the West Malaysian Peninsula belong within the S-type of Chappell and White (1974) and a uniquely subduction origin for these rocks is debatable. The Upper Carboniferous granites, e.g. the Bintang and Kledang Ranges and the Dinding areas of Perak and Penang Islands in the Western Belt are more differentiated than their counterparts of the Eastern Belt, (Hutchison, 1973a). Hence they would be considered distal granites according to the classification of Kuno, (1966).

The Upper Triassic granites of the Main Range have been interpreted as having been formed by anatexis of a sialic crust in response to anomalously high heat flow associated with subduction of the Sumatran plate during the Triassic, (Fig.3). This increased heat flow was also responsible for the metamorphism of the metasediments of the shallower levels to the greenschist facies, (Hutchison, 1973a).

There are, no doubt, considerable areas of uncertainty regarding the precise tectonic framework and petrogenetic processes governing the genesis of the three belts of eruptives in the West Malaysian Peninsula. It is, however, certain that the intrusives of both the Eastern and Western Belts possess certain special features of petrochemistry in common which have led to the generation of tin deposits of economic interest.

1.2. Regional distribution of Tin and Iron Mineralisation.

The distribution of both primary and secondary tin deposits, and primary iron deposits as shown in figure 2 indicates clearly that they are spatially closely related to the granitic intrusives of the Eastern and Western Belts. Thus these belts should be referred to as Iron-Tin Belts. However, they are popularly known as Tin Belts.

The tin and iron deposits were essentially emplaced in the vicinity of the granite contact: the tin deposits within the intrusives are sparse and small, (Hosking, 1973a). Thus, it can be inferred that the granitic intrusives could have either acted as the source of the mineralising fluids or have acted in a secondary role to remobilise and reconcentrate pre-existing sedimentary ores. However, the style and the intensity of tin

mineralisation are different in the two tin belts. The Western Belt is much richer in primary and, in particular, in secondary alluvial tin deposits than the Eastern Belt. These deposits concentrate largely along the western flank of the Main Range of the Western Belt with the richest occurrences in the Kinta District and the Kuala-Lumpur Area where Karst limestone (Upper Palaeozoic) bedrocks have been eroded to Karst topography and have trapped vast amounts of alluvial and colluvial cassiterite released as a consequence of extensive erosion during the Quaternary Period. In contrast, the Eastern Belt is less mineralised with respect to tin as shown in figure 2. This difference may not be real, as the thick and inacessible tropical jungles together with the presence of the Communists' activities in the jungles have discouraged tin mining activities in the Eastern Belt. Furthermore, the Eastern Belt has been subject to erosions obviously much less intense than those experienced by the Western Belt. In addition the fact that there was an almost complete lack of limestones in this belt to produce Karst topography to trap the alluvial/colluvial cassiterites.

The two well known alluvial tin fields are at Gambang and Kota Tinggi, but they are in no way comparable in size or grade to the Kinta and Kuala Lumpur alluvial tin fields.

Despite the less intense overall tin mineralisation in the Eastern Belt, the Sg Lembing hydrothermal tin deposits mined by the Pahang Consolidated Company Limited are by far the largest hypogene lode deposits presently known in this belt and perhaps they are also the largest in the whole South East Asian Tin Province, if not the world. These cassiterite-chlorite lodes are very extensive down dip (2,000 feet) and also variable along strike (440 feet to 1,750 feet). They occur within the Quartz-Muscovite-chlorite-biotite hornfelses near the granite contact. Most of the important economic iron deposits occur in the Eastern Belt and they are the Bt. Besi and Machang Satahun of Trengganu: Ulu Rompin of Pahang and Pelapah Kanan und Pelapah Kiri of Johore. Thus it gives an impression that this belt is richer in iron mineralisation than the Western Belt as can be seen in figure 2. Magnetite and haematite are the ore minerals in these deposits except for the ferromanganese ore of Machang Satahun. Martite forms a cap rock over the magnetite deposits. The iron mineralisation of these deposits pre-dates the associated cassiterite mineralisation although some cassiterites were formed contemporaneously with the iron minerals. A Carboniferous-Triassic age for the iron deposits has been suggested by Bean (1976) who has also postulated a hydrothermal replacement origin related to subjacent/nearby granitic intrusives for these deposits. Only the martitised magnetic skarn ore deposit of the

Waterfall Mine at Pelapah Kanan was selected for mineralogical and fluid inclusion investigations during the present study.

CHAPTER 2.

The Sg. Lembing Tin Field.

2.1. Introduction.

The Sg. Lembing tin field is located near the mid-point of the Eastern Belt which extends from latitude 7° north in Southern Thailand to latitude 1°30' north in South East Johore, (Western Malaysia), (Fig. 2).

This tin field has been the property of the Pahang Consolidated Company Limited since 1906 and it is one of the largest underground tin mines in the world with over 300 miles of underground workings in about 46 tin lodes covering an area of six sq. miles. Since the First World War the annual production from this tin field has amounted to 5% of the national total or 1½% of the world's total, (Fitch, pg. 68, 1952). About 8,691,000 tons of ore have been mined during the years from 1891 to 1966 yielding 121,000 tons of tin concentrates of a value of £36,489,000, (P.C.C.L. pg. 70, 1966). Up-to-date recorded production exceeds 11 million tons of ore, (Pun and Singh, 1978). The current cut off grade for the ore mined is 0.8% Sn over a width of 48 inches, but the average assay of the lodes is 1.2% SnO_2 over an average width of 36 inches, (Pun and Singh, 1978).

The tin lodes of the Gakak, Willinks and Hantu

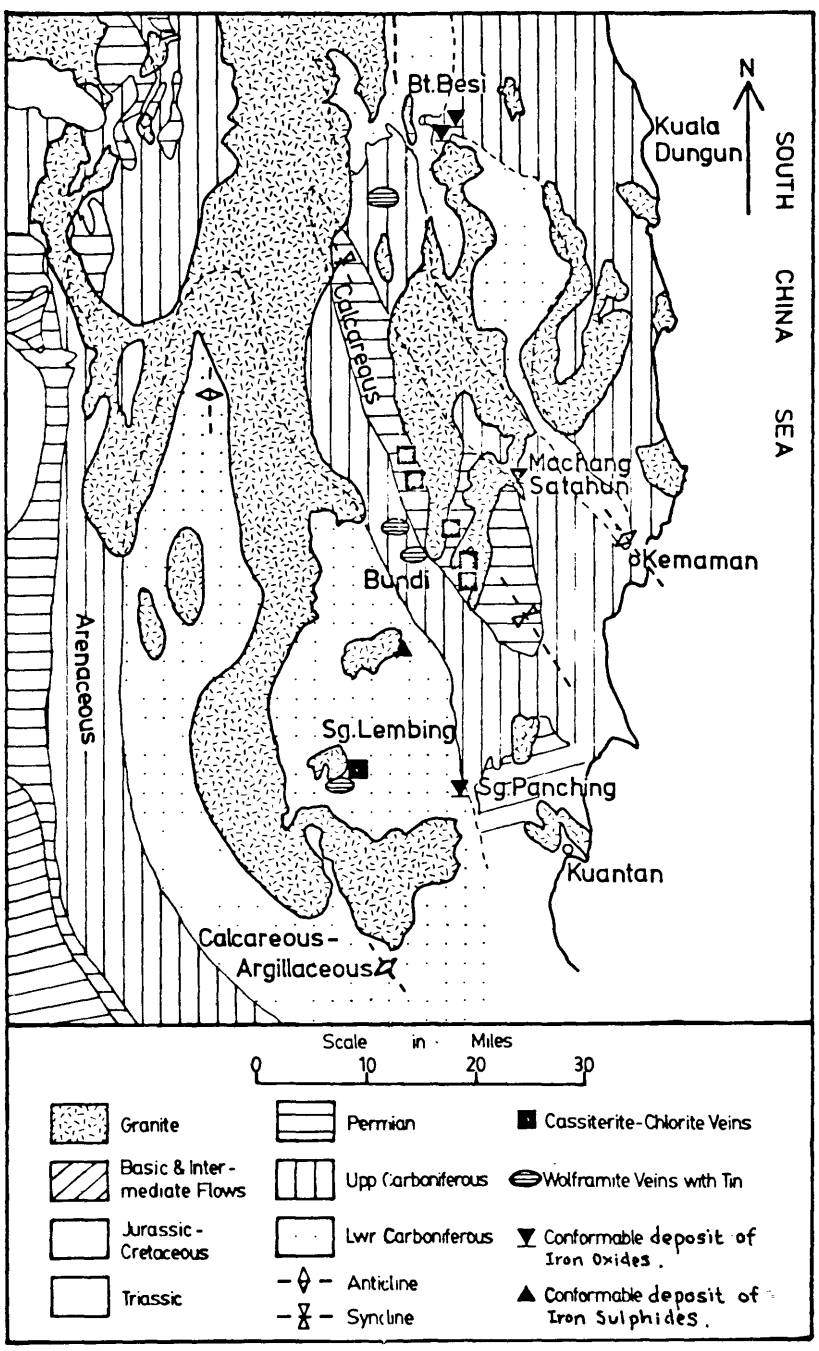

Fig 4. The Geology Of Pahang-Trengganu Tin Field.

After Garnett, 1966.

Mines were selected for detailed study by a range of methods because those lodes revealed typical and well developed mineralisation and most of the operating faces of these lodes were accessible and safe during the writer's visits. Structural and mineralogical study was concentrated on the lodes from the Gakak and the Hantu Mines; fluid inclusion studies were made on the Willinks Main Lode System and the Hantu Lode System of the Willinks and the Hantu Mines respectively. This study was made possible because of the abundance of suitable primary fluid inclusions in the minerals of these lodes; a geochemical investigation was made on cassiterite and gangue ferroan chlorite from the veins of the Gakak III Lode and the Hantu Lode Systems respectively.

2.2. Regional Geology.

The cassiterite-chlorite lodes of the Sg. Lembing and the neighbouring Bundi tin fields were located in an almost north south trending anticline and syncline respectively, (Garnett, 1966), in the vicinity of the contacts of the granitic intrusives of Upper Carboniferous Age, (Fig. 4). The host rocks of the Sg. Lembing tin lodes are Lower Carboniferous calcareous-argillaceous metasediments whereas those of

the Bundi tin field are calcareous shales and have a Permian Age. From figure 4 it is apparent that the tin lodes are preferentially developed in the calcareous metasediments which evidently responded to the regional tectonic stresses in a more brittle fashion than the granitic intrusives. The calcareous shales may also have provided a more favourable chemical environment for the precipitation of cassiterite and its gangue minerals.

2.2.1. Sedimentary Rocks.

The Lower Carboniferous, (Visean), metasedimentary rocks of the Sg. Lembing Area are largely calcareous shale interbedded with subordinate siltstone and quartzite all dipping generally about 30 degrees to the east-northeast. The quartzites are known to form beds up to 20 feet thick between bands of shale, (Fitch, 1952).

According to Fitch, (1952), the sedimentary rocks in general have not been strongly metamorphosed by the heat of nearby granitoids. Even the sedimentary rocks from the granitoids/

PLATE 1.

Transmitted light photomicrograph of a typical quartz-biotite (green) hornfels in section 80/W[a] of the 3rd level drive belonging to the Gakak III Lode System. This hornfels was collected from a local area free of lode mineralisation . The green biotite is pointed by an arrow. (Crossed Polars).

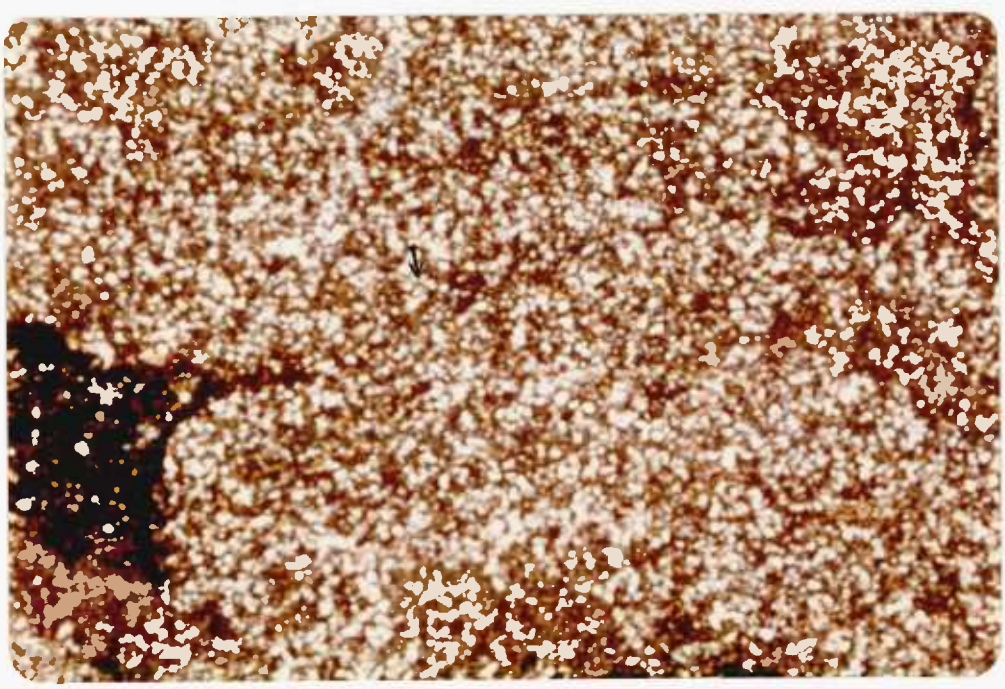

5X

shale contact do not show any sign of metamorphism and yet in places further away from the contact mica schist and chiastolite-bearing rocks are present. In contrast to the poorly developed hornfels as reported by Fitch, (1952), Yeap, (1966) has recognised the presence of a well developed hornfels around the granodiorite of the Gakak Mine. Yeap's finding is in agreement with that of Smith (1967) who has identified the presence of andalusite and chiastolite shales in drill cores from the Old Gakak Main Lode, (Gakak Lode), area. Smith (1967) has also recognised well developed Wollastonite, epidote and garnet, (brown), bearing hornfels in the lower eastern workings of Myah Mine. The writer has also recorded andalusite hornfels, in the 10th Level cross cut, (S.E.), at section $77/A^{b}$ of the Gakak Mine, but the common metamorphic facies of the metasedimentary rocks at the Gakak Mine inclusive of those at the granodiorite/shale contact is a muscovite-chlorite-magnetite-biotite-quartz hornfels, (Plate 1). Thus it can now be stated that well developed muscovite and andalusite/chiastolite hornfels are widespread around the granodiorite of the Gakak Mine.

2.2.2. Granite.

The Upper Carboniferous porphyritic medium grained biotite granite of the Sg. Lembing Area, (Fitch, 1952), is spatially, and by inference, genetically related to

the tin lodes there. However, economic deposits have never been traced into the granitoids and this is in marked contrast to the tin deposits in the Western Belt of Western Malaysia and also those of Cornwall. The emplacement of tin lodes within the endocontact zones of a granitoid would require the impounding of the tin rich mineralising fluids by impervious envelope rocks such as limestones or marbles. Marbles are common envelope rocks of granitic intrusions in the Western Belt, but they are very rare in the Eastern Belt, consequently the emplacement of tin lodes in the endocontact environment of granitoids in the Western Belt can be, to some extent, expected. In the Sg. Lembing and neighbouring areas marble is virtually absent although a few isolated marble hills do occur along the Kuantan end of the Kuantan-Sq. Lembing road. Perhaps the granitoids here may be mineralised and, therefore, deserve investigation.

The biotite granite occurs underground in the west of Willinks Mine, below the Kabang and Simons lodes in the east, (Fitch, 1952). Muscovite-biotite granodiorite has been intersected by the Gakak Shaft to the west of the Gakak Mine. Thus it is apparent that variations in the grain size and in the petrographic composition of the granitoids in the Sg. Lembing Area do exist. The actual configuration of the granitoids is at present imperfectly known. An investigation into the overall configuration of the

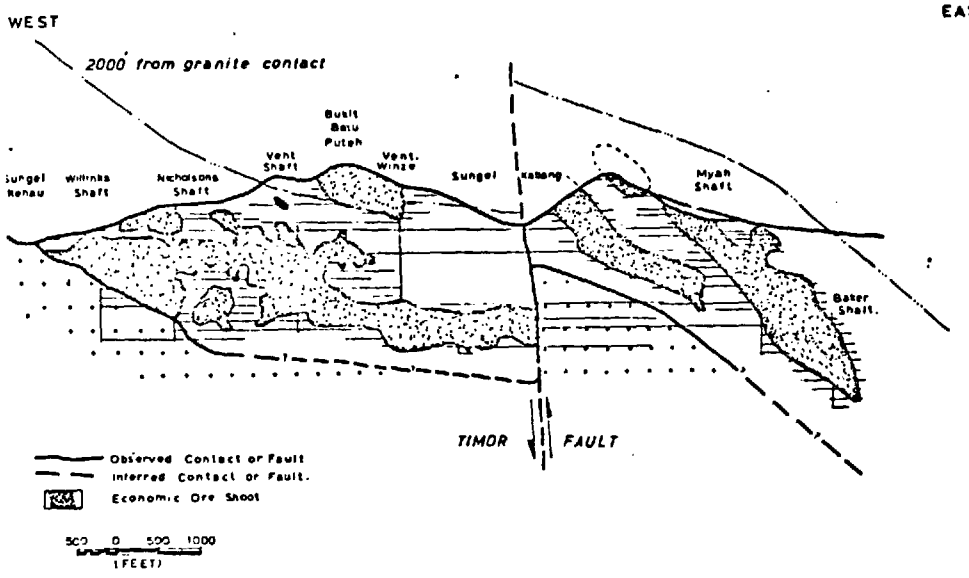

Figure 5. The present positions of the granite and the tin zone after late faulting. After Fitch, 1952.

PLATE 2.

A. The granodiorite from the 10th level shaft of the Gakak Mine shows a hollocrystalline texture composing of plagioclase (a), orthoclase (b) and quartz (c) with veinlets of calcite filling the fractures of the rock. Note the predominant abundance of the plagioclases over the orthoclases. (Crossed Polars).

B. Low magnification veiw of the Gakak Mine granodiorite showing its medium grained hollocrystalline texture and the presence of micas (a) and euhedral and subhedral pyrite grains, (b). (Crossed Polars).

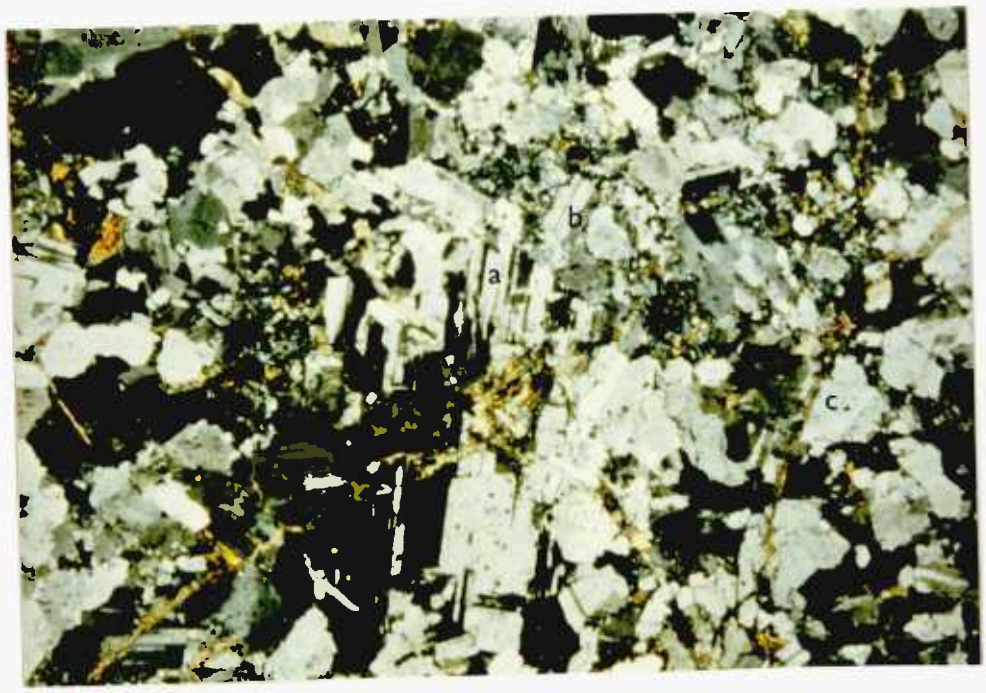

4X

1.5X

Sg Lembing granitoids by geophysical methods, (gravimetry), would be valuable as this would also help to search for tin lodes which are known to be spatially and by inference, genetically, related to the granitoids in this area, (Fig. 5). Although the granite/shale contact to the west of the Willinks Mine is irregular, it is generally dipping about 30° to the east which is more or less parallel with the dip of the bedding of the metasediments, (Fitch, 1952). The writer has recorded a dip of 40° northeast for the unfaulted granodiorite/shale contact of the Gakak Mine granodiorite exposed at the 9th level of the Gakak Shaft. Fitch, (1952), has described the fresh granites of Willinks, and Kabang and Simons sections as porphyritic medium-grained biotite granite with an increase of muscovite and feldspar and a corresponding decrease of biotite as the granite approaches the granite-shale contact. Chloritisation at shear zones and next to quartz veins imparts a greenish look to the otherwise grey granite. However, the Gakak granodiorite is medium grained hollo-crystalline, (Plate 2A), and it contains a predominant amount of sodic plagioclases, (Plate 2A), and minor amounts of euhedral and subhedral pyrite, (Plate 2B), with chloritization and muscovitization of brown biotites as its distinctive features. Rutile laths and subhedral plates were formed as alteration products of chloritization and they often occur aligned parallel to the cleavage planes of chloritised biotite, (Plate 3A). These features are to be expected since it is the contact facies of the Gakak granodiorite which is in those

samples examined in this present study. Fitch, (1952), has also recognised these features in the contact facies of the porphyritic, medium-granied biotite granite. The green coloration in nearly all the contact facies of the granite intersected in various mines as reported by Smith, (1967), is to be considered a result of chloritisation of biotite and this, according to Smith, (1967), only occurs in granite in contact with argillaceous or calcareous shale. The contact phase of the Gakak granodiorite which has a shale contact is, in fact, greenish in colour confirming the trend observed by Smith, (1967). The ubiquitous plagioclase in the Gakak granodiorite was identified as Oligoclase ($Ab_{70}An_{30}$) by the Michel-Levy Method; only small amounts of orthoclase are present. The feldspars, in particular, together with the muscovite and biotite were sericitised. The biotites have been variously chloritised and sericitised in places making it impossible to study the trace element geochemistry of the respective altered biotites.

The roof zone of the Gakak granodiorite at the 9th Level of the Gakak Shaft and the deeply weathered granitoid at the Jeram Batang road cutting were mineralised by barren white quartz veins. The Gakak granodiorite has been extensively mineralised by calcite which occurs as veinlets or as fillings in the intergranular spaces or fractures. The calcite was largely derived from calcium and carbonate-enriched ground waters which had their source in the calcareous shales. The granodiorite

PLATE 3.

A. Laths of rutile interleave with the cleavages of chlorite from the granodiorite of the Gakak Shaft in Gakak Mine. (Plane Polarized light).

B. The granodiorite sample right next to the granodiorite/shale contact fault at the Gakak Shaft of the Gakak Mine shows an increase in its quartz contents which has evidently resulted from the sericitisation of feldspars. The effect of the fault movement has fractured larger grains of quartz and the resultant fractures are filled by calcite (a) and sericite (b). (Crossed Polars).

200μm

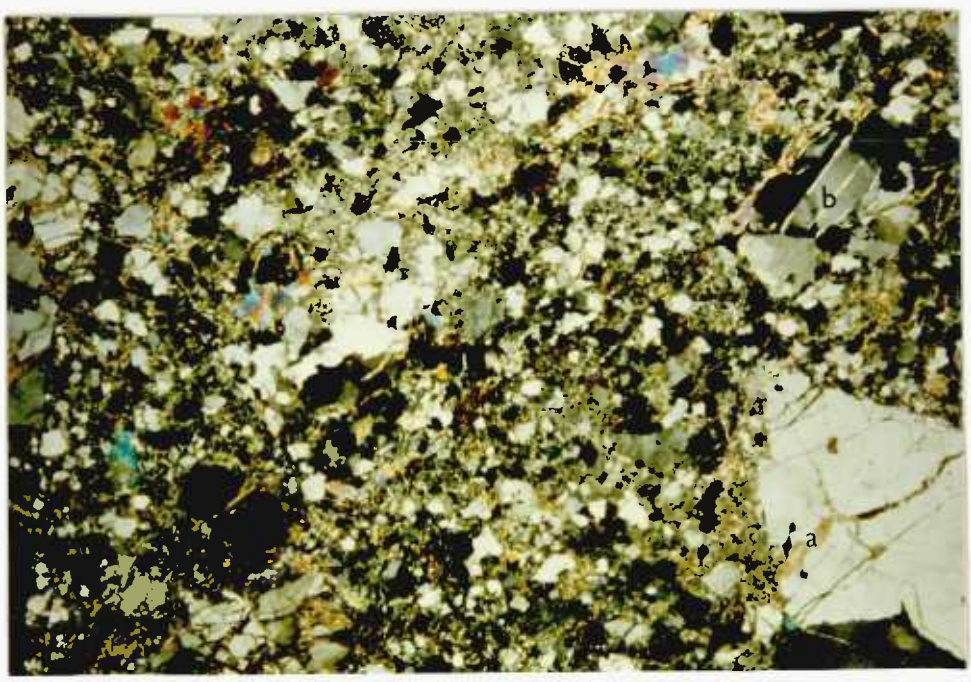

1.5 X

shale contact at the 10th Level Shaft is faulted and consequently the quartz grains in the granodiorite right next to the fault were brecciated and fractured and were subsequently cemented by calcite and muscovite, (Plate 3B); the feldspars were all virtually altered to sericites and secondary quartz , (Plate 3B).

A study of the major, minor and trace element chemistry of the Gakak granodiorite was undertaken by the author and its results are discussed in section 8.1.6 Yeap (1966) in his doctoral project has studied the trace element pattern of Rb, Sn, Nb, W, Sr, Zr and Ba in the granitoids of the Sg. Lembing Area and he found that a progressive enrichment of Rb, Sn, Nb,and W, and a corresponding progressive impoverishment of Sr, Zr and Ba in granitoids which are nearer to the tin lodes. This potentially useful geochemical trend has also been recognised in the Kuala Lumpur and Gambang Areas by the same author, (as reported in Hosking et. al., 1975). Yeap interpreted this trend as a secondary, (epigenetic with respect to the host granite), geochemical pattern imposed on the granitoids by the mineralisation event.

2.3. Mineralisation Events and their associated tectonic hydraulic structures.

Underground field observation together with detailed thin and polished section studies of the tin lodes in

the Gakak and Hantu mines have led to the recognition of five main mineralisation events in the respective mines. These are listed as shown below:-

1. Cassiterite + Ferroan Chlorite mineralisation with minor sulphides ± quartz.

2. Barren white quartz mineralisation emplaced in a sequence of dilational events.

3. Sulphide mineralisation with minor cassiterite.

4. Emplacement of Amphibole-pyroxene andesite dykes.

5. Calcite mineralisation.

2.3.1. Cassiterite-ferroan Chlorite mineralisation with minor sulphides.

This mineralisation event was the first to occur in the lode systems studied and also in other lode systems in the Sg. Lembing Area. This mineralisation event has deposited large economic amounts of cassiterite intimately intergrown with green ferroan

chlorite and minor amounts of sulphides. The detailed mineralogy and paragenesis of this stage are described in Chapter 3.

A single phase of cassiterite mineralisation was recognised in the Gakak Lode System, two phases were recognised in the Hantu and Gakak III Lode Systems and finally three phases in the Gakak III Extension Lode System.

This mineralisation takes the following forms:-

1. (a) Wallrock replacement ore.
   (b) Wallrock Stringer ore.
   (c) Quartz cassiterite chlorite vein-fillings with typical textures of hydrothermal deposition.

2. Breccia ore with cockade texture.

1(a). Wall replacement ore.

This is the commonest form of cassiterite mineralisation and it was emplaced symmetrically within both margins of the lode fault structures as the tin rich fluids diffused from the opened vein into the wallrocks assisted by microfissures created by the

tectonic, (and hydraulic?) stresses. This first important phase of tin-rich fluids have deposited economic quantities of fine-grained cassiterites and at the same time they have also almost totally chloritised the primary hornfels biotites and muscovites in the wallrock. Sparse relicts of biotite and muscovites can be seen (Plate 16B), in most places. Where the influx of tin-rich fluids was intense, anhedral cassiterite masses were formed within a matrix of green ferroan chlorite-recrystallised hornfels quartz. However, cassiterite also occurs very commonly as granular disseminations and granular aggregates and microveinlets/veinlets in a matrix of green ferroan chlorite with or without quartz. The granular disseminations are often found nearby veinlets of cassiterite. In quartzite host rock, quartz is the dominant phase of the matrix whereas in shale chlorites become the dominant mineral. Euhedral quartz grains from the quartzite have been seen to be the nucleii of crystallization of granular cassiterites, (Plates 17A). Cassiterites, being brittle in nature, together with their early deposition were vulnerable to later imposed deformation and consequently they are well fractured except for the tiny disseminated grains. These fractures are commonly infilled by simultaneously formed green ferroan chlorites which could have been physically injected into them by the deformation processes. As mentioned earlier the processes of cassiterite mineralisation and chloritization were

PLATE 4.

B. The cassiterite-chlorite-quartz bearing selvedge at the right hand margin of the later quartz veins complex is cut by a quartz vein which branches out from the quartz veins complex. Note the development of stylolites (arrowed) and the incorporation of chloritic wallrock within the quartz veins complex. This section of the Gakak III Extension Lode System was exposed at a 8th level drive in Section $86/S^{a}$.

contemporaneous in age which also supported by both chemical and mineralogical evidence.

The cassiterite-chlorite bearing wallrocks of lode fault structures were later mineralised by minor amounts of sulphides occurring as veinlet fillings. Since this stage of mineralisation was largely confined to the wallrocks of the lode fault structures, it can be inferred that the latter, which were acting as channel-ways for the mineralising tin-rich and sulphide-rich fluids, must either not have afforded much open space during the cassiterite-forming episode or the fluid pressure of the mineralising fluids exceeded the pore fluid pressure in the wall rock thereby allowing the mineralising fluids to diffuse into the porous wall rock and the microfractures where the chief body of tin mineralisation occurred. These lode-fault structures were subsequently centrally filled in multiple stages by barren milky white quartz and consequently the quartz vein complexes which formed can be used as 'leaders' in the pursuit of cassiterite-bearing lodes. These quartz veins have in places branched out to cut into the cassiterite-chlorite bearing borders, (Plate 4 and they have also impregnated the mineralised selvedges there. Thus, the cassiterite-chlorite-minor sulphides mineralisation event had occurred before the quartz veins.

(b) Stringers.

Two generations of cassiterite stringer occur in the intensely sheared shale between the quartz filled gashes at the 10th Level drive of Gakak III Extension Lode System in section 84/T[a]. The earlier generation occurs along the series of sub-parallel stylolites and along the borders of earlier quartz and chlorite veinlets. This was followed by a later generation which cut the stylolites, but which has in places followed them briefly, (Plate 22C). These cassiterite stringers also cut the chlorite veinlets. Furthermore, the two generations of cassiterite have also diffused into the host rocks as disseminated grains which are, unfortunately, not abundant.

Discontinuous stringers of cassiterite have been observed to penetrate the fine parallel bedding planes of a chlorite-rich rock from the 1200' Level drive of the Hantu Lode System in section 42/m". Here they are associated with later rutile which has in places surrounded the cassiterite grains, (largely non-pleochroic), (Plate 27B). Disseminated cassiterite grains also occur in the chlorite shale in between the stringers. Some of these cassiterite grains have suffered almost total pseudomorphism by quartz.

PLATE 5.

A. This cassiterite-bearing 'black-dyke' is believed to be initially a cassiterite-quartz vein with quartz occupying the central zone of the vein. The texture of this 'black dyke' does, however, suggest that the cassiterite-quartz vein was disrupted violently with the result that fragments (a) of quartz were cemented in a matrix composed of chlorite, sericite, biotite and quartz which is believed to be material largely derived from the hornfelsed wallrock. The presence of cassiterite, (arrow b), mineralising around fragments of the matrix and the clasts of quartz suggests that the fluid medium which accompanied this event of violent disruption was tin rich. (6th level Stope of the Gakak III Lode System in Section $75/A^{b}$).


b
a
3cm

(c) Vein.

Cassiterite-chlorite-quartz vein fillings often occur as veins which are ½" to 1 3/4" wide, (Plate 27A). They represent mineralisation of the first cassiterite-chlorite$^{+}_{-}$quartz stage on dilated extension fractures which were created by fault movements. These fractures are normally orientated obliquely to associated planes of movement defining the principal lodes.

2. Cockade Ore.

Cockade ore is essentially a mineralised tectonic/hydraulic breccia. This form of cassiterite-chlorite mineralisation occurs in the Hantu Lode System, (600'/35/N"), and the Gakak III Lode System, (9th Level Stope/76/A^{b}).

This form of mineralisation is not suprising as the shale country rocks are fissile which means that a shale band bounded by two parallel active fractures or intersected by a fault would become brecciated as a result of movements in these structures. The resultant breccia fragments were mineralised and cemented together by tin-rich hydrothermal fluids to

PLATE 6.

A. A cassiterite and quartz-bearing mineralised breccia ore from the 600 ft. drive of the Hantu Lode System in Section 35/N" shows the presence of well-rounded breccia shale fragments in various sizes. These fragments are used as centres of crystallisation for cassiterite (a). The cassiterite mineralisation is followed by a phase of white quartz mineralisation which occurs as veinlets (b).

B. A cassiterite-quartz-bearing mineralised breccia ore from the 9th level stope of the tin lode belonging to the Gakak III Lode System in Section 76/A^b displays the presence of angular breccia shale fragments, (arrowed), of various sizes cemented together by cassiterite. It is apparent that this phase of cassiterite mineralisation was cut by a fault plane which was later mineralised by quartz, (a). This mineralised rock is cut by a series of thin veinlets of calcite, (arrow b), which are seen to cut across the breccia fragments.

C. Quartz filling the interstitual spaces between the mineralised breccia fragments and also the fractures within the cassiterite-bearing mineralised breccia.


1 2 3 4 5 6 7 8 9 10 11 12 13
cm

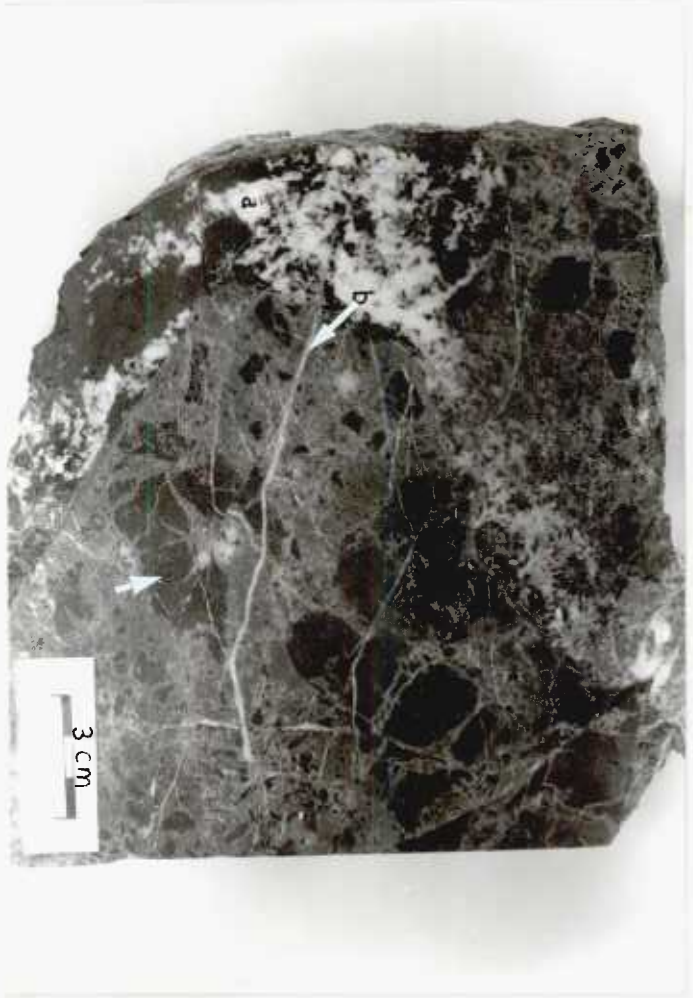
a
b
3 cm


a
b
3 cm

form a minerlaised rock with a cockade texture.

The cockade ore exposed at 600'/35/N" in the Hantu Lode System is comprised of well-rounded breccia shale fragments with shiny surfaces, (Plate 6A), in contrast to the angular shale fragments, (Plate 6B), seen in the cockade ore from the 9L stope/76/A^b of Gakak III Lode System. This difference in the roundness of fragments indicates that the former were probably constituents of a fluidised system supported by the tin rich hydrothermal fluids. In both examples cassiterite was deposited around the margins of the breccia fragments and sometimes also in the fractures developed within the fragments. These cassiterite-chlorite bearing breccia ores were fractured and dilated by continued movements of the faults concerned. The resultant fissures and spaces created were mineralised by quartz which can be seen to form veinlets cutting across the breccia fragments, (Plate 6C), and also as interstitial materials infilling the spaces between the mineralised breccia fragments.

PLATE 7.

A. A quartz veins complex bifurcates to incorporate a lens of chloritic pelite wallrock. The growth of the quartz veins complex was assymmetrical as indicated by a greater concentration of slivers of chlorite wallrock on one side of the quartz veins complex. This complex is cut by lenses of calcite (arrowed). This section of the Gakak Lode System was exposed at the 5th level drive.

B. Sphalerite-galena-cassiterite bearing wallrock fragments are incorporated in a composite quartz vein during its emplacement. This hand sample of the Gakak III Lode System was collected from a 6th level stope at 40 ft. above the 6th level drive in section $76/77/Y^a/Z^a$.


1
2
3
4
5
6
7
8
9
10
11
12
13
14
15
16
cm

2.3.2. Barren white quartz mineralisation.

This mineralisation event succeeded the economic cassiterite-chlorite$^{+}_{-}$quartz mineralisation event. It has many phases which were emplaced largely as a steeply dipping, (55^{o} to 85^{o}), non-crustified massive vein complex in the lode fault structures during multiple episodes of hydraulic/tectonic dilation with the result that numerous thin slivers of mineralised chlorite wallrock were incorporated in the quartz veins, (Plate 7A The quartz veins are also characterised by the presence of stylolites, (Plate 7A), which must have been formed by lateral compression either along the contacts of successive phases of quartz fill or within a single phase of quartz deposition when the pressure of the silica-bearing hydrothermal fluids supporting the dilation of the lode fault structure was exceeded by the horizontal confining stress and the opening collapsed so that the stress was transmitted directly to the mineral filling in the lode. Breccia fragments rich in cassiterite have been seen just inside the bottom left margin of an almost vertical dipping quartz vein of the Gakak III Extension Lode System at the 10th level drive in Section $86/S^{a}$. At a 6th level stope in section $76/77/Y^{a}/Z^{a}$, the multiple nature of a 10" wide composite quartz vein of the Gakak III Lode System is clearly shown by the presence within it of a series of more or less parallel discontinuous stringers of chloritic wallrock bearing sphalerite, galena and cassiterite, (Plate 7B). The texture of

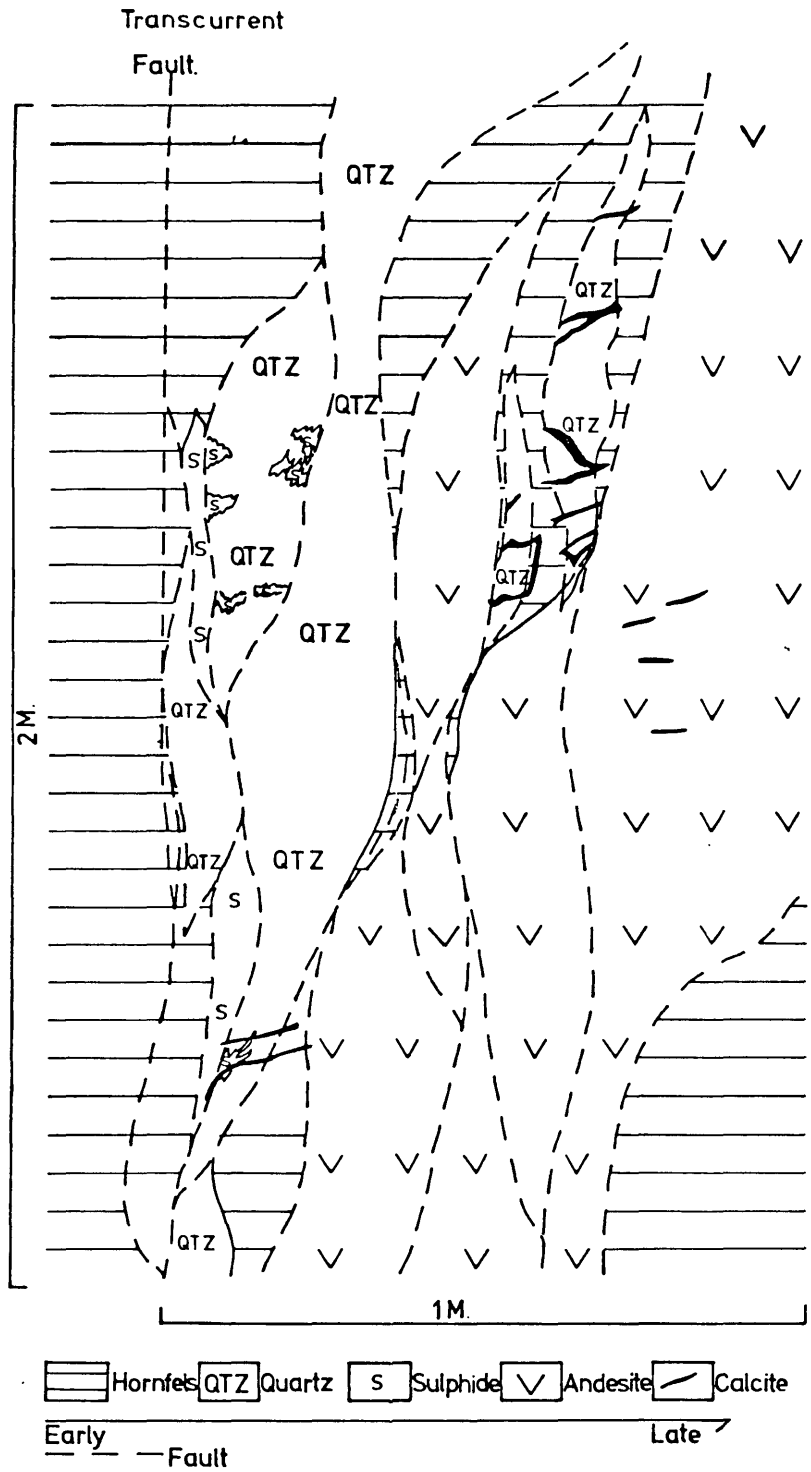

Figure 6. Structural and paragenetic relationship of the mineralisation events belonging to the Gakak Lode Extension System as seen in a face section on the 8th level drive in section 89/R[a].

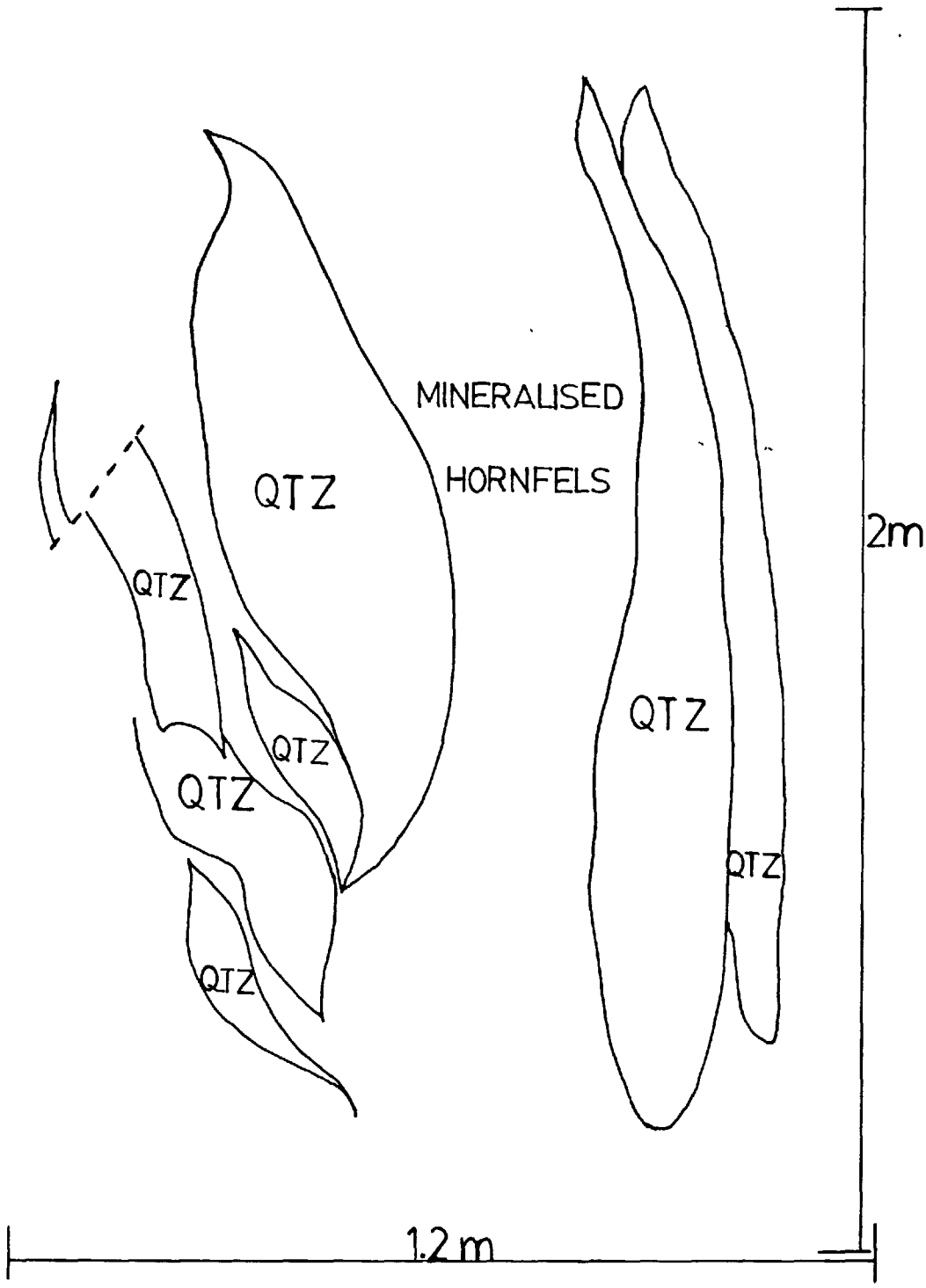

Figure 7. Structural and paragenetic relationships between the cassiterite-chlorite lode and the barren white quartz veins of the Gakak III Extension Lode System as seen on a face section on the 10th level drive in Section 84/U[a].

PLATE 8.

A. Two parallel complexes of quartz veins are linked by oblique quartz veins emplaced in oblique fractures created by drag movement. The quartz veins complexes show a braided 'streaky-bacon' texture with the incorporation of slivers of chlorite wallrock. Limonitic stains are also seen on the surfaces of the quartz veins complex. This section of the Gakak Lode System was exposed at the 3rd level branch S.W. at 175 ft. in section $75/j^{a}$.

B. Subhorizontal slickensides, (arrowed), developed across the black pelites, the quartz vein and the andesite dyke of the Gakak III Extension Lode System at the 10th level drive in Section $86/S^{a}$. This indicates that the formation of the slickensides occurred after the emplacement of the andesite dyke by a strike slip fault movement. Note planes of the slickensides are mineralised by calcite. It is possible to determine the nature of the fault movement responsible for the formation of the slickensides. The slickensides-forming fault movement was in an anti-clockwise fashion.

the chlorite slivers-bearing quartz veins indicates that the amount of each dilation of the mineralised fault lode structure was not uniform. This variation in the magnitude of the dilation of a fault was likely to be due to changing fluid pressures of the silica-bearing fluids and the geometry of fractures. The asymmetrical pattern of the chlorite slivers in the quartz veins, (Plate 7A), indicates that the emplacement of the quartz during the successive dilational episodes of the lode-fault structure was asymmetrical. A complex of thin, (approximately ½" wide), quartz veinlets were emplaced in oblique extension fractures of both the hanging and footwalls of a 4" wide quartz vein of the Gakak III Lode System at a 5th Level stope in section $76/Y^a$. At the 3rd Level branch drive at 175 feet of the Gakak Lode System in section $75/j^a$ two parallel quartz veins were linked by oblique quartz veins which were emplaced in fractures created by drag resulting from a sinistral vertical wrenching movement of the two quartz veins, (Plate 8A). In two locations, one at 8th Level drive in section $89/R^a$, (Fig. 6), and another at 10th Level drive in section $84/u^a$, (Fig. 7 the quartz phases of the Gakak III Extension Lode System were seen to be emplaced in a complex of almost vertically orientated en echelon tension gashes, (Fig. 6 and 7), of varying sizes from the largest of 6.5' by 1' to the smallest of 1' by 3". These gashes were evidently created by lateral and vertical wrench faulting which is no doubt common as indicated by the

PLATE 9.

A. A ramifying network of quartz filled hydraulic fractures in pelites. This section of the Hantu Lode System was exposed at the 500 ft. intermediate level drive west in section 33/M.

B. A series of more or less parallel calcite veinlets cutting the quartz veins complex of the Gakak III Extension Lode System as seen on the wall of the 10th level drive in Section 86/S^{a}.

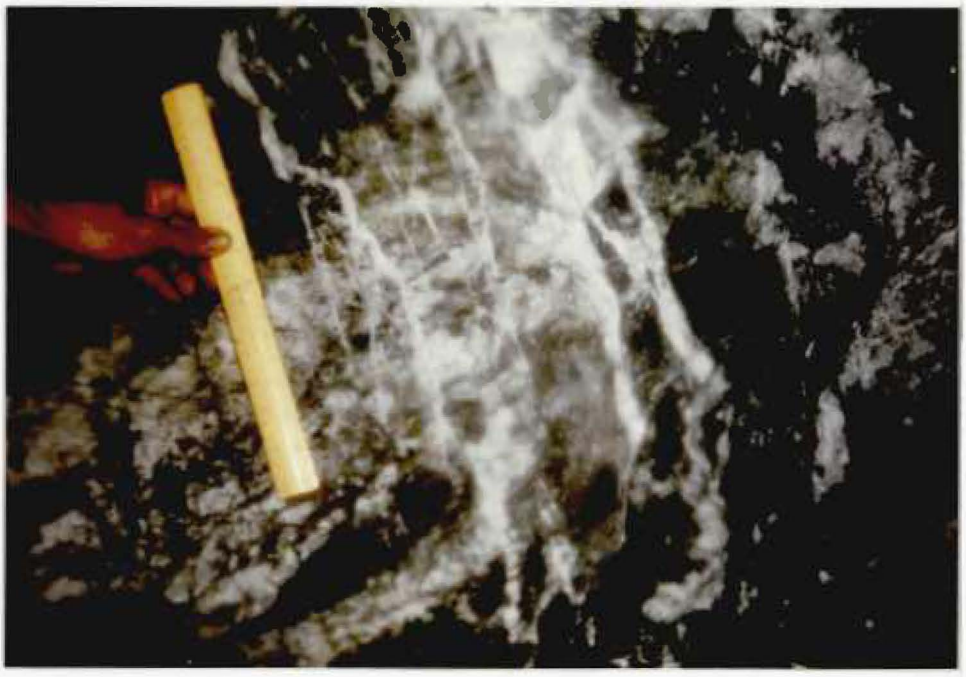

abundance of horizontally or vertically orientated slickensides, (Plate 8B), some of which were mineralised by calcite. Apart from the quartz veins and quartz gashes, quartz was also deposited as a stockwrok of veinlets, (Plate 9A), in hydraulically fractured shale mineralised by cassiterite observed at the 500' intermediate level drive of the Hantu Lode System. This is the only occurrence observed by the writer. Furthermore, quartz veinlets have cut the cockade cassiterite ore, cementing and cutting across the mineralised breccia fragments. It was common for silica-bearing solutions to intrude along the fractured centre of cassiterite-chlorite veins and veinlets, (Plate 27A), forming cassiterite-chlorite-quartz veins.

The notable difference between the style of the cassiterite-chlorite-minor sulphides$^{+}_{-}$quartz mineralisation and that of the barren white quartz is the confinement of the generations of barren white quartz to the space giving rise to a distinctive banded quartz vein complex in which the evidence for the restoration of intense horizontal confining stresses in between dilatant episodes is provided by stylolitic solution surfaces. The intense mineralisation of the permeable wallrock of the lode fault structure by cassiterite, chlorite and minor amounts of sulphides plus earliest quartz phase of the barren white quartz mineralisation event has drastically reduced the permeability of the wallrock and thus preventing further migration of later

PLATE 10.

A. A complex of steeply dipping quartz veins is displaced by a pair of low angle reverse (a) and normal (b) faults. Note the bedding planes of the pelites, (arrowed). This complex of the Gakak North Lode System was exposed at a 3rd level stope.

B. A quartz vein is cut by a low angle reverse curved fault. The fault is marked by a distinct sheared zone showing the incorporation of fragments of pelites and quartz. The fault movement has also created parallel undulating fractures (arrowed) in the fissile pelites which were filled by quartz. This suggests that the faulting event occurred before the end of the quartz mineralisation event. This section of the Gakak Lode System was exposed at the 2nd level intermediate drive S.W. at 15 ft. in section $65/S^{a}$.


a
b

silica-bearing quartz fluids into the wallrock.

Quartz being deposited early in the mineralisation sequence, it was, therefore, susceptible to transection by later sulphide veins, Amphibole-pyroxene andesite dykes, and calcite veins/veinlets. The sulphides were seen to fill fractures in the quartz veins, (Plate 11A), and an andesite dyke was seen cutting across a quartz vein, (Plate 12B), belonging to the Gakak III extension Lode System at the back of the 10th Level drive in section $84/T^{a}$. Calcite veinlets were also observed to cut into the fractured quartz veins, (Plate 9B).

The quartz veins of the Gakak North Lode System which were exposed at a 3rd Level stope, (Plate 10A), and those of the Gakak Lode System at the 2nd level intermediate drive southwest at 15' in section $65/S^{a}$, (Plate 10B), were displaced by low angle faults.

All the observed field evidence indicated that the barren white quartz mineralisation event had followed the cassiterite-chlorite-minor sulphides mineralisation event, but it was itself followed by the major sulphides mineralisation event.

2.3.3.Sulphide mineralisation with minor cassiterites.

This mineralisation event has associated

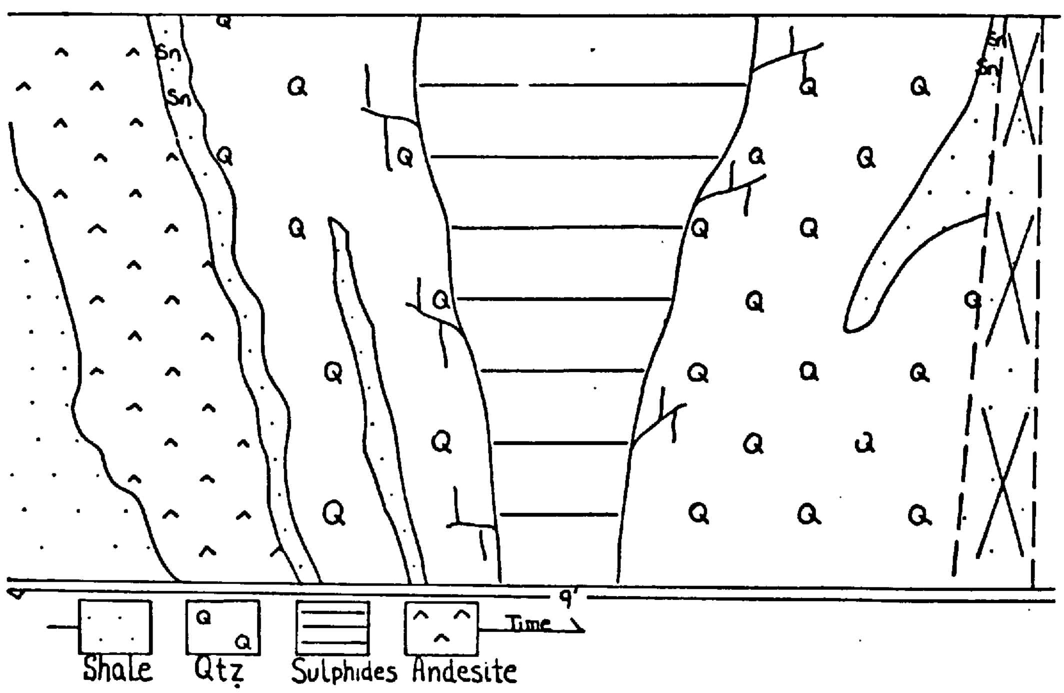

Figure 8. Structural and Paragenetic Relationships between the mineralisation events of the Gakak III Lode System as seen on a face section on the 9th level stope, (1st lift), in section 87/88/S[a].

sub-economic amounts of cassiterite and following the white quartz vein mineralisation. The Sulphide-Cassiterite Lodes occur commonly as massive veins, (Fig. 8), but they were also emplaced in en echelon gashes, (Fig. 6). The Sulphide-Cassiterite Lode of the Gakak III Extension Lode System was observed in three localities:

1. 8th Level drive in section 86/S^a, (Chalcopyrite-galena-Sphalerite lode).

2. 8th Level drive in section 89/R^a, (Pyrite lode) and

3. 9th Level Stope, (1st Lift), in section 87/88/S^a, (Pyrrholite-Pyrite lodes).

The detailed mineralogy, texture and paragenesis of the sections of the sulphide lode mined at the above mentioned locations are described in section
Only the latter two lode sections were sufficiently well exposed to enable detailed structural and paragenetic studies to be made. Even within a short vertical distance of less than a 100 feet, (between 8th Level drive and 1st lift of 9th Level Stope), the sulphide-cassiterite lode shows a distinct upward enrichment in copper content as indicated by the presence of chalcopyrite as the major phase in the sulphide-

cassiterite lode of locality "1" while the Fe-Sulphides, (Pyrrhotite and Pyrite), become the dominant phases of the sulphide-cassiterite lode of locality 3". This is an observation which may have only local significance.

No Sulphide-Cassiterite Lode was seen associated with the Cassiterite-Chlorite-Quartz paragenesis of the Gakak Lode System. A large sphalerite-cassiterite lode belonging to the Gakak North Lode System was intersected at the 3rd Level drive and in its stopes in sections $63/64/65/I^a/j^a$. This lode has enclosed and replaced the margins of its neighbouring barren white quartz vein). A sphalerite, (non-exsolution bearing variety) - Cassiterite Lode has been reported by Ang, (1974), to be present in the Gakak Hill Lode System. A chalcopyrite-pyrrhotite lode of the Hantu Lode System is assumed to be present on the 400 foot drive as suggested by the presence of fallen sulphide pieces in workings on that drive. Based on these observations there seems to be an apparent radial mineral zonation around the Gakak granodiorite with a sphalerites-rich outer zone and a chalcopyrite-pyrrhotite-pyrite enriched inner zone.

The pyrite lode at the 8th level in section $89/R^a$ and the pyrrhotite-pyrite lode at the 9th level stope, (1st lift), in section $87/88/S^a$ showed clear evidence of their post-quartz age based on the fact that they have infilled the fractures developed in their

PLATE 11.

A. A massive 'V' shaped pyrrhotite vein cuts into a complex of quartz veins with the result that the fractures of the quartz veins are filled by sulphides as indicated by an arrow. This section of the sulphide lode in the Gakak III Extension Lode System was exposed at the 1st lift of the 9th level stope in Section 88/S^{a}.

B. This sample shows the relative ages of the barren white quartz vein (a) and the sulphide (pyrite and chalcopyrite) - cassiterite lodes (b). The filling of fractures in the quartz vein by the sulphides is strong evidence suggesting that the deposition of sulphides followed the quartz mineralisation event. The sulphide-cassiterite lode is deformed into a gentle fold over the andesite dyke (c). This spatial relationship suggests that the tectonic event which folded the lode occurred after the emplacement of the andesite dyke. This section of the Gakak III Extension Lode System was exposed at the first lift of the 9th level stope in Section 88/S^{a}.

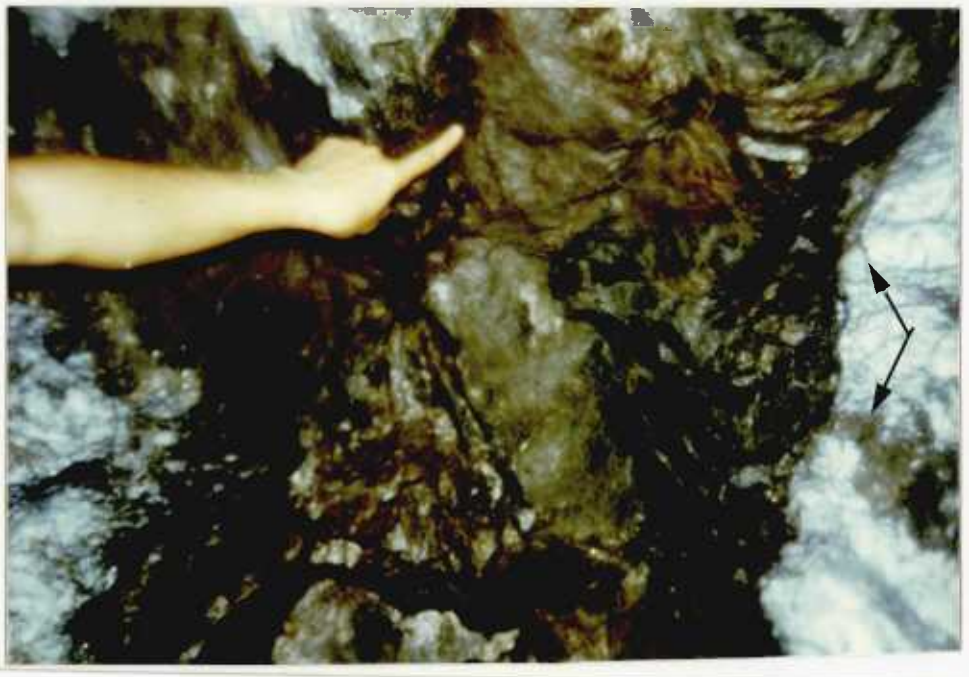

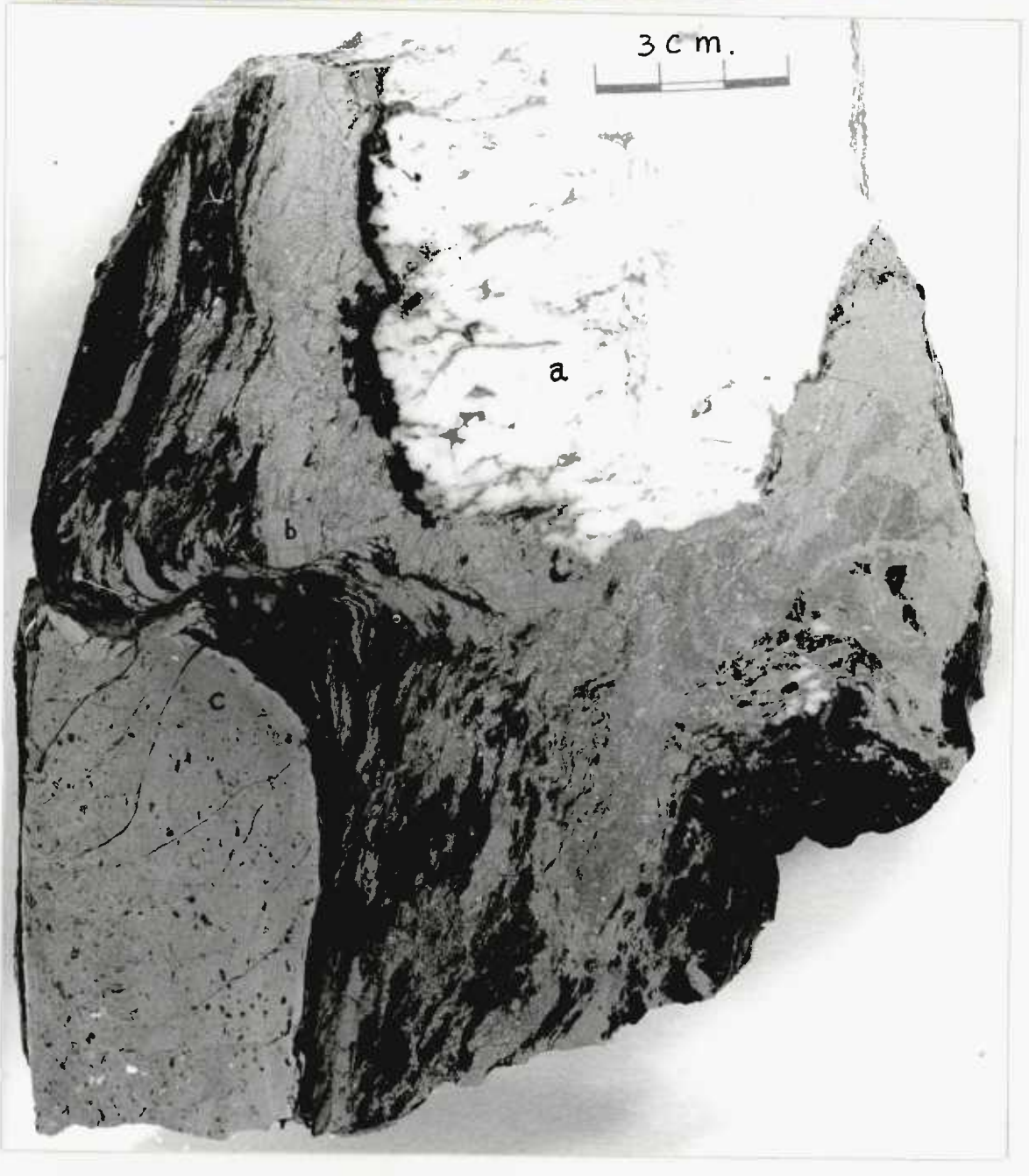
3 c m.
a
b
c

neighbouring barren white quartz veins, (Plate 11A and Fig. 6). The age of this mineralisation event can be further narrowed down to post-quartz and pre-andesite age by the fact that the Amphibole-pyroxene andesite dyke occurring right next to the gently folded pyrite-cassiterite lode at the 1st lift of the 9th Level stope in section $87/88/S^a$ had not been cut by the sulphide lode, (Plate 11B).

2.3.4. Emplacement of Amphibole-pyroxene andesite dykes.

Amphibole-pyroxene andesite dykes are common components of the lode systems in the Sg. Lembing Area. They were emplaced, following the Sulphide-Cassiterite lode, in the fissures and tension gashes developed along the strike of the lode fault structures. This spatial relationship with the tin lode system can be potentially useful in guiding the programme of the mine development.

Amphibole-pyroxene-andesites dykes associated with the Gakak Lode and Gakak III and its extension Lode Systems occur as massive one to two feet wide dykes, (Plate 12A), as well as in a complex of tension gashes, (Fig. 6). An Amphibole-pyroxene andesite dyke of the Gakak III extension Lode System when traced along a drive does change its relative position with respect to the selvages of the tin lode. This observation suggests that the dyke must have cut the

PLATE 12.

A. A massive andesite dyke with its adjacent smaller branch dyke cut the black pelites. The dyke shows two sets of joints, one subhorizontal and the other subvertical. The latter joints are in places filled by the later calcite. This section of the andesite dyke was exposed at the 8th level drive of the Gakak III Lode System in sections $77/78/Y^{a}/Y^{b}$.

B. The quartz vein complex of the Gakak III Extension Lode System is cut by later andesite dyke as seen on the back of the 10th level drive in section $84/T^{a}$.

PLATE 13.

A. Transmitted light photomicrograph of a pervasively altered andesite dyke of the Gakak III Lode System at the 10th level drive in section 85/T[a]. The feldspar phenocrysts (a) and microlites are completely altered to albite and minor calcite; the pyroxene and amphibole (b) phenocrysts are completely altered to calcite. Minute magnetite grains (arrowed) are distributed evenly within the groundmass of feldspar microlites. (Crossed Polars).

B. Transmitted light photomicrograph of a relatively unaltered andesite dyke of the Gakak III Extension Lode System at the 8th level drive in Section 86/S[a]. This dyke is composed of euhedral and subhedral phenocrysts of plagioclase (a); orthoclase (b); microcline (not present on photo); pyroxene (not present in photo) and amphibole (c) set in a fine-grained hyalopilitic groundmass of feldspar microlites glass (brown colour); calcite (difficult to see on photograph); magnetite and minor quartz. Note the feldspar phenccrysts are unsericitised, but some (arrowed) show internal replacement by the groundmass material. (Crossed Polars).

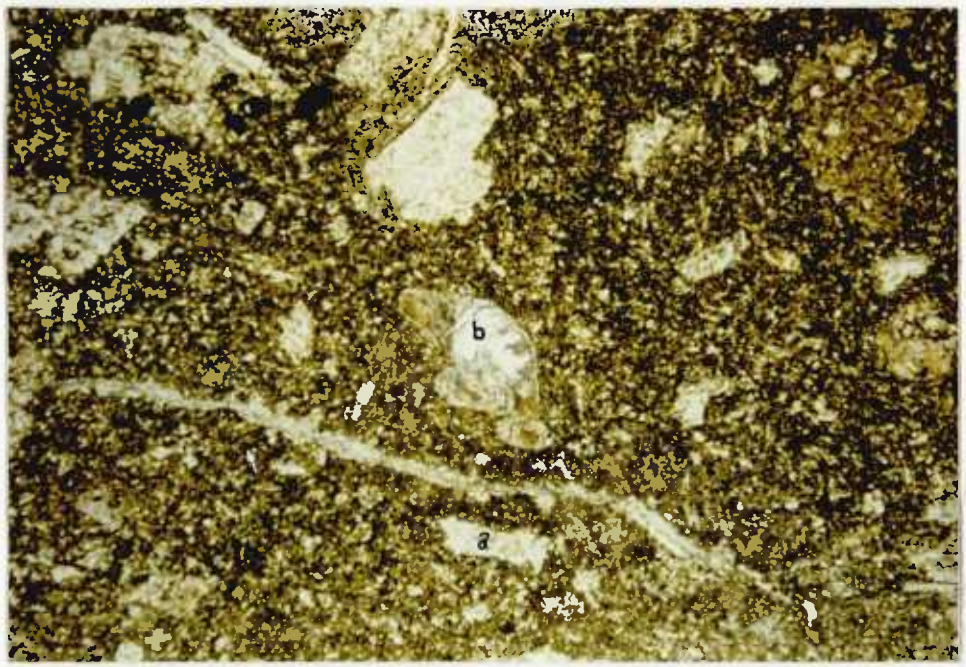

1.5X

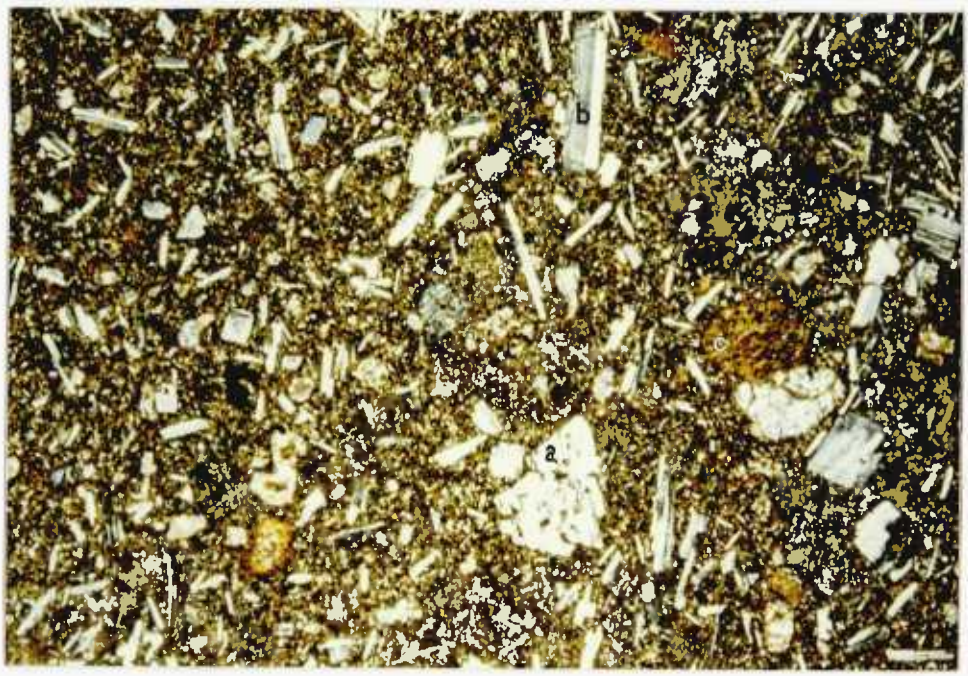

1.5X

tin lode somewhere along its strike and this suggestion has been confirmed by the discovery of the point of intersection, (Plate 12B), between the dyke and the quartz veins by Dr. Halls and the writer at the specially water cleaned back of the 10th level drive of the Gakak III Extension Lode System in section $84/T^{a}$. This finding indicates the age of the Amphibole -pyroxene andesite dyke to be post-quartz.

The Amphibole-pyroxene andesite dykes have almost everywhere suffered pervasive alteration with the result that feldspar phenocrysts and microlites were completely altered to albite and minor calcite; the pyroxene and amphibole phenocrysts were completely altered to calcite and minor chlorite and magnetite. The shapes of these phenocrysts have survived as 'ghost pseudomorphs'. Tiny magnetite grains and calcite patches are distributed evenly within the groundmass of feldspar microlites, (Plate 13A). However, a relatively unaltered portion of an Amphibole-pyroxene andesite dyke at the 8th level drive of the Gakak III Extension Lode System in Section $86/S^{a}$ was seen and its petrography was investigated using polished and thin section microscopic techniques. This investigation showed that the relatively unaltered Amphibole-pyroxene andesite is composed of euhedral and subhedral phenocrysts of plagioclase, orthoclase, microcline, pyroxene and amphibole set in a fine-grained hyalopilitic groundmass of feldspar microlites, glass, calcite, magnetite and minor quartz, (Plate 13B). The

plagioclase phenocrysts are more than 2/3 of the total feldspar content, whereas the microcline is present in trace amount. Thus the classification of these dykes as Amphibole-pyroxene andesite is correct according to the classification scheme of Hatch, Wells and Wells, (1975). These feldspars were not sericitised, but their fractures were mineralised and replaced by calcite. In some cases the feldspar phenocrysts were intensely replaced internally by calcite. The amphibole and pyroxene phenocrysts were altered to chlorite and calcite along their cleavages making it possible to recognise the characteristic set of cleavages of the amphibole and pyroxene. Some of these phenocrysts are euhedral in shape making it possible to confirm the distinction between pyroxene and amphibole. However, the majority of the pyroxene and amphibole phenocrysts are subhedral in form. This feature suggests that the phenocrysts were not in equilibrium with their host magma and consequently they suffered magmatic corrosion, (Hatch, Wells and Wells, 1975).

The Amphibole-pyroxene andesite dykes were commonly fractured into rectangular blocks by two sets of joints, one subvertical and one subhorizontal at almost 100^{o} to each other, (Plate 12A), and also by irregular fractures. These fractures were commonly infilled by calcite. At the 8th level drive of the Gakak III Extension Lode System in section $89/R^{a}$ the

PLATE 14.

A. Fractures of andesite dykes are filled by calcite. Calcite veinlets also occur in the black pelites within a complex of andesite dykes. Note the igneous contacts of the dykes. This complex of andesite dykes as part of the Gakak III Extension Lode System was exposed at the 8th level drive in section 86/S[a].

B. Calcite veinlet (arrowed) cut both the andesite and the quartz indicating a post andesite age for the calcite veinlets as seen on a face section of the Gakak III Extension Lode System at the 10th level drive in Section 86/S[a].

Amphibole-pyroxene andesite filled gashes there have parts of their faulted margins mineralised by calcite. The latter has also in places filled one of the horizontal joints developed within one of the andesite gashes, (Fig. 6). This relationship between the andesite dykes and the calcite veinlets indicates that the dykes were emplaced prior to the calcite mineralisation event.

2.3.5. Calcite mineralisation.

This event was the last to occur in the mines concerned as well as in the other mines within the Sg. Lembing Area according to Fitch, (1952), and Smith, (1968). The source of the calcite is undoubtedly the hornfelsed calcareous shales as suggested by the common presence of stalactites of calcite on the backs and walls of cross-cut and drives. The calcite commonly occurs as veinlets filling fractures in the pre-calcite phases and tension gashes, (Plate 14A). Some of the calcite veinlets cut straight through more than one phase of the former, (Plates 14B and 15A). Since calcite has filled fractures in andesite dykes, (Plates 14A and 14B), this must indicate that the calcite mineralisation took place after the emplacement of the andesite dykes. However, where the voids created were sufficiently large, crystalline vug calcites were formed. In addition, calcite has also commonly mineralised

PLATE 15.

A. A cassiterite-chlorite-quartz-bearing selvedge at the margin of the quartz vein complex of the Gakak III Extension Lode System is cut by thin calcite veinlets (arrowed) as seen on a face section along the 10th level drive in section 86/S^{a}.

B. Almost horizontally orientated slickensides occur on the wall of the 10th level drive of the Gakak III Extension Lode System in Section 86/S^{a}. The formation of these slickensides is accompanied by the deposition of calcite along the planes of the slickensides as indicated by the presence of slickenside-striations on the calcite. The slickensides-forming strike slip fault movement was in an anticlockwise fashion.

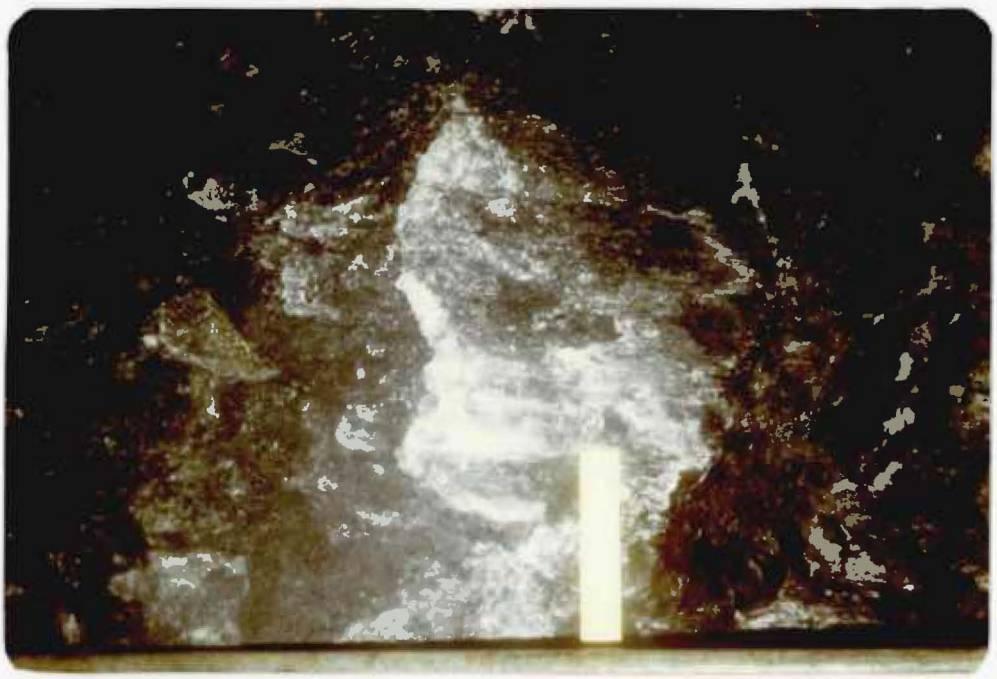

planes of slickensides seen where the walls of the drives coincide with the plane of the lode margin, (Plate 15B). This made it possible to deduce the nature of the fault movements responsible for the formation of the slickensides.

2.4. Tectonisism and associated mineralisation in the Sg. Lembing Area.

This study was based on the field data provided by Fitch (1952); Garnett (1966); Smith, (1967) and the writer.

The lode fault structures of the Sg. Lembing Area are located on the eastern limb of an almost north-south trending anticline the axis of which parallels the contact of the Sg. Lembing granitoid pluton. This pluton has a width of 3 miles and a length of 3 miles and it forms part of the train of the Eastern Belt intrusives of Upper Carboniferous age which displays a north-south elongation.

The geometric relationship of the lode fault structures to the anticline infers that the former were initiated by the same deformation process which formed the anticline. This suggestion is also supported by the similarity of the systematic pattern of the lode fault structures, (Fig. 9), to that of the master joints, (Fig. 10), typically developed in

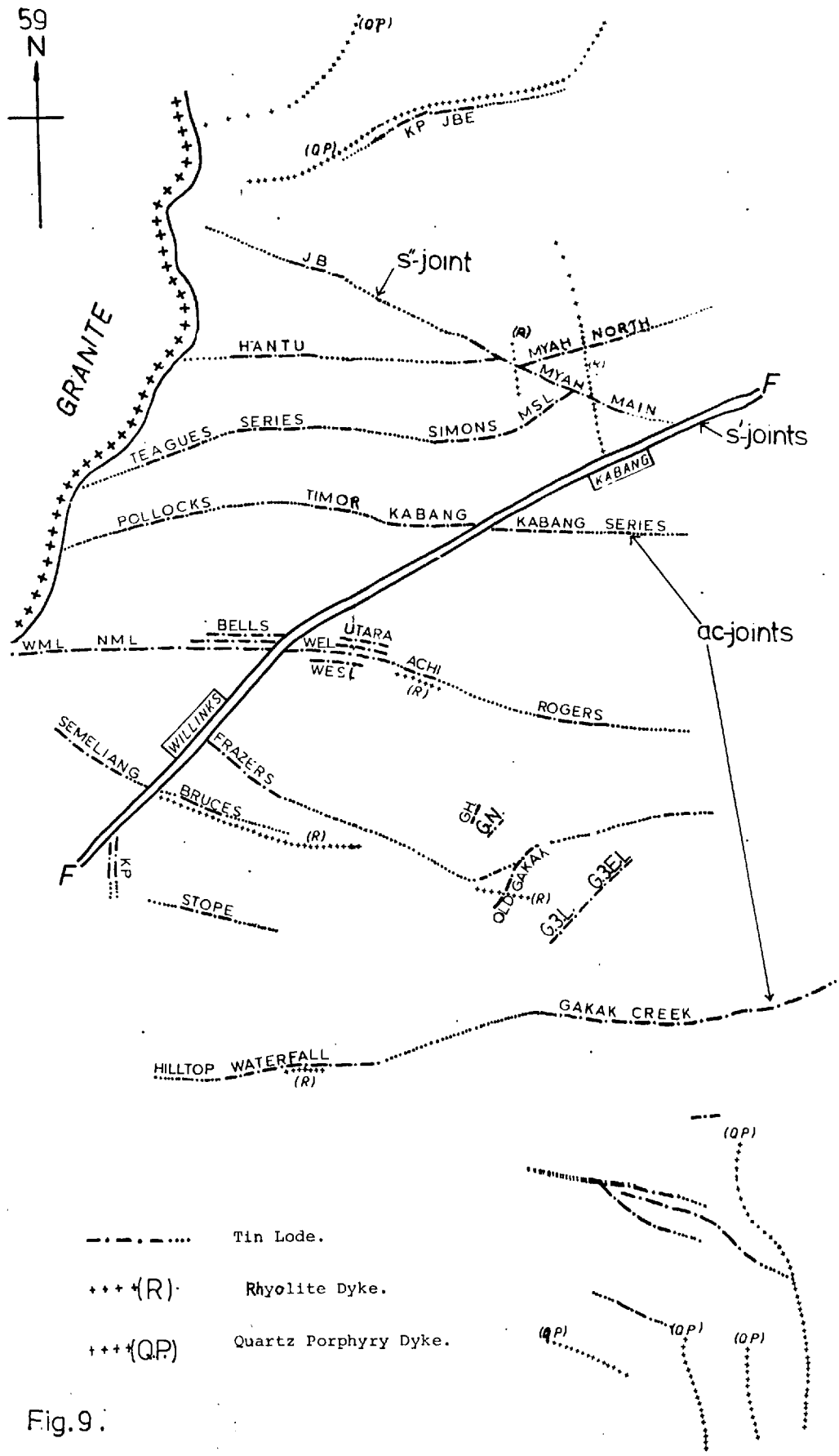

Fig.9.

RECONSTRUCTED FRACTURE PATTERN AS IT EXISTED BEFORE THE FINAL FAULT PHASE

After Smith, 1967. SCALE 1:10,560

an anticline as figured by Price, (1966). This shows best in the reconstruction of the fracture geometry prior to the final stage of faulting as made by Smith, (1967). For example, the east-west trending lode fault structures are the ac —joints since they cut the axis of the anticline at right angles; the northeast-southwest trending lode fault structures, (e.g. the Willinks-Kabang Fault; the Gakak North Lode System; the Gakak Lode System; the Gakak III and its extension systems; the Jeram Batang East Lode System), are the S'-joints since they cut the ac-joints at an oblique angle. The S"-joints are represented by the lode fault structures of the Jeram Batang and the Myah Main Lode Systems plus a few unnamed structures near the Gakak Mine Area. The steeply dipping nature of the planes of the three sets of lode fault structures lends further support to the suggestion that they were created initially as joints during the formation of the anticline, (Price, 1966). These joints were later used as escape routes as well as sites of mineralisation by mineralising hydrothermal fluids.

The braided 'streaky-bacon' texture of the quartz vein complex and the cockade and breccia ore textures of the cassiterite-chlorite $\pm$ quartz lodes of the Gakak and Hantu Mines, P.C.C.L., as described in detail respectively in sections 2.3.2 and 2.3.1 indicates that mineralisation took place under physically energetic conditions along fault zones. Furthermore, the braided 'streaky-bacon' texture of the quartz vein

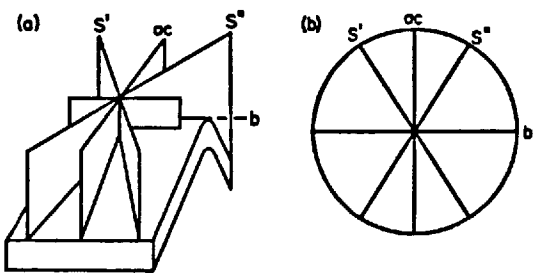

After Price, 1966.

Figure 10(a). Block diagram showing typical relationship of master joints to an anticline.

(b) Steoreogram of master joints shown in (a).

complexes indicates that the deposition of barren white quartz occurred episodically following episodes of hydraulic/tectonic shear dilation of the lode fault structure, (Sibson et. al., 1975). Such episodic flow of mineralising quartz-forming hydrothermal fluids in and around fault zones is best explained by the dilatancy/fluid diffusion model of Scholz, Sykes and Aggarway, (1973), for energy release in shallow earthquakes. This model supposes that prior to seismic shear failure along an existing fault, (such as those in Sg. Lembing), the region for some considerable distance around the focus of the subsequent failure dilates in response to rising tectonic shear stress (T) by the opening of extension cracks and fractures normal to the least principal compressive stress (σ_3). The development of this fracture porosity causes the fluid pressure (p) in the dilatant zone to decrease inducing a slow inwards migration of fluid from the surrounding volume of rocks. In the Sg. Lembing Area a major source of fluids at depths would have been the granitoids. At the onset of dilatancy, the drop in fluid pressure causes a rise in the frictional resistance to shear along the fault, ($T_f = \mu(\sigma_n - p)$), where μ = is the coefficient of static friction and σn is the normal stress across the fault). As the migrating mineralising hydrothermal fluids fill the cracks, fluid pressure rises again and frictional resistance decreases. Seismic failure eventually occurs when the rising shear stress equals the frictional resistance. At such

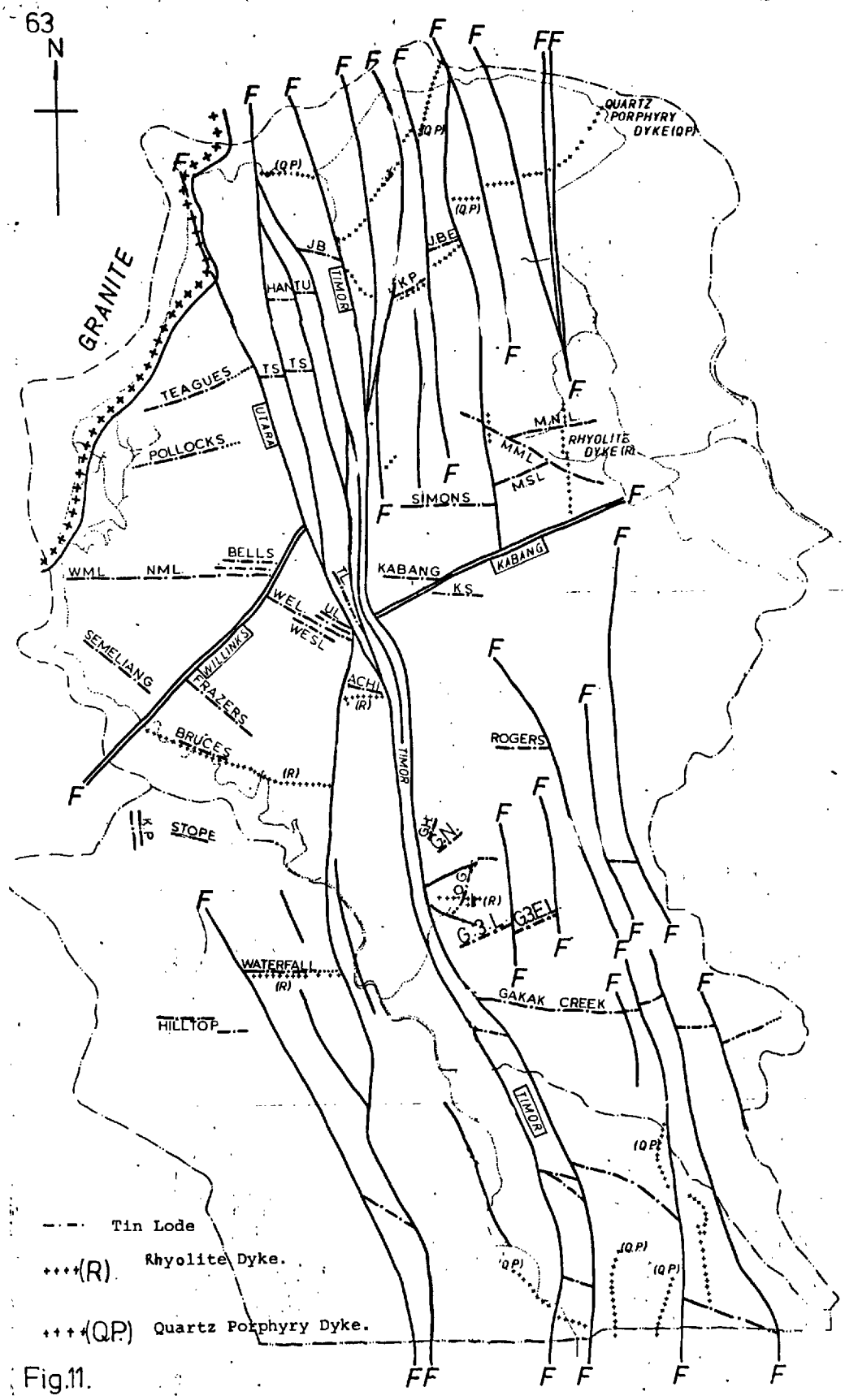

Tin Lode

+++(R) Rhyolite Dyke.

+++(QP) Quartz Porphyry Dyke.

Fig.11.

THE LODE FRACTURE PATTERN AS INTERPRETED FROM FIELD DATA

After Smith, 1967.

SCALE 1:10,560

moments the mineralising fluids in the dilatant zones are expelled rapidly along the lode fault structures and, consequently, the cracks within the dilatant zones collapse. Thus seismic faulting acts as a pumping mechanism whereby individual episodes of earthquakes are capable of moving significant quantities of mineralising fluid rapidly from one crustal en environment to another.

After the cessation of the mineralisation events at the Sg. Lembing Area, the lode fault structures were truncated and displaced by the north-south trending Timor fault and its associated parallel extension faults, (Fig. 11). These late faults were not mineralised, (Fitch, 1952). The nature of displacement by these faults is difficult to assess because there are no marker beds present within the hornfelses.

CHAPTER 3.

Petrography of ore samples from the Hantu and the Gakak Mines of the Pahang Consolidated Company Limited at Sg. Lembing.

3.1. Introduction.

A detailed textural and paragenetic study of thin and polished sections using microscopic techniques was made on ore samples from the Hantu and Gakak Mines. The purpose of this study was to reveal the mineral paragenesis and the tectonic events governing the mineralisations. This detailed petrographic study was also aimed at identifying mineral species which have not been identified previously. This was thought necessary because no extensive detailed mineralogical study has ever been made for the cassiterite associated mineralisations within the Sg.Lembing Area.

The mineragraphic relationships of the mineral components in the tin, and the sulphide-cassiterite lodes are described and interpreted in order of paragenesis.

3.1.1. The Gakak III Lode Systems.

The tin lode.

Mineralogy.

The minerals present in this economically important phase of mineralisation are listed as shown below:-

Biotite
Muscovite
Fe-Chlorite
Rutile
Anatase
Cassiterite

Arsenopyrite
Pyrite
Chalcopyrite
Exsolution-bearing ferroan Sphalerite
Exsolution-free Ferroan Sphalerite
Galena
Marcasite

Quartz
Calcite

PLATE 16.

A. Massive aggregates of fractured cassiterites are interspersed with disseminated grains and smaller aggregates of cassiterite set in a chloritic matrix. (Plane Polarized light).

B. A biotite-muscovite-chlorite bearing fragment is rimmed by cassiterites. The cassiterite and the fragment are cut by thin calcite veinlets (arrowed). Note the twinned cassiterite crystals (arrowed). (Crossed Polars).

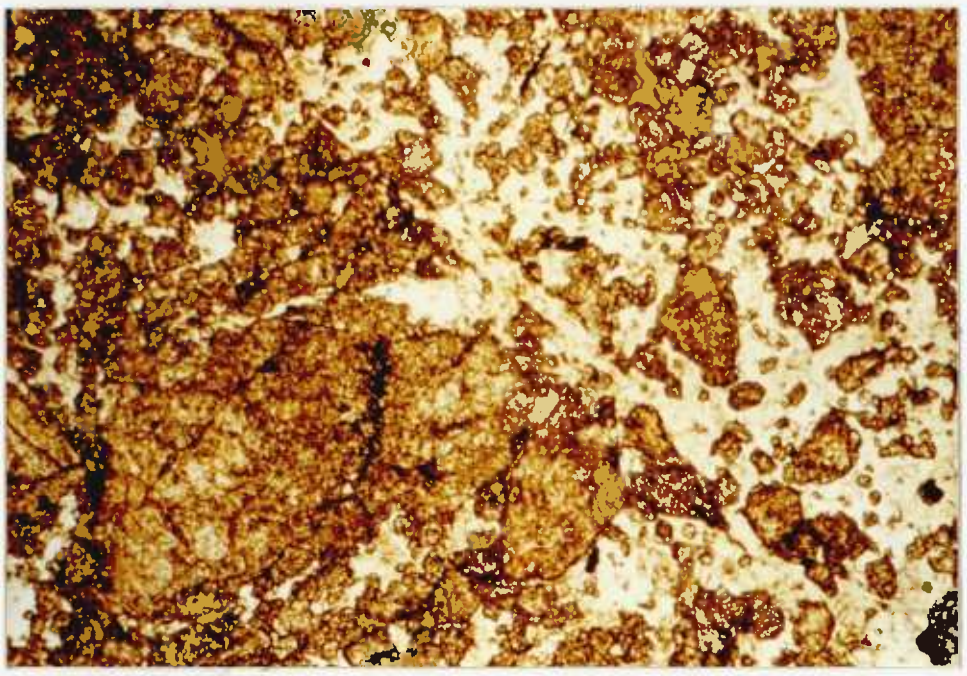

200μm

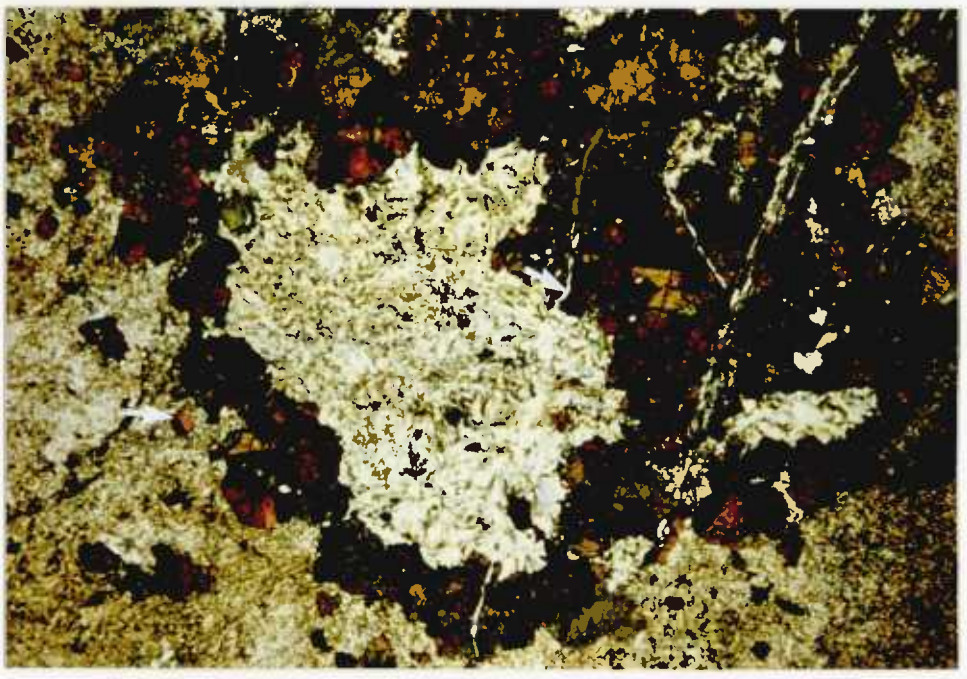

1.5X

Covellite

Chalcocite

Textures and Paragenesis.

Cassiterite-Fe Chlorite-Rutile Assemblage.

The first group of minerals to be deposited in this phase of mineralisation includes cassiterite, green ferroan chlorite and rutile/anatase. These minerals were deposited contemporaneously judging from the evidence provided by mineralogy, textures, and chemistry. The cassiterite occurs in the following forms:

1. Disseminated unfractured grains, (Plate 16A).

2. Massive and fractured anhedral aggregates, (Plate 16A).

3. Intensely fractured irregular veinlets; and, finally

4. As fractured rim materials around chloritised breccia fragments, (Plate 16B), and also around euhedral quartz, (Plate 17A).

These various forms are always intimately associated with

PLATE 17.

A. An euhedral quartz grain within a quartzite acts as a centre of nucleation for the crystallisation of granular cassiterites, (arrowed). (Crossed Polars).

B. An intensely fractured grain of cassiterite in chalcopyrite matrix whose fractures are filled and replaced by the latter. Irregular inclusions of stannite,(arrowed), are present in places around the margin of the cassiterite inclusion. (Plane Polarized light).

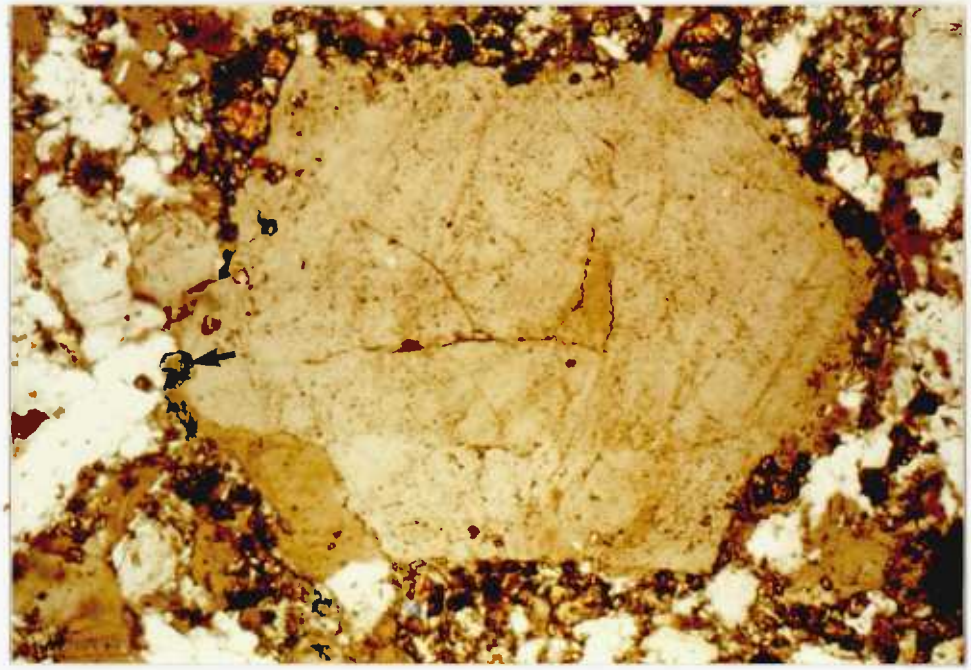

200μm

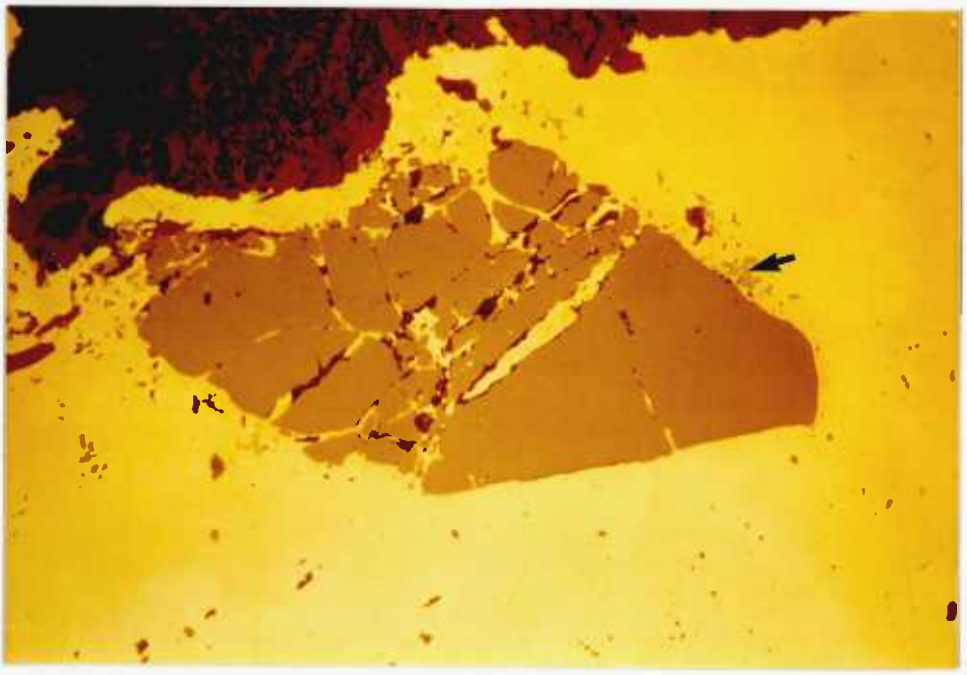

200μm

a matrix of green ferroan chlorite, (Plate 16B). Furthermore cassiterite also occurs as isolated and fractured subhedral inclusions in chalcopyrite matrix (Plate 17B). Located at the margins of such cassiterite inclusions are anhedral stannite inclusions, (Plate 17B). This important gangue chlorite occurs as fan shaped and interlocking aggregates forming the matrix, (Plate 16B), and also filling the fractures in cassiterite, (Plate 16B). Chlorite is associated with relict biotite and muscovite, (Plate 16B), and rutile which suggests that the micas were, in part, the precursor minerals from which chlorite was produced by alteration. This suggestion is confirmed by the presence of rutile as disseminated laths and anhedral plates within the chlorite matrix, (Plate 18B), and also occasionally as long laths located along the cleavages of chlorite. Rutile is a common alteration by-product of Ti-bearing biotites. Rutile also occasionally occurs as inclusions, (some of which are orientated), in cassiterite. This association indicates that rutile formation was contemporaneous with cassiterite crystallization.

The early deposition of cassiterite and its brittle nature has given it ample opportunity to be fractured by the tectonic/hydraulic deformation processes which are known to have influenced the lodes as indicated by the abundance of well developed slickensides in e every sample studied and the local development of breccias. The filling of the fractures in cassiterite by minerals of different relative ages such as arsenopyrite, (rare), chlorite $\pm$ haematite, rutile,

PLATE

PLATE 18.

A. A massive aggregate of fractured cassiterite grains showing their chlorite fractures being cut along the middle and across by later quartz, (arrowed). (Crossed Polars).

B. A bundle of rutile laths set in a chloritic matrix. (Plane Polarized light).

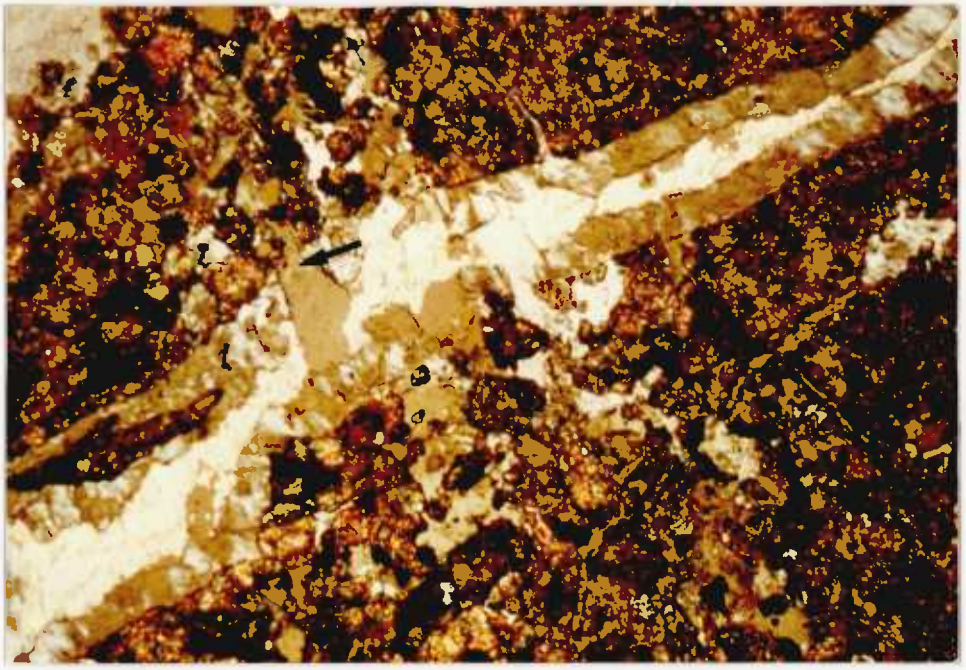

200μm

200μm

pyrite, chalcopyrite, (Plate 17B); quartz and calcite, (Plate 16B) indicates that the cassiterite has been repeatedly fractured throughout the mineralisation sequence.

The chlorites from a 2nd level stope of the Gakak III Lode System were oxidised to haematite and goethite by the acid ground waters. The oxidation process occurred preferentailly along the cleavages and the margins of chlorites. As with chlorite veinlets in the cassiterite, the alteration occurred along the cassiterite-chlorite veinlet contact or in some cases the alteration was pervasive.

Pyrite.

Pyrite was the first sulphide mineral to be deposited following the cassiterite-chlorite mineralisation and it has commonly been deposited in fractures developed within the cassiterites and their chloritic matrices. Pyrite also occurs in other forms such as

1. As anhedral masses with idiomorphic margins in places.

2. As disseminated idiomorphic grains in the chloritic matrix.

PLATE 19.

A. Pyrite cements and fills breccia fragments and fractures of cataclastic cassiterite respectively. The pyrite does not show any cataclastic texture. The cassiterite is partially replaced by quartz at margins and along fractures, (P/S G3.5, 4th level, Section $75/y^a$). (Plane Polarized light).

B. Sphalerite exsolves orientated exsolution bodies of chalcopyrite, (a), (major phase), and galena, (b), (minor phase). These bodies occur as droplets, ovoid, cigar-shaped, rods and trails. The galena bodies are similarly orientated as the chalcopyrite, (P/S G3.10, 6th level stope, (40 ft. 6Ld), Section $76/77/Y^a/Z^a$. (Plane Polarized light).

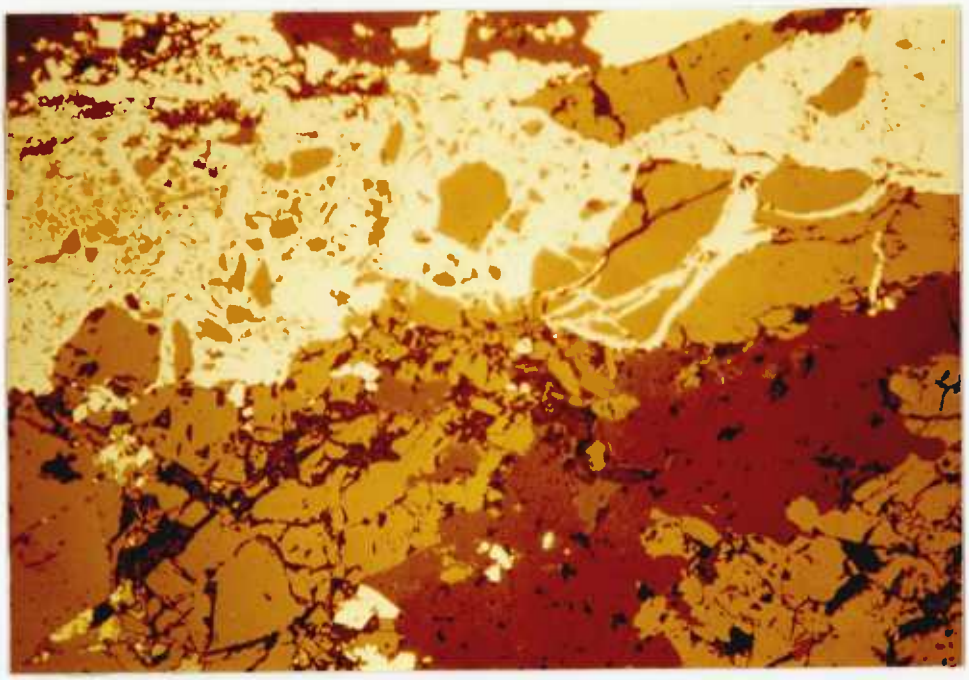

200μm

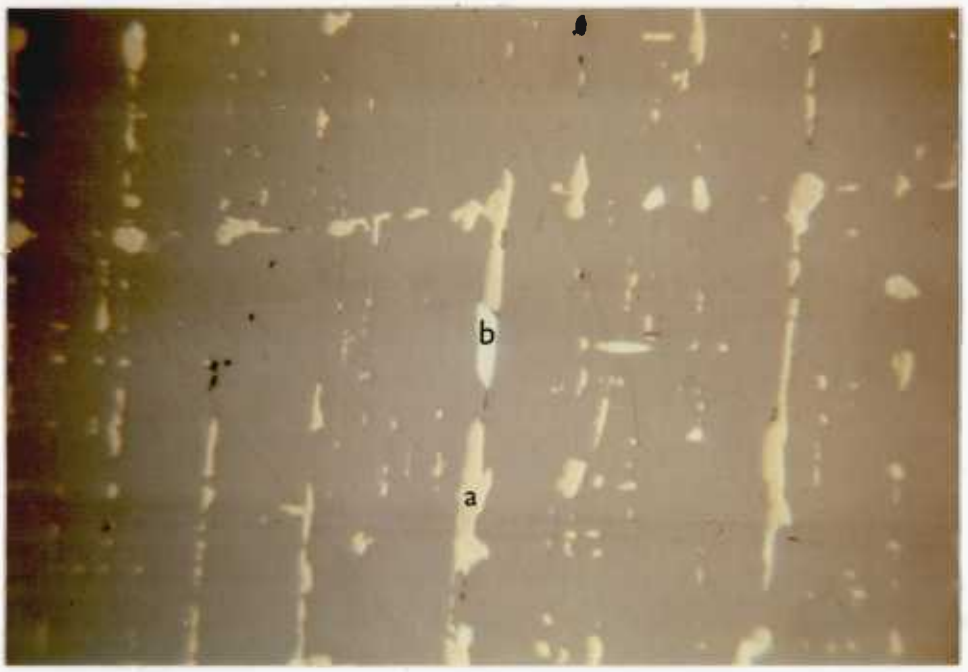

100μm

3. As disseminated inclusions in chalcopyrite, and, finally

4. As the cementing material of angular breccia fragments of cassiterite, (Plate 19A). The latter was only observed once.

Because of the position of Fe in the electrochemical series of elements and its early deposition, pyrite was very vulnerable to replacement and cataclasis respectively. Pyrite was partially replaced by chalcopyrite, marcasite, galena, exsolution-bearing sphalerite and quartz. Passive replacement of pyrite was facilitated by the development of both cleavage, (100) and irregular fractures, (Plate 28B), caused by cataclastic deformation. Along these fractures pyrite was vulnerable to replacement by sphalerite and chalcopyrite. The crystallization of the latter mineral has forced apart the fractures of pyrite. Brecciated pyrite was also cemented by rutile and quartz. The association of rutile with pyrite suggests that the chloritisation process of biotites and muscovites was still continuing during the deposition of the pyrite. The quartz cementing the breciated pyrite has also partially replaced the latter. Undeformed pyrite was also replaced by quartz and exsolution bearing sphalerite at margins and also along the zones bordering the cleavages. Pyrite has been seen to be pseudomorphically

PLATE 20.

A. Exsolution-free sphalerite is extensively replaced by chalcopyrite first and then by quartz. An euhedral quartz grain, (arrowed), grows on the sphalerite-chalcopyrite matrix enclosing inclusions of chalcopyrite and sphalerite, (P/S G3.16, 9th level stope, (just below 8Ld), Section 76/A^{b}). (Plane Polarized light).

B. A single grain of exsolution-bearing sphalerite inclusion in the chalcopyrite-pyrrhotite-pyrite-matrix shows an inhomogeneous distribution of orientated exsolution bodies of chalcopyrite. Polarized light).

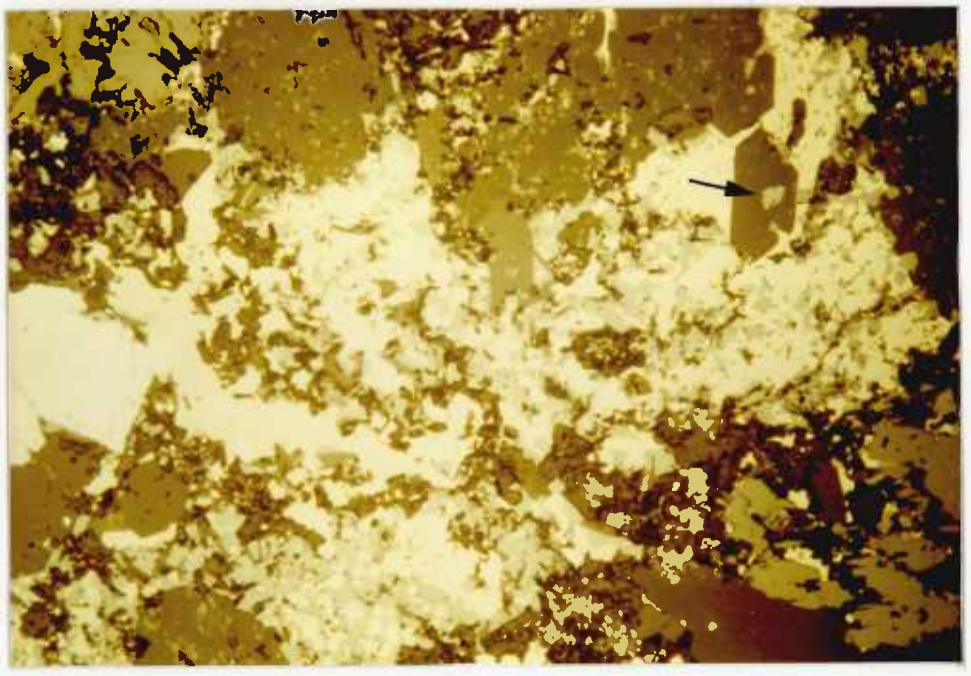

200μm

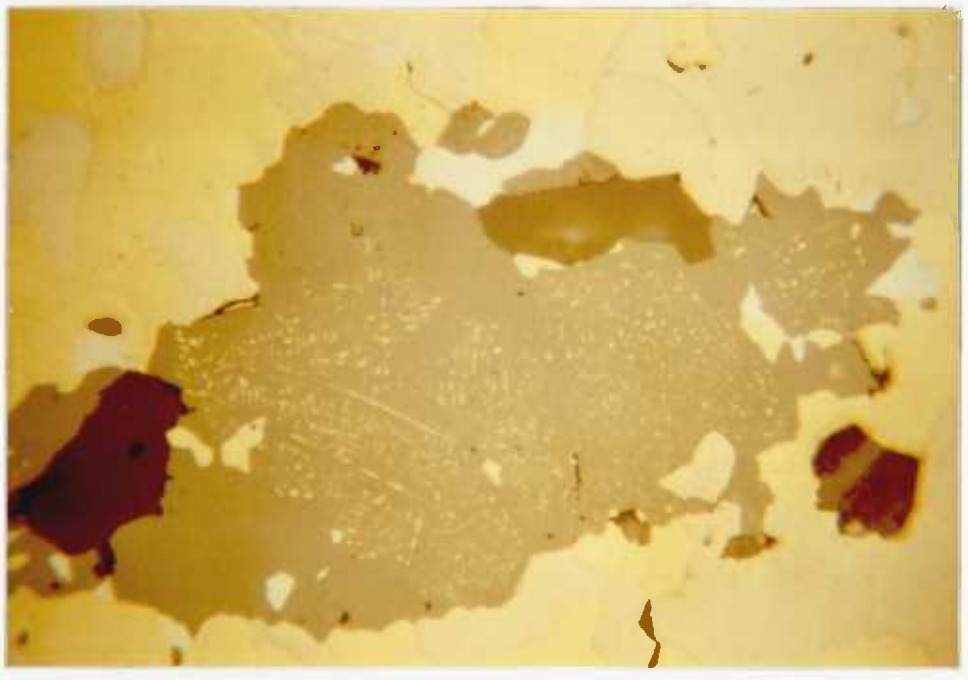

100μm

replaced by quartz, but this extensive replacement of pyrite was rare.

Sphalerite.

Two varieties of Ferroan Sphalerites, (5-7% Fe with Cu and Mn totally below 1%), were recognised and they are as follows:

1. Those which contain inclusions largely of chalcopyrite ± subordinate amounts of galena and/or pyrite, (Plate 19B), and

2. Those without any inclusions at all, (Plate 20A).

These inclusions occur as droplets, ovoid, cigar-shaped, rods and trails, (Plate 19b). The origin of these inclusions is difficult to identify as they can be f ormed either as exsolutions or as mutual intergrowths following cleavages. However, the formation of these inclusions as exsolution bodies is most likely if their host sphalerite is not surrounded by chalcopyrite as otherwise the alternative origin would equally be possible.

The inclusion-bearing sphalerite has been observed to occur together either with or without chalcopyrite. This spatial relationship suggests that the inclusions are probably exsolution bodies. The absence of these exsolution bodies in a population of exsolution-free sphalerite grains or in parts of a mass of sphalerites containing exsolution bodies or in portions of a single aggregate of sphalerite locally with exsolution bodies, (Plate 20B), could be due to the absence of tectonic stresses and/or the presence of impurities within the sphalerite, (Ramdohr, 1969). Tectonic stresses have been reported by Edwards, (1954),), and Ramdohr, (1969), to cause the initiation of exsolution.

Sphalerite is not an ubiquitous sulphide mineral as it was only found to be present in significant amounts in the fourth 6 Level stope in Section 76/77/ Y^a/Z^a and in traces in the ore samples from some 9 level stopes. This observation seems to suggest that there is an apparent zonation of sphalerite towards the lower levels of the lode.

The two varieties of sphalerite occur as:

1. Veinlets.

2. Inclusions in pyrite and chalcopyrite, (Plate 20B), and

PLATE 21.

A. Exsolution-bearing sphalerite is penetrated by tongues of galena, (P/S G3.10, 6th level stope, (40 ft. above 6L drive), Section 76/77/Y^a/Z^a). (Plane Polarized light).

B. Breccia fragments of cassiterite and silicate gangue inclusions are cemented by later quartz, (P/S G3E.14, 10th level, Section 85/T^a). (Plane Polarized light).

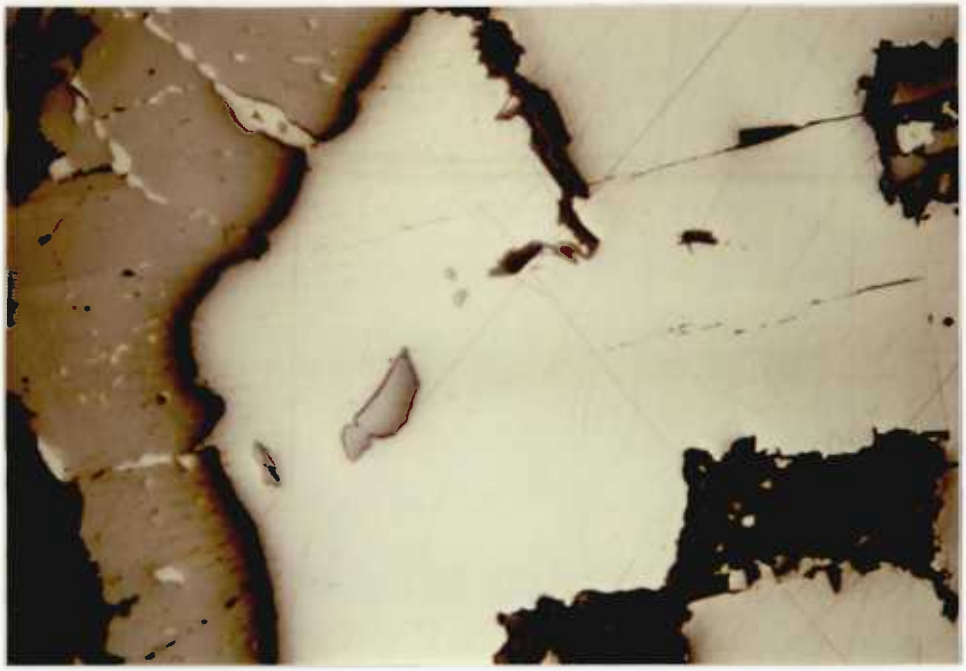

200μm

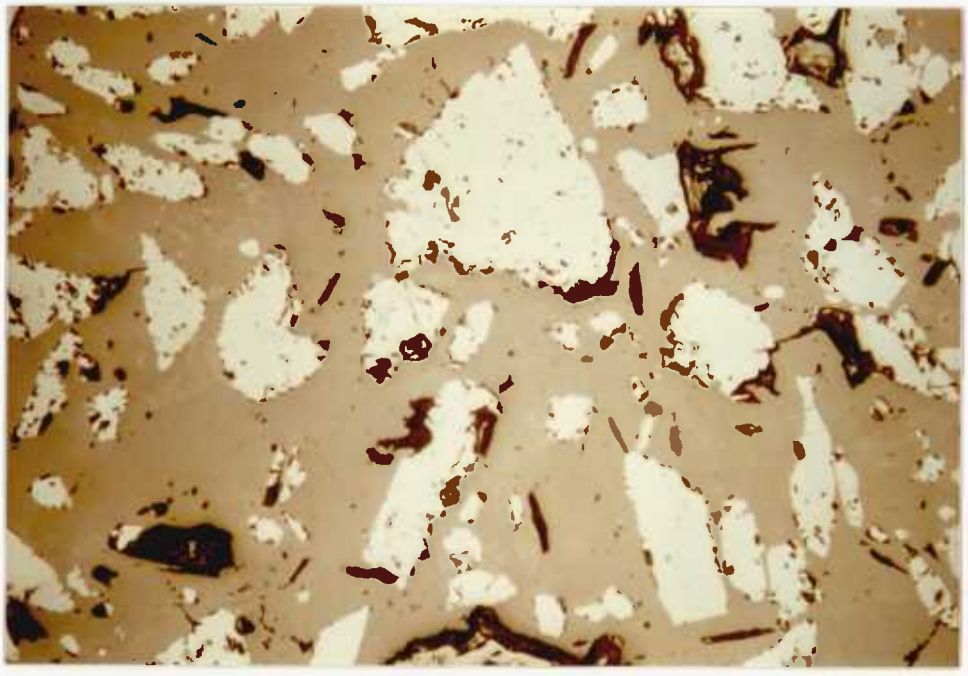

200μm

3. Disseminated anhedral grains in the chloritic matrix.

The sphalerites in pyrite can be interpreted as the product of a replacement process. This interpretation is supported by the observation of sphalerite progressively replacing pyrite starting from the margins. The sphalerite inclusions in chalcopyrite are unreplaced relicts of chalcopyrite. The above observations indicate that the sphalerites were deposited after the pyrite and prior to the chalcopyrite. The exsolution-bearing sphalerite from the 6 Level stope mentioned above was seen to have been penetrated by tongues of galena, (Plate 21A). The exsolution bodies in this sphalerite besides the predominant chalcopyrite also include a small amount of galena, (Plate 19B), orientated in the same way as their associated chalcopyrite. The origin of the chalcopyrite as exsolution bodies is most likely as chalcopyrite is absent in the sample, but that of the galena is uncertain as galena has been observed to replace into the sphalerite and this could have caused the selective replacement of the chalcopyrite exsolutions by galena. The galena inclusions could also be simultaneous mutual intergrowths governed by the favourable structural planes in the sphalerite structure.

It is not uncommon for the chalcopyrite

exsolution bodies to be altered to covellite when subjected to the oxidising conditions of mining activity.

Chalcopyrite.

The main period of chalcopyrite deposition followed the precipitation of sphalerites and it occurs as a matrix to cassiterite, (Plate 17B), and pyrite and as fracture fillings in the fractures of cassiterite, (Plate 17B), and pyrite veinlets. Chalcopyrite also occurs as disseminated anhedral flakes in the chloritic matrix and as inclusions in cassiterite and quartz. Replacement of pyrite, sphalerite, (Plate 20A), and cassiterite, (Plate 17B) by the chalcopyrite at their margins and along the fractures is evident. Besides being a replacement mineral, chalcopyrite was also replaced by later magnetite and quartz. The former replaces chalcopyrite along the intergranular contacts between chalcopyrite and pyrite. Such replacement was not common. The hydrothermal reaction of the silica-bearing solutions has corroded the chalcopyrite into rounded grains set in a matrix of quartz. The sparse chalcopyrite inclusions in cassiterite are fillings of voids between the cassiterite grains.

Chalcopyrites from the Upper Levels, (e.g. 2nd Level to 4th Level), were commonly oxidised to

covellite and chalcocite at their margins and along their fractures where the cu-bearing oxidising ground waters found access. Ramdohr, (1969), has given the sequence of progressive oxidation of chalcopyrite as follows: Chalcopyrite bornite covellite chalcocite. Covellite and chalcocite are occasionally present within a single polished section and this suggests that there was variation in the behaviour of chalcopyrite during oxidation even within the scale of a polished section.

Quartz.

Quartz in the cassiterite-chlorite-sulphides assemblage is believed to belong to the barren white quartz mineralisation event. Besides chlorite, quartz is another important gangue mineral and it occurs as:

1. Replacement veinlets in the chloritic matrix.

2. As veinlets cutting along the centre of chloritic fracture veinlets and then extending out into the cassiterite masses, (Plate 18A), and

3. As matrix to cassiterite, rutile, pyrite, sphalerite and chalcopyrite, (Plate 20A).

The latter form of occurrence is strong evidence that quartz was deposited after all the sulphide minerals. Quartz is common as fracture fillings in cassiterite masses and in cataclastic pyrite; in the former case lenses or slivers of cassiterite are incorporated into the quartz veinlets. Quartz also cements brecciated fragments of cassiterite and pyrite. The replacement of minerals in contact with quartz by quartz is ubiquitous and this event is indicated by the irregular intermineral grain boundaries. Complete pseudomorphic replacement of pyrite by quartz was observed. Quartz is itself frequently replaced by calcite, especially along fractures. This calcite replacement was facilitated by the cataclastic fracture of quartz which is very common owing to the repeated tectonism which has affected the lodes.

Calcite.

The emplacement of thin calcite veinlets across cassiterite-chlorite-quartz assemblages, (Plate 16B), indicates that calcite mineralisation was the last mineral to be deposited in the lode. Where dilatant fractures are absent in the chlorite matrix and the chloritic breccia fragments, calcite mineralisation is disseminated into the chlorites. The warped cleavages of some calcite veinlets are indicative of contemporaneous stresses of deformation imposed on the veinlets.

3.1.2. The Gakak III Extension Lode System.

The Tin Lode.

Mineralogy.

The minerals present in this economically important phase of mineralisation are listed as shown below:

Biotite
Muscovite
Fe-Chlorite
Rutile
Cassiterite
Tourmaline.

Pyrrhotite
Pyrite
Exsolution-bearing Sphalerite
Exsolution-free Sphalerite
Chalcopyrite.

Quartz
Calcite.

Textures and Paragenesis.

Cassiterite-Fe-Chlorite-Rutile Assemblage.

A single major and three minor phases of cassiterite mineralisation were recognised in the tin bearing stage of the lode system. One of the minor phases is post-quartz vein in age. The cassiterite of the major phase, like that of the tin lode in the Gakak III Lode System, is intimately associated with ferroan green chlorite and minor amounts of sulphides. Cassiterite occurs in several forms as follows:

1. Fractured massive anhedral masses with occasional brecciation in places.

2. Disseminated subhedral and anhedral grains set in a chlorite matrix or less commonly in pyrite, or in the two varieties of sphalerite in chalcopyrite, in quartz and in calcite.
   These disseminated grains have not suffered cataclasis.

Cassiterite has occasionally been seen to contain inclusions of rutile. The cataclastic fractures developed in cassiterite masses were commonly mineralised by chlorite, pyrite, chalcopyrite, quartz,

PLATE 22.

A. Massive aggregates of cassiterite are cut across by a composite quartz vein composed of two phases of quartz. Note the growth of acicular cassiterites, (arrowed), at the margins of the composite quartz vein. The interaggregate spaces are filled by green chlorite, (T/S G3E.14, 10th level, Section 85/T^a). (Crossed Polars).

B. The cataclastic grain of cassiterite, (a), is cemented together by a calcite veinlet, (b), which has replaced earlier quartz, (c). The cassiterite and quartz are replaced marginally by calcite, (P/S G3E.4, 9th level stope, (1st lift), Section 87/88/S^a). (Plane Polarized light).

C. A second phase discontinuous cassiterite stringer (a) cuts across the sheared biotite-quartz hornfels and follows only briefly the stylolitic surface, (arrowed), (T/S G3E $12^a(S_2)$, 10th level, Section 84/T^a). (Crossed Polars).

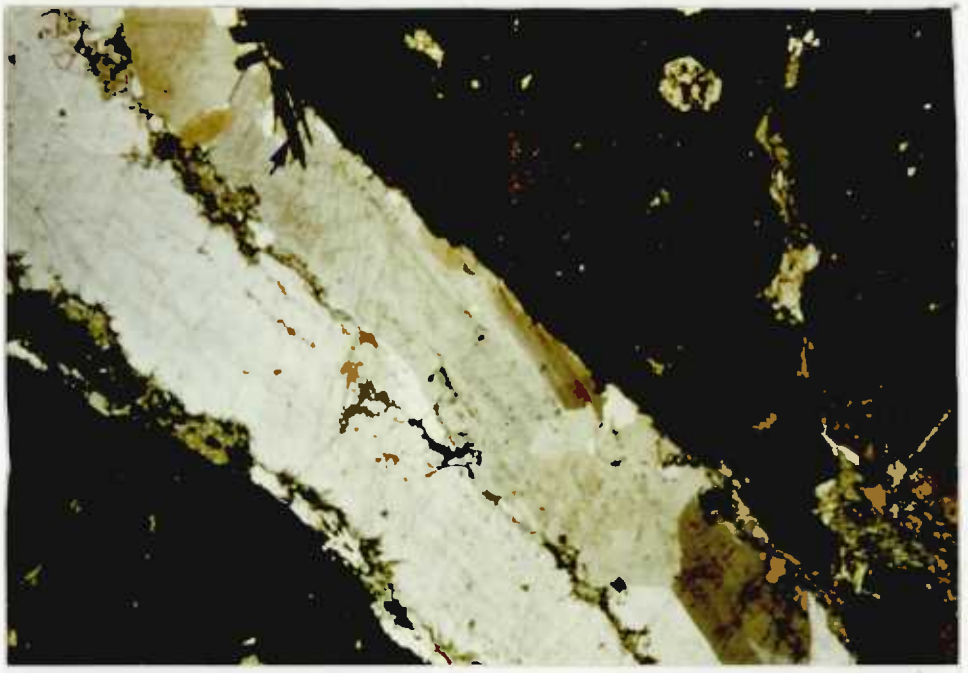

5X

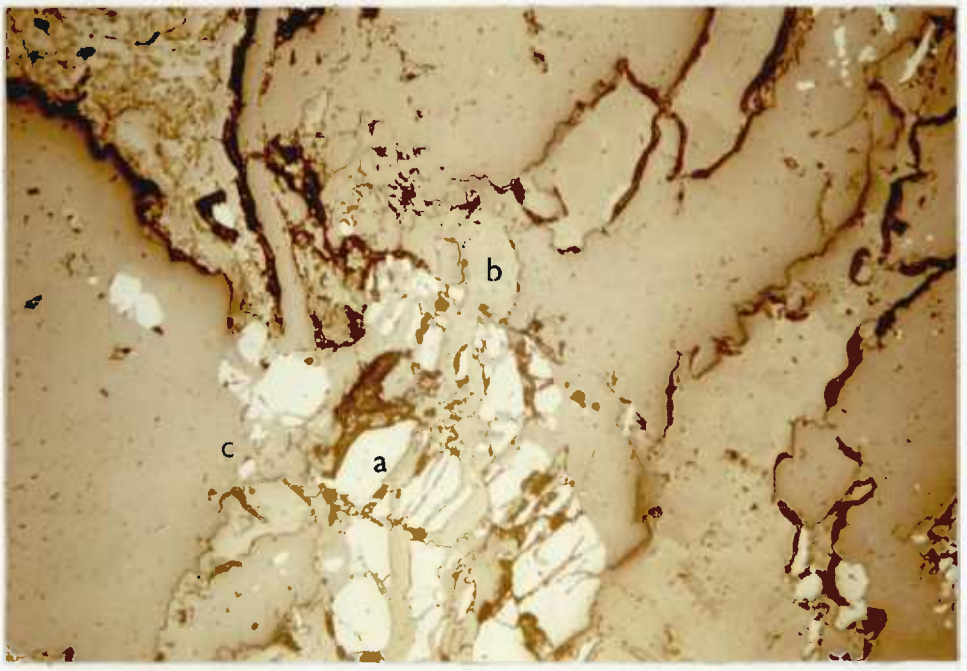

100μm

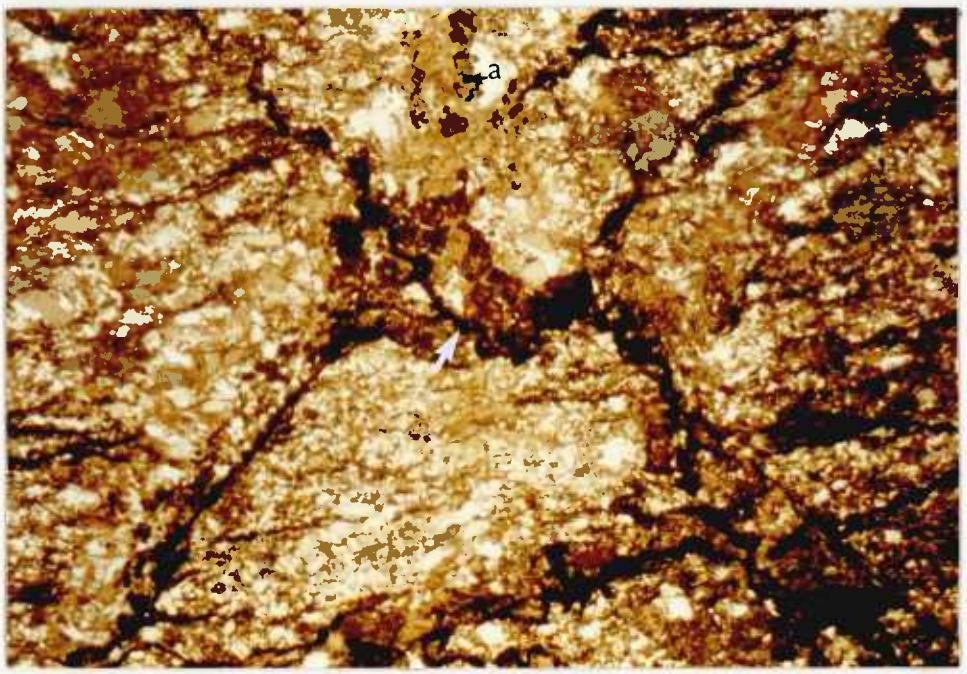

100μm

(Plate 22A) and calcite, (Plate 22B). Repeated fault movements in the tin lode have generated numerous small cassiterite breccia fragments around the larger unbrecciated cassiterite masses. Since these breccia fragments were cemented by chalcopyrite, the brecciation event must have occurred contemporaneous with or prior to chalcopyrite deposition. More than one deformation episode causing brecciation took place in the tin lode as indicated by the occurrence of a quartz cemented cassiterite breccia rock, (Sample G3E.14), (Plate 21B). This brecciation was probably caused by the high fluid pressure of the silica-saturated fluids, (i.e. hydraulic brecciation), during the stage of mineralisation by the barren white quartz. The well developed angularity of the cassiterite breccia fragments suggests that the silica-saturated fluids supporting the latter fragments were not turbulent enough to cause rigorous tumbling of the cassiterite fragments which can result in rounding off the fragments.

The two minor phases of cassiterite mineralisation were detected in the highly sheared biotite-quartz hornfels, (Plate 22C), between two massive white quartz veins. These cassiterites are not associated with green ferroan chlorite and minor sulphides like the cassiterites of the major phase are. Thus they are considered not to belong to the paragenesis of the main stage of tin mineralisation.

PLATE 23.

A. The early pyrite veinlets filling the fractures within the cassiterite mass are cut and replaced into by chalcopyrite. Relict fragments of pyrite, (arrowed), can be seen within the chalcopyrite veinlets. The latter, while filling the fractures within the cassiterite mass, also replace the cassiterite, (P/S H5, Adit level, section $67/O^a$). (Plane Polarized light).

B. Inclusions of pyrite, exsolution-bearing sphalerite and cassiterite are set in the chalcopyrite matrix, (P/S G3E.11, 10th level, Section $84/T^a$). (Plane Polarized light).

C. Irregular inclusions of exsolution-free sphalerite, (a), in chalcopyrite, (b), are due probably to its replacement by the latter. The chalcopyrite-sphalerite composite grain, is partially replaced by calcite, (arrowed), producing a 'worm-burrow-like' texture, (P/S G3.16X, 9th level stope, (30 ft. below the 8th level drive), Section $79/Y^a$). (Plane Polarized light).

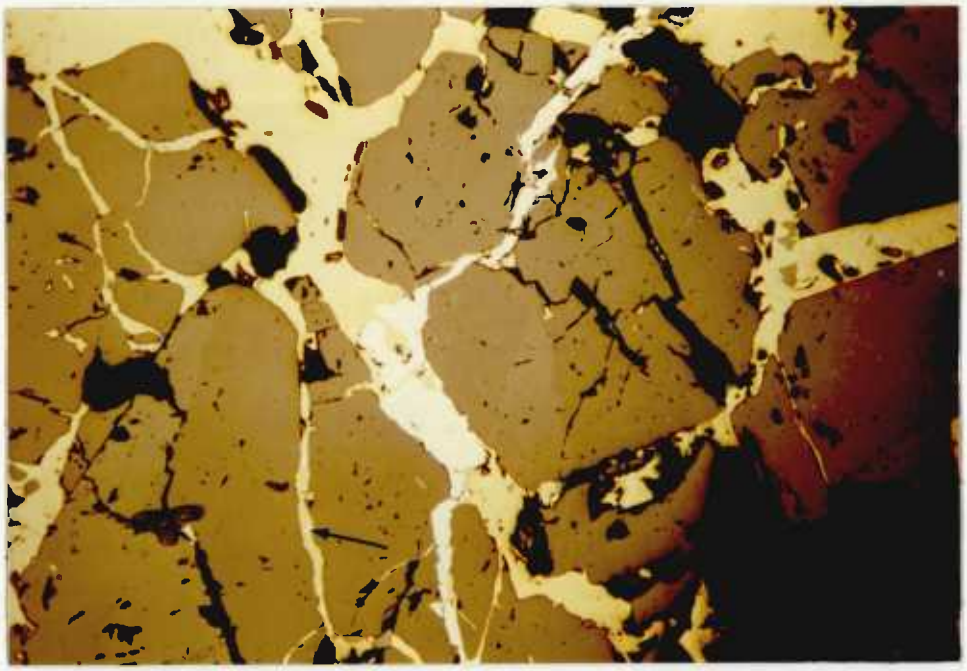

100μm

50μm

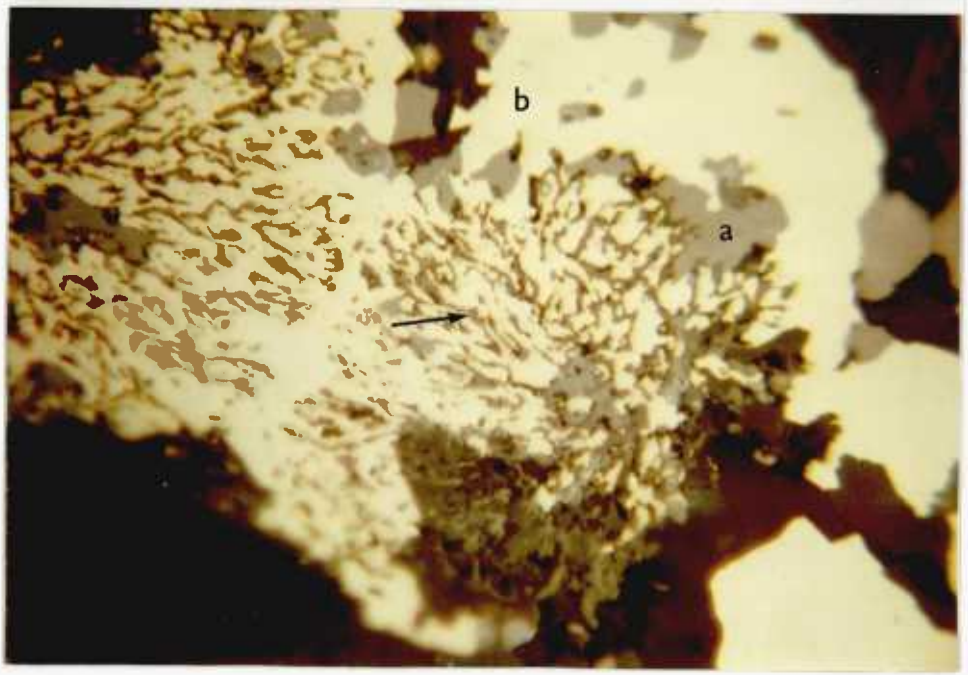

50μm

The first of the two phases occurs as discontinuous stringers following the stylolitic surfaces, and along the margins of quartz and chlorite veinlets. The second phase also occurs as discontinuous stringers, but they cut through the host biotite-quartz hornfels, (Plate 22C), and its associated stylolitic surfaces. They also cut the chlorite and quartz veinlets.

Pyrite.

Pyrite was the first sulphide mineral to be deposited following the cassiterite-chlorite mineralisation and it has been deposited in fractures which run through the chlorite matrix into the cassiterite masses. Pyrite also occurs as anhedral grains, some of which contain disseminated inclusions of cassiterite. A rare occurrence of anhedral pyrrhotite inclusions in pyrite was observed from ore samples collected from a face along the 10 Level drive.

In some instances the pyrite occupying the fractures in the cassiterite masses has been almost totally replaced by chalcopyrite, (Plate 23A). The cataclastic fractures of pyrite were mineralised and partially replaced by chalcopyrite and chlorite. The occurrence of chlorite in these fractures indicates that the formation of chlorite, in part by alteration of biotites and muscovites was still continuing during and after the deposition of pyrite as was also found to be the case in the tin lode of the Gakak III Lode

System. Pyrite was vulnerable to replacement by quartz especially along its cleavages and it can also be extensively replaced partially by calcite, (Plate 3.20).

Sphalerite.

The two varieties of ferroan sphalerite as recognised in the tin lode of the Gakak III Lode System were also present in this lode. The spatial relationship between the two varieties of ferroan sphalerite and their form of occurrence are similar to those observed in the tin lode of the Gakak III Lode System except for the absence of veinlets and disseminated grains in the chloritic matrix. Besides occurring in small amounts in inclusions in chalcopyrite, (Plates 20B and 23B), the two varieties of ferroan sphalerite have often grown around the margins of chalcopyrite grains. The exsolution-bearing sphalerite also occurs as anhedral inclusions in calcite veinlets and its replacement by the latter is ubiquitous. The two varieties of sphalerite have also been seen to enclose either partially or completely small cassiterite grains as in P/s G3E,4.

Chalcopyrite.

Like the chalcopyrite in the tin lode of the Gakak III Lode System, the main period of chalcopyrite deposition in this lode has also followed the

precipitation of sphalerites. The forms of occurrence of chalcopyrite in this lode are similar to those of chalcopyrite in the Gakak III Lode System. However, the presence of pyrr hotite inclusions in the chalcopyrite matrix was observed in this lode but not in the former case. The chalcopyrite inclusions in cassiterite as observed in the Gakak III Lode System have not been seen in the cassiterites from this lode. As mentioned in the description of pyrite relationships, chalcopyrite has extensively replaced the pyrite which occupied the fractures in cassiterite. The replacement of fractures in cassiterite and pyrite by chalcopyrite is evident, so also is the replacement of the latter mineral by quartz and calcite, (Plate 23C).

Quartz.

The paragenetic status and the relationships of quartz with respect to the earlier suite of minerals are generally similar to those displayed by quartz from the Gakak III Lode System. An important observation which is so far unique to this lode is the presence of small amounts of greenish tourmaline laths set in the margin of a quartz veinlet emplaced in cassiterite-chlorite masses. The occurrence of this mineral has never been reported either from the tin lodes within the Sg. Lembing Area, or from the mill run of the Mine. However, some detrital tourmalines were collected from the country

PLATE 24.

A. The irregular form of the pyrite (a) and chalcopyrite (b) grains has resulted from their replacement by calcite (c). The euhedral and subhedral grains of pyrite do not show much evidence of replacement by calcite. The latter shows a characteristic set of rhombohedral cleavages, (P/S G3E.1X, 8th level, Section 89/R^a). (Crossed Polars).

B. Lath-and diamond-shaped arsenopyrite inclusions (arrowed) in an unfractured anhedral grain of cassiterite, (P/S GL.11d, 2nd level, Section 65/66/S^a). (Plane Polarized light).

200μm

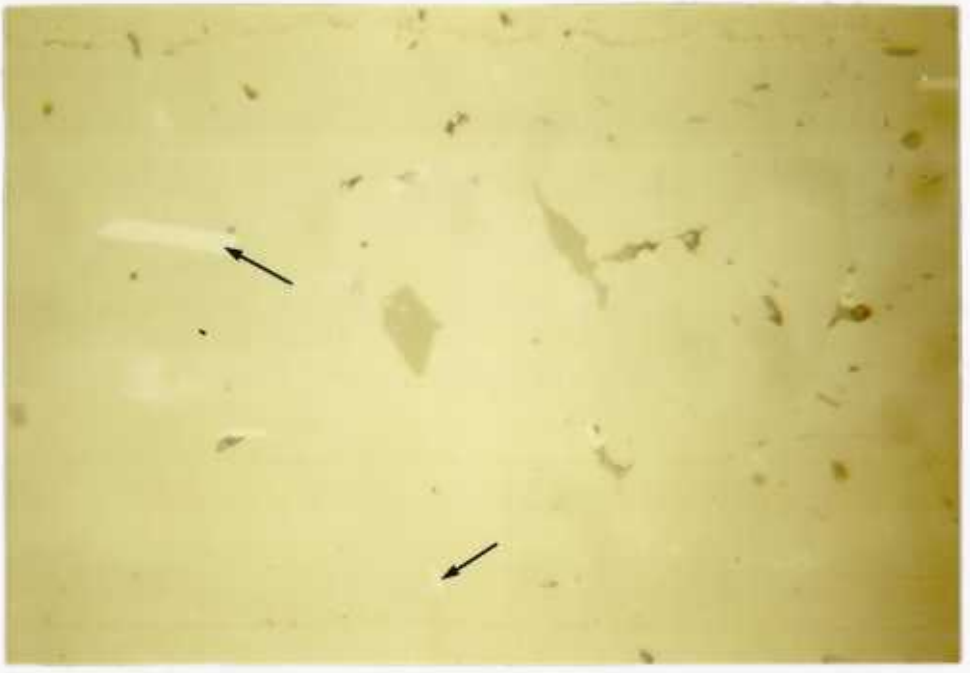

50μm

rock near Simons lode by J. B. Scrivenor as reported by Fitch, (1952). The rarity of occurrence of tourmaline as observed in this present field and laboratory study suggests that boron activity in the tin-rich mineralising fluids was not sufficiently high to cause precipitation of tourmaline in significant amount. The inferred low boron activity excludes B as an important element involved in the hydrothermal transport of Sn in the hydrothermal systems of Sg. Lembing.

Calcite.

The paragenetic and textural relationships of calcite with respect to the earlier suite of minerals are similar to those seen and described from the Gakak III Lode System. The replacement of cassiterite, pyrite and chalcopyrite inclusions by calcite matrix is evident, (see Plates 22B and 24A), and so is the replacement of quartz and cassiterite, (Plate 22B).

3.1.3. The Gakak Lode System.

The Tin Lode.

Mineralogy.

The minerals present in this economically important phase of mineralisation are listed as shown below:-

Biotite
Muscovite
Fe-Chlorite
Rutile
Cassiterite.

Arsenopyrite
Pyrite
Exsolution-bearing Sphalerite
Exsolution-free Sphalerite
Cosalite-Type Pb-Bi Sulphosalt
Chalcopyrite
Stannite
Quartz.

Goethite
Haematite
Covellite
Chalcocite.

Textures and Paragenesis.

Arsenopyrite.

This mineral was not detected in the polished sections made from the two previous tin lodes described. Its presence in this lode is not ubiquitous. The occurrence of arsenopyrite as marginally replaced idiomorphic inclusions, (laths, diamond-shaped and pseudohexagons), in cassiterite, (Plate 24B), indicated that the arsenopyrite was deposited prior to the precipitation of cassiterite. Such arsenopyrite inclusions were also observed in a quartz matrix.

Cassiterite-Fe-Chlorite-Rutile Assemblage.

The deposition of this mineral assemblage followed the precipitation of the small amounts of arsenopyrite. The styles of mineralisation seen in this mineral assemblage are broadly similar to those observed in the tin lodes of the Gakak III and the Gakak III Extension Lode Systems. The textural and the paragenetic relationships between the cassiterite and the sulphides and the quartz are also similar to those observed in the latter lode systems. However, that which has been observed in this lode and not in the other two lodes is the rimming of cassiterite grains by exsolution-bearing sphalerite and chalcopyrite.

The chloritic matrix of the outcropped portion

PLATE 25.

A. A fracture cutting across a mass of haematite is mineralised by colloform goethites. The haematites are the products of oxidation of ferroan chlorites, (P/S GL.2. Surface outcrops, Section $67/U^a$). (Plane Polarized light).

B. A pyrite veinlet within the cassiterite masses is cut by a veinlet of exsolution-bearing sphalerite. This is good evidence for the pre-sphalerite age of the pyrite veinlet. Note the alteration of the chalcopyrite inclusions within the sphalerite to covellite, (arrowed), (P/S GL.18S, 5th level stope, Section $73/74/K^a/L^a$). (Plane Polarized light).

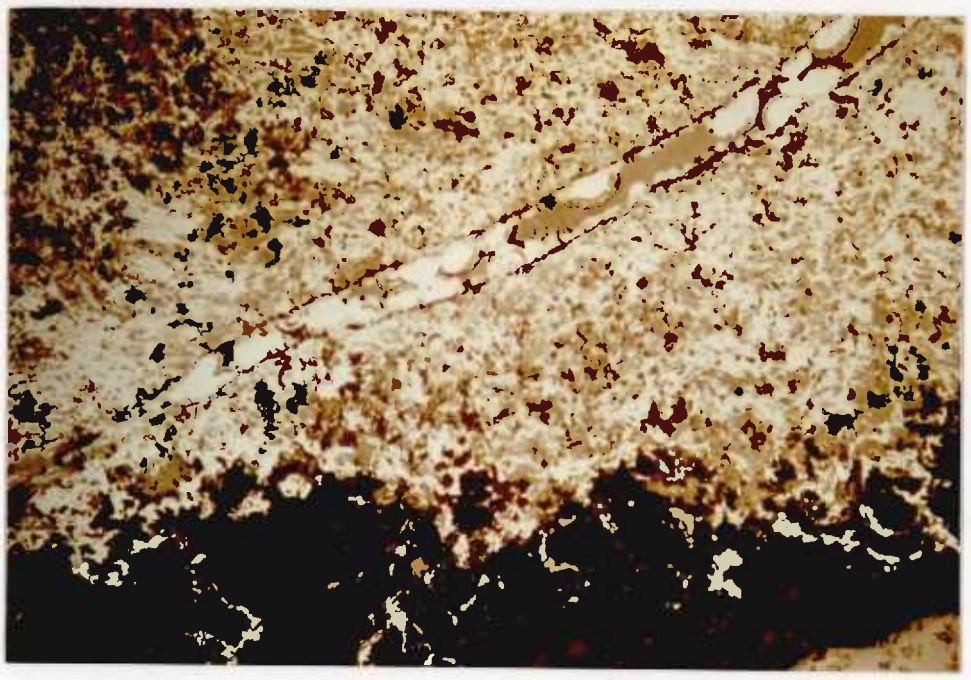

200μm

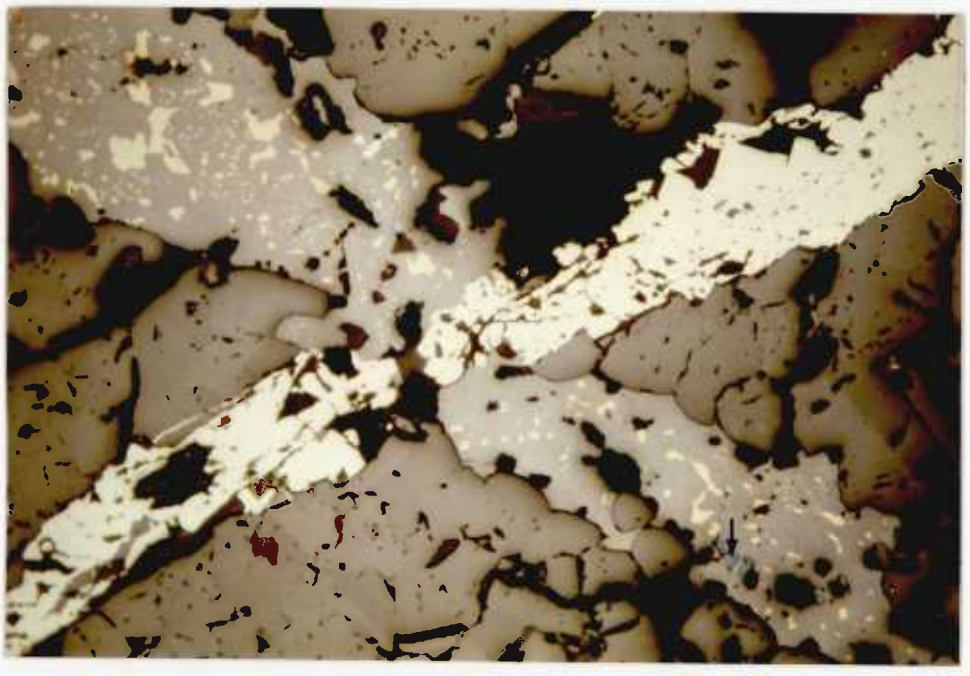

200μm

of this lode has been pervasively altered to haematite, (Plate 25A). The walls of small dilatant fractures cutting across the chloritic matrix were mineralised by colloform goethite, (Plate 25A). These supergene alteration processes were brought about by exposure at the surface to tropical weathering.

Pyrite.

In common with the other two tin lodes, pyrite was the first sulphide phase to be deposited after the precipitation of the cassiterite-chlorite-rutile assemblage and it is an ubiquitous constituent of this lode. In general the textural and paragenetic relationships between pyrite and its associated mineral phases are similar to those observed in the other two lodes. However, there are features which were not seen in the pyrites of the latter lodes and these are as follows:-

1. The truncation of pyrite veinlets located within the cassiterite masses by veinlets of exsolution-rich sphalerite, (Plate 25B), is strong evidence for the pre-sphalerite age of pyrite.

2. The inclusion of compact aggregate or disseminated idiomorphic grains of pyrite in the exsolution-rich

sphalerite veinlets occupying the fractures in cassiterite.

3. The pseudomorphic replacement of disseminated idiomorphic pyrite crystals by goethite, (Plate 26A) as observed in samples from the limonitised upper portion of the lode at the adit level in Section $67/O^{a}$.

4. The alteration of pyrite veinlets to goethite along fractures, even in the superficially fresh and unlimonitised lower portion of the lode at the 8th Level drive in Section $71/m^{a}$. This alteration process must, undoubtedly, have been brought about by the oxidising conditions admitted by mining activity and not by the oxidising acid ground waters from the upper levels.

5. The replacement of growth zones in unfractured idiomorphic pyrite grains and aggregates by sphalerite, both exsolution free and exsolution-bearing, where the pyrites occur within or at the margins of sphalerite aggregates.

Sphalerite and Cosalite-Type Pb-Bi Sulphosalt.

Two varieties of sphalerite were recognised in this lode as in the other two lodes described and they are distinctly more abundant overall in this lode than in the other two. However, the exsolution-bearing sphalerite variety differs from the similar variety of sphalerite in the other two lodes in that it contains exsolution bodies of Cosalite-Type Pb-Bi Sulphosalt and pyrite in addition to the chalcopyrite exsolution bodies. The Pb-Bi Sulphosalt is present in subordinate amounts together with chalcopyrite, whereas pyrite is present either in small amounts together with the latter or alone, (see P/s Gl 18s). The inhomogeneous distribution of these exsolution bodies in sphalerite is still characteristic. The presence of relict unreplaced sphalerite and later replacive sphalerite in chalcopyrite and pyrite respectively, and the dissemination of sphalerite grains in the chloritic matrix were typical of this lode as well as of the other two lodes so far described. However, the textural relationships between the sphalerite and its associated phases which were observed only in this lode are as follows:

1. Large anhedral sphalerite masses engulfed in chalcopyrite which has evidently progressively replaced the sphalerite masses.

2. Exsolution-bearing sphalerite veinlets filling fractures in cassiterite masses, (Plate 25B), These veinlets have cut and engulfed veinlets and idomorphic aggregates of pyrite respectively.

3. Sphalerite rims around breccia fragments of the chloritic matrix.

4. Infilling and replacement of the undulating margins of sphalerite aggregates by Cosalite-Type Pb-Bi Sulphosalt.

A grain of sphalerite was observed to have been transected by replacing Cosalite-Type Pb-Bi Sulphosalt. Thus on the basis of textural evidence the sphalerite was precipitated in sequence after the pyrite and prior to the Cosalite-Type Pb-Bi Sulphosalt. This Pb-Bi Sulphosalt was first identified by the writer in the tin lode of the Hantu Lode System and it has not been found to be present in the other two tin lodes so far described.

Chalcopyrite.

Chalcopyrite is not an ubiquitous mineral as its abundance progressively decreases with increasing depth; two polished sections made from lode materials

PLATE 26.

A. Subhedral grains of pyrite in the chloritic matrix are pseudomorphically replaced by goethite, (arrowed), (P/S GL.5, Adit level, Section $67/O^{a}$). (Plane Polarized light).

B. Exsolution bodies of stannite in chalcopyrite; these stannites also rim the margins of exsolution-bearing sphalerite inclusion in the exsolution-bearing chalcopyrite, (P/S GL.11.b^{2}, 2nd level, Section $65/66/S^{a}$). (Plane Polarized light).

C. The irregular margins of chalcopyrite are replaced by supergene covellite, (P/S GL.4, Adit level, Section $65/S^{a}$). (Plane Polarized light).

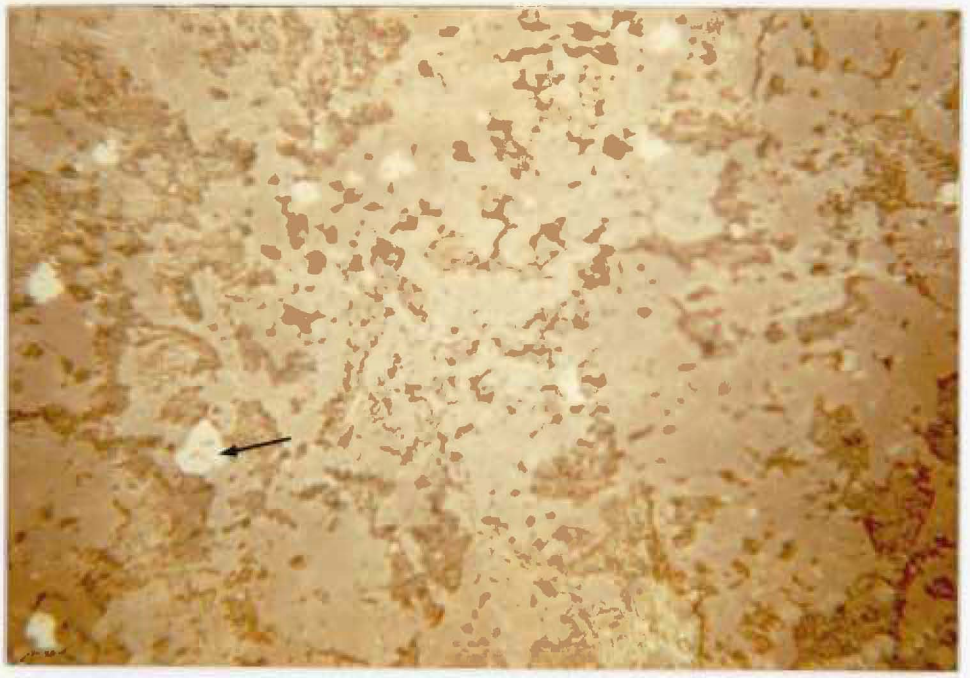

50μm

50μm

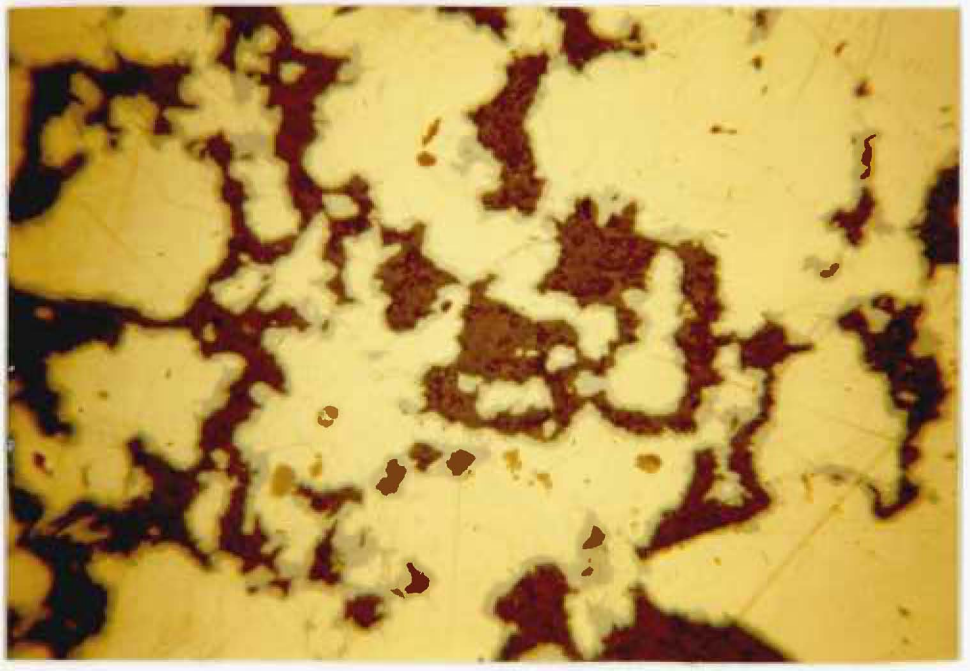

50μm

collected in section 71/M[a] of 8th Level drive revealed complete absence of chalcopyrite whereas those from the 2nd Level drive and adit level contain significant amounts of this material. Thus a copper enrichment in the upper levels, (i.e. adit - 5th Level stope), of the Gakak Lode System seems apparent. This zonation considered tentative at present should be confirmed by a more detailed study of polished sections from a wider range of localities.

The paragenetic and textural relationships of chalcopyrite with its associated mineral phases, as observed in this lode, are broadly similar to those observed in the other two lodes described. In addition to the chalcopyrite inclusions in cassiterite masses in pyrite was also commonly present as inclusions in cassiterites from this lode. These inclusions are fillings of interstitial spaces between cassiterite grains or grain aggregates. The chalcopyrites from this lode, unlike those of those of the other two lodes described, contain stannite exsolution bodies which occur as stars, droplets, rods, and anhedral and lenticular grains, (Plate 26B). In places the distribution of these stannite exsolution bodies is governed by structural planes and is inhomogeneous. It was frequent to observe stannite being exsolved to nucleate as margins surrounding exsolution-bearing sphalerite inclusions in the chalcopyrite, (Plate 26B). The chalcopyrite from the Upper levels of this lode,

(viz. adit to 5th Level stope), were oxidised to covellite and chalcocite at margins and along fractures, (Plate 26C), as are those from the upper levels of the tin lode belonging to the Gakak III Lode System. The margins of chalcopyrite veinlets within the cassiterite masses were also altered to covellite. It is not uncommon to find exsolution bodies of chalcopyrite in sphalerite from the upper levels of this lode oxidised to covellite.

Quartz.

Quartz being a later mineral has enclosed and replaced the idiomorphic sphalerite, quartz has replaced the growth zones of isolated compact idiomorphic pyrite aggregates around the margins of the sphalerite grains. Quartz has also replaced the chloritic matrix between anhedral masses of sphalerite, and also the margins of these sphalerite masses.

3.1.4. The Hantu Lode System.

The Tin Lode.

Mineralogy.

The minerals present in this economically important

phase of mineralisation are listed as shown below:

Biotite
Muscovite
Fe-Chlorite
Rutile
Cassiterite.

Pyrite
Marcasite
Exsolution-bearing Sphalerite
Exsolution-free Sphalerite
Chalcopyrite
Stannite
Cosalite-Type Pb-Bi Sulphosalt.

Quartz
Calcite.

Goethite
Covellite
Chalcocite.

Textures and Paragenesis.

Cassiterite-Fe-Chlorite-Rutile Assemblage.

Cassiterite is the principle ore mineral and the

PLATE 27.

A. A cassiterite-chlorite-quartz vein. Within the cassiterite are platy fragments of chloritic wallrock, (arrowed).

B. Parallel stringers of granular cassiterites,(arrowed), mineralising along the fine bedding planes of the chloritic pelites. (Crossed Polars).

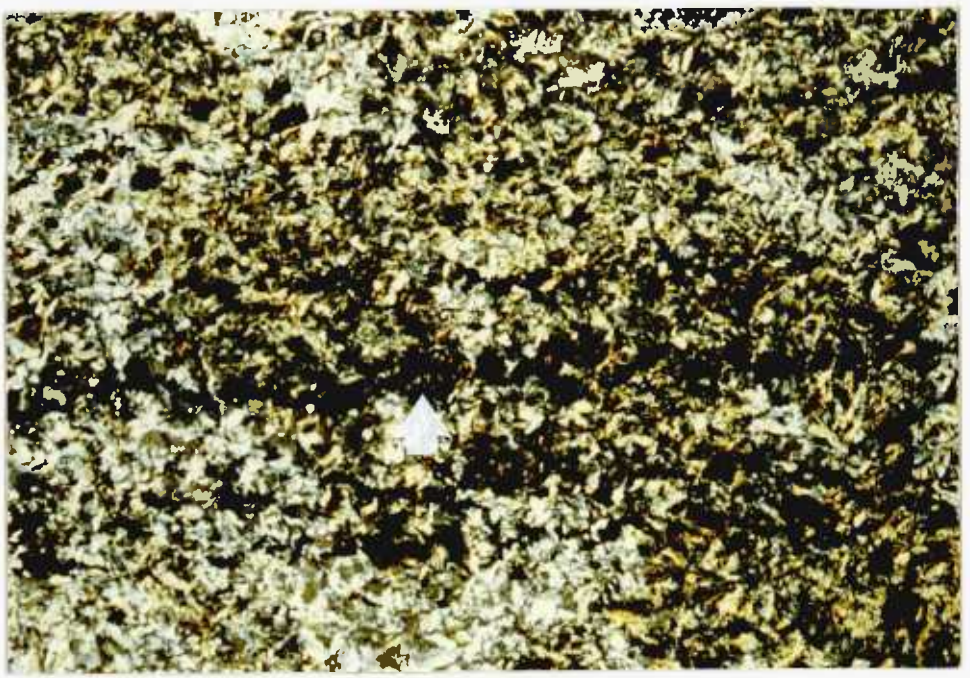

6X

only phase of economic significance in this lode and it occurs with quartz in cockage ore, and in veins 3/4" to 2" thick, (Plate 27A). Stringers of cassiterite are also present in the chloritic matrix away from the main lode, (Plate 27B), and much of the paying lode is composed by the replacement and stringer ore forming selvedges up to a foot outside the fracture walls. Cassiterite commonly occurs in bunchy masses and as rims around chloritised microbreccia fragments within the replacement selvedge, (Plate 16B). In between the massive patches are disseminations of largely unfractured cassiterite grains set within the chloritic matrix. This style of disseminated mineralisation was also seen in the margins of quartz veinlets which cut the chloritic matrix. Some disseminated cassiterite grains were caught up in quartz veinlets which cut across the cassiterite-chlorite-bearing replacement selvedge and hence some of the fractures in the cassiterite inclusions were filled by the later quartz. Partial replacement by quartz is evident. Some disseminated cassiterite grains in the chloritic matrix show almost complete pseudomorphic replacement by quartz. Cassiterite being the first mineral to be deposited in this lode and also partly due to its brittle nature was commonly fractured and locally brecciated. This is particularly typical of massive aggregates. In places where quartz and calcite veinlets cut through the massive cassiterite along fractures, angular and subhedral fragments and even slivers of cassiterite were subsequently included in these veinlets, (Plate 28.A).

PLATE 28.

A. Massive aggregates of cassiterite grains cut by ramifying veinlets of calcite, (T/S H20A, 1,200 ft. drive, Section 42/m"). (Crossed Polars).

B. Pyrite deformed into cleavage (100) (arrow a), and irregular fractures, (arrow b), which have been filled and replaced marginally by chalcopyrite, (P/S H10, 500 ft. intermediate drive W., Section 33/m"). (Plane Polarized light).

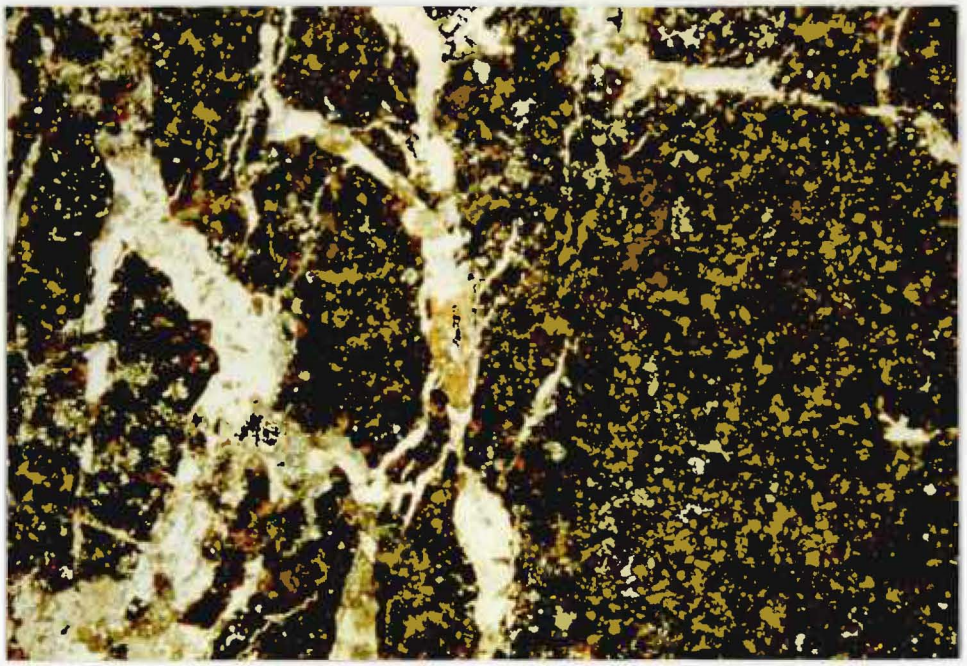

1.5X

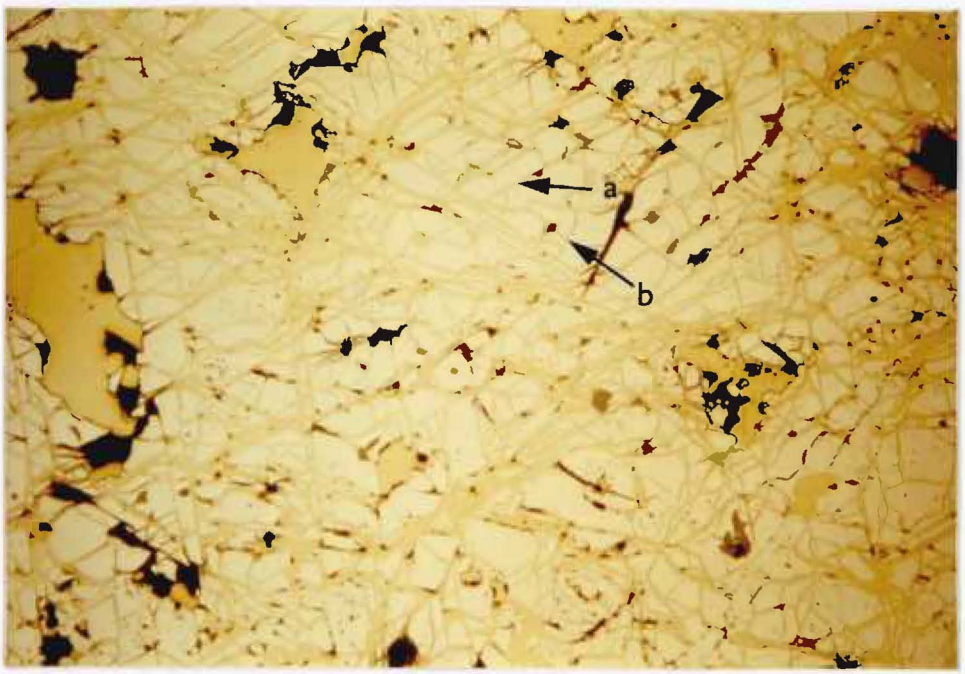

200μm

Subsequent replacement of these fragments by quartz may have played a part in rounding off some of the angular fragments. Additional rounding may have been caused by a natural fluid-supported tumbling process. As fractures were continously generated in the cassiterite, all the post-cassiterite minerals such as chlorite, pyrite, chalcopyrite, sphalerite, (the two varieties), Cosalite-Type Pb Bi Sulphosalt and marcasite have found their way into these fractures to form fillings and replacements. Being the earliest mineral cassiterite was embayed and enclosed by later minerals such as aggregates of idomorphic pyrite grains, euhedral chalcopyrite and quartz. Some cassiterite inclusions within chalcopyrite were rimmed by sphalerites, (the two varieties).

Pyrite.

Pyrite was the earliest sulphide phase which followed cassiterite mineralisation and consequently veinlets of pyrite veining through the fractures in the cassiterite and the chloritic matrix are to be expected. Pyrite is also present as granular aggragates set in chalcopyrite. Disseminated idiomorphic crystals of pyrite are occasionally present as inclusions in chalcopyrite. It was observed that there was a tendency for idiomorphic development at margins of either the pyrite veinlets or aggregates. It was common for the irregular and cleavage fractures in cataclastic pyrite to be filled and partially replaced

PLATE 29.

A. A cataclastic pyrite grain (a) within a matrix of cassiterite showing replacement by marcasite (b) from fractures inward, (P/S H18a, 800 ft. level, Section 36/P"). (Plane Polarized light).

B. Aggregates and individual euhedral grains of pyrite are set in the chalcopyrite matrix; both these pyrite forms are notably replaced by marcasite (a). Irregular inclusions of inclusion free sphalerite (b) are set in the chalcopyrite matrix, (P/S H.14, 600 ft., Section 35/n"). (Plane Polarized light).

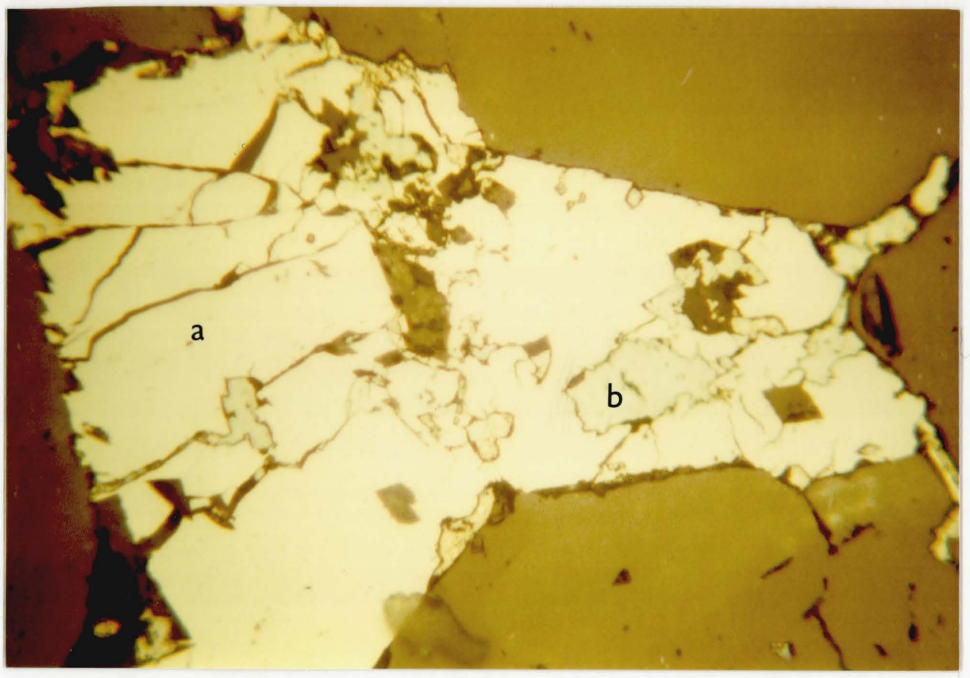

100μm

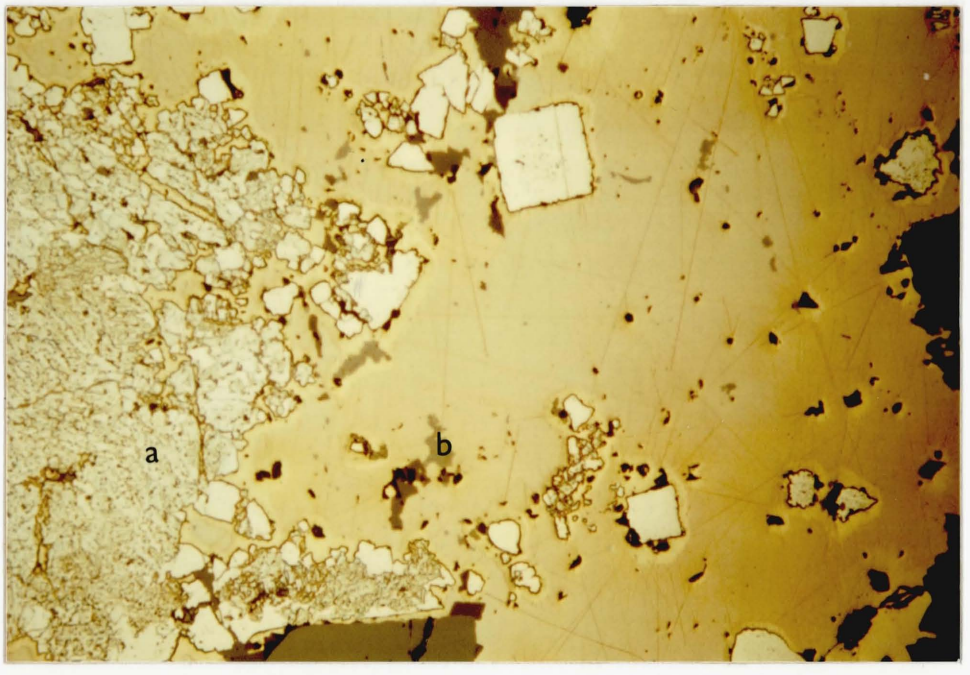

200μm

by chalcopyrite, (Plate 28B). This textural relationship indicates that pyrite was deposited prior to or during the precipitation of chalcopyrite. Replacement of pyrite by marcasite was very common at margins and within fractured masses, (Plates 29A and 29B). The unreplaced relict pyrite is often present as thin alternating lamellae within the marcasite. Quartz has also replaced pyrite along cleavages. Some of the marcasite-pyrite masses were veined through by exsolution-free sphalerite veinlets. Only pyrite from above the 400 foot drive has been oxidised to goethite at its margins by percolating acid ground waters.

Isolated pyrite inclusions in cassiterite as seen in P/S H_2 were replaced by cassiterite in some cases leaving behind a recognisable cubic rim, (Plate 30A Thus these pyrite inclusions were deposited prior to the precipitation of cassiterite. Rutile inclusions were commonly observed in the cassiterite and frequently showed alignment parallel to structural planes in the cassiterite grains. Rutile also occurs as disseminated laths and anhedral crystals set in the chloritic matrix; some of the rutile formsrims around cassiterite grains. The observed textural relationship between rutile and cassiterite suggests that the deposition of the former continued after the conclusion of the main phase of cassiterite deposition. If it is accepted on the basis of the petrographic evidence that the majority of the titanium was provided by chloritisation of

Ti-rich biotite in the wallrocks then it may be assumed that the release of Ti by this process overlapped the history of cassiterite deposition.

Sphalerite.

In common with the three lodes so far described, two varieties of sphalerite were recognised in this lode. The chalcopyrite inclusion-bearing sphalerite also contains subordinate amounts of pyrite, marcasite and galena as inclusions. The two varieties of sphalerite were often seen to coexist in close association. The distribution of the exsolution bodies in a single anhedral grain of sphalerite was observed to be heterogeneous, (Plate 20B). Domains with a high concentration of exsolved inclusions are often seen to lie adjacent to inclusion-free areas.

Sphalerite often occurs as relict unreplaced anhedral inclusions in matrix chalcopyrite and also as later replacive inclusions in pyrite. In addition it also occurs as rims around isolated cassiterite grains within the chalcopyrite. Furthermore, it also fills fractures in the cassiterite and evidence of replacement of the cassiterite outwards from the fracture margins was often seen. Massive sphalerite also enclosed cassiterite and occas ionally pyrite grains. Sphalerite also locally encrusts fragments of the chloritic matrix in the fractured wallrock selvedge of the veins and is

followed by quartz during subsequent reactivation of the fracture system. Some sphalerite grains were incorporated in the quartz vein with subsequent replacement to their margins as indicated by the presence of irregular margins. Small sphalerite inclusions in chalcopyrite were replaced by stannite exsolved from the chalcopyrite and nucleated at the boundaries between sphalerite inclusions and the host chalcopyrite.

Chalcopyrite.

The deposition of sphalerite was followed by the precipitation of chalcopyrite which is commonly present as veinlets filling fractures developed in the chloritic matrix, cassiterite and pyrite. The veinlets have also simultaneously replaced these minerals. Chalcopyrite veinlets have replaced some of the pre-chalcopyrite pyrite veinlets occupying the fractures in cassiterite, (Plate 23A). In some cases parts of these veinlets have suffered nearly total replacement leaving behind only a scattering of relict pyrite; in other cases replacement by chalcopyrite has followed along the pyrite/cassiterite contact of these veinlets. However, they have, themselves, occasionally been replaced by cosalite-type Pb-Bi-sulphosalt. Large and small anhedral and unfractured grains of chalcopyrite are present replacing the chloritic matrix. The larger chalcopyrite grains often contain inclusions of cassiterite, pyrite and sphalerite. Orientated

inclusions of sphalerite in chalcopyrite as seen in P/S H5 could be interpreted as mutual intergrowths since these two minerals share a comparable crystal structure. Some small flakes of chalcopyrite were enveloped and replaced by Cosalite-Type Pb-Bi Sulphosalt often leaving behind a relict core of chalcopyrite. Chalcopyrite veinlet in P/S H21a has partly exsolved numerous orientated rows of stannite in the form of elongate rods, ovoids and droplets, (Plate 26B). Stannite exsolution bodies have also replaced the coexisting sphalerite inclusions.

Chalcopyrite was commonly oxidised to form chalcocite or covellite. In certain cases the oxidation was complete while in others it was only partial, commonly at margins or along the intergranular boundaries between sphalerite and chalcopyrite where the Cu-bearing ground waters gained access to cause the oxidation process. Chalcopyrite was more frequently replaced by calcite than by quartz when the latter two minerals were in contact together with chalcopyrite.

Pb-Bi Sulphosalt: Cosalite type.

A Cosalite-Type Pb-Bi sulphosalt was detected for the first time in this lode and, as far as the writer is aware of also in other lodes within the Sg. Lembing Area. However, Bismuthinite has been recorded from

PLATES 30.

A. Inclusions of pyrite grains in cassiterite are partially replaced by cassiterite producing subhedral and skeletal forms, (P/S H.5, 400 ft. stope, (1st lift), Section 33/P"). (Plane Polarized light).

B. Cosalite-type Pb-Bi-sulphosalt occurs as aggregate of acicular laths in the chloritic matrix and as inclusions in the cassiterite grains. This sulphosalt also fills the fractures in the cassiterite, (P/S H.10, 500 ft. intermediate drive W., Section 33/m". (Plane Polarized light).

100μm

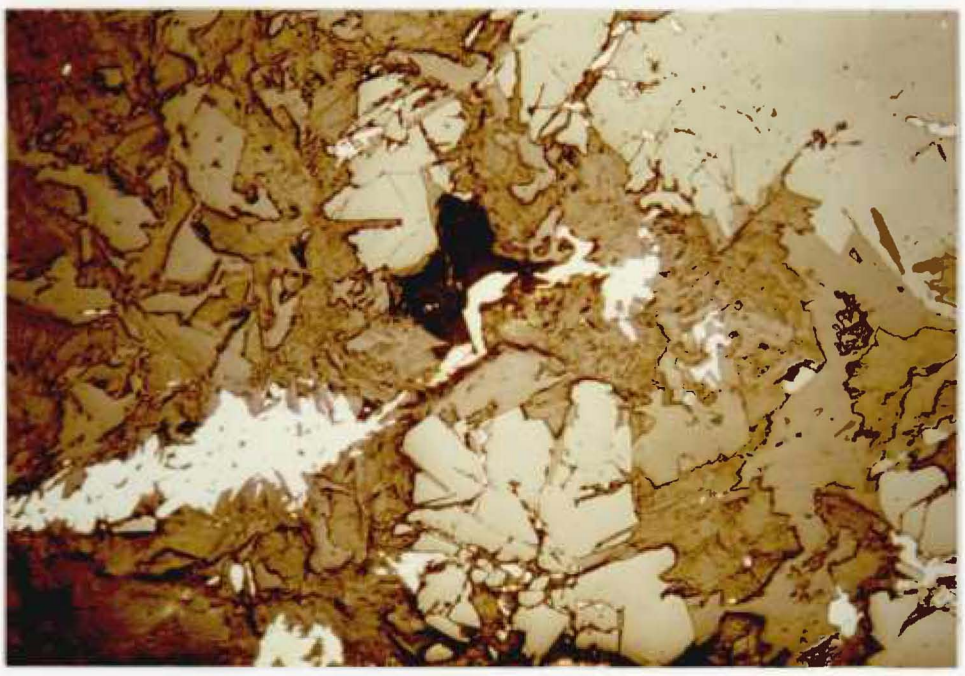

200μm

the tin lode of the Gakak Lode System by Ang, (1974). The identification of this mineral was made using the Electron Probe X-ray Microanalyser and ore microscopic technique. The former technique gave the qualitative major chemical composition of this mineral as rich in Pb and Bi; Pb was slightly more abundant than Bi. This result indicates that the mineral is a Pb-Bi sulphosalt and its optical properties as listed below compared best with those of Cosalite given by Uytenbogaardt and Burke, (1971):

Colour:	Grey with bluish tint when in chalcopyrite matrix. Grey white when set in chloritic matrix.
Reflection Pleochroism	Strongly pleochroic
Anisotropy:	Strongly anisotropic.
Internal reflection:	Not present.

This Cosalite-Type Pb-Bi sulphosalt mineral occurs as:

1. Aggregates of prismatic laths, (Plate 30B), and

PLATE 31.

A. Cosalite type Pb-bi-sulphosalt occurs as lensoid inclusion in chalcopyrite, (P/S H10, 500 ft. intermediate drive W., Section 33/m"). (Plane Polarized light).

B. Cosalite-type Pb-bi-sulphosalt fills the fractures of cassiterite masses, and also partially replaces a chalcopyrite veinlet which runs along the inter-cassiterite spaces, (P/S H.10, 500 ft. intermediate drive W., Section 33/m"). (Plane Polarized light).

100 µm

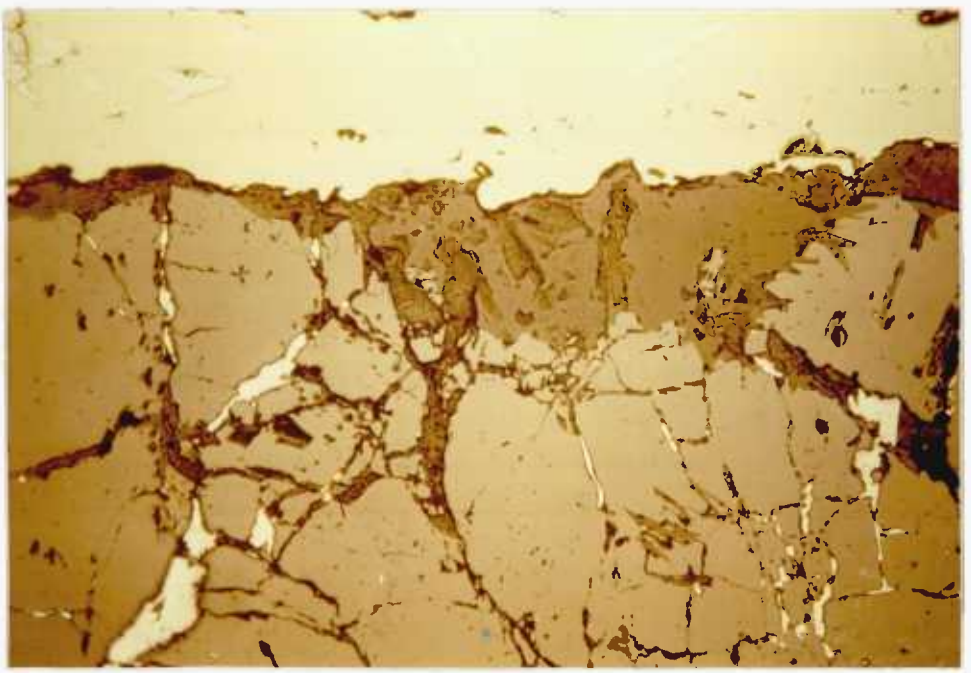

200 µm

2. As lensoids with sharply terminated tails, (Plate 31A).

This mineral occurs around the margins and in the fractures of cassiterite masses, (Plate 31B). It also occurs as aggregate of prismatic laths set in the chloritic matrix and it replaces chalcopyrite frequently, (Plate 31B). However, it has been seen to be enclosed and replaced by quartz.

Quartz.

Quartz is an important gangue mineral and is ubiquitously present in the cassiterite-chlorite lode, (Hantu lode), as veinlets and veins which were emplaced in a series of dilatant episodes which followed the main cassiterite-chlorite-sulphide mineralisation. Thus it is not suprising to expect the quartz veinlets/veins to have filled and cemented respectively the fractures and breccia fragments developed in the cassiterite-chlorite-sulphide rock. Quartz was also seen to replace the chloritic veinlets in the fractures of cassiterite. In the case of mineralised breccia cockade ore even the breccia fragments are clearly cut across by quartz veinlets, (Plate 6C). Thus the main quartz mineralisation must have been accompanied by a new phase of disruptive fracturing. In previous chloritised wallrock matrix, quartz also occurs as irregular. replacements so that the pre-existing chlorites,

sulphides or cassiterite grains in the wallrock are enclosed and subsequently replaced marginally. Minerals that were enclosed and partially replaced were cassiterite, chlorites, pyrite, chalcopyrite and cosalite. Quartz was fractured to allow the emplacement of calcite in ramifying veinlets which locally replaced the quartz.

Calcite.

The last phase of mineralisation in this lode is calcite which was only found present in levels between the 500 foot intermediate level and 1,200 foot level. Calcite occurs commonly as thin ramifying veinlets cutting through the chloritic matrix, cassiterite masses, (Plate 28A) and quartz veins and veinlets and their enclosed cassiterite grains. In places where the quartz veinlets, (those in cassiterite fractures), have no fractures developed across them, the calcite veinlets followed the cassiterite/quartz contacts utilising the pre-existing weakness. Besides occurring as veinlets, calcite is also present as a replacive mineral in the pockets of chloritic matrix within and beyond the cassiterite masses. Cassiterite, quartz and chalcopyrite masses and veinlets, (those occupying cassiterite fractures), which were in contact with calcite masses or veinlets have been replaced locally by calcite. It was observed that while quartz and chalcopyrite were both in contact with calcite it was the latter which was more readily replaced.

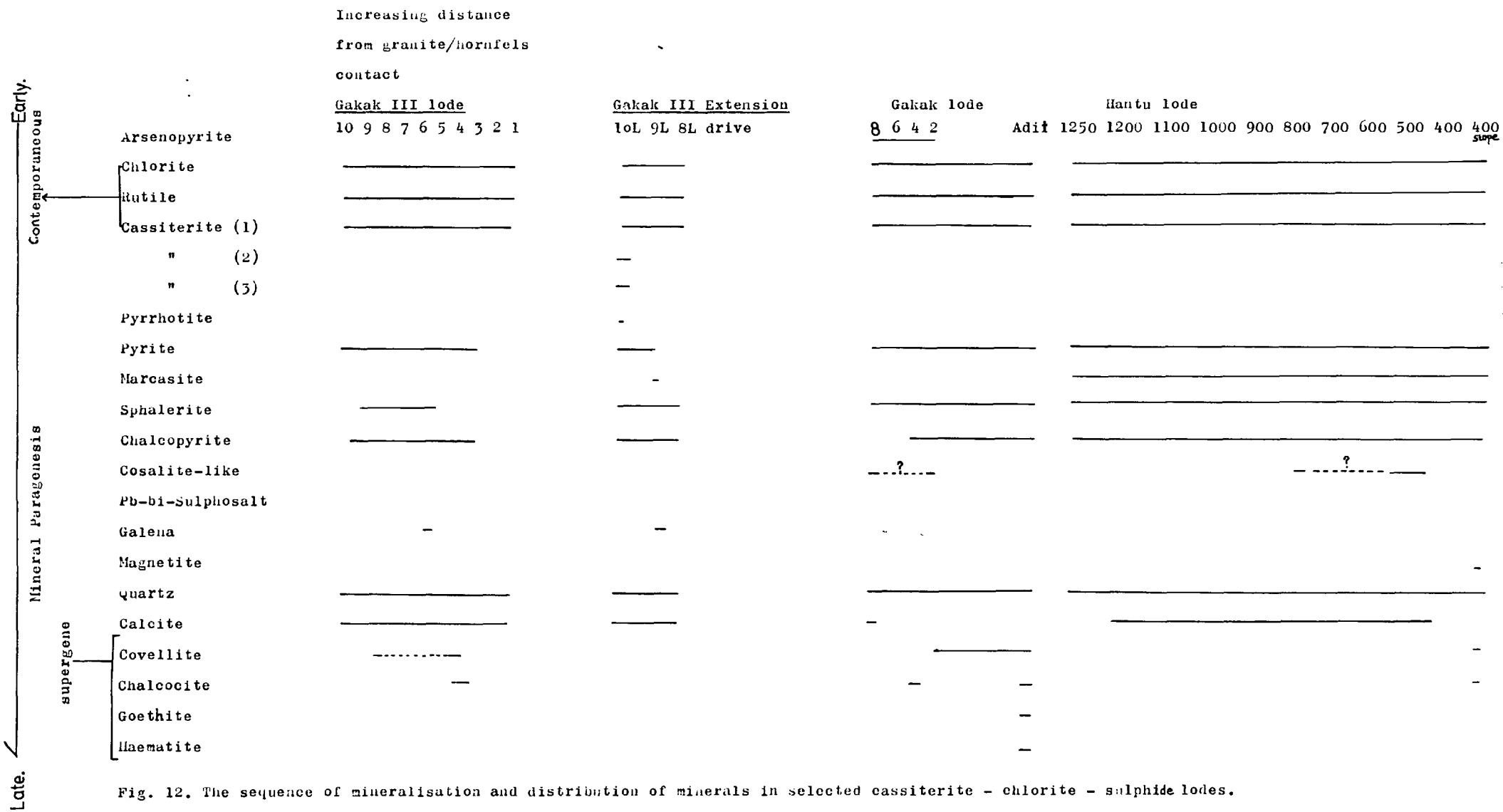

Fig. 12. The sequence of mineralisation and distribution of minerals in selected cassiterite - chlorite - sulphide lodes.

General Conclusions.

The sequence of precipitation of the minerals present in the four tin lodes described above is graphically shown in figure 12 . As can be seen in Fig. 12 , chlorite, rutile, cassiterite, pyrite, sphalerites (the two varieties), chalcopyrite, quartz, and calcite are consistently present in the five tin lodes.

The cassiterite-chlorite-rutile assemblage forms the main component of the tin lodes whereas the sulphides are present in minor amounts. The rarity of occurrence of tourmaline and fluorine-bearing minerals as observed in this present field and laboratory study and, also, by Fitch, (1952), suggests that boron and fluorine activities in the tin-rich mineralising hydrothermal fluids were not sufficiently high to cause precipitation of tourmaline and fluorine-bearing minerals in significant amounts. The inferred low boron and fluorine activities exclude B and F as important elements involved in the hydrothermal transport of Sn in the hydrothermal systems of the tin lodes in the Sg. Lembing Area. The inferred insignificance of F in the latter hydrothermal systems is confirmed by the low F content of the gangue ferroan chlorite.

A cosalite-like Pb-bi-sulphosalt is present only in

the tin lodes of the Gakak and Hantu Lode Systems. Galena is present only in the tin lodes of the Gakak III and its extension Lode Systems. Pyrrhotite and magnetite are very rare as they are detected only in minor amounts in the Gakak III Extension and Hantu Lode Systems respectively. Since chalcopyrite from the upper levels of three tin lodes, (Fig. 12), was commonly altered partially to covellite and chalcocite it can be inferred that the alteration process was brought about by percolating acid ground water. Unlike the sulphide $\pm$ cassiterite lodes the late carbonate phase in the tin lodes is calcite. This calcite fills and replaces fractures develpped in the precalcite mineral phases. It also encloses and replaces earlier mineral grains both marginally and internally.

Pyrite and cassiterite have preserved their cataclastic texture whereas chalcopyrite, sphalerite, cosalite-like Pb-Bi-sulphosalt and galena have evidently undergone recrystallisation and annealment after deformation. Because of their ductile mechanical properties they do not preserve obvious cataclastic textures.

CHAPTER 4.

Petrography of ore samples from the Sulphide±Cassiterite lodes of the Hantu and the Gakak Mines.

4.1. The Chalcopyrite-Pyrrhotite Lode from the 400 foot drive of the Hantu Lode System.

This phase of mineralisation was observed in hand specimens collected from fallen rock in workings on the 400 foot drive of the Hantu Lode System. The phase relationships in situ could not be observed but it is inferred from the relationships observed in the lodes of the Gakak Mine that the sulphide phase in the Hantu Lode System also postdates the initial cassiterite mineralisation and also the multiple episodes of barren white quartz mineralisation. The mineralogy of this sulphide lode is summarised in the following list:

Rutile.

Pyrite

Pyrrhotite

Chalcopyrite

Exsolution-free sphalerite

Exsolution-bearing sphalerite

Marcasite

Siderite

Quartz.

The mineragraphic relationships of the mineral components of this lode are described and interpreted in order of paragenesis as follows:

Sphalerite.

Ferroan Sphalerite is predominantly free of exsolved inclusions except for a few grains which contained chalcopyrite globules. The ferroan sphalerite shows brownish red internal reflection which is suggestive of its iron rich nature. This sphalerite occurs as tiny rounded and irregular anhedral inclusions frequently set in chalcopyrite except for a few grains in the mutually intergrown pyrrhotite. The irregular shape of these inclusions suggests that a marginal replacement by both chalcopyrite and pyrrhotite has occurred. Sphalerite inclusions, some of which contain chalcopyrite exsolution bodies, have also been observed within pyrite and they are interpreted as a selective replacement of the interior of the pyrite. According to the textural relationship of sphalerite with chalcopyrite-pyrrhotite and pyrite, the deposition of sphalerite was post-pyrite but prior to chalcopyrite-pyrrhotite.

PLATE 32.

A. Bands composed of intergranular growth of pyrrhotite (a) with chalcopyrite (b) are separated by a thin band of pyrrhotite-free chalcopyrite. The latter contains of a subhedral grain of siderite (c). (P/S H400A, 400 ft. drive). (Plane Polarized light).

B. Chalcopyrite (a) is intergrown with pyrrhotite (b) and pyrite (c). The latter is extensively replaced by marcasite (arrowed), (P/S H400A, 400 ft. drive). (Plane Polarized light).

200μm

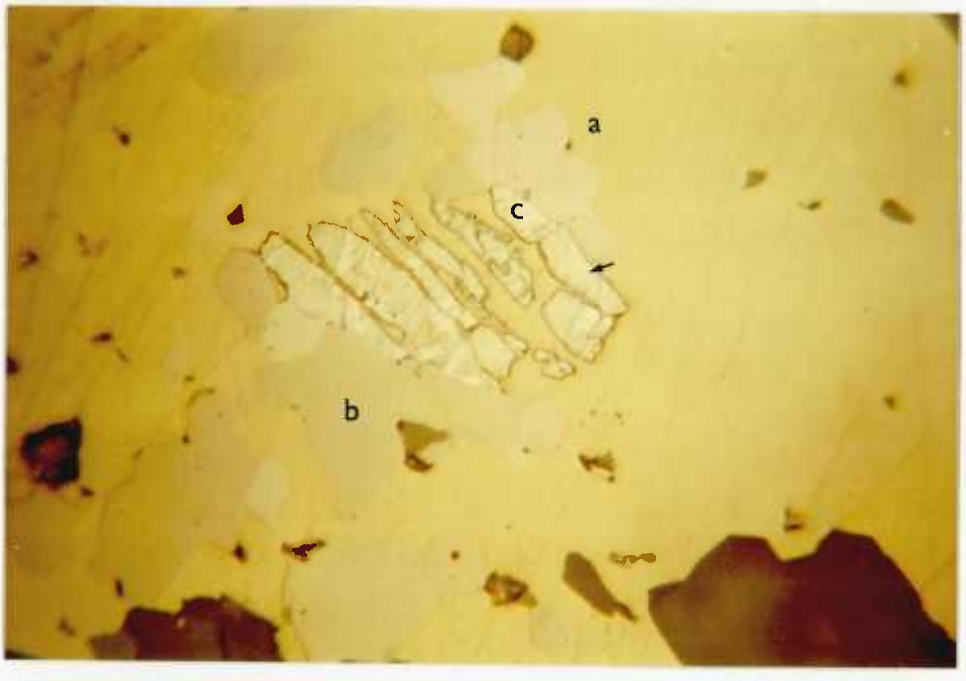

100μm

Chalcopyrite-pyrrhotite-pyrite intergrowths.

The main component of this lode is composed of bands of chalcopyrite composing a granular intergrowth with pyrrhotite and minor pyrite and these are separated by thinner bands of chalcopyrite, (Plate 32A), mutual intergrowth of pyrrhotite in chalcopyrite is suggested by the subhedral to euhedral form of the pyrrhotite grains and also the absence of replacement features between these two phases. The banding mentioned above is believed to have been produced by shearing during post-sulphide movements on the lode followed by annealment of the pyrrhotite-chalcopyrite fabric. This is confirmed by the parallel development of siderite-pyrite veinlets. Isolated early pyrite grains within the annealed chalcopyrite-pyrrhotite matrix have preserved a cataclastic texture and have partially or completely suffered alteration to marcasite, (Plate 32B).

Pyrite veinlets.

The fractures produced by the shearing movements were favourable sites for the emplacement of pyrite veinlets which cut across both the chalcopyrite and the early pyrite aggregates. The pyrite veinlets were fractured. The contact between the pyrite veinlets, the pyrite aggregates and the chalcopyrite, and the fractures within the pyrite veinlets were

planes of weakness favourable for the migration of siderite ($FeCO_3$) solutions which have marginally replaced these minerals. The early pyrite and the pyrite in the veinlets have also been subjected to replacement along growth zones. However, chalcopyrite has also simultaneously been replaced by siderite. The replacement of pyrite veinlets by marcasite is also evident in places.

Marcasite.

Marcasite occurs only in minor amounts and it occurs exclusively as a replacement of pyrite veinlets and early pyrite inclusions and aggregates, (Plate 32B). In some cases the replacement was only marginal whereas in others it was completely pseudomorphic. This is a relatively rare phenomenon and it is also thermodynamically a complete absurdity, (Ramdohr, pg. 830 and pg. 170, 1969).

Siderite.

Siderite is abundant and was recognised by its rhombic crystal habit, strong anisotropy and milky white internal reflection. The identity of siderite was confirmed by Electron Probe x-ray microanalysis.

Siderite commonly occurs as a mineral pervasively replacing pyrite veinlets and also along the pyrite

veinlet chalcopyrite-pyrrhotite contact as a result of which it formed distinct veinlets. It is also present as discontinuous lensoid stringers which are aligned parallel and subparallel to each other and also to the chalcopyrite-pyrrhotite banding. However, some did cut across the chalcopyrite-pyrrhotite banding. Isolated euhedral, (Rhombic), and subhedral inclusions of siderite also occur randomly in the chalcopyrite-pyrrhotite matrix of the lode, (Plate 32A). siderite was the last phase to be deposited Relict inclusions of sphalerite, chalcopyrite and pyrrhotite in siderite naturally occur. Furthermore, siderite has also replaced some idiomorphic pyrite grains marginally as well as from within forming poikilitic siderite intergrowths.

4.1.1. The chalcopyrite-pyrrhotite-galena Lode at Eight Level Drive, (Section 86/S^{a}), of the Gakak III Extension Lode System.

This phase of mineralisation was emplaced next to the barren white quartz vein complex. The phase relationships in situ could not be observed, but it is inferred from the relationships observed in other localities of this lode system that the sulphide phase postdates the multiple episodes of barren whitequartz. The mineralogy of this lode is summarised in the following list:

Cassiterite

Pyrite

Pyrrhotite

Chalcopyrite

Exsolution-bearing Sphalerite

Exsolution-free Sphalerite

Galena

Siderite

Quartz.

The minera graphic relationships of the mineral components of this lode are described and interpreted in order of paragenesis as follows:

Cassiterite.

Cassiterite was the first mineral to be deposited in the lode and it occurs only in trace amounts as isolated subhedral and anhedral inclusions set in chalcopyrite, some cassiterite inclusions were rimmed by exsolution (chalcopyrite)-bearing sphalerites and also those without exsolution bodies.

Pyrite.

Pyrite was the first sulphide phase to be deposited in the form of veinlets and irregular anhedral masses set in a chalcopyrite matrix. This fact, together

PLATE 33.

A. Exsolution (chalcopyrite)-bearing sphalerite is replaced by chalcopyrite (a) and galena (b) and later cut by veinlets of siderite (arrowed), (P/S G3E, 8th level, section 86/S^{a}). (Plane Polarized light).

B. Inclusions of exsolution and non-exsolution bearing sphalerite (a) and pyrrhotite (b) in chalcopyrite.Quartz (c) replaces a pyrrhotite inclusion along cleavages. It has also replaced the chalcopyrite, (P/S G3E, 8th level, section 86/S^{a}). (Plane Polarized light).

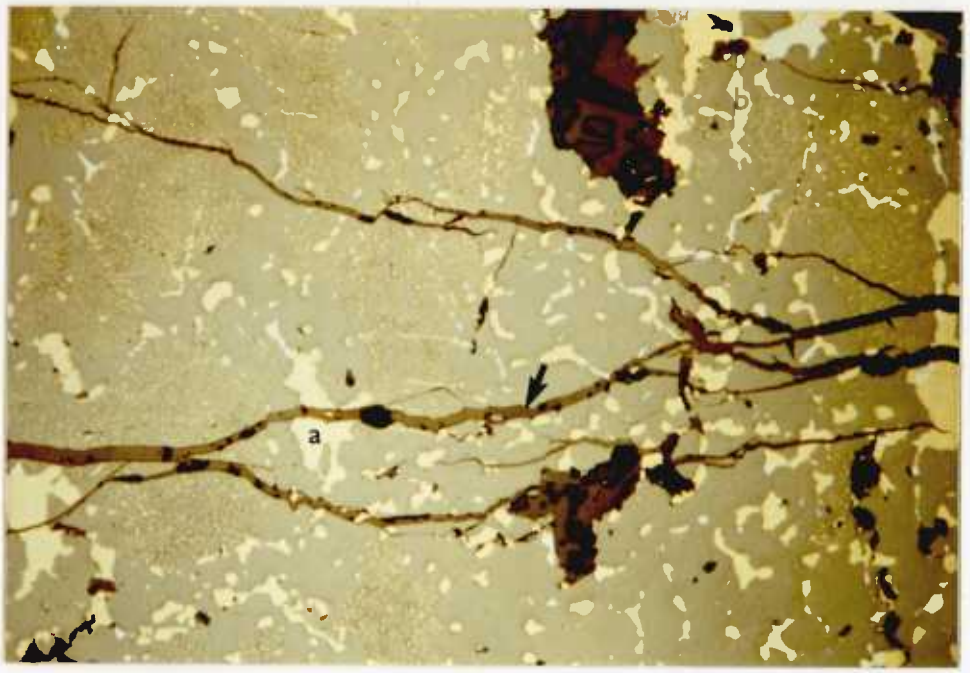

200μm

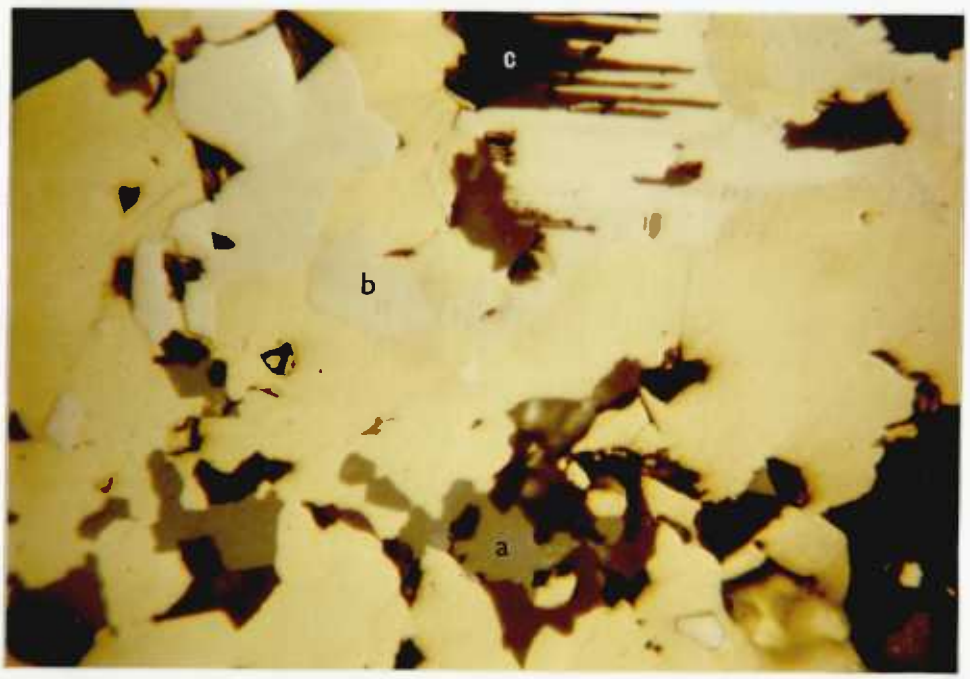

100μm

with its frequently fractured form has led to the replacement of pyrite by later minerals, (e.g. exsolution-bearing and exsolution-free sphalerite, chalcopyrite, pyrrhotite, galena, quartz and siderite), which followd cleavages and fractures. Thus inclusions of chalcopyrite and siderite are present in some pyrite veinlets; poikilitic intergrowths of pyrrhotite, sphalerite, galena, chalcopyrite, quartz and siderite also occur in idiomorphic pyrite. The most common and effective replacement of pyrite is by siderite which migrated into the pyrite via fractures developed in chalcopyrite and then into the contact between pyrite and chalcopyrite. In places the replacement of pyrite by siderite was so extensive that the siderite now forms pseudomorphs after pyrite.

Sphalerite.

Two varieties of sphalerite are present:

1. Sphalerite which bears exsolution bodies of chalcopyrite, (major phase), and inclusions of galena and pyrrhotite, (minor phases), (Plate 19B). The exsolved phases occur in both globular and thin rod-like forms, (Plate 33A), and the distribution pattern of these phases is heterogeneous even within a single sphalerite grain, (Plate 20B).

2. Sphalerite free of any exsolution bodies.

The first variety is more abundant than the second variety. The two types of sphalerite occur as anhedral inclusions of varying sizes set in chalcopyrite or chalcopyrite-pyrrhotite matrices, (Plate 33B). In places they have rimmed around isolated cassiterite inclusions in chalcopyrite and they have also replaced pyrite. They were, however, replaced by chalcopyrite at their margins as well as internally, (Plate 33A). The occurrence of anhedral inclusions of chalcopyrite in the sphalerite confirms its internal replacement by chalcopyrite, (Plate 33A). Exsolution-bearing sphalerite had also been replaced by galena, (Plate 5 and quartz, and it was transected by siderite veinlets, (Plate 33A). It seems that the sphalerites were not as susceptible to replacement by siderite as pyrite was.

Chalcopyrite-pyrrhotite.

This combination of phases forming a granular intergrowth, (Plate 33B), followed the sphalerites and they form the major component deposited in this lode. In places it consists of coarse mutual intergrowths of pyrrhotite with chalcopyrite. As a late phase it has enclosed and partially replaced inclusions of cassiterite, pyrite and sphalerites,

PLATE 34.

Galena replaces sphalerite (a) chalcopyrite (b) and pyrite (c) both marginally and internally. (P/S.G3E. 8th level, section 86/S[a]). (Plane Polarized light).

200μm

but it has also been replaced by galena, (Plate 34 and siderite. Chalcopyrite has also been fractured and the fractures filled by siderite veinlets.

Galena.

Galena is the last sulphide phase to be deposited in this lode and has mineralised the wallrock selvedge and replaced the earlier sulphide phases, (chalcopyrite-pyrrhotite, the sphalerites, (Plate 34 pyrite, (Plate 34), and cassiterite. One inclusion of cassiterite was seen to have been replaced a little from within. Galena replaced chalcopyrite forming penetrating apophyses and irregular inclusions with the result that relict inclusions of chalcopyrite were enclosed in galena, (Plate 34). It was, however, enclosed and replaced by quartz. Quartz pseudomorphs after galena were also seen.

Quartz.

Quartz occurs in minor amounts and it has enclosed and partially replaced pyrite, exsolution-bearing sphalerite, chalcopyrite and galena. In the case of the latter mineral pseudomorphic replacement by quartz is evident in places.

Siderite.

Siderite was the last phase to be deposited in this lode and it was introduced into the lode via the pyrite/chalcopyrite contact and also along fractures in the chalcopyrite-pyrrhotite phase. Siderite replaced pyrite and chalcopyrite and pyrrhotite inclusions spreading from the pyrite/chalcopyrite contact. The siderite veinlets which occupy the fractures in the chalcopyrite-pyrrhotite phase have been seen to cut across the exsolution-bearing sphalerite inclusions in the latter, (Plate 33A).

4.1.2. The Pyrite Lode at Eight Level Drive, (Section 89/R^a) of the Gakak III Extension Lode System.

The mineralogy of this lode is summarised in the following list.

Cassiterite

Pyrite
Chalcopyrite
Exsolution-bearing sphalerite
Exsolution-free sphalerite

Quartz

Calcite

PLATE 35.

A. Pyrite vein showing cataclastic texture. The fractures within the vein are filled and replaced in places by chalcopyrite (a). A subhedral cassiterite inclusion (b) within the pyrite is replaced marginally by chalcopyrite, (P/S G3E.IX, 8th level, section 891Ra). (Plane Polarized light).

B. Disseminated grains of pyrite in between the massive aggregates of pyrite grains. (P/S G3E.IX, 8th level, section $89/R^a$ (Plane Polarised light).

C. Breccia fragments of pyrite are cemented by calcite veinlets. Note some fractures in the pyrite brec breccia fragments are filled by chalcopyrite (arrowed). (P/S G3E.IX, 8th level, section $89/R^a$ (Plane Polarized light).

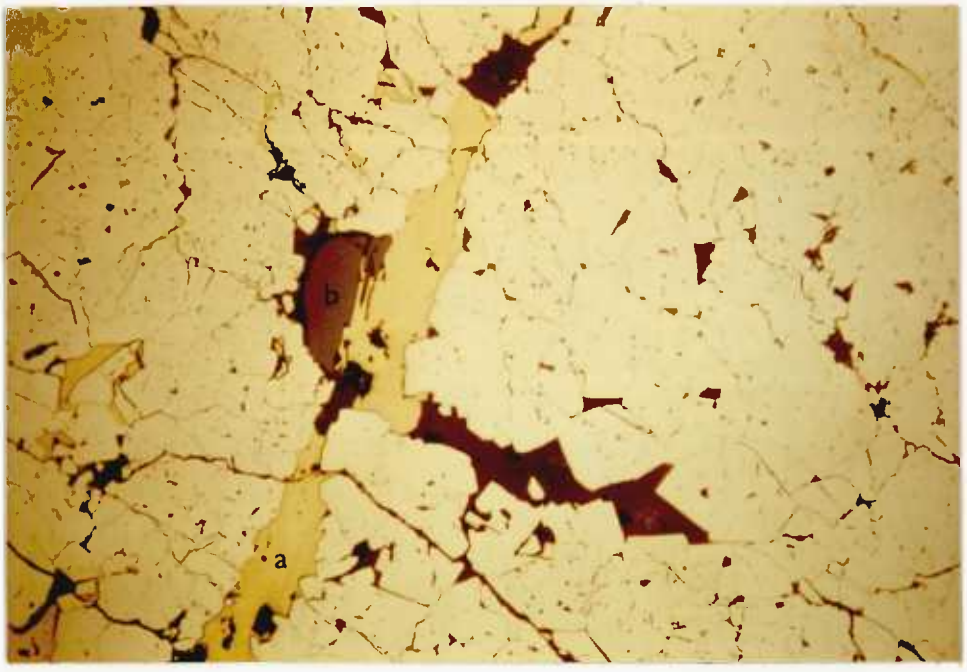

100μm

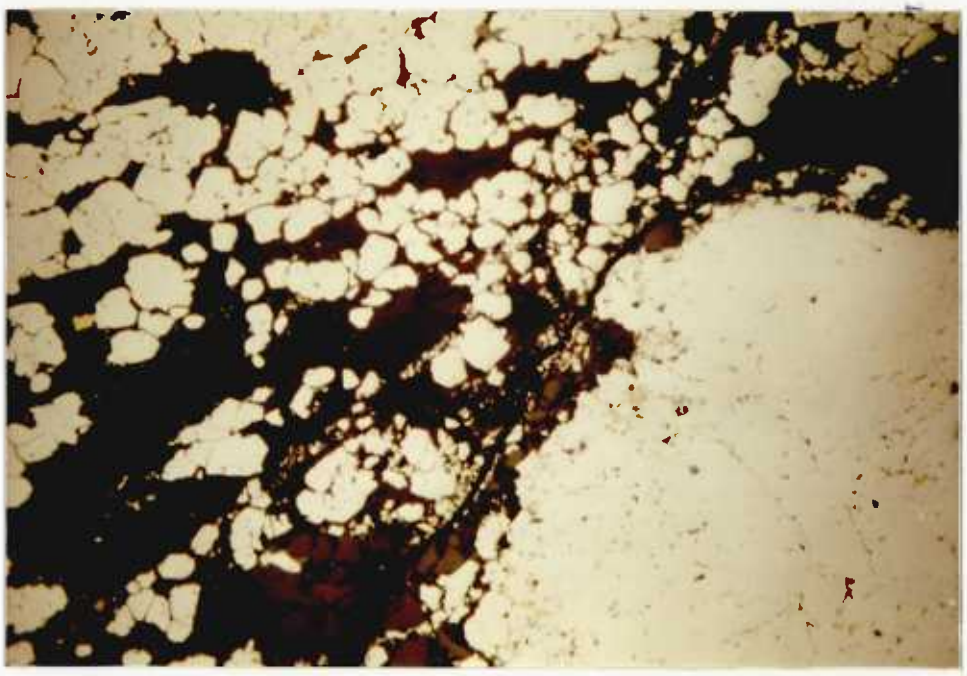

100μm

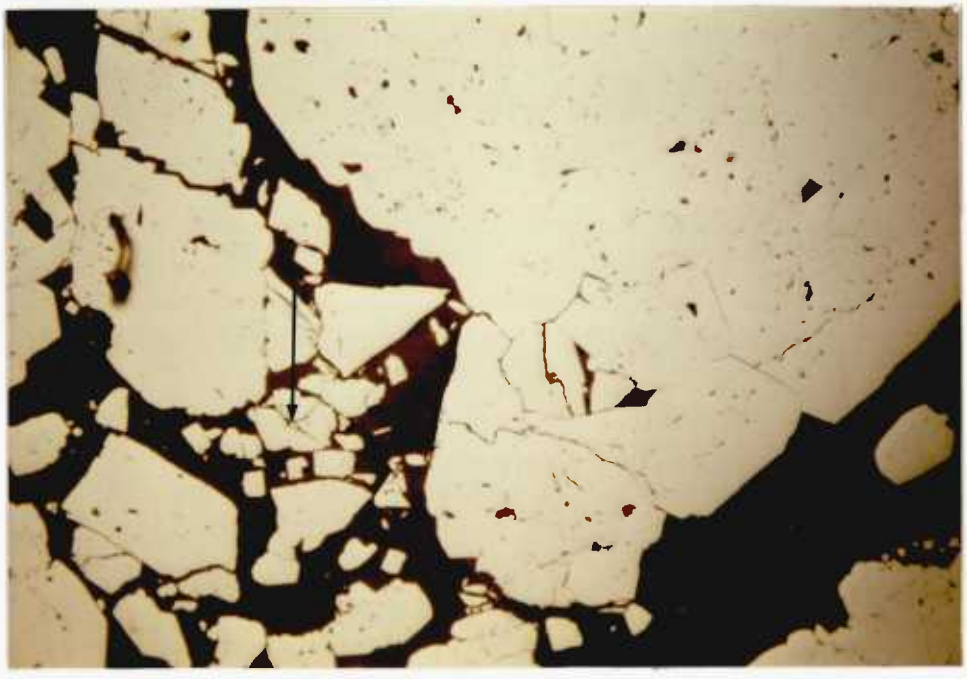

100μm

The mineragraphic relationships of the mineral components of this lode are described and interpreted in order of paragenesis as follows:

Cassiterite.

Cassiterite was the first mineral phase to be deposited in this lode, but it occurs in very small amounts as isolated, small unfractured subhedral and anhedral grains set in pyrite, (Plate 35A), chalcopyrite, calcite and the included silicate gangue. In one instance a larger anhedral cassiterite inclusion in pyrite shows intense fracturing but none of these fractures were infilled by the surrounding pyrite which suggests that the fracturing event has occurred after the pyrite was deposited. Another large cassiterite grain shows brecciation. These breccia fragments were cemented by a pyrite veinlet. An unfractured subhedral inclusion of cassiterite within the pyrite vein was also replaced at margins by a chalcopyrite veinlet, (Plate 35A).

Pyrite.

Pyrite is the major phase in this lode and it was emplaced in en echelon tension gashes just next to the quartz veins. It occurs in a massive form with idiomorphic margins at places particularly at the contact with the wallrock- it is also present as

disseminated idiomorphic grains in pockets of the silicate gangue, (Plate 35B), and in calcite within the pyrite vein. Some of these idiomorphic pyrites were enclosed by chalcopyrite.

The pyrite vein was intensely fractured and the resultant fractures were infilled and partially replaced by chalcopyrite, (Plate 35A). Hydraulic fracturing and brecciation in the pyrite vein caused by the fluid pressure of the calcium and carbonate-rich fluids is evident, (Plate 35C). The pyrite vein has small amounts of sphalerite inclusion with exsolved chalcopyrite. These inclusions are believed to have been produced by partial replacement of pyrite along growth zones.

The Sphalerites.

The two varieties of sphalerite are present but in very small amounts. The exsolution-bearing variety is present as replacement inclusions in the pyrite vein and the exsolution-free sphalerite, (though a few contain chalcopyrite inclusions), always spatially associated with chalcopyrite veinlets as well as with the disseminated chalcopyrite within the calcite gangue. The sphalerite in the chalcopyrite veinlets could be interpreted as relict unreplaced grains. These textural relationships indicated that the sphalerites are post-pyrite and pre-chalcopyrite in age.

Chalcopyrite.

Chalcopyrite occurs in minor amounts. It is present as a matrix for disseminated idiomorphic pyrite and also as disseminated flakes in the wallrock and in calcite gangue. The chalcopyrite inclusions within calcite could be interpreted as unreplaced relict grains.

In addition to the two forms just described, chalcopyrite also occurs as thin veinlets occupying the fractures in pyrite, (Plate 35A).

Quartz.

Quartz is not common in this lode as it has only been observed in one place where it has enclosed cassiterite breccia fragments.

Calcite.

Calcite is abundant and it was the last phase to be deposited in this lode. Hence, it has replaced the pockets of host facies with subsequent enclosure of pyrite, the sphalerites and chalcopyrite as inclusions. These inclusions do show signs of replacement by the calcite matrix. Furthermore, it also fills brecciated fractures in the pyrite vein forming an interconnected network of veinlets, (Plate 35C).

4.13. Pyrrhotite Lode at Ninth Level Stope - First Lift, (section 87/88/ ^{a}), of the Gakak III Extension Lode System.

The mineralogy of this lode is summarised in the following list:

Pyrite
Pyrrhotite
Exsolution-free sphalerite
Chalcopyrite

Siderite

The mineragraphic relationships of the mineral components of this lode are described and interpreted in order of paragenesis as follows:

Pyrite.

Pyrite was the first phase to be deposited in this lode as isolated euhedral grains and anhedral aggregates enclosed by the pyrrhotite in the lode. The early deposition of pyrite is indicated by two textural features:

1. Its replacement by pyrrhotite, (Plate 36A).

2. Some of the isolated pyrite inclusions

PLATE 36.

A. Calcite (a) fills and replaces fractures in in the pyrrhotite (b). The calcite veinlet encloses aggregates of euhedral and subhedral pyrite grains (c) and small inclusions of chalcopyrite (d). The fractures within these aggregates are filled by pyrrhotite (arrowed) suggesting that they were inclusions in the pyrrhotite. Inclusion of pyrite aggregate in the pyrrhotite shows extensive alteration to marcasite (arrowed e). (P/S G3E.4, 9th level stope, (1st lift), Section 87/88/S^a). (Plane Polarized light).

B. Exsolution-free sphalerite veinlet (a) within the pyrrhotite vein is replaced along cleavages by siderite (b) producing a parallel banded texture. (P/S G3E.4, 9th level stope (1st lift), section 87/88/S^a). (Plane Polarized light).

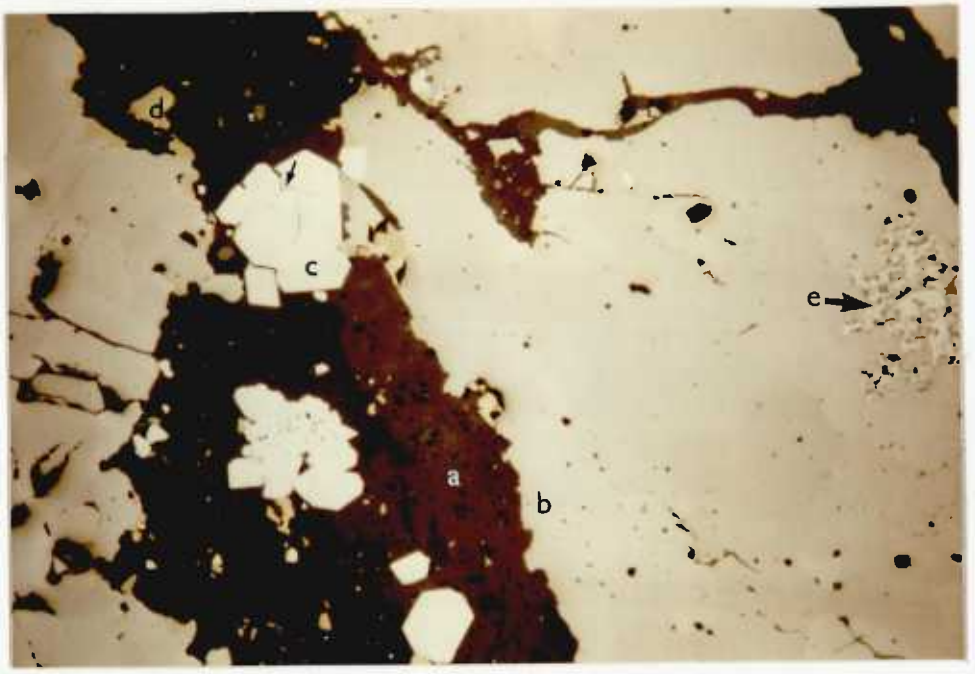

200μm

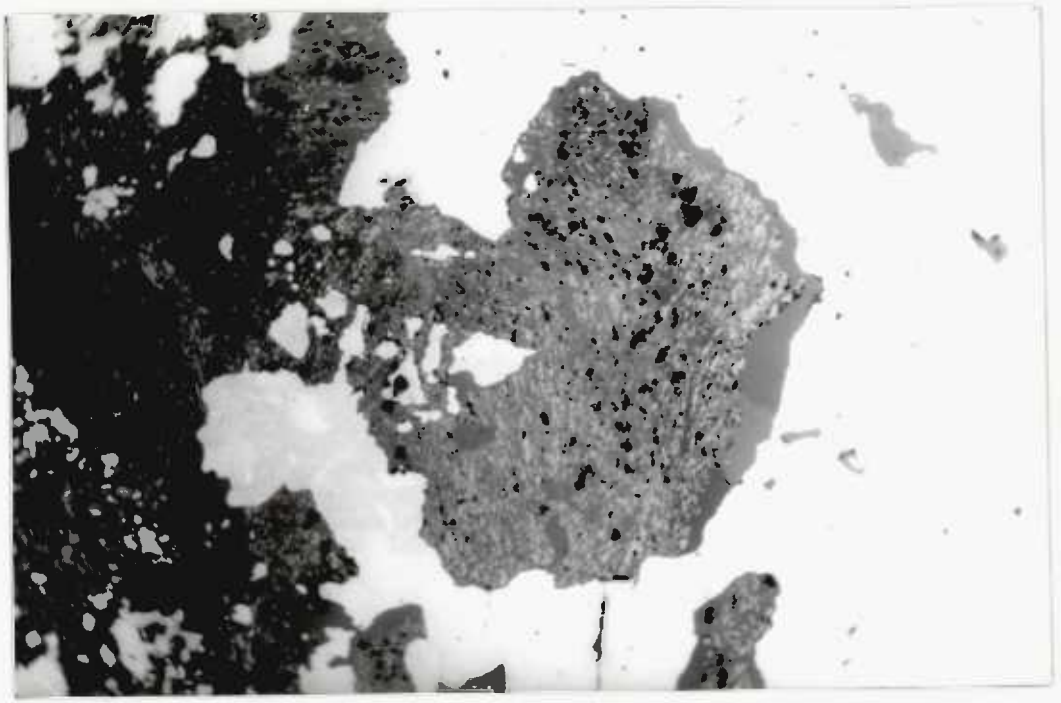

200μm

within the pyrrhotite were rimmed around by sphalerite.

Pyrrhotite.

Pyrrhotite is the major phase in this lode. It occurs in a massive form composing a mosaic of anhedral grains of variable dimensions, (Plate 36A). This phase followed the first pyrite generation as indicated by the replacement features, but it was cut by later pyrite veinlets. Lensoid slivers of later veinlets were incorporated into the pyrrhotite margins next to the pyrite veinlets and this is good evidence that there may have been a phase of disruption followed by annealment of the pyrrhotite grain fabric around the pyrite. The pyrrhotite contains inclusions of pyrite, sphalerite and chalcopyrite. The pyrite inclusions are incorporated phases while the other two are apparently replacement phases. The pyrrhotite vein was cut by a network formed by two sets of fractures roughly at 45° to each other. These fractures were easy channel-ways for sphalerite, chalcopyrite and siderite solutions. The latter has extensively replaced the pyrrhotite walls forming irregularly embayed margins.

Pyrite Veinlets.

Pyrite veinlets cut the pyrrhotite and they show

evidence of shearing and brecciation at their margins and within. The fractured and brecciated margins of the veinlets were infilled and cemented by pyrrhotite, probably by a process of ductile flow and annealment in the pyrrhotite grain fabric. Slivers of pyrite at the margins of pyrite veinlets were included in the pyrrhotite matrix by a process of shearing and annealment. Pyrite veinlets were replaced by exsolution-free sphalerite, chalcopyrite and siderite along cleavages and fractures and also at margins.

Sphalerite.

It is important to note that only the exsolution-free sphalerite is present in this lode and it succeeded the pyrite veinlets. It migrated into the pyrite veinlets along the contact between the veinlets and their pyrrhotite host to replace the veinlets along their cleavages and fractures, and also at margins. Where no pyrite is present, the sphalerite has probably completely replaced the pyrite. Sphalerite is also known to rim around and to replace marginally the pyrite inclusions in pyrrhotite. The filling of fractures in sphalerite by chalcopyrite and the presence of irregular chalcopyrite replacement inclusions in sphalerite are good evidence of the pre-chalcopyrite age. The sphalerite was, however, subject to replacement by siderite.

Chalcopyrite.

Chalcopyrite filled and replaced pyrite fractures. It has also replaced sphalerite as indicated by the presence of relict inclusions of chalcopyrite. Furthermore, it has replaced the pyrrhotite wallrock of the sphalerite-chalcopyrite-siderite composite veinlets. Chalcopyrite was, however, replaced by siderite as indicated by the presence of irregularly shaped inclusions of chalcopyrite in the siderite.

Siderite.

Siderite is abundant and it filled and replaced the fractures in the pyrrhotite vein as well as along the pre-existing veinlets of sulphides. The replacement occurred marginally, and along cleavages particularly in the case of pyrite and sphalerite. Siderite pseudomorphs after pyrite are characteristic, Sphalerite which has been replaced by siderite along one set of cleavages shows a parallel texture with alternating zones of siderite. The curved parallel texture, (Plate 36B), as seen in some sphalerites indicates that the sphalerite was selectively replaced while under stress. In the thicker siderite veinlets, relict inclusions of pyrite and chalcopyrite are present. In one place a siderite veinlet has developed into a radiating fan of acicular crystals.

4.1.4. The sphalerite-cassiterite lode of the Gakak.

North Lode System.

This approximately three feet wide sphalerite-cassiterite lode occurs adjacent to the barren white quartz vein complex as seen in the second level drive and the third level stope in sections S.W. from rise 65 and 64/65/I^a/J^d respectively. The mineralogy of this lode is summarised in the following list:-

Cassiterite

Pyrite
Pyrrhotite
Exsolution-bearing sphalerite
Exsolution-free sphalerite
Chalcopyrite
Galena

Quartz

Siderite.

The minera graphic relationships of the mineral components of this lode are described and interpreted in order of paragenesis as follows:

PLATE 37.

A. Anhedral grains of cassiterite are surrounded by chalcopyrite. The fractures in these cassiterites are also filled and subsequently replaced by chalcopyrite. (P/S GN.3b, 3rd level stope, section $64/65/I^{a}/j^{a}$). (Plane Polarized light).

B. Exsolution-bearing sphalerite showing coarse and fine twins. The exsolved chalcopyrite bodies (arrowed) are located along the intergranular boundaries and also occasionally along the twin planes. (P/S GN4, 3rd level, section $63/j^{a}$). (Plane Polarized light).

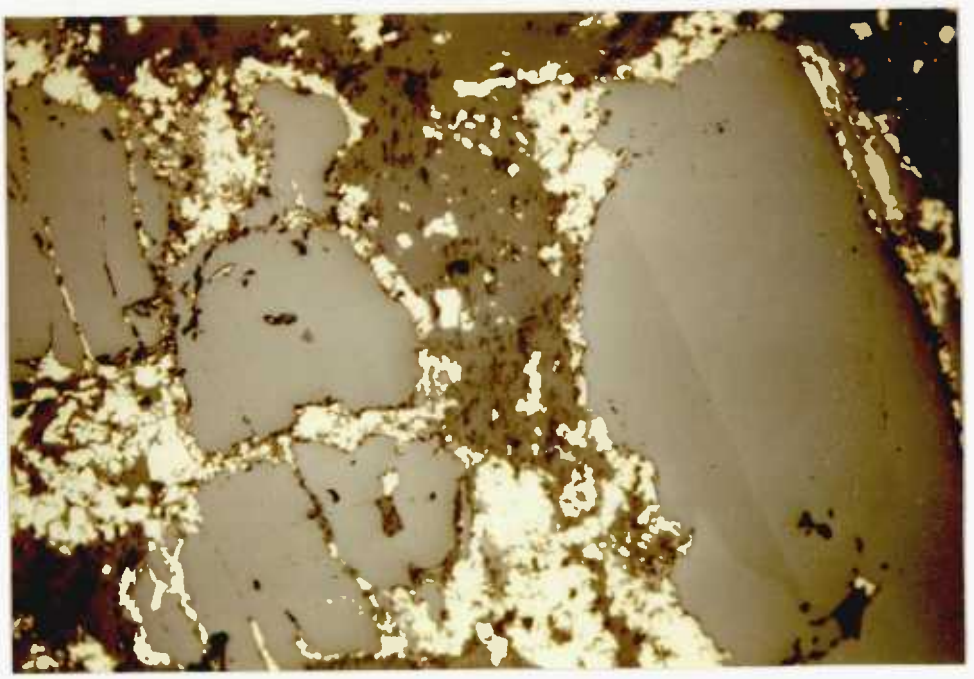

200μm

200μm

Cassiterite.

Cassiterite is present in this lode from the second level drive down to the third level stope, but it was not detected at the third level drive in Section 63/j^{a} or at the fourth level drive in Section 63/i^{a}.

Cassiterite occurs as bunchy granular aggregates in the silicate gangue as well as in the form of individual grains frequently with a partial or complete rim of sphalerite of the two varieties set in the chalcopyrite matrix. Occasionally large subhedral cassiterite grains in the wallrock silicates were rimmed and their fractures mineralised by aggregates of tiny chalcopyrite flakes, (see Plate 37A). Cassiterite grains are also set in large pyrite grains and also occur included in idiomorphic quartz.

Fractures commonly cut the cassiterites, particularly the aggregate masses and they invariably contain sulphides which have partially replaced the host cassiterite.

The fracture-filling sulphides observed are:

1. The exsolution-bearing sphalerite.

2. Pyrite and

3. Chalcopyrite.

Besides the replacement of cassiterite along fractures, marginal and internal replacements by these sulphides have also occurred as indicated by the presence of irregular inclusions of sphalerite and chalcopyrite in cassiterite. Quartz also replaced cassiterite at margins as suggested by an irregular contact between these two minerals.

Pyrite.

Cassiterite mineralisation was followed by early pyrite which occurs as aggregates of euhedral grains. These early pyrite aggregates were enclosed in a chalcopyrite-pyrrhotite-sphalerite matrix and they were replaced at grain margins and along fractures and cleavages by the components of the matrix. Interior replacement of pyrite by quartz, galena and sphalerites has produced a poikilitic fabric in the pyrite. Characteristic zonal replacement of pyrite euhedra by quartz has been observed only once in P/S GN3.C_2.

Pyrrhotite.

Pyrrhotite following early pyrite occurs as anhedral to subhedral mosaic aggregates and isolated grains in the chalcopyrite matrix. The irregular forms of the pyrrhotite inclusions locally suggest

replacement by the enclosing chalcopyrite matrix. One subhedral pyrrhotite inclusion was cut by chalcopyrite-bearing fractures and the chalcopyrite has replaced the pyrrhotite from fracture margins. The margins of some of these pyrrhotite inclusions are the locus for the nucleation of sphalerite which has subsequently included a few pyrrhotite grains. Early pyrite aggregates were occasionally replaced along the cleavages by pyrrhotite.

Sphalerite.

The usual varieties of sphalerite are present cogenetically in this lode as veins, and also as large and small irregular shaped inclusions set in the chalcopyrite and the wallrock silicate gangues. The exsolution-bearing sphalerite contains largely chalcopyrite and minor galena and contains lesser amounts of pyrrhotite as inclusions; the inclusions were observed to occur in linear trains in which the chalcopyrite alternates with galena and pyrrhotite. Pyrite and arsenopyrite are rare as inclusions and are only present in P/S GN3.C and GN3.a, the two sphalerites show a distinct set of twin lamellae parallel to (111) and (211) and the width of these lamellae is variable; the exsolution-bearing sphalerite exsolved its chalcopyrite exsolution droplets and stringers along the boundaries of the twin lamellae, (Plate 37B), whereas in the other variety of sphalerite

the chalcopyrite droplets, (probably exsolved phases), are distributed along the intergranular boundaries and only occasionally along the boundaries of the twin lamellae, (Plate 37B). The difference here may be a reflection of a differential stress pattern acting on the sphalerite. The possible causes which have led to the formation of these cogenetic exsolution-bearing and exsolution-free sphalerites are believed to be:

1. Differential tectonic stress and

2. Major element chemistry, (e.g. Cu, Fe and Sn).

The action of the former in the presence of appropriate amounts of Fe and Cu in sphalerite are known to initiate the exsolution process, (Moh, 1974).

The sphalerites occur as veins as well as irregular grains of various dimensions set in matrices of wallrock silicate gangue,chalcopyrite and quartz. The vein sphalerite has enclosed inclusions of wallrock silicate gangue very often replaced by the early pyrite and quartz and it was cut by late pyrite veinlets with the result that angular fragments of sphalerite were incorporated in the veinlets. The pyrite veinlets have also replaced the sphalerite at the walls of the fractures. The irregular grains of sphalerite set in the chalcopyrite matrix suffered

PLATE 38.

A pyrite veinlet cutting through the exsolution-bearing sphalerite and pre-sphalerite pyrite aggregate (arrowed), (P/S GN.4b, 3rd level section $63/j^{a}$). (Plane Polarized light).

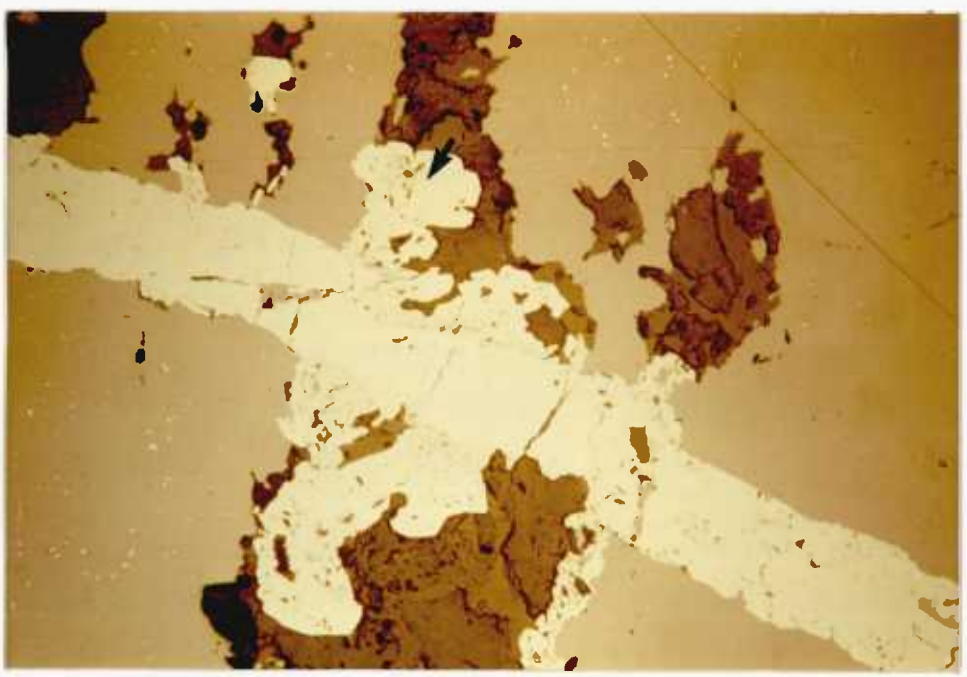

200μm

replacement by chalcopyrite at their margins, within the grain interior and also along fractures; they were also similarly replaced by galena. In contrast, the sphalerites have replaced the early pyrite at margins and along cleavages.

Pyrite (2).

The late pyrite occurs only as veinlets cutting the sphalerite, (Plate 38). These veinlets have, in places, branched into much thinner parallel and subparallel veinlets. At places along the thicker veinlets fragments of sphalerite can be seen to be incorporated within the pyrite. At one place as observed in P/S GN4.b the early pyrite aggregate was cut by a late pyrite veinlet, (Plate 38).

The late pyrite veinlets from P/S GN4.a and b locally replaced by marcasite. In some cases this replacement was complete thus giving an impression of marcasite veinlets cutting the host sphalerite. The incontestably observed replacement of pyrite by marcasite is indeed rare and it is also thermodynamically a complete contradiction, (Ramdohr, pg. 830; pg. 170, 1969).

Chalcopyrite.

Chalcopyrite is not ubiquitous throughout this

lode; chalcopyrite occurs in minor amounts as tiny inclusions in cassiterite and quartz from the sphalerite rich portions of this lode. These could be interpreted as a replacement and enclosed phase respectively. In contrast, chalcopyrite is the major phase when sphalerite occurs as a minor constituent of the lode. This relationship is well-illustrated by ore samples collected from a Third Level Stope in Section $64/65/I^{a}/j^{a}$. Thus there appears to be an antipathetic relationship between the abundance of sphalerite and chalcopyrite in this lode.
Chalcopyrite as a major phase occurs as massive veins and disseminated anhedral flakes in wallrock silicate gangue and also as tiny aggregates rimming large and small subhedral cassiterite grains in the wallrock silicate gangue. These grains also have their fractures mineralised by chalcopyrite, (Plate 37A). Chalcopyrite veins have enclosed inclusions of cassiterite, sphalerite, idiomorphic pyrite, pyrrhotite and idiomorphic quartz. All except the quartz inclusions are pre-chalcopyrite in age as indicated by marginal replacement features and the infilling of fractures of these inclusions by the enclosing chalcopyrite. The idiomorphic quartz is post-chalcopyrite and this is confirmed by the presence of inclusions of chalcopyrite, cassiterite, pyrite and sphalerite in the quartz. Idiomorphic quartzs replaced the chalcopyrite in preference to pyrite and sphalerite. The presence of stannite occurring in

PLATE 39.

A. A subhedral inclusion of cassiterite, (a), within the chalcopyrite matrix is partially surrounded by irregular shaped inclusions of stannite, (b). The chalcopyrite matrix also consists of inclusions of exsolution (chalcopyrite)-bearing sphalerite, (c), (P/S GN.3b, 3rd level Stope, Section $64/65/I^a/J^a$). (Plane Polarized light).

B. High magnification view of the irregularly shaped inclusion of stannite in chalcopyrite showing twin lamellae, (arrowed), (P/S GN.3b, 3rd level Stope, Section $64/65/I^a/J^a$). (Crossed Polar).

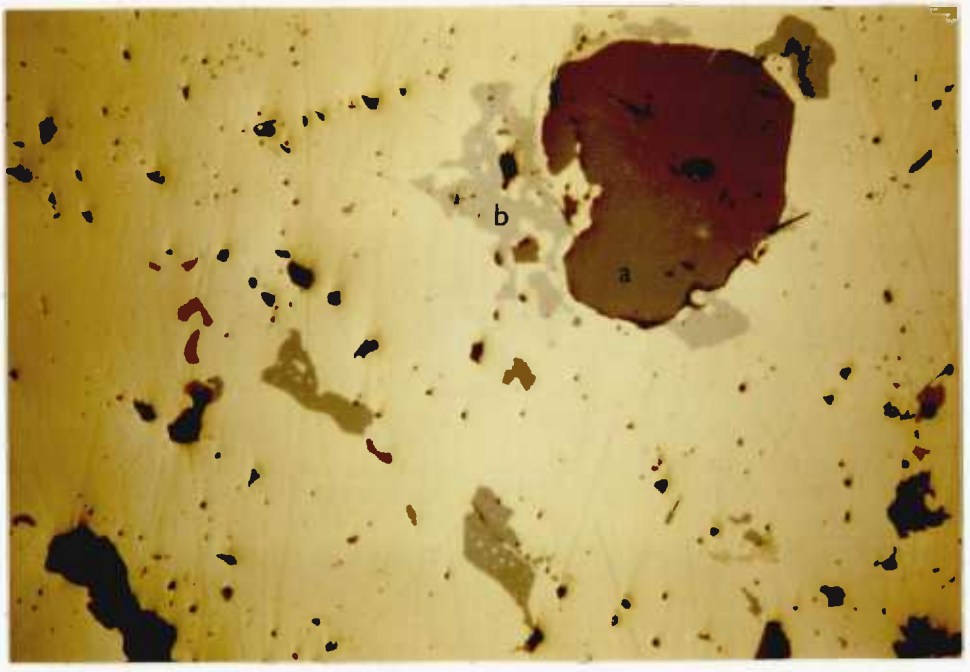

200μm

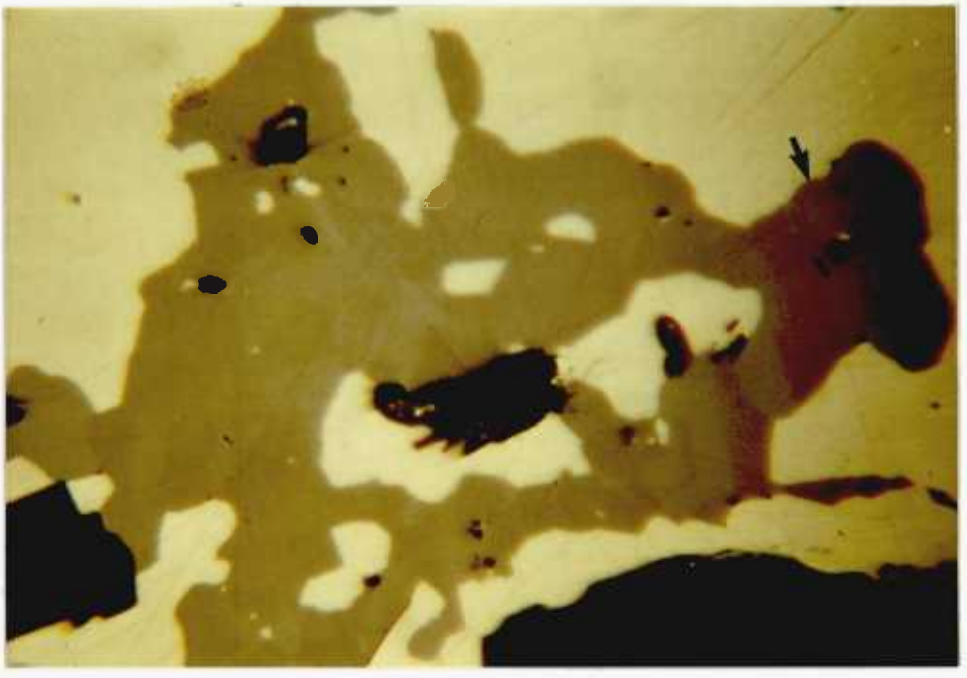

50μm

irregular form surrounding isolated cassiterite inclusions, (Plate 39A), and showing coarse twinning, (Plate 39B), in a chalcopyrite vein seen in P/S GN3.b suggests that the stannite is probably the product of a chemical reaction between the cassiterite and chalcopyrite during which Sn was released to combine with the Fe, Cu and S from the chalcopyrite to form stannite, (Cu_2, Sn, Fe, S_4). Thus stannite was formed contemporaneously with chalcopyrite. Chalcopyrite in P/S GN3.c, and c_2 is unique in that exsolved sphalerite stars and globules are distributed in orientated fashion,

Galena.

Galena was the last sulphide phase to be deposited in this lode and it is present only in P/S GN3.c and c_2. Galena occurs as shred-like intergrowths, (Plate 40), randomly distributed in the chlorite-silicate gangue of the wallrock and it has also replaced early pyrite, sphalerite and chalcopyrite at grain margins, and interiors, and along cleavages. In the case of pyrite, poikilitic intergrowths of galena in pyrite grains are abundant and they are commonly present together with quartz poikilitic intergrowths. Galena has replaced chalcopyrite in the form of irregular inclusions. Galena was, however, enclosed and subsequently replaced at margins by quartz.

PLATE 40.

Galena occurs in irregular and shredded forms. The latter form is common in the silicate gangue matrix. On the upper right hand corner the galena replaces into sphalerite (a) and chalcopyrite (arrowed b). (P/S GN.3C, 3rd level stope, section $64/65/I^{a}/J^{a}$). (Plane Polarized light).

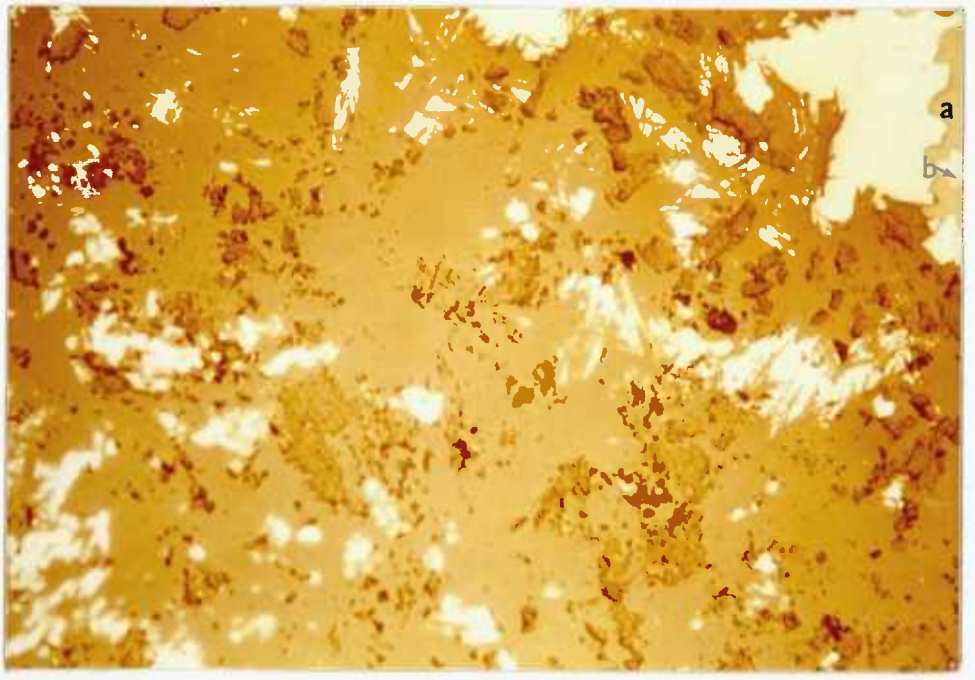

200μm

Quartz.

Quartz is a major gangue oxide in this lode and it is predominantly present as veinlets enclosing and replacing early pyrite, the sphalerites and galena. Zonal and marginal replacements of early aggregates of idiomorphic pyrite grains by quartz are present. Idiomorphic quartz is present within the chalcopyrite matrix and they may have formed by replacement of the chalcopyrite host, but sphalerite inclusions were not similarly affected. Quartz is also found mineralising the pockets of wallrock within the sphalerite vein.

The presence of relict sphalerite inclusions in quartz, together with the fact that the quartz veinlets cut across the post-sphalerite pyrite veinlets, as can be seen in P/S GN4.b, all points to a post-sulphide relative age for the mineralisation by quartz.

Siderite.

Siderite is present only in P/S GN3.c_1 and c_2 and it occurs as irregular patches having replaced the chalcopyrite matrix and its enclosed anhedral early pyrite masses, and sphalerite.

4.2. General Conclusions.

The mineralogy of the sulphide ± cassiterite lodes described above is generally similar with the consistent presence of pyrite, exsolution-bearing sphalerite, exsolution-free sphalerite, chalcopyrite, pyrrhotite and siderite. Although both the exsolution-bearing sphalerite and exsolution-free sphalerite are present in the lodes described, the latter appears to be more abundant than the exsolution-bearing variety as observed in the sphalerite-cassiterite lode of the Gakak North Lode System. Cassiterite when detected occurs only in minor amounts and, therefore, it is of no economic interest. Pyrite always show a tendency to form idiomorphic margins. Siderite is a common carbonate mineral and it fills and replaces fractures developed in the pre-siderite mineral phases. It also encloses and replaces earlier mineral grains at margins and in the interior forming poikilitic inclusions.

Pyrite and cassiterite have preserved their cataclastic texture whereas pyrrhotite, chalcopyrite and sphalerite have evidently undergone recrystallization and annealment after deformation. Because of their ductile mechanical properties they do not show obvious cataclastic textures.

Chapter 5.

The martitised magnetite-fluorite skarn and the hydrothermal tin deposit within the hornfels of the Waterfall Mine at Pelapah Kanan.

5.1. Location.

The martitised magnetite skarn and the associated hydrothermal tin deposit of the Waterfall Mine Limited are located ten miles north of Kota Tinggi town in Southeast Central Johore at co-ordinates $1^{o}51'$ north and 103^{o} 15' East, (Figure 2).

5.1.1. The Geology of the Fe-and Sn-mineralisation.

The martitised magnetite skarn and the underlying associated tin deposit were emplaced in shales and pyroxene-and-biotite- (sericite-quartz-chlorite) hornfels respectively at the immediate contact zone of an Upper Carboniferous fine grained porphyritic granodiorite. This porphyritic grandiorite rock is composed of phenocrysts of plagioclase; orthoclase, (minor amount); quartz and biotite set in an equigranular groundmass of quartz, plagioclase laths and minor amounts of biotite and orthoclase. accessory magnetite grains are also present in the

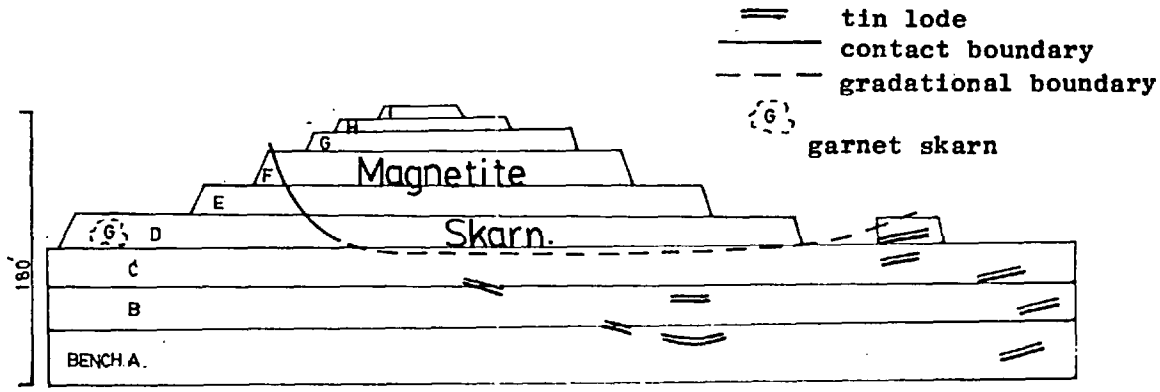

Figure 13. A cross section of the magnetite skarn and its underlying tin deposit at the Waterfall Mine in Pelapah Kanan.

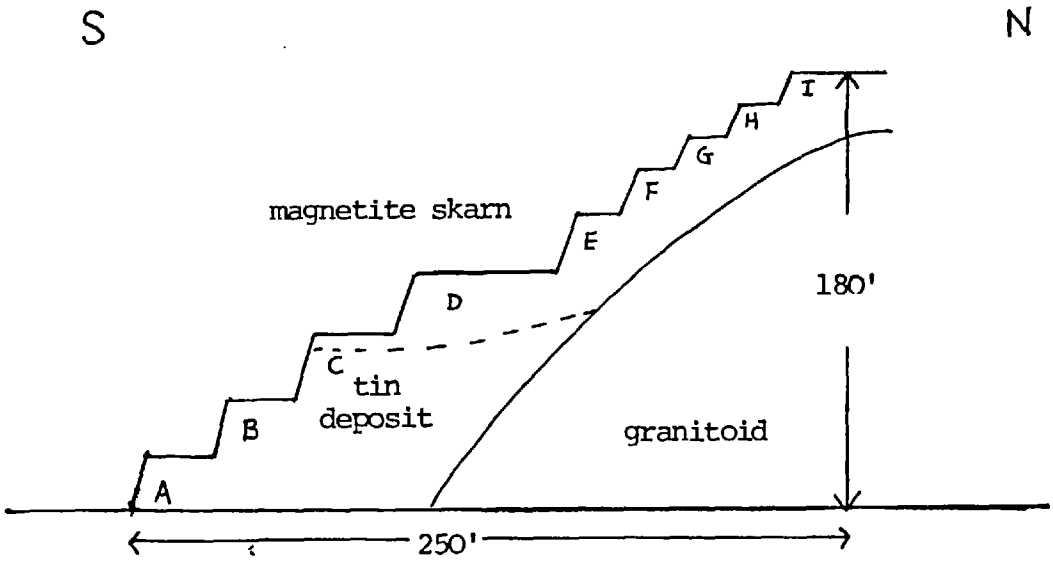

North South Section of the Fe-and Sn-deposits of the Waterfall Mine at Pelapah Kanan.

PLATE 41.

A. A chicken-wire mesh like network of magnetite veins in the top portions of the magnetite skarn ore body, (Bench F, Waterfall Mine, Pelapah Kanan).

B. Massive stratiform magnetite skarn at the bottom portions of the magnetite skarn ore body. (Bench D, Waterfall Mine, Pelapah Kanan).

groundmass. The plagioclase phenocrysts are replaced by quartz at margins and in the interior. They have also been partially sericitised. The green-brown biotite phenocrysts are unaltered. The amount of plagioclase present is greater than 2/3 that of the total feldspar content. On this basis this rock can be classified as a granodiorite according to the classification scheme of Hatch, Wells and Wells, (1975).

The host rocks of this complex ore body formed an open syncline with a shallow southward plunge. This is shown up distinctly by the convergent dips of the sedimentary bedding planes, (about 30^{o}). The feldspar-quartz-fluorite-cassiterite-löllingite veins were emplaced in a sequence of dilatant fractures formed along bedding planes and these also trace distinctly the synclinal structure, (Fig. 13). This synclinal structure has also previously been recognised by Burton, (1959); Garnett, (1966) and Bean, (1969 p. 93).

The emplacement and geometry of the magnetite mineralisation were controlled by the lithology and structures respectively of the metasedimentary host rocks. Thus the magnetite mineralisation varies from a massive-stratiform style, (Plate 41B), at the bottom of the ore body to a chicken-wire mesh stockwork of coarse-grained magnetite veinlets, (Plate 41A), towards the top. The development of this network of veinlets may have been due to the hydraulic fracturing of the

host rock when the fluid pressure of the mineralised fluids exceeded the confining pressure, (σ_3), and the tensile strength, (T), of the host rock, (Fyfe, Price and Thompson, 1978), during the initial hydrothermal history of the wallrocks. Garnett, (1966), suggested that the magnetite skarn was formed by the remobilisation and reconcentration of the iron from the host which he assumed to be ferrigenous. However, Hosking, (1973b pp. 350), believed that the source of the iron lay in the granitic intrusive. Some consideration of the cycle of heating and cooling in relationship to the stages of hydrothermal activity lead to the inferrence that the iron necessary to create the metasomatic magnetite body could be more easily provided by the primary hydrothermal residue from the crystallizing granodiorite.

As in other iron skarn ore bodies in Western Malaysia, this magnetite ore body was strongly martitised in the near surface sections by deep tropical weathering to form a haematitic capping.

Roe, (1941) and Burton, (1959) both considered that the hornfelses were developed by contact thermal metamorphism of a mixed sequence of calcareous shales, siltstones and mudstones, and their mineralogy varies accordingly from place to place.

Burton, (1959), has recognised the following

PLATE 42.

A. A quartz-pyroxene hornfels of the Waterfall Mine at Pelapah Kanan showing the intergrowth of pyroxene crystals, (a) and quartz, (b), together with disseminated cassiterite grains, (c). Plane polarized light.

B. A predominantly quartz rich part of the same sample of quartz-pyroxene fornfels as above, showing the presence of disseminated cassiterite grains/aggregates of various sizes, (Plane Polarized light).

C. This photomicrograph also shows the same features as Plate 42B, (Plane Polarized light).

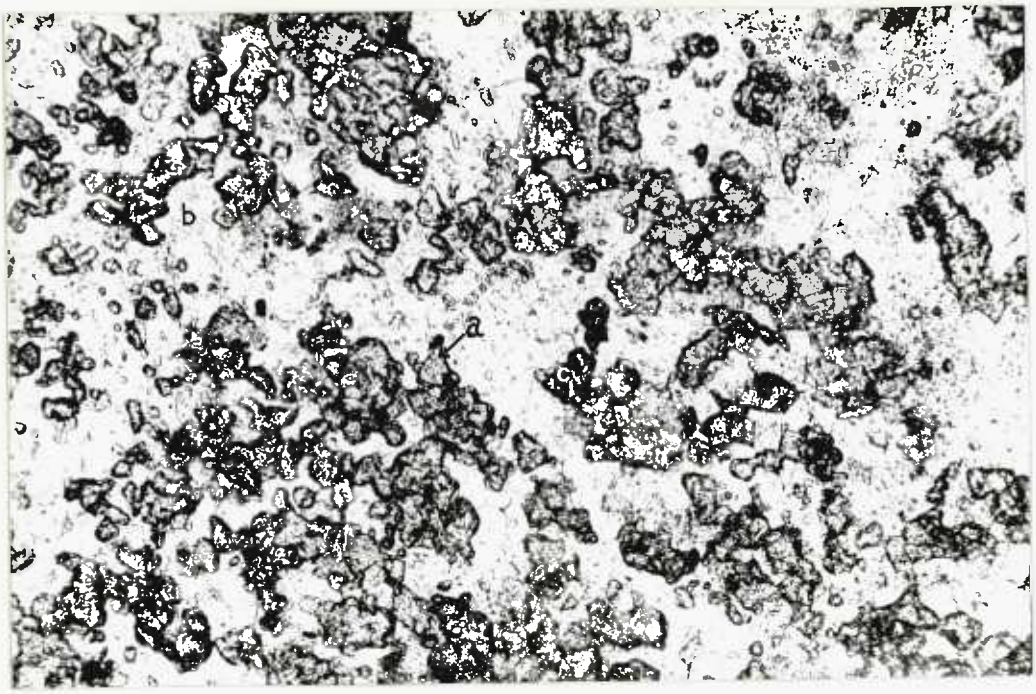
b
a
100μm

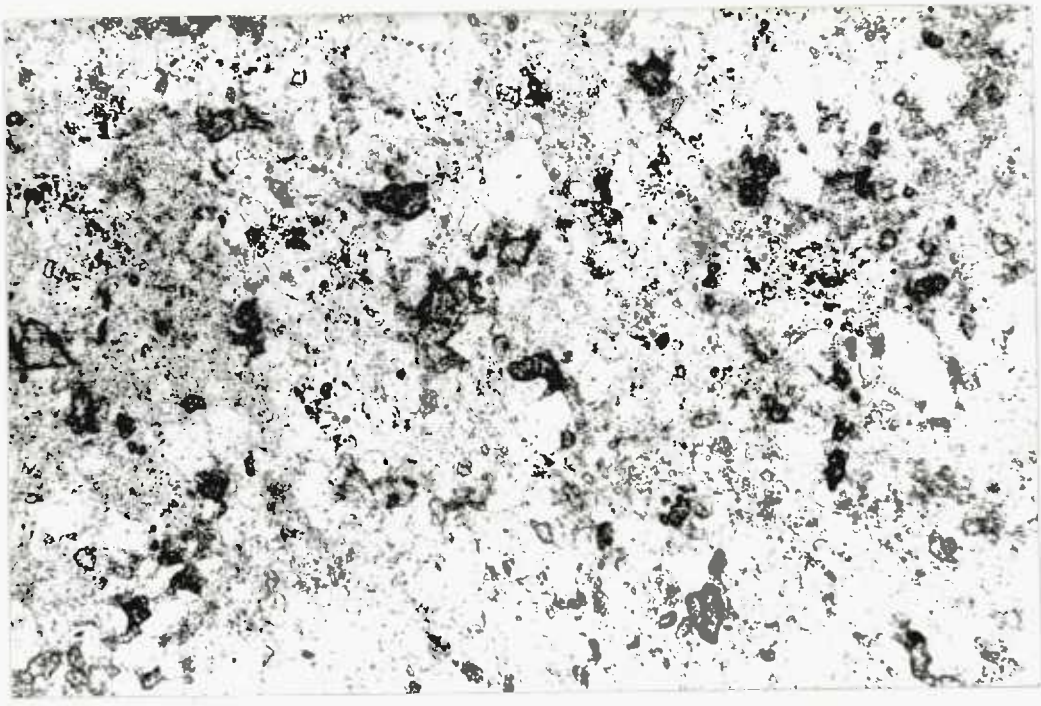
100μm

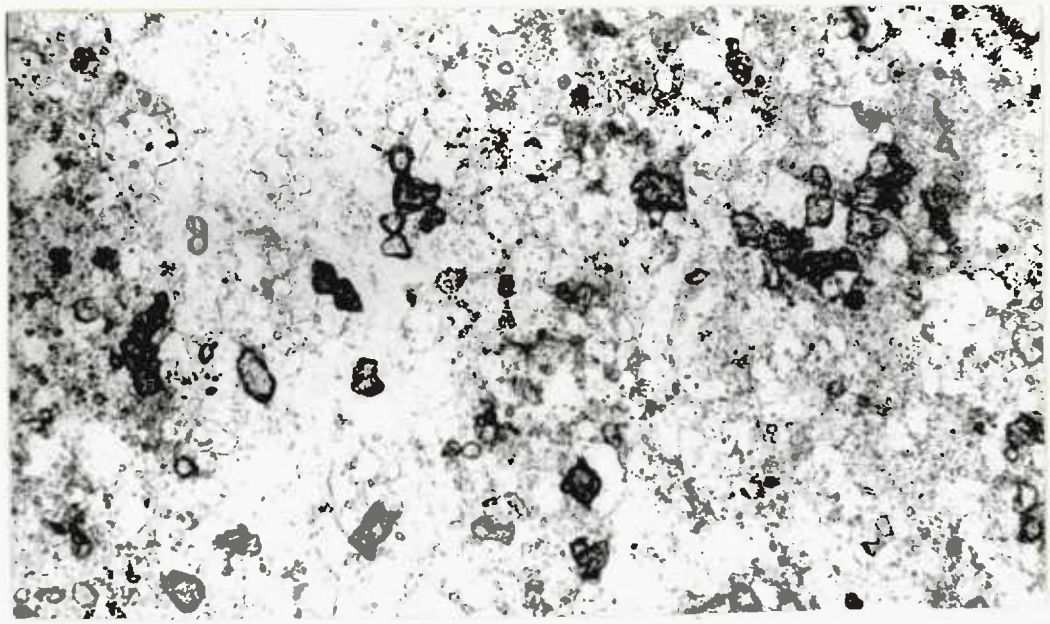
100μm

mineral assemblages within the hornfelses: quartz-epidote-sericite, quartz-diopside-epidote-sphene, and quartz-diopside. The author has recognised mineral assemblages such as quartz-hedenbergite, (Plate 42A), quartz-biotite-sericite, and quartz-chlorite. The quartz-chlorite assemblage with relict biotites is usually found in a narrow zone, (about 2 mm), immediately next to feldspar-quartz-flourite-cassiterite veins and it gradually grades into a quartz-biotite hornfels. These chlorites are products of hydrothermal metamorphism of biotites. However, quartz-chlorite hornfels assemblages are also known to develop away from hydrothermal veins. Ganesan, (1969), has noted a "metasomatised porphyroblastic cordierite rock" immediately overlying the granite of the hill. The great variety of mineral assemblages recognised in the hornfels suggests that the pre-hornfelsed rocks were of variable chemistry from place to place.

The development of these hornfelses was accompanied by a metasomatic introduction of tin rich fluids which has led to the formation of fine-grained disseminations of a distinctly pleochroic reddish brown/neutral coloured cassiterite in the respective hornfelses, (Plates 42B&C). The presence of these cassiterites in the pyroxene hornfelses, collected from the north of the mineralised hill where vein mineralisation is totally absent suggests that they

PLATE 43.

A. A large loose block of garnet-hornblende (arrowed) skarn showing the development of the skarn mineralisation following the primary lithology during phases of metasomatic hydrothermal replacement. Note the replacement of the skarn by calcite, (white mineral), (Bench D, Waterfall Mine, Pelapah Kanan).

B. Euhedral poikiloblasts of garnet set in a decussate matrix of interlocking hornblende laths. These garnet crystals show birefrigence and they contain abundant poikilitic intergrowths of quartz, (arrowed a), brown biotite, (arrowed b) and green chlorite, (Bench D, Waterfall Mine, Pelapah Kanan), (Crossed Polars).

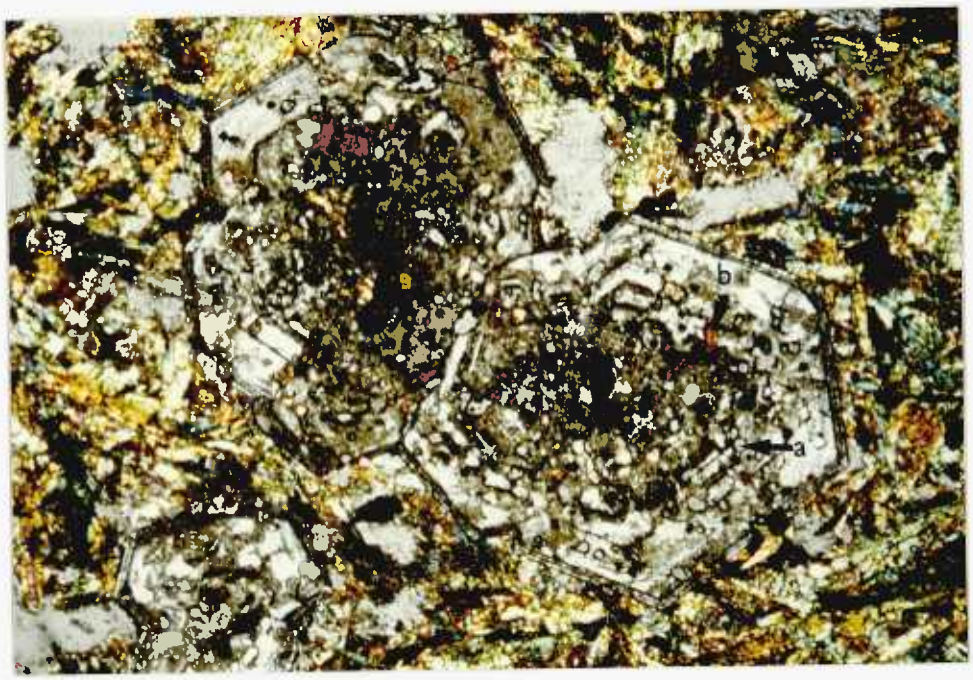

5X

PLATE 44.

A. Euhedral and subhedral poikiloblastic garnet crystals set in a decussate matrix of interlocking laths of hornblende, (Bench D, Waterfall Mine, Pelapah Kanan), (Plane Polarized light).

B. Hornblende-free aggregate of birefringent garnet crystals shows their fractures filled and replaced by quartz (a) and calcite (b). The latter also replaces the garnets along the growth zones, (arrowed), (Bench D, Waterfall Mine, Palapah Kanan) (Crossed Polars).

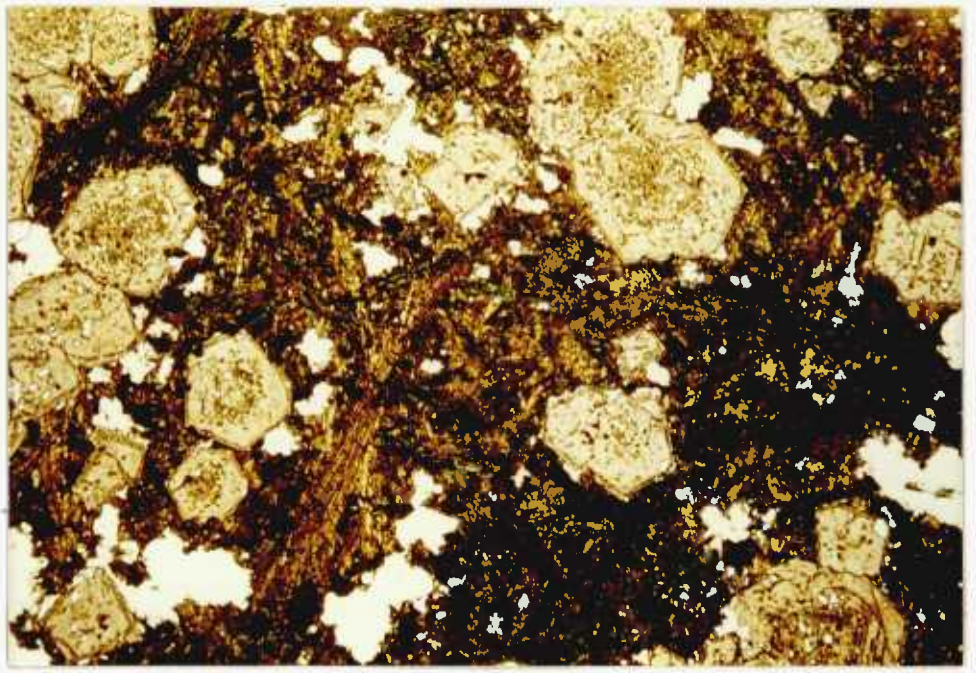

1.5X

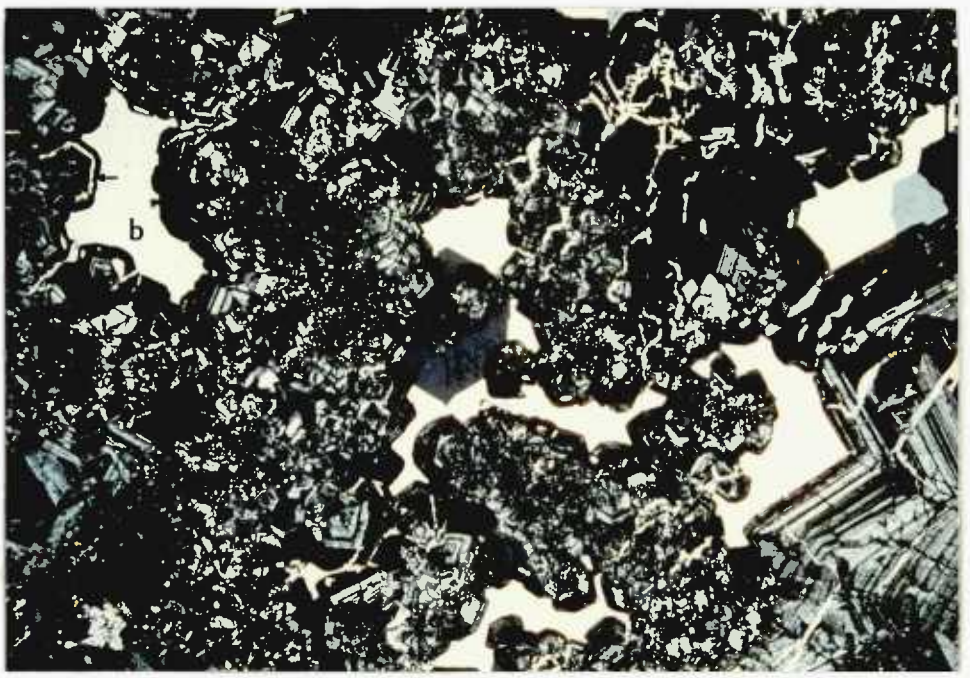

4X

were emplaced in a hydrothermal event predated and independent from the vein mineralisation. An efficient mineral processing technique would be necessary to recover most of this cassiterite, but, nevertheless, the disseminated tin mineralisation has an unknown future potential for mining.

The development of these hornfels was also accompanied by the formation of a localised minor silicate facies of the skarn. This consists of birefringent andradite garnets and hornblende with minor quartz and calcite. This garnet hornblende rock is located on the western limb of the open syncline where it is overlain by the magnetite skarn ore body, (Fig.13). The development of this garnet-hornblende skarn followed the primary lithology during the phases of metasomatic hydrothermal replacement, (Plate 43A). A thin section petrographic study of this skarn showed it to be largely composed of aggregates of euhedral birefrigent poikilitic garnet crystals, (Plate 43B), rich in quartz, brown biotite and green chlorite inclusions, (Plate 43B), the garnets are locally set in a decussate matrix of interlocking hornblende laths, (Plate 44A), with quartz veinlets penetrating and replacing the garnet grains where these are transected, (Plate 44B). Calcite has also filled and replaced the garnet aggregates along later fractures. Furthermore calcite has also partly selectively replaced the garnet crystals along the growth zones, (Plate 44B).

PLATE 45.

A. A feldspar-quartz-fluorite-cassiterite vein in pyroxene hornfels is emplaced parallel to bedding planes. Feldspar (a); quartz (b); cassiterite (c). Note that the quartz replaces into the white K-feldspar of the vein, (indicated by arrow). (Bench C, Waterfall Mine, Pelapah Kanan).

B. The contact between the bottom of the magnetite skarn ore body and the mineralised pyroxene hornfels is marked by a persistent quartz vein, (arrowed). Note the feldspar vein branches out into thinner veins and veinlets. (Bench C, Waterfall Mine, Pelapah Kanan).


a
b
c

PLATE 46.

A. The contact between the magnetite skarn and mineralised pyroxene hornfels is marked by a quartz vein, (arrowed). The skarn is cut by quartz veins. The feldspar vein in the hornfels branches out to form thinner veins and veinlets and in places it is intensely stained by haematite, (Bench C, Waterfall Mine, Pelapah Kanan).

B. A sequence of parallel and subparallel gently dipping, (about 30°), mineralised veins are emplaced along the dilated bedding planes of the pyroxene hornfelses, (Bench B, Waterfall Mine, Pelapah Kanan).

The gently undulating bedding planes in the hornfels were hydraulically opened by an overpressure of the mineralising fluid. The dilatant fractures created were mineralised in a symmetrical fashion by vein minerals commonly with löllingite and K-feldspar, (both the pink and white varieties), occupying the outer zones of veins while the cassiterite, fluorite and quartz phases occupy the central zones, (Plate 45A). The adjacent wallrocks of these fractures have created, in places, oblique extension fractures and branching of the veins is a common feature, (Plate 45B). The veins, (e.g. feldspar-quartz-fluorite and quartz-cassiterite), are seen cutting banded magnetite skarn, ('wrigglite'), (Askin, 1975), (Plate 50A), and along the boundary between the magnetite ore body and the mineralised hornfelses, (Plate 46A), and also across massive magnetite. The detailed paragenetic succession of these veins is discussed later in Section 5.4.. The width of these veins varies from 1 cm to as much as 8 cms. The veins on both limbs of the syncline dip gently between 20° to 30° towards the axis, (Plate 46B), and those in the axial region of the gentle syncline were almost horizontal, (Plate 47A). Thus the attitude of these veins is concordant with the bedding of the shallow syncline. However, the intensity of the vein mineralisation was uneven with an overwhelming concentration of veins east of the axis of the syncline reflecting the inequalities of stresses affecting the syncline during access of the mineralising fluid.

PLATE 47.

A. A reverse fault displaces a horizontally emplaced feldspar-quartz vein at the axis of an opened syncline. Faulting must have occurred along one of the joints of the hornfelses since the fault plane, (mineralised by quartz), is orientated parallel to the joints, (arrowed). (Bench A, Waterfall Mine, Pelapah Kanan).

B. A ramifying network of quartz veins and veinlets in a highly weathered granitoid, (Waterfall Mine, Pelapah Kanan).

The main phase of vein mineralisation was followed by a minor phase of reverse faulting which is evident at the axis of the shallow syncline where the veins an and bedding are lying horizontally. The fault strikes northeast-southwest and it has truncated and subsequently displaced a feldspar-quartz-fluorite-cassiterite vein by twenty-six centimetres, (Plate 47A). It dips strongly towards a west-northwest direction. The fault was mineralised by a barren quartz vein of five centimetres thick which has a temperature of formation between 70^{o}c and room temperature as indicated by the presence of monophase liquid inclusions in the respective vein quartz.

The subjacent highly weathered intrusive, (Plate 47B), is assumed to be originally a biotite-bearing porphyritic granodiorite similar to that at the nearby waterfall. Judging from the high temperature homogenisation temperatures given by the cassiterites and the presence of pyroxene hornfels it can be concluded that the intensely weathered rock subjacent to the magnetite skarn is a deeply weathered granitic intrusive.

All the geological evidence observed suggests that both the massive skarn-like magnetite body and the cassiterite-bearing vein mineralisation originated from hydrothermal fluids genetically connected with the porphyritic granodiorite. In all probability

PLATE 48.

Concentric step-like growth surfaces of a large crystal of magnetite, (Bench G, Waterfall Mine, Pelapah Kanan).


3 cm.

the intense metasomatic activity leading to the formation of the magnetite skarn took place during the peak of the thermal cycle, (Heating-Cooling), of the aureole rocks while the tin-bearing veins were formed subsequently in the early stages of the cooling history. The high $Th^{o}c$ value of the vein minerals, in particular cassiterite, and the relatively high salinity of the inclusion fluids together with the presence of feldspar as a major gangue species suggest that the porphyritic granodiorite was the source of the mineralising hydrothermal fluids.

5.2. Magnetite Ore Body.

A. Upper Martite Capping.

A.1. Mineral Textures and Martitisation.

The massive well formed magnetite crystals, (Plate 48), from the top parts of the magnetite skarn ore body were intensely martitised and consequently this has led to the formation of a martite cap over the ore body. Since martitisation was largely confined to the top parts of the ore body, it can be concluded that the case of alteration was a supergene process which was initiated by the tropical climatic conditions. However, it is important to realise that martitisation can also be a hypogene process, (Ramdohr, 1969).

PLATE 49.

A. Martitisation in the magnetite is concentrated in areas cut by fractures (arrowed) while it is absent in unfractured areas, (the centre of this photograph). (Plane Polarized light).

B. Martitisation of the magnetite occurs along and also extends from both the intergranular boundaries, (arrowed a), and fractures, (arrowed b), into the octahedral planes producing a triangular pattern of mutual intergrowth of martite lamellae, (c). The variation in the thickness of the martite lamellae suggests differences in the extent of martitisation in different octahedral planes. (Plane Polarized light).

C. The partially martitised magnetite was also altered to goethite along fractures,(arrowed a), and at margins, (arrow b). The supergene goethite forms non-banded veinlets cutting across the aggregate of magnetite grains. (Plane Polarized light).

200μm

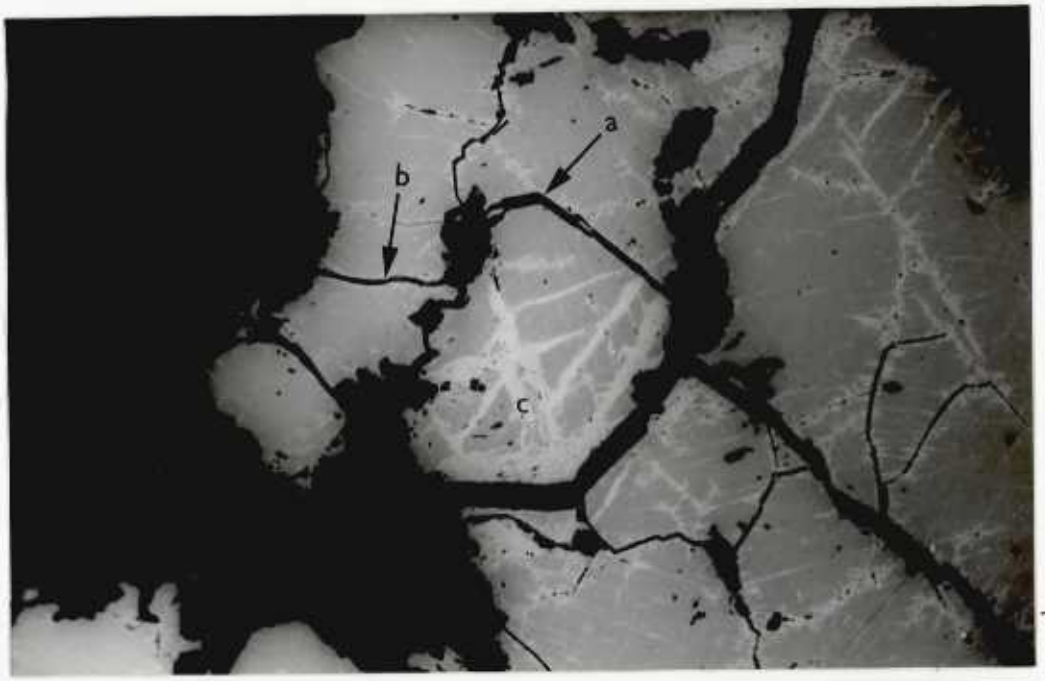

200μm

200μm

Alternatively the undulatory banding of the magnetite rock could also be produced by diffusion of iron-rich mineralising hydrothermal fluids into the host lithology.

Martitisation of magnetite was almost complete except for sparse relicts in these grains free of fractures or holes, (Plate 49A). Martitisation is usually initiated from fractures, holes and intergranular boundaries and then extends into the octahedral planes of the magnetite host with the result that the martite lamellae display a triangular pattern of mutual intergrowth, (Plate 49B).

The magnetite was also altered to goethite along fractures and margins, (Plate 49C). This goethite as veinlets, (largely non-banded), in fractures and as marginal rims is common in martitised magnetite.

B. Lower banded magnetite-fluorite-löllingite 'Wrigglite' rock.

B.1. Mineral textures and paragenesis.

This banded magnetite-fluorite-löllingite rock is typical of ore samples from the lower portion of the magnetite skarn ore body. The folded banding of this rock, (Plate 50A), gives it a similar look as the magnetite 'wrigglite' rock from Herberton, Queensland in Australia, which has been described by Askins, (1975). The magnetite bands of the 'wrigglite' were produced by hydrothermal metasomatic replacement of the original folded beddings by Fe-bearing metasomatic fluids. Such 'wrigglite' rock has also been discovered in Northwest

PLATE 50.

A. Banded magnetite-fluorite 'wrigglite', (arrowed), cut by quartz and fluorite-bearing veins.

B. Fluorite-bearing magnetite 'wrigglite' showing its banded texture. This texture is more conspicious in the field when the zones between the magnetite bands are infiltrated by K-feldspar, (arrowed), which must have originated from the neighbouring kaolinised K-feldspar vein, (Bench C, Waterfall Mine, Pelapah Kanan).


3 cm

Tasmania and at Lost River in Alaska, (quoted in Taylor, 1978). It is worth noting that the löllingite-fluorite-bearing 'wrigglite' magnetite at the Waterfall Mine of Pelapah Kanan is the first of its kind to be described from Western Malaysia.

The mineral fabric of this banded rock is composed of magnetite and fluorite intergrowth with accessory intergrown sphalerite, chalcopyrite, cassiterite, löllingite, quartz, K-feldspar, chlorite, siderite and supergene chalcocite and covellite. The fine banding is due to partial segregation between fluorite and magnetite. Löllingite is the most abundant sulphide phase and it is exclusively confined to the lower portions of the magnetite skarn ore body. This apparent zonation is considered likely to be due to the infiltration into the lower portions of the magnetite skarn by As-rich fluids which are believed to be parts of the mineralising fluids of the later cassiterite vein stage.

This banded magnetite rock when cut by a large feldspar-quartz vein was seen in the field to be infiltrated by feldspar along the zones folded bedding planes, (Plate 5OB).

Magnetite.

Magnetite is the ore-mineral in this rock and it

PLATE 51.

A. Cassiterite (a) and quartz (b) mineralise the porous fabric of martitised magnetite and silicates, (Bench D, Waterfall Mine, Pelapah Kanan). (Plane Polarized light).

B. Magnetite occurs as tiny grains arranged in a mesh of veinlets with a chicken-wire appearance in the silicate matrix; it also occurs around the margins of quartz (arrowed), (Bench C, Waterfall Mine, Pelapah Kanan). (Plane Polarized light).

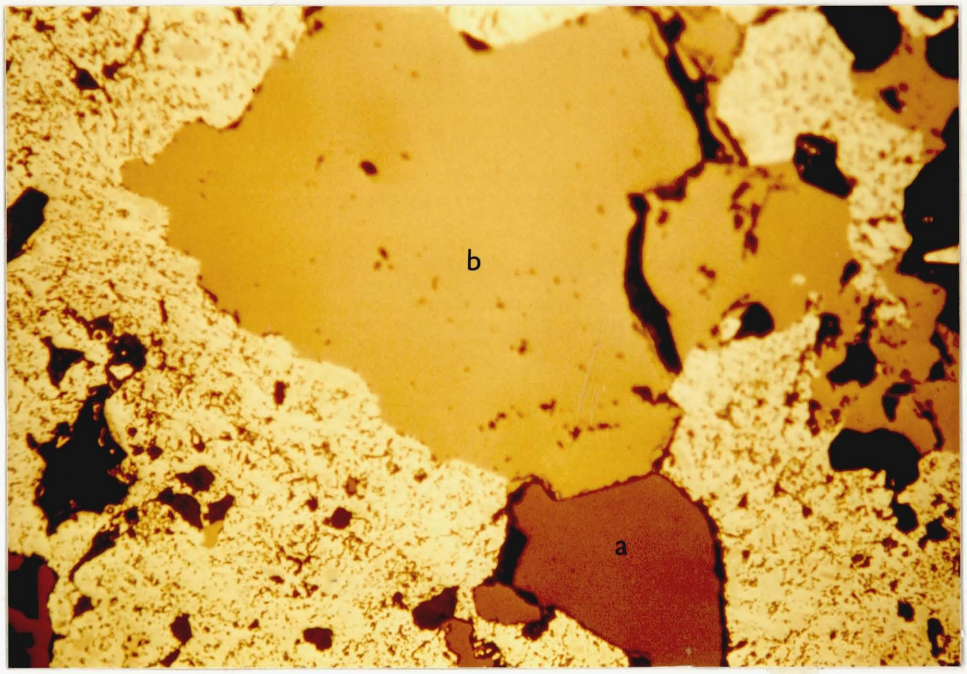

200μm

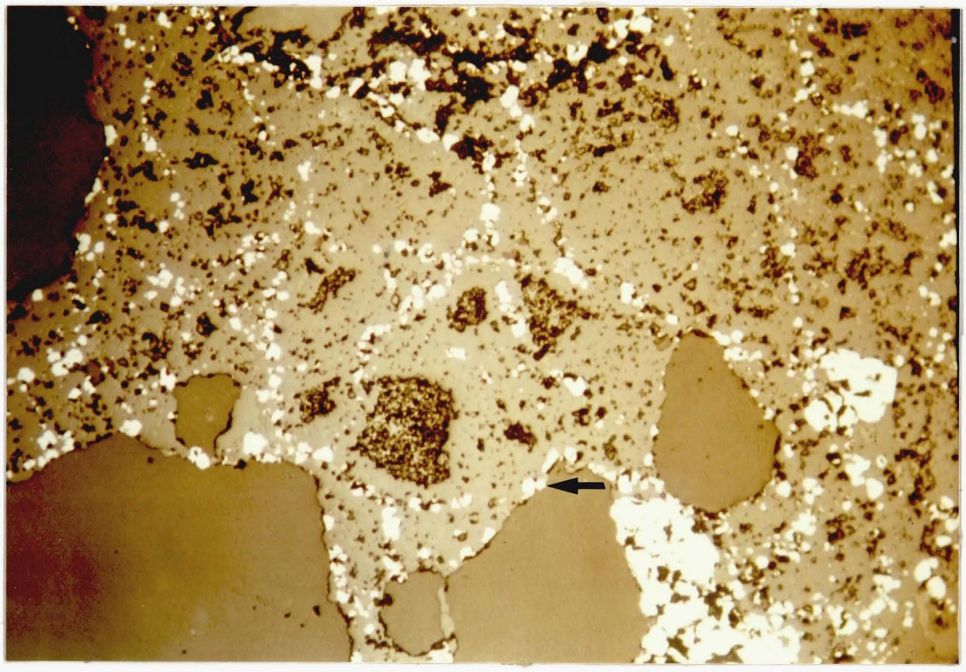

200μm

commonly occurs in mutual intergrowth with gangue minerals including chlorite, green biotite, fluorite, quartz, feldspar and cassiterite. The green biotite is generally characteristic of both the skarn and hornfels rocks. Chlorite has been formed by the alteration of the green biotites. The other four gangue minerals occur in the later hydrothermal mineralisation and it appears that the gangue mineralogy of the two mineralisation episodes was similar. In the porous facies of the magnetite ore, cassiterite was seen encrusting the margins of the cavities in the magnetite and it was followed by quartz, (Plate 51A).

Magnetite also occurs, (but much less commonly), as tiny grains distributed in a disseminated fashion, or as a mesh of veinlets with a chicken-wire appearance, (Plate 51B). Furthermore, it occurs as tiny grains around host rock fragments, (Plate 51B). and as veinlets in the fractures developed within the host rock.

In general the magnetite from the lower portions of the 'wrigglite' was unmartitised, (Plate 52A). There are, however, some magnetites which have been martitised in the common way with alteration starting from margins, fractures and holes and extending into the octahedral planes of the magnetite. Martitisation here was the result of the deep-reaching effects of tropical supergene weathering.

PLATE 52.

A. Irregular unmartitised masses of magnetite intergrowth with silicate gangue consist of inclusions of löllingite (arrowed),(Bench C, Waterfall Mine, Pelapah Kanan). (Plane Polarized light).

B. Mutual intergrowth of silicate gangue, (chlorite, feldspar and quartz), and magnetite is cut by a later quartz veinlet, (arrowed), (Bench C, Waterfall Mine, Pelapah Kanan). (Crossed Polars).

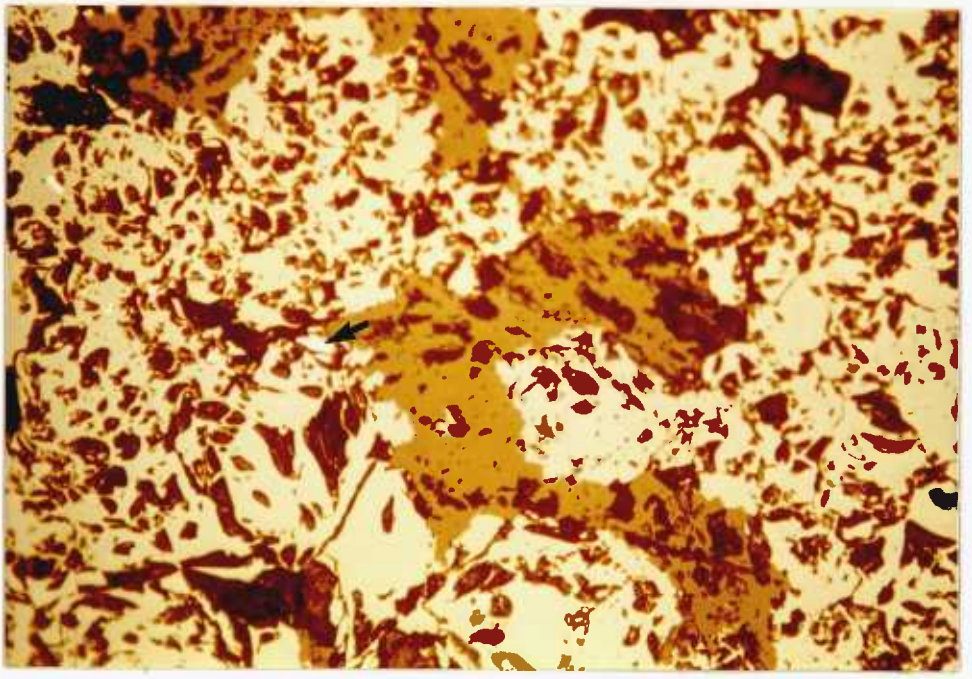

200μm

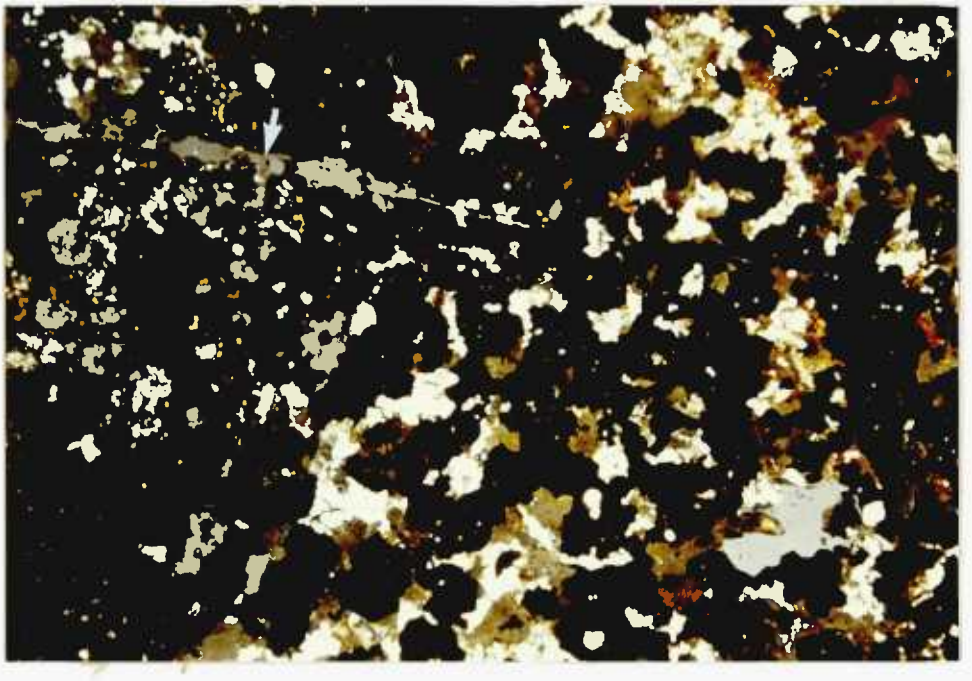

1.5 X

Tiny magnetite grains were occasionally observed as inclusions in cassiterite. The mutually penetrating intergrowths of magnetite and gangue also contain idioblastic and skeletal löllingite crystals, and anhedral chalcopyrite. These two minerals have replaced the magnetite-gangue mutual intergrowth. Some of the magnetite-gangue mutual intergrowths were cut and replaced by quartz veins/veinlets, (Plate 52B). In one instance brecciated fragments of magnetites were seen incorporated in parallel alignment in the margins of a quartz vein. Magnetite in places has suffered extensive replacement by siderite in the matrix resulting in skeletal relict forms.

Cassiterite.

The distribution of cassiterite in the martitised magnetite is irregular. The cassiterite occurs as isolated grains and aggregates in cavities within the porous fabric of magnetite and silicates, apparently replacement boundaries between cassiterite and the enclosing magnetite host together with the frequency of silicate inclusions in the associated quartz, (Plate 51A), suggests that the quartz-cassiterite mineralisation was superimposed upon the earlier magnetite mineralisation resulting in partial replacement.

PLATE 53.

A. An aggregate of poikiloblastic löllingite crystals (a) set a matrix of quartz (b) and silicate gangue (c) in between the magnetite bands of a 'wrigglite', (Bench C, Waterfall Mine, Pelapah Kanan). (Plane Polarized light).

B. Concentric-spherulitic supergene goethites, (arrowed a), corrode into the associated quartz (b), löllingite (c) and silicate gangue (d), (Bench D. Waterfall Mine, Pelapah Kanan). (Plane Polarized light).

800μm

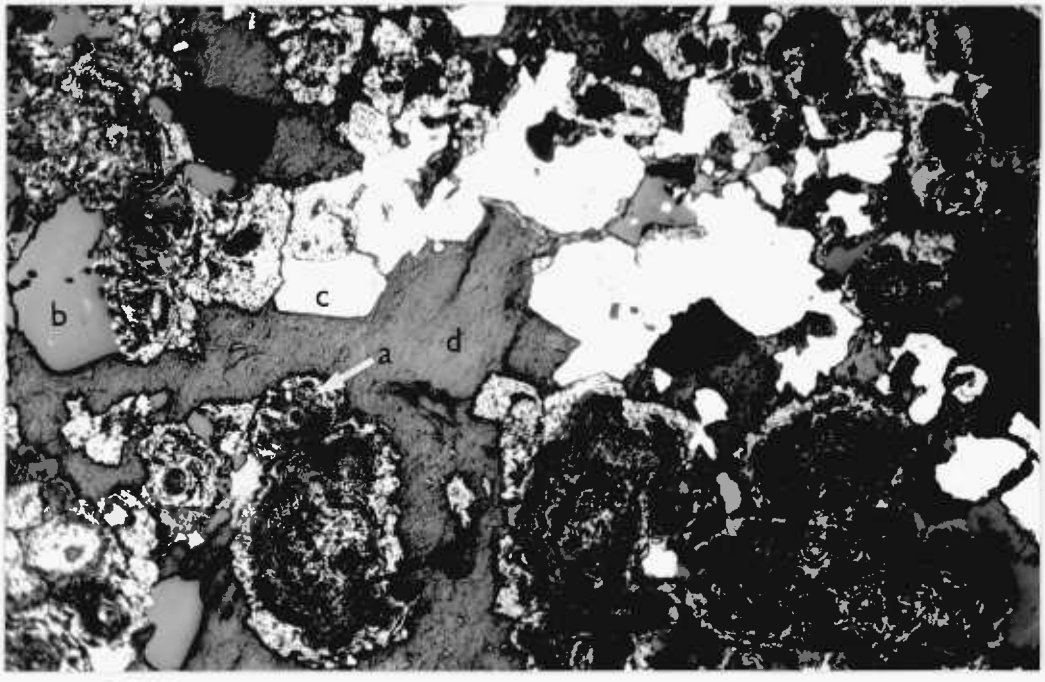

200μm

Löllingite.

Löllingite was the first major sulphide phase to be deposited in the magnetite skarn and it commonly occurs as idioblastic crystals within the magnetite-gangue mutual intergrowth, (Plate 53A), and along cross-cutting fractures in the gangue matrix. The intergrowth inclusions in the idioblastic lollingite are magnetite, quartz and chlorite which locally produce a poikilitic texture. Löllingite is also present as euhedral and subhedral inclusions and in quartz occurring between the martitised magnetite bands.

As an early mineral, löllingite was subsequently subject to replacement by stannite, chalcopyrite, quartz, siderite and goethite, (Plate 53B). Quartz, stannite(?) and colloform goethites have replaced lollingite crystals to produce skeletal relics. For some löllingites, replacement by goethite was pseudomorphic. Löllingite was also replaced at margins and also along fractures by chalcopyrite which was later locally oxidised to chalcocite or covellite.

Löllingite crystals occasionally enclose euhedral and subhedral sphalerite inclusions, some of which still have some gangue material at the margins; the inclusions do not show evidence of replacement by the enclosing löllingite. In one instance löllingite

PLATE 54.

A. Magnetite (a)-silicate gangue (arrowed b) intergrowth is partially replaced by later chalcopyrite (c) with subsequent enclosure of silicate gangue inclusions. Note the alteration of chalcopyrite to covellite (arrowed). (Bench C, Waterfall Mine, Pelapah Kanan). (Plane Polarized light).

B. Spherulitic goethites corroding both the löllingites (a) and the quartz (b). Greenish mineral probably scorodite (c) is formed at the margins of the löllingite grains and is probably the alteration product of löllingite, (Bench D, Waterfall Mine, Pelapah Kanan). (Plane Polarized light).

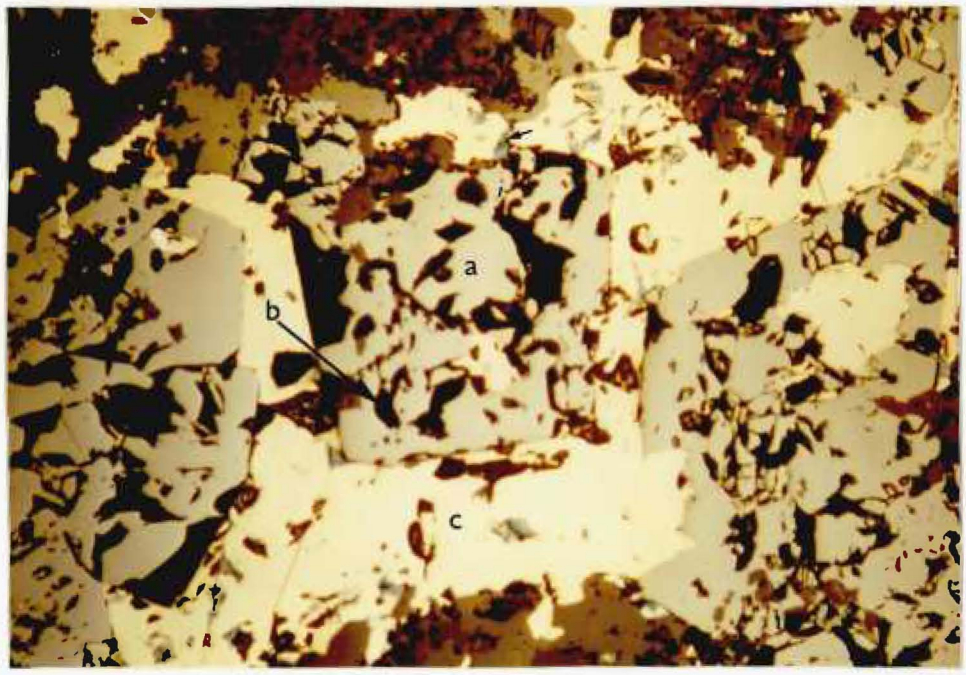

200μm

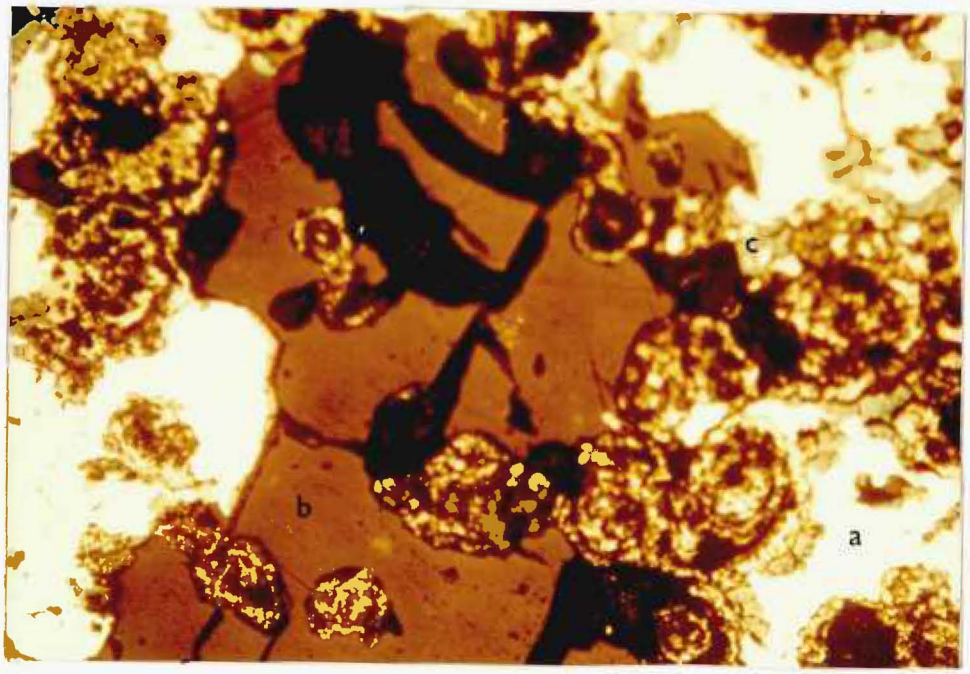

200μm

has partially rimmed and filled fractures in cassiterite grains.

Chalcopyrite.

Chalcopyrite is present generally in trace amounts as inclusions in interstitial quartz matrix and also as disseminated grains in the chloritic-silicate gangue. Larger anhedral grains of chalcopyrite have replaced the magnetite-gangue intergrowth thereby enclosing subhedral and euhedral grains of magnetite, (Plate 54A). Some of these chalcopyriteswere altered to covellite/chalcocite at margins and along fracture contacts with adjacent magnetite while others were completely altered. Chalcopyrite has also replaced lollingite idioblasts at margins and within. The former chalcopyrite has all been altered to chalcocite while the latter remained unaltered. Some lollingites contain two-phase inclusions of chalcopyrite intergrown with bornite,

Galena.

Galena is very rare as it was only seen in one polished section. It occurs as anhedral to subhedral grains containing relict inclusions of magnetite, inclusions of bornite-chalcopyrite intergrowth and chalcopyrite which has been partially altered to covellite.

Quartz.

Quartz is an ubiquitous gangue mineral and it is commonly present as veins/veinlets traversing and partially replacing the magnetite-gangue (intergrowth) intergrowth. It has replaced the gangue intergrowths with magnetite or the bands that interbed with the magnetite-gangue. Thus the pre-quartz minerals such as chalcopyrite/covellite, lollingite, magnetite and cassiterite were subsequently enclosed by the quartz. These inclusions do show signs of marginal replacement by the quartz. Not uncommonly the quartz veins that cut across lollingite-bearing magnetite-gangue intergrowth have included crystals of lollingite and brecciated fragments of magnetite. These included phases were partially replaced by the quartz; in the case of the lollingite the replacement has resulted in the production of poikilitic relicts and skeletal forms. Some lollingite crystals set in the quartz veins were partially or pseudomorphically altered to goethite which was likely to have been brought about by the oxidising action of the solution that formed the quartz veins.

Irregular anhedral quartz in polished section (PKD_3) shows distinct corrosion by cellular goethite, and its fractures were filled by hematite.

PLATE 55.

A. Core of a subhedral magnetite initially replaced by chalcopyrite which is altered to supergene covellite (a): this magnetite grain is oxidised to haematite (arrowed(at its margins. (Bench C, Waterfall Mine, Palapah Kanan). (Plane Polarized light).

B. A löllingite crystal (a) is replaced internally by goethite (b)- its margins and fractures are replaced by quartz. (Bench C, Waterfall Mine, Pelapah Kanan). (Plane Polarized light).

100 µm

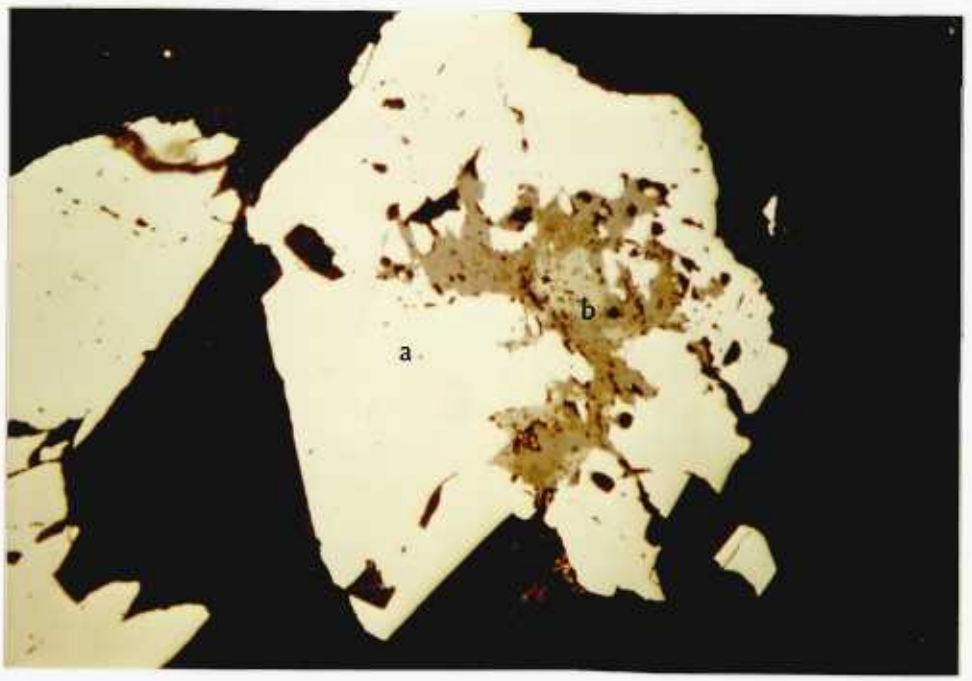

200 µm

Siderite.

Siderite is rare and it occurs as a matrix phase to magnetite masses and also together with magnetite it rims around the rounded clasts of the host rock. Siderite replaced magnetite both marginally, and extensively to the extent of skeletal forms. This replacement was much more common than that of lollingite by siderite. Siderite succeeded the quartz phase as it was seen to have replaced into quartz.

Goethite.

Goethite was the last phase to be deposited and it has resulted from the supergene alteration of magnetite or martite or lollingite.

Besides occurring as veinlets in fractures, goethite is commonly present in a concentric-spherulitic form as a matrix to skeletal and idioblastic lollingite, (Plates 53B & 54B) and quartz, and also rimming margins of cavities within martitised magnetite masses. As a matrix phase it corroded into quartz, (Plate 54B), and lollingite. Thus the latter mineral became anhedral or skeletal in form. In addition to these two modes of occurrences, goethite is also present as narrow rims around euhedral magnetite grains which have been extensively replaced by chalcopyrite which has, in turn, been altered to covellite, (Plate 55A).

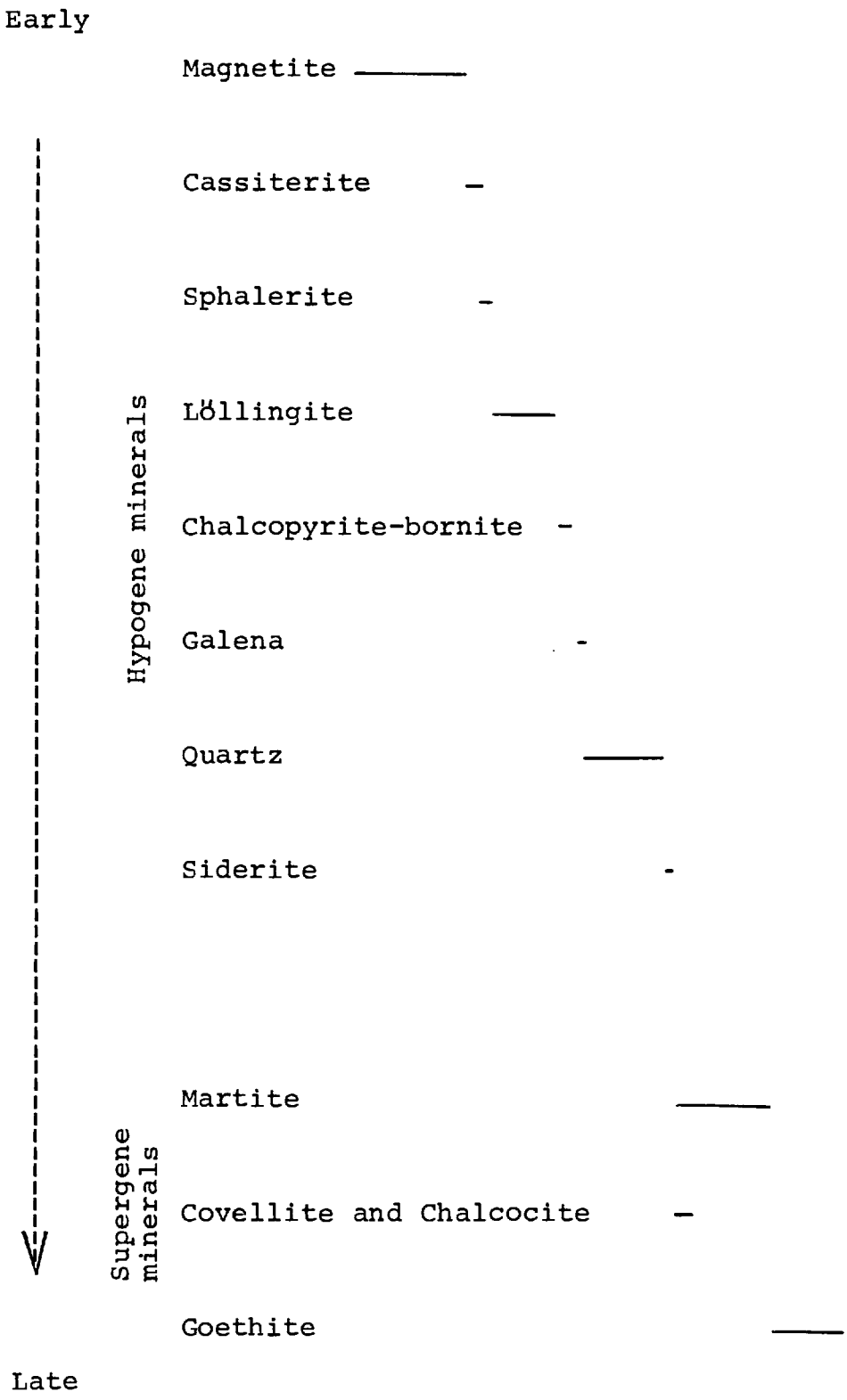

Figure 14. The sequence of mineralisation of the magnetite skarn ore body.

This covellite is confirmed to be the supergene alteration product of chalcopyrite by the presence of relicts of chalcopyrite within the covellite.

Goethite is also known to have formed from the oxidation of the löllingite idiomorphs caught in the quartz veins, (Plate 55B), or those in contact with quartz. Some of the löllingite crystals were completely pseudomorphed by goethite and scorodite through the process of alteration. It is interesting to note that löllingite crystals which are not in contact with quartz are free of goethite.

5.3. General Conclusions.

The conclusions which are drawn from the above mineragraphic description are as follows:

1. The sequence of precipitation of minerals present in the magnetite skarn ore body is shown in Fig.14.

2. Since martitisation was largely confined to the top parts of the ore body, it can be concluded that the cause of alteration was a supergene process which was initiated by the tropical climatic conditions.

3. The above description of the magnetite-fluorite-löllingite 'wrigglite' from the skarn ore body was the first of the its kind from Western Malaysia.

4. The presence of a suite of gangue minerals, (e.g. fluorite, quartz, feldspar, cassiterite and löllingite), only in the bottom parts of the skarn ore body which is similar to those of the later vein mineralisation stage suggests that the suite of gangue minerals was deposited from mineralising hydrothermal fluids which are believed to be parts of the mineralising fluids of the later vein mineralisation stage and which have infiltrated up into the bottom parts of the skarn ore body.

PLATE 56.

The border zones of a fractured quartz veinlet are mineralised by magnetite occurring as laths, (arrowed). These laths may be pseudomorphs of haematites. (Plane Polarized light).

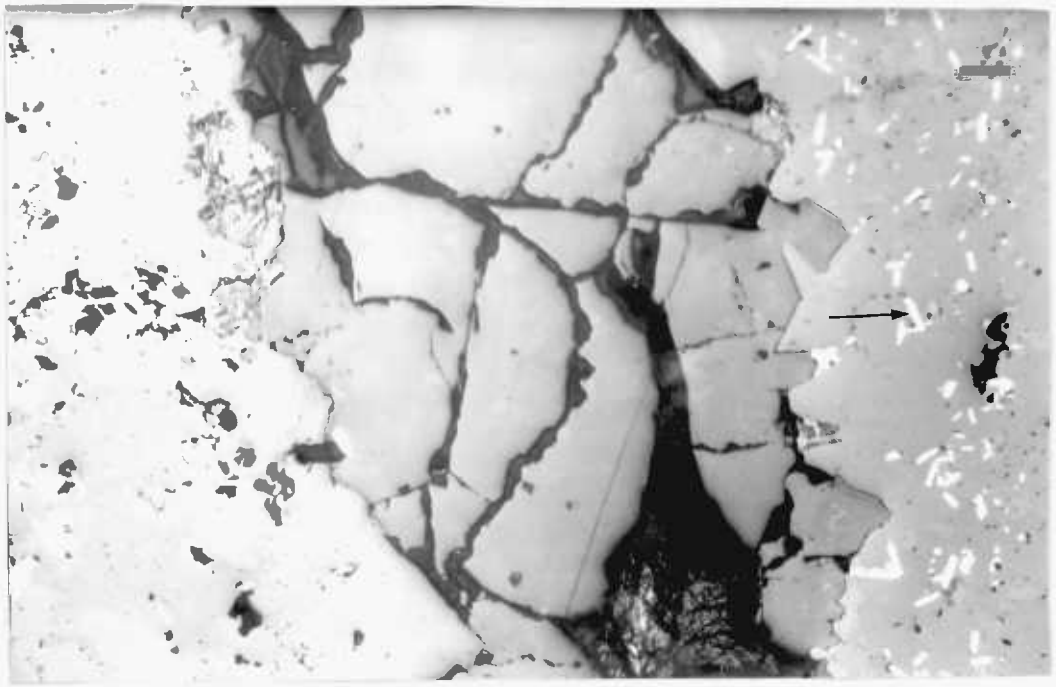

400μm

5.4. The Vein Mineralisation Stage.

A study of many selected hand specimens, thin sections and polished sections together with field observations has provided a basis for description of the paragenetic sequence of mineralisation, both in the veins and their margins. The minerals deposited in the hornfelsed margins of the hydrothermal veins are magnetite, (Plate 56A); löllingite, fluorite veinlets and disseminations, and quartz veinlets respectively in order of decreasing age. A single phase each of quartz and magnetite deposition and two phases each of cassiterite,fluorite, K-feldspar and calcite deposition were recognised in the veins. The commonest mineral assemblage in the veins consists of K-feldspar, fluorite, quartz, löllingite and cassiterite. However, the recognised phases of deposition of these minerals were not invariably present in all the veins studied. This is attributed probably to the timing of fissure development in each vein in relation to the arrival of each of the mineralising fluids and the sequence of mineral precipitation. The K-feldspars are unique to the veins from the hornfelses underneath the magnetite ore body. This zonation is a reflection of the earlier age of the K-feldspar as compared to the quartz phase which was deposited higher in the lower portion of the magnetite ore body.

5.4.1. Mineral Textures and Paragenesis of the Main Vein Mineralisation Stage.

Cassiterite, (Phase One).

This earliest vein cassiterite phase has been observed in a fluorite-löllingite-K-feldspar-quartz vein at Bench D. Here it occurs as granular crystals lining the margins of the vein and also around the margins of lenticular inclusions of the host rock incorporated within the vein. Irregular aggregate masses of phase one cassiterite have partly replaced the wallrock lens and the associated pre-cassiterite magnetite which belongs to the paragenesis of the earlier magnetite skarn ore body. The deposition of this vein cassiterite within the wallrocks and symmetrically in the margins indicates that it was the first mineral in the paragenetic sequence formed in the veins. Field observation has shown that the cassiterite of this phase is not widely distributed in the veins.

Magnetite.

Magnetite is ubiquitous within the marginal zones, (a few mm. wide), bordering the veins, (Plate 56), and it occurs both as laths and subhedral to anhedral plates interspersed with idiomorphic löllingite grains. In places, euhedral and subhedral magnetite crystals

were enclosed by löllingite; their subhedral form has resulted from marginal replacement by the löllingite. In some veins, the magnetite has also formed inclusions within quartz. In a polished section of a vein long magnetite laths, (0.15mm), were seen occurring next to the margins of partially replaced cassiterites within the vein and this suggests that magnetite was the second mineral phase of the paragenetic sequence.

Löllingite.

Löllingite is the most common sulphide mineral. It commonly occurs as cataclastic grains at the selvedge and wallrock contacts of the veins and also as disseminated idiomorphic and irregular poikiloblastic grains in the hornfelsed borders of the veins.

The fractures in the cataclastic löllingite have been filled and replaced by quartz and K-feldspar. The disseminated idiomorphic and subhedral löllingite crystals in the hornfelsed borders were interspersed with lath-shaped and anhedral magnetite grains. The subhedral poikilitic löllingite crystals contain included magnetite laths and anhedral magnetite grains which suggests that they were present prior to growth of the löllingite crystals. The löllingite crystals incorporated in the quartz and early fluorite of the veins was commonly replaced marginally and internally to produce anhedral and poikilitic forms. In some cases the löllingites trapped by quartz were either partially or totally altered to goethite by the hydrothermal action of the later fluids. Furthermore, löllingite crystals were enclosed and marginally replaced by phase two cassiterite, quartz and calcite-chlorite to give subhedral to anhedral forms and more rarely skeletal relics when replaced by quartz.

PLATE 57.

A. A composite quartz(a)-K-feldspar(b)-fluorite (c)-veinlet in pyroxene hornfels with K-feldspar occupying the outermost zones of the veinlet. Fluorite was deposited on dilation of the fractured K-feldspar veinlet and it was followed by the deposition of quartz in the central zone of the veinlet. The fluorites show some sign of disruption by the later quartz. Note the unidentified isotropic brownish minerals, (arrowed), growing along the fractures of fluorite. They are probably some alteration products of fluorite. (Bench A, Waterfall Mine, Palapah Kanan). (Crossed Polars).

B. Fractured fragments of fluorite (a) in a quartz veinlet. Fluorite shows features of replacement by the quartz at margins and along fractures, (arrowed), (Bench D, Waterfall Mine, Pelapah Kanan). (Crossed Polars).

4X

5X

PLATE 58.

A. The parallel white K-feldspar-quartz-cassiterite bearing veins in this loose block of pyroxene hornfels are emplaced parallel to bedding planes and they show a variation of their widths and their mineral composition. For example, vein 'a' does not contain any feldspar whereas vein 'b' does. The marginal white K-feldspars in vein 'b' show replacement features by later quartz. (Waterfall Mine, Pelapah Kanan).

B. Pink K-feldspars form the outer margins of a k-feldspar-quartz-fluorite vein. The initial pink feldspar vein is fractured and dilated by the fluid pressure of the quartz-forming fluids along both its centre and at one of its margins. (Bench C, Waterfall Mine, Pelapah Kanan).


a
b

Fluorite, (Phase One).

The consistent presence of this early fluorite phase within the outermost zones of veins as a contact layer and also as isolated aggregates produced by disruption, (Plate 57A), shows that this pale green fluorite was deposited prior to the k-feldspar and quartz phases. This fluorite extends into the hornfelsed borders of veins as thin veinlets and as disseminations. These veinlets were often the focus of dipositions of later quartz thus forming thin composite quartz-flourite veinlets. The early fluorites have inevitably been replaced marginally and along cleavage fractures by K-feldspar and/or quartz, (Plate 57B).

Although there is an occurrence in which the earliest fluorites were marginally surrounded and penetrated along the cleavage direction by löllingite. It is more commonly observed that löllingite occurs as inclusions in the fluorites suggesting that the fluorites mostly postdate the löllingite.

K-feldspar, (Phase One).

A pink, (Plate 58B), and a white,variety, (Plate 58A), of gangue feldspar were recognised and they both have been identified as a K-feldspar using the S.E.M. and x-ray microanalytical technique. Since the chemical investigation has shown them to be similar in the

PLATE 59.

A. A composite K-feldspar(a)-cassiterite(arrowed b)-quartz(c) vein in pyroxene hornfels showing the incorporation of thin and thicker slivers of K-feldspar some of which with cassiterite grains in later quartz. This braided 'streaky-bacon' texture indicates that the quartz phase was deposited episodically following the dilation of the K-feldspar-cassiterite bearing vein structure, (Bench C, Waterfall Mine, Pelapah Kanan). (Crossed Polars).

B. A composite vein consisting of K-feldspar (a); cassiterite (b); fluorite (c); quartz (d)- biotite (e) and an unidentified fluorite-associated mineral (arrowed). The fluorite fragments show replacement by quartz at margins and along fractures, (arrowed). Note the twig-like form of the unidentified brown mineral and also the colour zonation of the cassiterite. The order of occurrence towards the centre of the vein is as follows: K-feldspar-cassiterite-fluorite-quartz. (Bench A, Waterfall Mine, Pelapah Kanan). (Plane Polarized light).

1.5 X

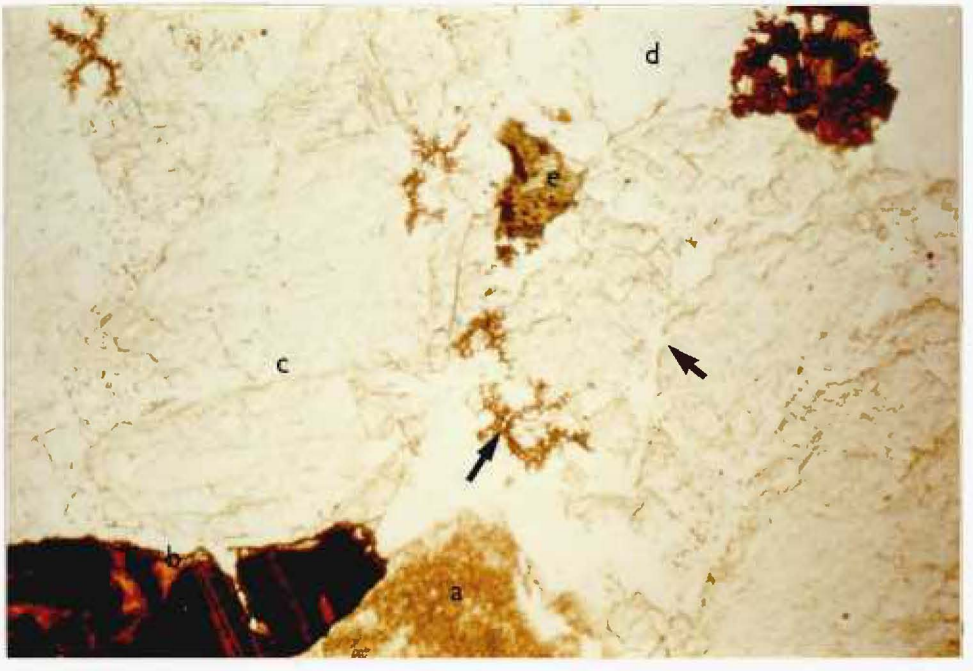

200µm

major-element chemistry, the colour difference must be purely a superficial effect due probably to the presence of finely disseminated haematite grains in the pink K-feldspar. This probability is considered likely in view of the fact that the k-feldspar-bearing veins are located beneath a massive magnetite skarn ore body which could be the source of the iron in Fe-enriched waters percolating down into the k-feldspars.

The K-feldspar is also a common, but not an ubiquitous gangue mineral of the veins. It commonly occupies the outer zones of the veins and encloses earlier fluorite and löllingite. This phase of K-feldspar has been seen in the field to be partially replaced by later quartz, (Plates 45 and 58), which was deposited during continued dilational opening of löllingite-fluorite-bearing veins.

Cassiterite, (Phase Two).

This cassiterite constitutes the main economic mineralisation of the veins. This cassiterite succeeded the K-feldspar, (phase one), being deposited during the progressive dilation of the veins. The cassiterite of this phase forms distinct grains and aggregates next to the fractured margins of K-feldspar, (phase one), (Plates 59A and 59B), and also occurs as inclusions in the later quartz gangue. This generation of cassiterite provided suitable populations

of primary and pseudosecondary fluid inclusions for homogenisation temperature determinations.

Fluorite, (Phase Two).

This phase of fluorite is nearly always closely associated with phase two cassiterite encrusting the K-feldspar, (Plate 59B) and as loose fragments in the later quartz-gangue, (Plate 57B). The relationship of these two associated minerals suggests that the second generation of fluorite was deposited in sequence with the second generation of cassiterite and prior to the introduction of the final quartz phase. It was common for the fluorite to be replaced by the quartz along margins and cleavage fractures. In non-cassiterite (2) bearing veins with K-feldspar this fluorite generation succeeds the K-feldspar phase directly.

The consistent discrepancies in the paragenetic sequence observed in the samples collected from different veins within the group of structures suggests that the history of mineral deposition was accompanied by episodic dilation which did not affect all veins uniformly.

Quartz, (Phase One).

Quartz is the most abundant gangue mineral in the

PLATE 60.

A quartz-K-feldspar bearing vein in the pyroxene hornfels showing the infilling of a K-feldspar(2) (a) in the cavity formed by vug quartzs, (b). Associated with the white K-feldspar are minor amounts of greenish mineral which has not been identified, (Bench D, Waterfall Mine, Pelapah Kanan).


a
b
3 cm

veins. The symmetrical dilation of the pre-quartz K-feldspar-bearing veins, (Plate 59A), locally also along one or both of the marginal contacts during the pressure episodes of the later hydrothermal solution led to the deposition of significant amounts of quartz. This generation of quartz formed thick veins, (≏ a few cms. wide), and also thin, (≏ a few cms. wide), and microscopic veinlets.

The mineralisation was accompanied by the partial replacement of K-feldspar,(Plate 45A), fluorite and löllingite. The latter shows irregular poikilitic shapes as a result of this replacement. The quartz veinlets were seen to extend into the hornfelsed border zones of veins where they cut across and also along the middle of fluorite veinlets.

This generation of quartz has also been seen to form vuggy crystals in a fractured and dilated fluorite-bearing vein.

K-feldspar, (Phase Two).

This K-feldspar phase is rare and it occurs as fillings in the irregular surfaces provided by the vuggy quartz (1), (Plate 60). This demonstrates that hydrothermal fluids of the later stages are of the appropriate composition to allow crystallization of potash feldspar.

Calcite.

This calcite phase followed the earlier quartz phase, replacing it and also filling in the voids in quartz as vug linings and crystalline masses. This calcite was itself cut by later calcite veinlets. The straight set of rhombohedral cleavages observed in this calcite suggests that the vein which contained it has not suffered deformation post deposition.

Post-vein Mineralisation Stage Quartz Phase.

This final hydrothermal quartz phase is evidently post-vein mineralisation stage in age as it was emplaced almost vertically along a reverse fault which has displaced the veins of the main vein mineralisation stage. Another vertical quartz vein observed on the floor of Bench C displays local vuggy quartzs which contain only monophase aqueous inclusions. These inclusions indicate that this quartz was deposited within a temperature range from 70^{o}c to room temperature.

The borders of this quartz-hematite vein are quartz-chlorite hornfels which contain disseminated metasomatic subhedral cassiterite grains almost always spatially associated with green chlorite, and also located in the interstices between quartz grains. Some of these very weakly pleochroic cassiterites were rimmed by supergene hematite.

The quartz vein was intensely fractured and the fractures and the inter-granular quartz spaces were infilled by supergene hematite some of which shows a colloform banded texture especially where it lines the walls within the vein.

The green chlorites within the vein and in the wall rocks, particularly those nearer to the vein were mineralised by supergene hematite at margins and along cleavages. Haematite veinlets have also filled fractures developed in the border zones of the quartz vein.

The source of the Fe-oxide solution was undoubtedly the overlying martitised magnetite skarn ore body, the iron having been transported by the descending oxidising solutions.

Supergene Haematite/Goethite Phase.

These supergene phases are the products of

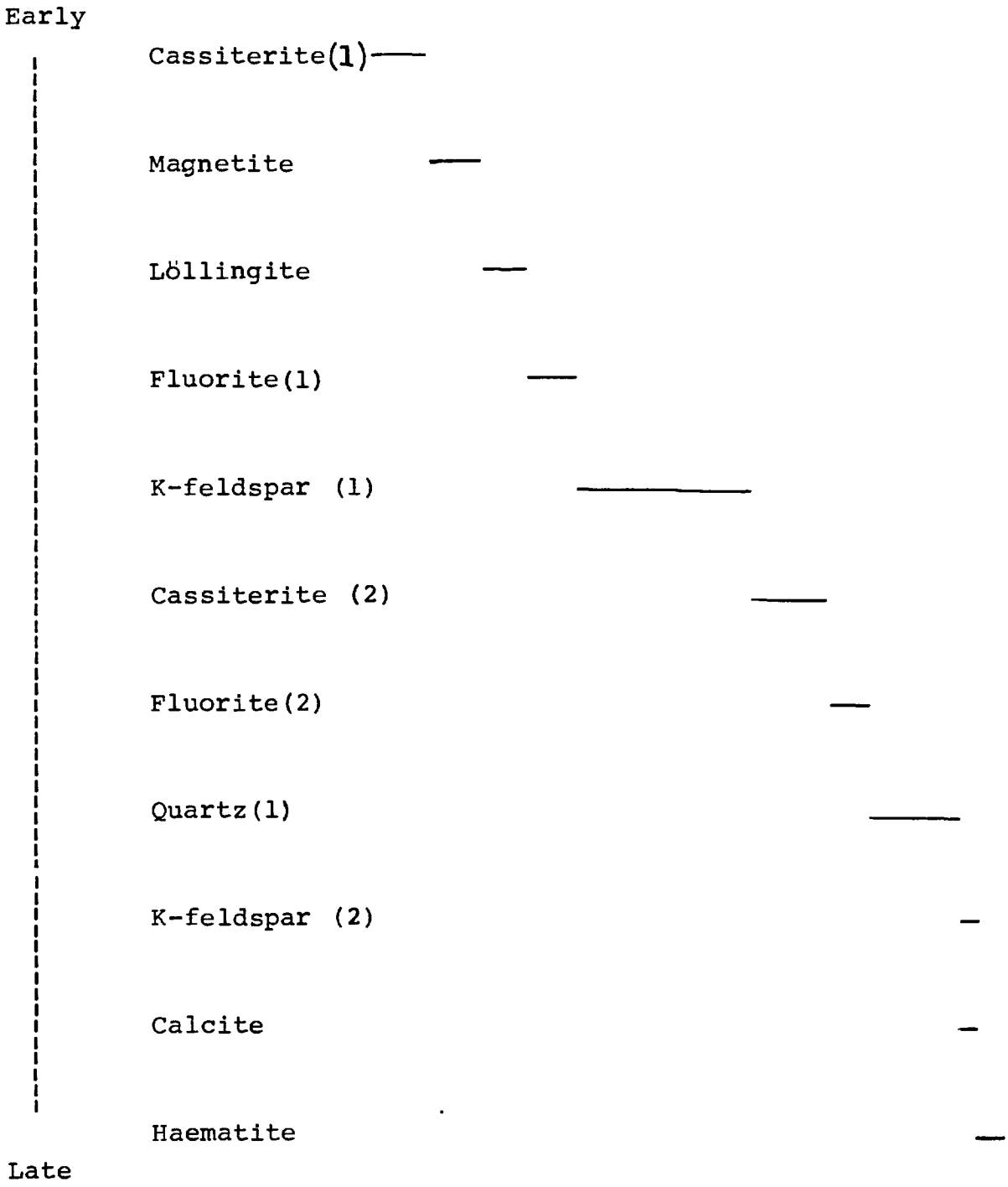

Figure 15. The sequence of mineralisation in the tin veins.

tropical weathering processes. Goethite was seen to form concentric-spherulitic bodies usually around a central fragment of gangue material, (probably fluorite?); these were formed in the border zones of the mineralised veins and corrode the lollingite, quartz and fluorite(?). Haematite formed from downward percolating iron solution was deposited in fractures developed within the veins and in their border zones as described in page

This supergene phase was cut and partially replaced by the later calcite veinlets and this shows that calcium-bearing solution was also generated during the process of supergene weathering.

5.5. General Conclusions.

The conclusions which are drawn from the above mineragraphic description are as follows:

1. The commonest mineral assemblage in the veins consists of quartz, K-feldspar, fluorite, cassiterite and löllingite.

2. The sequence of precipitation of the mineral components of the veins and their border zones is graphically shown in figure 15.

3. The consistent descrepancies in the paragenetic sequence observed in the samples collected from the different veins within the group of structures suggests that the history of mineral deposition was accompanied by episodic dilation which did not affect all veins uniformly.

4. The economic mineral in the veins is cassiterite.

5. The presence of cataclastic texture in the löllingites indicates that there was a phase of cataclastic deformation after the deposition of löllingite and also that the löllingites did not recrystallise or anneal after the deformation.

CHAPTER 6.

Studies of fluid inclusions from cassiterite and associated gangue minerals.

6.1. Introduction and aims.

Except for some preliminary fluid inclusion data on the West Malaysian tin deposits gathered by Little in 1960, fluid inclusion data on the respective deposits are confined to within unpublished work done by Yeap, (Personal communication, 1976) on the Kuala Lumpur tin field. It was, therefore, necessary to carry out a petrographic, thermometric and chemical study on the primary and pseudosecondary fluid inclusions in cassiterite and associated gangue quartz, fluorite and calcite from a range of deposits. The minerals were collected from accessible hypogene tin veins emplaced in the following geological settings:-

a. Within the granite (e.g. Sg Pari tin lodes, and the tin lodes of Eu Tong Seng Mine at Tekka Hill).

b. In the contact zone next to the granite (e.g. the tin lodes of Waterfall Mine at Pelapah Kanan, and the tin lodes of Eu Tong Seng Mine at Tekka Hill).

c. Further distance away from the granite contact

(e.g. the Hantu and Willinks lode systems of Pahang Consolidated Mine at Sg. Lembing and the tin lode of Siputeh at the Kinta Valley).

In addition, samples were also collected from a cassiterite-bearing quartz-muscovite greisenised granite at Gambang and stanniferous colluvial and alluvial deposits, (e.g. Chenderiang Tin S.E.A. Mine Limited at the Chenderiang Valley, Gopeng Consolidated Mine, Timah Gaya Mine, Dato Sherri and Sons Mine, Lian Pong Mine Ayer Hitam Mine and Sg. Besi Mine). The geographic locations of these deposits are shown in Fig. 2.

The purpose of this study was to reveal the physico-chemical conditions of deposition for the mineral parageneses in the various tin-bearing environments specified above: these conditions were evaluated with relationship to the geological settings.

The petrographic study was done by means of a polarizing transmitted light microscope, (Vickers. M. 70), the thermometric measurement was done using a Leitz microscope heating stage (Leitz 1350), and finally chemical (largely salinity) determinations were carried out by using the heating stage (Leitz 1350) to determine the temperature of solution of halite and

Sylvite in the halite/sylvite-bearing fluid inclusions in cassiterite and quartz from the tin lodes of Waterfall Mine at Pelapah Kanan.

An evaluation of the thermometric data from fluid inclusions in cassiterite in relationship to the primary geological settings of the tin lodes has given trends which may be useful as an environmental indicator for alluvial cassiterite and hence making it easier to select prospective source areas of the respective alluvial cassiterite.

A special study was made of fluid inclusions in Pegmatitic topaz from the Chenderiang Tin S.E.A. Mine Limited, Chenderiang Valley, in order to specify the physico-chemical nature of the fluids responsible for the crystallization of topaz-bearing pegmatites. This was also considered of interest in order to test the genetic relationship between the topaz and associated colluvial cassiterite.

In conclusion a comparative review of fluid inclusion data from other tin provinces was made and the results are discussed in relation to the author's results from the West Malaysian deposits.

6.1.1. Previous fluid inclusion studies in Western Malaysian tin deposits.

The first study of fluid inclusions from Western Malaysian cassiterite and associated gangue quartz and beryl was made by Little (1960). This study was, however, of a reconnaissance nature investigating only a few mineral samples from tin veins of different origins (e.g. pegmatite, hydrothermal veins and replacement lodes (pipes) in limestones) at the Kinta Valley, Kuala Lumpur and Chenderiang tin fields. Little observed the common presence of both H_2O-CO_2, and H_2O fluid inclusions in beryl, cassiterite and quartz from the range of deposits specified above except for the replacement lodes in limestones in which in addition to the H_2O inclusions a single H_2O-CO_2 fluid inclusion was recorded in cassiterite. Little had recorded the presence of salt crystals only in some H_2O inclusions.

Homogenisation temperatures of 346°C and 361°C and 366°C were measured (using the Microscope Heating Stage) in coexistent pegmatitic beryl and cassiterite respectively. These two minerals were collected from a pegmatite vein at the Chenderiang Valley. From comparative petrography and homogenisation temperatures of the fluid inclusions in the two

Mineral from pegmatites

Sample No	Mineral	Locality	Types of fluid inclusions	Eqt T°c	(vol of Incl)/(vol of liq)	Calc T°c	Th°c
22	Beryl	Chenderiang Valley	H_2O.S(?). Very few.	110	-	-	-
			H_2O-CO_2 III - Abundant. (A few H_2O-CO_2 I and II).	-	1.89	?	346(9) (334-358)
23	Cassiterite	Chenderiang Valley	H_2O P(?). Some with large Salt x'tals. 4 smaller anisotropic x'tals.	300	1.30	270	361(3)
			H_2O-CO_2 I P(?)	-	2.22-4.83		366(3)

Minerals from hypogene in tin veins

91	Cassiterite	Kinta Valley	H_2O.S(?)	180	1.11	170	-
			H_2O P(?). Some with salt x'tals.	260	1.24	250	-
			H_2O-CO_2(?) P(?)	-	2.33	-	-
	Quartz	Kinta Valley	H_2O.S(?)	150	-	-	-
			H_2O.P(?). Some with salt x'tals.	260	-	-	-
			H_2O-CO_2 (?) P(?)	-	-	-	-
92	Cassiterite	Menglembu	H_2O.S(?)	150	-	-	-
			H_2O P(?). Some with salt x'tals.	260	1.19	230	-
			H_2O-CO_2 (?) P(?). Few.	-	-	-	-

Minerals from hypogene tin veins, (continued).

Sample No	Mineral	Locality	Types of fluid inclusions	Eqt T°c	(vol of Incl)/(vol of liq)	Calc T°c	Th°c
93	Cassiterite	Selangor	H_2O P(?) Few	-	-	-	-
	Quartz	Selangor	H_2O S(?)	100	-	-	-
			H_2O P(?). Some with salt x'tals.	220	1.11	170	-
			H_2O-CO_2(?) P(?)	-	-	-	-
94	Cassiterite		H_2O S(?)	-	1.11	170	-
			H_2O P(?)	240	-	-	-

Minerals from replacement lode in limestones

119	Cassiterite	Ipoh district (Kinta Valley)	H_2O P(?)? Most with salt x'tals	220	1.19	215	-
120	Cassiterite	Ipoh district (Kinta Valley)	H_2O CO_2(?) P(?). Only one.	-	-	-	-

( ) = no. of fluid inclusions measured.

Table 1. Fluid inclusion data from Western Malaysian cassiterite and associated gangue quartz and beryl obtained by Little, (1960)

respective minerals Little has proposed a hypothesis that two immiscible phases (one CO_2 rich and the other H_2O rich) have separated from a homogeneous H_2O-CO_2 fluid phase on cooling. The beryl had crystallised from the homogeneous H_2O-CO_2 phase while the cassiterite crystallised from both the CO_2 rich and H_2O rich phases.

Besides the three measured Th^oc values mentioned above those for the rest of the samples were calculated from the phase ratio (i.e. $\frac{\text{volume of inclusion}}{\text{volume of inclusion liquid}}$) and they are listed in Table 1.

6.2 Genesis and Classification of fluid inclusions

A. Genesis.

Any process that produces irregular crystal growth would cause fluid inclusions to be formed. The ubiquitous presence of fluid inclusions in minerals (at least the transparent minerals) suggests that small scale irregularities during crystal growth are the rule rather than the exception. An understanding of the mechanisms of trapping of the fluid inclusions in a crystal will be indication of the changing physical conditions and perhaps also the chemical conditions during the growth of the crystal.

Some possible causes of irregular crystal growth

are as follows:

1. A period of rapid crystal growth can produce a feathery, dendritic layer with many very irregular reentrants, which succeeding slower growth covers with solid, impervious layers, thereby trapping many inclusions, (e.g. in fluorite). (Roedder, 1967).

2. Temporary starvation of nutrient solution at the centres of growth faces due to uneven flow patterns. (Zerfoss and Slawson, 1956; Sheftal, 1957).

3. Temporary interruption of the supply of nutrient solution by solid particles or oil globules adhering to crystal growth faces. (Khaimov - Mal'kov, 1959).

4. Changes in the chemical composition of the fluids, for example traces of Pb or Mn have been experimentally shown to prevent irregularities during the growth of synthetic Halite crystals, (Buckley, 1951; Schlichta, 1968).

PLATE 61.

A. A large 2 phase (L+V) primary/pseudosecondary fluid inclusion with its long axis aligning obliquely to the growth zones of its garnet host.

B. Three isolated 2 phase (L+V) primary fluid inclusions (arrowed) in vein fluorite intergrowth with cassiterites from the tin lode of the Waterfall Mine at Pelapah Kanan. Note the planes of tiny pseudosecondary/ secondary inclusions formed on cleavage planes of fluorite.

C. A few scattered 3 phase (L+V+halite (arrowed)) primary fluid inclusions in cassiterite from the Waterfall Mine at Pelapah Kanan.

100μm

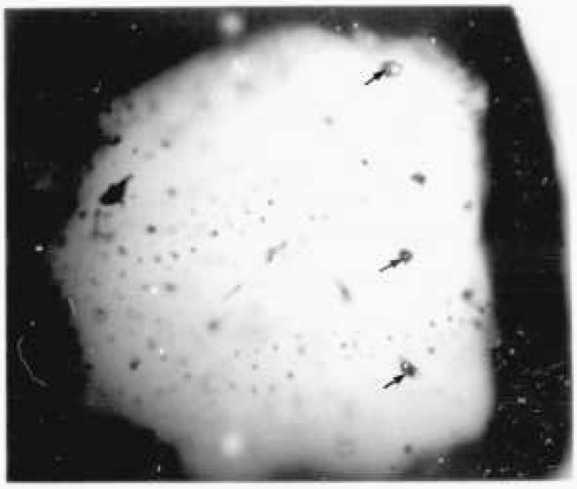

100μm

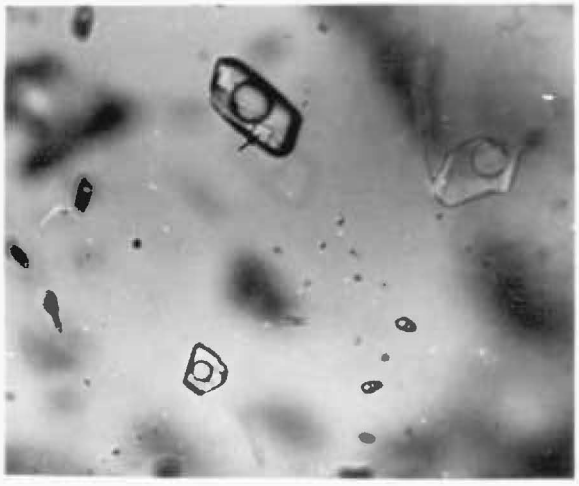

10μm

B. Classification.

Fluid inclusions in transparent minerals can be classified into primary, pseudosecondary and secondary types according to the criteria described below. The primary and pseudosecondary fluid inclusions are formed during the process of growth of the host crystal and consequently their fluids are representative of the mineralising fluid medium responsible for the crystallisation of the host crystal. The secondary fluid inclusions are formed after the growth of the host crystal on fracture planes.

The primary fluid inclusions were recognised as follows:

1. Large and small isolated fluid inclusions. (Plates 61A and B).

2. A small scattered group of fluid inclusions that are not related to any planes in the host crystal. (Plate 61C).

3. Inclusions that aligned themselves parallel to coloured growth zones or crystal margins as in cassiterite, (Plate 62A) and topaz, (Plate 62B), fluorite, vug quartz, (Plate 62C). and garnet respectively.

PLATE 62.

A. A population of cogenetic 3 phase (L+V+halite) (a) and 4 phase (L+V+halite + an unidentified daughter phase) (b) primary fluid inclusions with their long axis aligning parallel to the coloured growth zones of cassiterite.

B. A population of cogenetic Types I, II and III fluid inclusions with long axis aligning parallel to the growth margins of their pegmatitic topaz host.

C. A population of 2 phase (L+V) primary fluid inclusions with their long axis more or less aligning parallel to the growth margins of their pegmatitic topaz host.

D. A population of cogenetic 2 phase (L+V) pseudosecondary fluid inclusions in the central part of a vug quartz.

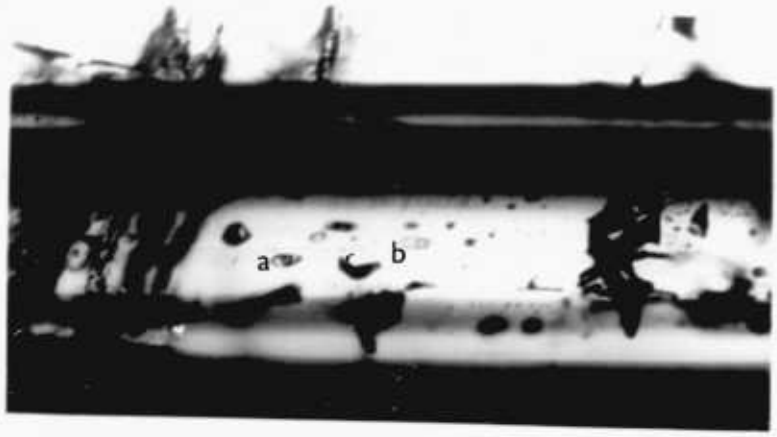

10μm

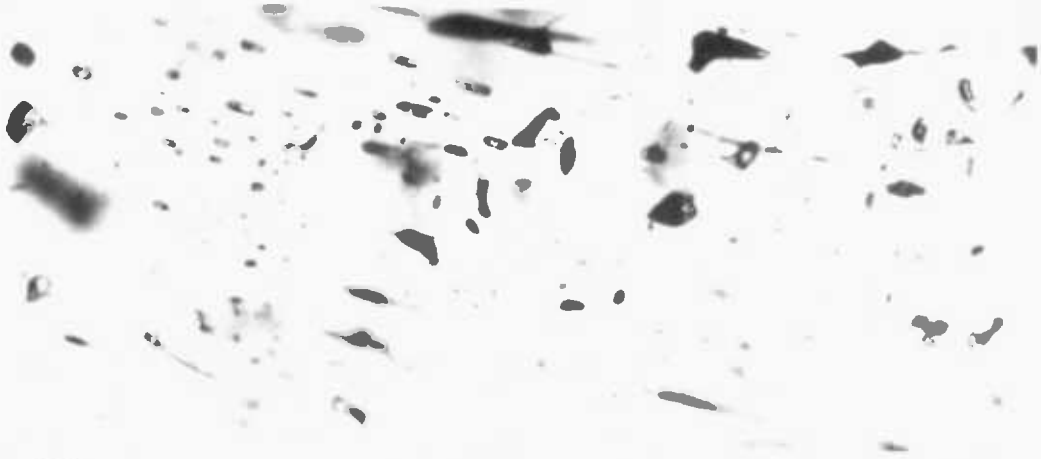

100μm

25μm

100μm

The pseudosecondary fluid inclusions were recognised as follows:

1. Inclusions on a plane that does not terminate at crystal margins, (Plate 62D).

2. Inclusions are generally much smaller in size than the primary inclusions,

The secondary fluid inclusions are formed after the growth of their host crystal often on fracture planes that transect crystal faces. Thus they fill with fluids representative of post-crystallization conditions and were consequently not used to provide genetic criteria for this study.

6.3. The principles and methods of fluid inclusion geothermometry and theoretical discussion of the pressure correction for the $Th^{o}c$ data.

A. Principles.

Sorby (1858) was the first to propose that the gas bubbles in most fluid inclusions are the consequence of differential shrinkage of the liquid and its host mineral during cooling from the higher temperature of trapping to the temperature of observation. Sorby reasoned that an estimate could be made of the temperature of trapping of the fluid in the inclusion. This could

be obtained by heating the inclusion until the vapour bubble disappeared. The temperature at which this took place could be defined as the temperature of homogenisation ($Th^{o}c$) and sets a minimum limit on the temperature of trapping of the fluids in the inclusion. However, the validity of this method is based on the following assumptions:- (Roedder, 1967).

1. The fluid in the inclusion was trapped as a homogeneous phase.

The uniform phase ratio shown by the majority of fluid inclusions in a sample is strong evidence suggesting the inclusion fluids were trapped as a homogeneous phase, However, fluid inclusions formed from a uniformly heterogeneous fluid such as a colloidal dispersion would also show a uniform phase ratio, (Roedder, 1967). Inconsistency of phase ratios in a population of fluid inclusions can be attributed to either trapping of fluids from a heterogeneous system, (e.g. boiling fluid (liquid + coexisting vapour) or Co_2 gas in H_2O). Leakage or necking down may also be responsible. In the case of a boiling fluid when primary gas and liquid may be trapped together in one inclusion the homogenisation of such an inclusion will give an anomalously high $Th^{o}c$ value. Thus inclusions of a

boiling assemblage which have minimum Th^{o}C value are the ones which have not trapped primary gas and they are, therefore, considered reliable. Fortunately the trapping of primary gas phase in inclusions is a relatively rare event, (Roedder, 1967).

2. The inclusion cavity does not change in volume after sealing.

Changes can and do occur by several mechanisms:-

a. Due to crystallization on the walls of the inclusion or in the liquid itself.

b. Due to thermal contraction of the host mineral, (and daughter minerals) on cooling and

c. Due to dilational change as a result of internal or external pressures. The first mechanism does reduce the volume of the inclusion cavity but as these minerals (daughter) do redissolve on heating the original volume is restored. Hence the homogenisation temperatures should not be affected. The author considers this reversible phase change as theoretically sound but in practice it is difficult to observe this phase change. Therefore this uncertainty may

well be the reason which Ermakov (1950), Lemmlein (1950) and others used for their disagreement against the hypothesis described above. The second mechanism would have a negligible effect on the size of the bubble at room temperature even for minerals with large thermal coefficients of expansion since their fluid inclusions have somewhat smaller bubbles. Since the volume change by contraction of the host mineral on cooling is reversed exactly on heating, the $Th^{o}c$ values should be unaffected. Dilational change resulting from internal pressure during heating work has a negligible effect on the inclusion volume even though it is twice that which has resulted from nominal external pressures. This is because the volume change resulting from external pressure is very small.

3. The inclusion contents after sealing do not leak out or have something added to them.

There is much experimental evidence provided by the works of Kennedy (1950), Skinner (1953) and McCulloch (1959) to show that fluids can be leaked out of or into the fluid inclusions by establishing both large inward and outward pressure gradients (pressure

differences used ranged from 4,000 psi to 23,000 psi). These severe pressure gradients used are considered to be unlikely to exist in a natural geological environment (by Richter and Ingerson (1954)). The degree of leakage of fluids from and into fluid inclusions must partly be controlled by the thinness of the wall of the host mineral supporting the confining pressures. In Kennedy's work (with fluorite) the thinness of the wall was 1mm; in Skinner's work (with quartz) 0.75mm in most and 0.5mm in some; in McCullum's work (with NaCl) 0.5mm. (as quoted in Roedder, 1960).

Natural in-situ deformation, sawing and grinding of the sample can all cause leakage (Bond and Andrus, 1952, Brody, 1953). Heating the fluid inclusions well beyond their homogenisation temperature can also cause breakage, but this can be recognised by the change in the size of a bubble before and after heating runs and also by the poor reproducibility of the $Th^{o}c$ values. Minerals susceptible to such leakage are those with good cleavages such as topaz, fluorite and calcite, especially at higher temperatures.

Solid state diffusion of elements such as hydrogen through the crystal (in the case of H in quartz) can be a serious problem for the determination of D/H isotope ratio in inclusion fluids. Hydrogen diffusion can also change the oxidation state of the inclusion fluids, (Roedder, 1972).

Although leakage can and does occur, it is, however, not a common phenomenon and the main arguments for this are as follows:-

(a) The uniform phase ratio present amongst the non-boiling fluid inclusions of a given population is strong evidence for the absence of leakage in these inclusions; leakage would affect the liquid/vapour phase ratio.

(b) Reproducible liquid/gas $Th^{o}c$ values of fluid inclusions which have been heated to well above their homogenisation temperatures, (Roedder and Skinner, 1968). Leakage in these cases is dependent on the amount of overheating, (i.e. that increment of temperature above the liquid/gas $T_h{}^{o}c$ value) and the development of cleavage of the host mineral. In this study a random check on the reproducibility of $Th^{o}c$ values has shown that leakage caused by heating is uncommon. In the case of pegmatitic topaz nearly all silicate/hypersaline complex inclusions when heated to above $500^{o}C$ showed leakage. This is chiefly due to the good basal cleavage of the topaz which can open as a consequence of heating to high temperatures; this will open fluid inclusions to cause them to leak.

(c) The frequently observed systematic relationship between crystal zoning and the temperature and salinity of primary inclusions.

(d) Pressure estimates of the contents of inclusions (from crushing experiments; Roedder, 1963). Since the estimated pressures of fluid inclusions are often dissimilar to their external pressures, leakage cannot have occurred.

4. The origin of the inclusion is known.

The identification of the origin of fluid inclusions is probably the greatest single source of ambiguity as most fluid inclusions are viewed in two dimensional situations only. Conclusive evidence for the primary (Cogenetic) origin of fluid inclusions is not always seen while evidence of secondary (post-crystallization) origins are usually clearly visible. The criteria used for the distinction of primary (inclusive of pseudosecondary fluid inclusions) and secondary fluid inclusions are discussed in pages 218 and 220.

B Methods.

The determination of the temperature of formation in fluid inclusions has been made using the homogenisation method pioneered by H. C. Sorby (1858). The principles of this method are described earlier on in this chapter.

The homogenisation method involved the use of Leitz microscope heating stage 1350. The instrumental assembly, including the systems of calibration and temperature recording are described in Appendix I.

The homogenisation procedure involved the heating of fluid inclusions under simultaneous optical observation until homogenisation in either the gas or liquid phase was achieved. The heating cartridge supplied the necessary heat by conduction to the sample which was in the form of parallel sided doubly polished plate or cleavage fragment. The mineral samples with their contained fluid inclusions were heated initially at a fast rate until homogenisation was about to occur. At this point the temperature was kept constant for the thinner sample plates/fragments

(≈ 0.1 to 0.3 mm thick) during a minimum period of 2 minutes, and for the thicker plates/fragments (≈ 0.3 mm to 0.6 mm) for a minimum period of 5 minutes. This interval was to allow the heating chamber and the sample to reach thermal equilibrium. The heating process was continued after this interval but at a slow rate less than 5°C/min until homogenisation of the fluid inclusions was achieved. In this way errors due to non-equilibrium thermal gradients were minimised.

The millivolt readings collected by this method were converted into temperature data (in °C) by reference to the calibration curves.

C. The associated problems.

The use of high power magnification (x 32 objective lens) necessary to observe small fluid inclusions (i.e. < 10μ) was not adequate to resolve the vapour bubble and consequently accurate homogenisation determination could not be made on these fluid inclusions. The large working distance intrinsic to the design of the Leitz optics used in conjunction with the heating stage meant that scattering of light reduced the brightness and resolution of the image. Some improvement was obtained by the use of directional fibre optics (Schott) but with limited success only.

Another problem was the frustrating habit of a bubble to hide itself in a dark corner or rim of the fluid inclusion so that observation of the precise temperature of disappearance was impossible. The heating run(s) had to be discontinued or repeated in these cases.

Fortunately, the occurrence of metastable vapour bubbles in fluid inclusions at temperatures well above the expected $Th^{o}c$ value was not a feature of this study.

Since a vertical thermal gradient is known to exist within the sample plates or cleavage fragments, it was considered important to take note of the approximate positions of the fluid inclusions within the sample plates or fragments the thickness of which were previously measured with a micronmeter. This helped the choice of the appropriate calibration curve by reference to which the $Th^{o}c$ values were deduced. Thereby the error caused by the vertical thermal gradient was minimised.

D After trapping changes that affect $Th^{o}c$ data.

Leakage.

Leakage in fluid inclusions will affect the $Th^{o}c$ values. Leaked fluid inclusions can be recognised by a non-uniform liquid-gas phase ratio in a given cogenetic population of fluid inclusions and also by the changes in the size of a gas bubble after each heating run is over. These inclusions can be distinguished from necked inclusions (which similarly have non-uniform liquid-gas phase ratios) by the poor reproducibility of the $Th^{o}c$ values. The leaked inclusions are also characterised by inconsistent $Th^{o}c$ values. In this study

any $Th^{o}c$ values were discarded if similar characteristics to those described above were shown.

Necking down.

Necking down is another phenomenon which can also affect the $Th^{o}C$ value. It is a process by which a simple large inclusion on cooling becomes divided up into a series of smaller ones through the process of recrystallization and solution of the walls of the original large inclusion. The rationalisation of the inclusion surfaces, often to negative crystal or spherical forms, thus reduces the surface free energy. The necking down process is expected to be more common for high temperature fluid inclusions particularly during the first 50 - $100^{o}C$ of cooling, (Roedder, 1967). If the necking down process is completed while the inclusion fluids involved are still homogeneous, the phase ratios and the chemistries of the necked inclusions will be uniform and their $Th^{o}C$ values consistent and valid. The opposite effect will result if the process of necking down occurs in a fluid inclusion that has already nucleated a gas bubble and, or precipated a daughter mineral phase in its fluids. The resultant erroneous inconsistent $Th^{o}c$ values in this type of necked inclusion can be used as an identification criterion in a situation when non-uniform phase ratios and characteristic 'tailed-off' shapes so typical of this type of necked inclusions are not observed. Some fluid inclusions which have undergone incomplete necking are seen to be linked by a tiny tube.

E. Pressure Correction.

The homogenisation temperature ($Th^{o}c$) and trapping temperature ($T_T{}^{o}c$) of an aqueous fluid inclusion are related as shown by the following equation:-

$$T_h + \Delta T = T_t$$

ΔT = Temperature Correction for pressure.

A pressure correction is needed because the homogenisation temperature of a non-boiling aqueous inclusion is only the minimum trapping temperature and consequently a positive temperature correction (ΔT) is needed for the effects of higher pressure which prevailed under the conditions in which the inclusion was trapped. However, an aqueous inclusion which was formed from a boiling liquid needs no such pressure correction because the vapour pressure of the boiling fluid must have been greater than, or equal to, the confining pressure at the time of trapping. Thus $Th = T_t$.

A pressure correction can only be applied if the salinity of the inclusion fluids and the depth and confining pressure regime, (lithostatic/hydrostatic) at the time of trapping are known. The methods for determining salinity of inclusion fluids are discussed

in detail in sections B2 and B3. The pressure of formation can be estimated from a knowledge of the depth of formation (or burial) of the host mineral (this may be provided by a stratigraphical evidence) using the following formula: hdg = Pressure, where h = depth; g = gravitational constant; d = density of the overburden.

In the above pressure estimation it is important to assess whether the pressure regime is dominantly lithostatic or hydrostatic because of the different densities of a column of aqueous fluid ($\sim 1 g/cm^3$) and a column of rock (average continental rocks $2.7 g/cm^2$). In general total lithostatic load will be 2.7 x hydrostatic pressure.

In determining whether the pressure of a mineralising fluid was lithostatic or hydrostatic or of an intermediate value between the two extremes, it is important to consider the following factors:-

1. The mechanism responsible for creating and dilating a fracture.

2. The attitude of the fracture.

When a horizontal fracture is opened hydraulically by the pressure of a mineralising fluid, the pressure,

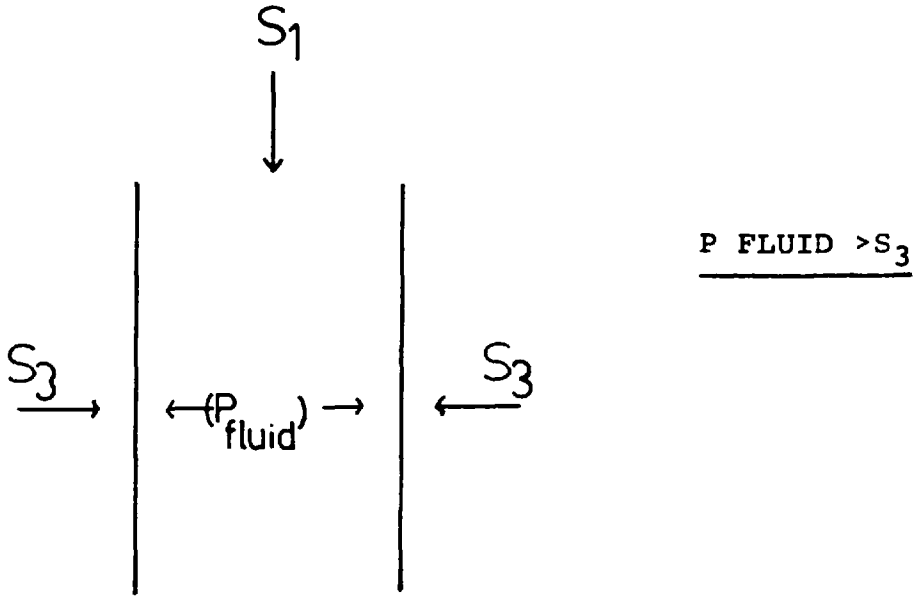

Figure 16. The relationship of fluid pressure, (P fluid) of fluids filling a vertical fracture with the confining (S_3) and lithostatic (Si) stress.

(P fluid) involved must be equal to or greater than the lithostatic load stress. However, when a vertical fracture is dilated by the hydraulic pressure of a mineralising fluid, the pressure involved (P_{fluid}) must be equal to or greater than the horizontal confining stress (S_3), (Fig. 16), which will normally be less than the lithostatic stress (S_1) (Rutter, 1970; Fyfe, Price and Thomson, 1978). Thus the maximum fluid pressure involved will normally be less than the calculated lithostatic pressure for the same depth. For an inclined fracture the effective normal stress (S_n), which must be opposed by the fluid pressure will be less than S_1 and greater than S_3. In the case of greisen-forming fluids impounded within the roof zone of a granite, the pressure of these fluids must be less than, or close to, the lithostatic confirming pressure. In situations where a fissure is supported by the strength of the host rock the pressure of the mineralising fluid can be due to a hydrostatic head assuming that the supported system is opened to surface. Subvolcanic systems and hot springs open to surface would be examples of mineralisation in which a hydrostatic head pressure would normally operate at shallow depths.

For fluid inclusions formed from boiling fluids, the depths of formation can be estimated with reference to the data of Haas (1971). Using Haas' data it is important to

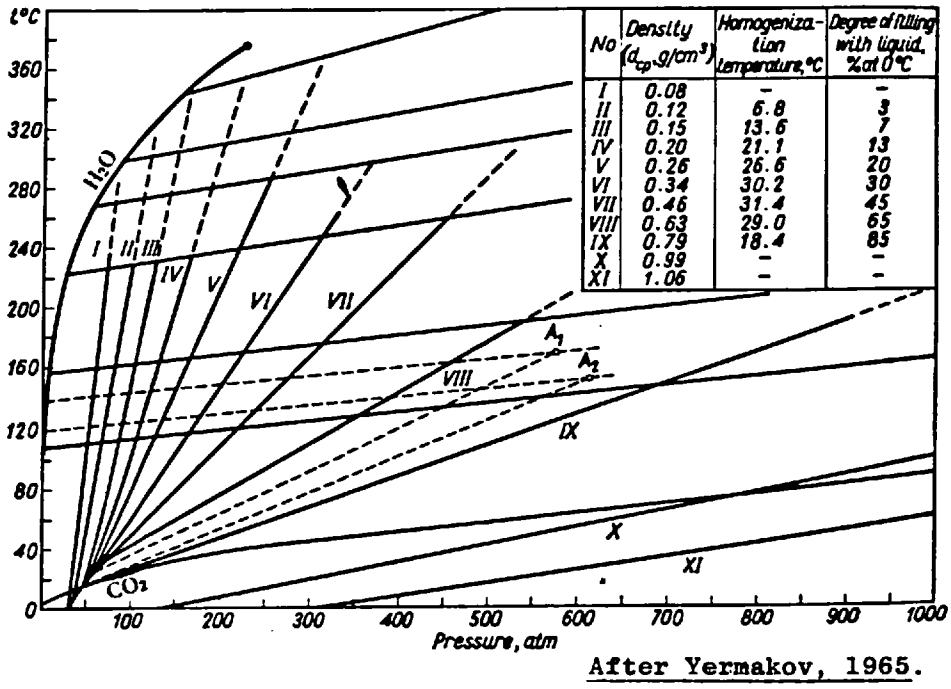

After Yermakov, 1965.

Figure 17. Combined PT diagram for water and CO_2.

realise that the pressure is assumed to be hydrostatic. An additional use of Haas' data is that it can be used to estimate the minimum depths of formation of the host mineral bearing fluid inclusions that were not boiling.

With a knowledge of the salinity and the pressure of formation it is possible to estimate the amounts of temperature correction needed by reference to the recently published pressure correction diagrams provided by Potter (1977). His diagrams are for NaCl brines from 0 to 25 weight percent NaCl and $T_h 0^{\circ}c$ up to $T_h{}^{\circ}c = 400^{\circ}c$. These diagrams can also be used to estimate the pressure of formation provided that salinity and T_h are known and that T_t can be determined using another pressure-independent geothermometer, (i.e. the $T_h{}^{\circ}c$ value of silicate melt inclusion = $T_t{}^{\circ}c$).

Another method of pressure correction involves the use of cogenetic pairs of CO_2 and H_2O inclusions. This method allows both pressure and temperature of trapping to be determined from the point of intersection of the isochores on a P-T plot (Fig. 17) of the heterogeneous system involved, (Roedder, 1967). However, the validity of this method is dependent on the assumption that the pairs of CO_2 and H_2O inclusions employed are cogenetic.

6.4. Identification and quantitative estimation of the daughter and liquid phases present in fluid inclusions.

A. Introduction.

Daughter mineral phases and liquid CO_2 are commonly encountered in fluid inclusions and their presence is an invaluable indicator of the saturation chemistry of the cogenetic inclusion fluids. The daughter phases are precipitated from inclusionsfluids saturated in their major elements during the cooling process. Because of the interest attached to these phases, it was thought relevant and important to make a study of the identity and the quantitative composition of the daughter mineral phases and liquid CO_2 by means of a combination of non-destructive methods using the Optical Microscope; the Microscope Heating Stage and the Microscope Freezing Stage.

Destructive methods involving wet chemistry such as the Crushing and Leaching Method, and the Drilling and Pipetting Method, were not applied in this study. These techniques and their associated problems are, however, described.

B. Non-destructive methods.

B.1. The Polarizing Optical Microscope.

Since mineral and liquid phases in fluid inclusions when examined under a polarizing petrographic microscope exhibit their diagnostic optical properties such as crystal habit, colour, refractive index (and relief), pleochroism, birefringence, and extinction angle, it becomes possible to identify or at least to limit the possible identities of these phases by using the above mentioned optical properties and it is also possible to make a semiquantitative volumetric analysis of the phases present.

Certain complications can arise with the use of birefringence and extinction angle properties since an accurate measurement of these respective properties in mineral phases present in fluid inclusions depends on the birefringence and extinction angle of the host mineral. For example, the birefringence of a mineral phase would be masked if the host mineral has a much stronger birefringence. In addition, the extinction angle of a mineral phase would be difficult to measure if it coincides with that of the host mineral. When two different minerals, for example, halite and sylvite, having similar optical properties could not be distinguished by this method, the Microscope Heating Stage was employed to resolve the problem.

The instrument used throughout this study was a Vickers polarizing petrographic microscope equipped with x 5, x 10, x 40 objective lens and a x 7 ocular lens. The fluid inclusion-bearing mineral samples under investigation were prepared in the form of parallel sided doubly polished plates, cleavage fragments and thin sections, the latter being suitable for qualitative examination only.

Results.

The daughter minerals identified in this study were halite, sylvite, calcite, anhydrite, opaques, (oxide/sulphide). The optical properties of these daughter minerals are as follows:

Minerals	Crystal habit	Colour	Relief	Pleochroism	Birefringence	Extinction Angle
Halite	Cubic	Colourless or white	Low to moderate	None	Isotropic	None
Sylvite	Cubic	Colourless or white	Low to moderate	None	Isotropic	None
Calcite	Rhombic	Colourless	High	None	Strong	Symmetrical to cleavage traces
Anhydrite	Prismatic lath	Colourless	Moderate	None	Strong	Parallel
Opaques	Cubic	Black	High	None	None	None
Opaques	Sphere	Black	High	None	None	None
Opaques	Speck	Black	High	None	None	None
Opaques	Plates	Black	High	None	None	None

Halite daughter phases were present almost exclusively in primary fluid inclusions from cassiterite and its gangue quartz and fluorite collected at the Waterfall Mine, Pelapah Kanan. A single halite daughter phase together with two unidentified birefrigent daughter phases were also recorded in cassiterite from the Sg. Besi Mine. Rare occurrences of halite were observed in primary fluid inclusions from cassiterites originating from the Chenderiang Valley tin field (Chenderiang Tin, S.E.A. mine) and the Sg. Lembing tin field (Willinks and Hantu Lode Systems, P.C.C.L.). The rarity of occurrence and the failure of this halite phase to dissolve at temperatures well above the liquid-gas homogenisation temperature. confirmed that the halite probably occurred as crystals suspended in the saturated mineralising fluids and these were subsequently trapped by the process of fluid inclusion formation. In addition to the halite daughter phases, the gangue fluorites from the Waterfall Mine also contained daughter anhydrite, calcite and opague plates, cubes and specks.

An unknown colourless and non-birefringent elongate lath shaped daughter mineral soluble at 175.5^{o}C was observed to coexist with a halite daughter mineral in a primary fluid inclusion from cassiterite, (Sample

A5, cass 1), collected at the Waterfall Mine.

Two birefrigent daughter materials, (one rectangular and the other pseudocubic) whose temperatures of solution are 146.5°c and 159°c respectively were unidentified. They are cogenetic with a duaghter halite phase because they occur in three primary cogenetic fluid inclusions from a cassiterite collected at the Sg. Besi Mine.

B2 Use of the microscope heating stage in determining the composition of fluid inclusions.

The occurrence of homogenisation phenomena of inclusion fluids and the solution of daughter phases upon heating the fluid inclusions can be used to provide important data on the identity of phases present in the respective fluid inclusions and their bulk composition, (Roedder, 1967). For example, the critical temperature for pure liquid CO_2 is +31°c and any deviation from this temperature indicates that the liquid is a mixture containing other organic and inorganic compounds such as methane, (critical point -82.1°c); ethane, (critical point +32.3°c); H_2S and H_2O. The high coefficient of thermal expansion of liquid CO_2 (32 times that of H_2O) is another useful criterion for the identification of liquid CO_2 in inclusions. The chemical composition of inclusion has an important effect on the homogenisation temperature,

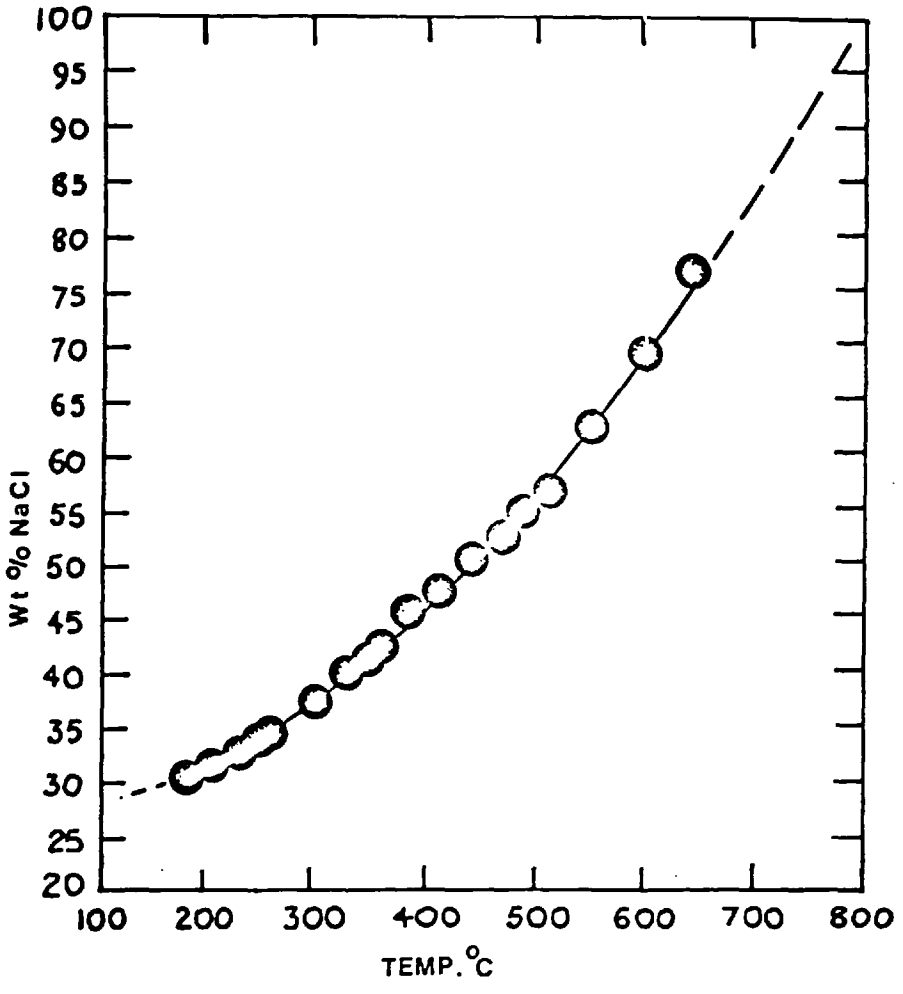

Fig. 18 Composition of the liquid phase of saturated aqueous sodium chloride solutions (From Sourirajan & Kennedy, 1962)

for example, the maximum $T_h{}^{o}c$ value for pure water is $374^{o}c$, (the critical temperature), but for brines it becomes much higher, (critical temperature of $471.5^{o}c$ was recorded for inclusion fluids with 34 equivalent weight % NaCl), (Sourirajan and Kennedy, 1962). The $T_h{}^{o}c$ value may be lowered if the inclusion fluids are low pressure gas or certain organic substances, (Roedder, 1967).

B.2.1. Apparatus and methods.

The instrument used was a Leitz 1350 heating stage mounted on a Leitz Nr. 494425 petrographic microscope equipped with x 10; x 22; x 32 objective lens and a x 7 ocular lens.

This method involved a slow progressive heating of fluid inclusions contained in thin parallel sided doubly polished mineral plates while at the same time observing and recording the temperatures and the rates of phase changes which occurred within the respective inclusions.

Using the temperature of solution of halite, it was possible to estimate the concentration of NaCl in that halite-bearing solution by reference to the NaCl concentration versus temperature of solution graph

POINT	KCl	NaCl	H_2O
O	13.0	39.0	48.0
P	6.96	22.54	70.50
Q	5.81	20.17	74.02

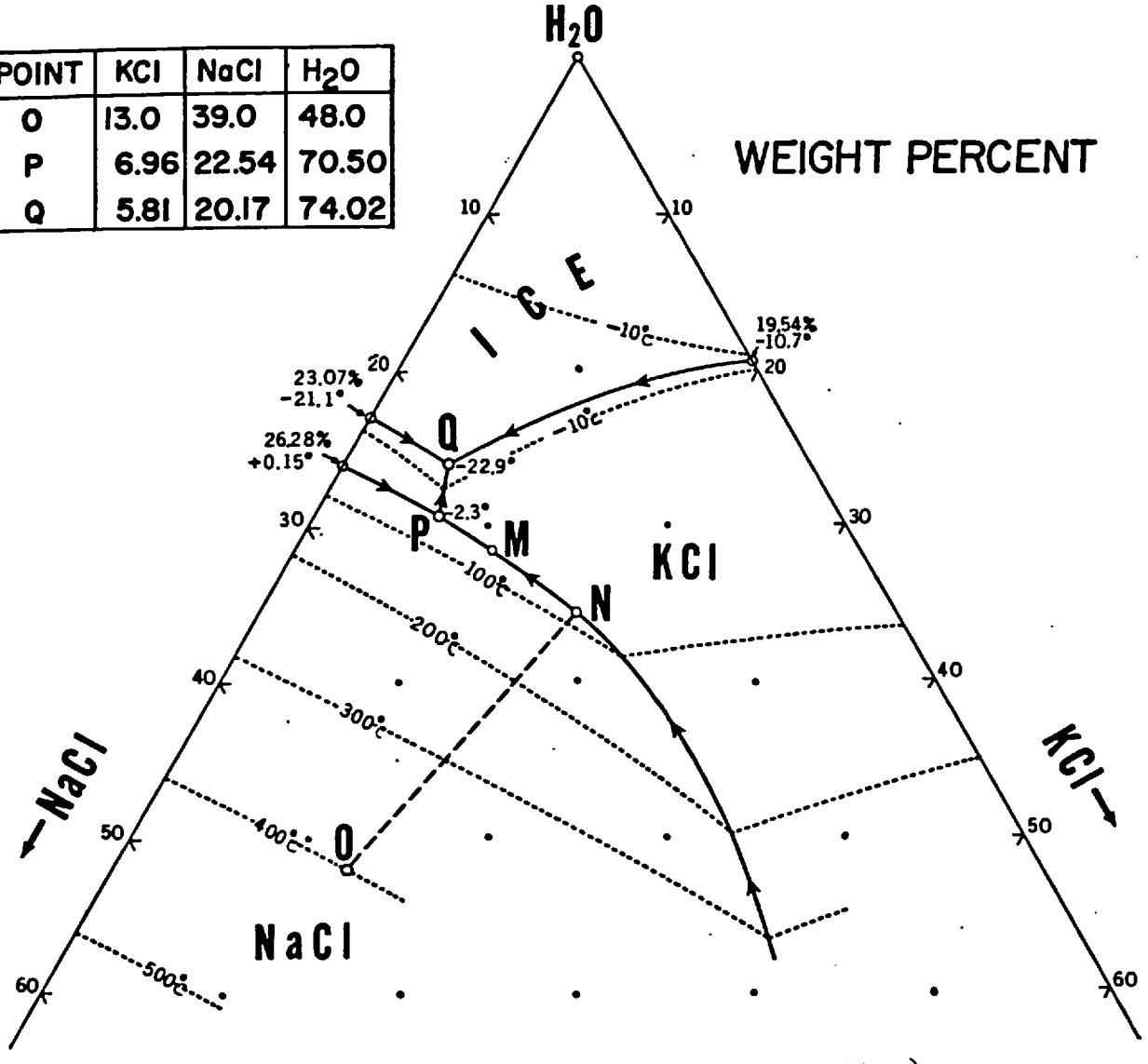

FIG. 19. Phase diagram for part of the system NaCl-KCl-H_2O. (After Roedder, 1971)

(Fig.18) provided by Sourirajan and Kennedy, (1962). Similarly, it was also possible to estimate the concentration of KCl in sylvite by reference to the NaCl-KCl-H_2O system phase diagram, (Fig.19) given by Roedder, (1971). Because of the very different temperatures of solution for coexisting halite, (200°c to 250°c) and sylvite (<150°c), it is possible to distinguish them by their T_{sol} values. In addition, the eight times higher coefficient of solubility for sylvite was also employed as a guide and additional criterion in distinguishing the latter from halite.

B.2.2. Results.

The presence of impure liquid CO_2 in cogenetic fluid inclusions from a colluvial/alluvial cassiterite from the Timah Gaya Mine, Kinta Valley was suggested by the high coefficient of thermal expansion and the homogenisation temperatures, (29.5°c, 19°c and 17°c), of the respective liquid. Judging from the low T_h°c values, the liquid was suggested to be an impure liquid CO_2 with admixtures of CH_4 and H_2O which were responsible for the depression of the T_h°c value of pure liquid CO_2. On the basis of the properties described in the previous section, all the isotropic cubic daughter phases were identified as halite with the exception of one occurrence of sylvite. The temperatures of solution of the halites and sylvite are listed in Table.2.

	Sample No.	T sol°c (Halitè)	Salinity (equiv. wt% NaCl)
	PK_3	156	29
	DIC_3	270.2	35
	PK1a	223	32.87
	A5	257.5	34.3
		250.5	34
Cassiterite		207	31.5
		222.75	32.5
		222.75	32.5
		242.5	33.58
	A5	134*	38 wt% Kcl
$^{\Delta}$Cassiterite	SB1.7	248	35
	D1Q1	224	32.87
$^{+}$Quartz	D1Q1	226	33
	D1Q1	224	32.87
$^{+}$Flourite	A1.F_4	224.5	33

* = Sylvite (wt% deduced from the phase diagram for part of the NaCl-KCl-H_2O System given by Roedder, (1971)).

\+ = Minerals from Waterfall Mine, Pelapah Kanan.

Δ = Minerals from Sg. Besi mine, Sg. Besi.

Table 2 shows the temperatures of solution for daughter halites and sylvite and the salinities of inclusion fluids which contain these daughter phases.

The salinities of the halite and sylvite-bearing inclusion fluids were determined by the methods described in the previous section and they are given in table 2. . From the table, it is clear that the salinity of halite-bearing solutions varies from 29 to 35 equivalent weight % NaCl.

Calcite and $CaSO_4$ daughter minerals recorded in the primary fluid inclusions from the gangue fluorites of the Waterfall Mine were insoluble even at temperatures well above the liquid-gas $T_h{}^oc$ value. This finding confirmed the identities of the respective daughter minerals as suggested by the optical microscope method.

Daughter opaque phases common in primary fluid inclusions from the gangue fluorites of the Waterfall Mine were also found to be insoluble even at temperatures well above that of liquid-gas homogenisation. This did not exclude them from being considered as daughter phases because of their consistent presence in the primary fluid inclusions.

B.3. The Microscope Freezing Stage Method.

The validity of measuring the salinity of inclusion fluids by the Microscope Freezing Stage Method is based

on the fact that the freezing point of a liquid lowers in proportion with increases in the salinity expressed as the equivalent weight % of NaCl in that liquid.

The instrument used for the measurement of salinity was a specially designed freezing chamber, (Rankin-Ferriday), on a Vickers ortholux petrographic microscope equipped with x 10 and x 22 objective lens and a x 7 ocular lens. The complete instrumental assembly including the systems of calibration and temperature recording are described in Appendix

The method of salinity determination involved the complete freezing of the inclusion liquids with cold N_2 gas passing over the parallel sided doubly polished sample plates or cleavage fragments and then allowing them to approach the thaw point, quickly at first and then very slowly at the rate of $0.1^{o}c$ per minute especially at temperatures within $15^{o}c$ of the expected freezing point. The melting process was controlled by progressive reduction in the flow of the coolant gas. During the warming up process, phase changes were observed optically. The temperatures of the occurrences of phase changes were also recorded. The freezing point of a liquid is considered as the temperature at which the last ice crystal melts. Using the freezing point data the salinity of inclusion fluids can be estimated

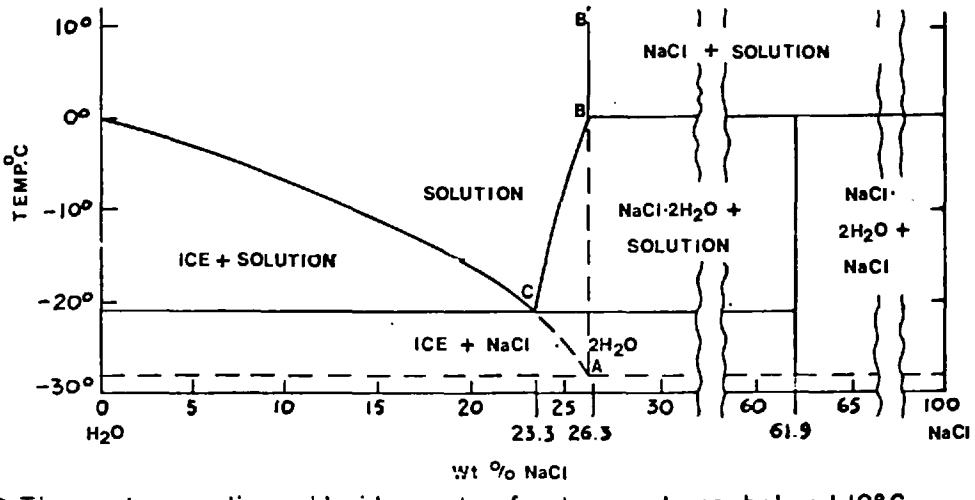

Fig.20.The system sodium chloride-water for temperatures below +10°C (From Roedder, 1962)

by reference to the phase diagrams for the NaCl-H_2O system for temperatures below +10°c, (Fig. 20) given by Roedder, (1962). The observation for the appearance of a liquid CO_2 phase in a previously two-phase gas-liquid filled inclusion during the freezing process is important as its appearance at temperatures below the normal room temperature does suggest that the CO_2 concentration in the inclusion fluids at room temperature was unsaturated. This phenomenon was observed particularly in Topaz from the Chenderiang Valley deposits.

B.3.1. Results.

The primary fluid inclusions from three cassiterite samples, (one from the Hantu Iode (P.C.C.L.) and the other two from the Timah Gaya Mine) were measured for salinity, but only the isolated single 2 phase vapour liquid primary fluid inclusion from the cassiterites of the Hantu Iode has given a freezing point of -0.2°c which gave a corresponding salinity of 0.3 equivalent weight % NaCl. The CO_2 and H_2O inclusions from the other two cassiterite samples could not be frozen at all even after being subject to 'shock' freezing overnight in an approximately -100°c cold alcohol bath. This kind of metastability indicates that the inclusion fluids were devoid of particles which could act as

nucleii for crystallization. Such physical purity of the inclusion fluids in turn suggests that the inclusion fluids were probably trapped from a slowly flowing column of mineralising fluids.

C Destructive methods.

C.1. Introduction.

A knowledge of the total chemistry of the inclusion fluids would help to understand better the chemical environment of transportation and deposition of minerals. There are three methods, (e.g. Crushing and Leaching, Drilling and Pipetting, and SEM and its energy dispersive x-ray analyser) available to achieve this aim but with only some success depending on the method used and the nature of the sample studied. The first two of the techniques mentioned above have not been applied to this study. However, the scanning electron microscope plus its energy dispersive x-ray analyser was used in the chemical investigation of the complex hypersaline and silicate melt inclusions from the pegmatitic topaz of the Chenderiang Valley tin field.

C.1.1. The Crushing and Leaching Method.

The crushing and leaching method is by far the commonest method of extraction of inclusion contents for chemical analysis. For gas analysis, simple crushing or ball-milling of a large, (several grams), sample in a vacuum have been used to open the contained fluid inclusions to release the gases to be analysed

by various freezing and absorption techniques, using volume and/or pressure measurements, (Roedder, 1967), and also by mass spectrometer, (Murray, 1957; Preisinger and Huber, 1964). The results of gas analysis can be invalidated if there is contamination of other gases from other sources, (Goguel, 1963). Surface adsorption of gases onto the walls of the instrument can be a problem in the gas analysis by mass-spectrometer. For analysis of the chemistries of inclusion fluids simple crushing or ball-milling in air followed by water or acid leaching followed by separation of the leachate from the host mineral by simple filtration, or membrane filtration and electrodialysis if ball-milling has been used, (Roedder, 1958; Goguel, 1963). Sensitive methods are required for analyses because of the very large dilution of the very small volume of inclusion fluids; therefore the favoured techniques are flame photometry; colorimetry, emission spectrometry specific ion electrolysis; wet chemistry; x-ray fluorescence spectrometry; neutron activation spectrometry and lastly atomic absorption spectrometry. The latter method is widely used for the analysis of major cations or cation ratios; flame photometry for K and Na; specific ion electrolysis for F; and neutron activation analysis for some heavy metals, (Czamanske et. al., 1963), and Cl, (Roedder, 1972).

Chemical contamination of the leachate from solution of ions from the broken surfaces of the host mineral or even very minute amounts of impurity minerals, (Correns, 1940), or even from 'Analar' grade reagents and apparatus, (Roedder et. al., 1963, p. 359 - 360), can give gross error to the results since the volume of inclusion fluids involved is very small and its dilution by the leach solution is very large. Similar error can also arise from the loss of ions from inclusion fluids through surface adsorption on the large surface area provided by the crushed host mineral, (Roedder, 1972). The multiplicity of origins of fluid inclusions so typical of most minerals can be a major limitation on the interpretation of the results. Thus published chemical data on inclusion fluids can only be meaningfully interpreted if sufficient details of techniques, such as blank analyses of reagents and water, volumes of leachates used, analytical accuracy and the nature of the sample are provided.

C.1.2. Drilling and Pipetting Method.

Large single inclusions, (more than a few millimetres^3 in volume), can be opened by drilling into them and their fluids extracted for analysis by simple pipetting, (Davy, 1822; Roedder, 1967 and 1972). Smaller inclusions may be cracked open and a micropipette,

(Roedder, 1967) used. The errors resulting from these two methods of extraction are minor as compared to those of the Crushing and Leaching Method. This is because the inclusion fluids involved are larger in volume and they display increased solute concentrations.

Geological settings of tin lodes.	Tin lodes emplaced within the margins of granitoids.			Tin lodes emplaced close to the margins of granitoids.			Tin lodes implaced further away from the margins of granitoids.					Primary environments of unknown relationship to granitoids.		Colluvial/Alluvial environments.						
Sample Locations	Sg. Pari	Gambang	Sg. Besi	Pelapah Kanan	Tekka Hill	Chenderiang Valley	400' stope	Hantu 600' stope	Lode 600' stope	(P.C.C.L., Sg. Lembing) 1200'	Willinks Lode	Hock Hing Leong Mine, near Pusing.	Siputeh	Tg. Tualang Area. Timah Gaya Mine	Dato Sherri & Sons	Foong Seong Mine	Anglo Oriental Mine.	Gopeng	Liang Pong Mine, Gambang.
Sources of Cassiterites.	Cassiterite-quartz veins in biotite granite.	Cassiterite-bearing greisenised quartz-muscovite granite.	Cassiterite-quartz veins in granite(s).	Cassiterite-K-feldspar quartz-flourite veins in hornfels.	Cassiterite-Wolframite--Arsenopyrite-quartz veins in marbles.	Probably the topaz-bearing pegmatites in marbles.	Cassiterite-chlorite hypogene lodes in hornfels.					Cassiterite-quartz vein in marble.	Cassiterite-quartz veinlets in hornfels.	The nature of the sources for these colluvial/alluvial cassiterites in not known.					
TYPES OF INCLUSIONS IN CASSITERITES 2 phase L + V	✓	✓	✓	✓	✓	✓	✓	✓	✓	-	✓	✓	✓	✓	✓	✓	✓	✓	✓
3 phase L + V + halite.	Rare	-	Rare	✓	Rare	Rare	Rare	Rare	-	Rare	Rare	Rare	-	-	-	-	-	-	-
3 phase L + V + S Solid phases.	-	-	Rare. 1 Biref P cubic? 1 Biref Rectangular?	Rare. 1 Non-biref lath? (Soluble).	-	Rare 1 Non-biref mineral? (Insoluble).	-	-	-	-	✓ 2 lath(?) 1 sphere	-	-	Rare 1 calcite (insoluble)	-	-	-	Rare 1 A opaque	Rare 1 non-biref Nacl(?) 1 biref-P. cubic calcite.
3 phase CO_2 rich inclusion.	-	-	-	-	-	-	-	-	-	-	-	-	-	✓	-	-	-	-	-
Monophase gaseous inclusions.	-	✓	✓	✓	✓	✓	✓	✓	✓	-	✓	-	✓	✓	✓	✓	-	-	✓
Monophase aqueous inclusion	-	-	-	-	-	-	-	✓	-	-	-	-	-	-	-	-	-	-	-
Solid inclusion	-	qtz	-	Magnetite Tourmaline	-	-	-	-	-	-	-	-	-	Tourmaline a Ca and Si bearing phase.	-	qtz	-	-	-
Occurrences of boiling	-	✓	✓	✓	✓	✓	✓	✓	✓	-	✓	-	✓	✓	✓	✓	-	-	✓

Table 3 showing the petrography of primary fluid inclusions in cassiterites.

6.5. Petrography of the primary fluid inclusions from cassiterite, and gangue quartz, fluorite and calcite and their signficance.

A. Introduction.

The fluid inclusions in the minerals studied were classified on the basis of the phase proportions of liquid, vapour and solid phases which filled the inclusions as observed at room temperature.

B. Primary fluid inclusions in cassiterites from sixteen chosen tin deposits.

The probable primary and pseudosecondary fluid inclusions as observed in cassiterites collected from sixteen localities can be classified into five types whose distribution patterns in the respective cassiterites are shown in Table 3. The distribution pattern and the significance of the five types of primary fluid inclusions are described below:

Type 1. These are two phase inclusions consisting of vapour and liquid, (Plate 63A). They are common in all the cassiterites studied which suggests that the mineralising tin-rich hydrothermal fluids have a

PLATE 63.

A. A cogenetic group of 2 phase (L+V) primary fluid inclusions, (Types I & II), is orientated with their long axis parallel to the coloured growth zones of cassiterite from the Waterfall Mine at Pelapah Kanan. These inclusions show a variation in their phase ratios indicating they were formed from a boiling fluid medium.

B. A 4 phase (L+V+halite (a) + an unindentified daughter phase (b)) primary fluid inclusion (Type IV) in cassiterite from the Waterfall Mine at Pelapah Kanan.

C. A 3 phase (L+V+halite(arrowed)) primary fluid inclusion (Type IV) showing the presence of halite (arrowed) in cassiterite from the Waterfall Mine at Pelapah Kanan.

10µm

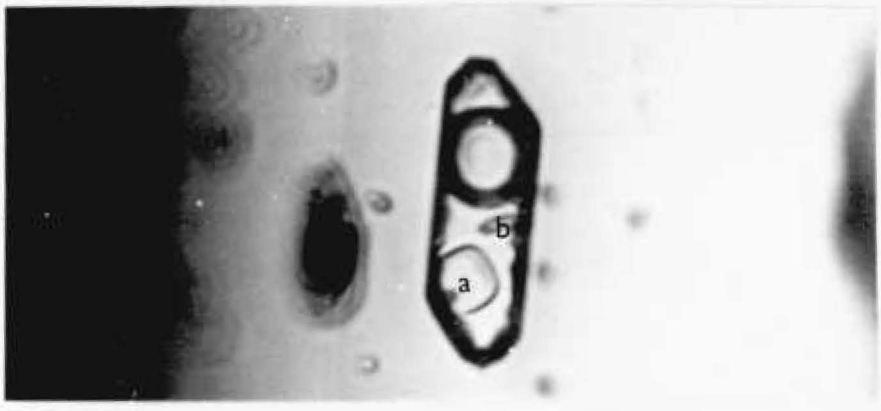

25µm

25µm

salinity not more than 26 equivalent wt% NaCl. Occasionally they are found cogenetic with gaseous inclusions, (Type II), in boiling assemblages. The occurrence of fluid inclusion assemblages indicative of boiling in cassiterites from lodes such as the Willinks and Hantu lodes, (P.C.C.L.) and the lodes of the Waterfall Mine, (Pelapah Kanan), which give evidence of episodic dilational opening suggests that these dilational episodes were accompanied by episodic pressure changes which led to boiling of the mineralising tin rich fluids

Type II. These are gaseous inclusions often with a thin rim of liquid, (Plate 63A). They are common in all the cassiterites studied which suggests that boiling was a widespread phenomenon.

Type III. These are monophase liquid inclusions and they are extremely rare as they are only present in some cassiterites from the Hantu lode, (P.C.C.L.). These liquid inclusions are likely to be metastable assemblages due either to insufficient cooling or the absence of nucleii for the nucleation of vapour bubbles.

Type IV. These are three phase inclusions consisting of liquid, vapour and an additional solid phase, (such as halite, sylvite, calcite, opaque, an unknown soluble non-birefrigent lath and lastly an unknown insoluble non-birefrigent lath). The three phase

PLATE 64.

Type V. H_2O-CO_2 fluid inclusions showing the presence of CO_2 vapour (a) CO_2 liquid, (arrow b), and aqueous liquid, (c). The largest inclusion, (arrowed), has also trapped a primary inclusion of calcite, (d), (Plane Polarized light).

100μm

(L+V+halite) inclusions, (Plates 63B and 63c), are generally rare but not for the cassiterites from the tin lodes at the bottom, (Bench A), of the Waterfall Mine in Pelapah Kanan. The rarity of the occurrences of some of the solid phases mentioned above combined with their failure to dissolve even at temperatures well above that of liquid/vapour homogenisation are evidence indicative of an origin as "captive" phases. One of the halite-bearing fluid inclusions from a cassiterite of the Waterfall Mine has an additional unidentified daughter phase which is non-birefrigent, lath shaped and has a solution temperature of 175.5^{o}c, (Plate 63B).

Type V. These are three phase fluid inclusions containing CO_2 vapour, liquid CO_2 and aqueous fluid, (Plate 64). The presence of liquid CO_2 in these inclusions indicates that the CO_2 content of the coeval inclusion fluids was greater than 2% by weight, (Alderton, 1977). The Type V fluid inclusions are extremely rare in the samples of cassiterite investigated by the writer. They were observed only in the cassiterites from two neighbouring mines, (Timah Gaya and Dato Sherri and Sons Mines), located at the south western flank of the Kinta Valley tin field near Kampong Timah Gaya. This type of inclusion has been recorded by Little, (1960), in Western Malaysian berly, cassiterite and quartz from pegmatites and hypogene tin veins. He has also recorded an isolated

H_2O-CO_2 inclusion, (Type V), in cassiterite from a vein emplaced in limestone.

The CO_2 content in tin rich fluids can be derived from the metamorphism of carbonate bearing rocks or as a primary component separated from a previously homogeneous CO_2-H_2O mixture on cooling, (Poty, Stalder and Weisbrod, 1974). The CO_2 may have acted as a ph buffer which could adjust the ph in tin rich fluids to an alkaline condition favourable for the breakdown of a tin complex which could have subsequently led to the precipitation of tin as an oxide (SnO_2) phase. Alternatively the CO_2 could have also formed a bicarbonate complex with Sn which can transport Sn in hydrothermal fluids.

B.1. Primary fluid inclusions of post-cassiterite vein quartz from Hantu lode (P.C.C.L.) and the lodes from the Waterfall Mine, (Pelapah Kanan).

The primary fluid inclusions in vein quartz can be classified into two main types. The criteria used for assessing the primary origin of fluid inclusions in non-crystalline milky vein quartz are as follows:

1. The inclusions should occur isolated and

2. The inclusions should occur as isolated

PLATE 65.

A. An isolated 2 phase (L+V) primary fluid inclusion (Type I) in vein quartz from the tin lode of the Waterfall Mine at Pelapah Kanan.

B. An isolated 3 phase (L+V±halite (arrowed)) primary fluid inclusion (Type II) in vein quartz from the same deposit as above.

C. A large 3 phase (L+V+ a birefringent rhombic mineral phase (arrowed) which is probably calcite) primary fluid inclusion (Type II) in fluorite from the same deposit as above.

25µm

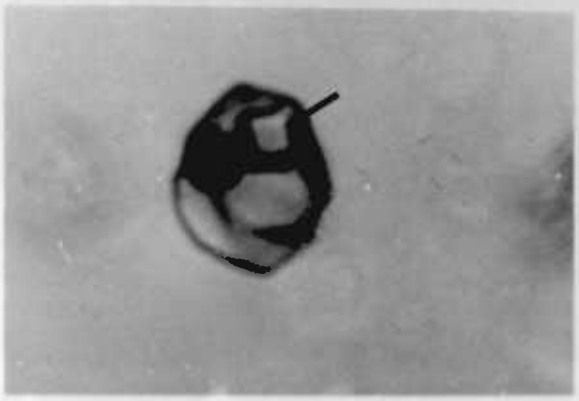

25µm

100µm

groups not associated with any planar systems.

Type 1. These are two phase inclusions consisting of vapour and liquid, (Plate 65A), and they are common in the quartz from the Hantu, the Waterfall Mine and the Tekka lode systems. The inclusion fluids in these fluid inclusions have a salinity of less than 26 equivalent wt % NaCl as indicated by the absence of daughter halite in these fluid inclusions.

Type 2. These are three phase inclusions containing vapour, liquid and a solid phase, (Plate 65B). The solid phase is often halite, but it is very rarely found together with a captured opaque or calcite phase. This type of fluid inclusion is cogenetic with Type 1 fluid inclusions and it is common in vein quartz from the Waterfall Mine. This suggests that the post-cassiterite quartz fluids were diluted as a consequence of inefficient mixing between the less saline cooler meteoric waters and the denser and hotter saline brine.

B2. Primary fluid inclusions of post-cassiterite late vug quartz from the Hantu lode (P.C.C.L.) and the lodes from the Waterfall Mine.

These inclusions can be classified into two types as follows:

Type I. These are two phase inclusions containing

vapour and liquid and they are associated with equivalent number of monophase Type II fluid inclusions in the vug quartz from the Hantu lode. In the case of the vug quartz from the tin lodes of the Waterfall Mine, they are distinctly less abundant than Type II monophase liquid inclusions and they represent inclusions which were formed at higher temperatures than the latter fluid inclusions.

Type II. These are monophase liquid inclusions which are equally as common as their coexistent Type I fluid inclusions in the vug quartz from the Hantu lode, and they are likely to be metastable assemblages formed as a consequence of the absence of nucleii in the inclusion fluids for the nucleation of vapour bubbles. Thus the coexistence of these two types of fluid inclusions suggests that the physical cleanliness of the inclusion fluids was inhomogenous. In contrast, the Type II fluid inclusions are distinctly more abundant than the coexisting Type I inclusions in the vug quartz from the tin lodes of the Waterfall Mine at Pelapah Kanan. The predominant abundance of these fluid inclusions suggests that they are stable assemblages indicating a low range of formation temperatures from 70^{o}c to 20^{o}c, (Personal communication, Rankin, 1977), while the coexistent Type I fluid inclusions were formed at a relatively higher temperature.

B3. Solid inclusions in the vug quartz from the Hantu lode.

Calcite. These primary solid phases are recognised by their rhombic habit and strong birefringence. They are present only in some of the vug quartzs from the Hantu lode as expected in view of the calcareous nature of the pelitic country rock in the Sg. Lembing Area. The calcite rhombs aligned more or less parallel to the crystal margins of the euhedral vug quartz crystal. This distribution pattern could have been formed by the trapping of primary calcite rhombs suspended in calcium and carbonate saturated silica-bearing solutions. The latter interpretations is considered likely since calcite inclusions are not invariably present in all the vug quartzs examined.

B4. Primary fluid inclusions of vug quartz from the martitised magnetie skarn of the Waterfall Mine, (Pelapah Kanan).

The primary fluid inclusions in the two samples of the quartz studied can be classifed into three types as follows:

Tvpe I. These are two phase inclusions containing liquid and vapour and they are the main type in the vug quartz. The absence of halite daughters in these fluid inclusions indicates that they have a salinity

of less than 26 wt % NaCl.

Type II. These are three or four phase fluid inclusions containing liquid, vapour, and one or two solid phases. This type of fluid inclusion is extremely rare. The solids observed are:

1. A birefringent grain.

2. A non-birefringent phase.

3. Birefringent calcite and

4. A halite.

The first two of these were too small for microscopic observation of their crystal habit. The rarity of the occurrences of these phases in the Type I fluid inclusions suggests that they are probably captive phases.

B5. Solid inclusions in vug quartz from the martitised magnetite skarn of the Waterfall Mine, (Pelapah Kanan).

1. Calcite. These are common in the vug quartz developed within the martitised magnetite skarn ore body.

2. Green Chlorite. This mineral is common as

inclusions in the vug quartz and occurs as euhedral green crystals. Sometimes they are found togehter with solid inclusions of calcite within a single vug quartz. The presence of calcite and green chlorite solid inclusions in vug quartz indicates that the silica-bearing fluids were saturated in Ca, CO_2, Fe, Mg, Mn, Al and OH at the time of crystallization.

3. Unidentified red-brown neddles. These are also common and they are likely to be goethite needles mineralising along fractures in the vug quartz and thus they are epigenetic with respect to the host vug quartzs.

B6. Primary fluid inclusions of pale green fluorite from the tin lodes of the Waterfall Mine, (Pelapah Kanan).

The primary inclusions in the pale green gangue fluorites from the tin lodes at the Waterfall Mine are those which are isolated; these inclusions are not common and are of two types.

Type I. These are liquid and vapour-filled fluid inclusions which have only been seen in the late vug fluorite. Two such fluid inclusions from a population

PLATE 66.

A. An isolated Type II inclusion showing the presence of an opaque daughter phase and a rectangular isotropic daughter phase, (arrowed).

B. An isolated Type II inclusion showing the presence of two insoluble weakly birefringent hexagonal daughter phases (a) probably quartz, and also two opaque daughter phases. Note one of these opaques is cubic (arrowed) while the other is a granular form.

C. An isolated Type II inclusion showing the presence of a perfectly cubic halite daughter mineral (a) and an opaque phase (b) above it.

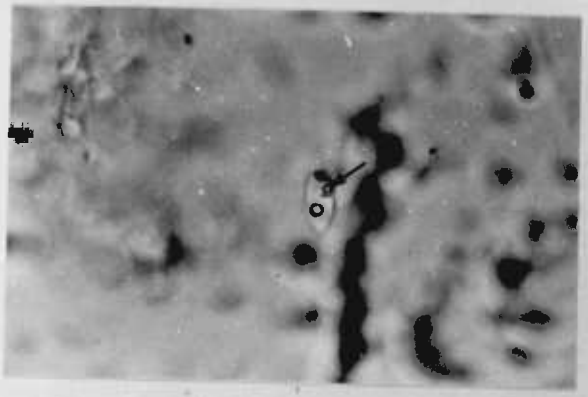

10µm

25µm

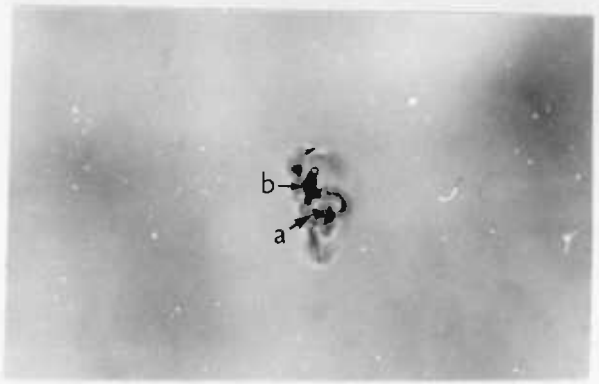

25µm

PLATE 67.

A. An isolated Type II inclusion containing at least 3 tiny opaque specks and four cubic halite phases. This inclusion was observed in fluorite.

B. A large isolated Type II inclusion in fluorite showing 3 opaque phases; two of these phases (arrowed) are cubic looking while the remaining opaque is elongate.

C. The same inclusion as above showing a poorly recrystallised halite daughter mineral. Note the poor crystalline form of the recrystallised halite, (arrowed).

10µm

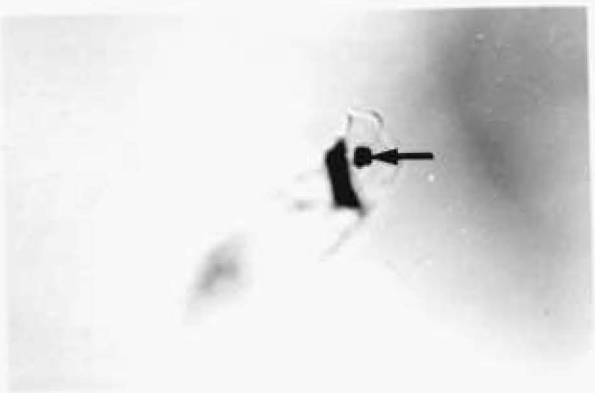

2.5µm

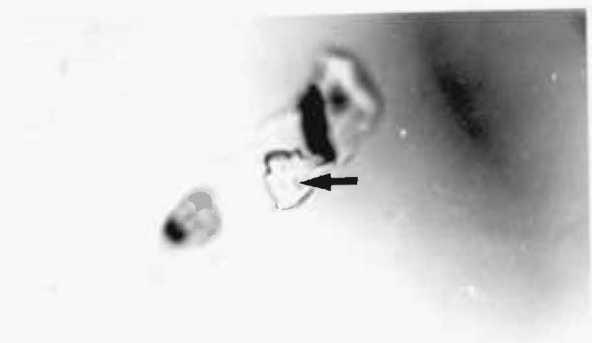

2.5µm

of five were found to be metastable as they each precipitated a daughter phase following a homogenisation heating run.

Type II. These are inclusions with a filling of liquid plus vapour plus one or more solid phases, (Plates 65C, 66A and B). Halite, calcite and $CaSO_4$ daughter phases were optically and thermally identified in some Type II fluid inclusions. Halite is always present together with primary opaque phases which occur as cubes, plates, spheres and tiny specks in isolated Type II fluid inclusions. (Plate 66C, 67A, B and C).

PLATE 68.

A. Transmitted light photomicrograph of a mutual intergrowth of cassiterite, quartz and muscovite in a greisenised granitoid from Gambang, (Crossed Polars).

B. This shows the divided inner, (G.T.F.1.a), and outer zone, (G.T.F.1.b), at the greisenised border of a quartz vein, (arrowed), (Gambang, Pahang State).

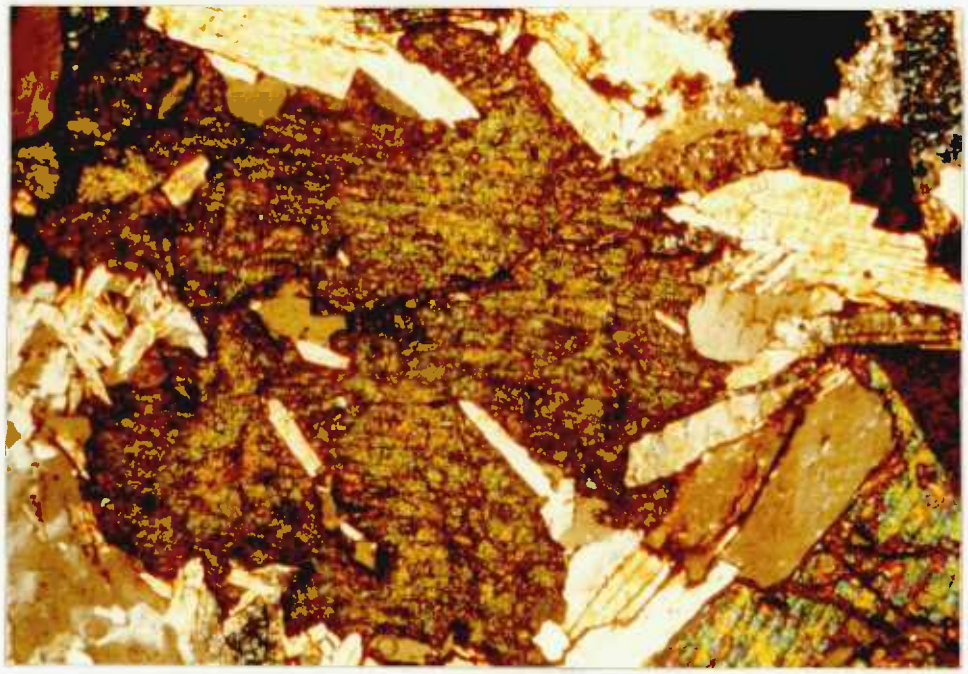

200µm

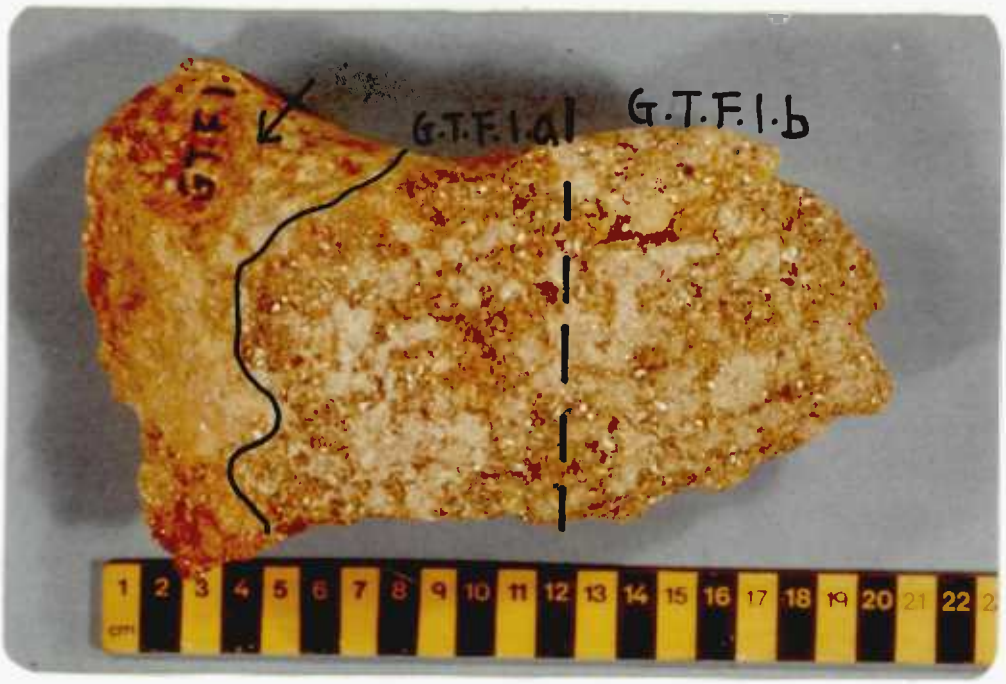
G.T.F.1
G.T.F.1.a
G.T.F.1.b
1 2 3 4 5 6 7 8 9 10 11 12 13 14 15 16 17 18 19 20 21 22
cm

6.6. The thermal history of the hydrothermal systems as reflected in the primary fluid inclusions from cassiterite and associated gangue minerals.

6.6.1. The $Th^{o}c$ values of primary fluid inclusions from cassiterites in lodes emplaced within the granites.

A. The Cassiterite-bearing quartz-muscovite greisenised granite of the Tong Huat Mine at Gambang.

A.1. Geological Setting.

This pervasively greisenised granite contains economic concentrations of cassiterite and it is now being mined by a gravel-pump method. The greisenised granite is composed of muscovite and cassiterite phenocrysts evenly distributed in a fine grained ground mass of muscovite and quartz, (Plate 68A). The homogeneous distribution of the cassiterite crystals together with the mutual muscovite cassiterite intergrowths indicate that they were formed contemporaneously with the greisenization process, hence the $Th^{o}c$ values measured on the primary fluid inclusions from these respective cassiterites would give an indication of the thermal conditions prevalent during the greisenization process. In addition to the greisenization process

Table 4. Showing the types of primary fluid inclusions and their Th°c values from the greisen-associated cassiterite of the greisenised granite of the Tong Huat Mine at Gambang.

Sample no.	Inclusion types	Th°c	σ
G.T.F.1.a			
	2 phase (L+V)	199.75	
C1	2 phase (L+V)	202.75	
	Gaseous inclusion	307*	
	2 phase (L+V)	199	
C2	2 phase (L+V)	219	
	2 phase (L+V)	250	36.7°c
C3	2 phase (L+V)	270	
C4	2 phase (L+V)	202.5	
	2 phase (L+V)	202.5	
		$\bar{x}$=228.1	
		n= 9	
G.T.F.1.b			
	2 phase (L+V)	305	
	2 phase (L+V)	333	
	2 phase (L+V)	333	
CO	2 phase (L+V)	333	
	2 phase (L+V)	332	
	2 phase (L+V)	332	
	2 phase (L+V)	303	
	2 phase (L+V)	303	
	2 phase (L+V)	307.1	
C1	2 phase (L+V)	319.6	
	2 phase (L+V)	323.6	
	2 phase (L+V)	330.6	
	2 phase (L+V) (leaked inclusion?)	405	9.9°c
	2 phase (L+V)	322.25*	
	2 phase (L+V)	323.25*	
C3	2 phase (L+V)	325.25*	
	2 phase (L+V)	324.25*	
	2 phase (L+V)	324.25*	
	2 phase (L+V)	329.5	
C4	2 phase (L+V)	322.5*	
	2 phase (L+V)	324.5*	
		$\bar{x}$=322.5	
		n= 20	

* = Th°c from inclusions indicative of boiling. Therefore, the Th°c = T_T°c.

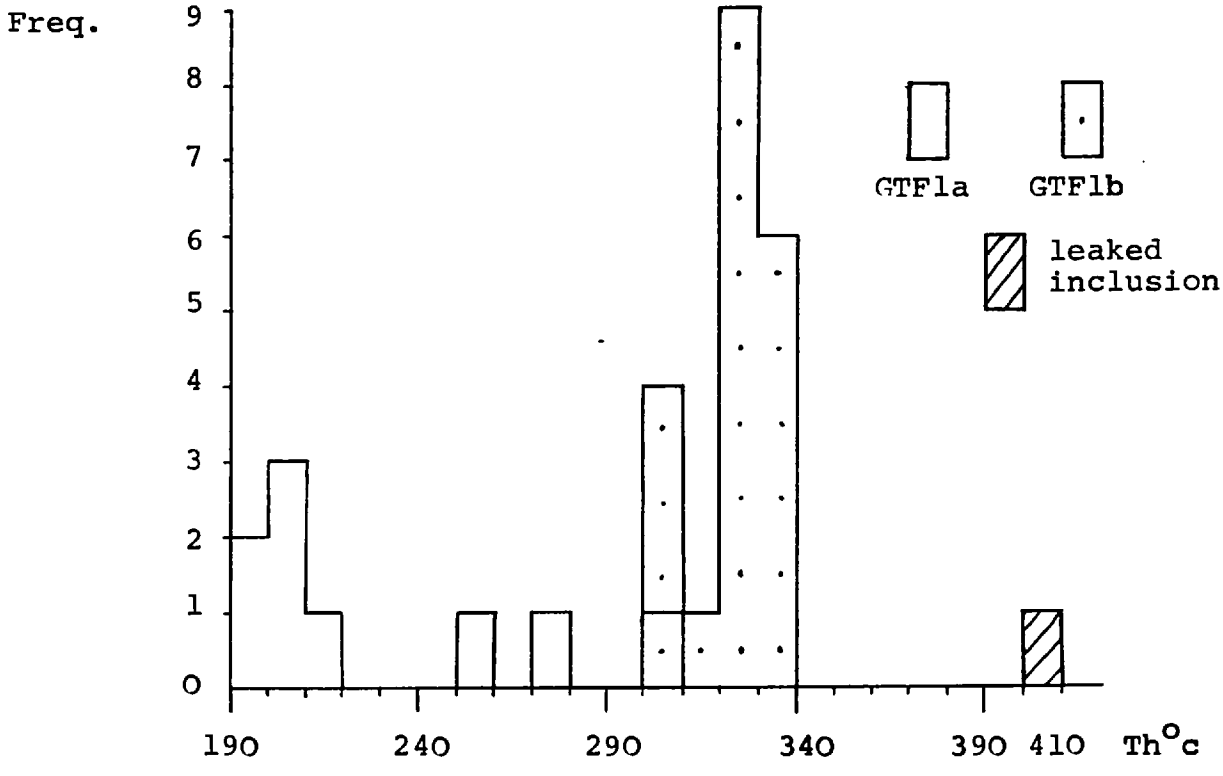

Figure 21 Frequency distribution histogram of Th°c values in primary fluid inclusions of greisen-associated cassiterite, (G.T.F.1.a and G.T.F.1.b), from the cassiterite-bearing quartz and muscovite greisenised granite of the Tong Huat Mine at Gambang.

the granite has also been cut by quartz veins following joints. It is known that vein and disseminated mineralisation except for the quartz veins, is totally absent in the contact rocks. This suggests that the country rocks were probably unfractured and impervious and consequently the greisenising fluids were impounded within the roof zone thereby producing confined pervasive alteration.

A.I.1. Interpretation of results.

Two samples of greisen-associated cassiterite crystals were taken from an arbitrarily divided inner, (GTF1a) and outer zone, (GTF1b), at the border of a quartz vein, (Plate 68B), for measurement of homogenisation temperatures. The Th^{o}c values for the non-boiling primary fluid inclusions have not been corrected for hydrostatic or lithostatic pressure effects because the depth of the mineralisation could not be reasonably estimated. The fluid pressure of the greisenising fluid must have been at maximum or less than the lithostatic pressure involved because there is no evidence of fracturing of the contact envelope. The Th^{o}c values from the inner zone are more scattered than those from the outer zone, (see Fig. 21 and Table 4). They range from 190^{o}c to 310^{o}c with a peak between 200^{o}c and 210^{o}c and they give a mean of 228.1^{o}c, (average of 9 determinations). This distribution is skewed strongly towards the high temperature end of the ranges. In

contrast, the Th°c values from the outer zone are less widespread, concentrating within a range of 40°c with the exception of one Th°c value (405°c) given by an isolated 2 phase (L + V) inclusion. This inclusion has probably leaked judging from its large vapour bubble. The Th°c values from this zone give a unimodal distribution ranging from 300°c to 340°c with the main grouping between 320°c and 340°c; a peak between 320°c and 330°c and a mean of 322.5°c were recorded. It is interesting to note that the Th°c values from the outer zone are distinctly higher than those from the inner zone; this difference is reflected by the chemistry of the cassiterites from the two zones. The negative temperature trend towards the quartz vein may have a genetic implication suggesting that the tin rich greisenizing fluids have migrated towards the cooling joints of the greisenised granite during the greisenization process. The joints were later infilled by quartz veins. The possibility of two generations of greisen-forming fluids of different temperatures is considered unlikely in this case because of the consistency of the Th°c values from each zone.

B. Cassiterite-chlorite-quartz veins with minor amounts of arsenopyrite in the biotite-granite of Sg. Pari Quarry.

B.1. Geological Setting.

The veins were emplaced along two sets of joints

in the medium grained porphyritic biotite granite exposed by quarrying for road metals, This exposure is a part of the granite forming the foot hills of the Kledang Range at the western flank of the Kinta Valley about 1½ miles north of Ipoh on the left hand side of the Ipoh-Butterworth trunk road.

These hypogene veins are composed of quartz, cassiterite, green chlorite and arsenopyrite. The quartz is massive and milky and it forms veins of 5 to 6 inches wide with intensely horisontally slickensided and crushed margins which were kaolinised at places. The veins are steeply dipping varying from 75^{o} to 85^{o} in both ESE and NNE directions and they have a strike of 022^{o} and 112^{o} east of north respectively.

Two phases of mineralisation were recognised at the Sg. Pari quarry and these were:

1. The early quartz veins with coeval coarse crystalline brown cassiterite and non-crystalline arsenopyrite, and

2. The cassiterite-green chlorite phase.

The quartz veins bear coarse crystalline brown cassiterites within their central portion at places.

The rare and non-crystalline arsenopyrite has only been observed once at the margin of a quartz vein where it occurs intergrown with quartz. This early phase of mineralisation was followed by the mineralisation of cassiterite and green chlorite which has consistently been deposited on only one margin respectively of the two quartz veins seen in the quarry.This observed asymmetric disposition of the cassiterite-green chlorite phase suggests that the latter phase was deposited after the formation of the quartz veins. The cassiterite-green chlorite phase was crushed by the post-mineralisation horizontal slickenside movements. Slickensides are common at the margins of the quartz veins observed.

B.1.1. Interpretation of $Th^{o}c$ values.

The cassiterites from these lodes were found to be lacking in suitable primary fluid inclusions for fluid inclusion study. Therefore only two fluid inclusions were measured for their $Th^{o}c$ values. The latter have not been corrected for pressure effect because the data required for pressure correction were not known.

The lower temperature, ($185^{o}c$ $Th^{o}c$) two phase (L + V) primary fluid inclusion is isolated and aligned parallel to growth zones. Thus this $Th^{o}c$ value should give an indication of the thermal condition of the mineralising tin rich fluids. In contrast to this $Th^{o}c$ value is the much higher $Th^{o}c$ value of $280^{o}c$ given by a

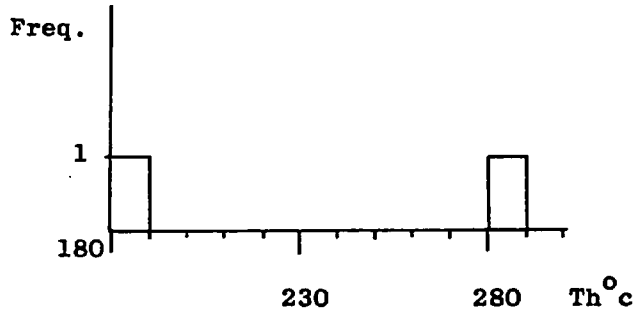

Fig. 22. Frequency distribution histogram of Th°c values from the primary fluid inclusions of cassiterites in the cassiterite-quartz lode of the Sg. Pari granite.'

two phase (L + V) fluid inclusion which is aligned almost at right angles to the growth zones, (Fig. 22). This inclusion is probably a pseudo-secondary fluid inclusion. The mean for these two Th°c values is 232.5°c.

C. Cassiterite-quartz-feldspar lode with minor sulphides from the Sg. Besi Mine.

C.1. Geological Setting.

The coarse colluvial cassiterites collected at the processing plant of the Sg. Besi Mine are believed to be from the coarse cassiterite bearing quartz-feldspar veins that traversed the decomposed stanniferous tourmalinised granite. These veins and granite have been described by M. P. Jones and M. M. Ghani, (1969, pg. 551 - 558).

C.1.1. Interpretation of Th°c values.

Measurements of Th°c values were made largely on the two phase (L + V) fluid inclusions and a few three phase (L + V + S) fluid inclusions. The uncorrected Th°c values give a unimodal distribution ranging from 320°c to 430°c. However, most of the Th°c values concentrate within 360°c and 400°c and they show a peak at 370°c to 380°c, (Fig. 23). The three phase (L + V + S) fluid inclusions give the highest Th°c values within 420°c and 430°c. The mean of these 16 Th°c values from

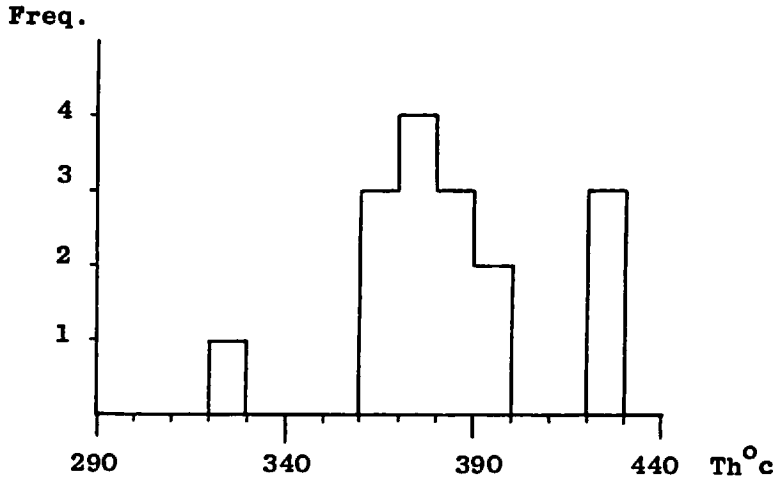

Fig. 23 showing the frequency distribution histogram of Th°c values from the primary fluid inclusions of the colluvial cassiterites from the Sg. Besi Mine.

Mineral	Sample Number	Inclusion types	Th°c	+ΔT°c	T_0°c	$(\chi-\bar{\chi})^2$	σ
Colluvial	SB1	2 phase (L+V)	377	?	-	34.81	
	SB1	2 phase (L+V)	384	?	-	1.21	
Cassiterite	SB2	2 phase (L+V)	387	?	-	16.81	
	SB3	2 phase (L+V)	370	?	-	166.41	
	SB4	2 phase (L+V)	364	?	-	357.21	
	SB5	2 phase (L+V)	383	?	-	0.01	
	SB6	3 phase (L+V)	329	?	-	2905.21	
	SB7	3 phase (L+V+S)	423.5	?	-	1648.36	
	SB7	3 phase (L+V+S)	426	?	-	1857.61	24.2
	SB7	3 phase (L+V+S)	420	?	-	1376.41	
	SB7	3 phase (L+V+S)	391	?	-	65.61	
	SB7	2 phase (L+V)	393.5(G)	?	-	92.16	
	SB7	2 phase (L+V)	379	?	-	15.21	
	SB8	2 phase (L+V)	374.5	?	-	70.56	
	SB9	2 phase (L+V)	362	?	-	436.81	
	SB10	2 phase (L+V)	364	?	-	357.21	
			$\bar{\chi}$=382.9			Σ9401.61	
			n= 16				

Table 5. Showing the inclusion types, the ΔT°c, the homogenisation

amongst ten individual colluvial cassiterite nuggets is 381°c, (Table 5).

Since the primary geological environment of these cassiterites is known it can be inferred that they had a similar depth of formation, (hence similar pressures of formation too), and consequently their Th°c values can be considered more or less proportional to the T_T°c values. This consideration allows a meaningful comparison of the Th°c values, (Rankin, 1978).

The close comparable Th°c values obtained give support to the belief that the cassiterites studied were derived from a common source.

6.6.2. The Th°c values of primary fluid inclusions from cassiterite, and its associated gangue quartz, fluorite and calcite of lodes emplaced either within or adjacent to the granite margins.

A. Alluvial cassiterites from the alluvial Timah Gaya Mine.

A.1. Geological Setting.

The primary source(s) of these cassiterites is not known, but their primary geological environments, (either endo or exocontact), were inferred by reference to their high Th°c values.

A.1.1. Interpretation of $Th^{o}c/T_{T}{}^{o}c$ values.

Two cassiterite crystals, one bearing CO_2 rich fluid inclusions and the other aqueous fluid inclusions, were measured for $Th^{o}c$ values.

The cassiterite-bearing the CO_2 rich inclusions contained interlocking aggregates of solid inclusions of Ferroan tourmaline and an unidentified calcium silicate phase. Thus the tin-rich fluids responsible for the crystallization of the respective cassiterite were supersaturated in Fe, Ca, Si and B together with CO_2.

The primary CO_2 rich fluid inclusions, (3 phase - CO_2-vapour-CO_2 liquid-aqueous liquid, show a variable gas-liquid phase ratio and they homogenised to both gas and liquid phase. This indicates that they are a boiling assemblage. This suggestion is further supported by the narrow range of $Th^{o}c$ values obtained which if otherwise would require an explanation in terms of necking down or leakage as being the cause for the variable gas-liquid ratio. Since the inclusions were boiling when trapped pressure correction is not needed here and consequently the $Th^{o}c = T_{T}{}^{o}c$. As experimental data for a boiling CO_2-H_2O system like that for boiling brines given by Haas, (1971), is not available at present, the depth of formation for the cassiterite cannot be estimated.

Mineral	Sample Number	Inclusion types	Th°c	+ΔT°c	ΣT_T °c	$(\chi-\bar{\chi})$	σ
Alluvial Cassiterite	KTG 1	3 phase CO_2 rich inclusion	403 (G)	0	403	64	
		3 phase CO_2 rich inclusion	398 (G)	0	398	169	
		3 phase CO_2 rich inclusion	507	0			
		3 phase CO_2 rich inclusion	390	0	390	441	
		3 phase CO_2 rich inclusion	394	0	394	289	
		3 phase CO_2 rich inclusion	429	0	429	324	17.42°c
		3 phase CO_2 rich inclusion	407	0	407	16	
		3 phase CO_2 rich inclusion	441.5	0	441	900	
		3 phase CO_2 rich inclusion	426	0	426	225	
					$\bar{\chi}$=411°c	Σ2428	
Alluvial Cassiterite	KTG 3	2 phase (L+V)	454	?		0.8464	
		2 phase (L+V)	464	?		50.13	
		2 phase (L+V)	479	?		579.85	
		2 phase (L+V)	439	?		253.45	
		2 phase (L+V)	439	?		253.45	
		2 phase (L+V)	446	?		79.57	14.9°c
		2 phase (L+V)	446	?		79.57	
		2 phase (L+V)	463	?		65.29	
		2 phase (L+V)	463	?		65.29	
		2 phase (L+V)	473	?		326.89	
		2 phase (L+V)	467.5	?		158.26	
		2 phase (L+V)	427.5	?		751.86	
			$\bar{\chi}$=454.92			Σ2664.46	
			n=12				

For KTG 1 CO_2 inclusion, Th°c = T_T°c because the inclusion fluids showed evidence of boiling.

Table 6. Showing the inclusion types, the ΔT°c, the homogenisation/trapping temperatures and their standard deviation (σ) of alluvial cassiterites from the Timah Gaya Mine.

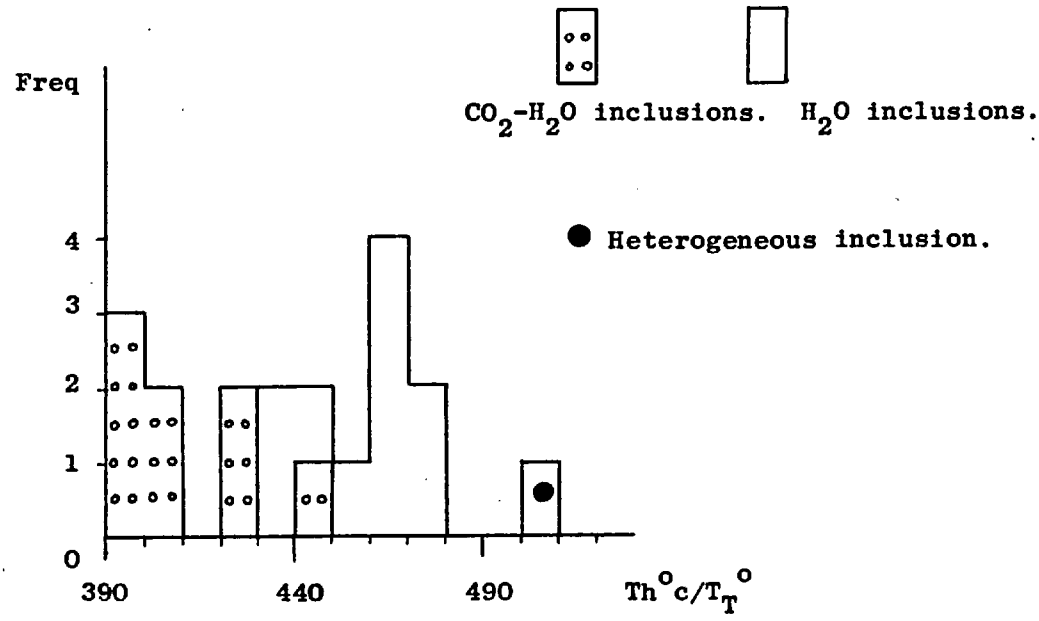

Fig. 24. Frequency distribution of the Th°c values from the primary fluid inclusions of coarse grained alluvial cassiterites from the Timah Gaya Mine near Kampong Timah Gaya.

The $T_T{}^{o}c$ values give a unimodal distribution which is skewed towards the high temperature end of the range and extends from $390^{o}c$ to $450^{o}c$ with a peak at $390^{o}c$ - $400^{o}c$, (Fig.24 and Table 6). The anomalously higher homogenisation temperature of $507^{o}c$ given by by a two phase (V+L) inclusion could have resulted from the inclusion having simultaneously trapped both vapour (gas) and liquid. Homogenisation of such inclusions can give anomalously high temperatures. The mean of these $Th^{o}c$ values is $411^{o}c$.

The other cassiterite-bearing aqueous fluid inclusions contains a cogenetic population of aqueous fluid inclusions which extends from the core towards the margin of the crystal. The $Th^{o}c$ values are not corrected for pressure effects because the depth of mineralisation and the salinity of the inclusion fluids are not known.

These $Th^{o}c$ values give a unimodal distribution which is skewed towards the lower temperature end of the range and extends from $420^{o}c$ to $480^{o}c$ with a peak between $460^{o}c$ and $470^{o}c$, (Fig. 24 and Table 6). From Table 6 it is evident that there was a variation in temperature as the cassiterite crystal grew. The temperature variation from margin to core is as follows: $465^{o}c$(Ave of 3$Th^{o}c$ values) $>449.3^{o}c$(Ave of 6$Th^{o}c$ values) $<470.25^{o}c$(Ave of 2$Th^{o}c$ values). The mean of these $Th^{o}c$ values is $454.9^{o}c$, (Table 6)

Since the $Th^{o}c$ values and the nature of the fluids of these two cassiterites are different, they are likely to be from lodes of different genesis which were emplaced close to their granitic sources as suggested by the high $T_T{}^{o}c/T_h{}^{o}c$ values recorded in them.

Inheritance of CO_2 from carbonate rich and marble host rocks cannot be a common phenomenon as CO_2 rich inclusions were not commonly seen in cassiterite or associated gangue minerals which have these types of host rocks, (Little, 1960). Thus the CO_2 content in KTG1 cassiterite is likely to be primary and related to the unmixing of a previously homogeneous CO_2-H_2O mixture into two immiscible liquid phases, (H_2O and CO_2 rich phases), as the ore fluids cool down, (Little, 1960; Poty et. al., 1974).

B. The tin lodes in the granite and its host rocks of the Eu Tong Seng Mine at Tekka Hill.

B.1. Geological Setting.

Tekka Hill sits on a "tin-granite" which forms part of the western margin of the Main Range Batholith. It is located midway on the right of the Gopeng to Simpang Pulai part of the Kuala Lumpur to Ipoh trunk road.

The heavily kaolinised granite of Tekka Hill was emplaced in Devonian Limestones, (now marble), and a

schist group, (Tekka Schists). Associated with the granite and its contact schist is a sequence of veins bearing different mineral assemblages as follows:

1. Cassiterite-Wolframite-arsenopyrite-quartz veins emplaced in the granite.

2. Wolframite-quartz veins in the granite.

3. Blue tourmaline (schorlite)-fluorite veins with traces of cassiterite emplaced in fluoritised-sericite-quartz host rock which is likely to be a fine grained fluoritised greisen.

4. Brown tourmaline -quartz veins.

5. Quartz veins in kaolinised granite.

6. Green fluorite veins and veins in kaolinised granite.

7. Muscovite-fluorite veins with traces of quartz in Tekka Schist.

8. Black tourmaline stringers in Tekka Schist and finally

9. A massive three feet wide Aplite vein with

disseminated tourmaline clots in kaolinised granite.

The greisen-forming process and the associated blue tourmaline fluorite-cassiterite veins mineralisation event must have occurred simultaneously. It was not possible to establish the paragenetic relationship between the various veins described above because the veins have not been seen to cross cut each other. Teh, (1974), has noted the absence of mineralisation in the highly jointed karst limestones, (marble), exposed by mining operations at the bottom of the no. 2 unit mine hole of Ee Tong Seng Mine Limited. The karst topography of the limestone was an efficient natural trap for the cassiterite-bearing colluvium and alluvium which have been the major economic source of the cassiterite.

Teh (1974) has observed that the tin lodes were emplaced in the Northern and Southern ridges of the southern flank of the Tekka Hills. These lodes are respectively known as the Northern Lodes and the Southern Lodes. These lodes were created as a system of mineralised dilatant fractures and joints in the host rock. The Northern Lodes strike in four directions, (035^{o}, 219^{o}, 213^{o} and 261^{o}). The most common strike is 261^{o} (WSW). The dips of these lodes vary from 42^{o} to 76^{o} towards the north-west,, but the commonest dip for these lodes is 54^{o} towards the North-Northwest. The Southern lodes also strike in four

Mineral	Sample number	Inclusion types	Th°c	ΔT	T_T°c	$(\chi-\bar{\chi})^2$	σ^2	σ
Vein	KT1.1	2 phase (L+V)	323.5	?	-	52.56	52.56	7.25°c
Cassiterite	KT1.2	2 phase (L+V)	338	?	-	52.56		
			$\bar{\chi}$=330.75 n=2			Σ105.12		
Quartz associated with Cassiterite	KT2.1	2 phase (L+V)	328*	?	-			
	KT2.1	2 phase (L+V)	245	?	-	20.25		
	KT2.1	2 phase (L+V)	241	?	-	.25		
	KT2.1	2 phase (L+V)	230.5	?	-	100		
	KT2.1	2 phase (L+V)	230.5	?	-	100	113.57	10.66
	KT2.1	2 phase (L+V)	230.5	?	-	100		
	KT2.2	2 phase (L+V)	244	?	-	12.25		
	KT2.2	2 phase (L+V)	262	?	-	462.25		
			$\bar{\chi}$=240.5 n=7	?		Σ795		

* leaked inclusion.

Table 7 showing the inclusion type, the homogenisation temperatures and their standard deviation (σ) of cassiterite and associated gangue quartz from the tin lodes of Eu Tong Seng Mine at Tekka Hill.

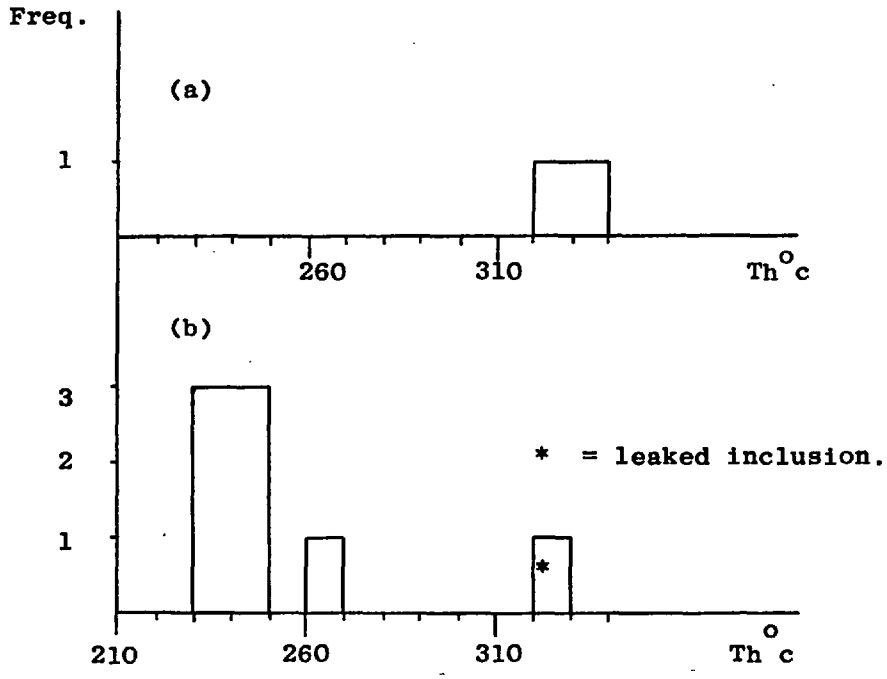

Fig. 25. Frequency distribution histogram of the Th°c values from the primary fluid inclusions of cassiterites (a) and quartz (b) in the cassiterite-wolfranite-arsenopyrite-quartz lodes of the Eu Tong Seng Mine.

directions, (312°, 351°, 245° and 277°), but the latter (277°) is the commonest of the four strike directions. The dips of these respective lodes vary from vertical to 62° towards the North-West, North-Northeast and North-East. However, a dip angle of 62° is most common for the Southern Lodes. An onservable strike length of up to 50 feet has been recorded by Teh, (1974), for some of these lodes.

The intensity of mineralisation appears to decrease towards the North-Western side of the Main Pit and also the Eastern end of the old mine workings. (Teh, 1974).

B.1.1. Interpretation of Th°c values.

Th°c values from the primary fluid inclusions in cassiterite.

The cassiterites in the tin lodes of the Eu Tong Seng Mine rarely contain suitable primary or pseudo-secondary fluid inclusions. Therefore only two, two phase (L+V) fluid inclusions were measured for their Th°c calues. The obtained Th°c values fall within a narrow range from 320°c to 340°c, (Fig. 25 and Table 7).

Th°c values from the primary fluid inclusions in cassiterite-associated gangue quartz.

Th°c values of the two phase, (L+V) fluid inclusions from the quartz associated with the cassiterite show a unimodal

distribution ranging from 230°c to 270°c; however, all but one Th°c value concentrate within 230°c and 250°c. The single anomalous temperature of 328°c (Th°c) is given by a member of an isolated group of three, two phase (L+V) fluid inclusions. This anomalous Th°c value is probably due to leakage.

The Th°c values for the cassiterite and quartz were uncorrected for pressure effects because the salinity of the fluids and the pressure of formation of these minerals are not available.

Judging from the higher Th°c values given by the primary fluid inclusions in the cassiterite as compared to those of quartz, it can be concluded that the deposition of cassiterite was before that of quartz. The decreasing temperature trend traced suggests that the hydrothermal fluids system of the tin lodes of Tekka Hill has undergone a progressive cooling throughout the mineral paragenetic sequence.

C. Colluvial cassiterites from the Chenderiang Tin S.E.A. Mine at the Chenderiang Valley.

C.1. Geological Setting.

The Chenderiang Valley tin field is located at the southeastern corner of the Kinta District and it extends from latitude 5°42½" north to latitude 5°45" north and from longitude 101.15" to longitude 101.17". This

valley has an area of 6 square miles and it is the property of the Chenderiang Tin S.E.A. Mine Sdn Bhd, a wholly owned subsidiary of Foo Yet Kai and Sons, (Malaysia), Sdn Bhd.

The Chenderiang Valley is flanked in the west by the Permain porphyritic biotite granite of the Bujang Melaka Mass and in the north and east by the Main Range batholith, (Dominantly U. Triassic). Karst limestone, (marble), bedrocks forming the floor of this valley have trapped large amounts of colluvial and alluvial cassiterite in the Quarternary sediments making the Chenderiang Valley a very productive tin field in the Kinta District of the Western Belt. In addition to the rich cassiterite-bearing colluvial and alluvial deposits occurrences of cassiterite-bearing pegmatites and cassiterite veins at the mine holes of Fook Wan Foh Kongsi and the Sg. Lah section have been reported by Ingham and Bradford, (1960); Yee, (Personal communication in Lee, 1971), and Lee, (1971). The well known Chenderiang Pegmatite had been exposed by mining operations at the mine holes of Fook wan Foh Kongsi, (lots 37, 38, 5929, 5988, 5989, 6017), and the Sg. Lah section. It was emplaced in the limestone close to the Bujang Melaka Mass. This pegmatite is composed of alkali felspar, quartz, muscovite, hydromica,(probably gilbertite), tourmaline, topaz, beryl, fluorite, zinnwaldite and cassiterite. It is also in part associated with jamesonite and galena. The cassiterites are coarsely crystalline, (Ingham and Bradford, 1960).

Another pegmatite was reported from a mine-hole at the Sg.Lah section by S. V. Yee, (Quoted in Lee, 1971, pg. 80), in the 1960s. It has a similar mineralogy to the above mentioned pegmatite and its widest exposed portion is about 2.5 m. This pegmatite was emplaced in the marble. Lee, (1971), has reported the occurrences of three non-cassiterite-bearing pegmatites emplaced in the marble at the mine hole of the number 1 unit of Fook Wan Foh Mine. These pegmatites are aligned parallel to each other and have a variable width of 50 cm to 1 m. They strike at 160^{o}E of North and dip vertically. At their contacts with the marble, greisen and some calc-silicate minerals, (especially vesuvianite and garnet), had developed. These pegmatites are composed mainly of quartz, lepidolite and feldspars together with minor amounts of phlogopite and tourmaline. The quartz is generally massive, but some are crystalline. The feldspars are heavily kaolinised. The large books of lepidolite showing a very pale purple tint are intergrown with quartz. Near these pegmatites in the marble were often found veins with large crystalline cassiterite. These pegmatites are presently not exposed by the mining activities.

The cassiterite-bearing pegmatites are believed to be the source of the coarse crystalline colluvial topaz and cassiterite collected by the author. An epigenetic origin for some or all the cassiterites from

these pegmatites has been suggested by Hosking, (personal Communication, 1976), who based his suggestion on three points:

1. That the pegmatites are brittle and hence they are readily fractured to form openings for hydrothermal mineralisation.

2. The association of cassiterite with sulphides, and

3. The cassiterite crystals are prismatic and singly terminated unlike the pegmatitic cassiterite which usually adopts a squat bipyramidal habit.

The present study of fluid inclusions from these topazes and cassiterites does aid some knowledge to help to resolve their genetic relationship.

C.1.1. Interpretation of $Th^{o}c$ values.

Homogenisation temperatures were measured only on two phase (L+V) fluid inclusions in several coarse grained colluvial cassiterites. These $Th^{o}c$ values were not corrected for pressure effects because the salinity and the pressure of formation of these cassiterites are not available. The $Th^{o}c$ values give

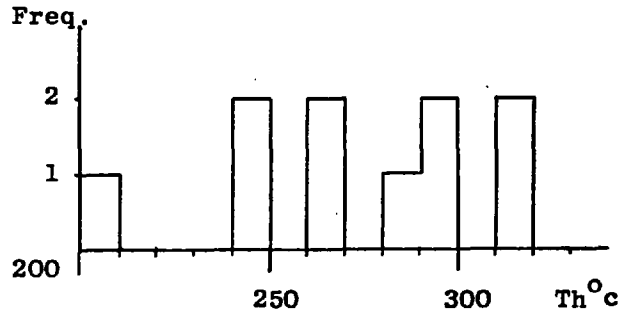

Fig. 26. Frequency distribution histogram of the Th°c values from the primary fluid inclusions of the coarse colluvial cassiterites from the Chenderiang Tin Mine at the Chenderiang Valley.

Mineral	Sample Number	Inclusion types	Th°c	+ΔT°c	=T_T°c	$(\chi-\bar{\chi})^2$	σ^2	σ
Colluvial	KCH2a	2 phase (L+V)	244.7	?	-	844.48		
	Chip 3	2 phase (L+V)	298.7	?	-	622		
cassiterite	Chip 3	2 phase (L+V)	283	?	-	85.37		
	Chip 4	2 phase (L+V)	296	?	-	494.61		
Colluvial	KCH2b	2 phase (L+V)	311.25	?	-	1405.50	1042.50	32.28°c
	Chip 1	2 phase (L+V)	261	?	-	162.81		
cassiterite	Chip 2	2 phase (L+V)	249.5	?	-	588.54		
	Chip 3	3 phase (L+V+S)	208	?	-	4324.37		
	Chip 4	2 phase (L+V)	268.5	?	-	27.66		
			317	?	-	1869.69		
			$\bar{\chi}$=273.76°c n=10			Σ10425.03		

Table 8 showing the inclusion types, the homogenisation temperatures and their standard deviation (σ) of colluvial cassiterites from the Chenderiang Tin Mine at the Chenderiang Valley.

a unimodal distribution which ranges from 200°c to 320°c. All the Th°c values with the exception of one are close to each other concentrating within 240°c and 320°c, (Fig. 26 and Table 8). It is believed that these cassiterites were derived locally from:

1. The cassiterite-bearing pegmatites emplaced in the limestones and the tourmaline granite and

2. The cassiterite veins in the marble as reported by Ingham and Bradford, (1960, pages 63 and 270 to 271), and Lee, (page 81, 1971), respectively.

The similarity in the Th°c values of the cassiterites studied indicates that they were deposited under similar thermal conditions and, therefore confirming the probable paragenetic similarity between the cassiterites in the sample studied.

The Th°c values from the primary fluid inclusions in the respective cassiterites are lower than the Th°c values recorded for the coexisting pegmatitic topaz. This temperature difference may indicate either that the cassiterites were deposited after the topaz or that they were epigenetic with respect to their pegmatite host. The latter explanation has previously been proposed by Hosking, (Personal Communication, 1976). Hosking's suggestion is supported by field evidence such as

the common occurrence of coarse grained cassiterite veins in marble near the cassiterite-bearing pegmatites, (Lee, 1971). Further support comes from the observed difference in the petrography of the primary fluid inclusions between the cassiterite and the topaz such as the common presence of CO_2 rich, silicate melt, and saline primary fluid inclusions which are unique to topaz and do not occur in cassiterite. However, Little, (1960), has observed the presence of CO_2 rich and H_2O rich primary fluid inclusions in cassiterite and beryl from a pegmatite in the Chenderiang Valley. He also obtained from these minerals $Th^{o}c$ values comparable to the liquid-gas $Th^{o}c$ values of the topaz, (300 - 400^{o}c). Thus it seems likely that the cassiterite studied by Little could be syngenetic with the topaz in the pegmatite host. From the combined fluid inclusion data of Little and those of the writer it can now be concluded with a measure of confidence that not all the cassiterites derived from the pegmatites are partly epigenetic in origin. This supports the suggestion made by Hosking, (1973b).

D. Cassiterite-feldspar-quartz-fluorite lode and its associated martitised magnetite-garnet skarn ore body of the Waterfall Mine at Pelapah Kanan.

D.1. Geological Setting.

The geology and the mineralogy of this mineralisation are described in detail in section 5.1.1.

Mineral	Level & Sample No.	Inclusion Types	Th°c	
Vein	Top Level			
Cassiterite	PK 3	3 phase(L+V+halite)	366.5	
		2 phase (L+V)	416	
		"	411.5	
		"	417.5	19.8°C
		"	411.5	
			$\bar{x}$=404.6	
			n=5	
	Middle Level			
	D I C 3	3 phase(L+V+halite)	472.8	
	P K 1 a	2 phase (L+V)	487	
		"	427	
		"	482	
		"	474	
		"	431	
		"	367	
		"	381	
		"	369	
		"	409	
		4 phase (L+V+halite + an unknown soluble phase)	498.75	
		2 phase (L+V)	487	
		"	483	
				33.7°C
	P K 1 b	"	444	
		"	446.5	
		"	439	
		"	437.45	
		" ($P2^{o}$?)	394	
		"	426	
	P K 1	"	433.45	
		"	478.45	
		"	476.45	
		"	460.45	
	P K 2	"	455.95	
		"	444	
		"	453.95	
		"	440.95	
		"	437.95	
		"	473.95	
		"	474.45	
		"	454.95	
		"	459.95	
			$\bar{x}$ =446.9	
			n =32	
	Bottom Level			
	A2	2 phase (L+V)	416.7	
		"	437.7	
	A5	3 phase (L+V+Sylvite)	478.5	
		2 phase (L+V)	469.5	
		"	448.5	
		"	493.5	
		"	491.5	
		"	490.5	
		"	491.5	
		"	478.5	
		"	470.5	23.2°C
		"	474.5	
	A5	4 phase (L+V+halite+ unknown non-brief phase).	473.5	
		3 phase (L+V+halite)	471.5	
		2 phase (L+V)	463.5	
		"	460.5	
		"	461.5	
		3 phase (L+V halite)	446	
		"	425.75	
		"	429.75	
		"	436.5	
		"	426.5	
			$\bar{x}$ = 460.7	
			n = 82	
			Grand ave (59) = 448.5°C	
			Grand n = 59	

Table 9 showing the inclusion types, the homogenisation temperatures and the standard deviation (σ) of Th°c values from cassiterites of the tin lodes at the Waterfall Mine (Pelapah Kanan).

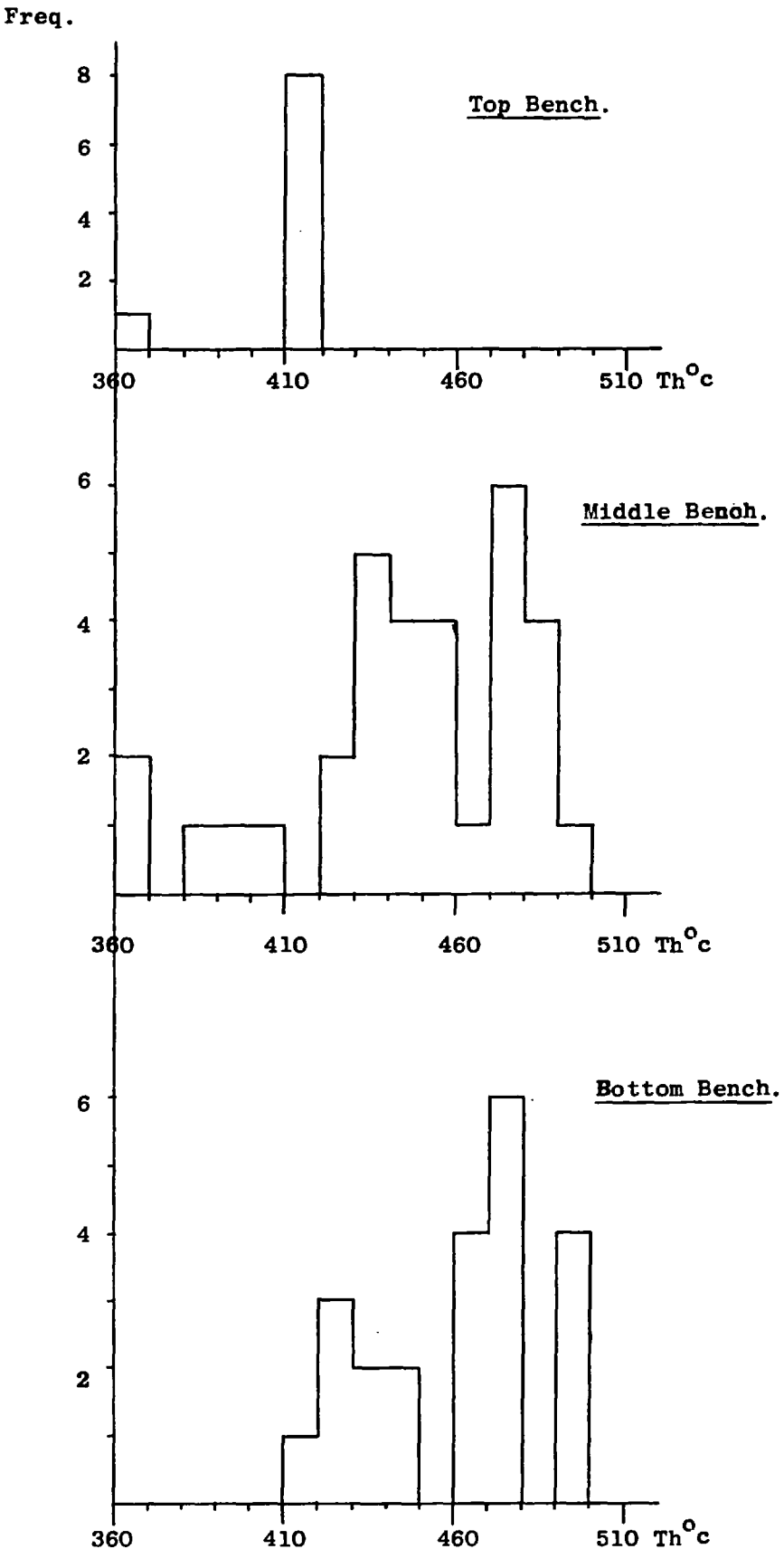

Figure 27A-C. Frequency distribution histograms of Th°c values in primary fluid inclusions of cassiterites from the three main benches of Waterfall Mine at Pelapah Kanan.

D.1.1. Interpretation of results.

Th°c values from the primary fluid inclusions in cassiterites from the Top Benches.

Two phase (L+V) and three phase (L+V+halite) fluid inclusions in the cassiterites, (Pk 3), which were spatially associated with the martitised magnetite skarn ore body were used for the measurement of homogenisation temperatures. The Th°c values were not corrected for pressure effects because the depth of mineralisation and the salinity of the inclusion fluids were not available. The Th°c values, (Table 9), show a bimodal distribution, (Fig. 27A). However, the main group occupies a range of temperat ures which extends from 410°c to 420°c, (T_h°c). The anomalously low T_h°c value, (366.5°c), is given by a three phase (L+V+halite) pseudo-secondary fluid inclusion the long axis of which is orientated perpendicular to the coloured growth zones. This decline in temperature must indicate that the primary fluid inclusions were formed prior to the pseudosecondary ones. The five T_h°c values obtained extend from 366.5°c to 417.5°c with a mean at 404.6°c.

Th°c values from the primary fluid inclusions in cassiterites from Benches C and D of the Middle Level.

Two phase (L+V) and three phase (L+V+halite) fluid

inclusions in the cassiterites collected from within Benches C to D were used for the measurement of their $Th^{o}c$ values. These values were not corrected for pressure effects due to the absence of necessary data. The $Th^{o}c$ values, (Table 9),), show a unimodal distribution, (Fig. 27B), which extends from $360^{o}c$ to $500^{o}c$ with a peak at $470^{o}c$ - $480^{o}c$; this distribution is skewed to the lower temperature end of the range. The thirty-two $T_h{}^{o}c$ values obtained range from $366.5^{o}c$ to $498.75^{o}c$ and they have a mean of $446.9^{o}c$.

<u>$Th^{o}c$ values from the primary fluid inclusions in cassiterites from Bench A of the Bottom Level</u>.

Two phase (L+V) and three phase (L+V+S) fluids inclusions in the two samples of cassiterites from Bench A were used for the measurement of $Th^{o}c$ values. The $Th^{o}c$ values were not corrected for pressure effects for the same reasons mentioned above. The $Th^{o}c$, (Table 9), values show a unimodal distribution, (Fig.27C), which extends from $410^{o}c$ to $500^{o}c$ with a peak at 470^{o} - $480^{o}c$. This distribution skewed to the lower temperature end of the range. The twenty-two $T\ ^{o}c$ values obtained range from $416.7^{o}c$ to $493.75^{o}c$ and they have a mean of $460.7^{o}c$,

From the means of the $Th^{o}c$ values and figures 28A, B, & C, is it clear that a progressive cooling and dilution of the hydrothermal fluids took place with shallowing

	Th°c (Y)	Salinity (in equiv. wt % NaCl) (X)	
Pk3	366.5	29	156
DlC_3	472.2	35	270.2
Pkla	498.75	32.87	223
A_5	473.5	34.3	257.5
	471.5	34	250.5
	446	31.5	207
	425.75	32.5	222.75
	429.75	32.5	222.75
	436.5	33.58	242.5
	$\bar{Y}$ = 446.72	$\bar{X}$ = 32.81	
	n = 9	n = 9	

Table 10 shows the salinities and Th°c values of the three phase (L+V+halite) fluid inclusions from the cassiterites of the Waterfall Mine at Pelapah Kanan.

$(X-\bar{X})$	$(X-\bar{X})$	$(Y-\bar{Y})^2$	$(Y-\bar{Y})$	$\Sigma(Y-\bar{Y})(X-\bar{})$
-3.81	14.5161	-80.22	6,435.25	305.64
2.19	4.7961	25.48	649.23	55.80
0.06	0.0036	52.03	2,707.12	3.12
1.49	2.2201	26.78	717.17	39.90
1.19	1.0908712	24.78	614.05	29.49
-1.31	1.7161	-0.72	0.52	0.94
-0.31	0.0961	-20.97	439.74	6.50
-0,31	0.0961	-16.97	287.98	5.26
0.77	0.5929	-10.22	104.45	7.87
Σ-0.04	Σ25,127971	Σ-0.03	Σ11,955.51	Σ454.52

Formula for calculating the coefficient of correlation:-

$$r = \frac{\Sigma(X-\bar{X})(Y-\bar{Y})}{+\sqrt{(X-\bar{X})^2\,\Sigma(Y-\bar{Y})^2}} = \frac{454.52}{+\sqrt{25.127971 \times 11955.51}}$$

$$= \frac{454.52}{+\sqrt{300417.7}} = \frac{454.52}{548.10}$$

$$= 0.83$$

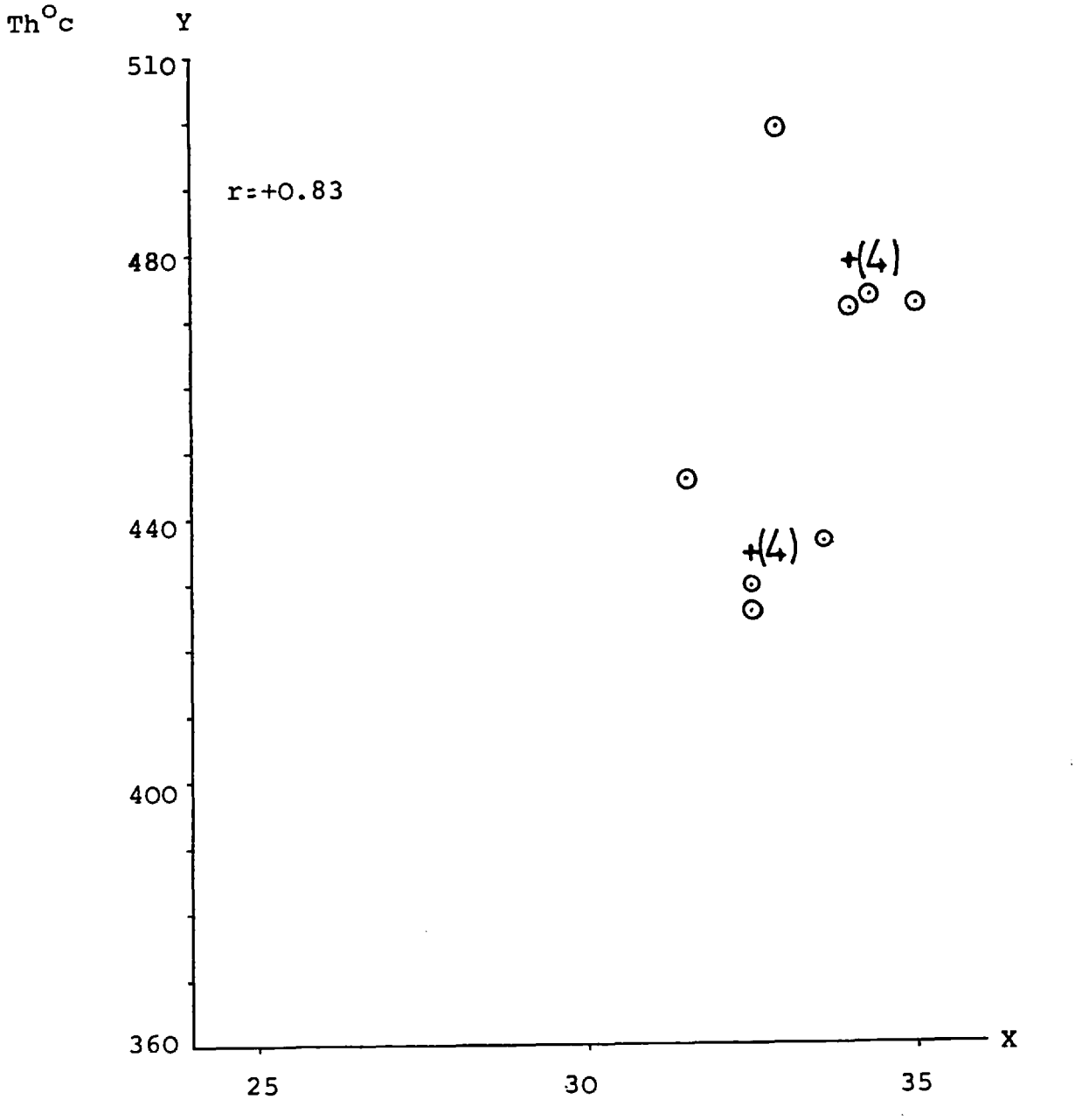

Figure 28 Plot of salinities versus homogenisation temperatures from the halite-bearing primary fluid inclusions in cassiterites of the Waterfall Mine at Pelapah Kanan.

depths. This trend is strong evidence suggesting an upward flow for the fluids. The salinities and $Th^{o}c$ values of seven, three phase, (L+V+halite+unknown S) fluid inclusions were found to be positively correlated with a correlation coefficient of +0.83, (Fig. 28; and Table 10). This realtionship is best explained by the dilution and cooling of the mineralising tin rich brines as a consequence of mixing with the less saline and cooler meteoric waters.

<u>$Th^{o}c$ values from the primary fluid inclusions in cassiterite-associated late vug fluorite of Bench B at the top of the Bottom Level</u>.

These vug fluorites filled a vug already lined by the third phase of cassiterite mineralisation. Thus they are post-phase three cassiterite in age.

Homogenisation temperatures were measured in a cogenetic population of two phase, (L+V) fluid inclusions. These $Th^{o}c$ values were not corrected for pressure effects because an independent estimation of the depth of mineralisation was not possible. The $Th^{o}c$ values give a unimodal distribution which ranges from $130^{o}c$ to $160^{o}c$.and it gives a small peak within 130 and $150^{o}c$, (Fig.29A and Table 11). The mean for these five $Th^{o}c$ values is $142.5^{o}c$.

Mineral	Sample number	Inclusion types	Th°c	σ
Late pale green	B1.F1	2 phase (L+V)	152	
fluorite.	B1.F1	2 phase (L+V)	144.5	
	B1.F1	2 phase (L+V)	136	5.6°c
	B1.F1	2 phase (L+V)	142	
	B1.F1	2 phase (L+V)	138	
			$\bar{\chi}$(Th°c)=142.5 n = 5	
Early pale	PK2	2 phase (L+V)	174.25	7°c
		2 phase (L+V)	160.25	
green flourite.			$\bar{\chi}$=167.25 n= 2	
	B_2.F1	3 phase (L+V+S)	165.5	
		3 phase (L+V+S)	142.5	
		3 phase (L+V+S)	136.5	
	$B_2.F_3$	5 phase (L+V+3S)	139.5	14.2°c
		2 phase (L+V)	145	
		3 phase (L+V+S)	157	
	$B_2.F_6$	3 phase (L+V+S)	117.5	
			$\bar{\chi}$=143.4 n= 7	
	A1.F1	2 phase (L+V)	154.5	
		2 phase (L+V)	177.	
		2 phase (L+V)	168.5	
	A1.F2	3 phase (L+V+S)	190.25	33.2°c
		2 phase (L+V)	250.25	
	A1.F4	7 phase (L+V+4OP + halite)	224.5	
			$\bar{\chi}$=194.2	
			n= 6	
			*$\bar{\chi}$=166.9	
			*n= 15	

Table 11 showing the inclusion type, the Th°c values and their standard deviations of the vein fluorites from the tin lodes of the Waterfall Mine at Pelapah Kanan.

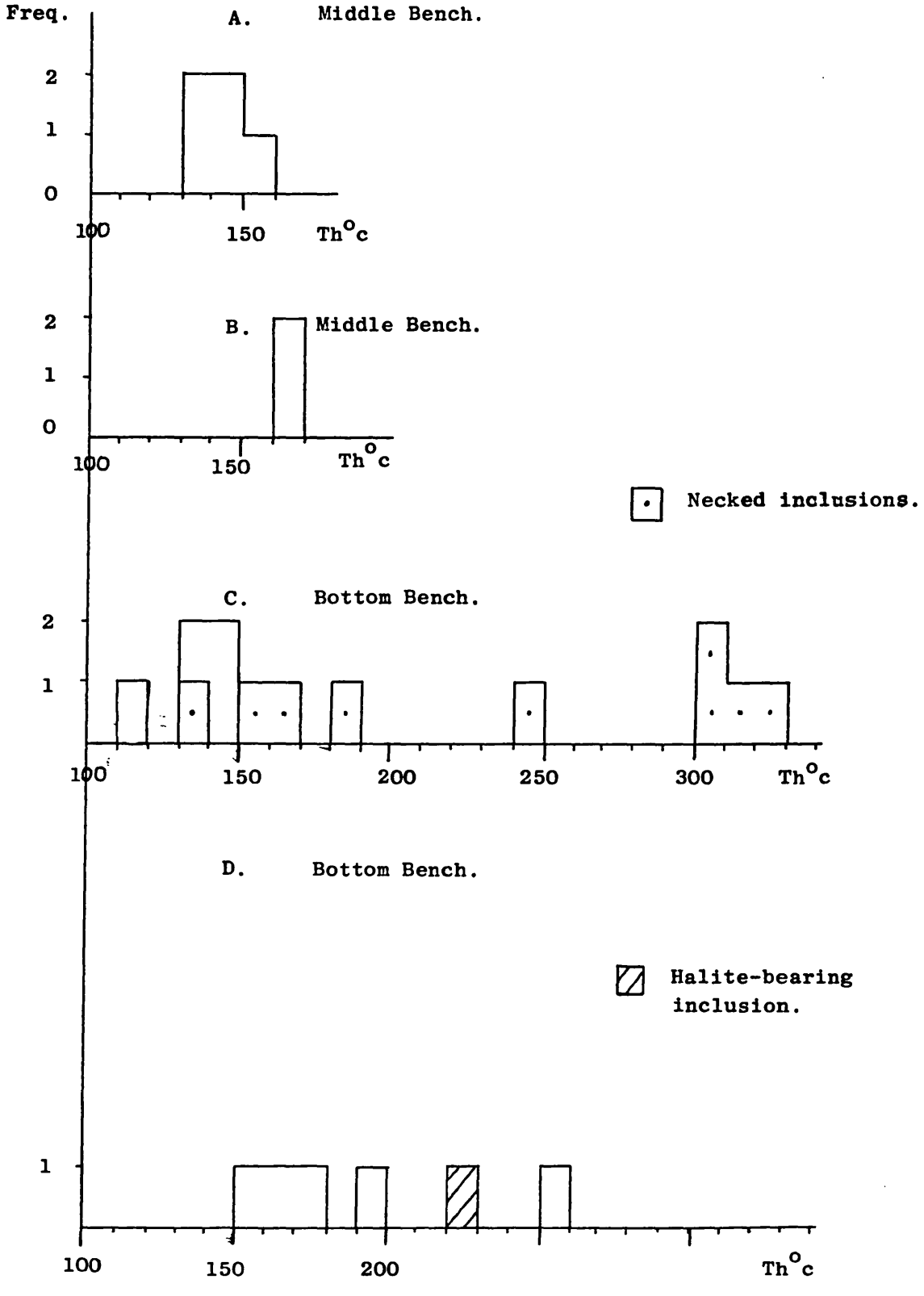

Fig.29A-D Frequency distribution histograms of Th°c values in primary fluid inclusions of fluorites from the main benches of Waterfall Mine at Pelapah Kanan.

Th°c values from the primary fluid inclusions in cassiterite-associated early gangue vein fluorite of Benches C-D at the Middle Level.

Only two Th°c values were measured on two, two phase (L+V) pseudosecondary fluid inclusions which are located on a tiny plane in the vein fluorite. These two Th°c values are very close to each other, (Fig. 29B). The mean of these Th°c values is 167.25°c.

Th°c values from the primary fluid inclusions in cassiterite-associated early gangue vein fluorite of Bench B at the top of the Bottom Level.

These fluorites are post-phase two and pre-phase three cassiterite in age.

Homogenisation temperatures were measured on three phase (L+V+S) fluid inclusions and also one, two phase (L+V) fluid inclusion in B_2 fluorites. The Th°c values give a unimodal distribution which ranges from 110°c to 190°c and it also gives a small peak within 130°c to 150°c. The mean for the 7 Th°c values obtained is 143.4.

The Th°c values obtained for two, four phase (L+V+2S) fluid inclusion and eight, two phase (L+V) fluid inclusions in B_3 fluorite were very widespread from 130°c to 330°c, (Fig.29C). This scattering of Th°c values can be interpreted as a consequence of

necking down of a large heterogeneous fluid inclusion. This group of inclusions does in fact show a non-uniform phase ratio and the characteristic tail off shape. Thus these inclusions show all the characteristic features (e.g. morphology, phase ratio and inconsistent $Th^{o}c$ values), of necked down fluid inclusions.

Th°c values from the primary fluid inclusions in cassiterite-associated early gangue vein fluorite of Bench A at the Bottom Level.

Homogenisation temperatures were measured on four, two phase (L+V), one, three phase (L+V+S) and one, seven phase (L+V+5S) fluid inclusions from these fluorites.

The $Th^{o}c$ values give a unimodal distribution which ranges from $150^{o}c$ to $260^{o}c$ but three out of six inclusions have homogenised at temperatures within $150^{o}c$ and $180^{o}c$, (Fig. 29D). The mean of these six $T_h{}^{o}c$ values is $194.2^{o}c$. It is necessary to note that the highest $Th^{o}c$ value is given, as is commonly the case, by the isolated halite-bearing seven phase (L+V+5S) fluid inclusion.

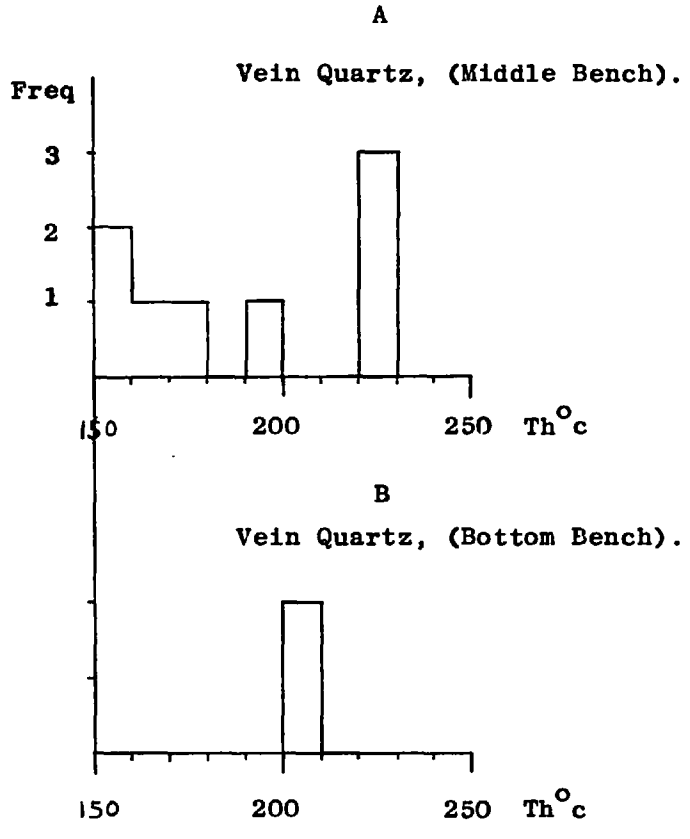

Fig. 30A-B. Frequency distrubition histograms of Th°c values in primary fluid inclusions of quartzs from the main benches of Waterfall Mine at Pelapah Kanan.

Conclusions.

It is apparent that the calcium and fluorine rich hydrothermal fluids had cooled with shallowing depths as indicated by the $Th^{o}c$ data, (Fig.29) from the primary inclusion in the gangue fluorites, (samples A and B_2).

$Th^{o}c$ values from the primary fluid inclusions in the gangue vein quartz of Bench D at the Middle Level.

Homogenisation temperatures were measured on five isolated 2 phase (L+V) fluid inclusions as well as in three other isolated 3 phase (L+V+halite) fluid inclusions. These $Th^{o}c$ values give a unimodal distribution with a small peak within $220^{o}c$ and $230^{o}c$ and it is skewed to the lower temperature end of the range, (Fig. 30A). All the three halite-bearing three phase fluid inclusions give notably higher $Th^{o}c$ values than the 2 phase (L+V) fluid inclusions. This is to be expected since the fluids of the three 3 phase halite-bearing fluid inclusions have higher initial (i.e. 26 equiv. wt% NaCl) salinities than the 2 phase inclusions, compatible with the model of progressive dilution parallelled by cooling.

Th°c values from the primary fluid inclusions in the gangue vein quartz of Bench A at the bottom level.

Only two Th°c values were measured on two two phase (L+V) fluid inclusions which may be pseudosecondary in origin as they are located on a short plane within the host quartz. These two Th°c values form a group within 200°c to 210°c, (Fig. 30B).

The ten Th°c values recorded in the vein quartz from benches D and A give a mean value of 193.4°c.

Th°c values from the primary fluid inclusions in the non-cassiterite-bearing vug quartz of Bench C at the Middle Level.

The vug quartz from the barren quartz veins contain abundant primary monophase aqueous inclusions. The presence of these inclusions indicates that the temperature of formation of their host vug quartzs was less than 70°c.

D.2. General Conclusions.

1. The temperatures of the tin rich hydrothermal fluids were high (400°c - 500°c) as expected since the tin lodes were emplaced at the immediate periphery of a porphyritic granodiorite. This high

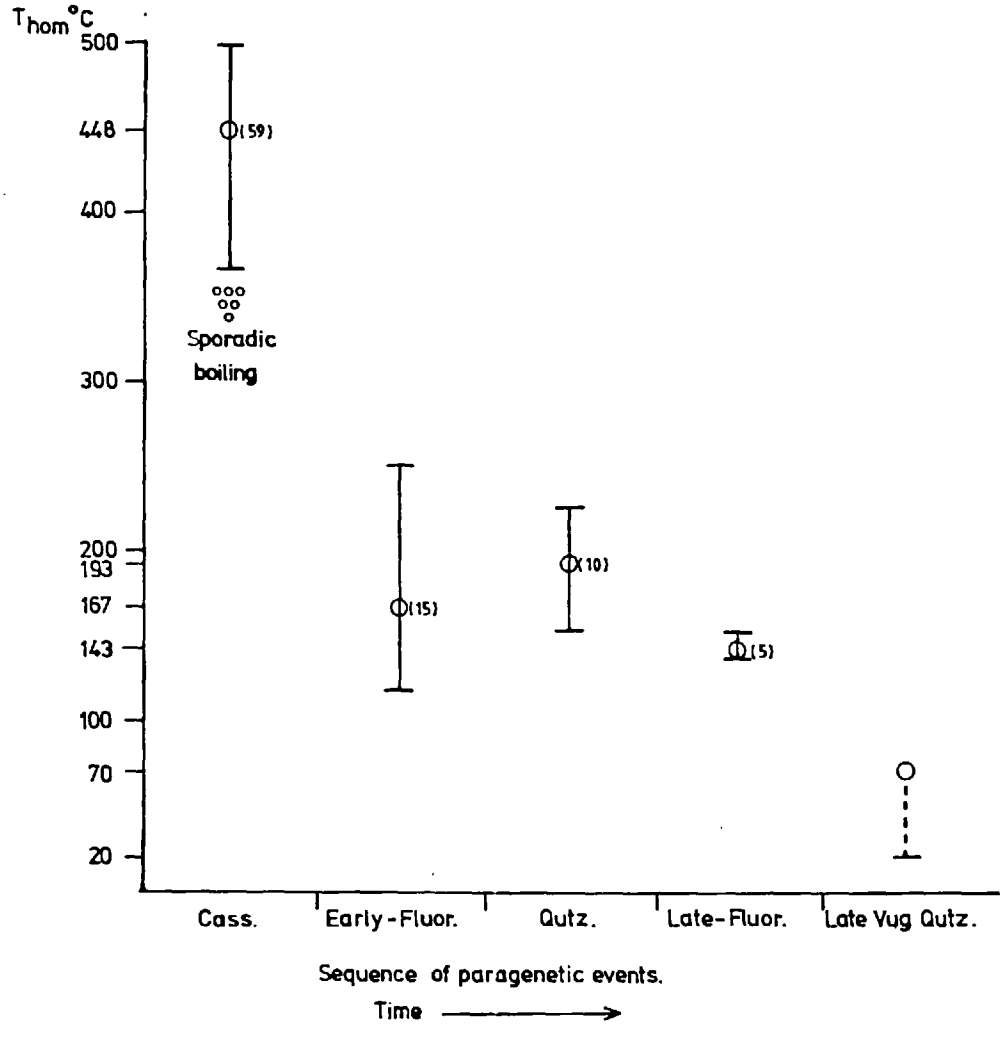

Figure 31 shows the variation of Th°c values in minerals from different paragenetic stages of the tin lodes at the Waterfall Mine, Pelapah Kanan.

PLATE 69.

The growth of vuggy quartzs, (arrowed a), in a pod-shaped area bounded by magnetite veins, (arrowed b), (Bench G, Waterfall Mine, Pelapah Kanan).

temperature suggests that the latter intrusive could have been the source of the mineralising tin rich fluids.

2. The mineralising tin-rich hydrothermal fluids has diluted as they anigrated towards the surface. The calcium and fluorine-rich hydrothermal fluids have also cooled with shallowing depths.

3. The hydrothermal system had cooled with time throughout the paragenetic sequence from 449°c (mean Th°c of cassiterite) to 167°c (mean Th°c value of early fluorite) to 193°c (mean Th°c value of vein quartz) to 143°c (mean Th°c value of late fluorite) and finally to 70°c - 20°c, (vug quartz), (Fig. 31).

E. The Th°c values of vug quartz within the magnetite skarn at Bench G of the Waterfall Mine.

E .1. Geological Setting.

The euhedral vug quartz were emplaced within a chicken-wire mesh stockwork of coarse grained magnetite veins. They were formed in pod-shaped cavities bounded by the magnetite veins, (Plate 6ª). Only two such quartz filled cavities were seen and they are separated

Figure 32.

Vug Quartz (Fe3).

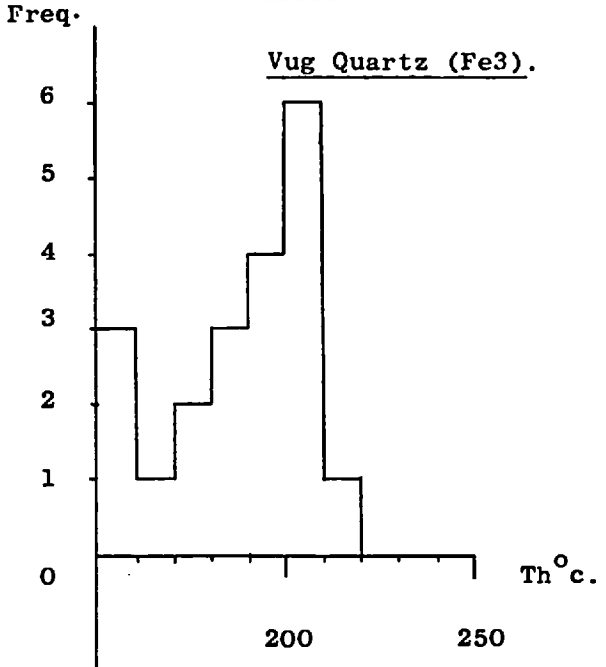

Figure 33.

Vug Quartz (Fe2).

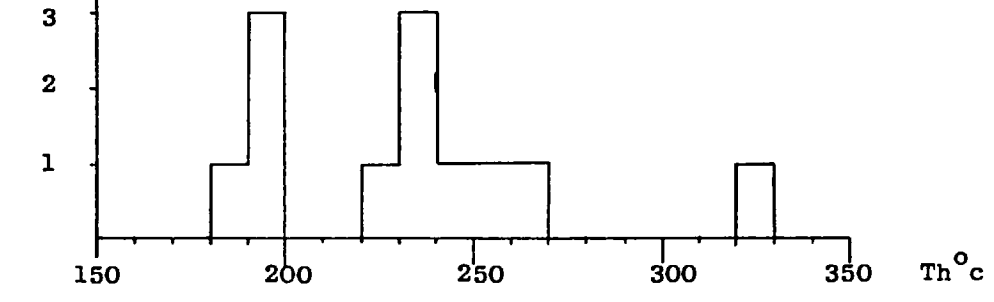

Figures 32 and 33. Frequency distribution histograms of Th°c values in primary and pseudosecondary fluid inclusions of Fe3 and Fe2 vug quartz from the upper part of the martitised magnetite skarn ore body of Waterfall Mine at Pelapah Kanan.

by a vertical distance of about ten feet. The lower down vug quartz (Fe 2) are much smaller in size than those vug quartz (Fe 3) above them. The vug quartzs of sample Fe 2 are about 1" to 1½" long and they have a diameter of about 1/4" to ½". The vug quartzs of sample Fe 3 are about 4" to 6" long and 1" wide.

These vug quartz contained suitable primary and pseudosecondary fluid inclusions for homogenisation study

E.1.1. Interpretation of Th values.

Th°c values from the primary fluid inclusions in the vug quartz (Fe 3) from the martitised magnetite skarn of the Waterfall Mine.

The Th°c values measured on 2 phase (L+V) primary fluid inclusions from the vug quartz give a unimodal distribution with temperatures ranging from 150°c - 220°c with a peak at 200°c - 210°c; the distribution is skewed to the lower temperature end of the range, (Fig. 32). The mean for the 20 Th°c values recorded is 187.3°c.

Th°c value from the primary fluid inclusions in the vug quartz (Fe 2) from the martitised magnetite skarn of Waterfall Mine.

The vug quartz (Fe 2) were collected about ten feet below those of (Fe 3) in the martitised magnetite skarn.

The $Th^{o}c$ values of 2 phase (L+V) primary fluid inclusions were measured giving a unimodal distribution which extends from $180^{o}c$ to $270^{o}c$ with a cleft peaks respectively at 190^{o} to $200^{o}c$, and $230^{o}c$ - $240^{o}c$. The distribution is skewed to the higher temperature end of the range, (Fig. 33).. An anomalously high $Th^{o}c$ value, (330 $Th^{o}c$), is given by an isolated 2-phase (L+V) fluid inclusion. The mean for the 12 recorded $Th^{o}c$ values is $232.7^{o}c$. The latter mean $Th^{o}c$ value is $45.4^{o}c$ higher than the mean of the $Th^{o}c$ values from the upper vug quartz (Fe 3). Thus there is an apparent sharp thermal gradient over a vertical distance of about 3 meters.

The observed gradient may have been real or it may be false, resulting either from possible bias in sampling of two vugs with identical thermal paths during crystallisation or from the existence of two different generations of silica-bearing fluids crystallizing at different temperatures. If it was a real gradient it could only have existed during the heating up stage of the thermal history of the contact rocks as the cooling part of the cycle is marked by low thermal gradients. The heating up cycle in the immediate contact rocks can be modelled by time-dependent solutions of Laplaces Equation for a semi-infinite medium assuming instantaneous intrusion, (Carslaw and Jaeger, 1959; Personal Communication, M. Francis, 1979). In this model the heat transfer

is assumed to take place by conduction only. The constraints imposed in the application of this model mean that the thermal gradient, (notably 45°c taken over 3 m within 10 m of the contact) in the temperature range around 200°c could only have existed at this position in the aureole within approximately ten years of the time of intrusion. It would be expected that the conditions of heat transfer in this environment were dominantly convective in which case such a gradient would, in any case, be unreasonable and the field evidence is such that the quartz filled vugs closely postdate the formation of the magnetite skarn. In all probability the vugs were filled during the cooling-down part of the thermal history of the aureole rocks in a convective regime of heat transfer.

If there is no bias in the sampling of the quartz crystals from the vugs then the difference in the mean Th°c values must reflect filling at different times by separate pulses of silica-bearing fluids. Because there is a general paragenetic similarity between the fillings of the two vugs it is not unlikely that the difference in the mean Th°c values from the two vugs is a reflection of some bias in sampling although the writer took reasonable precautions to sample representatively.

6.6.3. Lodes emplaced within the thermal aureole of granitic intrusion.

A Cassiterite-chlorite vein, (Willinks lode).

A.1. Geological Setting

Two samples of cassiterite-chlorite vein of about an inch wide were collected from an old 300 foot level stope near the Nicholson shaft which was inaccessible during the writer's visit. Thus the paragenetic relationship between these two mineralogically similar vein samples could not be observed. These samples were emplaced at about 500 feet perpendicular to the nearest granite contact west of the lode.

A.1.1. Interpretation of results.

Homogenisation of temperatures were measured on the 2 phase (L+V) primary fluid inclusions of cassiterites from the two respective samples (a and b) of the Willinks Lode System. The $Th^{o}c$ values were not corrected for pressure effects because the data on the depth of mineralisation and the salinity of the inclusion fluids were not available.

The $Th^{o}c$ values of cassiterites from sample a vary from $190^{o}c$ to $280^{o}c$. However, there is an exception of an anomalously high $Th^{o}c$ value of $341^{o}c$

Mineral	Sample Number	Inclusion types	Th°c	ΔT°c	T_T °c		σ^2	σ
Vein	Wa	2 phase (L+V)	220.5	?	-	18.75		
Cassiterite		2 phase (L+V)	237	?	-	148.11		
		2 phase (L+V)	276.1	?	-	2628.61		
		2 phase (L+V)	193	?	-	1013.15	557.40	23.61
		2 phase (L+V)	200	?	-	616.53		
		2 phase (L+V)	220	?	-	23.33		
		2 phase (L+V)	224	?	-	0.69		
		2 phase (L+V)	228	?	-	10.05		
			$\bar{\chi}$=224.83 n=8			Σ4459.22		
Vein	Wb	2 phase (L+V)	357.5	?	-	29.59		
Cassiterite		2 phase (L+V)	344	?	-	64.96		
		2 phase (L+V)	356	?	-	15.52		
		2 phase (L+V)	335	?	-	291.04	278.40	16.69
		2 phase (L+V)	377	?	-	622.0		
		2 phase (L+V)	353	?	-	0.88		
		2 phase (L+V)	371	?	-	358.72		
		2 phase (L+V)	323	?	-	844.48		
			χ=352.06 n=8	?		Σ2227.19		

Table 12 showing the inclusion types, the ΔT°c, the homogenisation temperatures and their standard deviation (σ) of the vein cassiterite from the Willinks' lode.

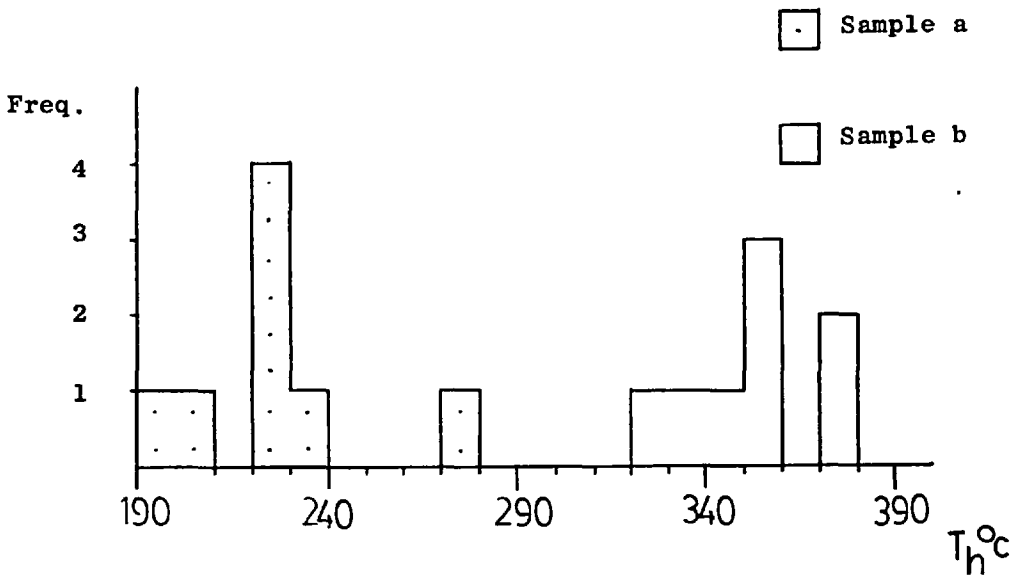

Fig 34. Frequency distribution histogram of Th°c values in priamry fluid inclusions of cassiterites, (Sample a and b), from the Willinks' lode.

given by a 2 phase (L+V) fluid inclusion which could have leaked. This anomalous Th°c value was, therefore, discarded. The range of Th°c values gives a peak within 220°c and 230°c and it is skewed weakly to the lower temperature end of the range, (Fig. 34). The mean Th°c value for the eight Th°c values obtained is 225°c, (Table 12).

In contrast to the above results, the Th°c values from the cassiterites of sample b have a narrower range which extends from 320°c to 380°c with a peak within 350°c and 360°c. The Th°c values are skewed to the lower temperature end of the range, (Fig. 34), they give a mean of 352°c, (Table 12).

Since they were emplaced at the same depth and pressure, the corrections to both sets of temperatures measured would be similar and the two ranges of Th°c values can be meaningfully compared. It is evident from figure 34 and the mean Th°c values obtained that a large temperature difference exists between the two sets of Th°c values. This difference is best explained if there were two phases of cassiterite-chlorite vein mineralisation which were formed from tin rich fluids of different temperatures passing through the structures at approximately the same times. This is evidence of a polyascendant history of tin mineralisation in these structures.

Mineral	Sample No	Inclusion Types	$Th^{o}c$	σ
Cassiterite	H7	2 phase(L+V)	261.5	
		"	268.5	
		"	269	
		"	363	
		Gascous inclusion	362.5(G)	
		2 Phase(L+V)	278	
		"	250.5	
			$\bar{x}(Th^{o}c)=$ 265.5(s)	$42^{o}C$
	H15	"	256.95	
		"	210.5	
		"	294	
			$\bar{x}(Th^{o}c)=$ 253.82	
	H116	"	272.5	
		"	301	
			$\bar{x}(Th^{o}c)=$ 286.75	
		Grand ave =	$282.3^{o}C$	
		n =	12	

Table 13 showing the inclusion types, the homogenisation/ trapping temperatures and their standard deviation (σ) of Hantu Lode's cassiterites.

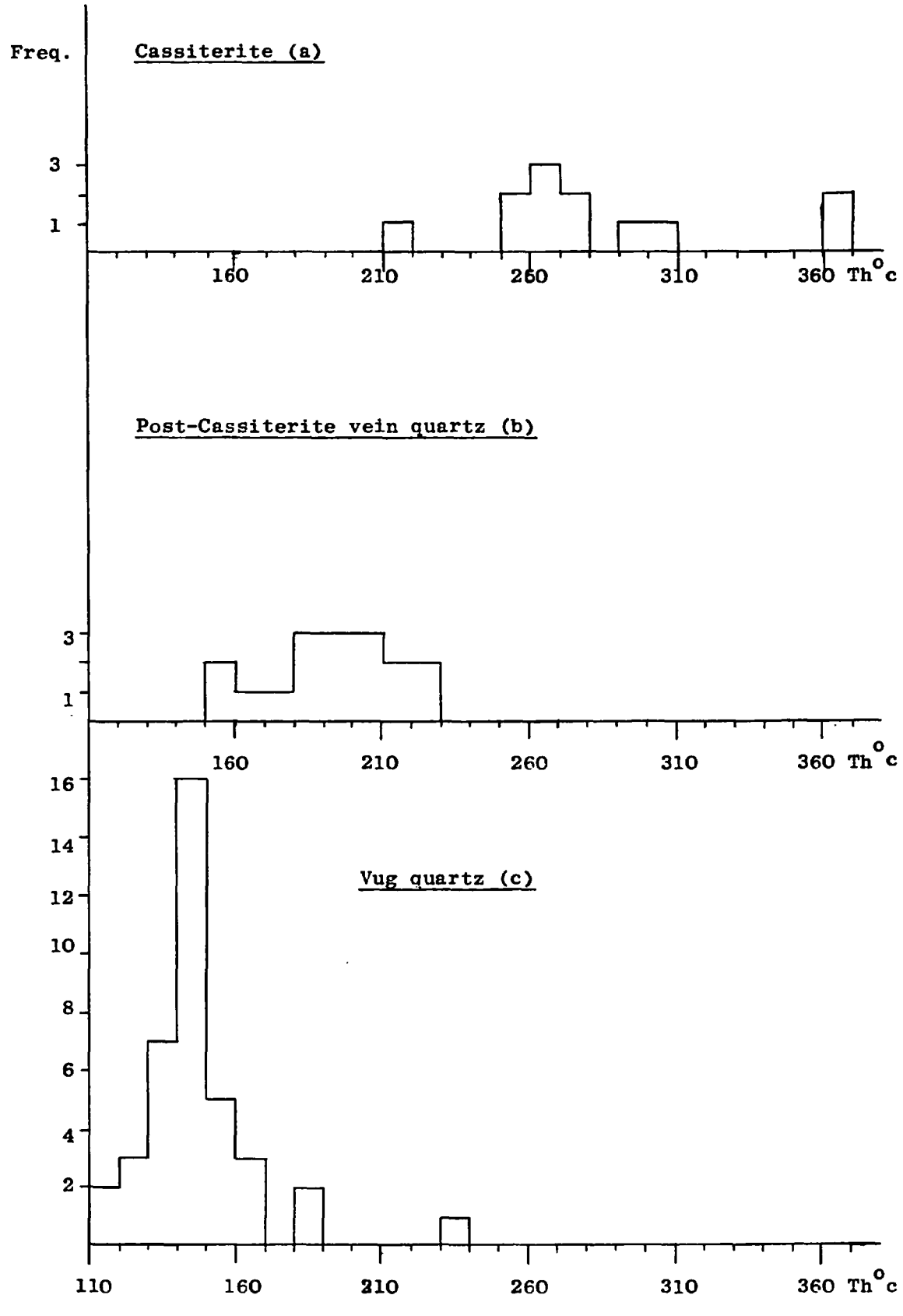

Figures 35A-C showing the frequency distribution histogram of $Th^{o}c$ values from the primary fluid inclusions of cassiterite (a), post-cassiterite vein quartz (b) and vug quartz (c) from the Hantu lode system, P.C.C.L.

B. Cassiterite-chlorite lode of the Hantu Lode System (P.C.C.L. Sg. Lembing).

B.1. Geological Setting.

The geology of this lode mineralisation is described and discussed in detail in Chapter 2.

B.1.1. Interpretation of Results.

Homogenisation temperatures were measured on primary 2 phase (L+V) fluid inclusions in the cassiterites of three samples, (H7, H15 and H11b), collected respectively from a 400 foot stope at Section 31/N", a 600 foot stope at Section 35/N" and a 600 foot stope at Section 35/M". Ten of the twelve $Th^{o}c$ values recorded were not corrected for pressure effects while the remaining two need no such correction because they are equal to the $T_T{}^{o}c$ values as the fluids in the inclusions from which these two $Th^{o}c$ were recorded showed evidence of boiling. The $Th^{o}c$ values show a bimodal distrubition, (Fig. 35A) with the main group occupying a range which extends from $250^{o}c$ to $310^{o}c$ while the other group, represented by the boiling assemblage, occurs within $360^{o}c$ and $370^{o}c$. The anomalously low $Th^{o}c$ value, ($210.5^{o}c$), given by a 2-phase (L+V) fluid inclusion may be due to leakage of the inclusion fluids. The twelve $Th^{o}c$ values, (Table 13), give a mean at $282.3^{o}c$.

Mineral	Sample No	Inclusion Types	$Th^{o}c$	σ
Post - Cassiterite Quartz	H7	2 phase(L+V)	172	
	H10	"	196	
		"	204.5	
		"	223	
		"	222	
		"	198	
		"	211	
		"	215	
		"	190	$21.36^{o}C$
		"	189	
		"	206	
		"	210	
		"	197	
	PCH 1	"	161	
		"	156	
		"	185	
		"	152.45	
			$\bar{x}(Th^{o}c)=$ 193.4	
			n = 17	

Table 14 showing the inclusion type, the $Th^{o}c$ values and their standard deviation (σ) of the Post - Cassiterite vein quartz from the Mantu Lode System.

Sample Number	Inclusion Types	$Th^{o}c$	σ
PCH4		146	
(500'inter/33/N')		146	
		146	
		131	
		150	
		148.5	
		143	
		140	
		134	
		150.5	
		144.1	
		117	
		125	
		132	
		135	
		148	
		158.5	
		146	
		152.5	$20.57^{o}C$
		150	
		144.1	
		149	
		128.1	
PCH 5		163.5	
(300'/36/M')		116	
		146.5	
		135	
		170	
		186	
		167	
H F 1.1.		147.45	
(400'/33/N')		127.45	
		142.25	
		153.25	
		142.25	
		139.5	
H F 1.2.		233.5	
(400'/33/N')		157.75	
		189.25	
		$\bar{x}$ ($Th^{o}c$)= 148.23	
		n = 39	

Table 15 showing the inclusion types, the homogenisation temperatures and their standard deviation (σ) of late vug quartzs from the Hantu Lode System.

Homogenisation temperatures were measured on primary 2-phase (L+V) fluid inclusions in the fairly milky vein quartzs from samples H7, H15 and H10. These vein quartzs are post-cassiterite in age as they have intruded into the cassiterite veins along the middle. The 17 Th^{o}c values, (Table 14), were not corrected for pressure effects and they show a unimodal distribution occupying a range which extends from 150^{o}c to 230^{o}c, (Fig. 35B). The mean Th^{o}c value for the 17 Th^{o}c values recorded is 193.4^{o}c.

Homogenisation temperatures were measured on primary and pseudosecondary 2 phase (L+V) fluid inclusions in vug quartzs from samples PCHS, (300'/36/M"); HF1.1 (400'/33/N"); HF1.2 (400'/33/N") and PCH4 (500' intermediate/33/N"). These vug quartzs were the last phase of the quartz mineralisation event as indicated by their occurrence at the margins of the massive barren white quartz veins. The 39 recorded Th^{o}c values with the exception of an anomalous high value, (233.5^{o}c), (Table 15), give a uniform unimodal distribution, (Fig. 35C), which extends from 110^{o}c to 190^{o}c and gives a distinct peak within 140^{o}c and 150^{o}c. The anomalous high Th^{o}c value is given by a large isolated 2 phase (L+V) fluid inclusion which may have leaked. The mean Th^{o}c value for the 39 Th^{o}c values is 148.23^{o}c.

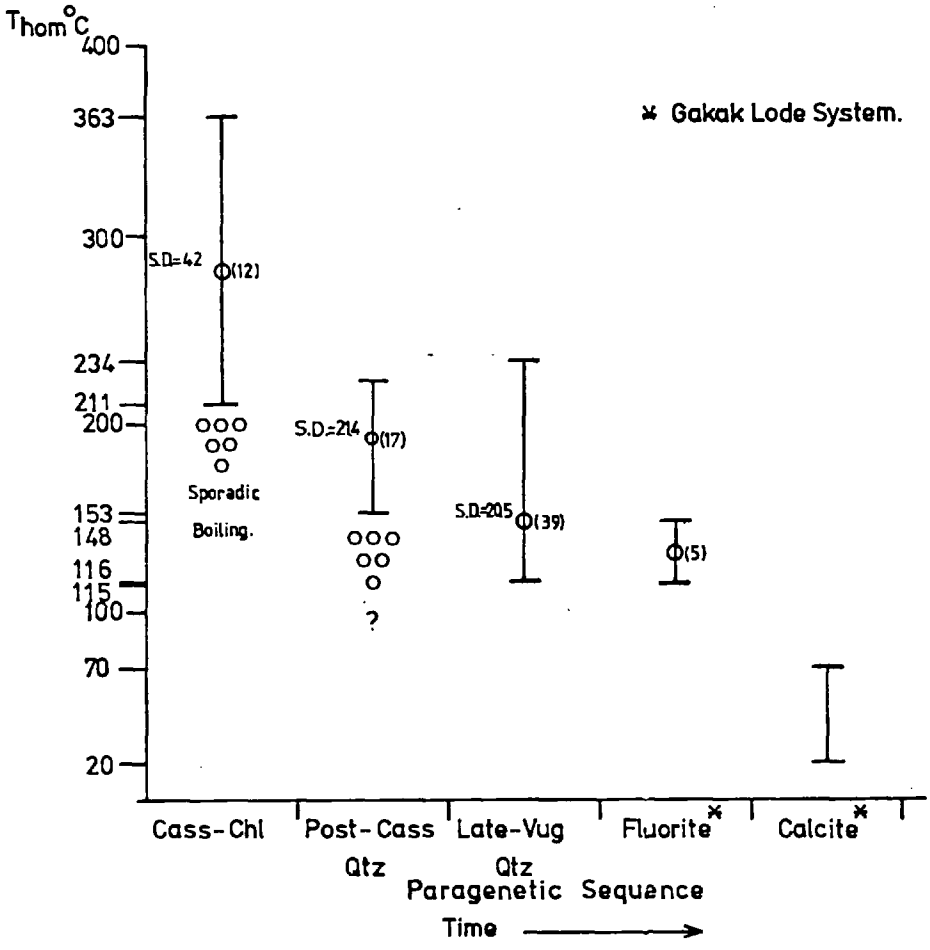

Fig.36. Variation in Th°C values. Hantu Lode.

Conclusions.

Judging from figures 35 and 36 it is clear that the hydrothermal mineralising fluids system which formed the Hantu Lode System had progressively cooled throughout the paragenetic mineralisation sequence- (Cassiterite (282.3°c (12)) → Post-cassiterite Vein Quartz (193.4°c (17)) → Late Vug Quartz (148.23°c (39)) → Fluorite (131.4°c (5)).

C. Cassiterite-quartz veins/veinlets in tourmaline hornfels, (Siputeh).

C.1. Geological Setting.

The cassiterite-quartz veins/veinlets of less than an inch wide occur in a ramifying network in tourmalinised hornfels. The ramifying nature of the network of mineralised veinlets suggests an origin due to hydraulic fracturing. Thus the fluid pressure involved must have exceeded the confining pressure, σ_3, plus the tensile strength, T, of the rock. This relationship is usually expressed as $\sigma_3 - p = T$ where T is, of course, a negative quantity, (Fyfe, Price and Thomson, 1978).

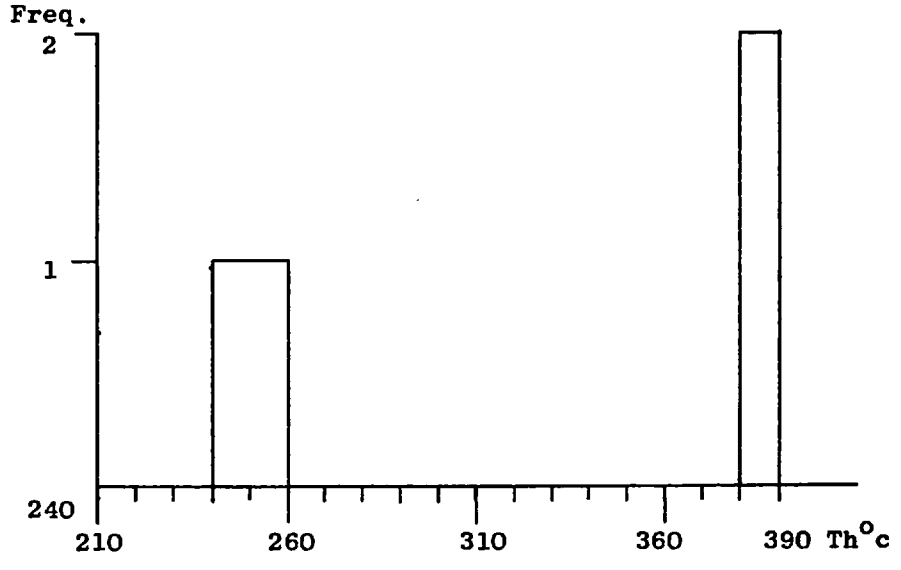

Fig. 37.Frequency distribution histogram of Th°c values in primary fluid inclusions of cassiterites from Siputeh's quartz-cassiterite lode.

Mineral	Sample number	Inclusion types	Th°c	+ΔT°c	T_T°c	$(\chi-\chi)^2$	σ^2	σ
Vein	KS1	2 phase (L+V)	248	?	-	4	4	2
cassiterite		2 phase (L+V)	252	?	-	4		
						8		

Table 16 showing the inclusion types, the ΔT°c, the homogenisation temperatures and their standard deviation (σ) of the vein cassiterites from the Siputeh lode.

C.1.1. Interpretation of Results.

Homogenisation temperatures were measured on four, two phase (L+V) fluid inclusions, but two of these inclusions are discarded because one of the two was necked while the other could be secondary in origin. The $Th^{o}c$ values of these two inclusions are anomalously high relative to the $Th^{o}c$ values given by two isolated primary two phase (L+V) fluid inclusions, (Fig. 37 and Table 16). The mean for the latter two $Th^{o}c$ values is $250^{o}c$. Even if these $Th^{o}c$ values were corrected for pressure effects by as much as 20^{o} - $30^{o}c$ the temperatures would still be within the medium temperature range. The intermediate $Th^{o}c$ values of the cassiterites suggests that the source of the tin-rich fluids responsible for the formation of these cassiterites must have been at some distance away from the lodes. This suggestion is based on the assumption that the initial temperature of the tin-rich hydrothermal fluids was close to that of granitic magmas.

6.6.4. Lodes whose primary geological environments are unknown.

A. Alluvial cassiterites, (Gopeng).

A.1. Interpretation of results.

Homogenisation temperatures were measured on 2 phase

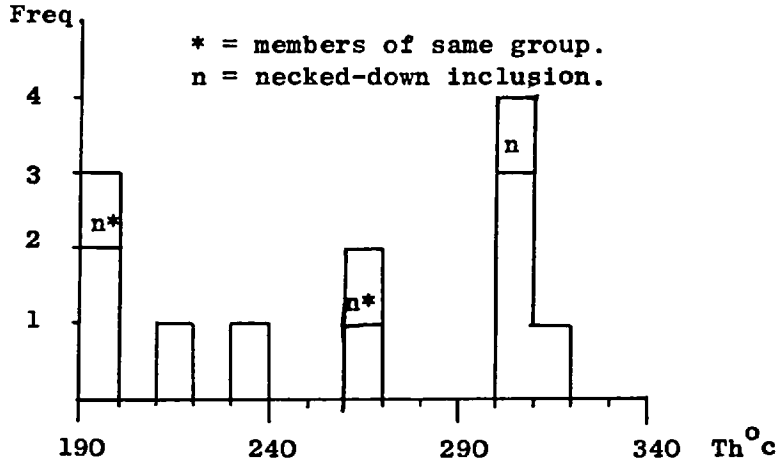

Fig. 38. Frequency distribution histogram of Th°c values in primary fluid inclusions of coarse alluvial cassiterites from the Gopeng Consolidated Mine.

Mineral	Sample number	Inclusion types	Th°c	+ T°c	T_T °c	$(\chi-\bar{\chi})^2$	σ
Alluvial	KGC1.1	2 phase (L+V)	303	?	-	1907.07	
Cassiterite	KGC.2	2 phase (L+V)	233	?	-	693.27	
	KGC.3	2 phase (L+V)	303	?	-	1907.07	
	KGC.3	2pphase (L+V)	309	?	-	2467.11	
	KGC.4	2 phase (L+V)	198	?	-	3761.37	47.1°c
	KGC.5	2 phase (L+V)	315	?	-	3099.15	
	KGC.5	2 phase (L+V)	198	?	-	3761.37	
	KGC.5	2 phase (L+V)	211	?	-	2335.79	
	KGC.5	2 phase (L+V)	264	?	-	21.81	
			$\bar{\chi}$ = 259.33			Σ19954.01	
			n = 9				

Table 17 showing the inclusion types, the ΔT°c, the homogenisation temperatures and their standard deviation (σ) of alluvial cassiterites from the Gopeng Consolidated Mine at Gopeng.

(L+V) fluid inclusions in five grains of alluvial cassiterites from the Gopeng Consolidated Mine Limited. The Th°c values are widespread ranging from 190°c to 320°c, (fig. 38 and Table 17), which is not expected in view of the fact that the cassiterites are alluvial and hence could have been derived from lodes of different genesis and geological settings. It is meaningless trying to compare the Th°c values obtained from alluvial cassiterites since their pressures of formation are not known. If the latter values of the alluvial cassiterites are similar, then the Th°c values would be more or less directly proportional to their T_T°c values and a meaningful comparison of the Th°c values could be made.

B. Alluvial cassiterite, (Liang Pong Mine, Gambang).

B.1. Interpretation of results.

Each of the two small alluvial cassiterite grains has two suitable two phase (L+V) fluid inclusions on which homogenisation temperatures were measured. The Th°c values were uncorrected for pressure effects as the necessary data required were not available. The two Th°c values from each cassiterite grain are consistent. The Th°c values from the two grains are comparable and they extend from 260°c to 290°c, (Fig. 39), with a mean value at 274.5°c.

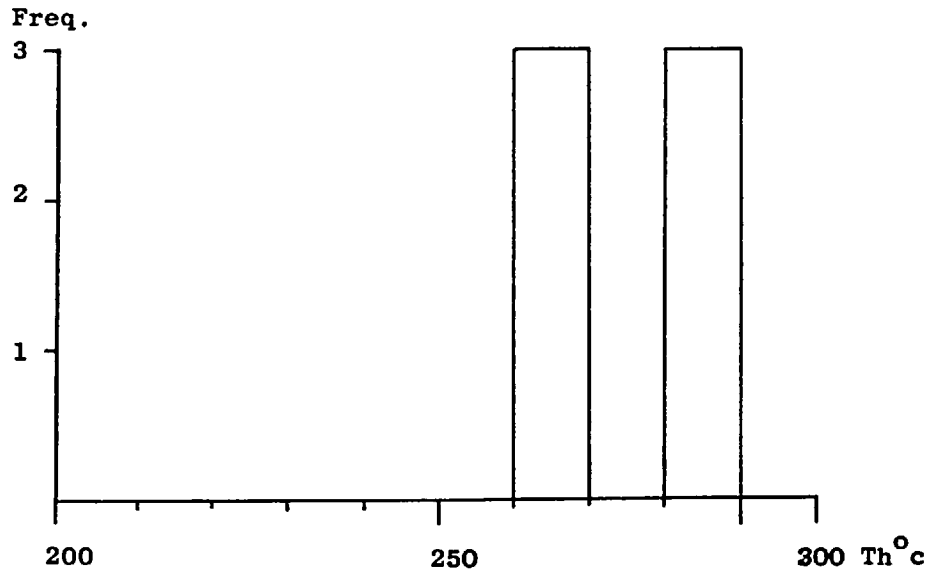

Fig.39. Frequency distribution histogram of Th°c values in primary fluid inclusions of alluvial cassiterites from Lian Pong Mine at Gambang's alluvial tin field.

6.6.5. General Conclusions.

The conclusions which can be drawn from this present study of the fluid inclusions in the selected Western Malaysian cassiterites and their associated gangue minerals are as follows:

1. The cassiterite-forming mineralising fluid medium in general has a salinity of less than 26 equivalent weight percent NaCl. The single exception to this generality is the cassiterite forming mineralising fluid medium from which the cassiterites of Bench A in the Waterfall Mine, (Pelapah Kanan), were deposited; this fluid medium has a salinity range which varies from 31.5 to 34.3 equivalent wt% NaCl.

2. The selected cassiterite samples were deposited in a broad range of te temperatures ranging from 180^{o}c to 500^{o}c.

3. The cassiterites from the tin lodes of the Waterfall Mine, the Sg.Besi Mine and the Eu Tong Seng Mine which

are emplaced either very close to or within the margin of granitoids were consistently deposited from a fluid medium with a temperature greater than 300°c.

4. Both the cassiterite-associated hydrothermal systems of the Hantu lode, (P.C.C.L.), and the tin lodes of the Waterfall Mine have progressively cooled throughout the sequence of mineralisations.

6.6.6. Comparative Study of the results of $Th^{o}c/T_{T}{}^{o}c$ values of Cassiterites from Western Malaysia and those from other tin fields.

A plot of all the ranges of $T_h{}^{o}c/T_T{}^{o}c$ values obtained for the Western Malaysian cassiterites from twelve lode systems, seven of which, (e.g. the Hantu Lode; the Willinks Lode; the Waterfall Mine Lodes; Sg. Besi Mine Lodes; Eu Tong Seng Mine Lodes; Siputeh Lodes and Sg. Pari Lode), belong to the cassiterite-quartz paragenesis and the remainder taken from colluvial/alluvial accumulations is shown in figure The original source of the colluvial/alluvial material can only be inferred. However, the data allows the cassiterites to be thermally classified into three groups according to the ranges of $T_h{}^{o}c/T_T{}^{o}c$ values as listed below:

1. Cassiterites with a range of $T_h{}^{o}c/T_T{}^{o}c$ values above $300^{o}c$ are from the Willinks Lode, (Sample b); the Zone b in cassiterite-bearing greisenised granitoid of Gambang; the Waterfall Mine Lodes; the Timah Gaya Colluvial/ Alluvial deposit; the Sg. Besi Mine and Eu Tong Seng Mine at Tekka Hill.

2. Cassiterites with a range of $T_h{}^{o}c/T_T{}^{o}c$ values below $300^{o}c$ are from the Willinks

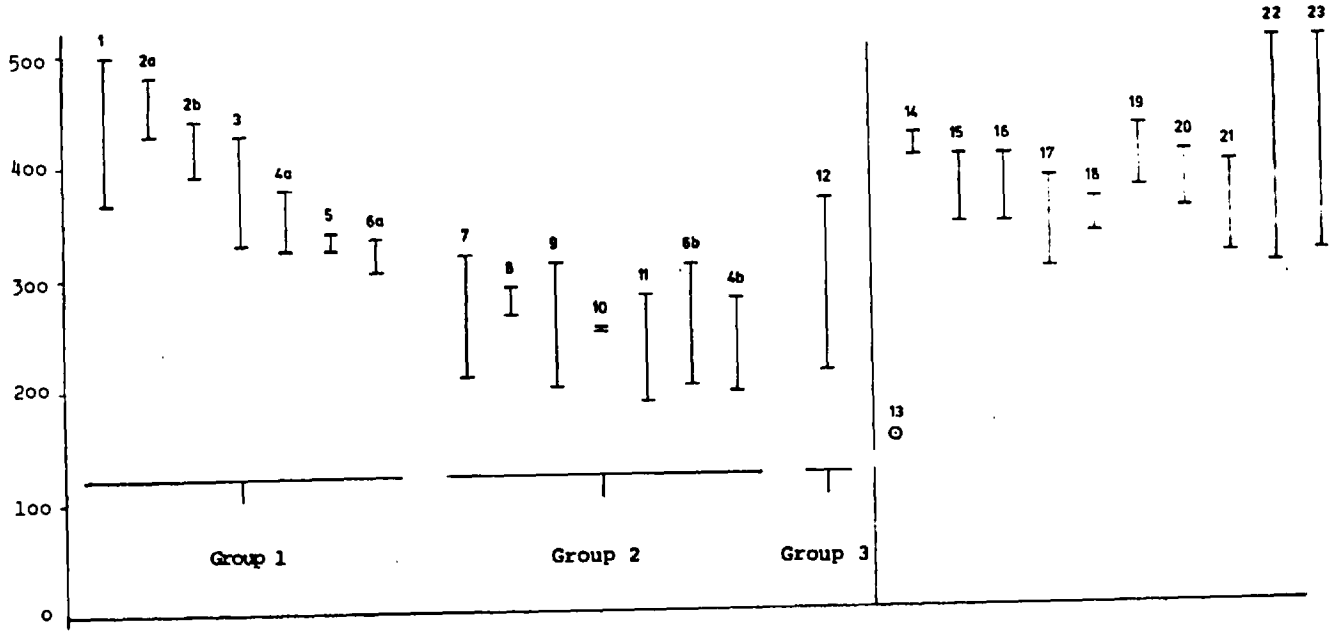

Figure 4o The ranges of Th°c values in cassiterites from Western Malaysia and other important tin fields.

1. Waterfall Mine, Pelapah Kanan.
2a. Timah Gaya Mine.
2b. Timah Gaya Mine.
3. Sg. Besi Mine.
4a. Willinks Lode, (sample b).
4b. Willinks Lode, (sample a).
5. Eu Tong Seng Mine.
6a. Greisenised granitoid of Gambang, (zone b).
6b. Greisenised granitoid of Gambang, (zone a).
7. Chenderiang Tin S.E.A. Mine.
8. Liang Pong Mine, Gambang.
9. Gopeng.
10. Siputeh.
11. Sg. Pari.
12. Hantu Lode.
13. Mexico. Pan and Ypma, 1973.
14. Bostraze Clay Pit.
15. St. Michael's Mount. } Jackson, 1976.
16. Cligga Head.
17. Hemerdon Ball.
18. Goonbarrow Clay Pit. } Jackson, 1976.
19. Preiselberg. Durisova, 1978.
20. Eastern Yakutia, U.S.S.R., (Greisen associated cassiterite). } Yakovlev, 1973.
21. Eastern Yakutia, U.S.S.R.
22. Bolivia. Kelly and Turneaure, 1970.
23. World Wide. Little, 1960.

Lode, (Sample a); the Lian Pong Alluvial Deposit; the Zone a in cassiterite-bearing greisenised granitoid of Gambang; the colluvial/alluvial deposits of the Gopeng Consolidated Mine; the Siputeh Lodes; the Sg. Pari Lode and the colluvial/alluvial deposits of Fook Wan Foh Kongsi, (Chenderiang Tin S.E.A. Mine Sdn Bhd).

3. Cassiterite with a range of $T_h{}^{o}c/T_T{}^{o}c$ values which extends from below $300^{o}c$ up to the lower end of the temperature range of the higher temperature group of cassiterites is from the Hantu Lode.

It can be seen from figure 40 that there is a distinct trend in which cassiterites from lodes which are emplaced either very close to, or within the margin of granitoids, belong to the higher temperature (i.e. > $300^{o}c$), group (1). The cassiterites from the colluvial/alluvial deposits of Timah Gaya Mine were also deposited within temperature ranges which are compatible with those of other cassiterites in Group 1 hence it can be inferred with a measure of confidence that they were deposited in lode structures created in or near to the contact of the parental granitoid.

However, the cassiterites from the Sg. Pari Granite Quarry have a range of T_h °c values below, 300°c and this may suggest that the granite wallrock was not the source of the cassiterite-forming fluids.

The cassiterites with a lower temperature range, (i.e. < 300°c), were probably emplaced in structures located at some distance from the 'source' granitoid intrusive. It is of interest to note that the Western Malaysian cassiterites under study were deposited in a broad range of temperatures ranging from 180°c to 500°c.

The observed correlation between the high temperature nature of the cassiterite-forming fluids and their emplacement within or at the immediate contacts of the margins of granitoids is also observed, (Fig. 40), in cassiterites of quartz-cassiterite paragenesis from the following deposits:

1. The Cornish sheeted vein systems, (e.g. St. Michael's Mount; Bostraze Clay Pits; Goonbarrow Clay Pit; Hemerdon Ball and Cligga Head, (Jackson, 1976).

2. The Eastern Yakutia ore district, (U.S.S.R.), (Yakovlev, 1973).

3. Preisselberg, Eastern Krusne hory Mountains, (Czechoslavakia), (Durisova, 1978).

It is interesting to note that the ranges of $Th^{o}c$ values fo cassiterite from the above mentioned three groups of tin deposits and those from the numerous Bolivian tin deposits, (Kelly and Turneaure, 1970), and also many deposits of the free world countries, (Little, 1960), all lay within the ranges obtained for the Western Malaysian cassiterites studied in this study. The only exception to all the ranges of $Th^{o}c$ values as shown in figure 40 is given by the cassiterites of the subvolcanic tin deposits in Mexico which are likely to have formation temperatures not greater than $150^{o}c$ as indicated by fluid inclusions data, (Pan and Ypma., 1973). In conclusion the data from the literature survey and the results of this present study all indicate that cassiterite precipitation can occur over a broad range of temperatures from $150^{o}c$ to $500^{o}c$ in hydrothermal systems. The data also indicates that the cassiterite-forming fluids that are emplaced in lode structures within or at the immediate contacts of granitoids are generally high temperature. This observation is strong evidence in favour of the inferrence that granitoids are the source of hydrothermal mineralising fluids. It is also possible for the cassiterite-forming hydrothermal fluids

which were emplaced in lode structures at some distance from the nearest granitoids to maintain their initial high temperatures if they were rapidly transported to the sites of deposition by seismic faulting which acts as a pumping mechanism, (Sibson et. al., 1975). This rapid transport would reduce the opportunity for the cooling of the cassiterite-forming fluids by wallrock conduction and mixing with cooler meteoric waters. Thus this possibility must be borne in mind when inferring the primary geological environment from thermal data.

CHAPTER 7.

Fluid Inclusion Study of Chenderiang Valley Pegmatitic Topaz.

7.1. Introduction.

This study was made inorder to specify the physico-chemical nature of the fluid system responsible for the crystallization of the topaz of the famous Chenderiang Pegmatite.

7.1.1. Geological Setting.

The colluvial pegmatitic topaz single crystals (≙ 3 cms.) collected at the Jig Plants of two nearby mine holes of Fook Wan Foh Kongsi, Chenderiang Tin S.E.A. Sdn Bhd., are believed to be derived from the famous topaz-bearing Chenderiang pegmatite which has intruded the Upper Palaeozoic limestone close to the Bujang Melaka granitoid massif. The pegmatite was described by Ingham and Bradford, (1960), while exposures were accessible, although now the progressive workings of the mine has led to its concealment. The pegmatite is mainly composed of alkali feldspar and quartz, and is rich in muscovite; hydromica, (probably gilbertite); tourmaline; topaz; beryl; fluorite; zinnwaldite and cassiterite, and is also associated with various metallic sulphides such as

PLATE 70.

A. An isolated 2 phase (L+V) primary fluid inclusion (Type I) in pegmatitic topaz.

B. A long tubular 2 phase (L+V) (Type I) primary fluid inclusion in pegmatitic topaz.

50µm

25µm

PLATE 71.

A. An isolated 3 phase (CO_2 vap. (a) + CO_2 liq. (b) + aqueous liq (c)) CO_2 poor primary H_2O-CO_2 inclusion (Type IV) in pegmatitic topaz.

B. A large 3 phase (CO_2 vap. (a) + CO_2 liq. (b) + aqueous liq. (c)) CO_2 rich primary H_2O-CO_2 inclusion (Type IV) in pegmatitic topaz.

25µm

25µm

jamesonite and galena. All these minerals may occur in coarsely crystalline form.

7.1.2. Previous work.

There has not been any fluid inclusion study done on topaz from Western Malaysia. This study is the first contribution in this field.

7.2. Petrography of fluid inclusions and their significance.

Using a Vickers polarizing petrographic microscope equipped with X5, X10, X40 objective lens and a X7 ocular lens polished and cleavage chips of pegmatitic topaz were examined. Six main types of primary and pseudosecondary fluid inclusions were recognised and they are listed as shown below:

I. Two phase (L+V), (Plates 70A and 70B).

II. Three or more phase (L+V+>1S),

III. Multiphase silicate melt inclusion $\pm$ saline brine and vapour bubble,

IV. Three phase CO_2 rich, (CO_2 vapour + CO_2 liquid + aqueous fluid), (Plates 71A and 71B).

V. Two phase CO_2 poor, (CO_2 vapour +

100μm

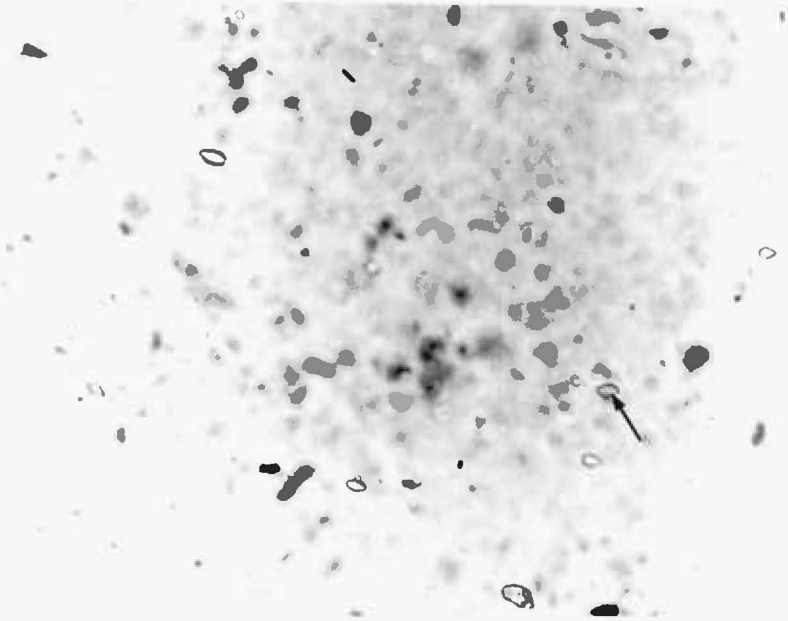

100μm

100μm

aqueous fluid) at RT°c, (Plate 72A).

VI. Primary mineral inclusion, (Plate 72B).

Type I. Two Phase (L+V) Fluid Inclusions.

These two phase fluid inclusions contain aqueous liquid and vapour and they commonly occur either isolated, (Plate 70A), or segregated as groups in a population, (Plate 72C). They have also been observed to coexist with Type II and Type III fluid inclusions, (Plate 73), in populations of cogenetic origin as indicated by the consistency of Th°c values in the fluid inclusions concerned, and the parallel alignment of their long axes with the growth margins of the host crystals. In addition to the above mentioned assemblages, the Type I inclusions also occur together with Type II fluid inclusions and also with Type IV fluid inclusions in cogenetic populations.

The observed coexistence of the Type I fluid inclusions with the other major types of fluid inclusions must be taken to indicate:

1. The existence of immiscibility between the silicate melt, (Type III), and the relatively dilute aqueous

PLATE 73.

The coexistence of Type I(a), II(b) and III(c) fluid inclusions in a cogenetic population of fluid inclusions. This population is orientated parallel to the crystal margin of the host pegmatitic topaz, thus indicating its primary origin.

100μm

fluid represented by the Type I fluid inclusion.

2. The immiscibility between CO_2 rich aqueous phase represented by Type IV fluid inclusion and the relatively dilute, (i.e. <26 equiv. wt.% NaCl), aqueous fluid represented by the Type I fluid inclusions and

3. The immiscibility between relatively dilute fluids, (represented by Type I fluid inclusion), and saline aqueous fluids, (represented by the Type II inclusion.

The latter form of immiscibility between two aqueous fluids, although apparently not easily explained, is commonly reported in the literature, (Roedder, 1972). The existence of such immiscibility even on the microscopic scale has often been explained in terms of inhomogeneous mixing between hot and dense brines and the cooler, less dense and less saline meteoric waters, (Groves and Solomon, 1969). In such a model mixing system it is, nevertheless, difficult to envisage the existence of inhomogeneous mixing on a microscopic sale.

Type II. Three or more phase (L+V+S(>1) fluid inclusions.

These fluid inclusions of three or more phases contain aqueous brine, vapour and 1 or more solid phases and they commonly occur together with Type I and Type III fluid inclusions in cogenetic populations, (Plate 73). Type II fluid inclusions also not infrequently occur with Type I fluid inclusions. The presence of these Type II inclusions, together with those of Types III and IV was also observed.

A great variety of crystal habits was observed amongst the solid phases present in the Type II fluid inclusions. These include birefringent and optically isotropic phases, most of which commonly dissolve in the inclusion fluids before the liquid-vapour homogenisation temperature is reached. This finding, together with their consistent presence within a population of fluid inclusions are strong evidence for their origin as daughter phases as opposed to captive incorporation during inclusion growth. Those which were insoluble, even at temperatures well above, (i.e. about 100°c - 150°c), that of liquid-vapour homogenisation, are likely to be silicate phases which are known not to reach solution thermal equilibrium readily, (Roedder, 1978), within the short heating times, (½ hour), employed during this study. A few hours or even a few days or weeks or heating

PLATE 74.

A. Necked Type III fluid inclusions showing birefringent and microlite silicate daughter phases as well as isotropic silicate glasses. (Crossed Polars).

B. The same inclusions as above showing crystalline (a); microlite (b) and glassy silicate daughter phases (c). (Plane Polarized light).

C. Type III fluid inclusions are packed with birefringent poorly crystalline silicate daughter phases.

100µm

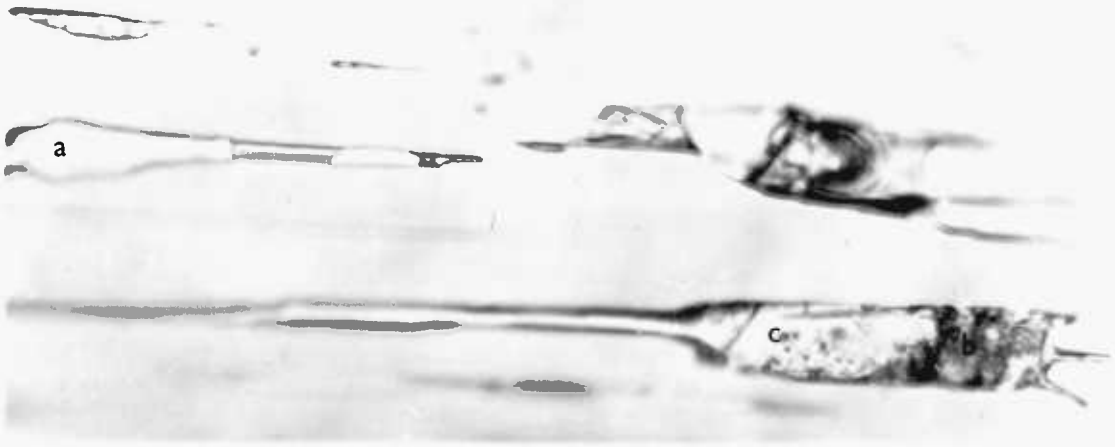

100µm

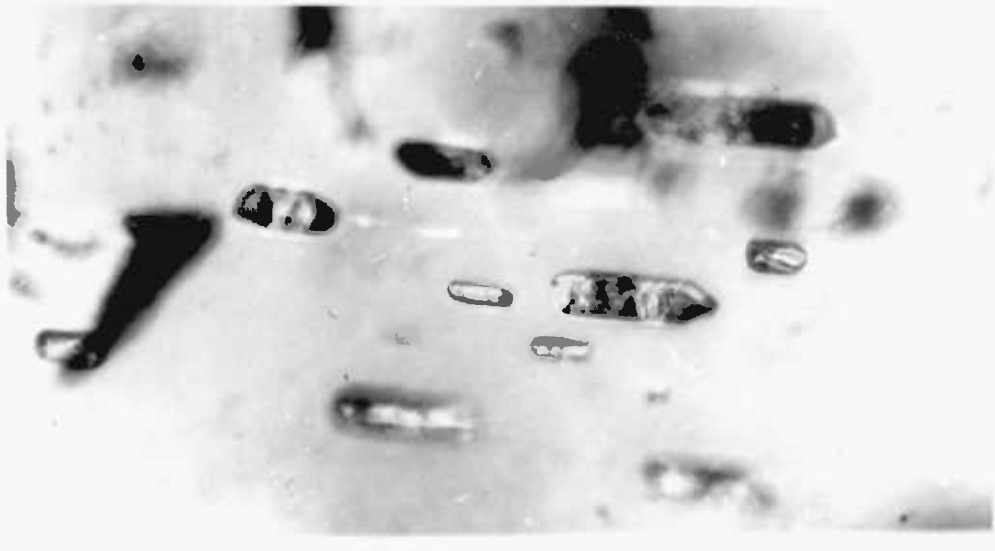

25µm

at high temperatures, (400°c-500°c), may be necessary before diffusion could allow equilibrium to be achieved, before the occurrence of solution of the insoluble phases, (Roedder, 1971). The presence of silicate and largely non-silicate daughter phases within a single fluid inclusion indicates that there was coexistence of silicate melt and saline aqueous brine even down to the microscopic scale of a fluid inclusion.

The coexistence of the Type II fluid inclusion with the other main types of fluid inclusion is strong evidence for the existence of a heterogeneous medium composed principally of silicate melt and aqueous fluids of different salinity and CO_2 content.

Type III: Multiphase silicate melt fluid inclusions ± saline brine and associated vapour bubble.

These multiphase silicate melt fluid inclusions contain largely silicate phases which occur as devitrified glass individual crystals and fine microlite aggregates with or without saline aqueous liquid and its non-silicate daughter mineral phase(s), (Plates 74A and 74B).
to be expected, as observed, that where aqueous liquid is contained within the Type III fluid inclusions one or more vapour bubbles are always present within each inclusion. Sometimes a small vapour bubble can

PLATE 75.

A. The Type III fluid inclusions are packed with birefringent silicate inclusions (arrowed) coexisting with Type I(a) and Type II(b) fluid inclusions. All these fluid inclusions are orientated with thier long axis parallel to the growth margins of their pegmatitic topaz host - thus indicating their primary origin, (Crossed Polars).

B. Three phase (CO_2 vap + CO_2 liq + aq. lig.) CO_2 poor fluid inclusions (Type IV), (arrowed), coexist and align parallel with Type III and Type II fluid inclusions. These fluid inclusions are orientated with their long axis parallel to the growth margins of their pegmatitic topaz host.

100μm

100μm

be easily overlooked in a fluid inclusions packed with silicate phases. The silicate phases are characterised by their failure to melt, even at temperatures 100°c - 150°c above that of the liquid-vapour homogenisation. The silicate phases besides being isotropic as in silicate glasses are largely distinctly to strongly birefringent, (Plate 74A).

The cogenetic association of Type III fluid inclusion with the other major types of fluid inclusions is as follows:

Type III	+	Type II	+	Type I	(Plate 73)
Type III	+	Type II			(Plate 75A)
Type III	+	IV			(Plate 75B)
Type III					(Plate 76B)

The presence of the Type III silicate melt inclusions naturally indicates that silicate melt was present during the crystallization of topaz and hence confirms that the crystallization occurred during the pegmatitic stage linking the magmatic to the hydrothermal stage of evolution of the system, (Jahns and Burnham, 1969). The coexistence of the Type III inclusions with the aqueous fluid phases as shown above, indicates that the silicate melt was immiscible with the aqueous fluid phases within a heterogeneous fluid system.

PLATE 76.

A. A very large Type III fluid inclusion is packed with birefringent crystalline (a) and microlite (b) silicate daughter phases. This inclusion has undergone necking.

B. Type III fluid inclusions is packed with crystalline and microlite silicate daughter phases.

C. Type II fluid inclusion consisting of devitrified silicate glasses (arrowed a) and a cubic daughter mineral (arrowed b) probably halite.

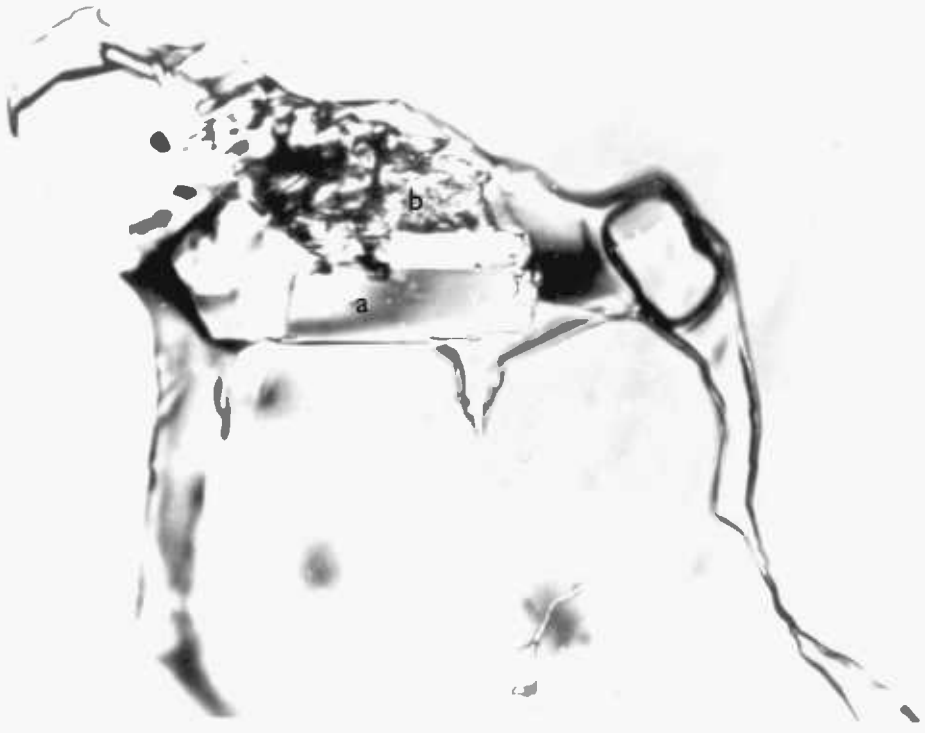

50µm

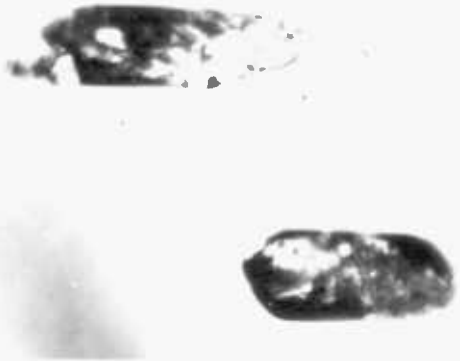

25µm

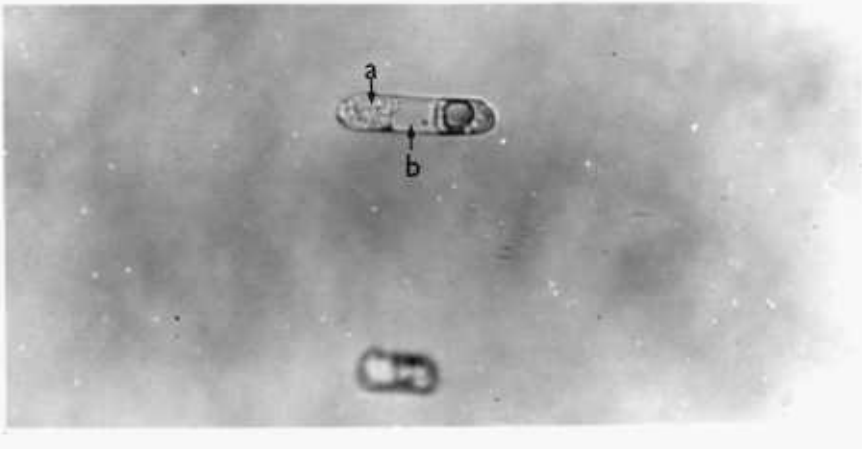

25µm

PLATE 77.

A. A large Type III silicate inclusion in pegmatitic topaz consisting of a vapour bubble, aqueous liquid and numerous crystalline silicate phases and two long dark coloured unidentified rods. These phases were not identified because they were lost as a result of the inclusion having exploded during the heating run. However, they are probably silicate phases since they have failed to dissolve before and well after the liquid/vapour homogenisation temperature.

30μm

The three main forms of crystallization of the silicate melt phase as mentioned earlier have all been seen either occurring together, (Plates 74A and B and 76A), or individually within a single Type III fluid inclusion, (Plate 77). The coexistence of silicate crystals and microlites $\pm$ minor amount of silicate glass was commonly seen in the large and irregular inclusions, (Plates 74A and 74B, and 76A and 76B), whereas the smaller and regular cigar-shaped or spherical inclusions tend to contain silicate glass $\pm$ minor amount of crystals, (Plate 76C). This observation has led to the conclusions that:

1. The crystallization of silicate melt as crystals and microlites was determined by the large surface areas and the availability of nucleation sites on the walls of large and irregular inclusions and, presumably, a slow cooling rate, (Roedder, 1971 and 1978).

2. The crystallization of silicate glass was the consequence of reduced surface areas, and in the number of nucleation sites in small and regular inclusions. Fast cooling rate can also be responsible for forming of the silicate glass, (Roedder, 1971 and 1978).

Type IV. Three phase CO_2 rich fluid inclusions containing CO_2 vapour + CO_2 liquid and aqueous liquid.

This type of fluid inclusion is common and it occurs in the following manners:

1. Isolated, (Plate 71A).

2. In segregated homogenous populations.

3. In coexistence with Type I fluid inclusions in isolated groups of few fluid inclusions.

4. In coexistence with Type II and Type III fluid inclusions.

5. In coexistence with Type III, (Plate 75B).

The Type IV CO_2-rich fluid inclusions have not been seen to contain any solid, (daughter), phases. This observation is to be expected as it has been shown by Takenouchi and Kennedy, (1965), that the solubility of halite decreases with increasing content of CO_2 in H_2O. It is presumed that other salts may have behaved like halite in a CO_2-H_2O fluid.

The coexistence of the Type IV CO_2 fluid inclusions with the other main types of fluid inclusion is strong evidence that immiscibility was present in the crystallising medium in which topaz formed. The presence of the Type IV fluid inclusions shows that the F-enriched topaz-forming medium was also enriched in CO_2.

Type V. Two phase, (CO_2 vapour + L), fluid inclusions.

These two fluid inclusions contain CO_2(?) vapour and aqueous liquid as observed at room temperatures, but a transition to a three phase state with the appearance of a thin rim of liquid CO_2 around the vapour bubble took place during the initial stages of the freezing process. This type of CO_2 poor fluid inclusion is very rare in the samples of the pegmatitic topaz studied and it was detected only in two instances.

1. In an isolated large inclusion, (Plate 72A), whose liquid CO_2 begins to separate from the aqueous liquid at $+21^{o}c$, and

2. In an isolated group of a few such inclusions, one of which has a partial $Th^{o}c$ value of $+14^{o}c$ for its liquid CO_2.

Type VI. Primary mineral inclusions.

These primary mineral inclusions of at least five different mineral species were commonly seen in the numerous samples of topaz studied. They occur as euhedral and subhedral crystals suspended in the topaz-forming crystallizing medium. The coexistence of mineral grains within the silicate melt-aqueous fluid heterogeneous system is a real possibility according to the results of experimental work by Smith, (1948); Quensel, (1956) and Jahns and Burnham, (1969).

The possible identities of these mineral inclusions are discussed in section

7.2.1. Conclusions.

The population pattern of the fluid inclusion types described above suggests that the topaz-forming fluid medium from which the pegmatitic topazes have crystallized was a heterogeneous system composed of the aqueous phases, (e.g. CO_2-rich; dilute; and saline fractions), and a silicate melt. The scale of the immiscibility varies from macro- to micro- scopic. This system was enriched in CO_2, in addition to F which is an essential element for the crystallization of the topaz structure.

The observed coexistence of an aqueous phase, (in this case it is comprised of CO_2 rich, and dilute and saline fractions), with silicate melt in the Chenderiang Valley pegmatitic topaz has also been observed in the primary fluid inclusions of pegmatitic topaz of Volynia in the Ukraine region, (U.S.S.R.), (Yermakov, 1965; Ivantishin, 1955; Kalyuzhny , 1956; Lemmleyn et. al., 1962; Sobolev et. al., 1964; Motorina, 1967; Voznyak, 1968; Dolgov, 1968; Pavlishin et. al., 1968; Yusupov and Dolgov,1970; Naumov et. al, 1977).and also in those topazes from the pegmatites at Dzun-Bain in Mongolia, (Lkhamsuren, 1970), and from the Amazonite pegmatites of Baga-Gazryn Massif in Mongolia, (Naumov et. al., 1977). It is, however, interesting to note that the CO_2-rich fraction of the aqueous phase common in the Chenderiang Valley pegmatitic topazes is absent in both the Russian and the Mongolian pegmatitic topazes mentioned above. Many other pegmatitic minerals have also been reported to contain silicate melt coexisting with an aqueous phase, (Cameron et. al., 1953, p. 257-259; Smith, 1954; Jahns, 1955,p. 1,090-1091; Roedder, 1958, 1963 and 1967). This immiscible coexistence of the aqueous phase and silicate melt has been regarded as a real possibility on theoretical grounds by the following authors namely Morey, (1922 and 1924); Niggli, (1937); Verhoogen, (1949) and Turner and Verhoogen, (1960), and it derives strong support from the results of

experimental work by Smith, (1948) and Jahns and Burnham, (1969).

7.3. Identification of solid phases.

7.3.1. Introduction

A combination of techniques such as optical microscopy; heating method and the Scanning Electron Microscopy plus its energy dispersive x-ray microanalyser was used to identify the solid phases present in the Type II and Type III fluid inclusions. The heating and freezing methods were used to identify the liquid CO_2 in Type IV and Type V fluid inclusions. The main purpose of this investigation was to reveal the chemical nature of the fluid medium from which the pegmatitic topazes have crystallized.

7.3.2. Optical and heating methods.

A Vickers polarizing petrographic microscope equipped with X5, X10, X40 objective lens and a X7 ocular lens was used to record the optical properties of the solid phases contained within the Type II and Type III fluid inclusions. A large majority of the solid phases examined were daughter minerals as suggested by:

1. Their consistent presence within

Minerals	Crystal habit	Colour	Pleochroism	Extinction angle	Birefrigence/ Isotropism	Range of T sol°c	Ave T sol°c	Number of determinations
Quartz	Hexagonal	Colourless	none	-	Isotropic/ Weakly birefrigent	insoluble	-	-
?	Lath	Colourless	none	Parallel extinction	Birefrigent	41 - 51	47	5
Opague	Speck	Opaque	-	-	-	321	-	1
paque	?	Opaque	-	-	-	273	-	1
Halite/ Sylvite	Cubic	Colourless	none	-	Isotropic	155 - 193	173.25	4
?	Rectangular	Colourless	none	-	Birefrigent	51 - 70	61.6	7
Calcite	Rhombic	Colourless	none	Symmetrical to cleavage traces.	Strongly birefrigent	56 - 158	122.75	4
?	Hexagonal	Colourless	-	Symmetrical to cleavage traces.	Birefrigent	65 - 83	67.33	3
?	Subhedral	Colourless	-	-	Birefrigent and isotropic	-	-	-
?	Octahedral	Colourless	-	-	Birefrigent	82 - 95	88.5	2
$CaSO_4$	Enhedral Lath.	Colourless	-	Parallel Extinction	Birefrigent	Insoluble	-	-
?	Tiny Granular	Colourless	-	-	Birefrigent	-	-	-

Table 18 showing the optical properties of daughter minerals present in Type II and Type III fluid inclusions of topaz from the Chenderiang Pegamtite.

populations of fluid inclusions, and

2. Their consistent dissolution at temperatures below that of liquid-vapour homogenisation. Those solid phases which were unaffected by heating even at temperatures well above, (i.e. by $\sim 100^{o}c$), the liquid-vapour homogenisation temperatures were likely to be silicate phases.

The optical properties and the thermal behaviour of the numerous daughter mineral phases largely from the Type II fluid inclusions are given in Table 18. The identification of quartz and halite or sylvite based on the optical and thermal properties was confirmed by the chemical and morphological data provided by the S.E.M. The strongly birefrigent rhomb is likely to be calcite. The presence of daughter calcite is to be expected in view of the presence of CO_2 and Ca in the inclusion fluids. The presence of Ca was detected by the S.E.M. The insoluble birefrigent euhedral lath with parallel extinction is probably a calcium sulphate phase. Again the presence of such phases is not unexpected as the S.E.M. study has shown the presence of sulphur and calcium in the evaporate residue from inclusion fluids. The

PLATE 78.

A. Two primary mineral inclusions in pegmatitic topaz show similar rhombic crystal form- they are probably calcite.

B. Two rhombic primary mineral inclusions in pegmatitic topaz are probably calcite.

C. A large platy rhombic primary mineral inclusion in pegmatitic topaz; it is probably a calcite.

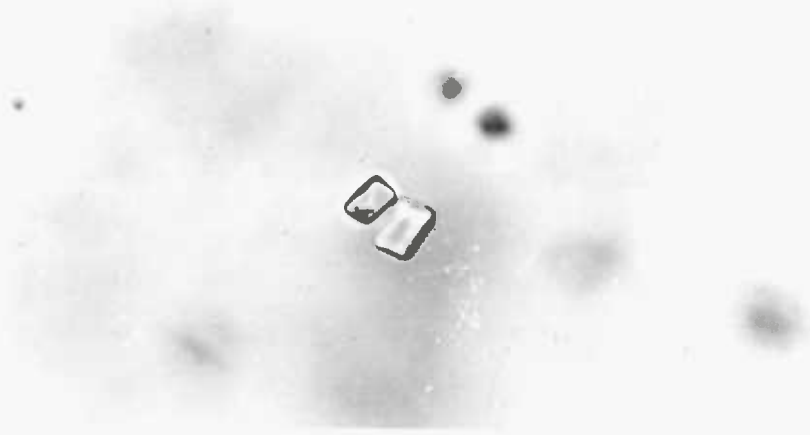

25µm

25µm

25µm

remaining seven daughter minerals remained unidentified pending more S.E.M. work.

The presence of silicate glass was recognised by its devitrified texture and optical isotropism, (Plate 74A). The birefringent crystalline silicate daughter minerals were recognised by their formation into acicular masses when quenched following melting at magmatic temperatures, 700°c - 900°c.

The mineral inclusions could not be positively identified by using the optical microscopic method alone. Nevertheless, the possible identities of the mineral inclusions may be inferred from their optical properties. The optical properties and the possible identities of these inclusions are described below as follows:

1. The rhombic crystals, (probably calcite), (Plates 78A, 78B and 78C). These colourless rhombic crystals are notably birefringent, but their refractive indices are lower than that of the host topaz. The most probable identity of those rhombs is the carbonate, calcite.

2. The prismatic crystals, (Plate 79A). (Probably an aluminium silicate of K, Ca or Cs or a mixed aluminium

PLATE 79.

A. A colourless birefringent prismatic mineral inclusion in pegmatitic topaz. This inclusion is probably an aluminium silicate of K, Ca or CS or a mixed aluminium silicate of all the 3 elements).

B. A pencil-like prismatic primary mineral inclusion (probably gypsum) in pegmatitic topaz.

C. A hexagonal primary quartz inclusion in pegmatitic topaz.

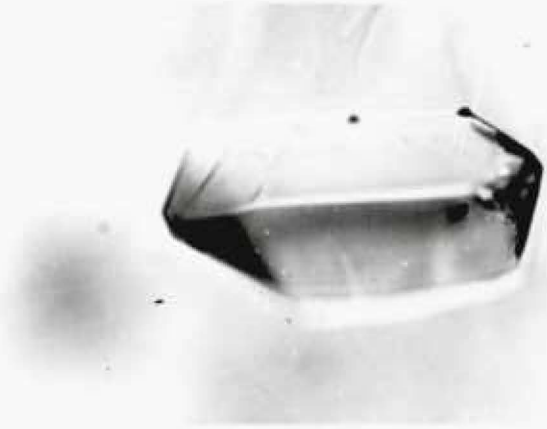

50 µm

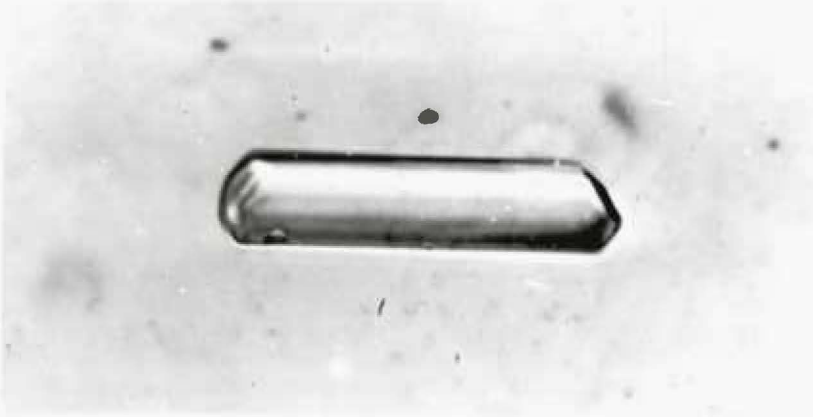

50 µm

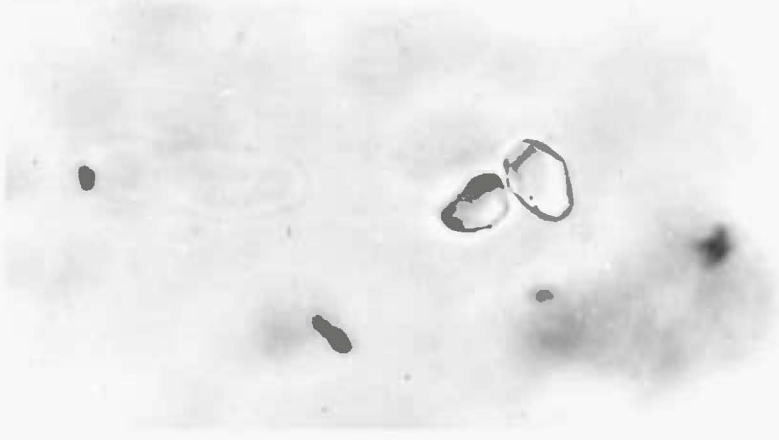

25µm

silicate of all the three elements). These colourless prismatic crystals are birefringent and their crystal habit is rather similar to that of the daughter minerals from Type II and Type III fluid inclusions which have been identified using the S.E.M. + x-ray microanalytical technique as aluminium silicates of K, Ca and Cs and also as mixed aluminium silicate of K and Cs and K, Ca and Cs.

3. The elongate euhedral prismatic laths, (Plate 79B), (probably gypsum). These colourless elongate pencil-like prismatic laths are weakly birefringent and they show parallel extinction. Elongate pencil-like laths have been reported by Dana, (1951), as one of the characteristic forms of gypsum. Thus these laths are tentatively identified as gypsum. This suggestion is reasonable in view of the fact that the topaz-forming fluids have been shown to contain Ca and S by the S.E.M. + x-ray microanalytical technique.

4. The hexagonal crystals, (Plate 79C), (probably quartz). These colourless

PLATE 80.

A. A large birefringent platy hexagonal primary mineral inclusion in pegmatitic topaz: two tiny mineral grains adhere on its surface. The platy inclusion is probably a mica.

B. An aggregate of birefringent platy primary mineral inclusions in pegmatitic topaz. These inclusions are probably micas.

100µm

100um

hexagonal crystals are birefrigent and they have a refractive index of less than that of the topaz host. Thus they are probably quartz as quartz daughter minerals have been identified by the S.E.M. technique.

5. The platy hexagonal crystals, (probably mica), (Plates 80A and 80B). These colourless platy hexagonal crystals are strongly birefrigent and they have a refractive index which is lower than that of the topaz host. These crystals are probably micas.

All the above mentioned mineral inclusions failed to melt even at around 550°c. The suggested identities of these mineral inclusions can be confirmed by the use of scanning electron microscopy in conjunction with an energy dispersive x-ray-analysis system or by using the Electron Probe on suitable polished plates.

7.3.3. Heating and Freezing Methods.

The second liquid phase which occurs as a thin ring around the vapour bubble in the Type IV and V fluid inclusions was seen to have a high coefficient

14.0

19.5

20.5

20.5

21.0

22.5

24.75

26.0

27.45

28.5

29.0

29.35

29.6

30.0

30.25

30.75

30.95

31.75

32.75

33.9

34.3

Table 19. Partial $Th^{o}c$ values of liquid CO_2 in the CO_2-H_2O fluid inclusions of the Chenderiang Valley pegmatitic topaz.

of thermal expansion and a low Th°c value often below 31.1°c, (the critical temperature for pure liquid CO_2), and a few even homogenise below ambient temperature, (Table 19). However, there were four out of the twenty-one determinations made which gave Th°c values, (Table 19), for liquid 'CO_2' within a range between 32°c - 34°c, (Table 19). These Th°c values are considered anomalous and they may be due to the presence of dissolved CH_4 and H_2S in the liquid CO_2 which could elevate the Th°c value. (CH_4 and H_2S are known to have higher critical temperatures than pure liquid CO_2, (Roedder, 1967).

The liquid CO_2 homogenises either to the vapour or liquid phase depending on the relative volume ratio between the liquid CO_2 and the CO_2 vapour. It homogenises to the vapour phase when the volume of liquid CO_2 < volume of CO_2 vapour, (Plate 71A), and Fig. 41), whereas the homogenisation to the liquid phase occurs only when the volume of the liquid CO_2 > vapour, (Plate 71B and Fig. 42). The former case of homogenisation to the vapour phase was most commonly encountered throughout this study. The occurrence of cogenetic CO_2-H_2O fluid inclusions with different ratios of volume of liquid CO_2/Volume of CO_2 vapour indicate that the aqueous inclusion fluids have different concentrations of dissolved CO_2. This difference could be the consequence of different salinities in the aqueous inclusion fluids as it has

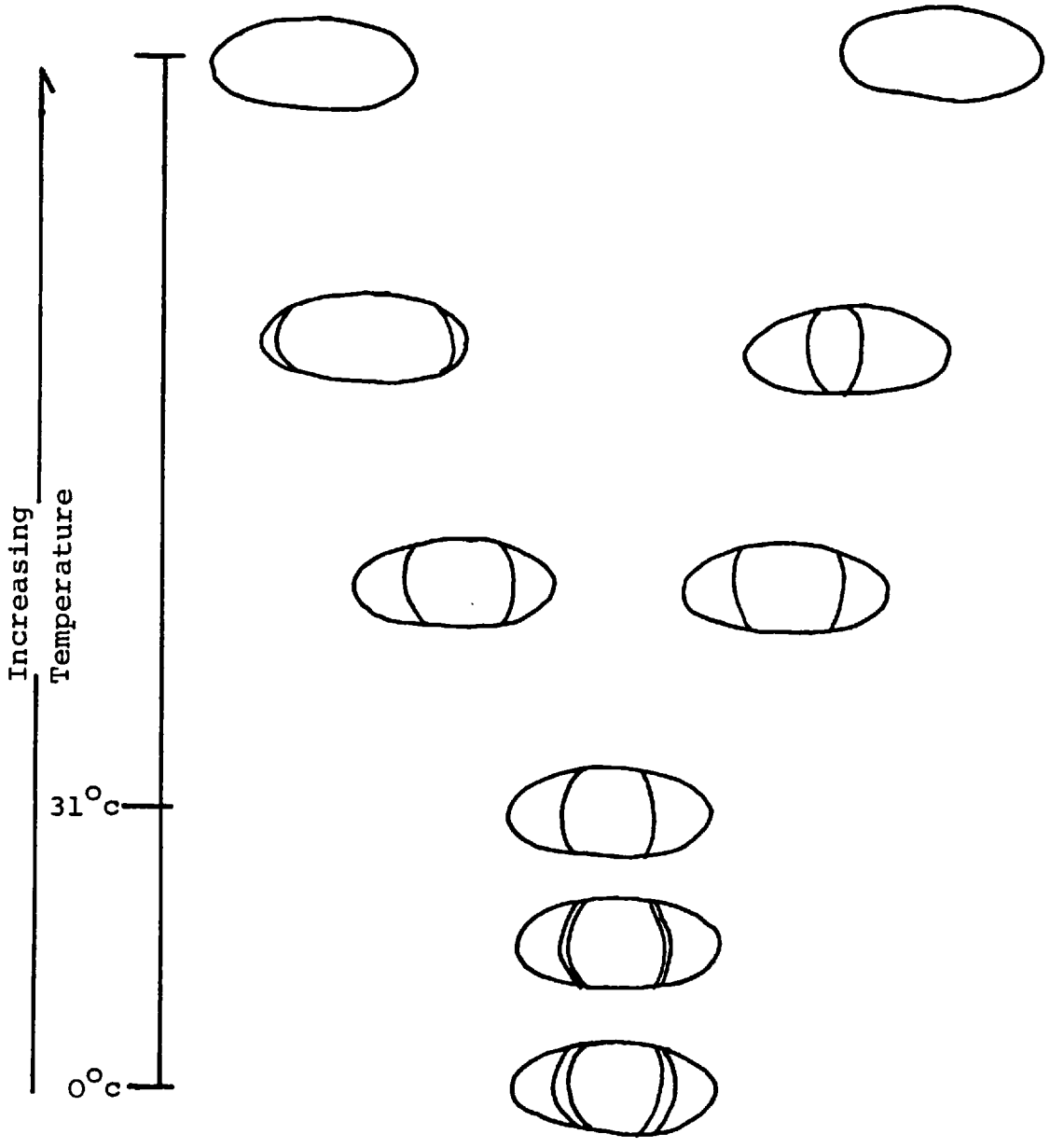

Figure 41. The homogenisation behaviour of CO_2 poor CO_2-H_2O fluid inclusions.

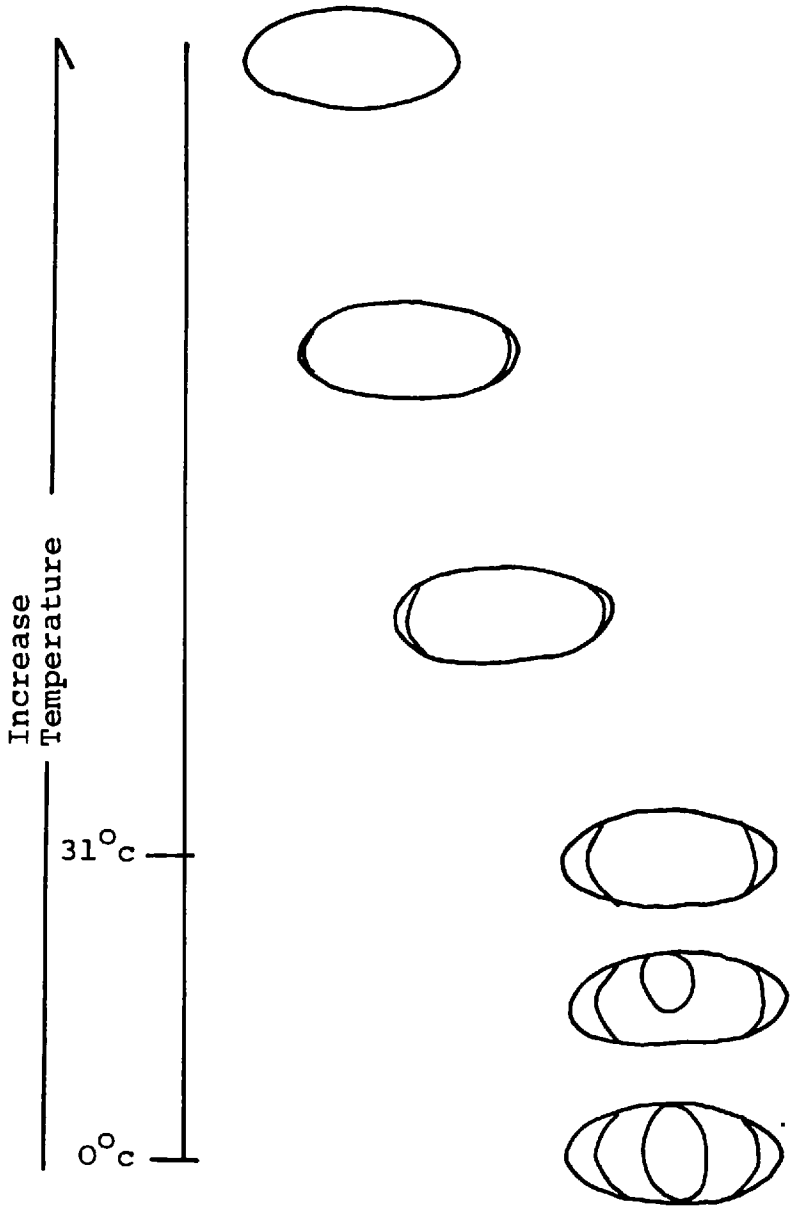

Figure 42. The homogenisation behaviour of CO_2 rich CO_2-H_2O fluid inclusions.

been shown by Takenouchi and Kennedy, (1965), that the solubility of CO_2 in aqueous fluids increases with decrease in salinity.

Besides these two criteria for the identification of liquid CO_2, the third criterion used in this study is the melting point of the CO_2 Clathrate compound, (CO_2-5 3/4 H_2O), which is known to be above 0^oc, (Roedder, 1967, 1972). The melting points of the CO_2 clathrates determined in this study are all above 0^oc and they are $+6.9^oc$; $+7.3^oc$; $+7.9^oc$ and $+8.6^oc$. Thus it can be confirmed that the second liquid phase in the Type IV inclusion is liquid CO_2.

7.4. The Scanning Electron Microscopy and its Energy Dispersive x-ray Microanalyser.

7.4.1. Previous Investigations.

In spite of the imaging capability of the S.E.M. with respect to small objects there has been little published S.E.M. work on fluid inclusions. The S.E.M. has, so far, being used to study the morphology of inclusion cavities, (Deicha, 1973), and of daughter minerals lifted from their inclusions by replica methods, (Boyarskaya, 1973). With the adaptation of an x-ray spectrometer to the S.E.M., it can become a valuable tool for the study of the morphology of daughter minerals in situ in opened fluid inclusions and simultaneously their qualitative major-element chemistry. Thus this tool is now the most reliable method for the identification of solid phases in fluid inclusions when used in combination with their diagnostic optical properties.

Three groups of users of the S.E.M. with energy dispersive x-ray analyser were rewarded with success in their attempts to identify the daughter minerals and 'evaporite' products of inclusion fluids. Grant et. al., (1976), identified NaCl, NaKCl and hydrous FeCl in saline inclusions of pre-cassiterite vein quartz; these results showed the major elements present in the fluids as iron,sodium, potassium,

Host Minerals and Localities	Type of fluid inclusions	Minerals identified	Authorities
Quartz	Polyphase fluid inclusions	Halite NaKCl Hydrous FeCl	Grant, Halls,
Quartz phenocrysts (Porphyry Cu deposit of Cerro Ver Verde/Santa Rosa of Southern Peru).		Silicates Chlorides Sulphates Phosphates Sulphides Oxides	Le Bel, (1976).
Fluorite, (Jamestown, Colorado).	Polyphase inclusions	Anorthite Arcanite Barite Celestite Ferroan Rhodocrosite Glaserite Gypsum Halite Phlogopite Sylvite Thenardite	Metzger, Kelly, Nesbitt and Essene, (1977).
Quartz, (Gold-quartz veins of of the Oriental Mine at Alleghany, California).		Muscovite(?) Dawsonite.	As above.
	A polyphase fluid inclusion	Sylvite Halite Gypsum Glauberite(?) Chlorocalcite (?)	As above.
Calcite (the Carbinatite at Magnet Cove, Arkansas.	Polyphase fluid in inclusions. Silicate melt inclusions.	Arcanite Thenardite Celestite Cs-La-carbonate A Calcium silicate, (larnite(?)) calcite magnetite.	As above.

Table 20 shows the list of mineral phases of fluid inclusions which have been identified by the S.E.M. and its x-ray microanalyser technique.

calcium, chlorine and sulphur. Le Bel, (1976), carried out a preliminary study of the solid phases in the fluid inclusions of the quartz phenocrysts from the porphyry copper deposit of Cerro Verde/ Santa Rosa of Southern Peru; he identified silicates, chlorides, sulphates, phosphates, sulphides and oxides. Metzger et. al., (1977), have established the presence of Anorthite, Arcanite, Barite, Celestite, Ferroan rhodochrosite, Glaserite, Gypsum, Halite, Phlogopite, Sylvite and Thenardite in polyphase inclusions in fluorite from Jamestown, Colorado; the precision of the S.E.M. method was tested with success in the identification of Dawsonite, $(NaAl(CO_3)(OH)_2)$, which had previously been identified by Coveney and Kelly, (1971). The Dawsonite is often accompanied by a potassium-aluminium silicate, possibly muscovite in fluid inclusions in quartz from gold-quartz veins of the Oriental Mine at Alleghany, California. Lastly Metzger et. al., (1977), also identified halite, sylvite, gypsum, glauberite(?) and chlorocalcite(?) in a multiphase hydrothermal inclusion; other phases identified in different inclusions are arcanite, thenardite, celestite and an unexpected phase is cesium-canthanum carbonate. All the mineral phases were found in multiphase saline inclusions in calcite from the carbonatite at Magnet Cove, Arkansas. Daughter minerals such as calcite, magnetite and a calcium silicate, probably larnite were identified in melt inclusions of the same deposit at Magnet Cove. The results described above are summarised in table 20.

7.4.2. The S.E.M. Method and Sample Preparation.

The S.E.M. with its energy dispersive x-ray microanalyser has been proved to be the most reliable method for the identification or at least for limiting the possible identity of solid mineral phases when combined with the optical properties. The great advantage of this method is that crystal morphology and major-element chemistry of the mineral phases can be studied simultaneously by display on a cathode-ray screen at various magnifications with clarity,if properly coated with carbon or gold. The carbon/gold coating is for discharging the current built up on the samples by the electrons from the electron-beam.

Sample preparation for the S.E.M. work involved careful fracturing by hand with tweezers of sample cleavage chips or polished plates which were previously seen to contain dense population(s) of Type II and Type III fluid inclusions. The line of fracture was chosen to cut through the area where the population of fluid inclusions was densest as this would statistically enhanced the chances of finding more solid phases retained in the inclusion cavities. The fracturing of the samples was done preferably a short time before the scanning work began as some solid phases may deliquesce when exposed to the moisture in the air. Unfortunately most of the fluid inclusions in the samples fractured by the manner

just described were found to be devoid of daughter phases and silicate inclusions. This could be partly due to the shock effect at the time of fracturing which could throw the solid phases from their matrix. However, this problem was successfully overcome by a gentler fracturing procedure which involved cutting a superficial line by diamond pen on the sample and then using two glass slides one on top and the other below the latter to apply a little pressure to fracture the sample. When S.E.M. work could not be done immediately after the fracturing, the fractured samples were stored in a dessicator to prevent deliquescence. The fractured samples were individually glued upright with their planes of fracture facing up on an aluminium stud using araldite glue. These samples were then coated with carbon. Gold and aluminium have been used for coating by other workers, but they produced interfering x-rays under electron bombardment, thus, while imaging was improved, semiquantitative analysis was hindered. For this reason carbon must be used.

7.4.3. The Interpretation of S.E.M. Results.

Topaz cleavage chips/polished plates bearing primary and pseudosecondary fluid inclusion populations consisting largely of Type II and Type III inclusions when fractured across and viewed under the Scanning Electron Microscope were often devoid of the largely

birefringent daughter phases described previously by examination using a polarizing petrographic microscope. The likely reasons for this loss of the daughter phases are the sudden release of high pressure which is to be expected in pegmatitic minerals when fluid inclusions are opened together with the method of fracturing the sample already been discussed earlier. The release of this high pressure has presumably ejected the daughter phases from their inclusion cavities. Although this loss of daughter phases caused disappointment to the writer, it has, however, given an important indication of the high pressure regime prevalent during the crystallization of the pegmatitic topaz.

Fortunately, the few solid phases which remained behind either in the inclusion cavities or on their rims still retained their crystal habits. The solid phases in the inclusion cavities which were well exposed above the plane of fracture, and those sitting near the rims, were scanned effectively by the S.E.M. electron beam. Combining the x-ray chemical data with the observed crystal habits and optical properties they were readily identified with a measure of confidence, those lacking good crytal habits and definitive optics were more difficult to diagnose. The minerals which were readily identified are described below as follows:

Figure 43.

SEM X-ray Scan of Halite daughter mineral in the fluid inclusions of Chenderiang Valley topaz.

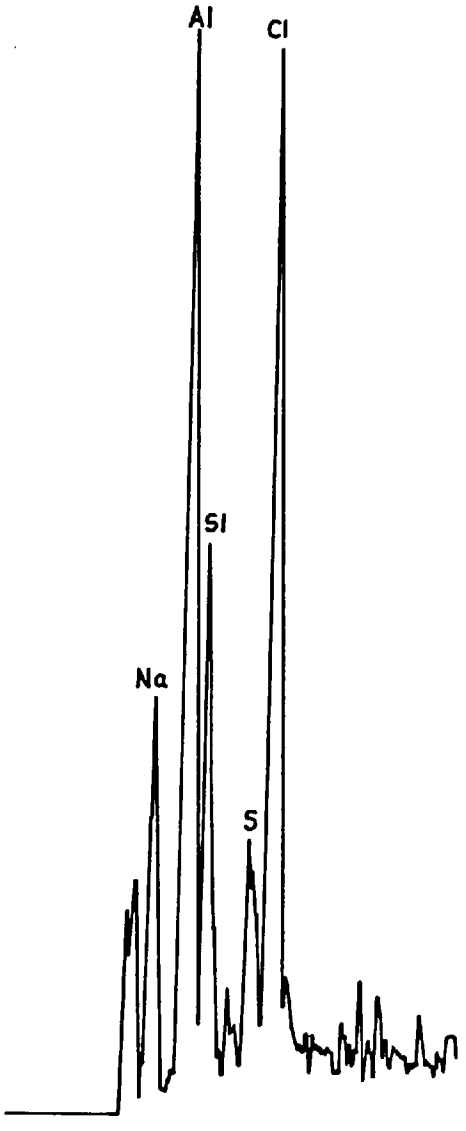

1. Halite. This cubic mineral was detected three times and its identification as halite was based on both the cubic crystal habit, (Plate 81A), and the x-ray analysis which gave Na and Cl as the major elements and S as a minor element, (Fig. 43). The accompanying Al and Si x-ray peaks were likely to be due to fluorescence from the host topaz $Al_2(F,OH)_2SiO_4$ as a result of electron scattering. The sulphur peak was probably caused by electron scattering onto sulphur precipitates which were formed during the evaporation of the inclusion fluids after the opening of the inclusion cavity.

2. Sylvite. This cubic mineral was detected once in an inclusion which also contained an euhedral prismatic anorthite. daughter phase. Like halite, it was identified on the basis of chemistry and crystal form. The x-ray analysis shows the presence of K, Cl, S, Al and Si. The presence of Al, Si and S peaks can be explained by the electron scattering effect as described above.

PLATE 81.

A. A subhedral halite (arrowed) sitting on a fractured surface of a pegmatitic topaz.

B. An euhedral hexagonal quartz daughter inclusion in an opened Type II fluid inclusion which is incompletely necked.

C. Another view of the same quartz inclusion.

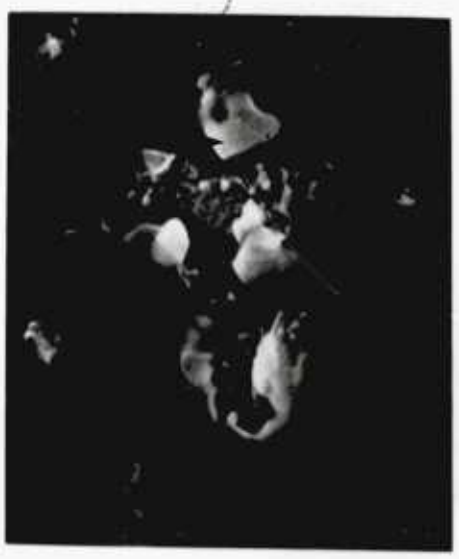

Mag. 2000 X

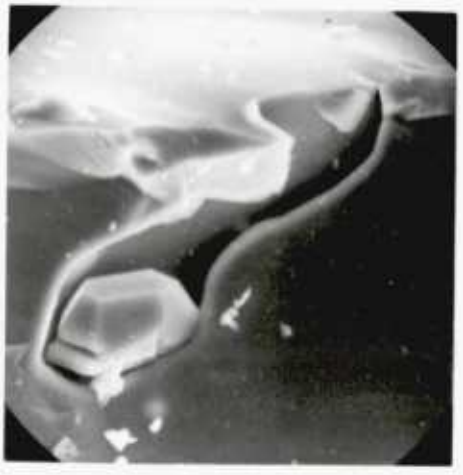

Mag. 2200X

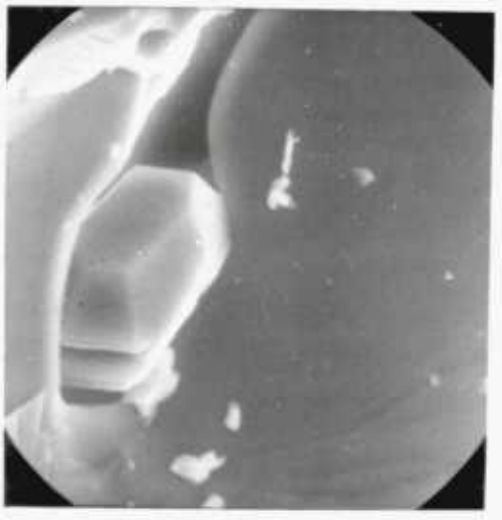

Mag. 4000 X

3. Quartz. A single euhedral quartz crystal was seen sitting in a partially necked inclusion cavity, (Plates 81B and C), and it was identified as quartz on the basis of the hexagonal crystal habit and, most important of all, its chemistry which consistently showed the presence of silica only on three point analyses from different angles.

4. A Calcium Aluminium Silicate, (probably zoisite). This mineral occurred associated with sylvite in a Type III inclusion as described above, and it was probably an anorthite judging on the basis of its tabular prismatic crystal habit and its chemistry which shows the presence of Ca, Al, Si and minor amounts of S and Cl. The latter two elements are produced by electron scattering on the surrounding matrix of the analysed Ca-aluminium silicate. The neighbouring sylvite was most probably responsible for the Cl peak.

5. A Potassium Aluminium Silicate, (probably a K-feldspar. This silicate phase was probably a k-feldspar judging from its

PLATE 82.

A. Two daughter mineral phases with poor crystal form in Type III fluid inclusion from the pegmatitic topaz. These phases shown to be potassium-aluminium silicates, (probably k-feldspar).

B. An opened Type III fluid inclusion in pegmatitic topaz packed with at least four poorly crystalline daughter minerals composing of k, Al and Si and traces of S. These minerals are probably k-feldspars.

C. Two prismatic daughter crystals of Cs-aluminium silicate in an opened Type III fluid inclusion from the pegmatitic topaz.

D. A prismatic daughter mineral of CS-aluminium silicate in an opened Type III fluid inclusion from the pegmatitic topaz.

Mag. 1100 X

Mag. 13000 X

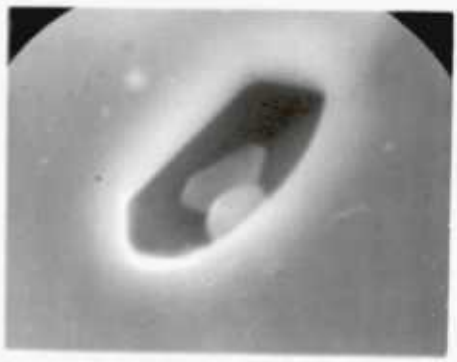

Mag. 6500 X

Mag. 10000 X

tabular prismatic crystal habit and major-element chemistry. The latter showed the presence of K, Al and Si. This silicate phase was seen in isolation in three inclusions of Type III, (Plates 82A and B), and also associated with three Cs-bearing potassium silicates in another Type III inclusion, all within one topaz crystal. In another topaz sample the presence of two similar silicate crystals was recorded in a fluid inclusion containing mixed crystals of Cs-K-Silicate and K-Ca-Cs Silicate, and three other crystals probably Na-Be-phosphates, (Beryllonites).

6. Iron chloride, ($FeCl_2.2H_2O$).

This mineral was identified by its rhombic crystal habit and major-element chemistry which showed the presence of Fe and Cl only. This mineral was only observed once during this study, and as far as the writer is aware it has not been recorded in pegmatitic topaz from Russia or Malaysia. However, this mineral was recorded in pagmatitic quartz from Russia, (Roedder, 1972), and also

in secondary quartz from the quartz-tourmaline alteration zone and in pre-cassiterite early vein quartz both from the Chorolque Mine of Bolivia, (Grant et. al., 1976; Grant, 1979).

7. A Cs-aluminium silicate, (probably pollucite-$Cs_{0.7}Na_{0.3}(AlSi_2O_6).3H_2O$).

This silicate phase was probably a pollucite judging from its tabular prismatic crystal habit, (Plate 82C), and its major-element chemistry, (Cs, Al and Si). Cs is known to behave as an incompatible element concentrating to a high level in pegmatite-forming fluids at which stage it tends to form its own mineral, namely pollucite. This silicate phase was found occurring alone in two fluid inclusions from one topaz crystal, (Plates 82C and 82D). Such Cs-silicate phase has not been recorded in pegmatitic topazes from Russia or Mongolia and this is the first time it has been identified as a daughter phase in fluid inclusion.

8. An unidentified phosphate mineral.

Three phosphate minerals occur together

PLATE 83.

A. High magnification view of a stacked aggregate of 3 daughter minerals in the same inclusion as that of Plate 83C. They are chemically similar composing of Na and P. Since a sodium phosphate mineral does not exist in nature, the most probable mineral phase which they can be identified with is beryllonite.

B. A pseudocubic mineral, (arrowed), besides an opened inclusion was shown to contain K, Ca and Cl as major components. Thus this mineral is a mixed crystal of Ca-k-chloride.

C. Low magnification view of an opened Type III fluid inclusion consisting of Beryllonite (?) (a); K-aluminium silicates, (probably feldspars), (b); K-Ca-Cslaluminium silicates (c) and lastly K-Cs-aluminium silicates (d).

D. Three 'dome-like' structures made up of dendritic leaf-like form material which has been shown to compose of Ca and Cl. Note each of the 3 domes shows a circular patch of thin film of 'evaporite', (arrowed), around it.

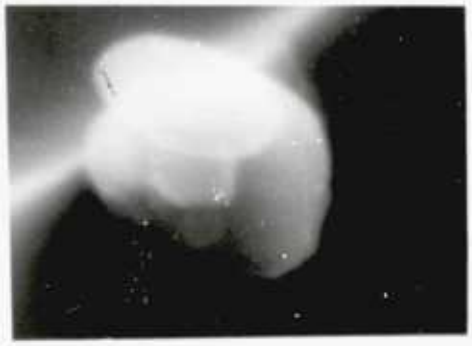

Mag. 11000 X

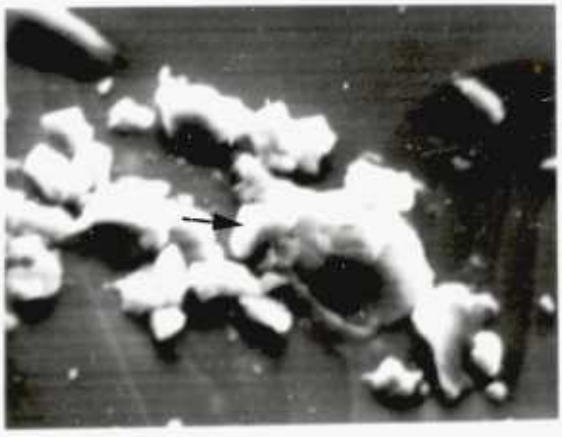

Mag. 1150 X

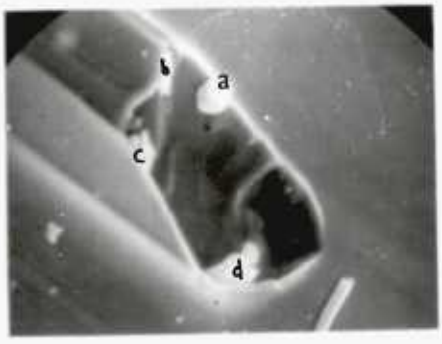

Mag. 2000 X

Mag. 1000 X

in a stacked aggregate, (Plate 83A), in which diagnostic crystal habits were, unfortunately, not conspicuous. The x-ray analyses of the three phases indicated the consistent presence of P, Na, Al and Si. The detection of Al and Si was assumed to be the result of electron scattering on the topaz host. Thus the unknown minerals are probably Na-bearing phosphate(s). A pure sodium phosphate is not known to occur in nature according to the detailed list of phosphorus minerals given by Koritnig in the Handbook of Geochemistry, Volume II-2, but a NaBe phosphate, namely beryllonite, does exist. Beryllonite was first discovered in a pegmatite vein composed of feldspar, smoky quartz, columbite, cassiterite, berly, apatite and triplite near Stoneham in Maine, U.S.A. by Mr. S. Andrews of Lawrence, massachusetts in 1886. It was later described and identified as Beryllonite, ($NaBe(PO_4)$), by Dana, (1888), and Dana and Wells, (1889). Beryllonite was also recorded at the Mills feldspar quarries in Hebron and Neville tourmaline Mine at Newry in Maine where it was found associated with smoky quartz, cassiterite and herderite, (Moore, 1973). Thus it

Figure 44.
SEM X-ray Scan of a Ca-K-chloride daughter phase in the fluid inclusions of Chenderiang Valley topaz.

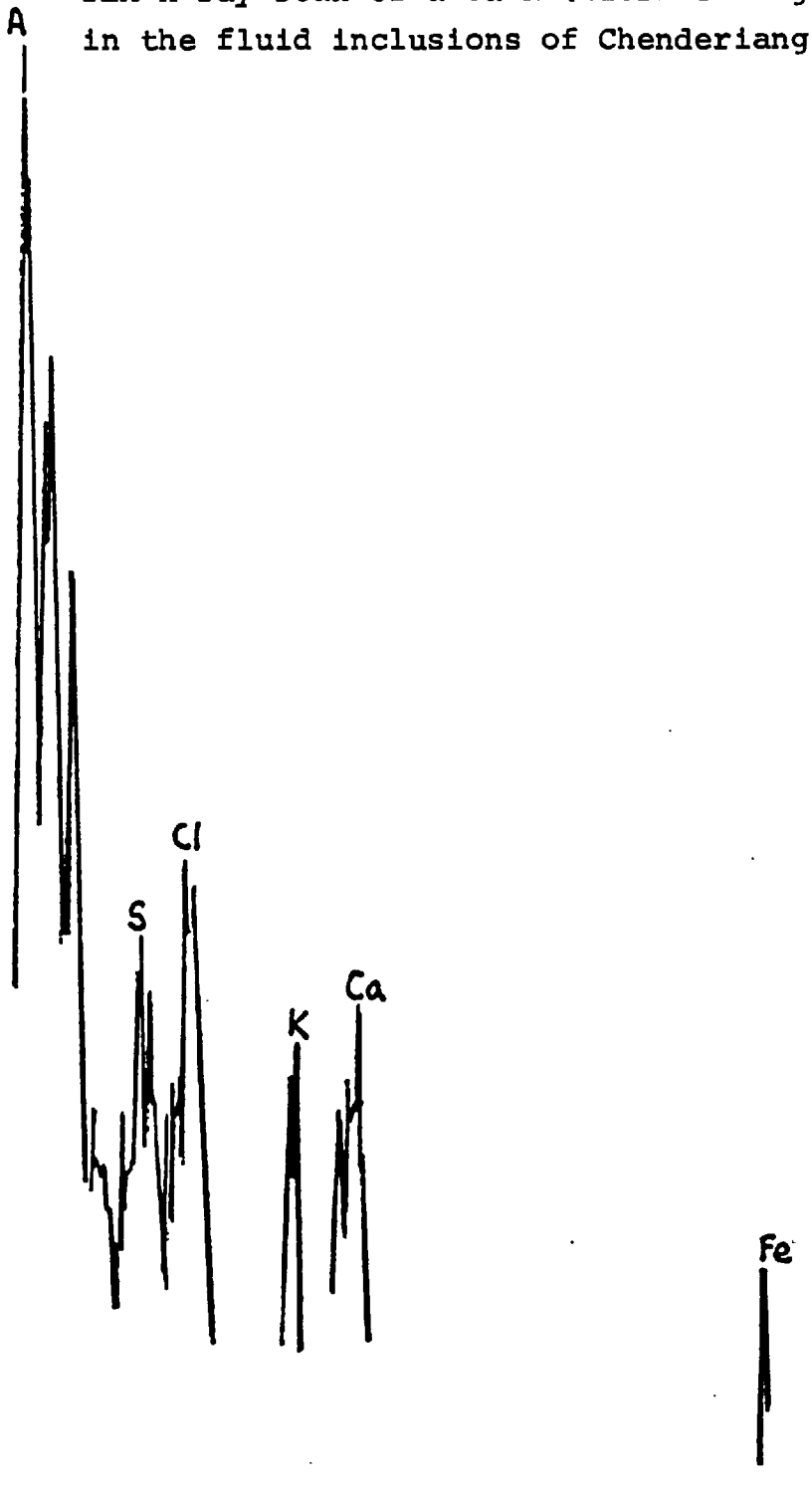

> appears that beryllonite always occurs in a paragenesis which includes tin minerals as well as beryllium and phosphate bearing phases. Since the three phosphate minerals also belong to a paragenesis which includes cassiterite and beryl, (Ingham and Bradford, 1960), it is possible that they may be beryllonite. This identification cannot be definitely confirmed without full structural and chemical analysis. The tentative identification seems reasonable, however, in view of the paragenetic association.

Mixed crystals such as K-Na-chloride, Ca-K-chloride, (Plate 83B and Fig. 44),and K-Fe-chloride, K-Cs-Al-Silicate, K-Ca-Cs-Al-silicate, (Plate 83C), and Ca-Cs-Al-silicate were also identified in this study. It is reasonable to expect that substitution of major elements in these mineral phases would be possible at temperatures in the range of 300°c - 400°c. An interesting phenomenon observed on opening some inclusions was the formation of 'domes', (Plate 83D), made up of leave-like dendrites which are believed to have been formed by rapid crystallization of inclusion fluids using fine debri produced by the fracturing

PLATE 84.

A. A platy primary mineral inclusion in pegmatitic topaz. This inclusion was shown to contain Al and Si as major constituents by the S.E.M. and x-ray microanalyser technique and hence it is probably a platy topaz.

Mag. 1000 X

process as nucleii for crystallization. These dendrites when scanned by an electron beam gave a composition with calcium and chlorine only. This data indicates that the host inclusion fluids contained signficant Ca and Cl. In other cases fine aggregates resulting from evaporation of inclusion fluids were scanned by the S.E.M. electron beam and the results showed the presence of Ca, K, Na, Cl, S, Al, Si, Fe and Mg, and less commonly Cr, P, Ni, Ti, Cs, Pb, Mn and Sn. Attempts were made to fracture primary mineral inclusions marked by their prior observation in topaz crystals, but this was generally unsuccessful except for one case in which a platy mineral inclusion, (Plate 84), was fractured broken with the other half still intact sticking out of its topaz host. The x-ray chemical data obtained for this mineral inclusion indicates that it is composed of Al and Si as major components, and, therefore it may be a topaz which is not unexpected since its host topaz has crystallised from Al and Si-saturated fluids. Platy topaz has been reported by Naumov et. al., (1977).

Judging from the chemical data obtained by the S.E.M. and x-ray microanalyser technique, it can now be concluded that the common major elements present in the inclusion fluids are K, Ca, Na, Al, Si, Cl, S, Fe, Mg, Cs while the less common elements are Cr, Ni, Ti, Pb, Mn, Sn and P.

7.5. The Homogenisation Temperature Data.

7.5.1. Introduction.

The purpose of this study was to determine the thermal condition of the heterogeneous fluid system from which the pegmatitic topaz crystallized. This study involved the use of a Leitz Microscope heating stage 1350.

Sixty-five, sixty-two, ten and thirty-nine determinations of homogenisation temperature were made on Type I, II, III and IV primary fluid inclusions respectively. A large majority of homogenisations was in the liquid phase. These $Th^{o}c$ values were not corrected for pressure effects by the usual method because the depth of mineralisation could not be assessed; also salinity determinations for the inclusion fluids were difficult to obtain. The alternative CO_2 method as described in section was not applicable either and this was due to the absence of pure CO_2 fluids coexisting with aqueous inclusions in the samples of topaz examined.

7.5.2. Interpretation of Results.

The $Th^{o}c$ values obtained for Type I fluid inclusions. The sixty-five $Th^{o}c$ values give a bimodal distribution ranging from $240^{o}c$ to $460^{o}c$ with two

Figure 45 The frequency distribution histogram of Type I fluid inclusions.

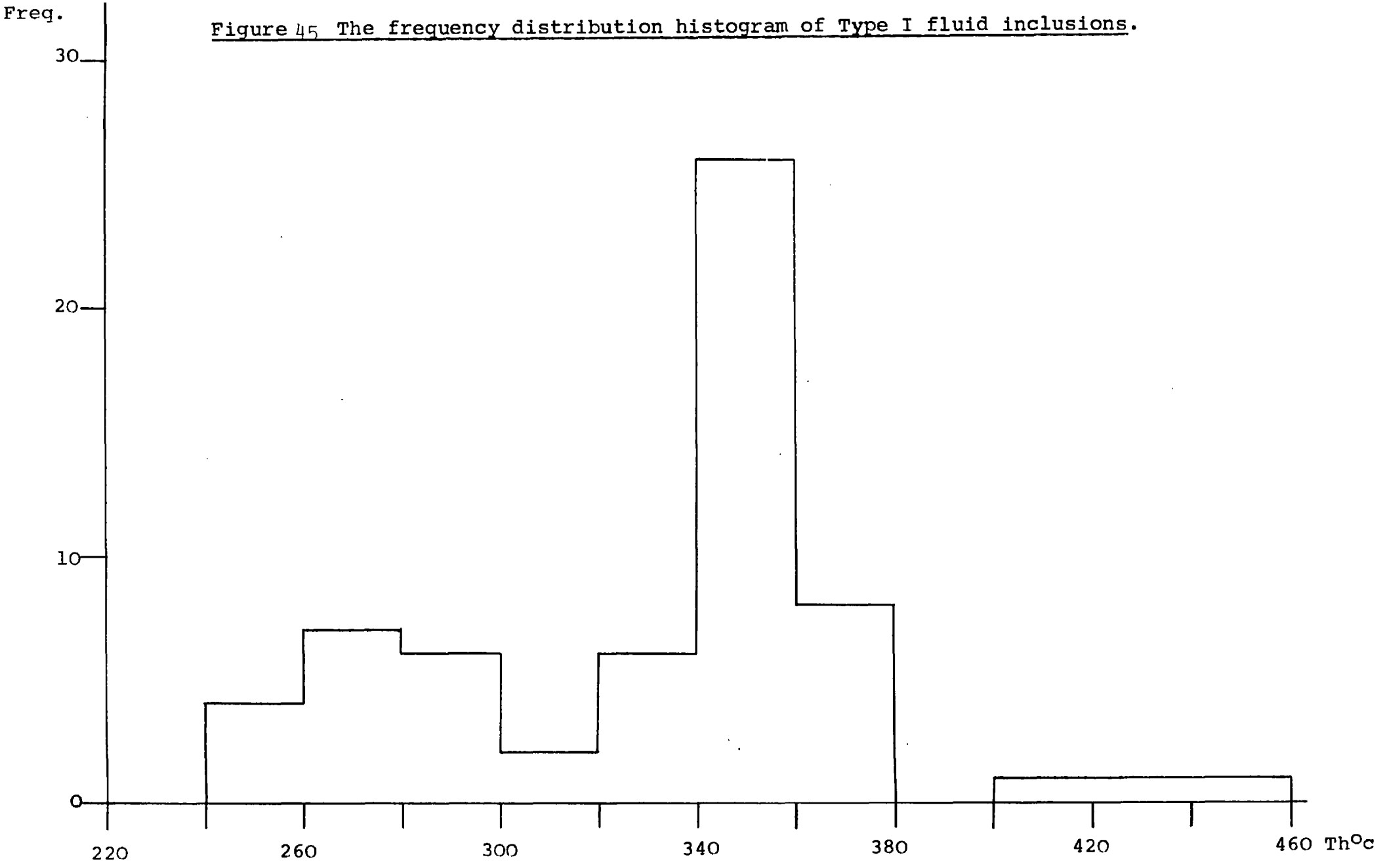

Figure 46 The frequency distribution histogram of Type II fluid inclusions.

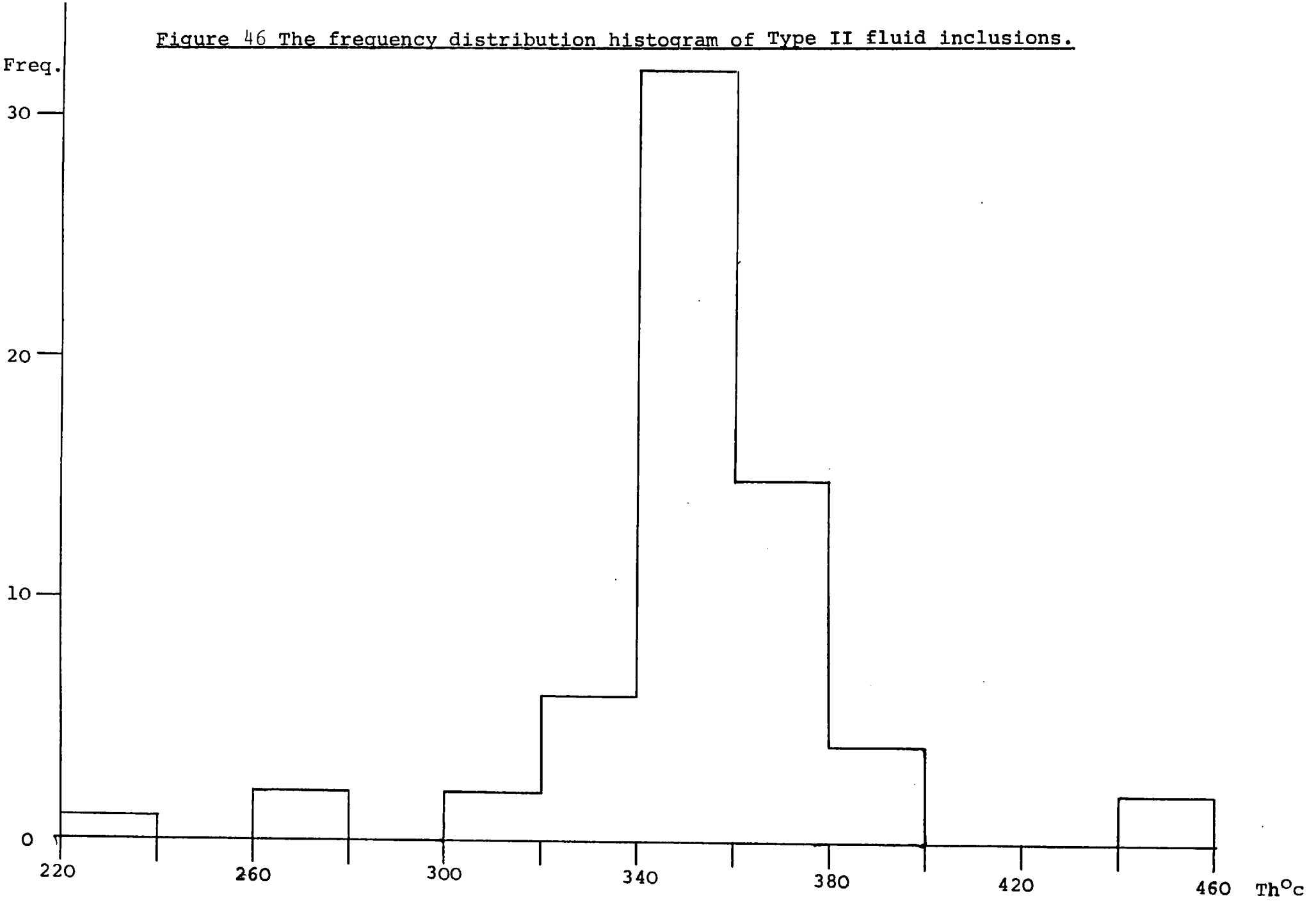

Figure 47 The frequency distribution histogram of Type III silicate inclusions.

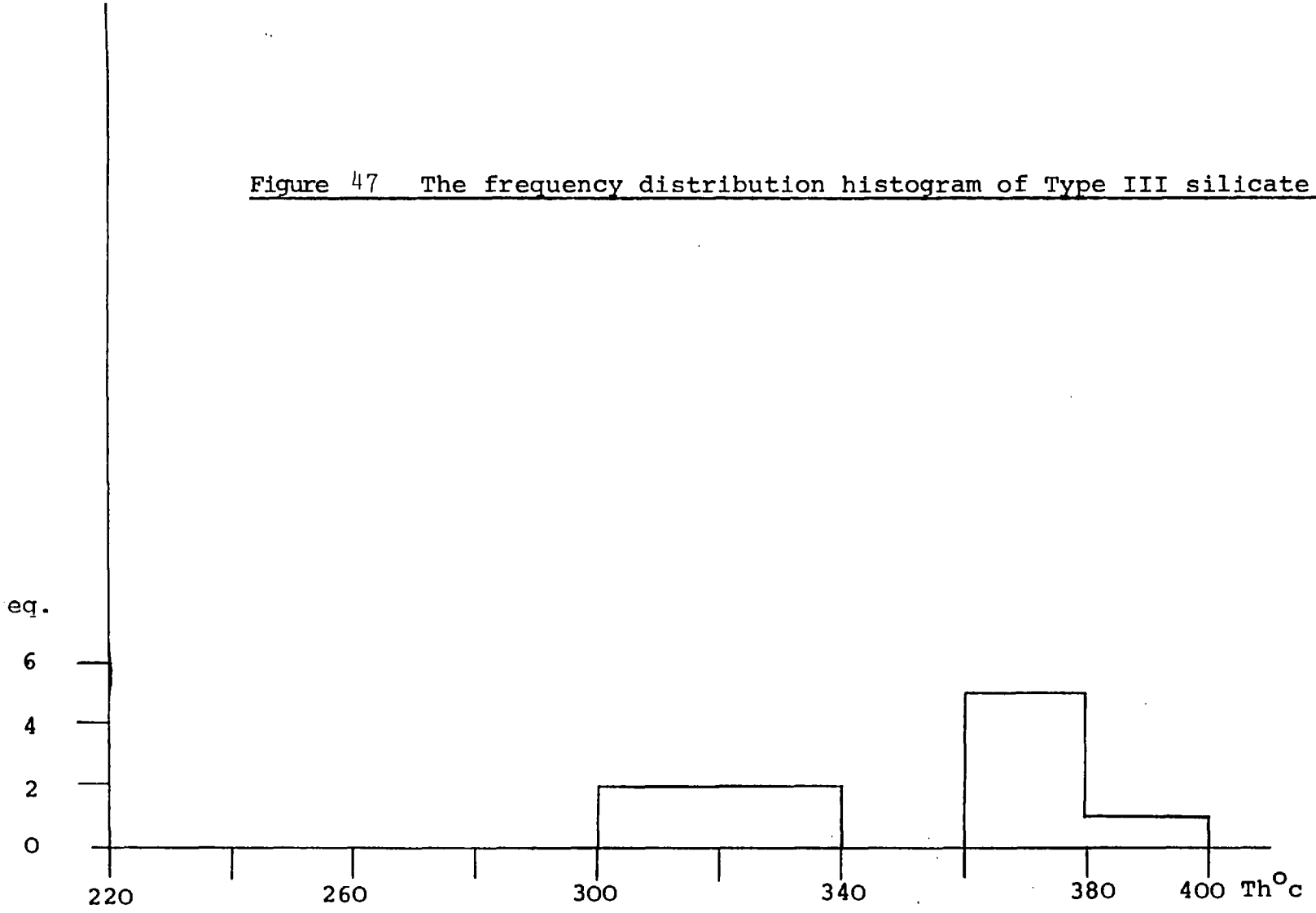

peaks at 260°c to 280°c and 340°c to 360°c respectively, (Fig. 45). The Th°c values for the lower temperature group may be interpreted as obtained from topaz crystallised from the cooler fractions of the topaz-forming fluids assuming a reasonable temperature range for the crystallisation history of the topaz

The Th°c values obtained for Type II fluid inclusions.

The sixty-four Th°c values display a wide range varying from 220°c to 460°c, but the large majority of these Th°c values are concentrated between 300°c and 400°c with a sharp peak within 340°c and 360°c with a slight tendency to skew towards the higher temperature end of this main range, (Fig. 46). This range of uncorrected Th°c values falls within the lower half of the total range of the uncorrected Th°c values, 200°c to 800°c), recorded for the Russian, Mongolian and Japanese pegmatitic topazes, (Naumov et. al., 1977).

The liquid/vapour Th°c values obtained for the Type III fluid inclusions.

Ten liquid/vapour Th°c values concentrate within a range from 300°c to 400°c, (Fig. 47). The silicate component in this type of inclusion always failed to melt before the liquid/vapour homogenisation and survived to temperatures in excess of around 500°c - 600°c,

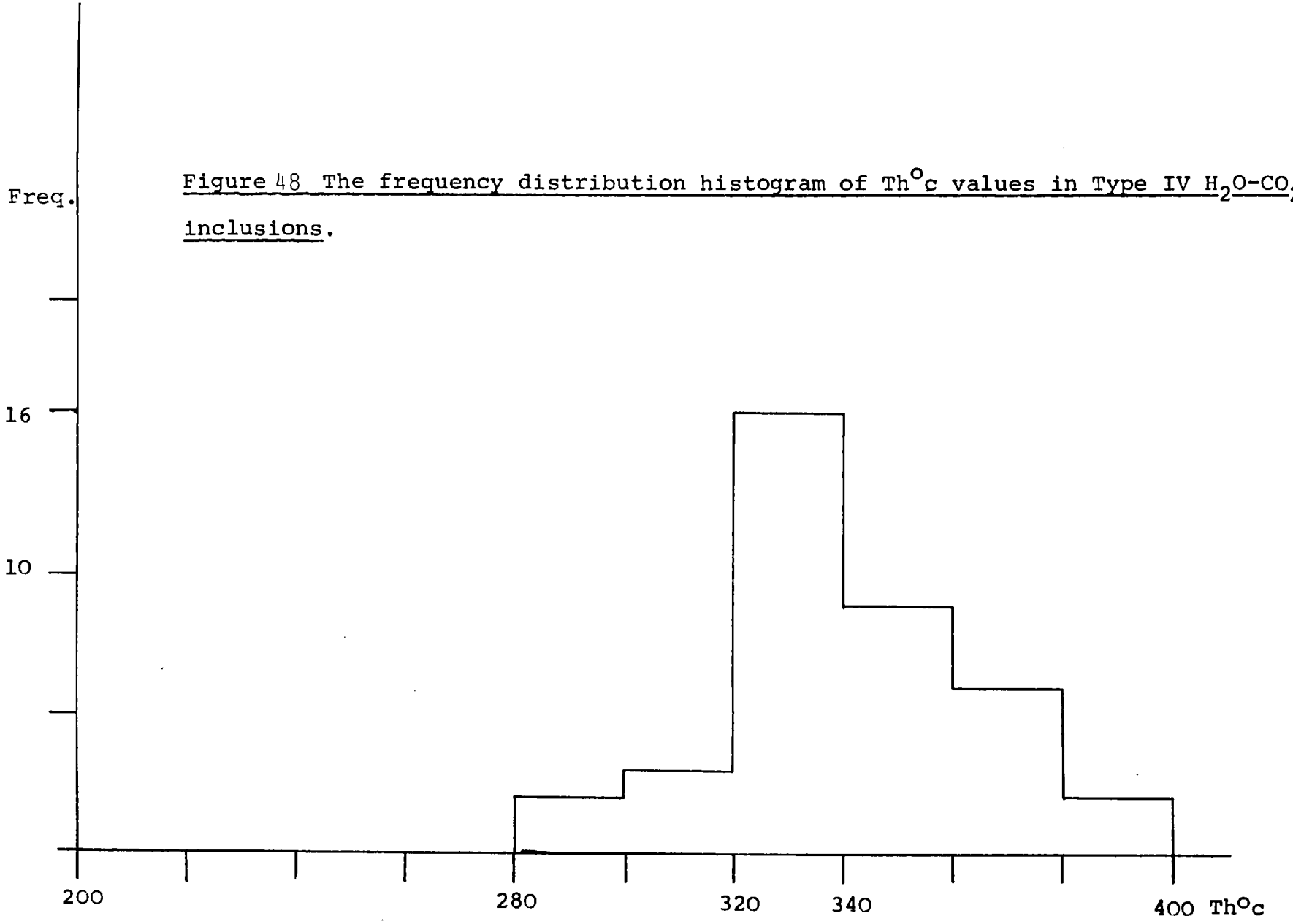

Figure 48 The frequency distribution histogram of $Th^{o}c$ values in Type IV H_2O-CO_2 fluid inclusions.

during the heating period of 30 to 45 minutes, (Roedder, 1971). The determination of the complete homogenisation temperature, (T_T°c), is obviously important in that this must be taken to be the closest approximation to the formation or trapping temperature of the topaz. Attempts to determine the total Th°c values ran into problems because of leakage and the kinetics of phase changes in the silicates at temperatures around 800°c - 1,000°c. Leakage was presumably accompanied by the loss of volatiles which would elevate the liquidus temperature of the silicate phases. Leakage in minerals with well developed basal cleavages is common especially at such high temperatures, (Rankin, 1973).

The Th°c values obtained for Type IV fluid inclusions.

The 39 Th°c values give a unimodal distribution which extends from 280°c to 400°c with a distinct peak within 320°c and 340°c, (Fig. 48). This distribution is skewed to the higher temperature end of the range. The range of Th°c values obtained is compatible with that (260°c - 440°c) recorded for pegmatitic topaz from Volynia in the Ukraine region, (Dolgov, 1968; Naumov et. al., 1977).

7.5.3. Conclusions.

It is interesting to note that the main range of the Th°c values for Type I, II and IV fluid inclusions and the range of the liquid-vapour Th°c values for Type III fluid inclusions are consistently similar within 300°c to 400°c. It is also important to note that Th°c values within 340°c and 360°c were most frequently encountered in the Type I and II fluid inclusions

but not for the CO_2 rich Type IV fluid inclusions. The Th°c values from the latter inclusions concnetrate most frequently within the range 320° to 340°c. This difference is to be expected since the presence of CO_2 can loser the Th°c value. The consistency of the Th°c values obtained from each type of fluid inclusion and the congruency of the ranges of Th°c values recorded for the four main types of fluid inclusions testify that the fluid inclusions chosen for homogenisation were cogenetic primary fluid inclusions. Thus the Th°c values obtained are valid and they represent the minimum thermal condition of the topaz-forming fluids at the time of trapping.

Kovalenko, (1977), has demonstrated experimentally that the solidus temperature of the granite-H_2O system can be reduced by about 150°c by interaction with fluorine (0.9 - 1.7 wt%). From this finding it may be inferred that the minimum solidus temperature of 450°c for a heterogeneous system of silicate melt + crystals + aqueous fluids as shown by Jahns and Burnham, (1969), can be considerably reduced especially if the system is enriched in fluorine as in the case of the topaz-forming heterogeneous fluid system from which the topaz of the Chenderiang Pegmatites crystallized. Thus the range of uncorrected Th°c values, (300°c - 400°c), obtained in this study is considered reasonable.

General Conclusions.

The petrographic evidence has shown that the system from which the topaz crystallized was heterogeneous and contained an immiscible silicate melt together with a CO_2-rich aqueous phase, an H_2O-rich aqueous phase, saline brine and crystals. The explanation for the concentration gradients in the aqueous fraction as shown by the inclusion populations is difficult.

The crystallization of topaz evidently took place during the transition from the magmatic to the hydrothermal stage of evolution of the system and is thus appropriately described as the 'pegmatitic stage of development' of the system, (Jahns and Burnham, 1969). The minimum thermal condition prevalent during the crystallization of topaz was within a temperature range from 300°c to 400°c.

CHAPTER 8.

Comparative Study of the Geochemistry of the "tin-granites" of Western Malaysia and other selected areas with the geochemistry of similar non tin associated granitoids from Western Malaysia, Southern Japan and Western Erzgebirge.

8.1. Introduction.

Researchers concerned with the problem of defining the geochemical and mineralogical characters essential to the recognition of a "tin-granite" have employed criteria based on several approaches as listed below:

1. The major element, (SiO_2, CaO, MgO). Composition. (Jones, 1925; Edwards and Gaskin, 1949).

2. The modal composition of the rock in terms of certain critical accessory mineral associations and the proportion of the main rock forming species, (Ishihara et. al., 1978; Jaafar, 1970; Suensilpong et. al. 1975).

3. The C.I.P.W. normative composition of the rock using the corundum-diopside boundary

as a critical indicator of peraluminous composition. (Chappel and White, 1974).

4. Critical observations on the initial $^{87}Sr/^{86}Sr$ ratio of the rocks, (Chappel and White, 1974).

5. Variation in the chemical composition of certain critical mineral species viz. biotite, muscovite and feldspar, (Jedwab, 1955; Jaafar, 1970; and Groves, 1972).

6. Concentrations of a range of trace elements (F, Li, Sn, W, Nb, Rb, Zr,and Sr) in rock, (Butler et. al., 1962; Bowden, 1966; Beus and Sitnin, 1968; Jaafar, 1970; Tischendorf, 1973; Groves and Taylor, 1973 ; Kozlov, 1974; Klominsky and Absolonova, 1974; Happala, 1974; Yeap, 1974; Ishihara and Terashima, 1978).

7. The ratios of pairs of critical elements, (Mg/Li and Zr/Sn) and the contents of Li and Sn, (Beus and Sitnin, 1968).

In the course of the present study major and trace element data from 84 existing analyses, (Alexander et. al., 1964) of granitoids from the Western Malaysian Peninsula, (the majority from the Western Belt, (46 samples); 8 from the Eastern Belt and 4 from the Central Belt), have

been compiled and the C.I.P.W. norms and certain critical differentiation indices have been computed. To this data have been added the analytical results obtained from "tin-granites" collected from the Gakak Mine at the P.C.C.L. property in Sg. Lembing, (8 samples of chloritised and sericitised muscovite-biotite granodiorites), the northern face of the Bujang Malaka biotite-granite pluton, (1 sample), and the chloritised biotite granite from Sg. Pari Quarry, (1 sample). Further, available major element data from 41 existing analyses, (25 analyses from Dartmoor granites, (Brammal and Harwood, 1932); 4 samples from St. Austell granites, (Brammall and Harwood, 1932); 11 analyses from Carn menellis granites, (Ghosh, 1934); and analysis from the Bodmin Moor, (Brammal and Harwood, 1932) from Cornwall have been treated similarly as those from Western Malaysian granitoids. Available major element data from 44 analyses, (Suensilpong et. al., 1975). of the adamellites from the Khuntan Batholith in Northern Thailand have also been treated in the same way as those from both Cornwall and Western Malaysia. Finally the analyses of some critical trace elements, (F, Li, Sn, W, Nb, Rb, Zr and Sr from "tin-granites" of Western Malaysia, Northern Thailand, South West England; Erzegebirge; the Karlovy Vary Massif; Southern Finland; Northeastern Tasmania, Central and Eastern Transbaikalia and finally Southern Japan), have been compiled in Table

The major and trace element analyses together with the plots for the computed C.I.P.W. norms have been used to provide a comparision between the "tin-granites' from the

Table 21

SiO_2 MgO and CaO contents (in %) of "tin-granites)

From Hunter, 1973 unless otherwise stated)

	SiO_2	MgO	CaO
Australia			
Elizabeth Creek Grainte, Queensland	77.24	0.06	0.46
Rossarden, Tasmania	75.85	0.26	0.20
[1] Anchor mine Biotite-muscovite granite, N.E. Tasmania.	75.0	0.06	0.39
Nigeria			
Riebeckite granite, Kudaru Hills	75.29	0.22	0.64
[2] Mayfield-Gona albite-biotite granite, JOS.	76.19	0.08	0.10
[3] U.S.S.R.			
Grodekovsk intrusive complex second phase, Kankaysk-Daubikhinsk district	70.88	0.55	1.83
Grodekovsk intrusive complex third phase, Kankaysk-Daubikhinsk district	73.2	0.38	0.81
Maryanovsk intrusive complex, Daubikhinsk district	75.29	0.23	0.68
Leucocratic granite, eastern slope of Sikhote-Alin	76.36	0.32	0.88
West Malaysia			
Main Range granite	73.29	0.08	0.70
Kledang Range granite	74.38	0.51	0.98

Saxony	SiO_2	MgO	CaO
Altenberg granite	74.68	0.35	0.09
South West England			
Carmenellis granite, Cornwall	71.95	0.69	1.47
Dartmoor Granite, Cornwall	71.20	0.60	1.60
Portugal			
Lagares do Estanho Granite	69.96	0.29	1.82
Bolivia			
Caracoles	65.39	1.87	3.02

1. Data from Groves and Taylor, 1973
2. " " Jacobson, Macleod and Black 1958
3. " " Gotman and Rub, 1961

different provinces while certain additional comparisons have also been made involving granitoids from the general vicinity of known tin belts but without known associated tin deposits. Chosen samples of such granitoids include granitoids from the tin-barren Central Belt of Western Malaysia and from the Japanese islands and from the Older Complex of the Kirchberg Massif in the Western Erzgebirge.

8.1.1. The major element composition, (SiO_2, CaO and MgO).

Jones, (1925), and Edwards and Gaskin, (1949), were the first groups of workers to suggest that the "tin-granites" are characterised by abnormally low CaO, (<2 wt %) and MgO (<2 wt %) and that they are more acidic, (i.e. SiO_2 = 70 - 77%) than the similar granites which have no known associated tin mineralisation. This argument has been challenged by Hosking, (1965), who pointed out the relatively lower silica contents of the "tin-granites" of Portugal and Bolivia and also the highly silicic, (76.70% SiO_2), Mountsorrel granodiorite of Leicestershire which has no known associated tin mineralisation. Table 21 shows a list of SiO_2, MgO and CaO contents of"tin-granites". From this table, in addition to the critical observations made by Hosking, (1965), the writer has observed that the Caracoles granite of Bolivia display relatively higher MgO and CaO contents than would be expected of a "tin-granite" according to the criteria used by Jones, (1925) and Edwards and Gaskin, (1949). The view of Jones, (1925), and Edwards and Gaskin, (1949) is not supported by the

more than 100 analyses of the granitoids from the Western, Central and Eastern Belts of Western Malaysia, (Alexander et. al., 1964; Jaafar, 1970; and Hutchison, 1973b and also most of the 45 analyses obtained for the adamellites of the Khuntan Batholith in Northern Thailand, Suensilpong et. al., 1975). The three anlaysed intrusive rocks from the Bolivian tin belt gave respectively low SiO_2 contents ranging from 60 wt% to 64 wt%, (Angus et. al., 1977). This finding gives further support to the argument against the views of Jones, (1925) and Edwards and Gaskin (1949).

It is concluded from the survey of the available analytical data that the simple criteria proposed by Jones, (1925), and Edwards and Gaskin, (1949) cannot be used alone as a reliable guide to granitoids bearing tin mineralisation of significance.

8.1.2. The modal composition of rock in terms of certain critical accessory mineral associations and the proportions of the main rock forming mineral species.

Aranyakanon, (1961, quoted in Ishihara et. al, 1978), was the first to notice that "tin-granites" do not contain magnetite whereas similar granitoids which have no known associated tin mineralisation do. The principle was successfully tested on the granitoids from Japan, Southern Thailand and the Western and Eastern Belts of Western Malaysia by Ishihara and his co-workers, (1978).

This discriminatory criterion was conceived by Ishihara and Terashima, (1978), having considered the possibilities for progressive enrichment or progressive depletion of Sn in the residual fraction of crystallizing granitic magma. In magnetite-series granitoids sphene and ilmenite were found to be commonly associated accessories whereas in the ilmenite-series granitoids sphene and magnetite were absent. In the magnetite-series magma Sn in the tetravalent state (Sn^{4+}) was considered to be substituted for Ti^{4+} and Fe^{3+} in the sphene and to a lesser extent in the magnetite and ilmenite. Thus the magnetite series granitoids suffered progressive depletion of Sn. In the ilmenite-series Sn, believed to be in the divalent state (Sn^{2+}) was concentrated as an incompatible element in the residual fraction of the melt.

Ishihara (1977) regarded presence of one magnetite grain in any polished section as a criterion for assigning the sampled granitoid to the magnetite series. Its absence is taken to indicate that the granitoid belongs to the ilmenite series. The field technique which Ishihara and co-workers employed involved the use of a portable magnetic susceptibility meter, (the Kappameter UGF-KT3), to identify the ilmenite and the magnetite series granitoids. This device reads magnetic susceptibility in SI units. The critical boundary separating the two series was taken as 60×10^{-3} SI units, (Ishihara et. al., 1978).

About 20 plutons of Southern Thailand (6-10^{o}N) were

investigated and the results showed that all the plutons except for the lineated granite along the Phucket Fault Zone, (Garson et. al., 1975)), gave magnetic susceptibility readings below 30 and this belonged to the ilmenite series. The lineated granite gave readings of 100 - 270 SI units equivalent to 0.13 to 0.32 vol % of magnetite content. The Main Range granitoids of the Western Belt in Western Malaysia are generally similar to those from Southern Thailand. In contrast to the Main range granitoids, the granitoids of the presently known less mineralised Eastern Belt were found to bear magnetite more frequently. This finding is not too suprising as some granitoids from the Eastern Belt are known to be genetically related to the contact magnetite skarns and hence the presence of magnetites in them is not unexpected. The findings of ilmenite in granitoids of the Western Belt is not suprising since this mineral has been a major common by-product of alluvial tin mines operating in the Western Belt. Until ten years ago it was discarded as tailing waste. Today, ilmenite is processed to be used as a source of Ti. The bulk chemistry of the Tak granitoids in Northern Thailand, (Pongsapich and Mahawa, 1977), suggests that the latter granitoids belong largely to the magnetite series. Bulk chemistry given by Suensilpong et. al., (1975) indicates that the Khuntan Batholith is composed generally of the ilmenite series.

Although the discriminant developed by Ishihara et. al, (1978), has been successfully tested on granitoids from the South East Asian Tin Province, it needs to be

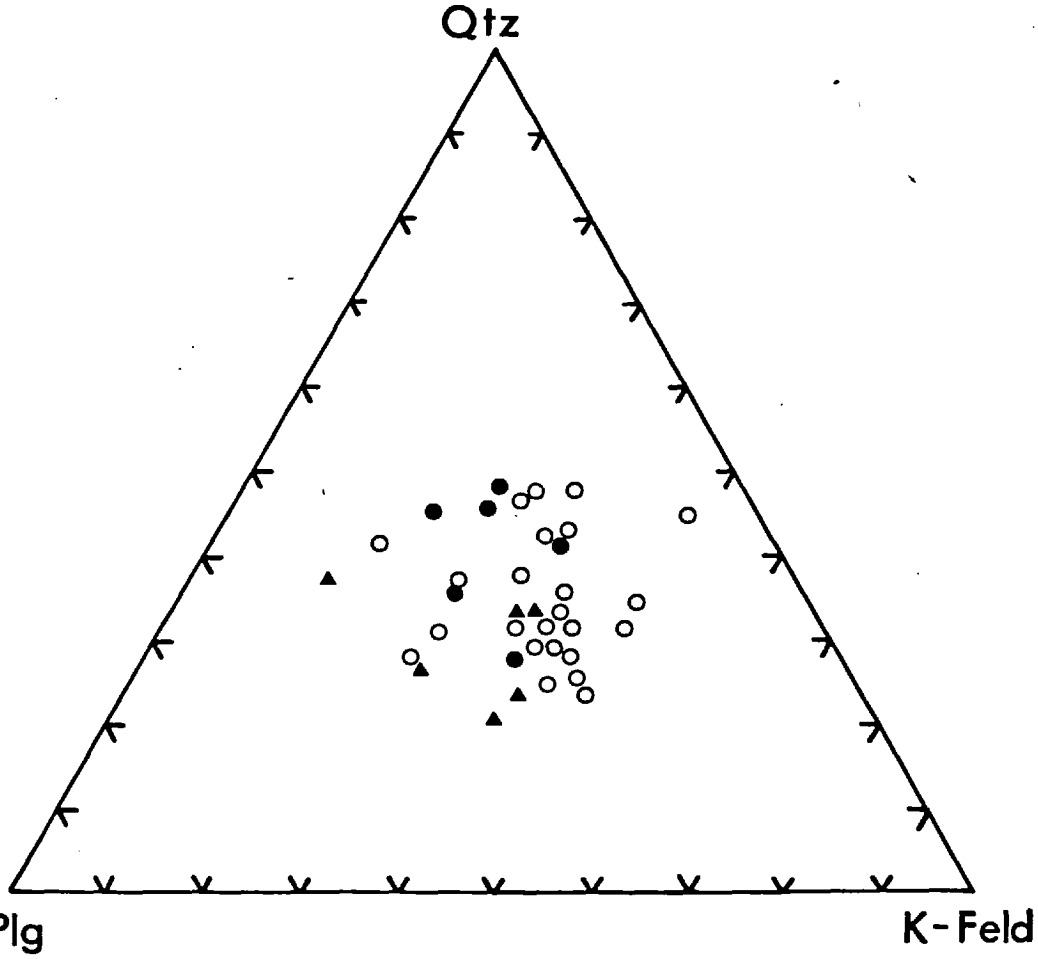

○ Western belt ▲ Central belt ● Eastern belt

Figure 49.
Modal amounts of quartz, orthoclase and plagioclase in granitic rocks from the three granitic belts in Malaya, plotted on quartz-plagioclase-orthoclase triangular diagram.

Reproduced from Jaafar, 1970

further tested on granitoids of tin provinces elsewhere in order to assess its universal validity in differentiating "tin-granites" from other granitoids with no known associated tin mineralisation.

Jaffar (1970) was the first to use the modal proportions of quartz, plagioclase and K-feldspar as a criterion to differentiate the "tin-granites" from granitoids with no known associated tin mineralisation. He plotted the modal proportions of the respective three minerals of 24 granitoids from the Western Belt and also those of the 6 granitoids respectively from the Central and Eastern Belts on a three component triangular diagram, (Fig. 49), defines the large majority of the granitoids from the Western Belt, as adamellites according to the classification scheme of Hatch, Wells and Wells, (1975), although both the alkali granite (3) and granodiorite fields (1) are represented. Six and five granitoids respectively from the Eastern and Central Belts were also identified as adamellites while the remaining single granitold sample from the latter belt belongs to the granodiorite class. Thus it is concluded that the granitoids from the Stanniferous Western and Eastern Belts and those from the tin-barren Central Belt are largely adamellites and hence there is no distinct difference in the petrographic composition of these granitoids. Jaafar (1970) has observed that although his plots were scattered they did, however, show that the majority of the adamellites from the Western

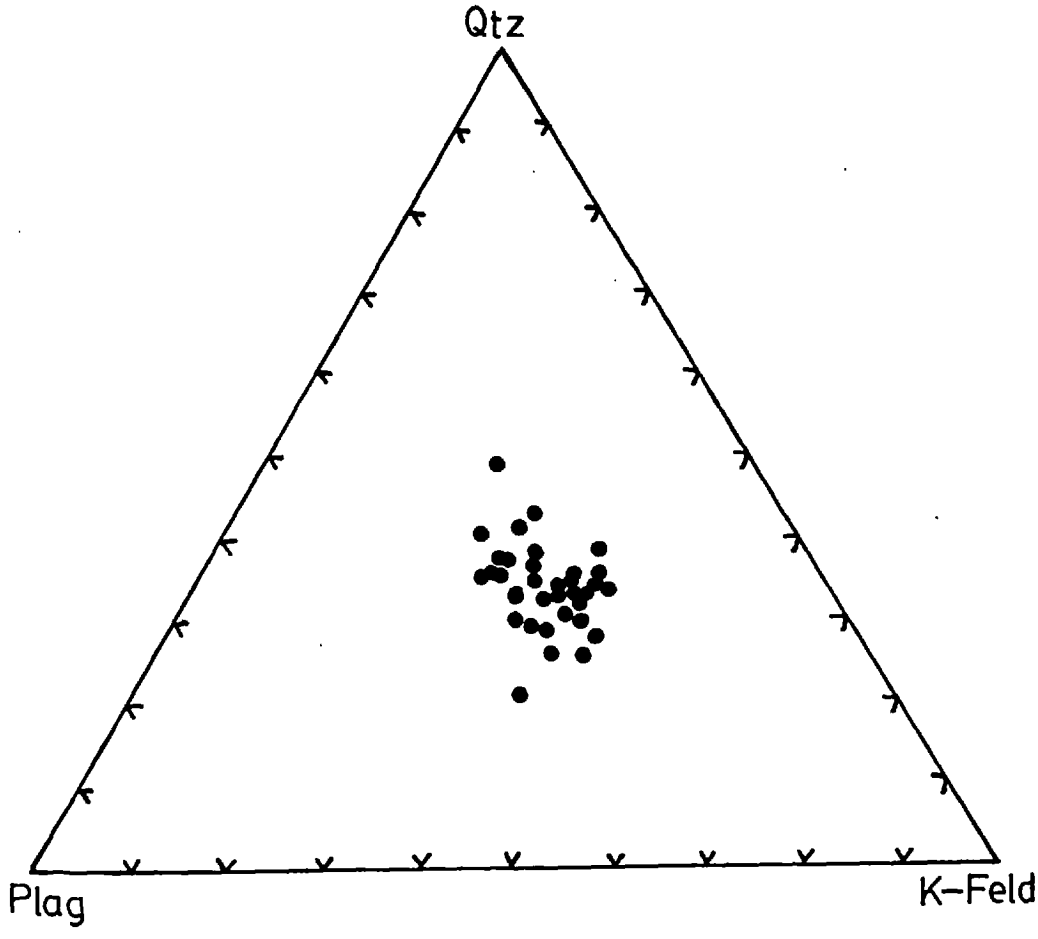

Figure 50. Modal amounts of quartz, orthoclase and plagioclase in granitoids.from the Khunton Batholith in Northern Thailand, plotted on quartz-plagioclase-orthoclase triangular diagram. Reproduced from Suensilpong et. al., 1975.

Belt tend to cluster towards the K-feldspar coner while two out of the six granitoids from the Central Belt showed an enrichment of the plagioclase content relative to that of K-feldspar. A meaningful comparison with respect to the enrichment of the K-feldspar content in the granitoids from the Western Belt and in those from the Central Belt cannot be made because of insufficient data for statistical evaluation.

Suensilpong et. al., (1975), made a similar three component plot, (Fig. 50), for 45 adamellites from the Khuntan Batholith in Northern Thailand from which it is possible to observe that the rocks have a tendency to cluster in the potassic area of the adamellite field. In this aspect the rocks of Khuntan batholith resemble the population of the adamellites and alkali-granites of the Western Belt in Western Malaysia.

The existing petrographic information on the granitoids from the Southern Thailand and Western Malaysian areas of the Southeastern Asian Tin Province shows that the tin mineralisation is clearly associated with adamellite showing enrichment in the potassium feldspar component. The available petrographic information, although limited, also suggests that true granodiorites and monzonites are not commonly associated with the tin-bearing batholiths, nor are more alkaline and highly silicic granites as the proposition of Jones, (1925), and Edwards and Gaskin, (1949), would suggest. It is not to be understood that all

FIGURE 51

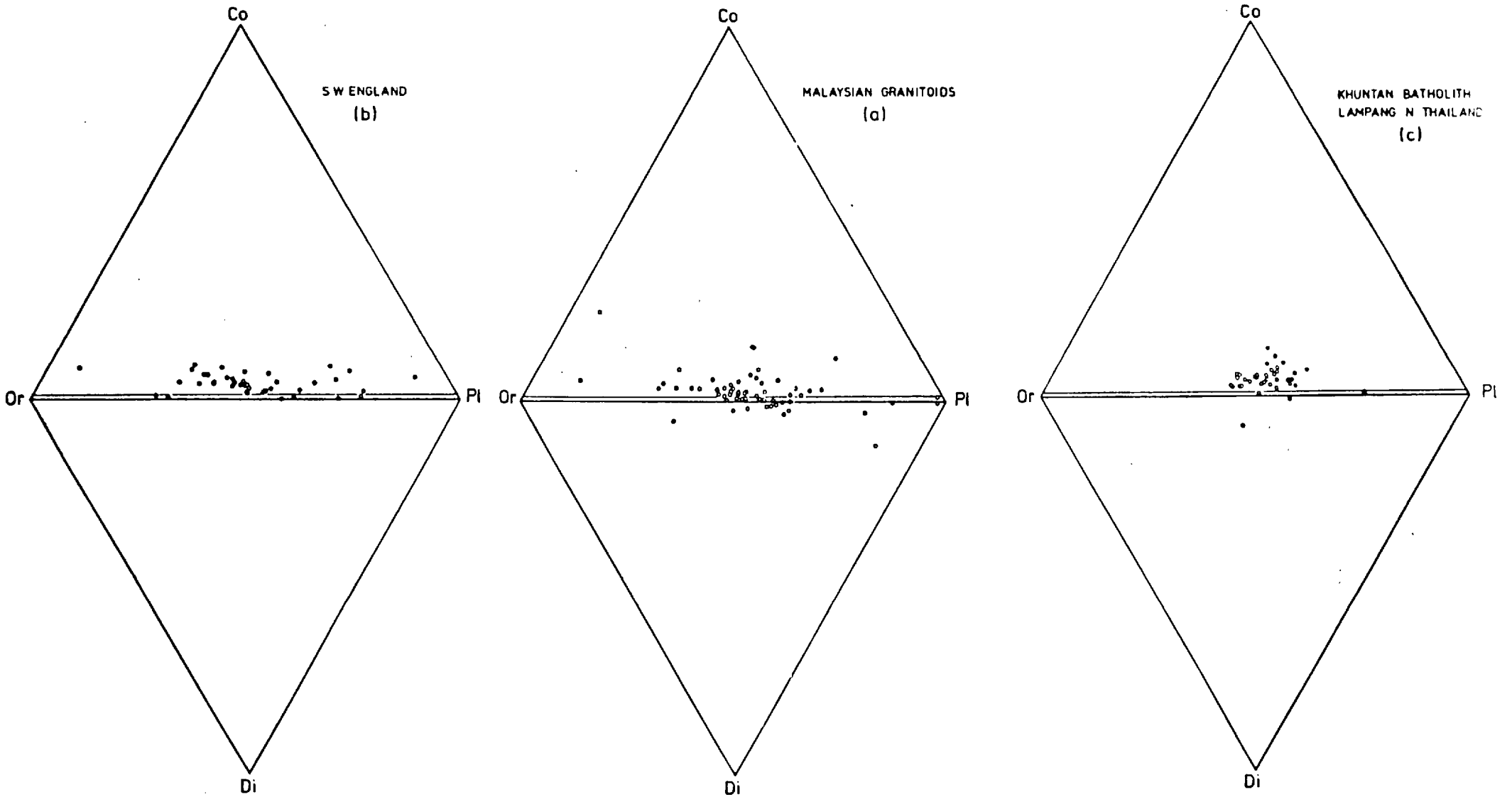

NORMATIVE PLOTS IN TERMS OF Orthoclase (Or) - Diopside (Di) - Plagioclase (Pl) - Corundum (Co) FOR POPULATIONS OF TIN-ASSOCIATED GRANITOID ROCKS FROM S.W. ENGLAND, THE MALAYSIAN PENINSULA AND N. THAILAND.

provinces with adamellitic rocks will have associated tin mineralisation but it is nevertheless interesting that the predominant tin-associated granitoids of the Southeast Asian Tin Province are potassic adamellites. To recognise specifically tin-associated adamellites amongst adamellites in general must depend upon more specific petrochemical criteria.

8.1.3. The C.I. P.W. Normative composition of the rock using the corundum-diopside boundary as a critical indicator of peraluminous composition.

The C.I.P.W. Normative mineral compositions of 84 Western Malaysian granitoids, (largely from the Western and Eastern Belts), 41 Southwestern England's granitoids and 42 Northern Thai granitoids were plotted on quarternary diagrams, (Figs. 51b, a and c respectively), using the four components Corundum-Plagioclase-Diopside-Orthoclase. From these figures, it is clear that the majority of the granitoids in the three tin provinces concerned are peraluminous, (1% normative corundum) and can be classified as of S-type according to the classi classification of Chappell and White, (1974). peraluminous character is taken to indicate a crustal origin according to Chappel and White, (1974), who used $^{86}Sr/^{87}Sr$ data in support of this argument.

The application of the S- and I- type classification as a criterion for the recognition of crustally derived

granitic melt has not yet been fully tested. However, it is certainly of considerable interest to find that the majority of the analysed tin-associated granitoids of the Southeast Asian Tin Province fall within the field of the S-type as defined by Chappel and White, (1974). The empirical recognition of this fact can easily be made but it is more difficult to explain.

8.1.4. Critical observations on the initial $^{87}Sr/^{86}Sr$ ratio of the rocks.

The observation of S-type granites from the Berridale Batholith to have an initial $^{87}Sr/^{86}Sr$ ratio >0.708, (Compston, Shirahase, Chappell and White in preparation, quoted in Chappel and White, 1974), typical of crustal material gives support to the crustal origin of the S-type granites as proposed by Chappell and White, (1974).

The validity of the above observation was successfully tested by the writer on the dominantly S-type granitoids from the Main Range Batholith of Western Malaysia which have an average initial $^{87}Sr/^{86}Sr$ ratio of 0.711, (Personal Communication, Snelling, 1974). The high initial $^{87}Sr/^{86}Sr$ ratio and the peraluminous nature, (S-type), of the granitoids from the Main Range Batholith of Western Malaysia both confirmed the crustal origin of the respective granitoids as suggested by Hutchison, (1973,a).

The discriminant developed by Compston, Shirahase,

Chappell and White cannot be used as a reliable indicator of the S-type granites because its universal validity has not been fully tested. The establishment of a discriminant such as this would be potentially useful as an indicator of "tin-granites" which have been suggested to be synonymous to S-type granites by Chappell and White, (1974).

8.1.5. The chemical variation in certain critical mineral species viz. biotites, muscovite and feldspar.

Biotite, muscovite and feldspar are mineral species which have been commonly chosen for trace element study. They were chosen for the following reasons:-

1. As they formed the major components of granitoids, their chemistries are expected to be partly representative of the chemistries in the melt from which they have crystallized hence their chemistries, (in particular the content of incompatible trace elements), may serve as differentiation indices for the melt, (Groves, 1972).

2. As they are the major components of granitoids, they can be effectively separated in amounts sufficient for chemical analysis. Biotite, in particular, is the principal femic mineral component and is

almost universally present in "tin-granites". micas have been chosen to be analysed for tin because of the high partition coefficient of Sn(>1) for the micas, (Jensen, 1973, and Pearce and Gale, 1977). Judging from the analysis of Li in biotite given by Jedwab, (1955), Li has also a high partition coefficient for biotite. Feldspar has not been chosen for the analysis of Sn because the partition coefficient of Sn for feldspar is low, (Jensen, 1973; and Pearce and Gale, 1977) and consequently their Sn content is usually low (<2 ppm), (Rattigan, 1964). Feldspar has been analysed for Li as the partition coefficient of this element is apparently high.

It is, therefore, not suprising that a considerable attention has been given to the use of the chemistry of biotite as criterion for the discrimination of "tin-granites". The interpretation of analytical results must, however, be tempered by consideration of the phases contributing to the total tin content of granitoids. Barsukov, et. al, (1966), has shown that 80% of the total tin in the "tin-granites" of the U.S.S.R. is present in the biotite lattice. However, this is not in agreement with the finding of Hesp, (1971), who was able to show that a general relationship existed between the modal content of the biotite in granitoids and the proportion of the total tin in granitoids which is present in the biotites. The data of Hesp, (1971), also showed that as the total Sn content of the granitoids decreases the percentage of the total Sn content in biotites increases. Hesp, (1971), has

The "tin-holding capacity" (THC) is defined as:

$$\frac{Fe^{3+} + Li^{+}}{Fe^{2+} + Mg^{2+}} - \frac{Ti^{4+} + Mn^{2+}}{10}$$

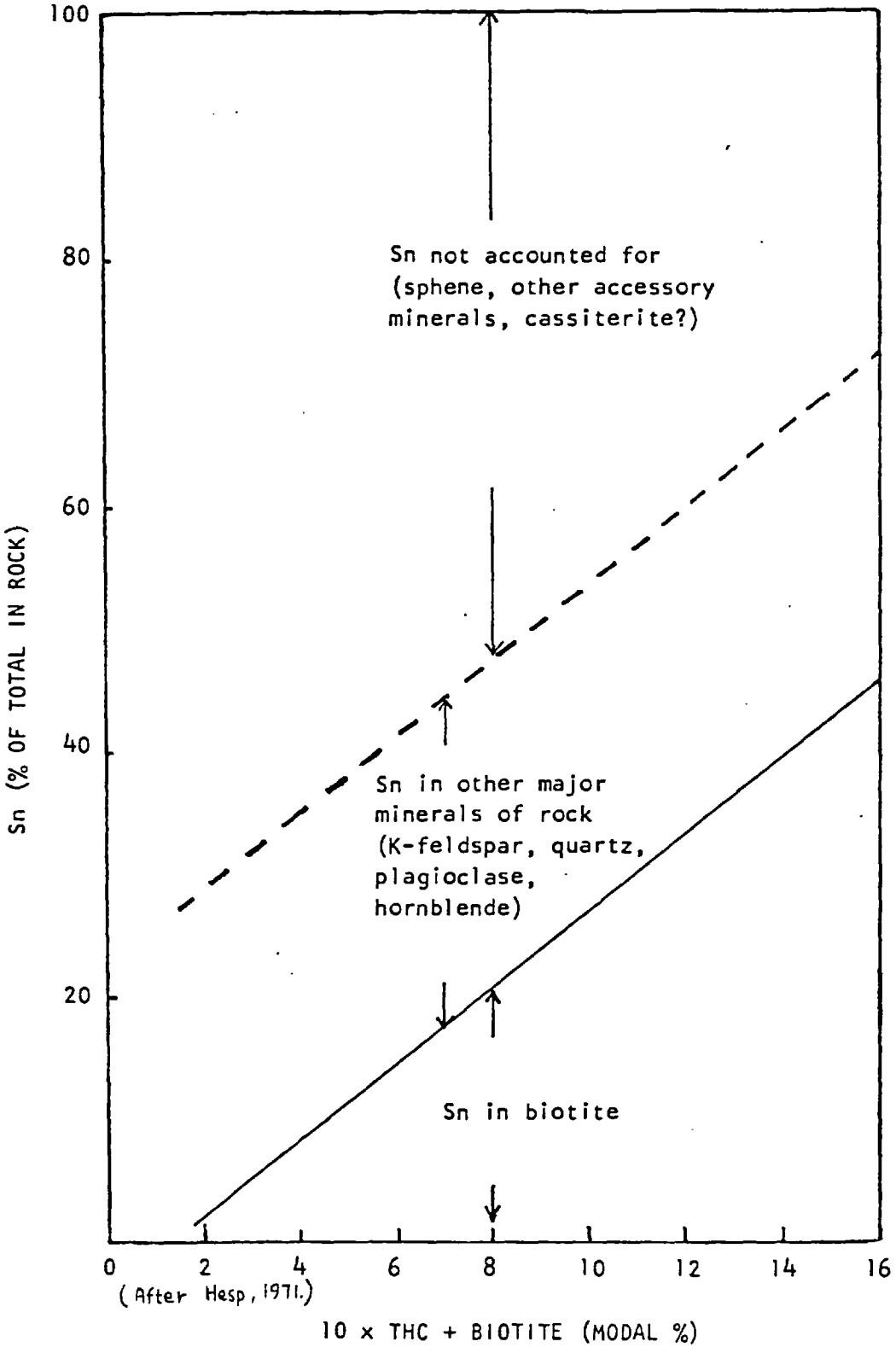

Fig. 52. The Overall Balance of Tin in Australian Granitic Rocks.

developed a concept of the "tin-holding capacity" (THC) of a biotite which is a factor chemically defined in terms of the ionic proportions as

$$\frac{Fe^{3+} + Li^{+}}{Fe^{2+} + Mg^{2+}} - \frac{Ti^{4+} + Mn^{2+}}{10}$$

Hesp, (1971), plotted the percentage of total Sn in Biotite from Australian granitoids against (10 x THC + Biotite (modal%) and a close straight-line correlation was obtained, (Fig. 52). Ivanov and Narnov, (1970), have also investigated the relationship between chemical composition and tin contents in biotites from Siberian intrusives and were able to show that increased tin contents were associated with increased F contents, higher iron indices, (Al/Si + Al + Fe^{3+} + Fe^{2+} + Mg), and decreased Ti contents. Groves, (1972), has used Hesp's factor to calculate the THC of two analysed biotites from the biotite adamellite and the muscovite biotite granite of the Blue Tier Batholith in Northeastern Tasmania and has found agreement with Hesp's plot of Rattigan's (1964) analyses.

Though it is clear that tin contents show positive correlations with cations occupying octahedral sites in the biotite, the apparent positive correlations with Fe^{3+} and Li^{+} and negative correlations with Ti^{4+}, Mn^{2+}, Fe^{2+} and Mg^{2+}, (Hesp, 1971), are not those predicted for selective substitution of tin from considerations of ionic radius, co-ordination number, ionization potential

and electro-negativity, (Hamaguchi and Kuroda, 1970). The change in composition of the biotites appears to be the result of crystal fractionation, with later melts having increased Fe/Mg and Li/Mg ratios. It is probable that the tin content is also related to crystal fractionation, and, therefore, may only be indirectly related to changes in biotite composition and not to preferential substitution for particular cations.

Hesp, (1971), has found that the tin content of the biotites from the Australian granitoids was generally less than 45% of the total tin content of the granitoids and in high-tin granitoids it was only 10% - 20%.
As shown in figure 52, besides biotites 20% - 25% of the total tin content of the granitoids were found to be accommodated by the major mineral components, (K-feldspar, plagioclase, quartz and in some cases hornblende). Although the partition coefficient of Sn for the respective major components except hornblende is low, (Jensen, 1973, and Pearce and Gale, 1977), the percentage of Sn accommodated by these mineral components as determined by Hesp, (1971), can still be accounted for because of the large modal % of the components concerned. The surplus 20% - 75% of the total tin content is likely to be accommodated by accessory minerals such as sphene, (Tauson et. al., 1968), and ilmenite, (1,500 - 2,000 ppm Sn) and zircon, (Hosking, 1970). This surplus tin can also concentrate to form cassiterite grains as they are known to occur as accessory minerals in some granitoids

from Australia, (Groves, 1972); Nigeria, (Bowden, 1970); Western Malaysia, (the present study) and Southern Finland, (Haapala, 1978). Hamaguchi and Kuroda, (1970), have also established the distribution pattern of Sn in co-existing minerals of a suite of granitic rocks from the Dzhida area, U.S.S.R. Thier findings indicated that 60% - 70% of the total tin content of the rocks was accommodated in the femic minerals and sphene. Amongst hornblende, biotite and sphene, the latter contains on average 40% and the other two minerals together contain 25% - 30% of the total Sn present in the rocks. As the modal % of the femic minerals decreases, the content of Sn in the sphene increases. Also, tin enters preferentially into the amphiboles rather than into the associated biotites. As amphiboles are rare and they occur in much less amount than biotites in granitoids associated with tin mineralisation, biotites are still the more important tin-bearing mineral owing to their high partition coefficient for Sn(>1) and their moderate to high modal % (<4% - 20%) in the rock, (Hesp, 1971). From the findings of Hamaguchi and Kuroda, (1970); and Hesp, (1971), it is clear that the interpretation of the Sn content of biotites in granitoids must be considered in relationship to the presence of other tin-attracting minerals such as sphene, hornblende, ilmenite, magnetite, allanite and zircon.

It is clear that in the absence of hornblende and sphene, the principal femic mineral which will

Table 22a

Trace-element content of micas and feldspar.

		Guehenno	La Villeder
Li in feldspar	no.of samples	11	30
	Extreme concentration in (P.P.M)	0-110	0-450
	Mean (P.P.M.)	36	141
Sn in biotites	no. of samples	10	25
	Extreme concentration in (P.P.M)	50-85-(165)	32-165
	Mean (P.P.M)	67 (77)	110
Sn in muscovites	no. of samples	9	23
	Extreme concentration in (P.P.M)	10-130(245)	60-400
	Mean (P.P.M)	71 (90)	120

Table 22b

Trace element concentrations in biotites (ppm)

Source of Trace-elements in biotite.	"Tin-granite".	Other granite.
Ni	10	30
Sn	455	200
Li	3,450	380

preferentially concentrate tin is biotite and thus it is appropriate that the tin content of this mineral should be used as a guide to the tin ore generating potential of granitoids.

Jedwab, (1955), analysed the Li and Sn contents of feldspars, and micas, (biotite and muscovite), respectively from two adjacent Hercynian plutons in Brittany, one being the La Villeder "tin-granite" and the other the Guehenno granite which has no known associated tin mineralisation. He found that:

1. Tin was always found in micas of granites.

2. The two granites studied showed a greater difference in the Sn content of their biotites than muscovites.

3. The Li content of feldspar, is higher in the "tin-granite".

The results of the above study are shown in Table 22a.

Jedwab claimed that tin-granites with associated staniferous pegmatites can be distinguished from other similar granites which have no known associated tin mineralisation by the Li and Sn contents of the biotite, (Table 22b), as it has been shown that the Sn content

in biotites from "tin granite" was about twice that of biotites from other granites while the Li content of the biotite has enriched by about 9½ times. Ni was found to be 3 times more in biotites from granites which have no known associated tin mineralisation as compared to the "tin-granites". Jaffar, (1970), has carried out a more comprehensive trace element, (e.g. Pb, Mo, Ni, Yb, Ga, Y, V, Sn Zr, La and Nb), study on biotites from the granitoids of the Western and Eastern tin belts of Western Malaysia and also on those biotites from the granitoids in the tin-barren Central Belt using XRF analysis. His results were in general agreement with the findings of Jedwab, (1955), for examples:

1. Tin was always found in biotites.

2. 75% of the biotite samples from the Western Belt had Sn content (20 - 550 ppm) higher than any biotites from the other two belts, (10 - 100 ppm) and

3. Ni content was highest from the tin-barren Central Belt as compared to the other two belts.

Groves, (1972), made a comparative trace element study, (Sn, Sc, Rb, Sr, and K/Rb), between the biotites and muscovites from the biotite-muscovite granites which are invariably associated with tin mineralisation, and

	Biotite-Muscovite Granite								
	682049B	682050B	682055B	682063B	682066B	682068B	Average	682055M	682068M
Sn	635	680	450	505	435	630	556	340	130
Sc	38	43	9	74	45	104	52		
Rb	6,795	6,940	6,810	7,570	6,790	7,520	7,070	2,370	2,400
Sr	4	8	8	15	4	3	7	10	13
K/Rb							10.8		

	Porphyritic Biotite Granite Adamellite					
	682046B	682047B	682048B	682059B	682062B	Average
Sn	60	67	58	65	72	64
Sc	74	68	74	74	73	73
Rb	1,935	1,550	1,685	1,520	1,840	1,705
Sr	21	3	4	18	21	13
K/Rb						39.5

Table 23. Trace Element Analyses (ppm) of Biotites (B) and Muscovites (M) from Biotite-Muscovite Granites and Porphyritic Biotite Granite/Adamellites, Anchor Mine, Blue Tier, N. E. Tasmania. Table from Groves, (1972).

those from the porphyritic biotite adamellites which are not associated with known tin mineralisation. Both of these granitoids are spatially and probably also genetically related and they formed part of the Blue Tier Batholith in Northeastern Tasmania. The average Sn content of the biotite in the biotite-muscovite granite is 556 ppm, (6 samples), in contrast to the average for the porphyritic biotite adamellite of 64 ppm, (Table 23), i.e., an enrichment factor in the former of about 9. The Rb content in the biotite of the biotite-muscovite granites is about 4½ times higher, (Table 23), than that of the biotite from the biotite adamellites. The Sr content in the former biotite is about 4 times lower, (Table 23), than that in the latter biotite. The two muscovite samples from the biotite-muscovite granites have distinctly lower Sn and Rb contents, (Table 23), as compared to those of biotites from the same granites. However, their Sc contents, (Table 23), are slightly higher than those of the biotites.

The results of various studies in widely separated areas, (Brittany, Western Malaysia, Northeast Tasmania, and Southwest England), have shown that the Sn, Li and Rb contents of biotites from "tin-granites" were notably higher than the respective values for granitoids with no known genetically associated tin mineralisation. The same trend was observed for the Li content of the feldspar although data is sparse.

The various studies discussed have shown a wide range of tin contents in the biotites of "tin-granites". The range of tin contents in the biotites of the La Villeder granite, ("tin-granite"), varies from 32 - 165 ppm with a mean value at 110 ppm (25),(Jedwab, 1955); that for the biotites from the granitoids of the Western Belt of Western Malaysia varies from about 25 - 550 ppm with a mean value at about 207 ppm (11), (Jaafar, 1970); and finally the range obtained for the biotites of the Biotite-muscovite granite, ("tin-granite") at the Anchor Tin Mine in Northeast Tasmania varies from 435 - 680 ppm with a mean value at 556 ppm (6), (Groves, 1972).

8.1.6. Concentrations of a range of incompatible, (F, Li, Sn W, Nb and Rb), and compatible, (Zr,and Sr), elements.

The following elements Li, F, Sn, W, Nb, Rb, Zr and Sr were chosen by the writer for this comparative literature survey because they are the most common set of elements which have been analysed by the numerous selected authors for the granitoids from several tin provinces around the world. The main reason for the analysis of the respective elements by the various authors is believed to be the consistent incompatible behaviour of Li, F, Sn, W, Nb and Rb during the differentiation of a granitic melt which may result in different concentrations of these elements in granitoids with different degrees of differentiation. Thus the level of concentration of these elements may be used as

an index of granitic differentiation. Another reason for the choice of F is its genetic association with Sn. It has also been experimentally and theoretically shown to form a fluoro-hydroxystannate complex, ($Na_2Sn(OH,F)_6$) with Sn. (Barsukov, 1957 and Suchchevskaya, Barsukov and Trusikova, 1965), and thus F is implicated as an important chemical associate in the transport of Sn in hydrothermal system. Li because of its positive correlation with F, (Klominsky and Absoloneva, 1974; and Tischendorf et. al., 1974), is also an important part of the chemical paragenesis. Li could thus also be involved in the formation of the fluoro-hydroxystannate complex. The not infrequent occurrence of wolframite in tin lodes naturally points to the selection of W as a geochemical associate of Sn. This association is also confirmed by the results of the present investigation of the geochemistry of West Malaysian cassiterites.

Zr and Sr are a pair of elements which do not behave incompatibly like the others in a differentiating granitic melt, (Pearce and Gale, 1977). Thus their depletion in granitoids may be used as an index of progressive differentiation of granitic magmas.

The significance of the level of the concentrations of the respective elements as indices of granitic differentiation has been made use of to distinguish "tin-granites" from granitoids with no known associated tin mineralisation. It is apparent that "tin-granites" are invariably more differentiated than the latter granitoids.

Elements analysed (in ppm) \ Sample No	PG1	2	3	3	Ave of Duplicate Analyses	4	5	5	Ave of Duplicate Analyses	6	7	8	Average of 8 samples (PG1 8)	SgP	BM	Approximate (standard deviation) over working range	Approximate mean "Precision" at 95% confidence level over working range
			Duplicate analyses				Duplicate analyses								1100 1160		
*P	980	388	600			600 596	208		598	604	416	536	541	2240		2.8	± .95% for sample PG1-8
Ti	424	251	234	251	242.5	245	186	193	189.5	227	261	179	252	443	2911	2.8 8.5	± 7.5% for sample Sg.P and BM ± 7.9%
Mn	367	344	394	407	400.5	338	379	387	383	353	346	408	367	126	497	7.45	± 3.8%
Pb	85	88	94	84	89	117	61	59	60	61	101	88	86	117	150	4.25	± 11.4%
Zn	66	75	41	44	42.5	50	91	95	93	70	89	53	67	27	91	2.45	± 7.2%
W	90	80	70	64	67	85	94	98	96	38	64	65	73	67	141	3.5	± 8.6%
Sr	37	37	34	40	37	26	27	32	29.5	32	27	39	33	24	66	3.85	± 23.2%
La	<28	<28	<28	<28	-	<28	<28	<28	-	<28	<28	<28	-	64	151	?	?
Ul	13.	25	24	26	25	24	40	39	39.5	21	23	25	24	22	49	1.1	±6.8%
Cr	35	28	39	38	38.5	39	27	26	26.5	35	38	36	34	41	35	.71	± 4.4%
V	7.8	7.2	7.2	7.2	7.2	6.9	16.1	15.6	15.85	6.1	7.2	5.7	8	9.	37.5	.35	± 6.1%
Zr	20	17	20	12	16	11	22	16	19	14	19	11	16	25	12	4.95	± 56.6%
Mo	7	9	7	6	6.5	9	6	6	6	<6	8	6	7.	15	19.	.71	± 22.7%
Co	4	7	8	6	7	10	7	5	6	4	6	5	6	12	18	2.8	± 86.2%
Cu	12	13	12	12	12	13	10	9	9.5	19	13	16	13	9	14	.71	± 13.2%
Cd	15	14	21	14	17.5	17	<10	<10	-	<10	<10	<10	15(4)	21	8.	4.9	± 56%
Ni	<34	<34	<34	<34	-	<34	43	50	46.5	34	34	34	-	34	45	4.9	± 21.1%
+Nb	27	22.2	21.5		-	25.5	16.9		-	27.7	23.3	16.5	22.6	-	-	-	-
Ca (%)	1.4	.72	1.72	1.79	1.76	1.01	.77	.77	.77	1.73	1.54	1.36	1.3	.65	1.66	.05	± 7.9%
Na "	21	1.	1.27	1.4	1.34	1.35	4.	3.99	3.995	1.47	1.7	1.66	1.6	1.56	1.46	.05	± 3.7%
K "	2.22	.97	.71	1.16	.94	1.53	.29	.32	.31	1.39	1.37	1.18	1.1	1.71	1.33	.17	± 54%
Mg "	.48	.27	.24	.26	.25	.17	.20	.22	.21	.21	.20	.22	.25	.36	.63	.014	± 12.2%
Fe	1.13	2.42	1.05	1.08	1.07	.93	2.83	2.85	2.84	.94	1.29	1.41	1.5	.92	3.36	.015	± 1.5%

Major and trace element analyses and their approximate precisions at 95% confidence level for granitoids from the Gakak Mine (PG1-8) the Sg. Pari Quarry (Sg.P) and the Bujang Melaka Massif (BM)

* = obtained by specific-ion electrolytic method

+ = obtained by XRF technique

All others are obtained by Plasma D-R Spectrometric technique

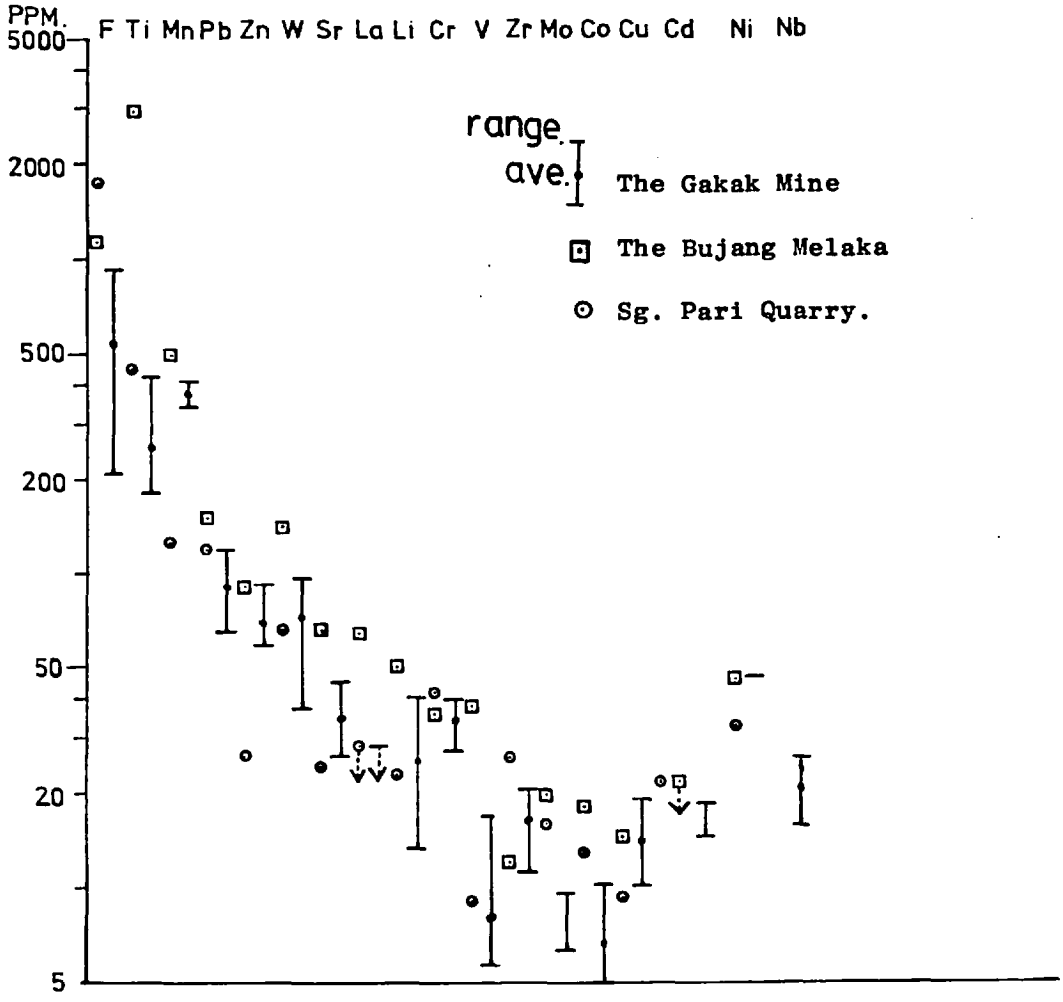

Figure 53 Trace element analyses of granitoids from the Gakak Mine, the Northern face of the Bujang Melaka Massif and the Sg. Pari Quarry.

Concentrations of a range of incompatible, (F, Li, Sn, W. Nb and Rb), and compatible, (Zr and Sr) trace elements in the whole rock.

The results of analyses carried out in the present study on granitoids from the Gakak Mine, Bujang Melaka Massif and the Sg. Pari quarry are plotted up as shown in figure 53 from which it is clear that the elements detected in the granodiorite from the Gakak Mine can be classified into four groups according to ranges of concentrations as follows:

1. 0 - 40 ppm: Li, Sr, La, Zr, V, Cr, Mo, Co, Cu, Cd, Nb, Ni, Sn (<6.3).

2. 40 - 120 ppm: W, Zn, Pb.

3. 180 - 900 ppm: Ti, Mn, F(208 - 920 ppm; with a mean of 534 ppm (8 samples)).

4. 0.09 - 4%: Ca, Na, K, Mg, Fe.

The Bujang Melaka and Gakak Mine granitoids show the highest values in F, Mn and Ti amongst the trace elements detected. The Khuntan "tin-adamellites" of Northern Thailand also show high F and Mn, (Suensilpong et. al., 1975). The Sg. Pari granite shows similarly high values for F and Ti but not for Mn. There are similarities as well as differences between the

concentrations of the elements detected in the granitoids from the Gakak Mine, the Bujang Melaka Massif and the Sg. Pari quarry as shown in figure 53. The contents of the following elements: Li, Sr, La. Zr, V, Cr, Mo, Co, Cu, Zn, Cd, Pb, Ni, Ca, Na, K, Mg and Al in the respective granodiorite are comparable, thus suggesting some chemical similarity between these analysed "tin-granites", (i.e. granites with associated tin lodes emplaced either within or peripheral to the contact environment). The contents of Ti, F and Mn in the respective "tin-granites" are, however, distinctly different. The Ti contents of the Bujang Melaka and the Sg. Pari granites are respectively 11.5 and 2 times higher than the average Ti contents, (253 ppm), of the Gakak Mine granodiorites. The F contents of the Sg. Pari and Bujang Melaka granitoids are respectively 4 and 2 times higher than the average F contents, (596 ppm), of the Gakak Mine granodiorites. Finally, the Mn contents of the Bujang Melaka granitoid are 1.4 times higher than the average Mn contents, (368 ppm), of the Gakak Mine granodiorites, but the Mn content of the Sg. Pari granitoid 3 times lower than that of the Gakak Mine granodiorite.

The F and Li contents of the respective granitoids were compared with those of the "tin-granites" from the Kinta Valley, (Western Malaysia); Cornwall; Western Erzgebirge, Karlovy Vary Massif, (Czechoslavakia); Southern Finland; Central and Eastern Transbaikalia, (U.S.S.R.). "Younger Granites" (Nigeria) and Southern

	Country and Location	Types of Granites	F	Li	Sn	W	Nb	Rb	Zr	Sr	no. of samples
	W. Malaysia										
1	Bintang Range										
	Taiping	Granites	-	-	11	720	7	738	64	41	5
2	Papan Quarry Kledang Range Kinta Valley	Porphyritic granite (GS. 19841)	2400	-	20	-	-	-	Tr	-	1
2	Telok Kruin Quarry Kledang Range Kinta Valley	Porphyritic granite (Gs. 19842)	900	-	20	-	-	-	Tr	-	1
2	Old Quarry at Merbau, Tronoh, Kinta Valley	Leucogranite (G.S. 19859)	1500	tr	30	-	-	-	nil	-	1
3	Sg. Pari Quarry Sg. Pari, Kledang Range, Kinta Valley.	Porphyritic Biotite granite	1130	22.81	-	67	-	-	26	25	1
3	P W D Quarry, Bujang Melaka, Kuala Dipang, Main Range, Kinta Valley	Porphyritic Biotite granite	8240	49.56	-	141	-	-	18	66	1
1	Main Range, Kinta Valley.	Granites	-	-	7	6.5	8	603	61	4	5
1	Kledang Range, Kinta Valley	"	-	-	6	9.2	8	624	77	13	5
1	Main Range Kuala Lumpur Area	"	-	-	8	5.7	7	658	69	25	30
1	W. Coast Range Lumut	"	-	-	817	5.3	7.5	652	77	4	4
3	E. Belt Batholith 10th Level Shaft, Gakak Mine (P.C.C.L.) Sg. Lembing	Hollocrystalline Muscovite - biotite granite	534 208-920	25 13-40	6.3	73.5 38.2- 96.6	22.6 16.5- 27.7	-	16	34 26-40	8
4	Thailand										
	Khuntan Batholith N. Thailand		Significantly high	-	483	Nil(27) 317(1)	-	-	-	-	28
	S.W. England										
5	St.Austell Cornwall	Porphyritic granite	2400	300	-	-	-	-	100	nil	1
5	Dartmoor Cornwall	Porphyritic granite	1600	260	-	-	-	-	130	50	1
6a	Cligga Head, Cornwall	Unaltered granite	3750	485	40	-	-	695	65	175	2
6b	S.W. England	90 unaltered granites	1395	-	-	-	-	-	-	-	90
7	Ehrenfriedersdorf	underground granite	-	-	83.8	-	-	1020	-	13	1
7	Vysoký Kámen (Younger Complex)	Drill core Granite	-	-	29.6	-	-	1140	-	9	1
	E. Germany										
7	Altenberg (Second phase intrusion Younger Complex)	Granite	-	-	11.2	-	-	1520	-	9	1
7	Altenberg N. Erzgebirge	Granite porphyry	-	-	52	-	-	503	-	100	1
7	Eibenstock Massif (Younger complex) (First phase)	Topaz - cassiterite bearing Protolithionite gran- ite	-	-	31.2	-	-	750	-	23	1
	(second phase)	" "	-	-	17.2	-	-	1050	-	16	1
	(Third phase) W. Erzgebirge	Topaz - cassiterite Li - bearing sidero- phyllite to protolithionite granite	-	-	15.8	-	-	1100	-	12	1
8	Eibenstock Massif (Younger complex) (Main phase)	Topaz - cassiterite bearing Li-bearing siderophyllite to protolithionite granite	3390	370	27	-	-	870	-	-	1
	(First phase)	Topaz - cassiterite bearing protolithionite granite	5590	435	37	-	-	1220	-	-	1
	(Second phase) W. Erzgebirge	" "	7280	490	32	-	-	1220	-	-	1
	Czechoslovakia										
9	Karlovy Vary Massif	autometamorphosed granites	4221	382	57(152)	-	-	677	55	31	155
10	S. Finland										
	Vakkara Eurajoki Area	Granite	8340	195	67(156)	-	38	698	112	27	5
	Kyni Area	granite	11100	279	17(?)	-	147	768	93	nil	2
11	Nigeria "Younger Granites"	Biotite granite	4200 (10)	110 (11)	76.7	-	-	341	210	-	variable
12	S. Australia Anchor Mine N.E. Tasmania Australia	Biotite - muscovite granite	10200	800	49	-	-	1033	-	5	6
13	U.S.S.R.										
	KUKULEISKII complex (Inner Main phase)	Leucocratic biotite granites (Hypabyssal)	2000	300	28	8	-	430	-	200	1
	Kharalginokii complex (Inner Main phase) C & E Transbaikalia	Leucocratic biotite granites (Hypabyssal - subsurface)	3000	84	9.4	5.9	-	380	-	100	1
14	Japan										
	Takakumayama, Japan	Biotite adamellite	390	153	8.8	-	-	-	-	-	7
	Naegi, Japan	Biotite adamellite	1330	77	4.4	-	-	-	-	-	3
	Okueyama, Japan	Biotite hornblende granodiorite	1640	100	3.8	-	-	-	-	-	5
	Otani, Japan	Biotite granodiorite	600	83	8.6	-	-	-	-	-	3
		Granites with no associ- ation of tin deposits									
	W. Malaysia										
15	C. Belt Johore (1) Singapore (1) Pahang (1)	Granitoids	-	-	5-5	11	5	190	155	124	5
14	Japan										
	Taishu	Biotite adamellite stock	510	33	1.2	-	-	-	-	-	3
	Hirase	" " "	420	24	0.7	-	-	-	-	-	3
	Yokota	" " batholith	240	32	2.1	-	-	-	-	-	3
	Busetsu	Biotite - muscovite adamellite "	520	56	1.6	-	-	-	-	-	5
	Sunikawa	Biotite - hornblende granodiorite batholith	520	27	1.8	-	-	-	-	-	7
	E. Germany										
8	Kirchberg Massif (Older complex) (Second phase) W. Erzgebirge	Magnetite bearing Febiotite granite	390	75	10	-	-	400	-	-	1
	Clark of average granites (Vinogradov, 1962)		750	40	3	1.5	20	180	200	300	

Table 24 Trace element analyses of selected "Tin-Granites" and "Wes - Tin - Granite".

Sources of data.

1 Yeap. 1974.

2 Alexander et. al., 1964.

3 The present study.

4 Suensilpong et. al., 1975.

5 Harding and Hawkes, 1971.

6a Hall, 1969.

6b Fuge and Power, 1969.

7 Ishihara and Terashima, 1978.

8 Tischendorf, 1973.

9 Klominsky and Absolonova, 1974.

10 Haapala, 1974.

11 Bowden, 1966, (Li and F); Butler et. al., 1962, (Nb); Bowden, 1970, (Sn).

12 Groves and Taylor, 1973.

13 Kozlov, 1974.

14 Ishihara and Terashima, 1978.

15 Jaafar, 1970.

Japan. The above F and Li data are tabulated in table 24. The F contents in the selected "tin-granites" are variable, ranging from 390 ppm, (in the Biotite adamellite of Takakumayama in Japan),to 11,100 ppm, (the "tin-granites" of the Kymi Area in Southern Finland (Table 24). Although variable these granitoids in general show significantly higher average F contents than the Japanese granitoids, (Ishihara and Terashima, 1978), and the second phase granite of the Kirchberg Massif in the Western Erzebirge, (Tischendorf, 1973), neither of which have any known associated tin mineralisation. The rocks are also distinctly higher than the F clark, (750 ppm), of world-wide average granites given by Vinogradov, (1962). There are, however, two exceptions to the above range in F contents. These are the values of 534 ppm and 390 ppm respectively obtained from the granodiorite of the Gakak Mine and the Biotite adamellite of Takakumayama in Japan. These values are comparable to those of Japanese and Western Erzgebirge granitoids which have no known associated tin mineralisation. The conclusions to be drawn from these findings is that the enrichment of F to the levels characterising many "tin-granites" is not a universal feature.

The Li contents of the selected "tin-granites" and "tin-eruptives" have a wide range of concentrations which extends from 22.8 ppm to 800 ppm, (Table 24). It was, however, interesting to observe that the Li contents of granites from the same tin field were fairly consistent

but this was not true for "tin-granites" from the different tin fields such as Cornwall, (260 - 490 ppm); Japan, (77 - 153 ppm); Western Malaysia, (22.81 - 49.56 ppm); Bolivia, (40 - 270 ppm) and Western Erzgebirge, (370 - 490 ppm). The value of 800 ppm Li at the higher end of the range is given by the Biotite-muscovite granite from the Anchor Tin Mine (Groves and Taylor, 1973). The values at the opposite end of the range are given by the Biotite-muscovite granodiorite of the Gakak Mine, (24.83 ppm of Li(8)) and the Biotite granitoid of the Sg. Pari quarry, (22.81 ppm of Li(1)). Both of these values are in fact lower than the Li clark (40 ppm) for granites given by Vinogradov, (1962). The Li contents of the selected "tin-granites" with the exception of Western Malaysian "Tin-granites" are clearly higher than those of Japanese granitoids and the second phase granites of the Older Complex in the Western Erzebirge neither of which have any known associated tin mineralisation. The average Li contents of the respective granitoids with two exceptions:

1. The Busetsu Biotite-muscovite adamellite batholith and

2. The latter granites are all below the Li clark.

Like F, Li tends to be enriched in "tin-granites".

The available Sn contents of the selected "tin-granites"

vary from 3.8 ppm (Bt-hbld-granodiorite of Okueyama in Japan) to as high as 76.7 ppm, (the Biotite granite of the Younger Granites of Nigeria), (Table 24). All the tin contents of the selected "tin-granites" are notably higher than the Japanese granites which bave no known associated tin mineralisation. The values (10 ppm) at the lower end of the range of Sn contents are given by "tin-granites" from Japan and Western Malaysia, but they are, however, comparable to the Sn content, (10 ppm) of the second phase granite, (Older Complex), of the Kirchberg Massif in the Western Erzebirge which have no known associated tin mineralisation.

The W contents of "Tin-Granites" from the Gakak Mine, the Northern face of Bujang Melaka and the Sg. Pari Quarry are considerably higher than the average W contents, (11 ppm), of the five granitoids from the Central Belt, (Table 24). This comparison is valid since the values obtained, (although by different methods of analyses - former by Plasma D.R.S. technique and latter by XRF technique), were quantitative. The results of the above comparison are in agreement with the findings of Jaafar, (1970) and Yeap, (1974). Comparison between the data given by Yeap and Jaafar is difficult because the data obtained by Yeap were semiquantitative whereas those analyses made by Jaafar were quantitative.

Similarly a rigorous comparison could not be made

between the semiquantitative values of the Nb concentrations given by Yeap, (1974) and the quantitative values given by Jaafar, (1970). However, a comparison could be made between the avarage Nb contents of the Gakak Mine granodiorites and those of the five Central Belt granitoids analysed by Jaafar, (1970). This comparison showed that the Nb contents of the granodiorites from the Gakak Mine, (22.6 ppm, average of 8 analyses, with a range of values from 16.5 ppm to 27.7 ppm) are significantly higher than the value for the Central Belt, (<5 ppm(5 samples)). This observation is in agreement with those of Jaafar, (1970) and Yeap, (1974).

The available Rb contents of the "tin-granites" vary from 341 ppm, (Nigeria's "Younger Granites"), (Butler et. al., 1962), to as high as 1,520 ppm, (the second phase intrusion of the "Younger Granites" at Altenberg), (Ishihara and Terashima, 1978), but they are significantly higher than the average Rb content, (198 ppm - average of five samples), obtained for the five granitoids from the tin-barren Central Belt of Western Malaysia, and the Rb clark (180) of the average granite given by Vinogradov, (1962), (Table 24). However, some of the values at the lower end of the range of the Rb contents are comparable or lower than the Rb content, (400 ppm), obtained for the Second Phase granitic intrusion of the Older Complex at the Kirchberg Massif in the Western Erzebirge. Although the latter Rb content is comparable to those of the selected "tin-

granites" from central and Eastern Transbaikalia, (430 ppm and 380 ppm), and Nigeria, (341 ppm), it is, however, significantly lower as compared to the Rb contents of the Younger Complex in the Erzegebirge. This observation suggests that local differences in the Rb contents of granitoids are important in differentiating a "tin-granite" from one which evidently has no associated tin mineralisation even though it is comparable to the Rb content of "tin-granite" elsewhere.

The Zr contents of "tin-granites" from Western Malaysia, Cornwall, Karlovy Vary Massif and Southern Finland vary from 12 ppm to 112 ppm, (Table 24), and they are lower than the average Zr contents, (155 ppm), of the five Central Belt granitoids of Western Malaysia and also the Zr clark, (200 ppm), of the average granite given by Vinogradov, (1962). This finding is in agreement with those of Jaafar, (1970) and Yeap, (1974). The "Younger Granites" of Nigeria show an anomalously high average Zr content of 210 ppm, (for 7 samples), which is not to be expected in "tin-granites" generated at destructive plate margins. This anomalous Zr content may be characteristic of mantle derived granite magmas which have formed the "Younger Granites". The latter were emplaced at "hot spots" within plates environment, (Sillitoe, 1974).

The Sr contents of the "tin-granites" that were selected for this comparative study, with two exceptions:

1. The Cligga Head granite in Cornwall, (175 ppm, (an average of two samples) and

2. The inner main granitic phase of the Kukulbeiskii Complex in Central and Eastern Transbaikalia, (200 ppm - mean average), vary from 4 ppm to 100 ppm, (Table 24), and they are consistently lower than the average Sr contents, (124 ppm) for the five samples of granites from the Central Belt of Western Malaysia which are not associated with any tin mineralisation.

The range of concentrations of Sr for the granitoids of the Central Belt extends from 20 ppm to 215 ppm. The normally higher concentrations of Sr in granitoids such as those of the Central Belt have also been recognised by both Jaafar, (1970) and Yeap, (1974).

This comparative study of the contents of some incompatible and compatible trace elements between the "tin-granites" and similar granitoids with no known associated tin mineralisation has indicated that, in general, the selected "tin-granites" are relatively enriched in F, Li, Sn, W, Nb and Rb and relatively impoverished in Zr and Sr as compared to similar granitoids with no known associated tin mineralisation.

The enrichment of incompatible trace elements, (F,

Table 25 - Geochemical criteria for determination of parent granites of rare-metals (Li, Be, Sn, W, Ta, Nb) deposits

Indicatory element or indicatory ratio (number of samples)	Average abundance (ppm) or ratio		Contents (ppm) or ratio selected as criteria	Probability of the indicatory value in sample populations	
	In ore-bearing granites	In barren granites		In ore-bearing granites	In barren granites
Li (60)	80-20	37-6	100 & more	0.23 & more	0.02 & less
Sn (75)	15-4	5-1	20 & more	0.16 & more	0.01 & less
Mg/li (40)	75-30	270-80	30 & less	0.27 & more	0.001 & less
			100 & more	0.30 & less	0.98 & more
Zr/Sn (40)	30-10	76-20	30 & less	0.46 & more	0.07 & less

*The error of the arithmetical mean was determined with probability of 0.95; Based on the following regions: Transbaikalia, Far East, Kalba, Altai, Ural and Central Asis (U.S.S.R.).

Reproduced from Beus and Sitin, 1968.

Li, Sn and Rb), in the mineralised roof contact phase as compared to the floor contact phase of the muscovite-biotite granites of the Blue Tier Batholith was interpreted by Groves and McCarthy, (1978), as a consequence of a continuous magmatic fractional crystallization. Fractional crystallization in granitic melts is a logical explanation for the enrichment of incompatible elements in "tin-granites" as observed in the present study.

Both the enrichment and depletion trends observed in the present study are potentially useful as indices of granitic differentiation. These indices may also be used as path finders for tin deposits.

Beus and Sitnin, (1968), studied the trace element geochemistry, (Li and Sn), and the element ratios, (e.g. Mg/Li and Zr/Sn), of Russian "tin-granites" from Transbaikalia, the Far East, Kalba, Altai, the Urals and Central Asia. They concluded that the "tin-granites" can be distinguished from granites with no known associated tin mineralisation by their significantly different average contents of Li and Sn and Mg/Li and Zr/Sn ratios, (Table 25). In addition to the above observation, they showed a sharp difference in the probability of appearance of the statistically valid geochemical criteria in the same sized sample populations from the two types of granites, (Table 25).

8.2. General Conclusions.

1. The major element geochemistry, (SiO_2, CaO and MgO), have been found to be an insensitive criterion for distinguishing the two types of granites.

2. The "tin-granites" were found to belong to the ilmenite-series of Ishihara et. al., (1978). While other similar granitoids with no known associated tin mineralisation belong to the magnetite-series. This sharp distinction is potentially useful for differentiating the two types of granitoids.

   The "tin-granites" from Western Malaysia and Northern Thailand are largely potassic adamellites showing enrichment in the potassium feldspar component.

3. The "tin-granites" from Northern Thailand, Western Malaysia and Southwest England are largely S-type, (i.e. peraluminous in composition and had a crustal origin).

4. Although the discriminant developed by Compston, Shirahase, Chappell and White (Quoted in Chappell and White, 1974.) has been successfully tested on

granitoids from the Western Belt of Western Malaysia, it needs to be further tested on granitoids of tin provinces elsewhere in order to assess its universal validity in distinguishing "tin-granites" from other granitoids with no known associated tin mineralisation.

5. There are distinct relative enrichments of Sn and Li in biotites and Li in feldspars from "tin-granites" as compared to those from other similar granitoids with no known associated tin mineralisation. Furthermore, Ni is relatively enriched in biotites from the latter granitoids. The above observed trends are potentially useful indicators of tin mineralisation.

6. "Tin-granites" in general are relatively enriched in incompatible trace elements such as F, Li, Sn, W, Nb and Rb, and relatively poor in Zr and Sr. These trends especially when recognised locally are invaluable indicators of a high degree of magmatic differentiation of the granitoids concerned. These trends may also serve to indicate the likely presence of tin deposits since the latter are often associated with highly differentiated granitoids.

7. The Russian "tin-granites" can be distinguished from other similar granitoids with no known associated tin mineralisation using the average contents of Li and Sn and the average ratios of Mg/Li and Zr/Sn, (Table 25). These distinct differences are further supported by a sharp difference in the probability of appearance of the statistically valid geochemical criteria in the same sized sample populations from the two types of granitoids, (Table 25).

CHAPTER 9.

Mineral Chemistry.

9.1. The Geochemistry of cassiterites from selected Western Malaysian tin fields.

9.1. Introduction.

This geochemical study of cassiterites from the Western Malaysian tin fields was undertaken in order to amplify the data compiled by Pryor and Wrobel, (1951), Venugopal, (1952) and the records of the Malaysian Geological Survey, (Alexander et. al., 1964). The material analysed by the author was selected chiefly from accessible cassiterite-quartz lodes, greisens and skarn-associated lodes giving clear evidence of the hypogene environment in which the mineralisation was emplaced. Aggregate cassiterite samples from selected alluvial deposits were also analysed for comparative purposes. The locations of all the lodes sampled are shown in Fig. 2. Using the geological evidence provided by the field setting and by geothermometric measurements made on fluid inclusions, the geochemical analyses are evaluated in terms of their significance in the interpretation of the environment of formation of the respective cassiterites. More detailed studies were carried out on selected lodes, (Gakak III and Hantu lodes), from the P.C.C.L. Mines at Sungei Lembing,

where, in addition, the chemistry of the associated gangue chlorites, (from the Gakak III Lode), was also examined in order to determine any significant variations in relationship to depth of formation. In the Sungei Lembing cassiterite associated paragenesis there is a notable lack of typical fluorine-rich gangue mineral species, (e.g. fluorite, micas, topaz and tourmaline), thus the chlorites were also analysed to determine whether or not any contained flourine in significant amounts.

9.1.2. Previous work.

The idea of relating chemical variation in the composition of cassiterite to the genetic origins dates back as far as 1936 with the work of Larionov and Tolmacev who investigated the minor and trace element geochemistry of cassiterite from Turkestan, (Russia), using Spark Source Emission Spectrometry. Their results revealed a distinct chemical difference between the cassiterite from pegmatitic and hydrothermal deposits which was considered a useful guide in the interpretation of the environment of derivation of alluvial cassiterite. Thus it was believed that the chemistry of cassiterite could be used as an exploration guide to the types of primary tin deposits in a given area.

Larionov and Tolmacev showed that the hydrothermal cassiterite, (two samples only), presumably of quartz

or quartz-feldspar vein origin, differed from the cassiterite of pegmatitic origin, (five samples), in containing a higher amount of As; the hydrothermal cassiterite also contained a high amount of V whereas it was undetected in the pegmatitic cassiterite. The latter contained notably large amounts of Nb and Ta, high amounts of Zr and Mn and also traces of Be, In, Ga, Y? Ni, Pb, Cu and Cr which showed no significant trends. The K, Na, Tl, Ba, Zn, Mo, Bi, Sb was not detected in any of the samples. The results produced by the study of Larionov and Tolmacev are interesting but the very limited number of samples analysed places restrictions on the general applicability of the observed chemical variation.

Borovick and Gotman, (1939), also investigated the minor and trace element geochemistry of cassiterites from pegmatites and quartz veins with the addition of material from sulphide-bearing cassiterite deposits. Wood-tin was also analysed. The most important difference between their investigation and that of Larionov and Tolmacev is that As was not detected in any of the samples. Chemical differences similar to those observed by Larionov and Tolmacev were noted for Nb, Ta, Zr, Mn and V in samples of the different genetic types of cassiterite. Their results can be summarised as follows:

Pegmatitic cassiterite: High Nb, Ta, Zr, Fe, Ga, Be and Hf.

Low In and W.

V undetected.

Quartz and guartz-feld: veins cassiterite: High V.

Increase of W.

Less Nb, Ta, Fe.

Low Be, Ga, In and Mn.

Hf undetected.

Sulphide bearing cassiterite: veins cassiterite:

Higher V.

Increase in W, Mn, and In.

Wood-tin: Zn, Pb, Mo, Sb and Ge are present.

The elements Ag, Cd, Co, Ni, K, Ba and Sb were not detected in any of the samples. Only Al, Si and Fe were detected in the colourless cassiterites. The Fe must be present only in trace amounts otherwise the cassiterites will be dark in colour. The relationship between the colour of cassiterite and the iron content was demonstrated by Clark et. al., (1976), who following the work done by Donaldson et. al., (1975) on SnO, have shown that the dark colour of tetragonal SnO_2 could be accounted for either by the population of the non-valence-shell bonds by d-orbital electrons from diadochically substituted Fe^{2+} or Fe^{3+} in the cassiterite Sn^{4+} structure, or by the non bonding electrons from Sn^{2+} formed in the SnO_2 lattice as a result of the

accommodation of the Fe^{3+} or Fe^{2+} impurity.

Itsykson and Russanov, (1946), analysed 72 cassiterite samples from 21 Russian tin deposits of pegmatitic, quartz vein and sulphide bearing vein origins in the southern part of the Soviet Far East by using Emission Spectrography. Their results were broadly in agreement with the data obtained by Boldyrev, (1941) and Gotman, (1941) on the character of the relationship between the elemental assemblages and the type of cassiterite deposits, but with some modification as follows:

a. V was detected in all groups.

b. Mo is concentrated in pegmatitic cassiterites and also partly in cassiterites from sulphide bearing veins.

c. W is most abundant in cassiterite from cassiterite-sulphide veins; the only exception being tin-bearing polymetallic veins where cassiterites contain no Wolfram.

d. In is present in all samples but it is the most abundant element in cassiterite-sulphide veins and especially in wood-tin.

e. Co also tends to be concentrated in cassiterites from cassiterite-sulphide veins.

The trends shown by W and In are also similar to those of Borovick and Gotman, (1939). V while present in all types of cassiterites is undetected in the pegmatitic cassiterites of both Larionov and Tolmacev (1936) and Borovick and Gotman (1939). The cassiterites from the southern part of the Soviet Far East are characterised by the presence of abundant V, W, Pb, Ga, In, Ag, Bi, Sb, Co and small amounts of Cu. The only exception is the absence of Ge which has been found by Papish et. al., (1927) and Venugopal (1952) to be present in small amounts (i.e. <50 ppm) in cassiterites from other tin fields such as Bolivia; Thailand; Lahat and Kuhun, (Western Malaysia); Nevada, U.S.A.; New South Wales; Tasmania; Nigeria; Japan; Alaska; Cornwall; Mexico; Sweden; Gold Coast; S.W. Africa and Swaziland. Venugopal, (1952), found Ge to be exclusively present in pegmatitic cassiterites.

In 1951, Pryor and Wrobel analysed 32 samples of acid cleaned cassiterites originated from pegmatites, quartz and quartz-feldspar veins and cassiterite-sulphide veins; they are from the tin fields of Western Malaysia; Bolivia; Australia; Europe; Africa and Canada. The results showed that the contents of Nb, Ta and Mn show a progressive decrease in the following order: pegmatites > quartz and quartz-feldspar veins >cassiterite-sulphide veins. V and As shownan opposite trend. Again Nb, Ta and V show trends similar to those obtained by the previous Russian workers.

Venugopal (1952) investigated the minor and trace

element contents of 141 samples of cassiterite, 8 samples of wood-tin and 13 samples of stannites all from the Free World countries using Spark-Source Emission Spectrography. These cassiterite samples were from pegmatites, gneisens, quartz veins and cassiterite-sulphide veins. Venugopal's results were semi-quantitative. He established that the cassiterites from pegmatites, gneisens quartz veins and sulphide deposits respectively have a decreasing content of Nb, Ta, Zr and Mn and an increasing content of V, In, W, Ga and As. These trends, especially those of Nb, Ta and V are in agreement with the finding of the Russian and British workers mentioned above. However, the W contents obtained by Pryor and Wrobel were a fifth to a tenth of those obtained by Venugopal.

Dudykina, (1959), has further confirmed the trend recorded for Nb and Ta.

Schneider et. al., (1978), analysed for 25 elements in 50 samples of Bolivian cassiterites representative of a range of tin deposits classified with respect to their geological age of formation in close relationship to their geotectonic position as follows:

1. PreCambrian pegmatites and greisen: Brazilian Shield, (Rondonia region).

2. Strata-bound ("Manto") deposits in Silurian sediments: Cordillera Oriental.

3. Discordant vein mineralisation resulting from Mesozoic granitic intrusions: Cord. Oriental, (e.g. Chojlla).

4a. Predominantly discordant vein swarms in connection with granitic intrusions of M-U. Miocene age, (Grant, Halls, Avila and Snelling, 1977); Cord. Oriental, (e.g. Viloco, Colquiri).

4b. Pipe shaped mineralisations and "tin porphyries" being linked with acid volcanism. ("Sub-volcanic" stages) of M-U. Miocene age, (Grant, Halls, Avila and Snelling, 1977): Cord. Oriental, (e.g. Llallagua, Potosi).

Their method of anlaysis was Spark-Source-Mass-Spectrometry. The results showed an increase of W and Ga and a decrease of Nb, Ta and Zr in cassiterites going from "PreCambrian group (1)" up to the "M-U. Miocene group (4b)". The analyses of type 2 cassiterites were not available at the time of publication of the results of this study. Ti contents did not show similar trends. Other elements like Zn, Pb, Sr, As and V were strongly correlated with the content of halogenes, (F, Cl). The trends obtained for Nb, Ta, Zr, W and Ga were in agreement with the findings Venugopal, (1952).

Haapala, (1978), has analysed cassiterites of different modes of occurrences from the granites of the Eurajoki

Area in Southern Finland for $Nb_2O_5Ta_2O_5$, FeO, MnO and TiO_2 using the electron microprobe. The cassiterites concerned occur

1. As an accessory mineral in topaz-bearing Vakkara granite.

2. In pegmatite veins emplaced within the latter granite and

3. In greisen and associated quartz veins within the Tarkki granite.

These cassiterites were checked for inclusions using the reflected light microscope and also the electron microprobe. Most of the cassiterites from type (1) and (2) modes of occurrences were found to be free of solid inclusions, but some were seen to contain small inclusions of Fe-Ta-Nb-Ti oxide and Fe oxide as identified by the electron microprobe. The distribution of Fe, Ta, Nb and Ti was found to be inhomogeneous and notably independent of the colour zoning in the respective cassiterites. The greisen-associated cassiterites contained some Nb- and Fe-bearing Ti oxide inclusions. The semiquantitative results of this study showed clear differences between the total contents of Nb_2O_5, Ta_2O_5, FeO and TiO_2 in the three types of cassiterites studied. Mo was not defected in any of the cassiterites.

The respective differences were as follows: for type

(1) cassiterites the Σ = Nb_2O_5, Ta_2O_5, FeO and TiO_2 = 10.5 - 6.4 wt%; for type (2) cassiterites Σ = 5.0 and 3.7% and finally for type (3) cassiterites Σ = 1.1 - 0.8%.

One interpretation for this observed chemical trend is that the fluids became progressively impoverished as they evolved from the magmatic, (higher temperature), to the hydrothermal, (lower temperature), fields. This could be regarded as a reflection of the progressive decrease with temperatures in the partition coefficients for the respective elements in cassiterite and other associated minor phases.

Other geochemical investigations of cassiterites involving analyses of one or a few elements are listed below:-

Analysts.	Elements detected.
Breithaupt (1872)	Sn, Fe.
Traube (1895)	Nb, Ta.
Hartley and Ramage (1897)	In.
Eberhard (1908, 1910)	Sc and rare earths.
Hadding (1922)	Ge
Papish, Brewer and Holt (1927)	Ge
Dekeyser (1931)	Y, Yb, Pt, Pb, Sb.

Analysts.	Elements detected.
Ida, Walter, Noddack (1931)	Pb, W, Ge, As, Mo, V, Cu and traces of Ru, Os, Rh, Ir, Pd, Pt, Re.
Goldschmidt and Peters (1931)	Sc.
Goldschmidt and Peters (1932)	Pt, An, Ag.
Brown (1934)	Cu, Zn, Ga, Nb, Zr, Sc, Mn and Fe.
Brewer and Baker (1936)	In.
Goldschmidt and Hormann (1937)	In.
Erametsa (1938)	In.
Fioletova (1940)	Sn, Nb, Ta, Ti, Si, Fe, Mn.
Prokopenko (1941)	In
Rankama (1944)	Ta
Pehrman (1945)	Sn, Nb, Ta.
Ivashentzov (1945)	Sn, Nb, Ta, Ti, Si, Fe, Mn.
Ahrens (1948)	In.
Cherdyntsev and Kozak (1949)	He.
Pecora, Switzer, Barbosa and Myers, (1950).	Mn, Fe, Nb, Ta, Ti, Si, Al, Mg, Ca, Cu.
Weibel (1956)	Sn, Nb, Ta, Ti, Fe.
Geological Survey of Malaysia (1903-1963)	Al, Fe, Ca, Mg, Ti, Mn, Cr, V, Ba, Ta, Nb, Zr, Be, Pb, Mo, W In, B, Sn.

Analysts.	Elements detected.
Fesser (1968)	Ga, In, Cd, Nb, Ta, Be, Ti, Ni, Y, Bi, Pb, Mo, Ag, Cu, V. (Rare earths - Yb, Dy, La, Sm). Zn.
Clark et. al. (1976)	Fe, Mn, Ti, Ta, Nb.

9.2. Methods.

Twenty eight cassiterite concentrates were prepared from selected primary tin lodes of various types, (e.g. cassiterite-quartz veins (chiefly); cassiterite-quartz-feldspar-fluorite veins, cassiterite-bearing quartz-muscovite greisenised granite and cassiterite-bearing sulphidic veins) and also from a number of the principal alluvial-colluvial tin mines of the Kuala Lumpur and the Kinta District tin fields. Preparation of the concentrates was achieved by using heavy liquid separations, cleaning using cold HF and hot aqua regia and finally hand picking, (Appendix III).

The concentrates were anlaysed for 21 elements using the Plasma Direct-Reading Spectrometer, (Appendix IV).

9.2.1. Results.

The elements detected were as follows: Na, K, Ca, Cu, Co, Fe, Ni, Mn, Cr, V, Ba, Zr, Ti, W, Al, Zn, Cd, La, Li, Sn and Sr. Not all the elements were detected in any sample because in some cases the contents were below the detection limits of the Plasma D.R.S. The chemical variation of the cassiterites can be discussed in terms of the contents of the elements grouped as follows, (see figure 54).

1. W, Ti and Fe. Their ranges of concentrations are as follows:-

   W - < 40 to 2,936. ppm

   Ti - 233. to 2,783. ppm

   Fe - 0.03% to 0.52 %

These elements are present in all the samples analysed.

2. Na, Al, Ca, Ni and Cr. Their ranges of concentrations are as follows:

   Na < 0.01% to 0.04 %

   Al < 0.01% to 0.085 %

   Ca < 0.01% to 0.13 %

   Ni < 40 to 133. ppm

   Cr < 43 to 130. ppm.

These elements are very variable in content.

3. Zr, V, Mn and Zn. Their ranges of concentrations are as follows:

Zr	-	<1.8	to 182.	ppm
V	-	<2	to 87.	ppm
Mn	-	<5	to 4,409.	ppm
Zn	-	<2	to 6,457.	ppm.

These elements occur in low abundance but are consistently present in detectable amounts.

4. La, Cu, Co, Cd, Sr, Li and Ba. Their ranges of concentrations are as follows:

La	< 1.8	to	56.	ppm
Cu	<11	to	697.	ppm
Co	<13	to	15	ppm
Cd	<10	to	60.	ppm
Sr	< 1.	to	4.	ppm
Li	<13	to	16.	ppm
Ba	< 0.2	to	129.	ppm.

These elements are frequently below the limits of detection and when detected they occur in trace amounts only.

5. K. Its range of concentrations is as follows:

K <0.07% to 0.09%

This element is frequently below the limit of detection (0.07%) and when detected it occurs in large amounts.

Na

K

Ca

Sr

Ba

La

Cd

The 7 elements which have cationic radii which differ by amounts greater than 0.2Å from that of Sn^{4+} (0.77 at co-ordination number VI) given by Whittaker and Muntus, (1970).

6. Sn. Its range of concentrations is as follows:

Sn 59. % to 78. %.

This element is the major constituent of the cassiterite structure.

Of the elements analysed above, 13 have ionic radii lying within 0.2Å of the ionic radius of Sn^{4+} (0.77Å) considered by Whittaker and Muntus (1970) as the maximum permissible difference compatible with diadochic substitution, (Whittaker, 1974. Personal communication). The remaining 7 elements have cationic radii which differ by amounts greater than 0.2Å up to 0.69Å (K^{+}) from that of Sn^{4+}. The presence of these elements in the octahedral sites in the tetragonal 'rutile type' lattice of SnO_2 must be explained as being due to the increased dimensional tolerance produced by elastic thermal expansion of the lattice under high formation temperature. Such effect has been considered by Jensen (1973) to be an important factor in increasing diadochic substitution in crystal structures.

An investigation into the relationship between temperature of formation and trace element content was made on twelve of the cassiterite concentrates. Two samples were taken from cassiterite-bearing quartz-muscovite greisenised granite at Gambang tin field, one sample from cassiterite-quartz-K.feldspar-fluorite veins at the Waterfall Mine, Pelapah Kanan; one sample from lodes

emplaced within the granite contacts in Sg. Besi Mines, Sg. Besi; and lastly eight samples from cassiterite-quartz veins at P.C.C.L., (Sg. Lembing), Tekka Hill, Sg. Pari and Siputeh, (Kinta Valley). Certain trends are evident. The contents of those elements with radii not differing by more than 0.2Å from that of Sn^{4+} (0.77Å) do not in general show systematic variation according to temperature of formation. Cr and Ti contents are higher in cassiterites with higher temperatures of formation while Ti contents increase with decreasing temperature and there thus appears to be an antipathetic relationship between Ti and Cr contents, which could be used as an environmental indicator. Analysed cassiterites from Tg. Tualang and Hock Hing Leong deposits, which unfortunately did not contain suitable primary inclusions for the determination of temperature of formation, contain high Cr (115. ppm and 54. ppm respectively) and low Ti (319. ppm and 233. ppm respectively). High Ca contents are correlated in two cases, (cassiterites from Tg.Tualang (200 ppm Ca) and Waterfall Mine (600 ppm Ca) with high Cr contents Tg.Tualang (115. ppm Cr) and Waterfall Mine (130. ppm Cr)) inferring that temperatures of formation in such cases were high. The cassiterite from the Waterfall Mine, Pelapah Kanan, (with Th°C values ≈ 400°C - 500°C) demonstrates this point. The cassiterites from the Gakak III and Willinks Lode Systems, (P.C.C.L., Sg. Lembing) with temperatures of formation in the lower range (200°C - 300°C), as determined by the homogenisation method, show high Ti (811. - 2,057 ppm and 690. ppm respectively) and low Cr (<43 ppm for both systems) contents.

Ca and La contents, when detected are significantly higher in the high temperature cassiterites, (e.g. those from Waterfall Mine, (600 ppm Ca and 2. ppm La) and Sg. Besi Mine (<100 ppm Ca and 23. ppm La) and Eu Tong Seng Mine (<100 ppm Ca and 3. ppm La). The ionic radius differences between Sn^{4+} (0.77Å) and Ca^{2+} (0.46Å) and La^{3+} (0.41Å) are 0.31Å and 0.36Å respectively according to ionic radii given by Whittaker and Muntus, (1970). The magnitude of the cassiterite lattice at high temperatures favours the incorporation of these elements.

Cr. Ti and Ca appear to have some value as indicators of the temperature of formation of cassiterites and could be used in conjunction with fluid inclusion studies to provide an indication of the primary environment of formation of alluvial/colluvial cassiterites.

The relationship between the temperature and the chemistry of greisen-associated cassiterites from the greisenised granitoid of Gambang was also investigated. The cassiterites from sample G.T.F.I.a gives a mean $Th^{o}c$ value of $228^{o}c$, (average of 9 $Th^{o}c$ values), which is significantly lower, (by $95^{o}c$), than the mean $Th^{o}c$ value of $323^{o}c$, (average of 20 $Th^{o}c$ values), obtained for the cassiterites of G.T.F.I.b.

This notable temperature difference is also followed by differences between the contents of

	Lower temp. Cassiterites (G.T.F.1.a).	Higher temp. Cassiterites (G.T.F.1.b).
Sn(%)	73.	70.
Fe(%)	0.09	0.07
Zn(ppm)	11.	<2.0
Ti(ppm)	1,184.	988.
W(ppm)	777.	634.
Zr(ppm)	137.	99.
Ba(ppm)	3.	1.
Na(%)	0.01	0.02
Mn(ppm)	15.	19.

Table 26. The contents of some elements in both low and high temperature greisen-associated cassiterites from the greisenised granitoid of Gambang.

certain trace elements. As can be seen in Table 26 the contents of Sn, Zn, W, Zr, Ti, Ba and Fe are higher in the low temperature cassiterites from sample G.T.F.1.a than in the high temperature ones from sample G.T.F.1.b. Amongst these elements, Zn shows the most significant difference with at least 6 fold enrichment in the lower temperature cassiterites as compared to the high temperature cassiterites. The Sn content of the lower temperature cassiterites is higher than that of the higher temperature cassiterites. The contents of Mn and Na show an opposite trend with relatively higher concentration in the higher temperature cassiterites from sample G.T.F.I.b. The content of Na in the latter cassiterites is two times higher than that of the lower temperature cassiterites, (G.T.F.I.a). Cu, Sr, Ca, Li, La, V, Cr, Co, Ni, Cd K and Al were undetected as their concentrations were below the analytical detection limit for these elements.

The observed correlation between the contents of detectable elements and the temperature of formation of the cassiterites is best explained in terms of the stability of the elements occupying the octahedral sites in the SnO_2 lattice under different temperature conditions.

The relatively higher concentration of the above mentioned seven elements in the lower temperature cassiterites, (G.T.F.1.a), may be the consequence of

a greater stability achieved by these elements occupying the octahedral sites in the tetragonal 'rutile type' lattice of SnO_2 which is expected not to expand significantly under a lower temperature condition. Whereas under a higher temperature condition, the SnO_2 lattice expands elastically with the result that the seven elements concerned, (especially Zn, Ti and Sn), were diadochically substituted by larger ions such as Nb, Ta, Mn and Na.

9.2.2. Regional and local comparison of cassiterite chemistry.

For purposes of regional comparison it is most appropriate to compare cassiterite deposits falling within the same genetic class. The evidence provided by the literature shows that cassiterites of different genetic origins may differ widely in the amounts of given trace elements which they contain. This principle is documented in the studies of Larionov and Tolmacev, (1936); Borovick and Gotman, (1939); Itsykon and Russanov, (1946); Pryor and Wrobel, (1951); Venugopal, (1952); Schneider et. al., (1978) and finally Haappala, (1978).

Certain regional differences in chemistry are evident when a comparison between the quartz and quartz-feldspar vein-associated cassiterites from the Western and Eastern Belts is made. The trace and minor element contents of 8 samples from the Western Belt,

Sample number and locality \ Elements analysed	W	Ti	Fe (in %)	Na (in %)	Al (in %)	Ca (in %)	Ni	Cr	Zr	V	Mn	Zn
1a												
16 Sq. Pari Quarry	197	2546	.05	.02	<.01	<.01	<40	43	137	17	6.	< 2
17 Hock Hing Leong Mine	349	233	.03	.02	<.01	<.01	<40	54	17	5	7	2
18 Si puteh	40	802	.06	.02	<.01	<.01	<40	43	6	19	8	< 2
19 Tg. Tualang	340	319	.17	.01	.02	.02	<40	115	4	25	25	< 2
20 Foong Seong Mine	1021	1208	.10	.02	.08	<.01	<40	43	138	19	7	< 2
D20 " " "	744	1092	.11	<.01	.09	<.01	58	43	106	18	6	< 2
Ave of duplicate (20)	882.5	1150	.105	-	.085	-	-	-	122	18.5	6.5	-
1b												
22 ChenderiangS.E.A. Mine	228	487	.04	<.01	.01	<.01	<40	43	15	14	<5	< 2
23 Gopeng	88	2598	.02	.02	.02	<.01	<40	43	174	40	29	8
D23 "	105	2968	.04	.02	.02	<.01	67	43	190	47	35	13
Ave of duplicate (23)	96.5	2783	.03	.02	.02	-	-	-	182	43.5	32	10.5
24 Eu Tong Seng Mine, Tekka	2936.	2473	.52	.03	.02	<.01	46.	43	131	37	4409	13
2a												
30 Ayer Hitam Mine	220	633	.05	<.01	.02	<.01	<40	43	10.	48	15	< 2
2b												
29 Sg. Besi Mine	602	631	.13	<.01	.05	<.01	133	53.	18	9	70	3.
3												
25 Greisenised granitoid of Gambang Zone a	777	1184	,09	.01	.01	.01	<40	43	137	<2	15	11
26 Same as above but Zone b	634	988	.07	.02	.01	<.01	<40	43	99	2	19	< 2
4												
28 Waterfall Mine	455	384	.36	.02	.01	.06	83.	130	16	62	32	10
5												
6 Willinks lode	1368	690	.21	<.01	.01	<.01	<40	43	18	70	41	6457
15 Sulphide + cassiterite lode of the Gakak III Lode Extension Lode System	1114	1455	.19	<.01	.04	<.01	<40	43	16	66	34	3.
6a												
7)	872	1648	.1	<.01	.01	<.01	<40	< 43	13	87	10	43
8)	1246	1777	.21	<.01	.04	.01	<40	< 43	22	68	38	49
9)	716	1222	.11	.03	.02	<.01	<40	< 43	23	59	23	29
10) Tin lode of Gakak III	1544	1750	.15	<.02	.02	<.01	<40	<43	25	82	35	11
11) Lode System	715	1045	.07	<.01	<.01	<.01	<40	<43	20	31	428	19
12)	1149	1474	.09	<.01	<.01	<.01	<40	<43	16	61	12	< 2
13)	882	811	.12	<.01	.02	<.01	<40	< 43	5	57	17	< 2
14)	921	2057	.13	<.01	.02	<.01	<40	< 43	33	97	25	18
6b												
1)	697	1422	.07	<.01	<.01	<.01	<40	<43	10	74	< 5	503
2) Tin lode of Hantu	1011	772	.09	.02	<.01	<.01	<40	< 43	<1.8	21	10	11
3) Load System	989	825	.08	<.01	<.01	<.01	<40	< 43	3	22	< 5	19
4)	667	1041	.08	<.01	<.01	.13	<40	43	8	37	60	13
5)	1435	688	.18	.04	<.01	<.01	109.	<44.	2.	26	35	2
Approximate σ (standard deviation) over working range	104	171.8	.011	0	.007	.005	20	21.5	17	2.83	2.5	3.5
Approximate mean Precision (%) at 95% confidence level over working range	±42.5	± 17.5	±32.4	0	±26.4	-	-	-	±22.4	±18.3	±26	66.7

Ca (in %)	Ni	Cr	Zr	V	Mn	Zn	La	Cu	Co	Cd	Sr	Li	Ba	K (in %)	Sn (in %)
<.01	<40	43	137	17	6.	< 2	<1.8	<11	<13	<10	<1.1	<13	.7	<.07	73
<.01	<40	54	17	5	7	2	<1.8	<11	15	<10	<1.1	15	1.	<.07	61
<.01	<40	43	6	19	8	<2	<1.8	<11	<13	<10	<1.1	<13	2	<.07	70
.02	<40	115	4	25	25	<2	8.	<11	<13	<10	<1.1	<13	.5	<.07	76
<.01	<40	43	138	19	7	<2	39.7	<11	<13	<10	<1.1	<13	3	<.07	75
<.01	58	43	106	18	6	<2	39.5	<11	<13	<10	<1.1	<13	4	<.07	70
-	-	-	122	18.5	6.5	-	39.6	-	-	-	-	-	3.5	-	
<.01	<40	43	15	14	<5	<2	<1.8	<11	<13	<10	<1.1	<13	1.	<.07	71
<.01	<40	43	174	40	29	8	4.	<11	<13	<10	<1.1	<13	1	<.07	72
<.01	67	43	190	47	35	13	5	<11	<13	<10	<1.1	<13	5	<.07	81
-	-	-	182	43.5	32	10.5	4.5	-	-	-	-	-	3	-	
<.01	46.	43	131	37	4409	13	3.	20	<13	18	1.5	<13	2	.09	71
<.01	<40	43	10.	48	15	<2	56	<11	<13	<10	<1.1	<13	2	<.07	67
<.01	133	53.	18	9	70	3.	23	11	<13	<10	1.8	<13	5	<.07	69
.01	<40	43	137	<2	15	11	<1.8	11	<13	<10	<1.1	<13	3	<.07	73
<.01	<40	43	99	2	19	<2	<1.8	<11	<13	<10	<1.1	<13	1	<.07	70
.06	83.	130	16	62	32	10	2	<11	<13	<10	<1.1	<13	2	<.07	73
<.01	<40	43	18	70	41	6457	<1.8	697	<13	60	<1.1	<13	.5	<.07	76
<.01	<40	43	16	66	34	3.	3	<11	<13	<10	2.	<13	3	<.07	76
<.01	<40	< 43	13	87	10	43	33	11	<13	<10	<1.1	<13	2	<.07	76
.01	<40	< 43	22	68	38	49	12	<11	<13	<10	<1.1	<13	<.2	<.07	59
<.01	<40	< 43	23	59	23	29	8	17	<13	<10	<1.1	<13	.5	.08	68
<.01	<40	<43	25	82	35	11	11	14	<13	<10	<1.1	16	1.	<.07	78
<.01	<40	< 43	20	31	428	19	4	47	<13	<10	<1.1	<13	1.	<.07	69
<.01	<40	< 43	16	61	12	<2	1.8	<11	<13	<10	<1.1	<13	<.2	<.07	75
<.01	<40	< 43	5	57	17	<2	1.8	<11	<13	<10	<1.1	<13	<.2	<.07	75
<.01	<40	< 43	33	97	25	18	2	17	<13	<10	1.5	<13	129	<.07	74
<.01	<40	<43	10	74	< 5	503	1.8	16	<13	<10	<1.1	<13	7	<.07	61
<.01	<40	< 43	<1.8	21	10	11	1.8	15	<13	<10	<1.1	<13	<.2	<.07	74
<.01	<40	< 43	3	22	< 5	19	1.8	14	<13	<10	<1.1	<13	<.2	<.07	69
.13	<40	43	8	37	60	13	1.8	<11	<13	<10	4.	<13	4	<.07	74
<.01	109.	<44.	2.	26	35	2	1.8	14	<13	10	< 1.1	<13	<.2	.09	77
7 .005	20	21.5	17	2.83	2.5	3.5	14.71	5.5	6.5	5	.55	6.5	1.76	.035	74.5
.4 -	-	-	±22.4	±18.3	±26	66.7	±.71 ±31.6 High Low Value Value	-	-	-	-	-	±108	-	±13.4

Chemical analyses of selected W. Malaysian Cassiterites:

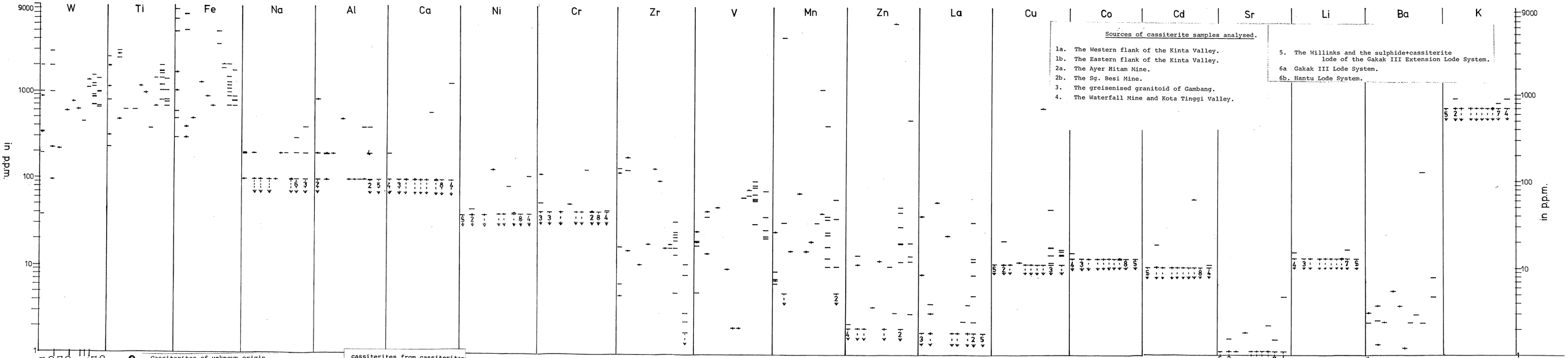

Table 54. Minor and trace element analyses of selected Western Malaysian cassiterites.

including 4 analysed by Pryor and Wrobel, (1951), taken from the Pulai Mine, Tekka Mine, Kacha Mine and Siputeh Mine respectively from the Kinta Valley, together with 16 samples from the Eastern Belt, including 1 analysed by Pryor and Wrobel, (1951), taken from the Kota Tinggi area of Johore State are shown graphically in Fig. 54, from which distinct differences in terms of Zn, Mn, V and Cu contents can be recognised. The cassiterites of the Eastern Belt are notably richer in these four elements than those from the Western Belt.

Difference in terms of minor elements such as Fe, Ti and W can also be recognised, (Fig. 54). The cassiterites from the Western Belt can be divided into two groups according to the Fe content.

1. A high Fe group, (5 samples), has a range of Fe contents varying from 5,000 to 8,000 ppm and

2. A low Fe group, (3 samples), has a range varying from 300 ppm to 600 ppm.

The cassiterites from the Eastern Belt can also similarly be divided into two groups.

1. A high Fe group has a range of Fe contents varying from 3,600 to 5,000

ppm and it consists of two samples respectively from the Waterfall Mine and Kota Tinggi area in Johore and

2. A low Fe group has a range of Fe contents varying from 700 to 2,100 ppm and it consists of 14 samples from the Hantu, Gakak III and Willinks Lodes.

Although the Fe contents of the two groups of cassiterites from the Eastern Belt are lower than those of the high Fe group from the Western Belt, they are, however, higher than the Fe contents of the low Fe cassiterites from the Western Belt. The cassiterites from the Western Belt can be divided into two groups according to the Ti content:

1. A high Ti group has a range of Ti contents varying from 2,000 to 3,000 ppm and it consists of 4 samples taken from the Sg. Pari quarry, Eu Tong Seng Mine, Pulai Mine and Siputeh Mine respectively, and

2. A low Ti group has a range of Ti contents varying from trace amounts to 800 ppm and it consists of 4 samples taken from the Tekka Mine, Kacha Mine, Siputeh Mine and Hock Hing Leong Mine respectively.

The cassiterites from the Eastern Belt can also be divided into two groups:

1. A high Ti group with a range of Ti contents varying from 685 to 2,055 ppm and it consists totally of cassiterites from the Hantu and the Gakak III lodes of the Pahang Consolidated Mines Limited, and

2. A low Ti group with a range of Ti contents varying from trace amounts to 385 ppm and it consists of 2 samples taken from the Waterfall Mine and the Kota Tinggi area respectively.

The range of Ti contents of the low Ti group is comparable with that of the low Ti group from the Western Belt while the cassiterites of the high Ti group of the Eastern Belt have lower values of Ti contents than the high Ti cassiterites from the Western Belt.

The range of W contents in cassiterites from the Western Belt extends from 38 ppm, (cassiterite from Siputeh), to 2,937, (cassiterite from the Eu Tong Seng Mine at Tekka Hill), which is distinctly greater than that of cassiterites from the Eastern Belt. The latter cassiterites have a more restricted range of W contents which extends from 455 ppm, (cassiterite from the

Elements analysed / Lodes of cassiterites analysed	Fe(%)	W	Ti	Zn	Zr	V	La
The tin lode of the Gakak III Lode System, (8 samples).	0.12	1,006.	1,473.	21. (6)	20.	68.	12. (6)
The tin lode of the Hantu Lode System, (5 samples).	0.1	960.	950.	12 (4)	6. (4)	36.	<1.

Table 27. The mean contents of some elements in the cassiterites from the tin lodes of the Gakak III and the Hantu Lode Systems. () no. in the bracket refers to the number of samples. All analyses are in ppm except for Fe.

Waterfall Mine), to 1,545 ppm, (cassiterite from Gakak III Lode). These differences may, perhaps, be a reflection of gross differences in the evolution of the chemistry of the hydrothermal fluids in the two tin belts.

It is also relevant to consider the variation between separate lodes, (e.g. the Hantu and Gakak III Lodes), from the Sg. Lembing tin field of the Eastern Belt. The mean contents of Fe, W, Ti, Zn, Zr, V and La, (Table 27), in the cassiterites from the Gakak III Lode are distinctly higher than those of cassiterites from the Hantu Lode.

Cassiterites showing distinct colour zoning from five different deposits, namely the Sg. Pari Lode; the Chenderiang Valley; the greisenised granitoid of Gambang; the Waterfall Mine and the Hantu Lode were investigated for their minor element chemistry, (Fe, Nb and Ta), as well as their Sn content using the S.E.M. and x-ray microanalyser technique. The samples analysed were in the form of thin parallel sided polished plates which have been previously used for fluid inclusion study. This investigation has shown that:

1. The colour zoning in these cassiterites bears no systematic relationship to the contents of Sn, Fe, Nb or Ta at the limits of detection as can be seen in

	Elements.	Sample Number. KSPL	GTF1		PK1bC1					
Light Zone	Sn	78.5	78.4	78,4	78.1					
	Fe	0.	0.	u.2	.3					
	Ta	.4	.4	.2	.4					
	Nb	.0	0.	.0	0.					
	O	21.2	21.2	21.2	21.2					
Coloured Zone	Sn	78.2	78.6	78.2	78.2	78.5	78.4	78.4	78.5	78.9
	Fe	0.0	0.	.3	.3	0.	0.	0.	0.	0.
	Ta	.4	.2	.3	.3	.3	.4	.4	.3	.4
	Nb	.2	0.	0.	0.0	0.	0.	0.	0.	0.
	O	21.3	21.2	21.2	21.2	21.2	21.2	21.2	21.2	21.2

	Elements.	PK3		KCH2				H7				H 11bC1			H20 a	
Light Zone	Sn			78.3	78.5	78.6	78.4	79.1*	78.3*	78.7†	77.6				80.3 *	
	Fe			0.	0.	0.	0.	0.	0.	0.	.3				.7	
	Ta			.3	.3	.2	.4	.4	.4	.4	.2				.3	
	Nb			.2	0.	0.	0.	0.	0.	0.	0.				0.	
	O			21.3	21.2	21.2	21.2	21.4	21.2	21.3	21.1				21.9	
Coloured Zone	Sn	78.5	78.5	78.4								81.1*	75*	81.1*	82*	81.6*
	Fe	0.	0.	0.								0	1.4	0.	0.	0.
	Ta	.3	.3	0.4								.4	2.8	.4	.4.	3
	Nb	0.	0.	0.								0	0	0		
	O	21.2	21.2	21.2								21.9	21.3	22.	0.	0.
														22.2	22.1	

* = non-normalised data

All data are normalised except for those marked by *

Table 28. The contents of Sn, Fe, Ta, Nb and O in some W. Malaysian cassiterites as analysed by the S.E.M. and X-ray micro-analyser technique.

Table 28.

2. Ta is consistently present in detectable amounts with a range of contents varying frim 0.2% to 0.4% within the light zones and from 0.2% to 0.4% with an exception of 2.8%, (from sample $H11_bC1$), within the coloured zones.

3. Nb was consistently undetected except for the coloured zone of cassiterite from the Sg. Pari Lode in which a Nb content of 0.2% was detected, and also for the light zone of a cassiterite plate from the Chenderiang Valley deposit in which a Nb content of 0.2% was also detected.

4. The ranges of Sn contents for the light zones and the coloured zones of the cassiterites analysed are 76. % to 78. % and 74% to 77. % respectively.

9.3. The geochemistry of the gangue chlorites from the Gakak III Lode of the Pahang Consolidated Mine Limited at Sg. Lembing.

Green chlorite is a common gangue mineral associated with cassiterite in the tin lodes of the Sg. Lembing Area. Chlorite is the dominant gangue silicate, apart from quartz, and contributes a distinctive character to the Sg. Lembing lodes which do not otherwise contain significant amounts of tourmaline or fluorite. Smith, (1967), has described the occurrence of two varieties of green chlorites in the tin lodes of the Sg. Lembing Area; the first is very dark green and is intimately associated with cassiterite. The second is much paler green in colour and it is generally to be found away from the tin lodes. In the course of the present study two varieties of green chlorites could be distinguished in the Gakak III Lode although the differences appear to be due to supergene alteration and leaching in the upper parts of the lode.

In the Gakak III Lode it was possible to distinguish visually the two varieties of green chlorites by their different shades of green colour. The first variety is pale green and is present in the heavily limonitised upper parts of the Gakak III Lode at the 2nd Level Stope in Section $^{73/y^a}$. The second is dark green and is present

in the intermediate and lower parts of the Gakak III Lode. The dark green chlorite has aslo been observed to be common in the Hantu, Willinks, Gakak and Gakak III extension Lode Systems.

Representative chlorites of the Gakak III Lode from the Second Level Stope (in Section 73/y^a), the Fourth Level Drive (in Section 75/y^a), the Fifth Level Stope (in Section 76/y^a), the Ninth Level Stope, (unknown locality) and finally the Ninth Level Stope (30 ft. below Eight Level Drive in Section 79/y^a) were analysed for 22 major, minor and trace elements and F, using Plasma Direct-Reading Spectrometry and Specific-ion-Electrolytic Methods, (Appendix IV for the former). This is the first analytical determination on chlorites from the tin lodes of the Sg. Lembing Area.

The results of these analyses can be grouped into three by virtue of the relative contents of the elements as as shown below:-

a.	10 - 32%	Fe > Al	(Fe 22.5 - 26.6 %)
b.	0.1- 2%	Mg > Mn > Na > Ca > W	(Mg 1.23 - 1.96%)
c.	0 - 900 ppm	Pb > Ba > Ti > La > Ni > F > Mo > Li > V > Co > Sr > Zr >	(F 116 - 156 ppm).

The above results showed that the chlorites studied were notably rich in Fe. The respective chlorites are

Chamosite dA° spacing	Ripidolite dA°	Thuringite dA°	Daphnite dA°	dA°	dA°	dA°	dA°	dA°	dA°	dA°
	14.1	13.6	14	13.936	14.01	14.012	13.94	13.936	14.05	14.08
7.12	7.07	6.90	7.08	7.0393	7.02		7.06	7.0107	7.04	7.0682
-	4.724									
4.68	4.620	4.63	4.68	4.6751	4.692	4.6751	4.69	4.6751	4.69	4.6961
4.305										
3.935										
3.553	3.537	3.49	3.523	3.5178	3.522	3.5131	3.51	3.5131	3.52	3.52
-	2.827	2.80	2.82	2.8145	2.822	2.8116	282	2.8145	281	2.82
2709					2.679					
-	2.664	-	2.682	2.6341	2.6217	2.6341	2.6367	2.6354	2.64	2.6405
-	2.599	2.61	2.619	2.6089			2.6114		2.61	2.6114
-	2.556	-	2.574	2.5624	2.577	2.5624	2.5806	2.5600	256	2.566
2.525										
2.151										
-	2.450	2.46	2.469	2.4536	2.471	2.4568	2.4557	2.4514	2.46	2.459
-	2.389	2.39	2.405	2.3981	2.408	2.4001	2.3981	2.3949	2.40	2.3981
-	2.265	2.26	2.279	2.2770	2.285	2.2742	2.2779	2.2770	2.28	2.2761
-	2.077									
-	2.009	2.00	2.014	2.0088	2.020	2.0124	2.0116	2.0095	2.01	2.0116
-	1.888	1.88	1.893	1.8867	1.897	1.8879	1.8891	1.8830	1.89	1.8848
-	1.826	1.81	1.828	1.8164	1.8137	1.8175	1.816	1.8147		1.8175
1778	1.749	-	1.765	1.7628	1.772	1.772	1.7634	1.7608	1.76	1.7644
-	1.716	1.72	1.722		1.729					
	1.665	1.66	1.666		1.6693	1.648	1.6725	1.6716	1.66	1.6615
1.563	1.566	1.55	1.560	1.5614	1.5614	1.568	1.5594	1.559	1.56	1.5602
				1.5399		1.5384	1.5399			
				1.4528		1.4528	1.4967			

Table 21 Shows the d spacings of identified chlorites and also those of unidentified chlorites from the Gakak III Lode System, P.C.C.L.

thus identified as ferroan species. Since the intensities of the first five orders of basal reflections (001, 002, 003, 004 and 005) of the seven chlorite samples, (inclusive of the five analysed chlorites plus two unanalysed samples respectively from 5th level stope (20 ft. above SL drive), in Section 76/y[a] and 9th Level Stope, (just below 8L drive) in Section 76/A[b]) were comparable to those characteristic of chlorites with less than 30% Fe contents, (Brindley, pg. 261)in Brown, 1961), the range of Fe contents (22.5 - 26.6%) obtained by the Plasma DRS technique were thus compatible. Chlorites which have an Fe content greater than 30% were reported by Brindley, (in Brown, 1961), to give relatively weak 001, 003 and 005 reflections and strong 002 and 004 reflections.

More detailed identification of the respective ferroan chlorites using the classification scheme of Hey, (1954), was not possible because the parameters (e.g. no. of Si ions; $\frac{Fe^{2+} + Fe^{3+}}{Fe^{2+}\ Fe^{3+} + Mg}$; and $Fe^{2+}\ Fe^{3+}$) used in the respective classification scheme could not be obtained owing to the absence of SiO_2, Fe_2O_3, FeO and H_2O^+ data which were necessary for calculating the number of ions each element has in a unit formula of chlorite.

The XRD powder patterns given by the two unanalysed chlorites and the five partially analysed ferroan chlorites were compared with those documented XRD powder patterns

	Green daphite* (bavalite) (%)	Green ferroan chlorites from Gakak III Lode System+ (%).
Al	11.32	10.77
Mg	1.42	1.7

* Data from analyses 23 on page 142 in Deer et. al., (1962).

\+ Average of four samples.

Table 30. The contents of Al and Mg in green daphaite and green ferroan chlorites.

of chemically analysed and fully identified ferroan chlorites such as daphnite, thuringite, ripidolite and chamosite, (oxidised chlorite). (See Table 29 for the above comparison). This comparative study showed that the spacing of the reflections of the seven chlorites were closely comparable to those of daphnite although the order of the relative intensities of the first five basal reflections of the respective chlorites was not in agreement with that of daphnite. The latter difference was not unexpected since there was a significant difference (by 9%) between the mean Fe contents of the five chlorites (average of 25%) and daphnite (34% (1)). Fe ions have scattering factors about twice that of Mg^{2+} and Al^{3+} ions and consequently their enrichment or impoverishment can change considerably the relative as well as the absolute values of the intensities of the x-ray reflections. (Brindley pg. 270 - 271 in Brown, 1961). The Mg and Al contents of the respective daphnites are comparable to those of the five chlorites, (Table 30). Judging from the results of the x-ray diffraction study and the the comparability of the contents of some major elements, (e.g. Al and Mg), it was very likely that the five chlorites studied were daphnite.

The average F content obtained from the five analysed chlorites, (daphnite), was 131 ppm with a range from the 116 ppm to 156 ppm. This mean (131 ppm) is anomalously low compared to the F analyses of two

metamorphic chlorites (600 ppm and 1,300 ppm) given by Lokka (1943) and Seraphim (1951) respectively. The F contents of the chlorites concerned could have been inherited from their precursors hornfels biotites and muscovites which are known to contain F contents varying from 600 ppm to as high as 20,000 ppm, (Deer et. al. (1967) and Seraphim (1951) and 450 ppm respectively, (Deer et. al. (1967)). The genessis of these chlorites was discussed on page 70. The anomalously low F contents of these chlorites can be ascribed to the loss of F during the process of hydrothermal chloritisation of F rich hornfels biotites and muscovites. The anomalously low F contents also suggest that the hydrothermal fluids responsible for the chloritisation process were poor in F. Otherwise the chlorites crystallising in equilibrium with the fluid would be expected to have a higher F content. Additional evidence for this point of view is the rarity of occurrence of fluorite, topaz and primary hydrothermal F-rich micas in the tin lodes of the Sg. Lembing Area, and secondly the anomalously low F contents of granodiorite from the Gakak Mine. The range of F concentrations in this granodiorite vary from 208 ppm to 920 ppm and it has a mean of 534 ppm).

The almost two-fold increase in the Fe contents of the the chlorites. (Average of 5 chlorites = 24.86%) from a mean of 14.3% Fe given by two hornfels biotites, (analyses no. 13 and 14 in Deer et. al., 1962) must

Elements analysed / Minerals	W	V	Cd	Cr
Ferroan Chlorite	1,389.	67.	<10	<6
Cassiterite	1,006.	68.	<10	<43

Table 31. The mean contents of W, V, Cd and Cr in gangue ferroan chlorites and cassiterites from the tin lode of the Gakak III Lode System.

Elements detected / Mineral sample and number and location	Pale Green Chlorite G3 1b 2nd level stope		Average of duplicate analyses of pale green chlorite	Dark Green Chlorites G3 4a 4th level	G3.8b 5th level stope	G3.17 9th level stope	G3.18 9th level stope	Average of 4 dark green Chlorites	Approximate ≤ (standard deviation) over working range	Approximate "Precision" 95% confidei level over working ran
Zr	10.	9	9.5	14	11	9	23	14.25	0.71	± 15%
Zn	515	523	519.	476	587	661	1219	735.75	5.65	± 2%
Mg (in %)	1.24	1.21	1.225	1.59	1.69	1.69	1.96	1.7	.02	± 3.3%
Mo	89.	90	89.5	149.	128	116	115	127.	.70	± 1.56%
W	1103	1122	1112.5	1424	1336	1378	1416	1388.5	13.43	± 2.4%
La	151	154	152.5	191	185	180	192	187	2.12	± 2.8%
Pb	500	514	507	572	572	582	646	593	9.9	± 3.9%
Fe (in %)	22.36	22.61	22.5	26.1	26	26	27	26.3	.18	± 1.6%
Ni	139	132	135.5	170	157	139	158	156	4.9	± 7.3%
K (in %)	.32	.25	.285	.35	.33	.30	.28	.32	.05	± 35%
V	62.4	63.9	63.2	67.4	61.6	63.3	78.	67.6	1.1	± 3.4%
Mn	4614	4694	4654	5637	4906	4537	4376	4864	56.6	± 2.4%
Co (in %)	.17	.16	.165	.11	.16	.21	.20	.17	.007	± 8.6%
Sr	15	12	13.5	23.	7	11	12	13.3	2.1	± 31.4%

Table 32 shows the chemical analyses and their averages and their approximate mean precision values at 95% confidence level obtained for the gangue ferroan chlorites. All analyses are in ppm unless otherwise stated.

Elements detected / Mineral and sample number and locations	Pale Green Chlorite G3.1b 2nd level stope		Average of duplicate analyses of pale green Chlorite	Dark Green Chlorites G3.4a 4th level	G3.8b 5th level stope	G3.17 9th level stope	G3.18 9th level stope	Average of 4 dark green Chlorite	Approximate σ (standard deviation) over working range	Approximate mean "Precision" at 95% confidence level over working range
Na (in %)	.44	.33	.39	.25	.22	.43	.34	.31	.08	± 40%
Al (")	12.79	12.85	12.8	11.1	10.56	10.59	10.83	10.77	.04	± .7%
Co (in ppm)	61	64	62.5	50	46	82	42	55	2.12	± 6.8%
Li (")	109	113	111	93	104	79	138.	103.5	2.8	± 5%

Table 33 shows the enrichment trends of four elements in the pale green ferroan chlorites of the Gakak III lode. This also shows the approximate Precision values of the data at 95% confidence level over the working range.

indicate that the extra Fe ions were derived from the hydrothermal fluids responsible for the chloritisation process. This indication led to the conclusion that the latter process was not isochemical. The contents of V. Cr, W and Cd in the chlorites were comparable to those of cassiterites, (Table 31). This finding suggests that the chloritisation process and the crystallisation of cassiterites were caused by the same hydrothermal mineralising fluids and hence the two respective events must have occurred contemporaneously. This conclusion is also supported by the textural evidence suggesting coeval formation of the two minerals.

The two varieties of green chlorites were found to be distinctly different in their major, minor and trace-element contents: The pale green chlorite was found to be distinctly poorer in Zr, Zn, Mg, Mo, W, La, Pb, Fe, Ni and K than the four dark green chlorites, (see Table 32 A lesser difference (i.e. <10%) was observed for V, Mn, Ca and Sr, (Table 32), between the two varieties of chlorites. As mentioned earlier these differences appear to be due to supergene alteration and leaching processes which were also responsible for the intense limonitisation with which the pale green chlorites are associated.

Accompanying these decreases, the Na, Al, Co and Li contents in the pale green chlorite were found to have increased compared to the means of these elements in the four dark green chlorites, (see Table 33).

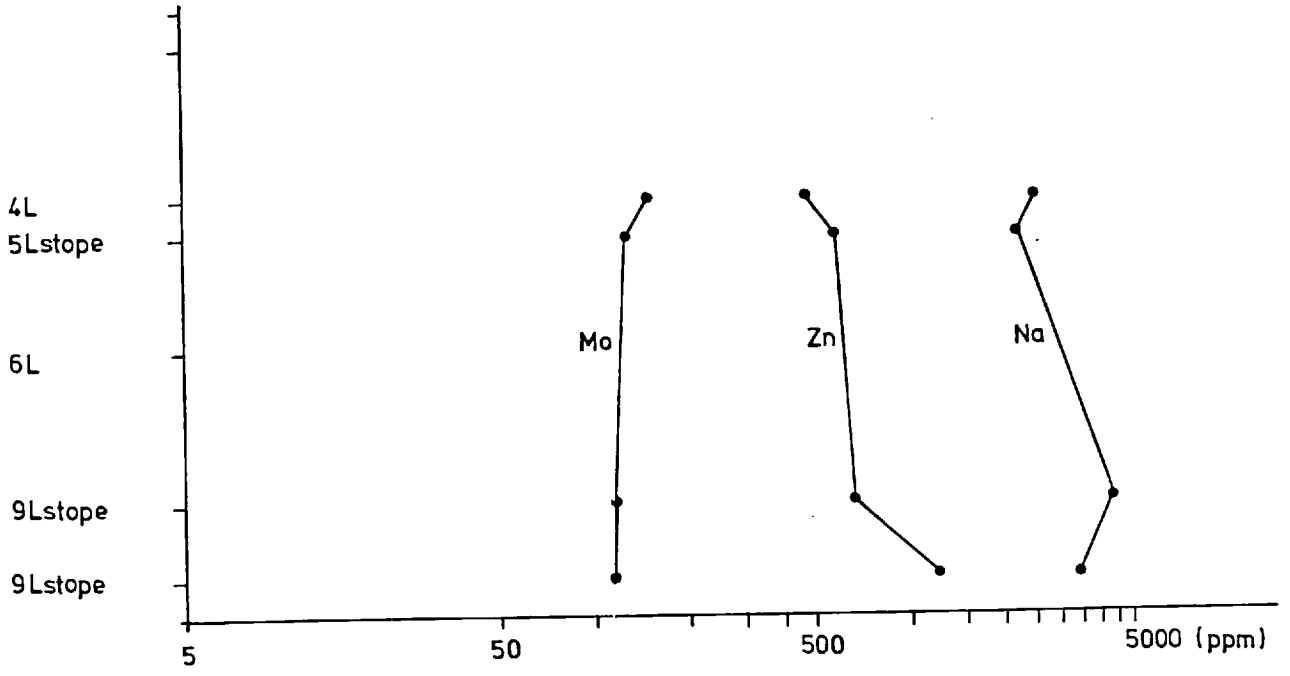

Figure 55. The variation with depth of Mo, Zn and Na contents in gangue ferroan chlorites.

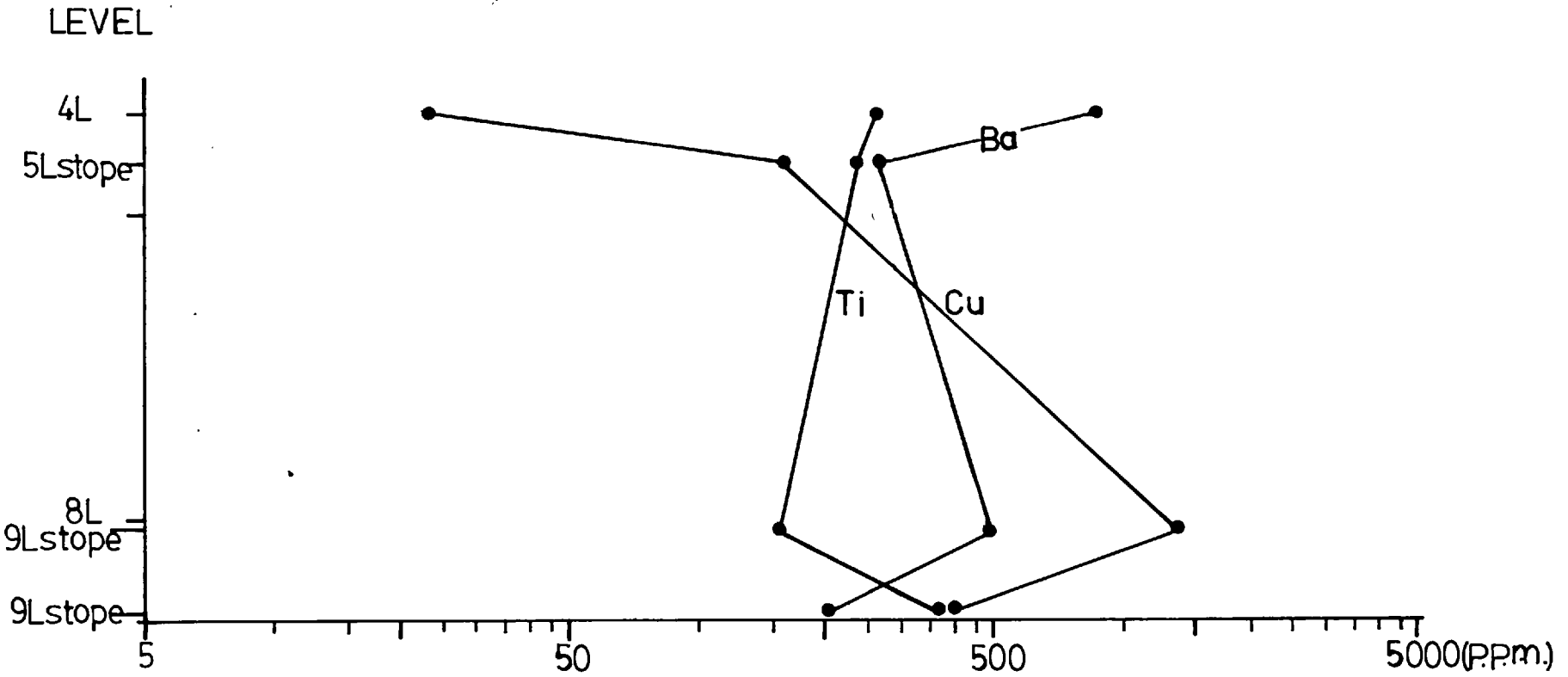

FIGURE 56. VARIATION WITH DEPTH DIAGRAM OF THE CONTENTS OF CU, TI AND BA IN GANGUE FERROAN CHLORITES.

The contents of certain elements in the dark green chlorites were found to vary with depths. For example, Zn and Na contents were found to increase towards the lower parts of the lode; Mo showed the opposite trend, (Fig. 55). As the number of chlorite samples analysed was small, it was difficult to draw any definite conclusion as to the applicability of the respective chemical trends to the mineral exploration drilling programme of a prospect. However, such trends if statistically valid may prove valuable as a depth indicator for chlorite-bearing lodes.

The major, minor and trace elements contents, (with the exception of Zn, Na, Mo, Cu, Ba and Ti), of the dark green chlorites were found to be consistent with depths. This uniformity suggests that there were no drastic changes in the physico-chemical conditions which prevailed during the hydrothermal chlorisation process in the Gakak.III Lode.

The large variation of the Cu and Ti contents in the four dark green chlorites, (see Fig. 56), may be ascribed to contamination of the samples by chalcocite and/or covellite, and rutile respectively. Rutile is an especially common alteration product of biotites, (Plate 18B) Barium variation, (Fig.56), was due to the very poor analytical precision (Percentage reproducibility of Ba in chlorite solutions is 59.7%) obtained for Ba by

the Plasma D. R. Spectrometry method.

9.3.1. Conclusions.

The main conclusions drawn from the above geochemical study are as follows:

1. The chemical and hence colour differences between the two varieties of green chlorites are due to supergene oxidation and leaching processes. There was, in fact, a single variety of dark green chlorite.

2. The single variety of dark green chlorite has been identified as ferroan chlorite with a composition close to daphnite.

3. The mineralogical and chemical evidence suggests that the fluids which were responsible for the hydrothermal chloritisation process were poor in F.

4. There is no evidence of drastic changes in the chemistries of the primary chlorites in the lodes according to depth. It may be inferred, therefore, that the conditions under which chlorisation took place were relatively uniform.

APPENDIX I.

The Leitz Microscope Heating Stage 1350.

Instrumentation.

The Leitz Heating Stage 1350 was mounted on the rotating stage of a Leitz optical microscope by means of two screws. Its main structiral elements are as follows:-

1. A set of milled screws for moving the sample for best optical observation.

2. A water cooling jacket.

3. The heating cartridge containing a metal support for a sapphire disc on which the sample plate or cleavage fragment was placed,

4. A platinum/rhodium-platinum thermocouple which was metal-joined to form a unit with the metal support.

5. Two quartz windows provided gas-tight seals for the top and bottom of the

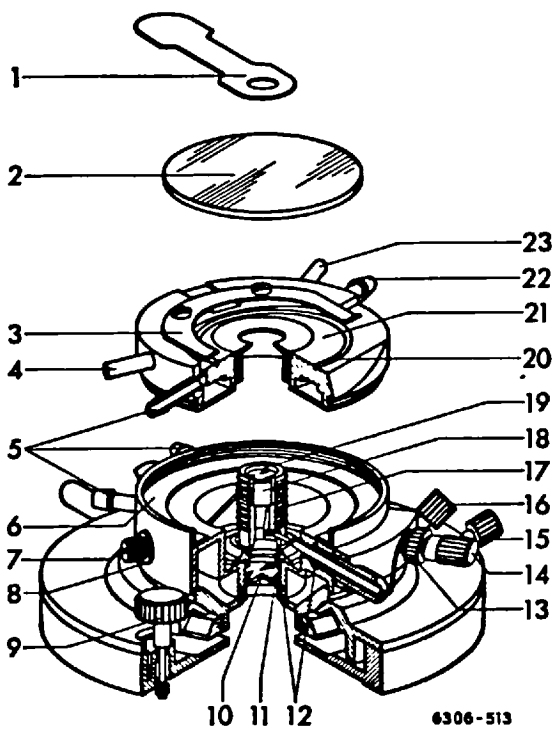

1 Slide stop
2 Quartz glass disc
3 Leaf spring
4 Socket for protective gas
5 Sockets for cooling water
6 Rubber ring
7 Current connection
8 Round cord ring
9 Clamping screw
10 Quartz glass disc
11 Clamping ring
12 Round cord ring
13 Nut for attaching the thermo-couple
14 Connection for the measuring instrument
15 Milled screw for the orientation of the object
16 Milled screw for the horizontal alignment of the object
17 Heating cartridge
18 Object holder with thermo-couple
19 Object carrier
20 Round cord ring
21 Diaphragm stop
22 Socket for cooling water
23 Socket for protective gas

Figure 57. Cross Section through the Heating Stage 1350°c.

heating vessel. The top quartz glass disc could be rotated in case of condensation on the disc which did impair optical observation of the sample. The structure of the Leitz Heating Stage 1350 is diagramatically illustrated in Fig. 57.

The techniques of calibration.

Throughout a period of two years. The Heating Stage was calibrated once at the beginning of each year to check whether or not the performance of the heating stage had changed significantly.

The calibration was done with pure inorganic and organic chemical standards with known melting points. The melting points of these chemicals are as follows:-

Chemicals	Melting Points.
Azobenzol	68°c
Benzil	95°c
Acetanilid	115°c
Salophen	190°c
Dicyandiamid	210°c
$K_2Cr_2O_7$	394°c
$BaNO_3$	593°c

The standards in the form of grains or chips were placed on the sapphire disc and subjected to slow (≈ 5^{o}/min) progressive heating until they melted. The temperature of melting was taken as the temperature at which the standard was just about completely melted. For each standard, three replicate determinations of the melting point were made. A similar procedure was repeated for all the standards. During the second run they were melted on top of a parallel sided polished quartz plate of known thickness which was placed on top of the sapphire disc in order to determine the vertical thermal gradient within the quartz plate and the variation with temperature. Experience has shown that the inconsistent thickness and size of the chips of the standards used can give inconsistent melting points and thus it is advisable to use chips or grains of closely similar size and thickness.

The parallel sided doubly polished quartz plates used in the first and second calibrations have a thickness of 0.505mm and 0.37mm respectively. During these two calibrations, the cold junction of the thermocouple was equilibrated with the room temperature which was recorded. At the first calibration the heating stage was zeroed at 'measured' whereas at the second calibration the stage was zero at 'short'.

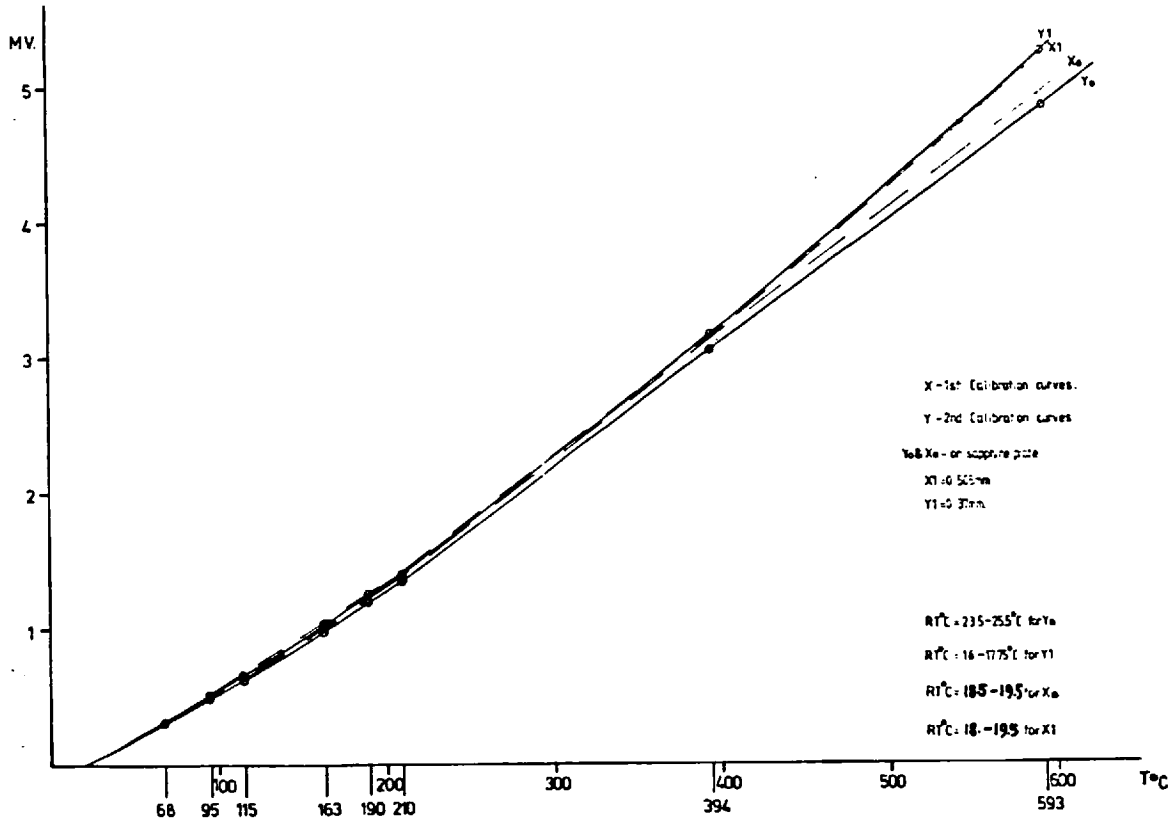

Fig.58. shows the calibration curves for the Leitz 1350 heating stage.

The calibration curves for the two calibrations are shown in Fig. 58. From this figure it is clear that the vertical thermal gradient within the quartz plate increases towards the higher end of the temperature range.

The determinable sources of error associated with the use of the Leitz 1350 Heating Stage were:-

1. Reproducibility of melting points and

2. Vertical thermal gradient in a sample plate.

The total errors for the heating stage at the first calibration were $\pm 4^{o}c$ for 100^{o}-$200^{o}c$, $\pm 13^{o}c$ for 300^{o}-$400^{o}c$ and $\pm 33.5^{o}c$ for temperatures around $593^{o}c$. The total error for the heating stage at the second calibration were $\pm 6^{o}c$ for 100^{o}-$200^{o}c$, $\pm 14^{o}c$ for 300^{o}-$400^{o}c$ and $\pm 44^{o}c$ for temperatures around $593^{o}c$. From the above data it is evident that the heating stage has changed its performance after a duration of one year.

<u>The system of temperature recording</u>.

The temperatures in the heater chamber were measured by a Pt(100%)/Rh(13%), Pt(87%) thermocouple which was metal joined to form a unit with the metal support of

the sapphire disc. The thermocouple had a common junction, (The Hot Junction), at which the conductors were in good thermal and electrical contact; this junction was located within the heating cartridge. The The "Cold Junctions" of the thermocouple at the opposite ends were maintained either at the room temperature as in this study or at $0^{o}c$ in ice water. When heat was supplied to the 'Hot Junction' by the heating cartridge, a temperature difference existed between the 'Hot Junction' and the 'Cold Junctions' and consequently an electro-motive force (EMF) was generated. Thus the magnitude of this EMF was dependent on the temperature difference between the "Cold Junctions" and the 'Hot Junction'. This EMF was recorded as millivolts (mv) on a moving chart recorder, (Hokushin) on which the chart speed was set at 120mm/min. This chart speed was chosen so that there would be minimum error in the recording of homogenisation temperature and other thermal events.

APPENDIX II.

The Freezing Stage.

Instrumentation.

The freezing stage is composed of four main elements. These are:

1. A short abestos cylinder within which sits a centrally holed gas chamber whose bottom was sealed by a glass slide.

2. An alcohol filled transparent freezing cell.

3. A copper-constantan thermocouple with a copper welded end and finally

4. A top abestos lid with a glass window.

The techniques for the calibration of the Freezing Stage and the thermocouple-thermometer system.

The Freezing Stage was calibrated with organic liquids of known freezing points. These standards and their freezing points are as follows:

Tetraclecane	(+5.86°c)
Water	(0°c)
Tridecane	(-5.5°c)
n-Dodecane	(-9.6°c)
Decane	(-29.7°c)

These liquid standards were sucked into closed end thin capillary tubes of 0.3mm in diameter and about 2 - 3mm long. The filled capillary tubes, one at a time, were placed in an alcohol filled transparent freezing cell and then subjected to cooling until frozen totally using cold oxygen free Nitrogen gas which has been previously through a copper coil submersed in very cold alcohol bath, (as low as -100°c has been recorded for this alcohol, (Personal communication, Rankin, 1976)). After being frozen, the standards were allowed to thaw slowly by increasing the temperature at the rate of 0.05 to 0.2°c/min until their freezing points were achieved. The freezing point was taken as the temperature at which the last crystal was completely

melted. The determination of freezing point was done in triplicate for each standard and the results were plotted to give the calibration curve shown in Fig. One disadvantage of using the alcohol filled cell was the problem of leakage of alcohol and its associated bubble formation inside the cell which has interferred the optical observation of the standards. The problem was overcome by putting another glass slide on top of the first one to improve the contact between the slide and the rim of the freezing cell. Another problem which arose during the use of this freezing stage was misting and condensation on the viewing window, but this was overcome by directing a stream of oxygen free N_2 gas onto the window.

The error involved in this measurement for a temperature range from $0^{o}c$ to $-10^{o}c$ is $\pm$ $0.2^{o}c$.

The thermocouple-thermometer system was calibrated with ice and warm waters of wide ranging temperatures. These temperatures were determined by two mercury thermometers. The result of this calibration has shown that the thermocouple-thermometer system was giving temperatures $2.5^{o}c$ in excess of the temperatures given by the mercury thermometers.

The system of temperature recording.

The temperature measurement was done using a Copper (100%)-Constantan (Ni. 40%, Cu. 60%) thermocouple which was connected to a direct reading digital thermometer, (Comark 5000), from which temperatures were read off directly.

APPENDIX III.

Preparations of minerals and solutions for chemical analysis.

Sample preparations of Cassiterites.

Cleaned cassiterites were separated and further concentrated and cleaned by a combination of methods using heavy liquid, (Tetrabromoethane Sg. 2.96), Cold HF treatment and hand picking. The HF treatment was used to remove coatings and veinlets of chlorite from the Pahang Consolidated Mines Limited 's Cassiterites. Alluvial/Collovial cassiterites (e.g. those from the mines of Foong Seong, Chenderiang Tin, Gopeng, Ayer Hitam and Sungei Besi) were cleaned with hot aqua regia solution to remove Fe Oxide coatings and metallic sulphides from their surfaces. Clean cassiterite concentrates were temaed to powder with an agate Tema Mill.

Sample preparations for Chlorites and Granites.

Green Ferroan Chlorites from P.C.C.L. were concentrated by conventional use of heavy liquids (TBE) followed by magnetic separation at 0.25 ampere.

Ten Gakak granite samples were jaw crushed and then

homogenised and quartered before being reduced to using agate tema.

For Nb, Ta and Sn amalyses, powder pellets were prepared from the temaed powder for x-ray flourescence analysis.

Techniques used in the preparation of solutions for the Plasma D.R.S. analysis of cassiterites.

A sample weight of 0.25g was placed in a teflon bomb to which was also added 5 ml of HI solution. The sample was allowed to decompose at 150^{o}c for four hours. The residue was dissolved in 6m HCl and then diluted to 25 ml with 6 m HCl.

Techniques used in the preparation of solutions for the Plasma D-R.s analysis of granites and chlorites.

A sample weight of 0.5g was placed in a teflon beaker to which was also added a total of 5ml of 40% HF solution, 5 ml of HNO_3 and 2ml of $HClO_4$. This mixture was evaporated down to dryness and the residue was then dissolved in 1m HCl. This solution was warmed until it became clear which is indicature of the complete dissolution of the residue. The clear solution was transferred to a 25ml volumetric flask and then topped up to the 25ml mark with 1 molar HCl.

APPENDIX IV.

Plasma Direct-Reading Spectrometry.

Previous Work.

Babat in 1946 pioneered the investigation into inductively coupled plasma as a result of which he published a paper on electrodeless discharges in high-frequency magnetic fields. This work was followed by Reed's pioneering work, (1961), in the field of high-frequency plasma generation. Such inductively coupled plasmas were first used as excitation sources for trace metal analyses by Greenfield et. al., (1964); shortly afterwards in 1965 Wendt and Fassell reported their independent studies using the plasma.

Instrumentation and methods.

(i) A.H.F. Plasma torch and direct reading spectrometer.

The plasma-direct reading spectrometer was composed of three main units:-

(a) The plasma torch.

(b) The nebulizer and

(c) The Spectrometer, (See Fig. 59 for a

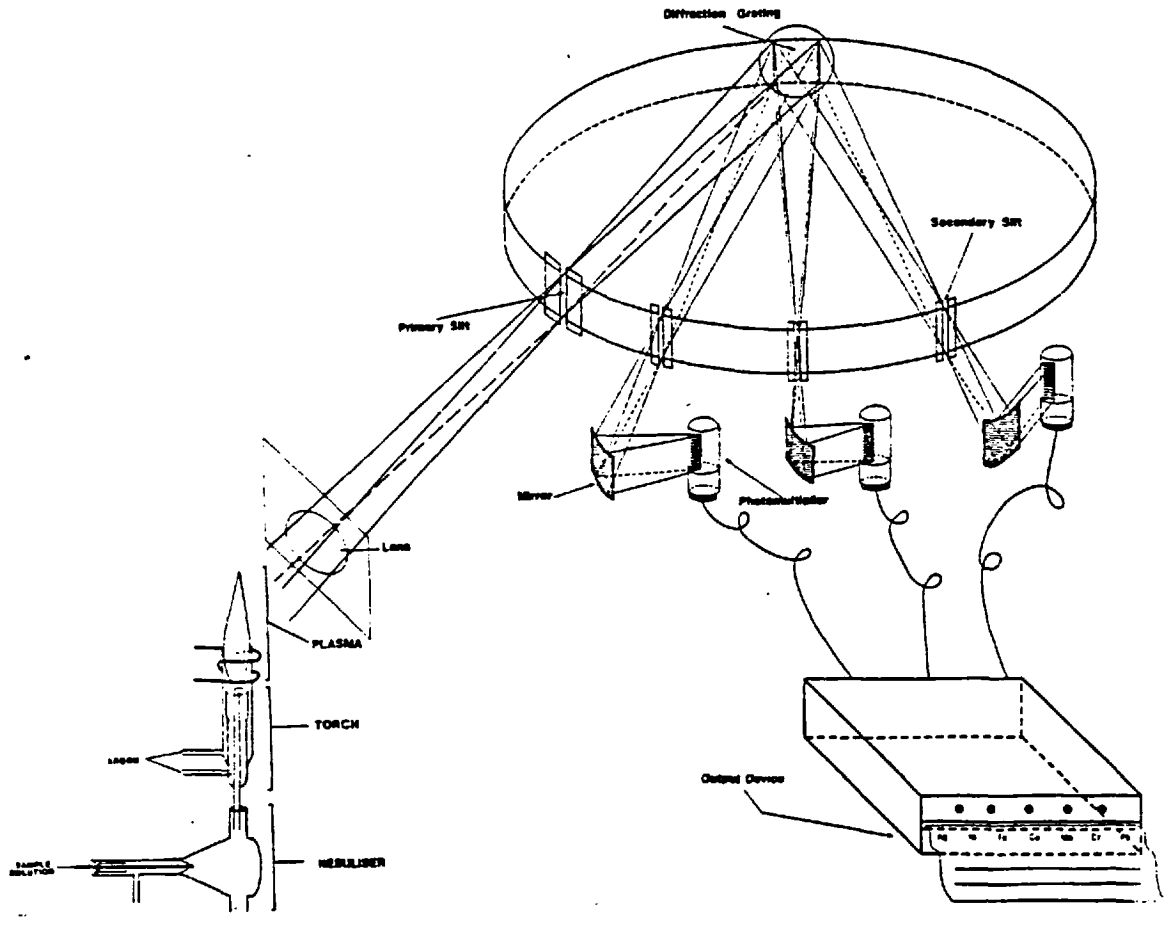

Figure 59. Schmatic diagram of the Plasma-Direct Reading Spectrometer.

diagramatic section of this plasma-direct reading spectrometer).

The Plasma Torch.

The torch consisted of three concentric tubes. The outer tubes were made from silica and were used to contain the plasma. The inner tube was made of borosilicate glass and was used to inject sample aerosol through the plasma once it has been formed. The top of the torch was concentric with the work-coil of the h.f. generator, (Raydyne R5OP).

Argon gas was fed tangentially into the central silica tube at 15ℓ/min^{-1} the h.f. field was applied by the work -coil and some free electrons were produced by a Telsa Coil. Once the gas was ionized and so made conducting, a current was induced and a plasma formed. 2.7kw was supplied to the coil to generate a plasma.

A hole was then punched through the flattened base of the plasma by introduction, through the injector, of a sample aerosol in argon gas at the rate of 0.7ℓ/min^{-1} at 25 psi with a Meinhard type pnumatic nebuliser. The aerosol entering the torch passed through a tunnel of plasma and consequently a long tail-flame was formed; it was this tail-flame which was used as a spectroscopic source.

The Spectrometer.

The direct-reading spectrometer used was the ARL 29000 B. This used a concave grating of 3-m radius and gave a dispersion of 0.173mm A^{-1} in the first order. Radiation from the source was focused on the entrance slit and then reflected by a plane mirror on the grating. The different wavelengths in the resulting spectrum were focussed at different points on a circle where a series of exit slits passed the wavelengths of interest. The radiation transmitted by an exit slit was focussed by a concave mirror to fall, after reflection by a plane mirror, on the cathode of a photomultiplier. There were thirty slits and photomultipliers.

When radiation strikes the photomultiplier, a current is set up proportional to the intensity of the radiation. The current from each photomultiplier charged a condenser for the duration of each exposure so that the resultant voltages on the condensers provide a measures of the integrated intensities.

Limits of detection.

One of the great advantages of the Plasma/D-R/ Spectrometry was the ability to detect a very low concentration of elements in the PPb range, either in

Elements detected in Cassiterite	Detection limit (in ppm/%)	Elements detected in granites and chlorites	Detection limit (in ppm/%)
Li	13	Li	0.4
Na	<0.01%	Na	0.01%
Ca	<0.01%	Mg	< 0.01%
SR	1.1	Ca	< 0.01%
Ba	0.2	S_R	0.25
La	1.8	Ba	0.65
Ti	1.6	La	28
Zr	1.8	Ti	0.6
V	2	Zr	0.2
Cr	43	V	1.3
W	40	Cr	6
Mn	5	Mo	6
Fe	<0.01%	W	10
Co	13	Mn	5.4
Ni	40	Fe	0.02%
Cu	11	Co	3.7
Zn	2	Ni	34
Cd	10	Cu	2.2
Al	<0.01%	Zn	3.6
Sn	-	Cd	10
k	0.07%	Al	0.02%
		Pb	29
		K	<0.01%

Table 34 — Showing the detectron limits of minor and trace elements in cassiterites, granites and chlorites.

Bulk or micro samples with the proviso that optimal operating conditions for each element were fulfilled. The detection limit was calculated as twice the standard deviation of the background intensities given by replicate readings of the blank. The limits of detection for the trace elements of cassiterites granites and chlorites are listed in Table 34.

BIBLIOGRAPHY.

Ahrens, L. H., 1948. "Evidence of geological age against decay of tin-115 to indium-115 by election capture". Nature, no. 4115, September 11, p.413-414.

Alderton, D. H. M., 1977. "The geochemistry of mineralisation at Pendarves and other Cornish areas". Unpublished Ph.D. thesis, King's College, University of London.

Alexander, J. B., Harral, G. M. and Flinter, B. H., 1964. "1903-1963, Chemical analyses of Malayan rocks, commercial ores and alluvial mineral concentrates". Malaysian Ministry of Lands and Mines, Prof. papers, E-64, pp. 295.

Ang., N. G., 1974. "The geology of Gakak Lode, P.C.C.L". B.Sc. Honours thesis, Department of Geology, University of Malaya.

Angus, J., Halls, C., Sillitoe, R. H., Meave, J., and Suarez, L., 1977. "The petrochemical characterisation of the eruptives in the subvolcanic province of the Bolivian Tin Belt: Comparative aspects and implications for exploration". Proceedings of the International Tin Symposium, La Paz. November 1978, (in press).

Askins, P. W., 1975. "Wrigglite, an unusual flourite bearing skarn, Mt. Garnet region, North Queensland, Australia". Unpublished M.Sc. thesis, James Cook University of North Queensland, Australia.

Barsukov, V. L., 1957. "The geochemistry of tin". "Geochemistry", no. 1, pp. 41-52.

Barsukov, V. L., and Kurichikova, G. Ye., 1966. "On the forms in which tin is transported in the hydrothermal solutions". "Geochemical International", vol. 3, no. 4, pp. 759-764.

Bean, J. H., 1969. "Iron-ore deposits of West Malaysia". Geological Survey of Western Malaysia, Economic Survey, vol. 2, p. 194.

Bean, J. H., 1976. "Iron ore deposits of Ulu Rompin, Malaysia". Unpublished Ph.D. thesis., University of Durnham, (Abstract in "Trans. Instn. Min. Metall, 85B, B305).

Le Bel, L., 1976. "Note preliminaire sur la mineralogie des phases solides contenues dans les inclusions des phenocristaux de quartz du porphyre cuprifere de Cerro Verde/Santa Rosa, Sud Perou". Bull. Soc. vaud. Sc. NAT., vol. 73, no. 350, pp. 1-8.

Beus, A. A. and Sitnin, A. A., 1968. "Geochemical specialization of magmatic complexes as criteria for the exploration of hidden deposits". 23rd Int. Geol. Cong, 6, pp. 101-105.

Boldyrev, A. M., 1941. "Zavismest morfologicheskikh fizicheskikh: khimichiskikh. Svoistv kassiterita at ego genezisa". Tr. Inst. Geol. Nauk. A.N.S.S.S.R. Vyp., 54. Min-geokhim. Seriya, 12.

Bond, A. F., and Andrus, J., 1952. "Structural imperfections in quartz crystals". Am. Mineral., v. 37, pp. 622-632.

Borovick, S. A. and Gotman, J. D., 1939. "Content of rare and other elements in the cassiterites of different genesis from U.S.S.R.". Compt. Rend. Acad. Sci., U.R.S.S., vol. 23, p. 351.

Bowden, P., 1966. "Li in Younger Granites of Northern Nigeria". Geochim. et Cosmochim Acta., vol. 30, no. 1, pp. 555-564.

Bowden, P., 1970. "Origin of the Younger Granites of Northern Nigeria". Contr. Miner. and Pet., vol. 25, pp. 153-162.

Boyarskaya, R. V., 1973. "Advantages of electron microscopy in studying fluid inclusions in minerals". (abs.). Regional Meeting of Thermobarogeochemistry of Mineral-forming Processes, 4th, Rostov-on-Don, September 24th - 30th, 1973, Rostov. Univ. Press, pp. 320-321.

Brammall, A. and Harwood, H. F., 1932. "The Dartmoor granites: their genetic relationships". Quart. Journ. Geol. Soc., vol. IXXX, viii, pp. 171-237.

Breithaupt, O. A., 1872. "Mineralogische Notizen". Neues Jahrb. Min., p. 814.

Brewer, F. M. and Baker, E., 1936. "Arc spectrographic determination of indium in minerals, and the association of indium with tin and silver". Jour. Chem. Soc. London, pp. 1286-1290.

Brindley, G. W., 1961. "Chlorite Minerals" in "The x-ray identification and crystal structures of clay minerals". Chapter VI. Edited by G. Brown. Mineralogical Society, (Clay Minerals Group), London.

Brown, J. C., 1934. "Lagerstattliche und Erzmikroskopische Untersuchung der Zinnerzgange der East Pool Mine bei Redruth in Cornwall". Neues Jb. Beil-Bd. Abt. H.2., pp. 298-336.

Brody, S. S., 1953. "A study of the surface structure of quartz crystals". Signal Corps Eng. Lab., Fort Monmouth, N.J. Eng. Rept. E-1133.

Buckley, E. N., 1951. "Crystal Growth". Wiley, New York, 571 p.

Burton, C. K., 1959. "Tin-iron deposits, Pelapah Kanan, Johore". Unpublished report of the Malaysian Geological Survey. Ref. no. GS:59/F/042/23.

Butler, J. R., Bowden, P. and Smith, A. Z., 1962. "K/Rb ratios in the evolution of the Younger Granites of Northern Nigeria". Geochim. et. Cosmochim. Acta, vol. 26, pp. 90-100.

Cameron, E. N., Rowe, R. B. and Weis, P. L., 1953. "Fluid inclusions in beryl and quartz from pegmatites of the Middletown district, Connecticut". Amer. Mineral., vol. 38, pp. 218-262.

Cann, J. R., 1970. "Upward movement granite magma". Geol. Mag., 107, pp. 335-340.

Carmichael, Ian, S. E., Turner, F. J. and Verhoogen, J., 1974. "Igneous Petrology". McGraw-Hill International Series in the Earth and Planetary Sciences. McGraw-Hill, New York, 739 p.

Carslaw, H. S. and Jaeger, J. C., 1959. "Conduction of heat in solids". Clarendon Press, Oxford. Second Edition. 510p.

Chappell, B. W. and White, A. J. R., 1974. "Two contrasting granite types". Pacific Geology, vol. 8, pp. 173-174.

Cherdynstev, V. V. and Kozak, L. V., 1949. "Sources of excess helium in some minerals". Dokl. Akad. Nauk. S.S.S.R., vol. 69, pp. 829-832.

Clark, A. M., Fejer, E. E., Donaldson, J. D. and Silver, J, 1976. "The ^{119}Sn Mossbauer spectra, cell dimensions and minor element contents of some cassiterites". Mineralogical Magazine, vol. 40, December, pp. 895-898.

Correns, C. W., 1940. "Die chemische Verwitterung der Silikate". Naturwissenschaften, vol. 28, pp. 369-376.

Coveney, R. M. and Kelly, W. C., 1971. "Dawsonite as a daughter mineral in hydrothermal fluid inclusions". Contr. Mineralogy Petrology, vol. 32, pp. 334-342.

Czamanske, G. K., Roedder, E. and Burns, F. C., 1963. "Neutron activation analysis of fluid inclusions for copper, manganese and zinc". Science, vol. 140, pp. 401-403.

Dana, E. S., 1888. Art XXXII. "Preliminary notice of Beryllonite". Am. J. Sci. vol. 36, pp. 290-291.

Dana, J. D. and Dana, E. S., 1951. "Dana's System of Mineralogy". 7th Edition by Palache, C., Berman, H. and Frondel, C. (Harvard University), John Wiley and Sons, Inc., (New York); Chapman and Hall Limited, (London), vol. II, 1124 p.

Dana, E. S. and Wells, H. L., 1889. Art II. "Description of the new mineral, Beryllonite". Am. J. Sci. vol. 37, pp. 23-32.

Davy, Sir Humphry, 1822. "On the state of water and deriform matter in cavities found in certain crystals". Roy. Soc. Lond. Phil. Trans., pt. 2, pp. 367-376.

Deer, W. A., Howie, R. A. and Zussman, J., 1962. "Rock-forming minerals". Sheet Silicates, vol. 3, Longmans, 270 p.

Deer, W. A., Howie, R. A. and Zussman, R. A., 1967. "Rock-forming minerals". vol. I-V. London, Longmans.

Deicha, Georges, 1973. "Scanning electron microscopy of cavities in gangue and rock minerals (abs.)". Soc. francaise Mineralalogie Cristallographic Bull., vol. 96, no. 4-5, pp. X-IX.

Dekeyser, 1931, (See Venugopal, 1952).

Dolgov, Yu, A., 1968. "Pressure and temperature in the process of formation chambered pegmatites". Doklady Akad, Nauk S.S.S.R., vol. 178, no. 5, pp. 1171-1174.

Donaldson, J. D., Silver, J. Haljiminolis, S and Ross, S. D., 1975. "Effects of the presence of valence-shell non-bonding electron pairs on the properties and structures of Caesium tin (11) bromides and of related antimony and tellurium compounds". Jour. Chem. Soc., Dalton Trans., pp. 1500-1506.

Dudykina, K. Y., 1959, "Paragenetic associations of element-admixtures in cassiterites of different genetic types of tin-ore deposits". Akad. Nauk. S.S.S.R., vol. 28, pp. 111-121.

Durisova, J., 1978. "Geothermometry in the minerals from the tin deposits of the eastern Krusne hory Mountains, (Czechoslavakia). I.G.C.P. Symposium, M.A.W.A.M., vol. 3, pp. 325-335.

Eberhard, G., 1908. "Uber die weite Verbreitung des Skandium auf der Erde, I. Sitzber. Kgl. Preuss. Akad. Wiss. p. 851.

Eberhard, G., 1910. "Uber die weite Verbreitung des Skandium auf der Erde, II". Ibid. p. 404.

Edwards, A. B. and Gaskin, A. J., 1949. "Ore and granitization". Econ. Geol. vol. 44, pp. 234-241.

Edwards, A. B., 1954. "Textures of the ore minerals and their significance". Australasian Inst. Min. Metall., Melbourne, 242p.

Erametsa, O., 1938. "On the distribution of indium in Finnish minerals and its association with other metals". Ann. Acad. Sci. Fennicae., Ser. A. 51., No. 1.

Fesser, von. H., 1968. "Spurenelemente in bolivianischen Zinnsteinen". Geol. Jb., vol. 85, pp. 605-610.

Fioletova, A. F., 1940. "The tantalo-niobates of the northern slope of the Twikestan range". Trans. Inst. Geol. Sci., Acad. Sci., U.S.S.R., no. 17, Min.-Geochem. Ser. no. 4, p. 33 (M.A. 3-430).

Fitch, F. H., 1952. "The geology and mineral resources of the neighbourhood of Kuantan, Pahang". Mem. Geol. Survey Dept., Fed., Malaya, 6, 144p.

Francis, M., 1979. Personal Communication.

Fuge, R. and Power, G. M., 1969. "Chlorine and fluorine in granitic rocks from S. W. England". Geochem. et Cosmochim. Acta., vol. 33, no. 7, pp. 888-893.

Fyfe, W. S., Price, N. J. and Thompson, A. B., 1978. "Fluids in the Earth's Crust". Elsevier, Amsterdam-Oxford-New York, 383p.

Ganesan, K., 1969. "Iron-tin mineralisation in the Gunong Muntahak area, Johore". Newsl. Geol. Soc. Malaysia, vol. 19, pp. 1-4.

Garnett, R. H. T., 1966. "Distribution of cassiterite in vein tin deposits". Trans. Inst. Min and Met., Appl. E. Sci., vol. 75, B245-273.

Garson, M. S., Mitchell, A. H. G., Bateson, J. H., Cooger, N., Jantaranipa, W., Johnson, R. L., Prewett, W. G., Rasrikriangrai, P and Stephens, E. A., 1975. "The geology of the tin belt in Penisular Thailand around Phuket, Phangnga and TakuaPa". I.G.S. Overseas Memoir No. 1. 112p.

Ghosh, P. K., 1934. "The Carnmenellis granite: its petrology, metamorphism and tectonics". Quart. Jour. Geol. Soc. XC. pp. 240-276.

Gmelin, L., 1959. "Handbuch der anorganischen Chemie". Flour Erganzungsband, 8, Auflage, Weinheim: Verlag Chemie, GmbH.

Goguel, R., 1963. "Die chemische Zusammensetzung der in den Mineralen einiger Granite und ihrer Pegmatite eingeschlossenen Gase und Flussigkeiten". Geochim. et. Cosmochim. Acta., vol. 27, pp. 155-181.

Goldschmidt, V. M. and Horman, 1937. "Geochemische verteilungsgesetze der elemente". IX. Skrifter Norske Videnskaps-Akad., Oslo, I. Mat.-Naturv. Klasse, no. 4.

Goldschmidt, V. M. and Peters, C., 1931. "Zur geochemie des Skandiums. Nachr. Des. Wiss. Gottingen, Math.-Physik. Klasse, III; IV p. 257.

Goldschmidt, V. M. and Peters, C., 1932. "Zur geochemie der Edel-metalle". Ibid. Maths-Physik. Klasse III: 24; IV: 26. p. 377.

Goncharov, V. I and Vorontsova, L. A., 1976. "Temperatures of formation of some Yakutian tin deposits". Geochemistry International, vol. 13, no. 3, pp. 71-76.

Goncharov, V. I. and Vorontsova, L. A., 1976. "Hydrothermal-solution compositions for some Yakutia tin deposits". Geochemistry International, vol. 13, no. 5, pp. 27-33.

Gotman, Ya, D., 1941. "Tipomorfnye osobennosti kassiterita olovorudnykh mestorozhdenii, S.S.S.R.". Tr. Inst. Geol. Nauk. A.N., S.S.S.R. Vyp. 46. min ser., 9.

Gotman, Ya, D., and Rub, M. G., 1961. "Comparative characteristics of the tin bearing granitoids of bearing granitoids of different ages". Int. Geol. Review, pg. 878.

Grant, J. N. M., 1979. "A study of ore genesis and geochronology in the sub-volcanic tin belt of the Eastern Andes, Bolivia". Unpublished Ph.D. thesis. Imperial College, London.

Grant, J. N. M., Halls, C., Avila, W. and Avila, G.,1977. "Igneous geology and the evolution of hydrothermal systems in some sub-volcanic tin deposits of Bolivia". "Volcanic Processes in Ore Genesis". The I.M.M. and the Geol. Soc. Lond., pp. 117-126.

Grant, J. N. M., Halls, C., Avila, W. and Snelling, N. J., 1977. "Edades potassio-argon de las rocas igneous y la mineralization de parte de la Cordillera Oriental Bolivia".Boletin del Servicio Geologico de Bolivia. Serie A. vol. 1, no. 1. La Paz, Diciembre, pp. 33-60.

Greenfield, S., Jones, I. L. L., McD.Mcgeachin, H. and Smith, P. B., 1975. "Automatic multi-sample simultaneous multi-element analysis with a H.F: Plasma Torch and direct reading Spectrometer". Analytica Chimica Acta, vol. 74, pp. 225-245.

Groves, D. I., 1972. "The geochemical evolution of tin-bearing granites in the Blue Tier batholith, Tasmania". Econ. Geol., vol. 67, pp. 445-457.

Groves, D. I. and McCarthy, T. S., 1978. "Fractional crystallization and the origin of tin deposits in granitoids". Mineralium Deposita, vol. 13. pp. 11-26.

Groves, D. I. and Solomon, M., 1969. "Fluid inclusion studies at Mount Bischof, Tasmania". Trans. Inst. Min. Metall. vol. 78, Bull. no. 747. B1-B11.

Haapala, I., 1974. "Some petrological and geochemical characteristics of Rapakivi granite varieties associated with greisen-type Sn, Be and W mineralisation in the Eurajoki and Kymi Areas, Southern Finland". I.G.C.P. Symposium, M.A.W.A.M., vol. 1, p. 159-169.

Haapala, I, 1978. "Petrographic and geochemical characteristics of Rapakivi granite varieties associated with greiden-type Sn, Be and W mineralisations in the Eurajoki and Kymi areas, Southern Finland". I.G.C.P. Symposium, M.A.W.A.M., vol. 3, pp.217-225.

Hadding, von. Assar., 1922. "Uber das vorkommen des germanium im kassiterit". Z. anorg. allgem. chem. vol. 123, pp. 171-172.

Hass, J. L. Jr., 1971. "The effect of salinity on the maximum thermal gradient of a hydrothermal system

at hydrostatic pressure". Econ. Geol. vol. 66. pp. 940-946.

Hamaguchi, H and Kuroda, R., 1970. "Tin", in "Handbook of Geochemistry". vol. II-2. Springer-Verlag Inc., Berlin.

Harding, R. R. and Hawkes, J. R., 1971. "The Rb:Sr age and K/Rb ratios of samples from the St. Austell Granite, Cornwall". I.G.S. Report No. 71/6.

Harris, P. G., Kennedy, W. Q. and Scarfe, C. M., 1970. "Volcanism versus plutonism - the effect of chemical composition", in "Mechanism of Igneous Intrusion". Edited by G. Newall and N. Rast. pp. 187-200.

Hartley, W. N. and Ramage, H., 1897. "The wide dissemination of some of the rarer elements, and the mode of their association in common ores and minerals". Jour. Chem. Soc., vol. 71, pp. 533-547.

Hatch, F. H., Wells, A. K. and Wells, M. K., 1975. "Petrology of the igneous rocks". Thomas Murby and Co., London. 13th Edition, 551p.

Hesp, W. R., 1971. "Correlations between the tin content of granite rocks and their chemical and mineralogical composition". Geochem. Exploration Spec., vol. 11. Canadian Inst. Min. and Met., pp. 341-353.

Hey, M. H., 1954. "A new review of the chlorites". Min. Mag., vol. 30, 277p.

Hosking, K. F. G., 1965. "The search for tin". Min. Mag., London, vol. 113, Oct. pp. 261-273(8p); Nov. pp. 368-383(9p); Dec. pp. 448-461(8p).

Hosking, K. F. G., 1970. "The primary tin deposits of southeast Asia". Minerals Sci and Engng., vol. 2, no. 4, October, pp. 24-50.

Hosking, K. F. G., 1973a. "The primary tin mineralisation patterns of West Malaysia". Geol. Soc. Malaysia, Bulletin 6, July 1973, pp. 297-308.

Hosking, K. F. G., 1973b. "Primary mineral deposits". In "The Geology of the Malay Peninsula", edited by Gobbett, D. J. and Hutchison, C. S., (1973). Wiley-Interscience, pp. 335-390.

Hosking, K. F. G., Santokh Singh, D., Jaafar, A. and Yeap, C. H., 1975. "The granitic intrusives of peninsual Malaysan with special reference to their trace element content and their relationship to the primary tin deposits". Unpublished paper.

Hosking, K. F. G., 1976. "Personal Communication".

Hunter, D. R., 1973. "The localisation of tin mineralisation with reference to South Africa". "Minerals, Science and Engineering",vol.5, no.1,Jan.pp53-77.

Hutchison, C. S., 1973a. "Tectonic evolution of Sundaland: A Phanerozoic synthesis". Geol. Soc. Malaysia, Bulletin 6, July 1973. pp. 61-86.

Hutchison, C. S., 1973b. "Plutonic Activity". Chapter 8 in "Geology of the Malay Peninsula, West Malaysia and Singapore", edited by Gobbett, D. J. and Hutchison, C. S. John Wiley-Interscience, pp. 215-252.

Hutchison, C. S. and Snelling, N. J., 1971. "Age determination on the Bukit Paloh adamellite". Bull. Geol. Soc. Malaysia 4, pp. 97-100.

Hutchison, C. S. and Jeacocke, J. E., 1971. "FORTRAN IV computer programme for calculation of the Niggli molecular norm". Bull. Geol. Soc. Malaysia, vol. 4, pp. 91-95.

Ida, Walter and Noddack, 1931. See Venugopal, 1952.

Ingham, F. T. and Bradford, E. F., 1960. "The geology and mineral resources of the Kinta Valley, Perak". Mem. Geol. Survey Dept., Fed. Malaya, vol. 9, 347p.

Ishihara, S., 1977. "The magnetite series and ilmenite series granitic rocks". Mining Geology, vol. 27, pp. 293-305.

Ishihara, S. and Terashima, S., 1978. "Tin contents of granitic rocks in Japan and its environs". I.G.C.P. Symposium, M.A.W.A.M., vol. 3, pp. 227-234.

Ishihara, S., Sawata, H., Arpornsuwan, A., Busaracome, P and Bungbrakearti, N, 1978. "The magnetite-series and ilmenite-series granitoids and their bearing on tin mineralisation, particularly of the Malay Peninsual region". Annex to Warta Geologi, Vol. 4, no. 2, March-April, pp. 33-36.

Itsykon, M. I. and Russanov, A. K., 1946. "Scattered elements in cassiterite". Izvest. Akad. Nauk. S.S.S.R. Ser. Geol., vol. 5, pp. 119-130.

Ivanov, V. S. and Narnov, V. S., 1970. "On the behaviour of tin in the granitoid intrusives of Northeastern U.S.S.R.". Geochem. Int., vol. 7, p. 424-431.

Ivantishin, M. M., 1955. "Geolog. Zh".,vol. 15, no. 4.

Ivashentzov, A. G., 1945. "Tin minerals in the Maikhura skarn deposit, (Ghissar range)". Doklady Acad. Sci., U.R.S.S., vol. 47, p. 494.

Jaafar bin Ahmad, 1970. "The geology of the Benom Igneous Complex and its relationship to tin mineralisation in Malaya". Unpublished Ph.D. Thesis, University of Leeds.

Jaafar bin Ahmad., 1976. "Personal Communication".

Jackson, N. J., 1976. "The geology and mineralisation of the St. Just District, with particular reference to Levant Mine". Unpublished Ph.D. thesis, King's College, Univeristy of London.

Jahns,R. H., 1955. "The study of pegmatites". Econ. Geol., Fiftieth Anniversary Volume, pp. 1,025-1,130.

Jahns, R. H. and Burnham, C. W., 1969. "Experimental studies of pegmatite genesis: I. A model for the derivation and crystallization of granitic pegmatites". Econ. Geol., vol. 64, pp. 843-864.

Jacobson, R. R. E., Macleod, W. N. and Black, R., 1958. "Ring-complexes in the Younger Granites of Northern Nigeria". Geol. Soc., Lond. Mem. no. 1.

Jedwab, J., 1955. "Caracterisation spectrochimique des granites". Bull. Soc. Belge. Geol., vol. 64, pp. 526-534.

Jensen, B. B., 1973. "Patterns of trace elements partitioning". Geochim. et. Cosmochim, Acta., vol. 37, pp. 2,227-2,242,

Jones, W. R., 1925. "Tin fields of the world". Mining Publs., Lond., 423p.

Jones, M. P. and Ghani, M. M., 1969. "The mineralogy of the Sg. Besi decomposed stanniferous granite". "A Second Technical Conference on Tin". Bangkok, vol. II, pp. 549-558.

Kalyuzhnyy, V. A., 1958. "The study of the composition of minerals of poliphasal inclusions". Mineralog. Sb. L'vovsk. geol. obshch., no. 12, pp. 116-128.

Kalyuzhnyy, V. A. and Yorysh, Z. I., 1962. "Roentgenometric study of microquantities of minerals". Mineralog. Sb. L'vovsk. geol. obshch., no. 16, pp. 403-407.

Kelly, W. C. and Turneoure, F. S., 1970. "Mineralogy, Paragenesis and Geothermometry of tin and tungsten of the Eastern Andes, Bolivia". Econ. Geol., vol. 65, pp. 609-680.

Kennedy, G. C., 1950. "Pneumatolysis and the liquid inclusion method of geologic thermometryP. Econ. Geol., vol. 45, pp. 533-547.

Khaimov-Mal'kov, V. Ya., 1959. "The thermodynamics of crystallization pressure; experimental measurement of crystallization pressure and the growth of crystals in contact with large obstacles". In "Growth of Crystals, 2 - Interim Reports". Edited by Shubmikov, A. V. and Sheftal, N. N., (3-28 in English translation), New York, Consultant Bureau.

Klominsky, J. and Absolonova, E., 1974. "Geochemistry of the Karlovy Vary granite massif, (Czechoslavakia)". I.G.C.P. Symposium, M.A.W.A.M., vol. 1. pp. 189-196.

Kovalenko, N. I., 1977. "The reactions between granite and agueous hydrofluoric acid in relation to the origin of fluorine-bearing granites". Geochem. International, vol. 14, no. 2. pp. 108-118.

Kozlov, V. D., 1974. "The sequence of phases and facies in the massifs of rare-metal granites in Transbaikalia and the problem of their ore-bearing capacity". I.G.C.P. Symposium, M.A.W.A.M., vol. 1, pp. 201-205.

Kuno, H., 1966. "Lateral variation of basaltic magma type across continental margins and island arcs". Bull. Volcanologique, vol. 29 pp. 195-222.

Larionov, J. and Tolmacev, J. M., 1937. "On the chemical composition of cassiterites". Comptes Rendus (Doklady) de l' Academie des Sciences de l'U.R.S.S. vol. XIV, no. 5. pp. 303-306.

Lee, C.Y., 1971, "The geology and mineralisation of the Chenderiang Valley. B.Sc. Honours thesis, Department of Geology, Univeristy of Malaya.

Lemmlein, G. R., 1950. "Ratio of the present and the original volumes of liquid inclusions in minerals". Akad. Nauk. S.S.S.R., Doklady, vol. 72, pp. 775-778, (in Russian).

Lemmleyn, G. G., Kliya, M. O and Ostrovskiy, I. A., 1962. "On the conditions of the formation of minerals in pegmatites according to data of the study of primary inclusions in topaz". Doklady Akad. Nauk. S.S.S.R., vol. 142, no. 1. pp. 81-83.

Lim, T. H., 1971, (MS). "Geology, mineralization and geochemical studies in the Western Gambang area, Pahang, West Malaysia". B.Sc. Honours thesis, Department of Geology, Univeristy of Malaya.

Little, W. M. C., 1960. "Inclusions in cassiterite and associated minerals". Econ. Geol., vol. 55, pp. 485-509.

Lkhamsuren, Zh., 1970. V sb.:"Materialy nauchn. konfer. posvyashchennoy XXX-letiyu geol. sluzhby MNR". In "Proc. of Scientific Conference Honoring 30th Anniversary of Geological Survey of Mongolian People's Republic". Ulan-Bator.

Lokka, L., 1943, see Gmelin, 1959.

McCulloch, D. S., 1959. "Vacuole disappearance temperatures of laboratory-grown hopper halite crystals". J. Geophy. Res., vol. 64, no. 7, pp. 849-854.

Metzger, F. W., Kelly, W. C., Nesbitt, B. E. and Essene, E. J., 1977. "Scanning electron microscopy

of daughter minerals in fluid inclusions". Econ. Geol., vol. 72, no. 2, March-April, pp. 141-152.

Moh, G. H., 1974. "Stannite solid solution and exsolution phenomena". I.G.C.P. Symposium, M.A.W.A.M., vol. 1, pp. 278-279.

Moore, P. B., 1973. "Pegmatite phosphates: Descriptive mineralogy and crystal chemistry". The Mineral Record, vol. 4, no. 3, pp. 103-130.

Morey, G. W., 1922. "The development of pressure in magmas as a result of crystallization". Washington Acad. Sci. Jour., vol. 12, pp. 219-230.

Morey, G. W., 1924. "Relation of crystallization to the water content and vapour pressure of water in a cooling magma". Jour. Geol., vol. 32, pp. 291-295.

Motorina, I. V., 1967. "Multiphase inclusions in topazes from the pegmatites of volynia". Doklady of the Academy of Sciences, U. S.S.R., vol. 175, nos. 1-6, pp. 135-137.

Murray, R. C., 1957. "Hydrocarbon fluid inclusions in quartz". Am. Assoc. Petrol. Geol. Bull., vol. 41, pp. 950-956.

Naumov, V. B., Kovalenko, V. I., Ivanova, G. F. and Vladykin, N. V., 1977. "Genesis of topaz according to the data on microinclusions". Geochemistry International. Vol. 14, no. 2, pp. 1-8.

Niggli, P., 1937. "Das magma und deine produkte unter besonderer beriichsichtigung des einflusses der leichfluchtigen bestandteile". I. Teil., Physikalisch-Chemische grundlagen. Leipzig, Akademische Verlagsgesellschaft M. B. H., 379p.

Pahang Consolidated Company Limited, 1966. "A history of the Pahang Consolidated Company Limited, 1906-1966". Pahang Consolidated Company Limited, 70p.

Pan, Y. S. and Ympa, P. J. M., 1973. "The Mexican type tin deposits - its occurrence, chemistry and physical

conditions of deposition. (Abstract). "Fluid Inclusion Research, Proc. of COFFI", vol. 6, pp. 117-118.

Papish, J., Brewer, F. M. and Holt, D. A., 1927. " "Germanium. XXV. Arc Spectrographic detection and estimation of germanium. Occurrence of germanium in certain tin minerals". Enargite as a possible source of germanium". Jour. Amer. Chem. Soc., vol. 49, pp. 3,028-3,033.

Pavlishin, V. I., Voznyak, D. K. and Melnikov, V. S., 1968. "Syngenetic inclusions of micas in topazes from Ukrainian pegmatites". Mineralog. Sb. L'vovsk. geol. obshch., vol. 22, no. 2, pp. 175-177.

Pearce, J. A. and Gale, G. H., 1977. "Identification of ore-deposition environment from trace-element geochemistry of associated igneous host rocks", in "Volcanic processes in ore genesis". The Inst. Min. and Met. and The Geol. Soc. of London, pp. 14-24.

Pecora, W. T., Switser, G., Barbosa, A. L. and Myers, A. T., 1950. "Structure and mineralogy of the Golconda pegmatite, Minas Gerais, Brazil". Amer. Mineral., vol. 35, pp. 889-901.

Pehrman, G., 1945. "Die Granitpegmatite von kimito, (S. W. Finland), und ihre minerale". Acta Acad. Aboensis, Math. Phys., vol. 15, no. 2, (M. A. pp. 9-202).

Pongsapich and Mahawa, 1977, see Ishihara et. al., 1978b.

Potter, R. W. II, 1977. "Pressure corrections for fluid-inclusion homogenization temperatures based on the volumetric properties of the system NaCl-H_2O". J. Research U. S. Geol. Sur. vol. 5, Sept-Oct., pp. 603-607.

Poty, B. P., Stalder, H. A. and Weisbrod, A. M., 1974. "Fluid inclusions studies in quartz from fissures of Western and Central Alps". Schweiz. Min. Petr. Mitt., vol. 54, 2/3, pp. 717-752.

Preisinger, A. and Huber, W., 1964. "Zur Bestimmung Kleinster Gaseinschlusse in Feldspaten (Abstract)". Fortschritte d. Mineralogie., vol. 41, p. 183.

Price, N. J., 1966. "Fault and joint development in brittle and semi-brittle rock". Pergamon Press, 176p.

Prokopenko, N. M., 1941. "Indium in cassiterite, (Transbaikalia):Compt. Rend. (DoKl) Acad. Sci. U.R.S.S., vol. 31.

Pryor, E. J. and Wrobel, S. A., 1951. "Studies in cassiterite flotation". Trans. Inst. Min and Met., vol. 60, no. 532, pp. 202-206.

Pun, V. T. and Singh, J., 1978. "Geology and mineralisation of Sg. Lembing tin deposits". Annex to Warta Geologi, vol. 4, no. 2, March-April, pp. 7-8.

Quensel, P., 1956. "The paragenesis of the Varutrask pegmatite". Arkiv fur Mineral. Och Geol., vol. 2, pp. 9-125.

Ramdohr, P., 1956. "The paragenesis of the Varutrask pegmatite". Arkiv fur Mineral. Och Geol., vol. 2, pp. 9-125.

Ramdohr, P., 1969. "The ore minerals and their intergrowths". Pergamon, Oxford, 1174p.

Rankama, K., 1944. "On the chemistry of tantalum". Bull. Comm. Geol. Finlande, no. 133.

Rankin, A. H., 1973. "Fluid inclusion studies in Apatite from some East African Carbonatites and inolites". Unpublished Ph.D. thesis, University of Leicester.

Rankin, A. H., 1976. "Personal Communication".

Rankin, A. H., 1978. "Course Notes for the User School on Fluid Inclusion Equipment and Mehtods". Applied Mineralogy Group, Mineralogical Society, London, U. K.

Reed, T. B., 1961. "Induction-coupled Plasma Torch". J. Appl. Phys., vol. 32, pp. 821-824.

Rattigan, J. H., 1964. "Geochemical characteristics

of Australian granitic rocks in relation to the occurrence of tin". Unpublished Ph.D. Thesis, Univ. of New South Wales.

Richter, D. H. and Ingerson, Earl, 1954. "Some considerations regarding liquid inclusions as geolo ic thermometers. Econ. Geol., vol. 49, pp. 786-789.

Roe, F. W., 1941. "Visit to Pelapah Kanan Mines, Johore".(GS:61/41). Unpublished report of the Malaysian Geological Survey.

Roedder, E., 1958. "Technique for the extraction and partial chemical analysis of fluid-filled inclusions from minerals". Econ. Geol., vol. 53, pp. 235-269.

Roedder, E., 1960. "Fluid inclusions as samples of the ore-forming fluids". Int. Geol. Congress, XXI Session, Norden, XVI., Genetic Problems of Ores, Copenhagen, pp. 218-229.

Roedder, E., 1962. "Studies of fluid inclusions, I-low temperature application of a dual purpose freezing and heating stage". Econ. Geol., vol. 57, pp. 1,045-1,061.

Roedder, E., 1963. "Studies of fluid inclusions, II. Freezing data and their interpretation". Econ. Geol., vol. 58, pp. 167-211.

Roedder, E., 1967. "Fluid inclusions as samples of ore fluids". In "Geochemistry of hydrothermal ore deposits". Ed. Barnes, H. L., Holt, Rinehart and Winston, Inc., New York. pp. 515-574.

Roedder, E., 1971. "Fluid inclusion studies on the porphyry type ore deposits at Bingham, Utah, Butte, Montana and Climax, Colorado". Econ. Geol., vol. 66, pp. 98-120.

Roedder, E., 1971. "Metastability in fluid inclusions". Soc. Mining Geol. Japan, Spec. Issue 3, pp. 327-334.

Roedder, E., 1972. "The composition of fluid inclusions", in "Data of geochemistry", Chapter JJ, sixth edition, ed. Fleischer, M. U.S. Geol. Surv.

Prof. Paper 440 JJ, 164p.

Roedder, E., 1978. "Origin and significance of magmatic inclusions". Session d'Automme De la Societe Francaise de mineralogie et cristallographie. Programme et resumes des communications. Nancy, p. 40.

Roedder, E. and Skinner, B. J., 1968. "Experimental evidence that fluid inclusions do not leak". Econ. Geol., 63, pp. 715-730.

Rutter, E. H., 1970. "An experimental study of the factors affecting the rheological properties of rock in simulated geological environments". Unpublished Ph.D. thesis. Imperial College, University of London.

Schlita, P. J., 1968. "Growth deformation and defect structure of salt crystals". Geol. Soc. Am. Spec. Paper, (in press).

Schneider, H. J., Dulski, P., Luck, J., Moller, P. and Villalpando, A., 1978. "Correlation of trace element distribution in cassiterites and geotectonic position of their deposits in Bolivia". Mineral Deposita, (Berl.), vol. 13, pp. 119-122.

Scholz, C. H., Sykes, L. R. and Aggarway, Y. P., 1973. "Earthquake prediction: a physical basis". Science, vol. 181, pp. 803-810.

Scrivenor, J. B., 1931. "The geology of Malaya". Macmillan, London, 217p.

Seraphim, R. H., 1951. "Some aspects of the geochemistry of fluorine". Thesis. Mass. Inst. of Techn.

Sheftal, N. N., 1957, "Real crystal formation" in "Growth of Crystals, 1 - Reports of the First Conference on Crystal Growth", edited by Shubnikov, A. V. and Sheftla, N. N., pp. 5-27. In English translation, 1959, Consultant Bureau, New York.

Sibson, R. H., Moore, J. Mc.M. and Rankin, A. H., 1975. "Seismic pumping - a hydrothermal fluid transport mechanism". Journ. Geol. Soc., vol. 131, pp. 653-659.

Sillitoe, R. H., 1974. "Tin mineralisation above mantle hot spots". Nature, April, vol. 248, no. 5448, pp. 497-499.

Skinner, B. J., 1953. "Some considerations regarding liquid inclusions as geologic thermometers". Econ. Geol., vol. 48, pp. 541-550.

Smith, F. G., 1948. "Transport and deposition of the non-sulphide vein materials. III, "Phase relations at the pegmatitic stage". Econ. Geol., vol. 43, pp. 535-546.

Smith, F. G., 1954. "Composition of vein-forming fluids from inclusion data". Econ. Geol., vol. 49, pp. 205-210.

Smith,C.W.E.H.,1967. "An unpublished report of the Pahang Consolidated Company Limited. 64p.

Snelling, N. J., 1974. Personal Communication".

Snelling, N. J., Bignell, J. D. and Harding, R. R., 1968. "Ages of Malayan granites". Geol. en Mijnb., vol. 47, pp. 358-359.

Sorby, H. C., 1858. "On the microscopic structure of crystals, indicating the origin of minerals and rocks". Geol. Soc. Lond. Quart. Jour., vol. 14, pt. 1, pp. 453-500.

Sourirajan, S and Kennedy, G. C., 1962. "The system H_2O-NaCl at elevated temperatures and pressures". Am. Jour. Sci., vol. 260, pp. 115-141.

Suensilpong, S., Meesok, A., Nakapadungrat, S. and Putthapiban, P., 1975. "The granitic rocks and mineralisations at Khuntan Batholith, Lampang". Paper presented at the I.G.C.P. Circum Pacific Geology Conference at Kuala Lumpur, West Malaysia.

Suskichevskaya, G. M., Barsukov, V. L. and Trusikova, 1965. "On the composition of inclusions in quartz from some sulphide-cassiterite deposits. Mineralogical thermometry and barometry. Nanka.

Takenouchi, S. and Kennedy, G. C., 1965. "The solubility of CO_2 in NaCl solutions at high temperatures and pressures". Am. J. Sci., Vol. 263, pp. 445-454.

Taylor, R. G., 1978. "Aspects of Australian tin environment, exploration models and their relationship to ore search". Unpublished paper.

Teh, G. H., 1974. "The geology and mineralisation of Tekka Hill, Kinta Valley". B.Sc. Honours Thesis, Department of Geology, University of Malaya.

Tischendorf, G., 1973. "The metallogenetic basis of tin exploration in the Erzgebirge". Trans. Inst. Min. Metall., Appl. E. Sci., vol. 82, no. 795, pp. B9-B24.

Tischendorf, G., Lange, H. and Schust, F., 1974. "On the relation between granites and tin deposits in the Erzebirge, G.D.R: I.G.C.P. Symposium, M.A.W.A.M., vol. 1, pp. 132-136.

Traube, H., 1895. "Ueher die Aetzfiguren einiger Minerale". Neues. Jahrb. Min. Geol. Beil-Bd., vol. 10, pp. 454-476.

Turner, F. G. and Verhoogen, John, 1960. "Igneous and metamorphic petrology". Second edition. McGraw-Hill Book Co., Inc., New York, 694p.

Uytenbogaardt, W. and Burke, E. A. J., 1971. "Tables for microscopic identification of ore minerals". Second revised edition. Elsevier. 430p.

Venugopal, K., 1952. "Trace elements in cassiterite and stannite". Unpublished Ph.D. Thesis. Imperial College, University of London.

Verhoogen, Jean, 1949. "Thermodynamics of a magmatic gas phase". Univ. of California Publs., Dept. Geol.Scis. Bull., vol. 28, pp. 91-136.

Vinogradov, A. P., 1962. "The average contents of elements in main igneous rocks of the earth's crust". Geochem., vol. 7, pp. 641-664.

Voznayak, D. K., 1968. "V kn.: "Tezisy dokl. III Vses. soveshch po mineralog. termobarometrii geokhimii glubinnykh mineraloobrazuyushchikh rastvorov", in "Abstracts of Papers. Third All-Union Conference on Mineralogical Thermobarometry and Geochemistry of Deep-Seated Mineralizing Solutions". Moscow.

Wedepohl, K. H., 1969. "Handbook of Geochemistry". Springer-Verlag, Berlin-Heidelberg-New York. Vol. II-1.

Wedepohl, K. H., 1974. "Handbook of geochemistry". Springer-Verlag. Berlin-Heidelberg-New York. Vol. II-4.

Weibel, M., 1956. "Amblygonite, cassiterite and associated minerals from Caceres, Western Spain". Amer. Min., vol. 41, pp. 41-48.

Whittaker, E., 1974. Personal Communication.

Whittaker, E. and Muntus, R., 1970. "Ionic radii for use in geochemistry". Geochim. et. Cosmochim. Acta., vol. 34, pp. 945-956.

Yakovlev, Ya, V., 1973. "Formation temperature of tin deposits of Yukutia, (on data of inclusion homogenisation in minerals)". Abstract in "Fluid Inclusion Research". Proc. of COFFI, vol. 6, pp. 169-170.

Yeap, C. H., 1966, (MS). "The geology of Gakak Lode, P.C.C.L. ". B.Sc. Honours Thesis. Department of Geology, Univeristy of Malaya.

Yeap, C. H., 1974. "Some trace element analysis of Western Malaysian and Singapore granites". Newsletter of the Geol. Soc. Malaysia, no. 47, March, pp. 1-6.

Yeap, E. B., 1976. Personal Communication.

Yermakov, N. P., 1965. "Research on the nature of mineral-forming solutions, with special reference to data from fluid inclusions". International Series of Monographs in Earth Sciences Vol. 22, 734p. Pergamon Press, New York.

Yusupov, S. Sh. and Dolgov, Yu. A., 1970. "Effect of dikes on the formation of quartz in chamber pegmatite". "Doklady of the Academy of Sciences, U.S.S.R.", vol. 190, nos. 1-6, pp. 125-128.

Zerfoss, S. and Slawson, S. I., 1956. "Origin of authigenic inclusions in synthetic crystals". Am. Mineralogist, vol. 41, pp. 598-607.

References to be included:

Babat, G.I., 1947, J. Inst. Elec. Eng., Vol.94, pp27

Groves, D.I., and Taylor, R.G., 1973 "Greisenization and mineralisation at Anchor tin mine, Northeast Tasmania": Trans. Inst. Min. Metall., Appl. E. Sci, Vol 82, No.804 pp. B135-146.

Hall, A., 1969. "The geochemistry of the Cligga Head granites". Proc. Usser Soc., Vol 2, pt. 1, pp 136-140

Sobolev, V.S., Yu. A. Dolgov, L. sh. Bazarov, I.T., Bakumenko and Z.V. Shcherbakova, 1964. Doklady Akad. Nank SSSR, vol 157, no 2.

Tauson, L.V., Kozlov, V.D., and Kuz'min, M.I., 1968. "Geochemical criterion of potential ore - content in granitoid intrusions; (abstr): Int. Geol. Congr., 23rd, Czech., Rep., Abstr. Vol., p 171

Wendt, R.H., and Fassel, V.A., 1965. Anal. Chem., vol. 37 pp920